ARABIDOPSIS JUMONJI HISTONE DEMETHYLASES REGULATE FLORAL TRANSITION THROUGH THE FLORAL REPRESSOR *FLC*

GAN ENG SENG

(*B.Sc.* (*Hons.*), *NUS*)

A THESIS SUBMITTED
FOR THE DEGREE OF DOCTOR OF PHILOSOPHY
DEPARTMENT OF BIOLOGICAL SCIENCES
NATIONAL UNIVERSITY OF SINGAPORE

2015

Declaration

I hereby declare that the thesis is my original work and it has been written by me in its entirety. I have duly acknowledged all the sources of information which have been used in the thesis.

This thesis has also not been submitted for any degree in any university previously.

Gan Eng Seng

21 January 2015

Acknowledgements

I would like to first express my most sincere gratitude and respect to my supervisor, Dr. Toshiro Ito, for his guidance and support throughout the years of studies in his laboratory. It has been an eye-opening and fruitful experience working with a man who is so passionate about science. His timely suggestions have kept the project running despite its ups and downs. For his kindness, I am forever in his debt.

I would also like to thank the members of my PhD Thesis Committee, Dr. Xu Jian, Dr. Toshie Kai, Dr. Shinichiro Sawa, and Dr Yin Zhongchao, and Qualifying Examination Committee, Dr. Frederic Berger, Dr. He Yuehui and Dr. Xu Tongda for their previous time in reading my thesis and their valuable comments and suggestions.

I am grateful to Temasek Life Sciences Laboratory Ltd for the financial support, and the Department of Biological Sciences, National University of Singapore for conferring me the degree.

Many thanks to my former and current colleagues in the Plant Systems Biology Laboratory, especially my first mentor Sun Bo who taught me to be independent, Xu Yifeng who selflessly taught me many experimental techniques and collaborated with me in several projects, Wee Wan Yi who assisted me in various experiments, and to Huang Jiangbo, Guo Siyi, Looi Liang Sheng, Norman Teo, Yuki Nakamura, Kazue Kanehara, Ng Kian Hong, Gan Siou Ting, and Zhou Jie for their friendship, advices, and assistances. I am thankful to be given the opportunity to guide three students, Jessamine Geraldine Goh, Wong Jie Yun, and Jievanda Ow Shu Ying. Their

involvements in the project had been a great help to me and I truly appreciate their contributions.

I am much obliged to the laboratory members from Dr. Yu Hao's group, Dr. Frederic Berger's group, Dr. He Yuehui's group and Dr. Xu Tongda's group for the many friendly discussions and sharing of equipment and reagents.

I would also like to extend my gratitude to my wonderful 'lunch kaki', Wee Wan Yi, Tan Yun Rui, Wong Jie Yun, Lim Xiao Fang, Nie Xin, Lim Pei Qi, Ng Qing Yong, Shawn Tan, Melissa Soh for those countless days of lunchtime chats and laughs. It has been a blessing to have my 'Ngongster' brothers, Chai Chu Ann, Chen Eng Pao, Kane Hansel Bong, Tan Boon Tiong, Tay Boom Seng, Kalvin Chong, Liu Sai Kwong, Jong Kuet Yung, 'Unity' sisters, Jennifer Ho, Sharon Chong, Voon Siew Hui, Pui Mei Phing, and all the friends I made during my undergraduate years in the King Edward VII Hall of Residence, to accompany me all these years. I would like to thank them for their companionship, encouragement and will truly treasure this friendship.

Walking the path of science can be lonely when your family do not understand what you are doing. Hence I would like to take this chance to say a great big heartfelt thank you to my parents and sisters, for their unwavering supports and encouragements, and my loving wife, Ng Huey Shin, for her love and understanding all these years.

-Gan Eng Seng-

"It is not the strongest of the species that survive, nor the most intelligent, but the one most responsive to change."

-Charles Darwin-

Table of Contents

Summary

As sessile organisms, plants are continuously exposed to the changing ambient environment and have thus evolved multiple mechanisms to respond to these changes to improve survival. *Arabidopsis* plants show accelerated flowering at increased temperatures which is considered to be an adaptive trait to increase reproductive success. Many developmental processes are regulated by epigenetic histone modifications, and one of them the trimethylation of histone H3 lysine 27 (H3K27me3) is shown to confer a repressive chromatin status and silence gene expression.

In this study, I show that Jumonji-C domain-containing protein JUMONJI30 (JMJ30) and its homolog JMJ32 function as H3K27me3 demethylases. JMJ30 directly binds to the floral repressor *FLOWERING LOCUS C* (*FLC*) locus and removes the repressive H3K27me3 mark. At elevated temperatures, the *JMJ30* mRNA and JMJ30 protein are stabilized. This increased accumulation of JMJ30 protein is proposed to maintain a permissive chromatin state at the *FLC* locus, thus keeping its expression at high levels to prevent extreme precocious flowering as too early-flowering may risk not having enough nutrients and resources to support seed maturation.

Accordingly, the double mutant of *jmj30 jmj32*, grown at elevated temperatures, exhibits an early-flowering phenotype similar to the *flc* mutant, which is associated with increased H3K27me3 levels at the *FLC* locus and decreased *FLC* expression. Furthermore, ectopic expression of *JMJ30* causes an *FLC*-dependent late-flowering phenotype. Hence, taken together, JMJ30/JMJ32-mediated histone demethylation at the *FLC* locus constitutes a

balancing mechanism in flowering control at warm temperatures to prevent premature early flowering.

FRIGIDA (*FRI*) is a strong activator of *FLC*. *Arabidopsis* plant with functional *FRI* requires a prolonged exposure to cold to epigenetically silence *FLC* expression via H3K27me3 deposition. Further observation of vernalization treatment on *FRI jmj30 jmj32* mutant shows that loss of the H3K27me3 demethylases causes the plant to be more sensitized for vernalization, both morphologically and molecularly. These results present a new view on the balancing mechanism at an epigenetic level on the expression of an important flowering regulator, *FLC*. Moreover, I also show that *FRI jmj30 jmj32* mutant is less tolerant to heat stress, suggesting that besides *FLC*, other stress-responsive genes are also affected in *jmj30 jmj32*.

List of Tables

List of Figures

List of Abbreviations and Symbols

Gene names

ABI3	ABSCISIC ACID INSENSITIVE3
AFR1	SAP30 FUNCTIONRELATED 1
AGL24	AGAMOUS-LIKE 24
AP1	APETALA1
ARP6	ACTIN-RELATED PROTEIN 6
ASHH	ASH1 HOMOLOG
ASHR	ASH1-RELATED PROTEIN
ATX	ARABIDOPSIS TRITHORAX
ATXR	ARABIDOPSIS TRITHORAX-RELATED
BX-C	Bithorax complex
CBF1	C-REPEAT/DRE BINDING FACTOR 1
CCA1	CIRCADIAN CLOCK ASSOCIATED 1
CDF1	CYCLING DOF FACTOR 1
CLF	CURLY LEAF
CO	CONSTANS
COP1	CONSTITUTIVELY PHOTOMORPHOGENIC 1
CRY	Cryptochrome
dRAF	dRing-associated Factors Complex
ELF6	EARLY FLOWERING 6
EMF2	EMBRYONIC FLOWER 2
ESC	Extra sex comb
E(z)	Enhancer of zeste
F3H	FLAVONONE 3-HYDROXYLASE
LHP1	LIKE HETEROCHROMATIN PROTEIN 1
FIE	FERTILIZATION INDEPENDENT ENDOSPERM
FIS2	FERTILISATION INDEPENDENT SEED 2
FKF1	FLAVIN-BINDING, KELCH REPEAT, F-BOX 1

FLC	FLOWERING LOCUS C
FLD	FLOWERING LOCUS D
FLM	FLOWERING LOCUS M
FT	FLOWERING LOCUS T
FUS3	FUSCA3
GAF	GAGA factors
GI	GIGANTEA
GID	GIBBERELLIC INSENSITIVE DWARF 1
HAM1	HISTONE ACETYLTRANSFERASE OF THE MYST FAMILY 1
JMJ	JUMONJI
LDL1	LSD1-LIKE 1
LEC2	LEAFY COTYLEDON2
LFY	LEAFY
LHY	LATE ELONGATED HYPOCOTYL
LSD1	LYSINE SPECIFIC DEMETHYLASE 1
LUX	LUX ARRHYTHMO
MEA	MEDEA
MRG1	MORF RELATED GENE 1
MSI1	MULTICOPY SUPRESSOR OF IRA 1
PADI4	PEPTIDYL ARGININE DEIMINASE 4
PcG	Polycomb Group
PHD	Plant Homeodomain
PHO	PLEIOHOMEOTIC
PhoRC	Pho Repressive Complex
PIF4	PHYTOCHROME INTERACTING FACTOR 4
PR-DUB	Polycomb Repressive Deubiquitinase Complex
PRE	Polycomb Repressive Element
PRC1	Polycomb Repressive Complex 1

PRMT	PROTEIN ARGININE METHYLTRANSFERASE
REF6	RELATIVE OF EARLY FLOWERING 6
RLE	Repressive LEC2 Element
SCF	Skp Cullin F-box
SOC1	SUPPRESSOR OF OVEREXPRESSION OF CONSTANS 1
SPA	SUPPRESSOR OF PHYA-105
SUC2	SUCROSE TRANSPORTER2
SUVH	SU(VAR)3-9 HOMOLOG
SUVR	SU(VAR)3-9-RELATED PROTEIN
Su(var)3-9	Suppressor of variegation 3-9
SUZ12	Suppressor of zeste 12
SVP	SHORT VEGETATIVE PHASE
SWN	SWINGER
TEK	TRANSPOSABLE ELEMENT SILENCING VIA AT-HOOK
TFL1	TERMINAL FLOWER 1
TOC1	TIMING OF CAB EXPRESSION 1
Trx	Trithorax
UTX	Ubiquitously Transcribed Tetratricopeptide Repeat X
VIN3	VERNALIZATION INSENSITIVE 3
VRN2	VERNALIZATION 2 (VRN2)
Z	ZESTE (Z)

Experiments, chemicals and reagents

α-KG	α-ketoglutarate
APS	Ammonium peroxodisulfate
BLAST	Basic local alignment search tool
CTAB	Cetyl trimethyl ammonium bromide
DTT	Dithiothreitol
EDTA	Ethylenediaminetetraacetic acid

GA	Gibberellin
NaCl	Sodium chloride
PCR	Polymerase chain reaction
PIC	Protease Inhibitor Cocktail, cOmplete (Roche)
RT-qPCR	Reverse transcription – quantitative polymerase chain reaction
TE	Tris-EDTA
TEMED	N,N,N',N'-tetramethylethylenediamine
TEAB	triethyl ammonium bicarbonate

Units and measurements

°C	degree Celsius
bp	base pairs
Ct	threshold cycle
g	gram(s)
hr	hour(s)
kb	kilo base pairs
kDa	kilo Dalton(s)
M	Molar
µg	microgram(s)
µl	microlitre(s)
µM	micromolar
min	minute(s)
rpm	revolutions per minute
rcf	relative centrifocal force (x g, gravitational force)

Others

3D	Three dimensions
a.k.a.	also known as
cDNA	complementary DNA

Col	Columbia
e.g.	*exempli gratia* (for example)
et al.	*et alii* (and others)
etc	*et cetera* (and the rest)
gDNA	genomic DNA
H3K27me3	Trimethylation of lysine 27 of histone H3
H2AK119ub	Monoubiquitination of lysine 119 of histone H2A
i.e.	*id est* (that is)
LB	Luria-Bertani
LD	Long day (16-h light/8-h dark)
lncRNA	long non-coding RNA
MS	Murashige and Skoog
ncRNA	non-coding RNA
SAM	shoot apical meristem
SD	Short day (8-h light/16-h dark)
WT	Wild-type

Chapter 1

Literature Review

Chapter 1 Literature Review

1.1 The epigenome at a glance

The DNA of the genome contains all the information for building the whole organism. However, not all the genes in the genome are similarly expressed in all cell types. The transcription of the gene depends not only on the presence of its *trans*-acting factor (e.g. transcription factor) and *cis*-regulatory elements (e.g. promoters, enhancer), but also its chromatin status or epigenetic landscape.

The term 'epigenetic' was first coined by Waddington more than half a century ago, which described the "the causal interactions between genes and their products, which bring the phenotype into being" (Goldberg et al, 2007; Waddington, 1942). In other words, epigenetics originally describes how a 'genotype' manifests itself into 'phenotype'. Nowadays, the text book definition of epigenetics is largely accepted as the study of heritable changes in gene expression without a change in DNA sequence (Berger et al, 2009). For example, in an organism, all the cells contain the same genetic information; however, as the organism develops, cells in various tissues differentiate into specific morphology and display distinct gene expression profiles, which is heritable as they divide. In broader effects, epigenetic changes in an organism may also be inherited by its offspring. Epigenetic regulation is involved in multitudinous developmental processes and exists in many, if not all, species. The human X chromosome inactivation by *Xist* RNA (Avner & Heard, 2001), heritable prion proteins in yeast (Liebman & Chernoff, 2012), the *cycloidea* epiallele of *Linaria vulgaris* that produces

peloric flowers (Cubas et al, 1999), centromeric histone H3 (CenH3) incorporation that establishes the self-propagating heterochromatic centromere (Folco et al, 2008) are a few classical examples of epigenetic phenomena.

In the nucleus, histone proteins help package the DNA into condensed chromatin. Both the DNA and histone can be modified with tags and these modifications serve as a second layer of information, which coincides with the literal meaning of epigenome ("epi-" means above in Greek). The epigenome shapes the physical structure of the genome. Tightly wrapped DNA inactivates genes by making them unreadable, while a relaxed chromatin allows easy accessibility to the active genes. As mentioned above, there exist multiple regulatory mechanisms that can affect the epigenome, including DNA methylation, histone modification, non-coding RNA (ncRNA), placement of histone variant, chromatin remodeling, etc. The histone modifications will be described in more details as the main topic of this study.

1.1.1 Histone modifications

In the nucleus, around 147 base pairs of DNA wrap around one octameric nucleosome core consisting of two of each core histone H2A, H2B, H3 and H4. The linker histone H1 binds the nucleosome, locking the DNA into place. Histones can undergo a wide array of post-translational modifications including, but not limited to, methylation, acetylation, phosphorylation, ubiquitination, sumoylation. The N-terminal tails of histones, post-translationally modified at selected residues, confers different regulatory

signals and some of the patterns have been shown to be closely linked to biological events (Strahl & Allis, 2000).

Approximately 30-40% of the core histone N-termini consists of the positively charged lysine and arginine residues. This fueled the spreading of the perception that the N-termini function primarily by binding to the DNA in the nucleosomes (Hansen et al, 1998). However, emerging evidence suggests that, rather than binding with DNA, the histone N-termini interacts with non-histone regulatory proteins and form multiprotein complexes. Many of these distinct histone H3 and H4 tail modifications lies close to each other that they act sequentially or in combination to regulate unique biological outcomes (Strahl & Allis, 2000). The histone code hypothesis predicts that these covalent modifications might provide specific binding platform, recruiting effector (or reader) proteins and allowing the inherent code to be interpreted into functional outcomes (Jenuwein & Allis, 2001; Lu et al, 2010). Hence, this highlights the importance of the enzymatic complex responsible for establishment, maintenance and removal of these types of epigenetic marks.

1.1.2 Histone methylation by writer proteins

One of the most well-studied histone modifications is histone methylation. Histone methylation plays an important role in diverse biological processes ranging from transcriptional regulation to heterochromatin formation (Lu et al, 2010). In plants, its importance is obvious in the loss-of-function mutants of components of this regulatory mechanism that many floral genes are mis-expressed in the leaves.

The histone mark is deposited by histone methyltransferase (HMTase), a family of proteins in the SET DOMAIN GROUP (SDG) that share the conserved SET domains. The SET domain has ~130 amino acids and was initially found in three *Drosophila melanogaster* proteins: Suppressor of variegation 3-9 [Su(var)3-9] (Tschiersch et al, 1994), Enhancer of zeste [E(z)] (Jones & Gelbart, 1993) and Trithorax (Trx) (Stassen et al, 1995), hence the name SET. These SET domain can catalyze histone lysine mono-, di-, or tri-methylation of several lysines and arginines in histones H3 and H4 (Figure 1)(Pien & Grossniklaus, 2007).

In *Arabidopsis thaliana*, there are 37 of these SET domain-containing HMTases, of which seven of them have truncated SET domains (Table 1) (Baumbusch et al, 2001; Thorstensen et al, 2011). They can be categorized into five classes based on their homology with the *Drosophila* SET domain proteins. Class I SDGs has three members, CURLY LEAF (CLF), SWINGER (SWN), MEDEA (MEA), and they are homologous to *Drosophila* E(z) protein which catalyzes the trimethylation on histone H3 lysine 27 (H3K27me3). Although not all the members have their functions analyzed, class II SDGs, ASH1 HOMOLOG 1-4 (ASHH1-4) and ASH1-RELATED PROTEIN 1-3 (ASHR1-3), are generally H3K4 and H3K36 HMTases. The *Drosophila* TRX protein are well-studied and reported as a H3K4me3 HMTase (Schuettengruber et al, 2011). Its homologs in *Arabidopsis*, ARABIDOPSIS TRITHORAX 1-5 (ATX1-5) and ARABIDOPSIS TRITHORAX-RELATED 1-7 (ATXR1-7), also generally target the same lysine residue on histone H3 and group together as the Class III SET domain proteins. However, ATXR5 and ATXR6 diverge functionally with the other ATX and ATXR proteins,

carry out H3K27me1 methylation, and are grouped together as Class IV HMTases (Jacob et al, 2010). The Class V HMTase is the biggest class which contains 15 members, SU(VAR)3-9 HOMOLOG 1-10 (SUVH1-10) and SU(VAR)3-9-RELATED PROTEIN 1-5 (SUVR1-5). Like the *Drosophila* Su(var)3-9 protein, members from Class V mostly catalyzes H3K9 methylation.

Besides the SET domain HMTases, the *Arabidopsis* genome contains another small family of proteins that catalyzes the methylation on arginine (Arg) residues, collectively known as the PROTEIN ARGININE METHYLTRANSFERASES (PRMTs)(Figure 1)(Lu et al, 2010). The type I PRMTs produces asymmetric dimethylated Arg, whereas type II PRMTs catalyzes symmetric dimethylated Arg.

Each of the histone methylation sites and their degree of methylation (mono-, di- or tri-methylation) confers different biological functions and roles. In general, these lysine and arginine methylation states can be experimentally classified into two categories. Methylation at H3K9, H3K27 and H4K20 are considered repressive epigenetic marks and associated more with transcriptionally inactive genes, whereas methylation at H3K4, H3K36 and H3K79, which correspond more with active genes, are considered activating marks (Pien & Grossniklaus, 2007). However, there are bound to be exceptions to every generalization, for example, H3K9 methylation are also found in transcriptional active regions (Vakoc et al, 2005) and H3K36 methylation represses spurious transcription from intragenic cryptic promoter (Carrozza et al, 2005).

Like histone lysine methylation, the distinct types of histone arginine methylation also regulate transcriptional activity differently (Litt et al, 2009). In human, asymmetrical dimethylation of H4R3 correlates with transcriptional activation, possibly by promoting histone acetylation (Huang et al, 2005a). On the other hand, symmetrical dimethylated H3R8 is associated with deacetylation of histone H3 and H4 (Pal et al, 2004), and asymmetrical dimethylation of H3R2 inhibits the recruitment of H3K4 methyltransferase complex (Guccione et al, 2007; Kirmizis et al, 2007), thus causing transcriptional repression. In *Arabidopsis*, the transcriptional regulation by methylated arginine is not as clear. AtPRMT4a/b asymmetrically dimethylate H3R17 (Niu et al, 2008), whereas H4R3 is symmetrically dimethylated by AtPRMT5 (Schmitz et al, 2008) and asymmetric dimethylated by AtPRMT1a/b (Yan et al, 2007) and AtPRMT10 (Niu et al, 2007). Interestingly, loss-of-function mutants of *atprmt4a atprmt4b*, *atprmt5*, and *atprmt10* all caused *FLC* up-regulation, suggesting that arginine methylation is required for *FLC* repression (Niu et al, 2007; Niu et al, 2008; Schmitz et al, 2008). It is unknown why the metazoan asymmetric dimethylation on H4R3 results in active transcription (Huang et al, 2005a) whereas the same mark in *Arabidopsis* appear to repress *FLC* (Niu et al, 2007). Detailed genome-wide methyl-arginine ChIP analysis and gene expression profile of their respective *prmt* mutant should better reveal their function.

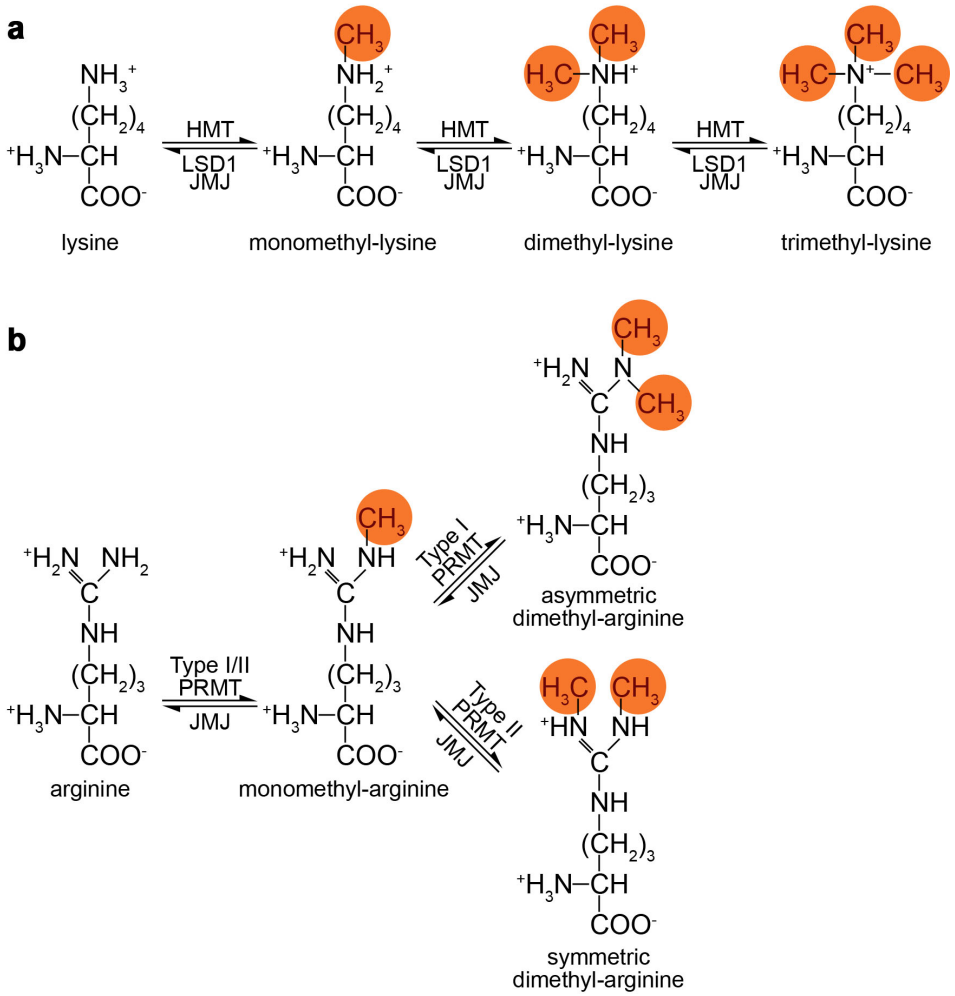

Figure 1. Histone methylation and demethylation on lysine or arginine residues.

(**a**) Histone methyltransferase (HMT/HMTase) acts as writer protein and deposits methyl groups on lysine residue on histone. The eraser proteins, LYSINE-SPECIFIC DEMETHYLASE1 (LSD1) and JUMONJI (JMJ) proteins, function as histone demethylases and remove these epigenetic marks. (**b**) The PROTEIN ARGININE METHYLTRANSFERASES (PRMTs) add the methyl groups onto arginine residues either symmetrically (type I) or asymmetrically (type II). JMJ proteins can also demethylate methyl-arginine, antagonizing the effect of PRMTs. Through the action of PEPTIDYL ARGININE DEIMINASEs (PADIs), the methyl-arginine can also be converted to citrulline rather than an unmodified arginine (not shown). Figure adapted from (Lu et al, 2010).

Table 1. *Arabidopsis* SET domain proteins

Class	Name	SDS number	AtG number	HMTase activity
I – E(Z)	CLF	SDG1	AT2G23380	H3K27me3
	SWN	SDG10	AT4G02020	H3K27me3
	MEA	SDG5	AT1G02580	H3K27me3
II – ASH1	ASHH1	SDG26	AT1G76710	H3K36me2
	ASHH2/EFS	SDG8	AT1G77300	H3K4me3; H3K36me2/3
	ASHH3	SDG7	AT2G44150	-
	ASHH4	SDG24	AT3G59960	-
	ASHR1	SDG37	AT2G17900	-
	ASHR2	SDG39	AT2G19640	-
	ASHR3	SDG4	AT4G30860	H3K4me2; H3K36me2
III - TRX	ATX1	SDG27	AT2G31650	H3K4me3
	ATX2	SDG30	AT1G05830	H3K4me2
	ATX3	SDG14	AT3G61740	-
	ATX4	SDG16	AT4G27910	-
	ATX5	SDG29	AT5G53430	-
	ATXR1	SDG35	AT1G26760	-
	ATXR2	SDG36	AT3G21820	-
	ATXR3	SDG2	AT4G15180	H3K4me1/2/3
	ATXR4	SDG38	AT5G06620	-
	ATXR7	SDG25	AT5G42400	H3K4me1/2/3
IV	ATXR5	SDG15	AT5G09790	H3K27me1
	ATXR6	SDG34	AT5G24330	H3K27me1
V – SU(VAR)3-9	SUVH1	SDG32	AT5G04940	-
	SUVH2	SDG3	AT2G33290	H3K9me1/2; H3K27me1/2; H4K20me1
	SUVH3	SDG19	AT1G73100	-
	SUVH4/KYP	SDG33	AT5G13960	H3K9me1/2
	SUVH5	SDG9	AT2G35160	H3K9me1/2
	SUVH6	SDG23	AT2G22740	H3K9me1/2
	SUVH7	SDG17	AT1G17770	-
	SUVH8	SDG21	AT2G24740	-
	SUVH9	SDG22	AT4G13460	-
	SUVH10	SDG11	AT2G05900	-
	SUVR1	SDG13	AT1G04050	-
	SUVR2	SDG18	AT5G43990	-
	SUVR3	SDG20	AT3G03750	-
	SUVR4	SDG31	AT3G04380	H3K9me2/3
	SUVR5	SDG6	AT2G23740	H3K9me2; H3K27me2

Adapted from (Baumbusch et al, 2001; Thorstensen et al, 2011)

1.1.3 Histone demethylation by eraser proteins

Antagonizing the effect of the SET domain proteins and PRMTs are the histone demethylases, which function as 'eraser' proteins of these histone codes. Unlike histone acetylation, which dynamism had been shown through the discovery of histone acetyltransferases and deacetylases, histone methylation was previously thought to be irreversible due to the lack of histone demethylases. The human PEPTIDYL ARGININE DEIMINASE 4 (PADI4) was the first enzyme shown to be able to antagonize histone arginine methylation (Cuthbert et al, 2004; Wang et al, 2004). However, there are arguments whether to consider PADI4 a histone demethylase because it catalyzes the conversion of methyl-arginine to citrulline instead of an unmodified arginine. The dynamics of histone methylation was finally rectified when the demethylation of lysine 4 of histone H3 (H3K4) was first demonstrated by human Lysine Specific Demethylase 1 (LSD1) in HELA cells (Shi et al, 2004).

Currently, there are three types of demethylases that have been characterized, PADI, LSD1 and Jumonji-C (JmjC) domain-containing proteins, each functioning through different biochemical mechanism. The mammalian PADI4 is a member of a gene family that catalyzes the citrullination/deimination of arginine residues of proteins such as histones. However, a protein-protein BLAST (blastp) search suggests that the *Arabidopsis* genome contains no PADI homolog. The existence of other proteins to carry out a similar enzymatic citrullination reaction is uncertain.

In the *Arabidopsis* genome, there are four LSD1 homologs, FLOWERING LOCUS D (FLD), LSD1-LIKE1 (LDL1), LDL2 and LDL3 (Table 2). LSD1

proteins are able to remove methyl groups from mono- and dimethylated histones through FAD-dependent amine oxidation (Figure 1) (Shi et al, 2004; Spedaletti et al, 2008). Oxidation of the methyl-lysine generates an imine intermediate, which is then hydrolyzed through a non-enzymatic process to produce the demethylated lysine and formaldehyde. Due to the property of the FAD-mediated reaction, LSD1 proteins cannot demethylate trimethylated lysine residues because a lone pair of electrons in the unprotonated state of N is required to generate the imine intermediate.

On the other hand, JUMONJI (JMJ) proteins are able to demethylate all three mono-, di- and trimethylated histone. All JMJ proteins contain the catalytic JmjC domain and within the JmjC domain, there are a few key amino acid residues: three of them bind to the Fe(II) cofactor and another two residues bind to the α-ketoglutarate (α-KG)(Figure 2)(Klose et al, 2006a; Klose & Zhang, 2007). Both cofactors, α-KG and Fe(II) ions are important for the oxidative demethylation reaction. The cofactor-bound JmjC domain forms a reactive oxoferryl species that hydroxylates the methyl-lysine or methyl-arginine. Similar to the LSD1 reaction, the unstable hydroxymethyl product then spontaneously degenerates to produce the demethylated lysine or arginine and formaldehyde (Lu et al, 2010; Tsukada et al, 2006).

The mammalian genome contains a large number (human, 30; mouse 30) of JMJ proteins which can be categorized into seven groups (Klose et al, 2006a). Members from the same group appear to targets a similar set of modified histone, e.g. the substrate specificity of the JHDM3/JMJD2 group for methylated H3K9 and H3K36 is not only conserved across all its members but also across species from human to mouse. Similarly, all three members of the

UTX/UTY/JMJD3 group targets H3K27 methylation specifically. The substrate specificity of the JMJ proteins partly relies on their JmjC domain, e.g. interaction of histone H3 with the Zn-binding domain within the C-terminal region of the JmjC domain of UTX/KDM6A bends the histone and extends the target residue H3K27me3 into the catalytic domain (Sengoku & Yokoyama, 2011). Moreover, additional domains such as the JmjN domain (Klose et al, 2006b; Whetstine et al, 2006), plant homeodomain (PHD) (Horton et al, 2010), and Tudor domain (Huang et al, 2006) also contributes to the JMJ proteins' target preferences. Hence, it is not surprising that members of the same group that has similar domain architecture may target a similar set of the substrates.

The *Arabidopsis* genome contains 21 JMJ proteins which can be categorized into five groups based on their JmjC domain sequences and overall domain architecture (Table 2)(Hong et al, 2009; Lu et al, 2008). Besides the JmjC domain, members of the same group of JMJ proteins share certain protein domains that set them apart from the other groups. Members of the KDM5/JARID1 and KDM4/JHDM3 group contain additional JmjN domain at its N-terminal not found in other groups, whereas most members of the KDM3/JHDM2 group has one or two RING domain(s) (Lu et al, 2008). One group of JMJ proteins comprises of no other recognizable protein domain besides its JmjC domain (further explained in section 1.1.5). In terms of the JmjC domains, almost all *Arabidopsis* JMJ proteins contain the conserved Fe(II) and α-KG-binding residues, while those that carry inactive variants are likely to abrogate their enzymatic activity. Like the animal counterparts, members from the same group of JMJ proteins show some degree of

conserved substrate specificity (Table 2). It is worth noticing that the *Arabidopsis* genome does not have members in the KDM4/UTX/JMJD3 group which catalyzes H3K27 demethylation, KDM2/JHDM1 group which target H3K36 methylation and the PHF group.

Table 2. *Arabidopsis* histone demethylases of the JMJ and LSD1 family

Group	Name	AtG number	Demethylase activity	Reference
JMJ family				
KDM5/ JARID1	JMJ15/MEE27	AT2G34880	H3K4me1/2/3	(Lu et al, 2010)
	JMJ18	AT1G30810	H3K4me2/3	(Yang et al, 2012)
	JMJ14	AT4G20400	H3K4me1/2/3	(Jeong et al, 2009; Lu et al, 2010; Yang et al, 2010)
	JMJ16	AT1G08620	-	-
	JMJ19	AT2G38950	-	-
	JMJ17	AT1G63490	-	-
KDM4/ JHDM3/ JMJD2	JMJ12/REF6	AT3G48430	H3K9me3; H3K4me2/3, H3K36me2/3; H3K27me2/3	(Yu et al, 2008b) (Ko et al, 2010) (Lu et al, 2011b)
	JMJ11/ELF6	AT5G04240	H3K9me3; H3K27me2/3	(Yu et al, 2008b) (Crevillen et al, 2014)
	JMJ13	AT5G46910	-	-
KDM3/ JHDM2	JMJ26	AT1G11950	-	-
	JMJ29	AT1G62310	-	-
	JMJ25/IBM1	AT3G07610	H3K9me1/2	(Inagaki et al, 2010)
	JMJ27	AT4G00990	-	-
	JMJ24	AT1G09060	-	-
	JMJ28	AT4G21430	-	-
JMJD6	JMJ22	AT5G06550	H3R2me2, H4R3me1/2s	(Cho et al, 2012)
	JMJ21	AT1G78280	-	-
	JMJ20	AT5G63080	H3R2me2, H4R3me1/2s	(Cho et al, 2012)
JmjC domain-only	JMJ30	AT3G20810	H3K27me2/3 H3K36me2/3	(Gan et al, 2014b) (Yan et al, 2014)
	JMJ31	AT5G19840		
	JMJ32	AT3G45880	H3K27me3	(Gan et al, 2014b)
LSD1 family				
LSD1	FLD	AT3G10390	H3K4me1/2	(Jiang et al, 2007)
	LDL1	AT1G62830	H3K4me1/2	(Jiang et al, 2007)
	LDL2	AT3G13682	H3K4me1/2	(Jiang et al, 2007)
	LDL3	AT4G16310		

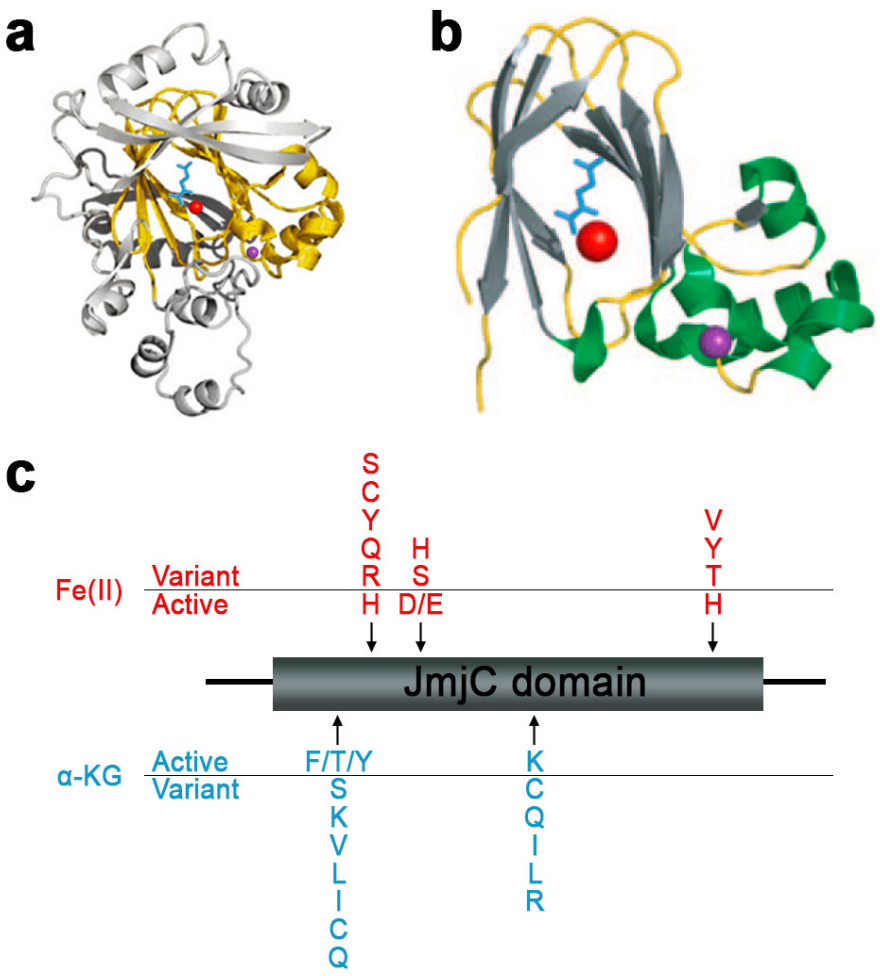

Figure 2. The catalytic JmjC domain contains key amino acid residues for its active function.

(**a**) Cartoon depicting the 3D structure of the N-terminal portion of JHDM3A/JMJD2A protein. The JmjC domain (yellow), α-ketoglutarate (α-KG) (blue), Fe(II) ion (red) and zinc ion (purple) are highlighted. (**b**) The JmjC domain of JHDM3A/JMJD2A is enlarged to show the catalytic β-sheets region (grey) that binds the cofactors α-KG (blue) and Fe(II) ion (red), and the α-helical region (green) that binds the zinc ion (purple). (**c**) Schematic diagram of the JmjC domain that shows the amino acid residues that binds α-KG (blue) and Fe(II) ion. Active and inactive amino acid variants are depicted based on their predicted biochemical properties. Figures adapted from (Klose et al, 2006a; Klose & Zhang, 2007).

1.1.4 H3K27 methylation targets a gene for repression

H3K27 can be methylated by two complexes, one that monomethylate H3K27, and another regulates di- and trimethylation of H3K27. H3K27me1 is a heterochromatic mark enriched in chromocenters (Mathieu et al, 2005b). It is conferred by the redundant H3K27 mono-HMTases, ATXR5 and ATXR6, and it protects genomic integrity by preventing over-replication of heterochromatin in *Arabidopsis* (Jacob et al, 2010). On the other hand, functioning in gene repression and developmental regulation, H3K27me3 is differently regulated throughout developmental stages, and is governed by the Polycomb group (PcG) proteins (Lafos et al, 2011; Zheng & Chen, 2011).

The PcG proteins were first described in *Drosophila* in which a mutation in a gene causes the fly to not only have sex combs on the first, but also the second and third pair of legs, hence the name *Polycomb* (*Pc*)(Lewis, 1949). It was nearly three decades later that the mechanism is slowly unfolded: *Pc* controls thoracic and abdominal development by acting as a negative regulator of the bithorax complex (BX-C)(Lewis, 1978). To date, five PcG complexes have been identified in *Drosophila*: Polycomb Repressive Complex 1 (PRC1), PRC2, Pho Repressive Complex (PhoRC), dRing-associated Factors Complex (dRAF), and Polycomb Repressive Deubiquitinase Complex (PR-DUB)(Kahn et al, 2014). Two of them, the PRC2 and PCR1, have been described in more detail.

In *Drosophila*, the PRC2 is composed of four core proteins, namely E(z), Extra sex comb (Esc), Suppressor of zeste 12 (SUZ12), and p55. Like *Drosophila*, *Arabidopsis* PRC2 also comprises four main proteins, but it has 12 homologs of Drosophila PRC2 subunits: three E(z) homologs CLF, MEA

and SWN; three SUZ12 homologs EMBRYONIC FLOWER 2 (EMF2), FERTILISATION INDEPENDENT SEED2 (FIS2) and VERNALIZATION2 (VRN2); one ESC homolog FERTILIZATION INDEPENDENT ENDOSPERM (FIE); and five p55 homologs MULTICOPY SUPRESSOR OF IRA1-5 (MSI1–5)(Pien & Grossniklaus, 2007). Genetic and molecular evidence suggests that these proteins form at least three PRC2-like complexes: the EMF, VRN and FIS complexes. Although these complexes have clearly distinct functions, they do share some target genes. For instance, the FIS complex, which contains MEA/SWN, FIS2, FIE and MSI1, silences target genes during gametogenesis and early seed development, whereas the EMF complex, which probably contains CLF/SWN, EMF2, FIE and MSI1, silences some of the same target genes during subsequent sporophytic development (Gan et al, 2013).

Around one fifth of the *Arabidopsis* genes are covered by the repressive H3K27me3 mark (Zhang et al, 2007). The process of methylation through the SET domain protein is well-defined, but knowledge on the process of recruitment to these sites is lagging behind. In *Drosophila*, there is a set of *cis*-regulatory elements called Polycomb Repressive Element (PRE) that recruits DNA-binding proteins such as PLEIOHOMEOTIC (PHO), ZESTE (Z), and GAGA factors (GAFs), which bring the PRC2 complex to these sites to exert transcriptional repression (Schwartz & Pirrotta, 2008). Similar PRE-like elements are found in mice and human (Sing et al, 2009; Woo et al, 2010), however the identification of PRE is not as successful in *Arabidopsis*, possibly because such conserved sequence is not found in the annotated H3K27me3 target regions in *Arabidopsis*.

LEAFY COTYLEDON2 (*LEC2*) is a master regulator of seed development that is specifically expressed in the embryo in a short time frame. Promoter bashing experiment showed that a 500-bp long sequence upstream of *LEC2* contains three *cis*-regulatory elements (Berger et al, 2011). Two of them are important for transcriptional activation, while the third one, named *Repressive LEC2 Element* (*RLE*) is necessary for the H3K27me3-mediated repression of *LEC2*. The *RLE* restricts *LEC2* transcription to the embryo. Furthermore, insertion of the 50 bp *RLE* to the *FLAVONONE 3-HYDROXYLASE* (*F3H*) promoter can trigger H3K27me3 deposition and repression of the *pF3H::GUS* reporter construct (Berger et al, 2011). Recently, we identified that a 153 bp fragment located upstream of *KNUCKLES* (*KNU*) is able to recruit H3K27me3 to the region (Sun et al, 2014). *KNU* encodes a C2H2 zinc-finger protein that regulates floral meristem termination and hence must be timely activated for its function (Sun et al, 2009). We showed mutation of this 153 bp fragment in the *pKNU::KNU-GUS* transgenic line causes ectopic expression of the GUS reporter (Sun et al, 2014). Moreover, like *RLE*, insertion of this fragment to the *pF3H::YFP* reporter is able to recruit H3K27me3 and suppress the *YFP* expression. This shows that *RLE* and the 153 bp *KNU* upstream fragment fulfilled the criteria of the PRE that it is able to generate a new binding site for PRC, create a site for H3K27me3 deposition, and induce repression of the corresponding gene (Schwartz & Pirrotta, 2008).

After PRC2 complex established the H3K27me3 repressive mark, it is generally accepted that H3K27me3 recruits PRC1 complex to reinforce the repression at the locus. The existence of a PRC2 complex in *Arabidopsis* is eminent because it contains all the core PRC2 components. However, whether

Arabidopsis has a functional PRC1 complex is unclear, because some of the metazoan homologs, such as Pc that binds H3K27me3, are not found in the plant genome (Goodrich & Tweedie, 2002). It is later revealed that *Arabidopsis* uses other proteins to carry out PRC1-like function. The LIKE HETEROCHROMATIN PROTEIN 1/TERMINAL FLOWER 2 (LHP1/TFL2) is shown to bind H3K27me3 *in vitro* and associate with genes that are marked by H3K27me3 *in vivo* (Turck et al, 2007; Zhang et al, 2007), fulfilling the role of the metazoan Pc. In animal, the PRC1 complex catalyzes the monoubiquitination of lysine 119 of histone H2A (H2AK119ub). It is recently reported that LHP1, AtRING1A/B (Chanvivattana et al, 2004), and AtBMI1A/B/C (Bratzel et al, 2010; Li et al, 2011b) interacts to form a PRC1-like complex in *Arabidopsis*. Moreover, this PRC1 complex also modifies histone with its RING subunit, catalyzing the deposition of H2AK119ub (Bratzel et al, 2010). Loss-of-function of *atbmi1a/b* causes dedifferentiation of vegetative tissues into callus-like structure. This phenotype mimics the double mutant of *clf swn* (Chanvivattana et al, 2004) and *vrn2 emf2* (Schubert et al, 2005), indicating that *AtBMI1* genes function in a similar pathway as PRC2 complex and are required to maintain the differentiated state of somatic cells.

Although the hierarchical model of PcG action in animal is well-accepted, in which PRC2-mediated H3K27me3 recruits PRC1 to establish the region of repression, this model is being challenged as recent findings again revealed exceptions to such generalization. There are genes targeted by H3K27me3 but lack PRC1 occupancy (Ku et al, 2008), and vice versa PRC1-mediated H2A monoubiquitination can occur independent of PRC2 activity, as in X inactivation mediated by *Xist* RNA (Schoeftner et al, 2006). Similar

H3K27me3-independent PRC1-like activity may also occur in *Arabidopsis*. Seed maturation genes *ABSCISIC ACID INSENSITIVE3* (*ABI3*), *FUSCA3* (*FUS3*), *LEC1* and *LEC2* are expressed in a short time frame during embryo development and must be silenced for proper vegetative growth. A recent study showed that mutant of the PRC1 components *atbmi1a/b/c* causes dramatic decrease of H3K27me3, whereas mutant of the PRC2 components *clf swn* increased H2AK119ub, highlighting the difference in repression mechanism of PRC1 and PRC2 on these seed maturation genes (Yang et al, 2013). Moreover, genome wide H2AK119ub level was not significantly affected in the *clf swn* mutant, suggesting that in plant PRC1 targeting may occur through pathways independent of PRC2 (Yang et al, 2013). The *Drosophila* non-canonical PRC1 complex, called the dRAF complex, comprises Sce (*Arabidopsis* homologs: AtRING1A/B), Psc (*Arabidopsis* homologs: AtBMI1A/B/C), and KDM2, but lacks two components of the canonical PRC1 complex, Pc and Ph. Interestingly, mutation of *Sce* or *Psc* significantly decreases H2AK119ub levels, whereas depletion of *Pc* or *Ph* yield no effect on global H2AK119ub levels (Lagarou et al, 2008). Thus, compared to the canonical PRC1 complex, the plant PRC1-like complex may more resemble the dRAF complex, and may be recruited to chromatin independently of H3K27me3 marks to catalyze the H2AK119 monoubiquitination (Calonje, 2014).

Although the HMTase of H3K27me3 has been reported for almost a decade, the discovery of its demethylase has not been as successful in plants. This is mainly because the H3K27me3 demethylase in animals, UBIQUITOUSLY TRANSCRIBED TETRATRICOPEPTIDE REPEAT X (UTX) and JMJD3

(Agger et al, 2007), do not have a homolog in plants. Only recently has JMJ11/EARLY FLOWERING 6 (ELF6)(Crevillen et al, 2014) and JMJ12/RELATIVE OF EARLY FLOWERING 6 (REF6)(Lu et al, 2011a) been reported as the H3K27me3 demethylase in *Arabidopsis*. A hypomorphic mutant allele of *elf6* causes defect in the epigenetic resetting of a floral repressor in which the H3K27me3 level at the locus is maintained at a higher level in the *elf6-5* allele (Crevillen et al, 2014). On the other hand, over-expression of *REF6* causes phenotype which resembles the PRC2 mutant, *clf swn*, showing defects in H3K27me3-mediated gene silencing (Lu et al, 2011a). However the fact that the phenotypes of *elf6*, *ref6* single mutants and the *elf6 ref6* double mutant are weaker than those of the metazoan counterpart hints that there might be more H3K27me3 demethylases waiting to be uncovered (Yu et al, 2008b).

1.1.5 Unique group of JMJ proteins that contains only the JmjC domain

In animals, most of the groups of JMJ proteins have at least one member whose function and enzymatic activity are characterized (Klose et al, 2006a). The group that contains only the JmjC domain is comparatively poorly understood. Some of them (sub-group: FIH, PLA2G4B, HSPBAP1) localize to the cytoplasm instead of nucleus. For example, Factor Inhibiting Hypoxia (FIH), the first JMJ protein shown to be enzymatically active, actually hydroxylates the asparagines residue of Hypoxia Inducible Factor α (HIFα), rather than targeting methylated histone (Lando et al, 2002). Members of other sub-group (JMJD5, JMJ4, L0C339123) has serine instead of a threonine or

phenylalanine in its first α-KG-binding residue (Klose et al, 2006a). From the studies of the crystral structure of the JmjC domain, these amino acid substitutions (serine in place of threonine/tyrosine/phenyalanine) may render them enzymatically non-functional, possible because a bulkier amino acid is inherently preferred in to form an enzymatically competent active site (Klose et al, 2006a). However, another recent report shows that JMJD5/KDM8 is still able to demethylate H3K36me2 specifically *in vivo* (Hsia et al, 2010).

Similarly, the members of the JmjC domain only group are also poorly characterized in plants (Table 2). There are three members in this group, namely JMJ30, JMJ31, and JMJ32. To date, only JMJ30 has been shown to be involved in circadian regulation (Jones et al, 2010; Jones & Harmer, 2011; Lu et al, 2011c) and flowering control (Yan et al, 2014). Hence, further investigations aim to reveal more functions of this group of JMJ proteins.

1.2 Flowering pathways that regulates the floral transition

Flowering is an important developmental process for angiosperms (flowering plants) because it ensures successful reproduction and propagation of its progeny. Hence, it is not surprising that a plethora of mechanisms have evolved to tightly control the flowering process. As a sessile organism, this poses a need for a plant to be able to respond to its ever-changing environment: day-night cycle, day length, light quality, temperature, nutrient availability, etc. The flowering regulatory pathways have evolved as adaptive traits to ensure successful reproduction.

Upon reaching a certain developmental stage and perceiving the right environmental cues, plants would undergo a floral transition, a major physiological switch from vegetative growth to reproductive development. In *Arabidopsis*, this switch from a vegetative to a reproductive phase is controlled by five genetically defined pathways, and all inputs congregate on a few key floral regulators: the floral repressor *FLOWERING LOCUS C* (*FLC*), which acts upstream and represses the downstream floral inducers *FLOWERING LOCUS T* (*FT*) and *SUPPRESSOR OF OVEREXPRESSION OF CONSTANS 1* (*SOC1*)(Figure 3)(Dennis & Peacock, 2007; He & Amasino, 2005; Liu et al, 2009; Srikanth & Schmid, 2011). The four classical flowering pathways are the photoperiod pathway, vernalization pathway, gibberellin pathway, and the autonomous pathway. In addition, recent findings have revealed a few players involved in a fifth flowering pathway that is responsive to ambient temperature changes and has been called the thermosensory pathway (Figure 3).

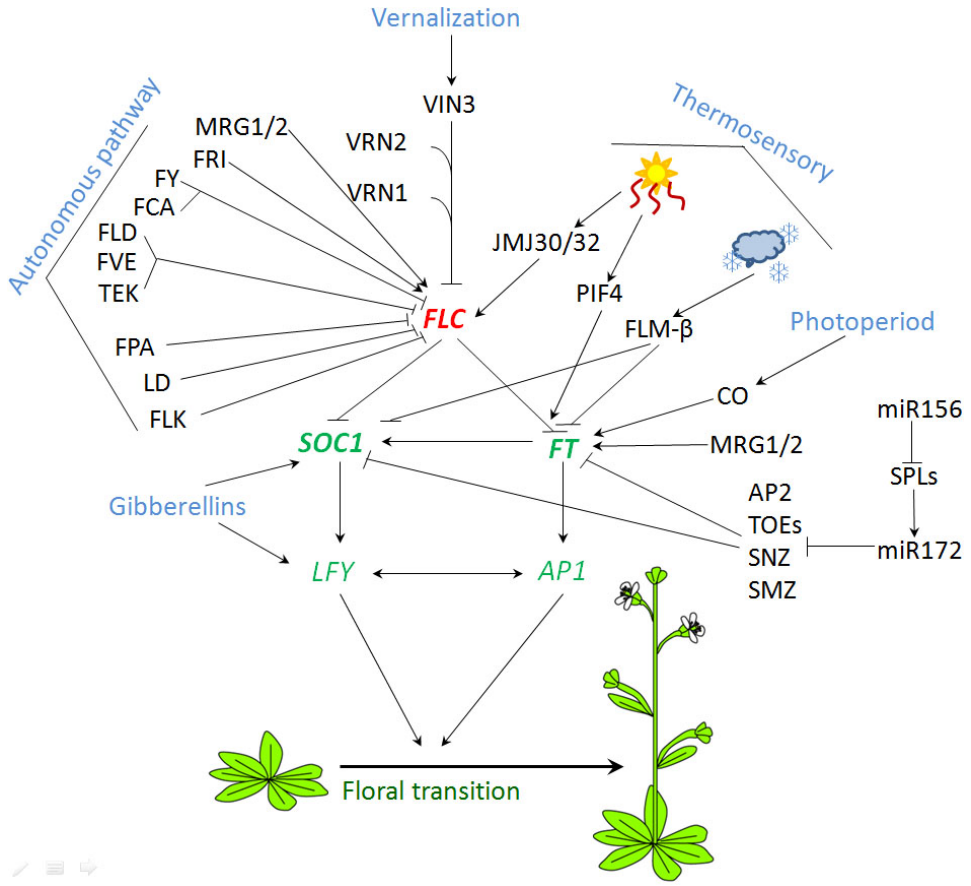

Figure 3. Multiple flowering pathways integrate to regulate the vegetative to reproductive phase transition.
The floral repressor *FLOWERING LOCUS C* (*FLC*) is repressed by players in the autonomous pathways, and activated by its potent upstream activator FRIGIDA (FRI). During a prolonged exposure to cold temperature, vernalization pathway kicks in and VERNALIZATION INSENSITIVE 3 (VIN3) recruits the PRC2 complex to silence *FLC*. Under long day conditions, *CONSTANS* is activated by the photoperiod pathway to up-regulated the floral inducer *FLOWERING LOCUS T* (*FT*) whereas under non-inductive short day conditions, the gibberellin pathway induced the expression of the other floral inducer *SUPPRESSOR OF OVEREXPRESSION OF CONSTANS 1* (*SOC1*) and the floral meristem identity gene *LEAFY* (*LFY*). Besides the four classical flowering pathways, the thermosensory pathway also plays a role in regulation of flowering time. At cold temperature, the functional spliceform of FLOWERING LOCUS M-β (FLM-β) represses the two floral integrators *SOC1* and *FT*. This repression is alleviated at a higher temperature. Moreover, elevated temperatures also trigger two seemingly antagonistic mechanisms: high temperature-induced PHYTOCHROME INTERACTING FACTOR 4 (PIF4) activates *FT* expression, while at the same time also stabilizes JUMONJI30 (JMJ30). The histone demethylase JMJ30 and its homolog JMJ32 delay the repression of *FLC* by removing H3K27me3 from the *FLC* locus. Another age-dependent pathway functions through a series of genetic interaction between *miR156* and *miR159*, the *SQUAMOSA PROMOTER BINDING PROTEIN-LIKE*s (*SPL*s) and the *APETALA2* (*AP2*) family genes. Figure adapted from (He & Amasino, 2005; Ito, 2014)

1.2.1 Regulation of the floral inducers by photoperiod and gibberellin pathways

One of the most obvious factors that contribute to flowering control is the day length or photoperiod. Based on their responses to day length, plants can be categorized as long-day (LD) plants which flower when days are long and night are short, short-day (SD) plants which flower in the reverse conditions or day-neutral plants which flower independently of photoperiod. Some of the LD plants include barley, pea, and oat; and the most important staple food in Asia, rice, is a SD plant. Other plants like cucumbers and tomatoes are day-neutral and initiate flowering based on internal hormonal control and developmental age. Nowadays, we know some of the molecular mechanisms that govern this photoperiod response, mostly through studies done in the model organism *Arabidopsis thaliana*. Unsurprisingly, the photoperiod pathway is governed by the plant's internal circadian clock that controls the oscillation of regulatory genes.

Arabidopsis is a facultative LD plant which flowers early under inductive LD photoperiod and flowering is delayed but not fully inhibited under SD conditions. Grown at an inductive LD conditions, CONSTANS (CO) is the key transcription factor that binds to and activates *FT* (Putterill et al, 1995), and is suppressed by a Dof transcription factor CYCLING DOF FACTOR 1 (CDF1) in the morning (Imaizumi et al, 2005). In the afternoon, GIGANTEA (GI) and a F-box protein FLAVIN-BINDING, KELCH REPEAT, F-BOX 1 (FKF1) gradually accumulate and form a FKF1-GI complex with its highest peak in the late afternoon (Sawa et al, 2007). This F-box protein-containing FKF1-GI complex targets CDF1 for degradation, facilitating *CO* daytime

expression by releasing *CO* from its CDF1-mediated repression. During SD, *FKF1* and *GI* expression peak at different phases of the day, resulting in the scenario where this small amount of FKF1-GI complex is unable to alleviate *CO* from its repression (Sawa et al, 2007).

Besides the transcriptional regulation of *CO* mRNA expression by FKF1/GI/CDF1 pathway, CO protein stability is also controlled by day length, particularly by the E3 ubiquitin ligase CONSTITUTIVELY PHOTOMORPHOGENIC 1 (COP1) and SUPPRESSOR OF PHYA-105 (SPA) protein family. During SD, COP1-mediated ubiquitination of CO protein targets it for the 26S proteasome-dependent degradation, thus unable to activate its downstream gene *FT* (Liu et al, 2008b). The COP1-mediated ubiquitination during SD appears to be assisted by the SPA proteins (Laubinger et al, 2006). In LD, the blue light photoreceptor cryptochromes (CRYs) might facilitate the translocation of COP1 from the nucleus to the cytoplasm, thus relieving CO from its degradation. Ultimately, these regulatory mechanisms allow the plants to differentiate SD conditions, and induces flowering when conditions are favorable during LD conditions.

The CO-dependent photoperiod pathway channels its flowering inductive signals through the florigen FT. Similar to *CO* expression in response to photoperiod, *FT* expression is induced in LD but almost undetectable in SD (Srikanth & Schmid, 2011). *FT* mRNA is produced in the phloem companion cells and transported to the shoot apical meristem (SAM), functioning as a long distance signal for flowering. Whether this systemic florigen signaling is contributed by the mobile FT protein (Corbesier et al, 2007) or *FT* mRNA (Li et al, 2011a) is still in debate. It is generally accepted that FT protein plays a

major role in floral induction. A phloem companion specific *SUCROSE TRANSPORTER2* promoter (*pSUC2*) induced FT-GFP is not only able to rescue the *ft* mutant, but this FT-GFP is also detectable in the apex, showing that FT protein moves long distances in the plant (Corbesier et al, 2007). However, although a previous report on mobile *FT* mRNA has been retracted (Huang et al, 2005b), a few recent studies showed that a viral-induced non-translatable *FT* mRNA in the leaf is able to move throughout the transformed tobacco plant and promote earlier flowering under SD conditions (Li et al, 2011a; Li et al, 2009). A grafting experiment using a *pSUC2* driven cell-autonomous RFP-FT fusion protein in *Arabidopsis* also show that while the RFP-FT protein is retained in the vasculature, *RFP-FT* mRNA is detected in the grafted tissues and induce an early-flowering phenotype, albeit to a lesser extent (Lu et al, 2012). These results suggest that *FT* mRNA may act redundantly and supplement the major effect of flowering promotion by FT protein. Nonetheless, once in the SAM, FT protein interacts with a meristem-specific bZIP transcription factor FD and activates their downstream target, a floral meristem identity gene *APETALA1* (*AP1*)(Abe et al, 2005). *AP1* together with another floral meristem identity gene *LEAFY* (*LFY*) triggers the formation of flower at the flank of the inflorescence meristem (Liu et al, 2009).

CO binding to the *FT* promoter not only activates *FT* expression, but also recruits SAP30 FUNCTION RELATED 1 (AFR1) and AFR2-containing histone deacetylase (HDAC) complex to the *FT* locus to moderate its expression (Gu et al, 2013c). The CO-induced transcriptional activity probably relaxes the chromatin structure, which then allows AGAMOUS-LIKE 18

(AGL18) to recruit AFR1/AFR2-HDAC complex to dampen the acetylation levels at *FT* locus (Gu et al, 2013c). This balancing mechanism promotes the expression of an adequate level of *FT* at dusk. Besides its transcriptional regulation by CO, *FT* also appears to be generally repressed by chromatin regulators, the PRC2 and PRC1 complex. Mutants of the PRC2 complex such as *clf*, *fie* and *emf2* (Jiang et al, 2008b) and PRC1 complex such as *lhp1* (Kotake et al, 2003; Turck et al, 2007) and *emf1* (Wang et al, 2014) all causes derepression of *FT* and an early-flowering phenotype.

The floral transition is also regulated by a phytohormone called gibberellin (GA). The GA flowering pathway functions in parallel to the photoperiod pathway in promoting flowering. The effect of GA is not as clear in LD, however, under non-photoinductive SD conditions, the GA pathway plays a major role in floral transition. In general, GA relay its flowering inductive signal through the receptor GIBBERELLIC INSENSITIVE DWARF 1 (GID1)(Mutasa-Gottgens & Hedden, 2009). Upon perception of the bioreactive GAs, GID1 undergoes a conformational change which promotes the binding of GID1 to the DELLA proteins. The GID1-bound DELLA proteins are targeted by E3 ubiquitin ligase and later degraded via the 26S proteasome pathway (Mutasa-Gottgens & Hedden, 2009).

DELLA proteins are transcriptional regulators that regulate floral transition through various pathways. Interaction of DELLAs with PHYTOCHROME INTERACTING FACTORS (PIFs) inhibits their ability to induce gene expression (Mutasa-Gottgens & Hedden, 2009). Integration of the GA-mediated DELLAs and light-sensing PIFs allows the two pathways to crosstalk and control the flowering time.

One of the key floral inducer regulated by the GA pathway is *SOC1*. Endogenous expression of *SOC1* requires GA activity to trigger flowering in SD (Moon et al, 2003). SOC1 and another MADS box protein, AGAMOUS LIKE 24 (AGL24) make a heterocomplex and autoregulate each other in a GA-dependent manner to increase their expression (Liu et al, 2008a). Moreover, a MADS heterodimer of SOC1 and AGL24 induces the transcription of a floral meristem identity gene *LFY*. Like *AP1*, induction of *LFY* triggers floral transition and formation of flower at the shoot apex.

LFY is also regulated by GAMYB transcription factors in a GA-dependent manner (Gocal et al, 2001). At one hand, GA relieves the DELLA-dependent repression of GAMYB protein, thus allowing GAMYB to bind to the GA-responsive element in the *LFY* promoter to enhance its expression (Gocal et al, 2001). On the other hand, GA-mediated DELLA proteins down-regulate *miRNA159*, which targets *MYB33* mRNA for cleavage, hence dampening *LFY* activation (Achard et al, 2004). This feedback loop thus provides multiple entry points for controlling flowering time.

1.2.2 Regulation of the floral repressor *FLC* by the vernalization and autonomous pathways

The effect of vernalization is originally studied in crop plants, in which winter cereal exposed to a prolonged period of cold temperature during winter is able to induce flowering when returned to warmer temperatures in spring (Chouard, 1960). In general, these genetic variations allow plants to be categorized into winter annual or biennial plants for their requirement for

vernalizing cold treatment to flower and summer annual which can flower without an extended cold exposure. Since the early reports, many genes and regulatory mechanism has been described mainly through studies done in the model organism *Arabidopsis*.

Most of the *Arabidopsis* ecotypes used in the laboratory are the rapid cycling ecotypes such as Columbia (Col), Landsberg *erecta* (L*er*), Wassilewskija (Ws). However, there are winter annual *Arabidopsis* ecotypes, such as the San Feliu-2 (Sf2) and Stockholm (St) which require a prior cold treatment to induce flowering. Most of these flowering differences can be attributed to the allelic variation in *FRIGIDA* (*FRI*) and *FLC* (Caicedo et al, 2004; Shindo et al, 2005).

As mentioned above, FLC is a MADS box transcription factor that directly represses two important floral inducers *FT* and *SOC1*. Thus, during floral transition, *FLC* need to be repressed. FRI function as an activator that up-regulates the expression of the potent floral repressor *FLC* (Michaels & Amasino, 1999). Moreover, *FLC* activation requires the H3K4 methylation. In yeast, the RNA polymerase II associated factor 1 (PAF1) complex recruits H3K4 methyltransferase to their target genes. In *Arabidopsis,* the PAF1 complex containing ELF7, ELF8, and VIP4 possibly also function to recruit H3K4 methyltransferase ASHH2/SDG8/EFS to deposit the activating H3K4me3 marks at the *FLC* locus (He et al, 2004; Soppe et al, 1999; Zhang & van Nocker, 2002). Similarly, a COMPASS-like complex containing RBL, WDR5a, ASH2R also function to up-regulated *FLC* expression by recruiting H3K4 methyltransferases such as ATX1 to the *FLC* locus to promote a transcriptionally permissive chromatin status at the locus (Jiang et al, 2011).

Recently we also show that a MORF RELATED GENE 1 (MRG1) and its homolog MRG2 may bind to both the *FLC* and *FT* locus through its chromodomain and recruit the histone acetyltransferases HISTONE ACETYLTRANSFERASE OF THE MYST FAMILY 1 (HAM1) and HAM2 to increase the acetylation level (Xu et al, 2014). This binding of MRG1/2 complex to the locus is dependent on H3K36me3 level, hence highlighting the crosstalk between different histone marks and their multi-layer reinforcement of the chromatin state.

In one of the earliest screen for flowering mutants, a group of autonomous pathway mutants are identified that showed delayed flowering phenotype irrespective of photoperiod (Koornneef et al, 1991). The autonomous pathway regulators function in multiple parallel pathways and all promotes flowering by repressing *FLC* expression. One of them, FLOWERING LOCUS D (FLD) functions as a histone demethylase that removes the activating H3K4me2 marks from the *FLC* locus, thus antagonizing the effects of PAF1 and COMPASS complex on *FLC* (Jiang et al, 2007). Moreover, FLD forms a repressor complex with a histone deacetylase HDA6, histone-binding proteins FVE or MSI5, and AT-hook DNA-binding protein TRANSPOSABLE ELEMENT SILENCING VIA AT-HOOK (TEK) which can reinforce the repressive chromatin state through histone deacetylation at the *FLC* locus (Gu et al, 2011; Xu et al, 2013).

Another three autonomous pathway players FCA, FPA and FY are important in RNA 3' processing (Ietswaart et al, 2012). However, they do not appear to regulate the 3' processing of the sense *FLC* mRNA. Besides the protein coding sense transcript, the *FLC* locus contains two long non-coding RNA

(lncRNA), *COLDAIR* which is expressed in *FLC* intron 1 in the sense direction (Heo & Sung, 2011), and *COOLAIR* which is expressed in the antisense direction and fully encompasses the coding *FLC* coding region (Swiezewski et al, 2009). These two lncRNAs participate in a few flowering pathway to modulate the expression of *FLC*. The *COOLAIR* transcript is alternatively terminated and polyadenylated (poly(A)): the proximal poly(A) site lies within sense intron 6 and the distal poly(A) site located at the sense promoter. The RNA-binding proteins FCA and FPA, and the RNA 3' processing protein FY appear to promote the use of the *COOLAIR* proximal poly(A) site (Baurle & Dean, 2008; Hornyik et al, 2010). However, the exact mechanism of how the choice of poly(A) sites of the antisense *COOLAIR* affect the transcription of the sense *FLC* is unclear. However, the utilizing the proximal poly(A) sites appear to promote the FLD-mediated H3K4 demethylation at the *FLC* locus, resulting in a repressed chromatin state (Liu et al, 2010).

In parallel with the autonomous pathway, the vernalization pathway also functions to repress *FLC* expression. During vernalization a cold-induced epigenetic silencing of *FLC* occurs to promote flowering upon returning to a warm condition. *FLC* silencing happen in a gradual and quantitative manner and this repression rely heavily on the PcG-mediated H3K27me3 deposition (Angel et al, 2011). One of the first event that occur is the accumulation of the *COOLAIR* antisense transcript that uses the distal poly(A) site which extend beyond each end of the sense *FLC* transcript (Swiezewski et al, 2009). This induction of *COOLAIR* peaks as early as 10-day after vernalization (Heo & Sung, 2011). However, the exact mechanism and importance of *COOLAIR* in

FLC vernalization-mediated silencing is debatable. While it is suggested that antisense *COOLAIR* transcription may interfere with its *FLC* sense transcription causing cold-induced silencing (Swiezewski et al, 2009), another report suggests otherwise and shows that production of *COOLAIR* transcript is not essential for vernalization-induced *FLC* repression (Helliwell et al, 2011). On the other hand, the sense transcript *COLDAIR* is expressed transiently at 3-week after vernalization from the cryptic promoter in the *FLC* intron, a region called vernalization response element (VRE)(Heo & Sung, 2011). Interaction between *COLDAIR* transcript and the PRC2 component CLF and SWN suggests that *COLDAIR* may recruit the PRC2 complex to establish the stable silencing epigenetic mark. Moreover, this promoter and first exon of *FLC* gene containing *COLDAIR* are sufficient to initiate repression during vernalization (Helliwell et al, 2011).

A PHD finger protein, VERNALIZATION INSENSITIVE 3 (VIN3), is then transiently induced by cold temperature at 20-day after vernalization and peaks around 40-day after vernalization (Heo & Sung, 2011; Sung & Amasino, 2004). VIN3 and another PHD finger protein VRN5 then forms a PHD-PRC2 complex with the core PRC2 proteins VRN2, SWN, CLF, FIE and MSI1 during vernalization and catalyzes the methylation of H3K27me3 at *FLC* locus, especially at intron 1 (De Lucia et al, 2008; Wood et al, 2006). Returning the vernalized plant to warm conditions causes the PHD-PRC2 containing VRN5 but not VIN3 to distribute more broadly over the *FLC* locus, which may further reinforce the repression by catalyzing increased level of H3K27me3 (De Lucia et al, 2008). The establishment of H3K27me3 on the locus requires further maintenance and enhancement by the PRC1 complex

containing LHP1 (Sung et al, 2006). Thus, plants acquire competency to flower during vernalization, which leads to flowering when return to warm conditions.

1.3 Temperature sensing as adaptive traits

Plants are sessile and thus have to adapt to their changing environment. Ambient temperature is one of the stimuli that affects the growth and development of plants. Temperature acclimation is an adaptation in which plant acquire tolerance as it perceive gradual temperature changes. A sudden drop to freezing temperature is usually fatal to plants. However, a pre-exposure to low non-freezing temperatures will increase their survival (Zhen et al, 2011). Similarly, a pre-exposure to non-detrimental high temperature can increase a plant's tolerance towards heat (Wu et al, 2013). Temperature fluctuations also affect various physiological responses such as seed yield, amount of chloroplasts, size of mitochondria, transpiration rate, etc (Capovilla et al, 2015).

Besides increasing survival, plants also respond to changing temperature by deciding the timing to produce offspring. Non-freezing cold temperature is known to delay flowering, possibly to anticipate a more favorable environment for flowering (Capovilla et al, 2015). On the other hand, if the surrounding gets hotter and unfavorable, plants may have to trigger premature flowering to prevent irremediable situation where they are unable to set seeds. Thus, the plant developmental plasticity and ability to sense and react to temperature fluctuation is an important evolutionary trait.

1.3.1 Non-vernalizing cold temperature exposure represses flowering

Decreased ambient temperatures can affect the timing of floral transition. The effect of vernalization to perceive winter and induce flowering in spring is a form of adaptation. However, plants need to distinguish between long and short exposure to cold temperature. The mechanism in which extended exposure to cold induces flowering had been reviewed in section 1.2.2. In response to reduced ambient temperature, two genes of the autonomous pathway, *FCA* and *FVE*, were initially shown to participate in the thermosensory pathway, as mutants of *fca* and *fve* showed temperature insensitivity to flowering (Blazquez et al, 2003). Unlike in the autonomous pathway, *FCA* and *FVE* function in cold temperature response seems to be independent of *FLC* (Blazquez et al, 2003), but rather act through another MADS box gene *SHORT VEGETATIVE PHASE* (*SVP*)(Lee et al, 2007). The cold-up-regulated *SVP* functions as a floral repressor and decreases the expression of the floral inducers *FT* (Lee et al, 2007). Besides the *SVP*'s transcriptional activity, SVP protein stability is also affected by temperature. SVP protein is stabilized at lower temperature and is targeted for 26S proteasome-mediated degradation at high temperature (Lee et al, 2013b).

Another MADS box protein FLOWERING LOCUS M (FLM) also participates in the temperature responsive flowering. *FLM* mRNA is alternatively spliced, with the *FLM-β* spliceform predominates at low temperature while the *FLM-δ* spliceform gradually being up-regulated as the

temperature increases (Lee et al, 2013a; Lee et al, 2013b). MADS box proteins frequently form heterocomplexes with other MADS proteins in gene regulation. In the cold-induced delayed flowering, SVP interacts with the functional form of FLM-β to form a MADS heterocomplex and repress *FT* and *SOC1* (Lee et al, 2013b). On the other hand, FLM-δ functions as the dominant negative form of FLM that competes with the functional FLM-β for the SVP interaction at higher temperatures, thus weakens or alleviates the SVP-FLM-mediated flowering repression (Lee et al, 2013a). Moreover, *MAF2*, *MAF3*, and *MAF4*, which are related to *FLM* and *FLC*, also contribute to the repression of flowering under cold ambient temperatures (Gu et al, 2013b). Like *FLM*, *MAF2* also shows alternative splicing with the *MAF2* var1 variant expressed at lower temperatures and *MAF2* var2 variant at higher temperatures (Rosloski et al, 2013). In a Llagostera-2 (Ll-2) *Arabidopsis* accession which is null for expression of *FLC*, *MAF2*, *MAF3*, and *MAF4* over-expression of the *MAF2* var1 transcript can produce a late-flowering phenotype, but the over-expression of the MAF2 var2 or var4 transcript show normal flowering time (Rosloski et al, 2013). Thus, the *MAF2* var1 transcript which encodes the full length MAF2 protein acts as a flowering repressor under low ambient temperature conditions. Coupling SVP's reduced stability and FLM's shift to a negative spliceform at high temperature, and formation of MADS heterocomplexes among homologs of FLM, *Arabidopsis* has evolved multiple mechanisms to fine-tune its flowering time in response to cold temperatures.

1.3.2 Elevated temperatures induce early flowering

Besides causing hypocotyl elongation and leaf hyponasty, it has been shown that exposure to elevated temperatures can induce early-flowering in *Arabidopsis* under SD conditions (Balasubramanian et al, 2006). One of the molecular responses to elevated temperatures is the change in nucleosome density. H2A.Z-containing nucleosome binds and packs DNA more tightly, making the region less accessible to RNA polymerase II (Kumar & Wigge, 2010). H2A.Z is incorporated into the genome by a SWR1 chromatin remodeling factor ACTIN-RELATED PROTEIN 6 (ARP6) and the H2A.Z incorporation is temperature sensitive. In response to higher temperatures, H2A.Z occupancy decreased significantly in *Arabidopsis*, which may facilitate the recruitment of RNA polymerase II and binding of other activators (Kumar & Wigge, 2010). This appears to play an important role for *FT* induction at elevated temperatures (Kumar et al, 2012).

The H2A.Z-mediated chromatin compaction at the *FT* locus was released at elevated temperature (Kumar et al, 2012). This allows the bHLH transcription factor PHYTOCHROME INTERACTING FACTOR 4 (PIF4) to bind to the *FT* promoter and activate its expression. The *pif4* mutant is insensitive to high temperatures and does not trigger the early flowering phenotype (Kumar et al, 2012). In the *arp6* mutant which attenuates the H2A.Z incorporation, the plant showed a constitutive heat-treated early-flowering phenotype (Kumar et al, 2012; Kumar & Wigge, 2010). Thus, the PIF4-mediated *FT* expression at elevated temperatures appears to be the main temperature-responsive mechanism.

PIF4 protein appears to be targeted for degradation in the presence of light (Kumar et al, 2012), which raises the issues of the timing of PIF4 effect on flowering. Recently, it is reported that warm temperature at night promotes flowering more than warm temperature in the day (Thines et al, 2014). This night-responsive thermal floral induction is partly contributed by PIF4 and its homolog PIF5, acting redundantly and additively to induce the expression of *FT* (Thines et al, 2014). The involvement of light responsive PIFs in the temperature responsive flowering regulation allows crosstalk between the photoperiod pathway and the thermosensory pathway.

1.4 Objectives of the study

The aim of this study is to understand the function of a class of JMJ proteins that contains only the JmjC domain in *Arabidopsis*. Histone methylation dynamics control many, if not all, aspect of growth and development. Hence, I am interested in uncovering which developmental processes JMJ30 and JMJ32 are involved in, what their downstream targets are, and how they exert their regulatory functions. Since JMJ30 and JMJ32 are enzymes, I also aim to study their biochemical properties, such as enzymatic activity, substrate specificity and protein stability. Through dissecting the exact functions of these enzymes, I hope to generate tools for molecular breeding or crop improvement in the future.

1.5 Significance of the study

In this study, I identified new functions of JMJ30 and JMJ32 as an active H3K27me3 demethylase *in vitro* and *in vivo*. The removal of this repressive H3K27me3 epigenetic mark promotes a transcriptional permissive state at the loci. More importantly, I showed that JMJ30 and JMJ32 target a potent floral repressor *FLC*, delaying flowering by maintaining its expression. *FLC* is developmentally regulated to be repressed for flowering. However, I showed that at elevated temperatures, *FLC* repression is delayed through the JMJ30/JMJ32-dependent mechanism, thus contributing to a parallel pathway to other known players in the thermosensory pathways. The JMJ30/32-regulated *FLC* derepression and PIF4-mediated *FT* activation may function in a balancing mechanism to fine-tune the timing of floral transition (Gan et al, 2014a). Moreover, I found that JMJ30 and JMJ32 also function as a buffering system during vernalization-induced *FLC* repression. In a nutshell, our findings presented a novel balancing pathway of flowering regulation. I hope that our improved understanding of floral transition will promote advancement in genetic manipulation of flowering time in response to the climate changes, to increase yield, and to take the big leap towards the next green revolution.

Chapter 2

Materials and Methods

Chapter 2 Materials and Methods

2.1 Plant materials

2.1.1 Plant materials and growth conditions

All *Arabidopsis thaliana* plants used in this study were of the Columbia (Col) ecotype unless otherwise stated. Plants were grown under either long day (LD, 16-h light/8-h dark) or short day (SD, 8-h light/16-h dark) conditions at standard growth temperature (22°C) or elevated temperature (29°C). For the vernalization treatment, plants were grown at 4°C in SD conditions.

Multiple alleles of the *JMJ* genes were isolated from the SALK, SAIL, GABI-Kat, and INRA collections, and were listed in Table 3.

Table 3. List of mutant alleles used in this study.

Gene	Locus	Allele in this research	Germplasm Name	Allele Previously described
JMJ30	AT3G20810	*jmj30-1*	SAIL_811_H12	(Lu et al, 2011c) a.k.a. *jmjd5-1* (Jones et al, 2010)
		jmj30-2	GK-454C10	(Lu et al, 2011c) a.k.a. *jmjd5-2* (Jones et al, 2010)
JMJ32	AT3G45880	*jmj32-1*	SALK_003313	
JMJ31	AT5G19840	*jmj31-1*	SALK_029755	
		jmj31-2	SALK_076996	
		jmj31-3	GK-175C06	
JMJ12/REF6	AT3G48430	*ref6-1*	SALK_001018	(Noh et al, 2004)
FLC	AT5G10140	*flc-3*		(Michaels & Amasino, 2001)

2.1.2 Plant selection

Transgenic plants harboring the Basta-resistant genes were sown on soil and allowed to grow for a week. Seedlings were sprayed with 0.2% Basta twice at one week interval, and screened for successful transformants which continue to grow.

Transgenic plants with the Kanamycin-, Sulfadiazine- or Basta-resistant gene were first seed-sterilized, and then sown on MS plates containing 50 μg/ml Kanamycin, 5.25 μg/ml Sulfadiazine or 15 μg/ml Glufosinate ammonium respectively. After stratification at 4°C for 3 days, the seeds were grown and screened under LD conditions. Successful transformants were transplanted to soil.

Transgenic plants with the Hygromycin-resistant gene were seed-sterilized and sown on MS plates supplemented with 20 μg/ml Hygromycin. After stratification at 4°C for 3 days, the seeds were allowed to germinate and grow at 22°C in dark conditions for 5 days. Successful transformants that showed elongation of hypocotyls were transplanted to soil.

2.1.3 Genomic DNA extraction and genotyping

Plant genomic DNA (gDNA) extraction was carried out using the CTAB (cetyl trimethyl ammonium bromide) method (Murray & Thompson, 1980). An adult leaf was removed from plants and ground with a pestle in a 1.5 ml microfuge tube. CTAB buffer (3% CTAB, 100 mM Tris, pH 8.0, 20 mM EDTA, 1.4 M NaCl, 0.2% β-mercaptoethanol) was added to the tube and incubated at 65 ºC for 30 min. After incubation, an equal volume of

chloroform was added to the tube, mixed, and then centrifuged at 9,000 rpm for 5 min. The upper aqueous layer was transferred to a new tube. 2/3 volume of isopropanol was added to the tube, mixed, and incubated at -20°C for 15 min for gDNA precipitation. Subsequently, the gDNA was pelleted by centrifugation (14,000 rpm for 5 min), washed with 70% ethanol, and dried in a SpeedVac vacuum concentrator. The gDNA was resuspended in TE-RNase (20 μg/ml), pH 8.0.

Genotyping PCRs of the various T-DNA insertion and deletion mutants were carried out using the primers listed in Table 4. For the T-DNA insertion mutants, the forward- and reverse-primer pairs (FP + RP) were used for testing the WT bands, while RP + respective LB primers were used for examining the mutant bands.

Table 4. Genotyping primers of T-DNA insertion and deletion mutants used in this study.

Allele	Germplasm	Primer name	Primer sequence
jmj30-1	SAIL_811_H12	jmj30-1GT-FP	TTCTACCTTGCAGGTCTTTAACTTG
		jmj30-1GT-RP	ATCCAACCCATCTTCTTATTAGCTC
jmj30-2	GK-454C10	jmj30-2GT-FP	CAAACTCTGCTGCAATCGATTTC
		jmj30-2GT-RP	GAAAATGTCACAAGCTCTTGCTTC
jmj32-1	SALK_003313	jmj32-1GT-FP	GACTGAGAAAACCTGAACTCAGC
		jmj32-1GT-RP	GTCGTGTAAAGGACTGAAGGTTG
jmj31-1	SALK_029755	jmj31-1GT-FP	CACATGGTATTACCTTAGCTGGAGT
		jmj31-1GT-RP	GTTCACACTCAACAAAGAGATGCTA
jmj31-2	SALK_076996	jmj31-2GT-FP	CTCTTAAGCTTTCCGTGGTTCTC
		jmj31-2GT-RP	GATTTAGCGGGAGAAAGAAAGAG
jmj31-3	GK-175C06	jmj31-3GT-FP	CATATGGAACGTCCAAGAATGATAC
		jmj31-3GT-RP	GTGATATCAGAAGCCATGAGAGG
ref6-1	SALK_001018	ref6-1GT-FP	TCATATACAAGGCGTTCGGTC
		ref6-1GT-RP	CAGTTGCAACTCTGGAGAAGG
		SALK-LBa1	TGGTTCACGTAGTGGGCCATCG
		SAIL-LB3	TAGCATCTGAATTTCATAACCAATCTCGATACAC
		GK-LB-8409	ATATTGACCATCATACTCATTGC
flc-3		flc-3GT-FP	TAGAAAGAAATAAAGCGAGAAA
		flc-3GT-RP	TATCGCCGGAGGAGAAGC
FRI-Sf2		FRI-GT-FP	AGATTTGCTGGATTTGATAAGG
		FRI-GT-RP	ATATTTGATGTGCTCTCC

2.2 Plasmid construction

2.2.1 Cloning

The constructs of *35S::JMJ30-HA* and *35S::JMJ32-HA* were produced as follows. To construct the *35S::JMJ-HA* plasmid, the full length *JMJ* gene coding sequences (*JMJ30*, *JMJ32*, *JMJ31*) were amplified from the cDNA by primer set XhoI-JMJ_F and XmaI-JMJ_R (Table 5) using KAPA HiFi HotStart DNA polymerase (Kapa Biosystems). The PCR products were separated by agarose gel electrophoresis and the bands with the correct sizes were excised. After gel extraction, the PCR products were digested with restriction enzymes XhoI and XmaI and cloned into vectors pGREEN-35S-HA (Hellens et al, 2000).

To make the plasmid constructs for the histone demethylase assays, *35S::JMJ30-HA* was further mutagenized in a key conserved amino acid using the primers JMJ30-H326A-F and JMJ30-H326A-R to produce the *35S::JMJ30H326A-HA* plasmid. Mutagenesis was also performed on the *35S::JMJ32-HA* plasmid using primers JMJ32-H174A-F and JMJ32-H174A-R to produce *35S::JMJ32H174A-HA*.

For the *pJMJ::JMJ-GUS* constructs used in the histochemical assays, genomic fragments of *JMJ* genes (6.1-kb *JMJ30*, -2,313 to +3,798; 5.3-kb *JMJ32*, -3,215 to +2,084; 7.5-kb *JMJ31*, -2,542 to +4,975; A of the start codon was set as +1) were amplified from gDNA by primer set JMJ-FL_F and JMJ-FL_R (Table 5) using KAPA HiFi HotStart DNA polymerase (Kapa Biosystems). The PCR products with the correct size were verified by gel electrophoresis and gel extracted. The *JMJ* genomic fragments were then cloned into pCR8

TOPO vector (Invitrogen). An SfoI restriction site was introduced in front of the *JMJ* stop codon through mutagenesis using primers JMJ-mut_F and JMJ-mut_R (Table 5). *GUS* fragments were then inserted into the restriction sites of the *pCR8-JMJ* plasmid. Finally, *pJMJ::JMJ-GUS* in pCR8 were recombined into pEarleyGate303 using LR Clonase II (Invitrogen).

The *pJMJ30::JMJ30-HA* plasmid were constructed similarly, differing only in that a *HA* fragment was inserted into the SfoI site of the *pCR8-JMJ30* plasmid, and the *pJMJ30::JMJ30-HA* in pCR8 were recombined into pHGW.

The DNA sequences of all plasmid constructs were verified by sequencing using BigDye Terminator Cycle Sequencing Kit (Applied Biosystems) following manufacturer's instruction.

Table 5. List of primers used for cloning.

***35S::JMJ-HA* construct**		
Gene	**Primer name**	**Sequence**
JMJ30	XhoI-JMJ30_F	GGCTCGAGACTTTCCCCAACTCATCATCAC
	XmaI-JMJ30_R	CCCCCGGGCGAGCTAGAAGATTCTGCTTCATTGC
	JMJ30-H326A-F	TGGGACAGTTACTCCGTTAGCCCATGATCCACATCATAAT
	JMJ30-H326A-R	ATTATGATGTGGATCATGGGCTAACGGAGTAACTGTCCCA
JMJ32	XhoI-JMJ32_F	GGCTCGAGGTCAATGGCTAAAGAGATAGAGAATTTATGG
	XmaI-JMJ32_R	CCCCCGGGGGGAGCAATCTCTGCATCACTG
	JMJ32-H174A-F	GACTCCGTGACTTCATTTGCTAAAGATCACTATGAGA
	JMJ32-H174A-R	TCTCATAGTGATCTTTAGCAAATGAAGTCACGGAGTC
JMJ31	XhoI-JMJ31_F	GGCTCGAGATGCCGACGGGATGCGAGTTTC
	XmaI-JMJ31_R	CCCCCGGGAATGTTTGTTGTTGGTGAAGCAATG
Nucleotides in red denote the inserted restriction sites, those in blue are mutated to change the codon from H to A.		

***pJMJ::JMJ-HA* and *pJMJ::JMJ-GUS* construct**		
Gene	**Primer name**	**Sequence**
JMJ30	JMJ30-FL_F	GCCAGATCCTGAAACAATTCTC
	JMJ30-FL_R	CTGATTTTGGGGTCTTTGGATTC
	JMJ30-mut_F	GCAGAATCTTCTAGCTCGGGCGCCTAGCGAATGGATTTATTT
	JMJ30-mut_R	AAATAAATCCATTCGCTAGGCGCCCGAGCTAGAAGATTCTGC
JMJ32	JMJ32-FL_F	GAGATCAGTTAAGCCAAGCCAAG
	JMJ32-FL_R	CATGATACACACATCAAAAAGACGG
	JMJ32-mut_F	GTCTCAGATTGCTCCCGGCGCCTGATTTAATGGTGGAAC
	JMJ32-mut_R	GTTCCACCATTAAATCAGGCGCCGGGAGCAATCTGAGAC
JMJ31	JMJ31-FL_F	CCCAAGCTTTGGAACATACTACA
	JMJ31-FL_R	CTTCCAGAGGATTTACTCCCACT
	JMJ31-mut_F	CACCAACAACAAACATTGGCGCCTGAagggtcttgggtgtg
	JMJ31-mut_R	cacacccaagaccctTCAGGCGCCAATGTTTGTTGTTGGTG
Nucleotides in red denote the inserted restriction sites.		

2.2.2 *Agrobacteria*-mediated transformation

Transgenic plants were generated by floral dipping with *Agrobacterium tumefaciens* (strain C58C1) (with additional *pSOUP* helper plasmid for transformation of *pGREEN-35S::JMJ-HA*)(Clough & Bent, 1998). Briefly, 3 µl of the construct plasmids were added to the *Agrobacteria* competent cells, and placed on ice for 2 min or until cells are thawed. The cells were frozen in liquid nitrogen for 5 min, then heat-shocked in 37°C water bath for 5 min. The transformed cells were incubated in a 28°C shaker for 1 hr for recovery. Subsequently, the cells were streaked on LB plates with corresponding antibiotics (pGreen vectors with pSOUP: 50 µg/ml Rifampicin, 30 µg/ml Gentamycin, 50 µg/ml Kanamycin, 5 µg/ml Tetracyclin; Gateway and pEarleyGate vectors: 50 µg/ml Rifampicin, 30 µg/ml Gentamycin, 100 µg/ml Spectinomycin,) and incubated at a 28°C oven for 2 days.

After 2 days, 5 – 10 colonies of *Agrobacteria* were picked and suspended in a small culture of 5 ml LB broth with antibiotics and incubated at 28°C on shaker overnight. The next day, the bacteria cultures were verified by culture PCR, and 2 ml of the bacteria culture were added to a big culture of 200 ml LB broth with corresponding antibiotics to be incubated at 28°C on shaker overnight.

Upon reaching the desired OD_{600} of 1.0 – 1.5 the next day, *Agrobacteria* were pelleted by centrifugation at 4000 rpm for 15 min and resuspended thoroughly in an equal-volume of infiltration medium (1/2 MS, 5% sucrose, 0.03% Silwet L-77). The inflorescences of plants were dipped into the agrobacteria infiltration suspension for 1 min with shaking. The inoculated plants were covered in a plastic bag and placed in the dark at 4°C overnight. The next day,

the treated plants were removed from the plastic wrap and grown under standard growth (LD, 22°C) conditions until seeds were ready to be collected. The T1 seeds were selected according to the resistance gene of the transformed plasmid. Refer section 2.1.2 for methods of plant selection.

2.2.3 PEG-mediated protoplast transformation

The protoplast isolation and transformation were conducted as previously described (Lee et al, 2013c). Briefly, 20 – 30 leaves of 3 weeks SD grown plants were harvested and cut into strips using a blade. The leaf strips were incubated in enzyme solution (0.25% macerozyme R-10, 1% cellulose R-10, 400 mM mannitol, 8 mM $CaCl_2$, 5 mM MES-KOH, pH 5.6) at room temperature for 90 min with gentle agitation of 50 rpm, then agitated at 80 rpm for 1 min to release the protoplasts. The protoplasts were filtered using Cell Strainers (BD Falcon) to remove undigested leaf tissues, and centrifuged at 100 rcf for 1 min to remove the supernatant containing the enzyme solution. The protoplasts were subsequently washed with ice-cold W5 solution (154 mM NaCl, 125 mM $CaCl_2$, 5 mM KCl, 5 mM glucose, 1.5 mM MES-KOH, pH 5.6) by gently resuspending the protoplasts and removing the supernatant after centrifuging the tube at 100 rcf for 1 min. The washing steps were repeated again but the protoplasts were incubated in W5 solution on ice for 30 min before centrifugation. The protoplasts were ready for PEG-mediated transformation or direct immunolocalization.

For PEG-mediated transformation, the protoplasts were resuspended in MaMg solution (400 mM mannitol, 15 mM $CaCl_2$, 5 mM MES-KOH, pH 5.6) at a

density of 5 x 10^6 protoplasts/ml. In each 1.5 ml microfuge tube, 200 µl of protoplasts and 20 µl (~20 µg) of construct plasmids were added and mixed. An equal volume (220 µl) of PEG solution (200 mM mannitol, 100 mM $CaCl_2$, 40% PEG 4,000) was added into the tube and mixed well by gently rotating the tube horizontally. The tubes were incubated at room temperature for 10 min to allow transformation to take place. After incubation, 0.8 ml of W5 solution were added, mixed, and centrifuged at 100 rcf for 1 min to remove the supernatant containing PEG solution. Finally, 1 ml of W5 solution was added to resuspend the protoplasts, and the tubes were incubated horizontally at 23 °C at low light conditions.

2.3 Expression analysis

2.3.1 RNA expression

For the tissue expression analysis of *JMJ30*, *JMJ32* and *JMJ31*, total RNA was isolated from young seedlings, rosette leaves, cauline leaves, stems and inflorescences. For the time course flowering time gene expression analysis, samples were harvested from aerial parts of 5 DAG to 13 DAG seedlings for WT, *jmj30*, *jmj32* and *jmj30 jmj32*, and 1 to 3-week old seedlings for *FRI* and *FRI jmj30 jmj32* (collected at the end of the light photoperiod). Collected plant samples were stored in -80°C freezer until analysis.

Total RNA was extracted using the RNeasy plant mini kit (Qiagen) according to the manufacturer's instructions. 2 µg total RNA was used for reverse transcription using the Superscript III RT-PCR system (Invitrogen). Semi-quantitative RT-PCR with gene-specific primers (Table 6) was performed

using HotStarTaq DNA Polymerase (Qiagen) on a Thermocycler (Bio-Rad) for 15-25 cycles.

Real-time RT-qPCR was performed on an ABI PRISM 7900HT sequence detection system (Applied Biosystems) using the KAPA SYBR FAST ABI Prism qPCR Master Mix (KAPA Biosystems). *Tip41-like* (AT4G34270) was used as an internal reference gene (Czechowski et al, 2005). The relative expression of a gene of interest is calculated as $2^{-\Delta\Delta CT}$ [$\Delta\Delta C_T = \Delta C_T$ (experimental sample) – ΔC_T (control sample); $\Delta C_T = C_T$ (gene of interest) – C_T (*Tip41-like*)]. Statistical analysis was performed using two-tailed Student's *t*-test. The primer sequences are shown in Table 6.

Table 6. List of primers used for expression analysis.

Semi-quantitative RT-PCR		
Primer name	**Primer sequence**	**Primer origin**
JMJ30-sqRT_F	ACTTGGACTACCTCAATGCTGTTG	This study
JMJ30-sqRT_R	TCATGGTGTAACGGAGTAACTGTC	
JMJ32-sqRT_F	GTTAGGCATGTACCTTGGTCTAGTG	This study
JMJ32-sqRT_R	TCCAAGAAAGAACTGGATTGAGTG	
JMJ31-sqRT_F	GATTACTCTTAACGCTGGTGATGC	This study
JMJ31-sqRT_R	CATTGCCTATATTATCATTCCCACC	
Tip41-sqRT_F	CATTATAGGTTTGGCGAAGATGAG	(Czechowski et al, 2005)
Tip41-sqRT_R	TGAAACCACCACAATAAGTCAGTG	

Real-time RT-qPCR		
Primer name	**Primer sequence**	**Primer origin**
JMJ30-RT-P1_F	GATTCTGTTTTGTTGGTCTCCTC	This study
JMJ30-RT-P1_R	GATTAGCCAAAACATGTCTCACC	
JMJ30-RT-P2_F	GAATCACTTGGACTACCTCAATGC	This study
JMJ30-RT-P2_R	CATTGGAGACGATTTATTGGTCC	
JMJ30-RT-P3_F	CAAGACGAACTTTACCCTTACTCTG	This study
JMJ30-RT-P3_R	GGATGTACAACATTTCACCTTCTTC	
JMJ32-RT-P1_F	CTCCAAAGCTATTACTCATTGGC	This study
JMJ32-RT-P1_R	GAAACAAAGATCACTATCTCCGG	
JMJ32-RT-P2_F	GTTTCATTGTACTGTCAAGGCTGG	This study
JMJ32-RT-P2_R	CATACTTGATGTCAAACTGCATGTC	
JMJ32-RT-P3_F	CTTCACTCAATCCAGTTCTTTCTTG	This study
JMJ32-RT-P3_R	GAACATATTGAACCAAACACAGCC	
JMJ31-RT-P1_F	CTAGTGTCTGGGATGCGTATTCTAAG	This study
JMJ31-RT-P1_R	CATGGCTTCTGATATCACCATTG	
JMJ31-RT-P2_F	GAGATTACTCTTAACGCTGGTGATG	This study
JMJ31-RT-P2_R	GATAATACGAATCCATGTGTTCAGG	
JMJ31-RT-P3_F	CCAACAGACTGGTGAAGAAGATAG	This study
JMJ31-RT-P3_R	CCCCAAAAACTTGTCTAGTACATTC	
FLC-RT_F	CCGAACTCATGTTGAAGCTTGTTGAG	(Jiang et al, 2007)
FLC-RT_R	CGGAGATTTGTCCAGCAGGTG	
FT-RT_F	CTTGGCAGGCAAACAGTGTATGCAC	(Liu et al, 2012)
FT-RT_R	GCCACTCTCCCTCTGACAATTGTAGA	
SOC1-RT_F	AGCTGCAGAAAACGAGAAGCTCTCTG	(Liu et al, 2012)
SOC1-RT_R	GGGCTACTCTCTTCATCACCTCTTCC	
SVP-RT_F	CAAGGACTTGACATTGAAGAGCTTCA	(Li et al, 2008)
SVP-RT_R	CTGATCTCACTCATAATCTTGTCAC	
CO-RT_F	TCAGGGACTCACTACAACGACAATGG	(Liu et al, 2012)
CO-RT_R	TTGGGTGTGAAGCTGTTGTGACACAT	
AGL24-RT_F	GAGGCTTTGGAGACAGAGTCGGTGA	(Liu et al, 2008a)
AGL24-RT_R	AGATGGAAGCCCAAGCTTCAGGGAA	
Tip41-RT_F	GTGAAAACTGTTGGAGAGAAGCAA	(Czechowski et al, 2005)
Tip41-RT_R	TCAACTGGATACCCTTTCGCA	

ChIP		
Primer name	**Primer sequence**	**Primer origin**
FLC-ChIP-P1_F	GCATTAGGTTGTTCCCTCCAAAC	(Yang et al, 2012)
FLC-ChIP-P1_R	GCCCTACCCATGACTAACGTGAG	
FLC-ChIP-P2_F	TGTTCTCAATTCGCTTGATTTCTAGT	(Yang et al, 2012)
FLC-ChIP-P2_R	GCCCGACGAAGAAAAAGTAGATAG	
FLC-ChIP-P3_F	CATCTCTCCAGCCTGGTCAAG	(Yang et al, 2012)
FLC-ChIP-P3_R	GGGCTATGAAAATTGCGGTATG	
FLC-ChIP-P4_F	CCTTGGATAGAAGACAAAAAGAGAAAGTG	(Yang et al, 2012)
FLC-ChIP-P4_R	AGGTGACATCTCCATCTCAGCTTC	
MU-ChIP_F	GATTTACAAGGAATCTGTTGGTGGT	(Sun et al, 2009)
MU-ChIP_R	CATAACATAGGTTTAGAGCATCTGC	

2.3.2 Microarray analysis

For the microarray genome-wide expression analysis, two replicates of WT, *jmj30-2 jmj32-1*, and *35S::JMJ30-HA* samples were collected from the aerial parts of 13 DAG seedlings. Microarray analysis was performed using the NimbleGen 12 x 135K arrays (Roche). Total RNA was extracted from plant samples using the RNeasy plant mini kit (Qiagen) following manufacturer's instructions. 5 µg of total RNA was used for double-stranded cDNA synthesis using the SuperScript double-stranded cDNA synthesis kit (Invitrogen). cDNA samples were Cy3-labeled and hybridized using the Maui Hybridization System following the manufacturer's instructions (Roche NimbleGen). After an overnight hybridization, the slide was washed in accordance to Roche NimbleGen's protocol. Finally, the slide was scanned using the Axon GenePix 4000B Scanner and the scanned image was analyzed by NimbleScan software. Both the Axon scanner and the NimbleGen workstation were located at the Biopolis Shared Facilities (Genomics). The NimbleGen 12 x 135K expression array data sets are deposited in the NCBI Gene Expression Omnibus (GEO) under the accession code GSE51898.

Gene expression was analyzed by Arraystar (DNAStar) software, and genes showing at least a 1.5-fold change within a 90% confidence interval were considered to be differentially expressed and were presented in Supplementary Data 1 and Supplementary Data 2. Gene enrichments with H3K27me3 target were tested with Fisher's exact test using R.

2.3.3 Histochemical β-glucuronidase (GUS) staining

GUS staining of plant tissues was performed as previously described (Sun et al, 2009). Plant tissues were harvested and fixed in ice-cold 90% acetone on ice for 20 min. The acetone solution was removed and tissues were then rinsed with rinse solution (50 mM $NaPO_4$, pH 7.2, 0.5 mM $K_3Fe(CN)_6$, 0.5 mM $K_4Fe(CN)_6$). Subsequently, the rinse solution were replaced with staining solution (50 mM $NaPO_4$, pH 7.2, 0.5 mM $K_3Fe(CN)_6$, 0.5 mM $K_4Fe(CN)_6$, 2 mM X-Gluc). Tissue samples were incubated in staining solution at 37°C for 4 hrs to overnight. After staining, the staining solution was replaced with fixative solution (50% ethanol, 5% acetic acid, 3.7% formaldehyde) and incubated at room temperature overnight. The fixative solution was decanted the next day and tissues were incubated with 100% ethanol at room temperature overnight to remove the chlorophyll. Finally, the tissues were dissected and mounted in clearing solution (7.5 g gum Arabic, 100 g chloral hydrate, 5 ml glycerol, 30 ml water)(Patton et al, 1998) on glass slides and observed under a microscope.

2.4 Chromatin Immunoprecipitation

Plant materials were ground in liquid nitrogen using mortar and pestle. M1 buffer (0.1 M NaCl, 1 M hexylene glycol, 10 mM $NaPO_4$, pH 7.2, 1x cOmplete Protease Inhibitor Cocktail (PIC)(Roche)) was added into the ground powder and mixed until homogenous. The cell lysate solution in M1 buffer was transferred into a 1.5 ml microfuge tube. Formaldehyde was added to the solution to a final concentration of 1% formaldehyde for fixation, and

incubated on a shaker at 4°C for 10 min. After fixation, the formaldehyde was quenched by incubating it with 125 mM glycine at 4°C for 10 min. After incubation, the cell lysate was filtered through a 10 µm cell strainer, and the flow-through was collected in new 1.5 ml microfuge tubes.

The flow-through was centrifuged at 14,000 rpm for 1 min at 4°C. The clear pale-yellowish supernatant was removed and 500 µl of M2 buffer (0.1 M NaCl, 10 mM $MgCl_2$, 0.5% Triton X-100, 1 M hexylene glycol, 10 mM $NaPO_4$, pH 7.2, 1x PIC) was added to the tube. The green pellet is resuspended in M2 buffer, and subsequently centrifuged at 14,000 rpm for 1 min at 4°C. The supernatant was discarded and new M2 buffer was added. The washing of the pellet with M2 buffer was repeated 4 – 5 times to remove the other organelles until the pellet turned white. Finally, the pellet was washed with M3 buffer (0.1 M NaCl, 10 mM $NaPO_4$, pH 7.2, 1x PIC) twice, and the crude nuclear extract was ready for the next sonication step.

The crude nuclear extract was suspended in 200 µl SDS lysis buffer (1% SDS, 10 mM EDTA, 50 mM Tris, pH 8.0), and incubated on ice for 10 min. After incubation, 700 µl ChIP dilution buffer (0.01% SDS, 1.1% Triton X-100, 1.2 mM EDTA, 16.7 mM Tris, pH 8.0, 167 mM NaCl) was added to the tube and the solution was equally separated into 300 µl in three 1.5 ml microfuge tubes. To shear the chromatin, the nuclear extract was sonicated in a Biorupter (Diagenode) sonicator at high power on ice for 20 min using the pulse rate of 30 sec on, 90 sec off. After sonication, the tubes were centrifuged at 4ºC for 10 min at 14,000 rpm. The supernatant was collected into a new 2 ml tube, and 1.1 ml of ChIP dilution buffer was added to achieve a 10x dilution.

30 µl of Protein-A agarose (Protein-G agarose for anti-HA ChIP) was added to 2 ml of nuclear lysate for pre-clearing and incubated at 4°C for 2 hours on a rotator. After incubation, the nuclear lysate was centrifuged at 4ºC for 1 min at 2,800 rpm, and the supernatant was transferred to a new 2 ml tube. The supernatant was divided into four tubes: 850 µl for each of the two antibodies (experimental and control), 250 µl for input, and 50 µl for western blot. 5 µl of antibodies were added into the antibody tubes, and incubated at 4°C overnight on a rotator. The input tube was kept at -20°C freezer. The chromatin complex was immunoprecipitated using anti-HA (Santa Cruz Biotechnology, #sc-7392) and normal mouse IgG as a control (Santa Cruz Biotechnology, #sc-2025), or anti-H3K27me3 (Millipore, #07-449) and anti-H3 as a control (Abcam, #ab1791). Antibody dilutions of 1:170 were used (5 µl antibody in 850 µl of immunoprecipitation reaction).

The next day, 50 µl Protein-A agaroses were added into the antibody tubes to bind the antibodies, and incubated at 4°C for 2 hr on a rotator. After incubation, the tubes were centrifuged at 4ºC for 1 min at 2,800 rpm, and the supernatant was removed. The agarose beads were resuspended in 500 µl of low salt buffer (0.1% SDS, 1% Triton X-100, 2 mM EDTA, 20 mM Tris, pH 8.0, 150 mM NaCl), and incubated on ice for 2 min for washing. These washing steps were repeated several times with high salt buffer (0.1% SDS, 1% Triton X-100, 2 mM EDTA, 20 mM Tris, pH 8.0, 500 mM NaCl), LNDET buffer (250 mM LiCl, 1% NP-40, 1% deoxycholate, 1 mM EDTA, 10 mM Tris, pH 8.0), and finally TE buffer (10 mM Tris, pH 8.0, 1 mM EDTA). After washing, 135 µl of SDS elution buffer (1% SDS, 100 mM $NaHCO_3$) was added to the tube and incubated at 65 °C for 10 min in a heat-block-

shaker to elute the bound proteins. Subsequently, the tube was centrifuged at room temp for 1 min at 2,800 rpm, and 125 µl of the supernatant was transferred to a new 1.5 ml tube. The elution steps were repeated one more time to obtain a total elution of 250 µl. The residual eluted supernatant was kept for western blot.

To reverse the formaldehyde crosslinking, the eluted antibody-bound supernatant and the input were treated with Proteinase K mix (200 mM NaCl, 40 mM Tris, pH 8.0, 10 mM EDTA, 40 µg/ml Proteinase K), and incubated in a thermocycler with the program: 42°C for 2 hr, then 65°C for 6 hr.

The next day after decrosslinking, the released chromatin was treated with 50 µg/ml RNase A at room temperature for 30 min. The released DNA was then ready for DNA cleanup. Briefly, 400 µl of phenol:chloroform:isoamyl alcohol (25:24:1) was added to each tube, mixed thoroughly on a vortex mixer, and centrifuged at room temp for 10 min at 14,000 rpm. The upper aqueous layer was transferred to a new tube. The extraction step was repeated with 400 µl of chloroform. The extracted DNA was precipitated with 0.8 M LiCl (final concentration), 2 volumes of 100% ethanol, and 1 µl of 20 mg/ml glycogen, incubated at -80°C for 1 hr. After incubation, the tube was centrifuged at 4 °C for 10 min at 14,000 rpm and the supernatant was decanted. The DNA pellet was washed with ice-cold 70% ethanol and centrifuged at 4°C for 10 min at 14,000 rpm. Subsequently, the supernatant was removed and the DNA pellet was dried in a SpeedVac vacuum concentrator. The dried DNA pellet was dissolved in TE buffer. The enrichment fold was analyzed by qPCR with gene-specific primers (Table 6), performed on an ABI PRISM 7900HT

sequence detection system (Applied Biosystems) using the KAPA SYBR FAST ABI Prism qPCR Master Mix (KAPA Biosystems).

The results were first normalized to an internal control *Mutator-like* transposon (AT4G03870). For the histone modification ChIP, the relative enrichment was calculated by taking the ratio of DNA immunoprecipitated with anti-H3K27me3 antibody with that of anti-H3 antibody. Similarly, the ChIP relative enrichment of JMJ30-HA binding was calculated from the ratio between anti-HA antibody and normal mouse IgG immunoprecipitated DNA. Statistical analysis was performed using two-tailed Student's *t*-test.

2.5 Biochemical analysis

2.5.1 Western blot

20 µl of protein sample was mixed with 4 µl of 6x SDS loading buffer (375 mM Tris, pH 6.8, 12% SDS, 60% glycerol, 0.06% bromophenol blue, 5% β-mercaptoethanol) and incubated at 95°C for 10 min in a heat-block. The denatured protein samples were then separated on denaturing polyacrylamide gels (10% Resolving gel: 2.67 ml 30% acrylamide, 2 ml 1.5 M Tris pH 8.8, 80 µl 10% SDS, 80 µl 10% ammonium persulfate (APS), 8 µl N,N,N',N'-tetramethylethylenediamine (TEMED), 3.2 ml ddH_2O; 4% Stacking gel: 0.67 ml 30% acrylamide, 1.25 ml 0.5 M Tris pH 6.8, 50 µl 10% SDS, 50 µl 10% APS, 5 µl TEMED, 3 ml ddH_2O) by electrophoresis in running buffer (25 mM Tris, 192 mM glycine, 0.1% SDS). Subsequently, the proteins were transferred onto a PVDF membrane through wet electroblotting at 100 V for 1 hr in transfer buffer (25 mM Tris, 192 mM glycine, 20% methanol).

After transfer, the membrane was pre-wash in PBST buffer (137 mM NaCl, 2.7 mM KCl, 10 mM Na_2HPO_4, 1.8 mM KH_2PO_4, 0.1% Tween-20), then blocked with blocking buffer (5% non-fat milk powder dissolved in PBST buffer) at room temperature for 1 hr with gentle agitation. Subsequently, the blocking buffer was removed, and the membrane was probed with primary antibody solution (1:1,000 dilution of antibody in 5% milk in PBST) at room temperature for 1 hr with gentle agitation. The membrane was then washed by gently agitating in PBST for 5 min for three times to remove excess primary antibody. The membrane was next probed with secondary antibody solution (1:10,000 dilution of antibody in 5% milk in PBST) at room temperature for 1 hr with gentle agitation. The washing steps were repeated by gently agitating the membrane in PBST for 5 min for three times to remove excess secondary antibody. The membrane was now ready for protein detection.

The immunoblot can be visualized by enhanced chemiluminescence (ECL) which detects the horseradish peroxidase (HRP) conjugated to the secondary antibody. Briefly, the Stable Peroxide solution and the Luminol/Enhancer solution were pre-mixed at a 1:1 ratio. The immunoblot was placed onto the exposure cassette with its protein side facing upwards. The pre-mixed ECL solution was transferred to fully cover the membrane and incubated for 5 min at room temperature. After incubation, excess reagent was removed. X-ray films (GE Healthcare) were placed over the immunoblot and exposed with various timing to determine the best exposure. The X-ray films were developed in Kodak M35 X-OMAT Processor (Kodak), and later scanned as a digital image for further quantitative analysis.

2.5.2 Immunolocalization

The isolation of nuclei and *in situ* immunolocalization of chromatin proteins were performed as described with minor modifications (Lysak et al, 2006). Briefly, young leaves from *pJMJ30::JMJ30-HA* transgenic plants were first fixed in ice-cold 4% formaldehyde in Tris buffer (10 mM Tris, pH 7.5, 10 mM EDTA, 100 mM NaCl) for 20 min, then rinsed in ice-cold Tris buffer twice for 10 min. The leaves were then chopped into a fine suspension in LB01 buffer (15 mM Tris, pH 7.5, 2 mM EDTA, 0.5 mM spermine, 80 mM KCl, 20 mM NaCl, 0.1% Triton X-100), and filtered with a cell strainer (BD Falcon). Subsequently, the filtered cell lysate was air-dried on glass slides. Each slide was blocked with 1% BSA in 1x PBS buffer (137 mM NaCl, 2.7 mM KCl, 10 mM Na_2HPO_4, 1.8 mM KH_2PO_4) in a moist chamber at 37°C for 30 min, and rinsed with PBS buffer at room temperature for 5 min for three times. Next, the slides were probed with mouse anti-HA antibody (Santa Cruz Biotechnology, #sc-7392) in a moist chamber at 37°C for 2 hr, and rinsed with PBS buffer at room temperature for 5 min for three times. The same probing steps were repeated with the secondary antibody CF555 goat anti-mouse IgG antibody (Biotium, #20030). A dilution of 1:200 is used for both primary and secondary antibodies. Finally, the slides were stained with DAPI and imaged with a Leica TCS SP5 confocal microscope (Leica).

Isolation of protoplasts were performed as described in section 2.2.3 while immunolocalization of protoplasts were performed as previously described (Lee et al, 2013c). Briefly, the transformed protoplasts were resuspended in W6 buffer (10 mM HEPES, pH 7.2, 154 mM NaCl, 125 mM $CaCl_2$, 5 mM

glucose, 5 mM KCl) and spread on a glass slide. The protoplast suspension was incubated at room temperature for 1 hr in a moist chamber to allow the cells to adhere. Subsequently, the excess cell suspension was removed using a pipette, and the adhered protoplasts were fixed in fixing solution (4% formaldehyde in W6 solution) by incubating at room temperature for 1 hr. After incubation, the slide was rinsed with TSW buffer (10 mM Tris, pH 7.4, 0.9% NaCl, 0.25% gelatin, 0.02% SDS, 0.1% Triton X-100) at room temperature for 10 min for three times. The TSW buffer also served as a permeabilizing agent and blocking agent for the protoplasts.

Next, the slide was probe with mouse anti-HA antibody (Santa Cruz Biotechnology, #sc-7392) and rabbit anti-H3K27me3 antibody (Millipore, #07-449) in a moist chamber at 4°C overnight. The next day, the slide was rinsed with TSW buffer at room temperature for 10 min for three times, and probed with the secondary antibodies CF555 goat anti-mouse IgG (Biotium, #20030) and CF488 goat anti-rabbit IgG antibodies (Biotium, #20012) at room temperature for 3 hr. Finally, after rinsing the slide with TSW buffer at room temperature for 10 min for three times, the slide was mounted with DAPI and imaged with a Leica TCS SPE confocal microscope (Leica). A dilution of 1:200 is used for both primary and secondary antibodies.

2.5.3 *In vitro* histone demethylase assay

Recombinant JMJ30-HA and JMJ30H326A-HA was transiently over-expressed in tobacco leaves and immunoaffinity-purified using anti-HA beads (Sigma, A2095). Histone demethylase assay was performed as previously

described (Lu et al, 2011b; Yang et al, 2010). Briefly, the purified JMJ30-HA enzymes and substrate calf thymus histone (4 μg) were co-incubated in a 20 μl reaction mix (20 mM Tris-HCl, pH 7.5, 150 mM NaCl, 50 μM $Fe(NH_4)_2(SO_4)_2$, 1 mM α-ketoglutarate, 2 mM ascorbate) for 4 hr at 37°C. The reaction products were analyzed by western blotting (described in section 2.5.1) using the following antibodies: anti-H3K27me3 (Millipore, #07-449), anti-H3K27me2 (Millipore, #07-452), anti-H3K27me1 (Millipore, #07-448), anti-H3K9me3 (Millipore, #07-442), anti-H3K9me2 (Millipore, #07-441), anti-H3K4me3 (Millipore, #07-473), anti-H3K4me2 (Millipore, #07-030), anti-H3K36me3 (Abcam, #ab9050), anti-H3K36me2 (Abcam, #ab9049), and anti-H3 (Abcam, #ab1791). A dilution of 1:1000 is used for primary antibodies and 1:10,000 for secondary antibodies. Band intensity of the scanned image was analyzed using ImageJ software.

2.5.4 *In vivo* histone demethylase assay

The *in vivo* histone demethylase assay was performed by modifying the protoplast isolation and transformation, nuclei isolation, and immunolocalization methods from various protocols (Lee et al, 2013c; Praveen et al, 1985). Briefly, JMJ30-HA, JMJ30H326A, JMJ32-HA, and JMJ32H174A were transiently over-expressed in *Arabidopsis* leaf protoplasts through PEG-mediated transformation (described in section 2.2.3)(Lee et al, 2013c). For nuclei isolation after one day, the protoplasts were resuspended in Nuclear Isolation Buffer (NIB) buffer (10 mM MES-KOH, pH 5.6, 0.2 M sucrose, 2.5 mM EDTA, 0.1 mM spermine, 0.5 mM spermidine, 10 mM NaCl, 10 mM KCl, 2.5 mM DTT, 0.01% Triton X-100) and incubated on ice for 7

min to allow deplasmolysis (Praveen et al, 1985). After incubation, the protoplasts were passed through a 26G gauge needle for four times, and filtered through a double-layered miracloth to remove larger debris. The cell lysate was centrifuged at 209 rcf for 5 min and the supernatant containing other cellular organelles was removed. The pelleted nuclei were resuspended in NIB buffer without Triton-X and spread on a glass slide for 30 min to allow the nuclei to adhere. Immunolocalization was performed as described in section 2.5.2 (Lysak et al, 2006) by incubating each slide with mouse anti-HA (Santa Cruz Biotechnology, #sc-7392) and rabbit anti-H3K27me3 (Millipore, #07-449) antibodies, and then with CF555 goat anti-mouse IgG (Biotium, #20030) and CF488 goat anti-rabbit IgG antibodies (Biotium, #20012). A dilution of 1:200 is used for both primary and secondary antibodies. The slides were stained with DAPI and imaged with a Leica TCS SP8 confocal microscope (Leica). The intensities of at least 50 pairs of closely-located JMJ-HA-transformed and non-transformed nuclei were analyzed using ImageJ software. Data were presented as a relative intensity of transformed/non-transformed nuclei. Statistical analysis was performed using two-tailed Student's *t*-test.

2.5.5 Protein expression assay

Samples for the time course JMJ30-HA protein expression experiment were harvested from aerial parts of 9 DAG *pJMJ30::JMJ30-HA* or *35S::JMJ30-HA* seedlings. The JMJ30-HA protein stability assay with CHX and MG132 was performed as described (Lee et al, 2013a). Total protein was extracted by grinding plant tissues in liquid nitrogen and resuspending in an equal volume

of 2x SDS loading buffer (4% SDS, 20% Glycerol, 0.125 M Tris, pH 6.8, 0.2% bromophenol blue, 200 mM β-mercaptoethanol). Protein samples were incubated at 95°C for 10 min and then centrifuged for 10 min at 14,000 rpm. The supernatant was used for western blots (described in section 2.5.1) using anti-HA-HRP (Santa Cruz Biotechnology, #sc-7392 HRP) using a dilution of 1:2000. Band intensity was analyzed using ImageJ software.

2.5.6 Immunoprecipitation-mass spectrometry

Plant materials were collected from 10DAG *pJMJ30::JMJ30-HA jmj30-2* plants grown at 22°C and 29°C at the end of the light photoperiod when JMJ30-HA was expressed at its highest level. Nuclear extract were prepared in a similar method as ChIP (section 2.4) except no fixation step is required (i.e. no addition of formaldehyde into M1 buffer after grinding). Immunoprecipitation was conducted by incubating the nuclear lysate with anti-HA beads (SIGMA) overnight at 4°C on a rotator. The next day, the beads were washed consecutively with low salt buffer, high salt buffer, LNDET buffer and TE buffer. Finally the bound proteins were eluted with 200 µl of SDS elution buffer (4% SDS, 125 mM Tris, pH6.0) at 85°C for 10 min. 5 volumes of acetone (i.e. 1 ml) were added to the eluted sample for precipitation at -20°C overnight. The following day, the tube was centrifuged at 4°C for 15 min at 14,000 rpm, and the supernatant was removed. Subsequently, the pellet was vacuum-dried on ice and resuspended in 30µl 100 mM triethyl ammonium bicarbonate (TEAB). The sample was casted in a tube gel (30 µl sample, 20 µl 20% SDS, 33.33 µl 30% acrylamide, 2.5 µl 10% APS, 0.25 µl TEMED, 13.92 µl water). After the gel solidify, the sample was

fixed in-gel with fixing solution (50% methanol, 12% acetic acid) at room temperature for 30 min. The tube gel was then cut into small pieces (~1 mm^3) and finally sent for mass spectrometry analysis in the Protein and Proteomics Centre, Department of Biological Sciences, National University of Singapore (PPC, DBS, NUS). Sample reduction and alkylation, in-gel digestion, followed by shotgun protein identification using TripleTOF 5600 System (AB SCIEX) were performed by the PPC staff.

Chapter 3

Results

Chapter 3 Results

3.1 *FLC* prevents precocious flowering at elevated temperature

The flowering time of the *flc-3* null mutant is indistinguishable from Columbia wild-type (Col WT) plants when grown at 22 °C under long day (LD, 16-h light/8-h dark) conditions (Figure 4a,b)(Michaels & Amasino, 1999; Michaels & Amasino, 2001). However, when grown at 29°C LD conditions, *flc-3* plants flowered earlier than WT plants with the leaf number ratio (29°C/22°C) of 0.51 for *flc-3* and 0.69 for WT (Figure 4a,b), suggesting that *FLC* contributes to preventing precocious flowering at elevated temperatures (Balasubramanian et al, 2006). Although *FLC* expression is low in WT plants that lack a functional *FRI* (Balasubramanian et al, 2006), expression analyses are still able to detect basal *FLC* expression, which gradually decreases during vegetative development (Figure 4c)(Yang et al, 2012). To determine whether *FLC* temporal expression level is affected by elevated temperatures, I analyzed *FLC* expression in plants grown at 22°C and 29°C under LD conditions at 5, 9, and 13 days-after-germination (DAG) before the plants undergo the bolting process. I observed that after shifting to 29°C at 3 DAG, *FLC* expression was initially comparable between plants grown at 22°C and 29°C at 5 DAG (Figure 4c). *FLC* expression decreases gradually at 9 and 13 DAG in plants grown under both the 22°C and 29°C conditions, but this *FLC* down-regulation is significantly attenuated in plants grown at 29°C (Figure 4c). This result showed that *FLC* repression during vegetative development was delayed during growth at elevated temperatures.

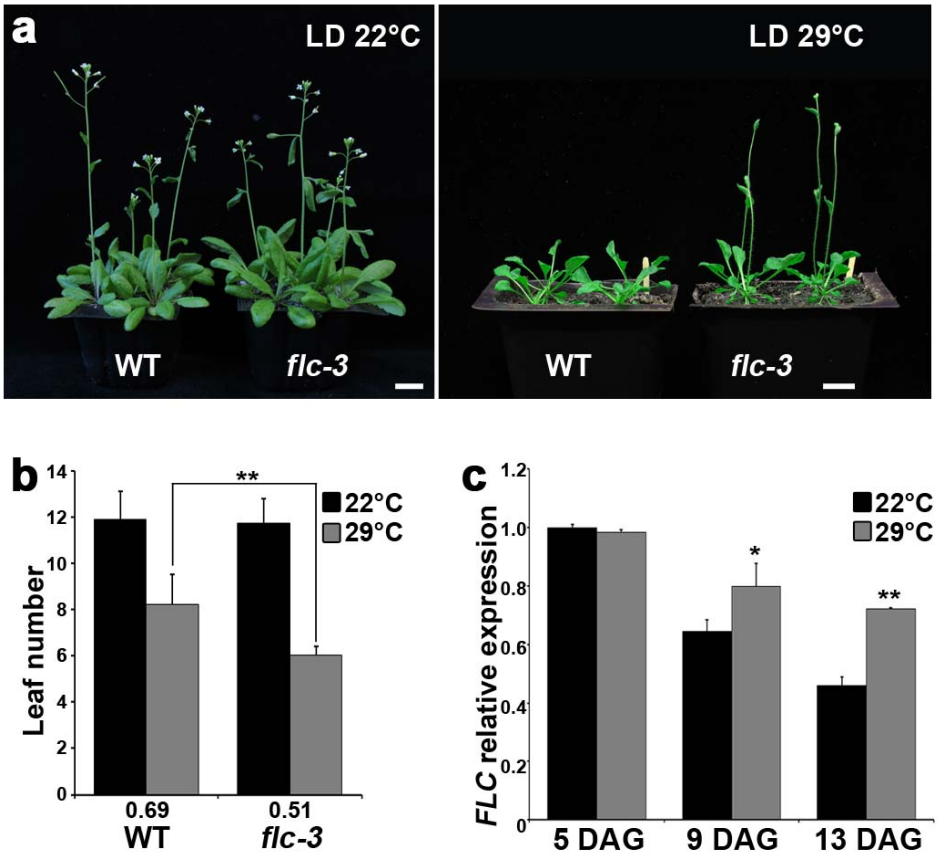

Figure 4. *FLC* is a suppressor of thermal induction of flowering.

(**a**) *flc-3* flowers at a similar time as WT when grown in LD 22°C, but flowering is accelerated in *flc-3* when grown under LD 29°C conditions. Representative 30-day-old plants (LD 22°C) or 23-day-old plants (LD 29°C) were shown as comparison. Scale bar, 1 cm. (**b**) Total primary rosette leaves before bolting in WT and *flc-3* plants grown under LD 22°C and 29°C conditions were counted (2 independent experiments with 15-20 plants each). Numbers below graph indicate leaf number ratio (29°C/22°C). Bars indicate standard deviation (s.d.); two-tailed Student's *t*-test, **P <0.01. (**c**) *FLC* mRNA levels in 5, 9 and 13 DAG seedlings grown under LD 22°C and 29°C conditions, analyzed by qRT-PCR. Relative fold changes to 5 DAG seedlings grown under 22°C conditions are presented. Bars indicate s.d. of three biological replicates; two-tailed Student's *t*-test, *P<0.05, **P<0.01.

I next wondered whether this *FLC* delayed repression is regulated at the chromatin level. As *FLC* reduction during the developmental switch from vegetative to reproductive phase is known to be regulated by the repressive H3K27me3 (Angel et al, 2011; Jiang et al, 2008a), I performed chromatin immunoprecipitation (ChIP) assays to assess the level of H3K27me3 at the *FLC* locus at 8 DAG, which is on the brink of floral transition occurring at 9 DAG (Figure 5a)(Li et al, 2008). Compared with WT plants grown under 22°C LD conditions, WT plants grown at 29°C showed reduced H3K27me3 enrichment at the *FLC* locus (Figure 5b). This finding indicates that delayed *FLC* repression at elevated temperatures is associated with the reduction of the repressive H3K27me3 at the *FLC* locus. Taken together, these results suggest that H3K27me3-associated histone modifiers may participate in the thermosensory pathway by regulating *FLC* expression at elevated temperatures to control flowering in moderation.

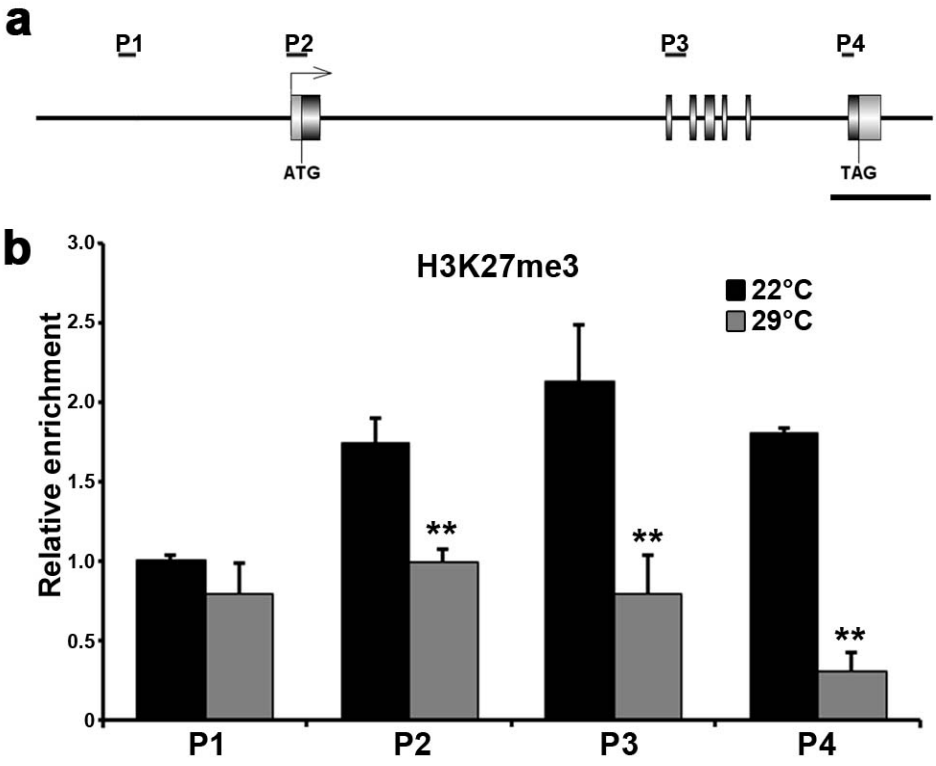

Figure 5. The H3K27me3 repressive mark at *FLC* locus was decreased at elevated temperatures.

(**a**) Schematic drawing of the *FLC* genome structure showing regions amplified by primers used for ChIP analysis. Scale bar, 1 kb. (**b**) ChIP analysis of H3K27me3 enrichment at the *FLC* locus in 8 DAG WT seedlings grown under LD 22°C and 29°C conditions. An anti-H3 antibody was used as a control. Bar indicates standard error of the mean (s.e.m.) of three biological replicates; two-tailed Student's *t*-test, **P<0.01.

3.2 Phylogenetic analysis of the JMJ proteins

The lower levels of H3K27me3 at the *FLC* locus at elevated temperatures and the increased level of *FLC* expression led us to conjecture that the effect may be maintained through the action of H3K27me3 demethylases. In *Arabidopsis*, the LSD1 class of histone demethylases mainly catalyzes the removal of H3K4me2 (Jiang et al, 2007). Thus, I hypothesized that this high temperature regulated removal of H3K27me3 should be mediated by JMJ proteins. However, *FLC* expression is up-regulated rather than down-regulated in the loss-of-function mutant of the only known *Arabidopsis* H3K27me3 demethylase, *REF6* (Lu et al, 2011b; Noh et al, 2004). Hence, I reasoned that there might be other JMJ proteins that may remove the H3K27me3 repressive marks at the *FLC* locus.

A blast on the *Arabidopsis* genome shows that it contains 21 JmjC domain-containing proteins (http://blast.ncbi.nlm.nih.gov/Blast.cgi). I carried out a domain analysis using SMART (http://smart.embl-heidelberg.de/) and multiple sequence alignment using Multiple Alignment using Fast Fourier Transform (MAFFT, http://mafft.cbrc.jp/alignment/server/), with scoring matrix of BLOSUM62, and gap opening penalty of 1.53. Neighbor-joining analysis was done with the Poisson substitution model. Bootstrap test was performed using 1,000 resampling. Based on the phylogenetic analysis of the full-length protein sequence, these 21 genes can be categorized into 5 groups (Figure 6a). Despite some minor differences, my results are agreeable with two previous studies (Hong et al, 2009; Lu et al, 2008).

The main disagreement between the two previous studies lies in whether to place JMJ20 in the JMJD6 group or the JmjC domain only group (Hong et al, 2009; Lu et al, 2008). Lu et al (2008) appeared to emphasize more on the domain architecture and placed JMJ20 in the JmjC domain only group, whereas Hong et al (2009) categorized JMJ20 into the JMJD6 group together with JMJ21 and JMJ22. My phylogenetic analysis also yield ambiguous results depending on whether I used their full-length protein sequences or only their JmjC domains (Figure 6a,b). Howover, a recent report showed that JMJ20 and JMJ22 function as histone arginine demethylases (Cho et al, 2012), thus suggesting their homology and functional conservation. Whether JMJ21 has similar functions as JMJ20 and JMJ22 in the JMJD6 group remains to be eludicated.

Taking into account previous studies in animals which reported that proteins with similar JmjC domain are more likely to have the same specificity towards certain methylated histone, we would expect similar substrate specificity for *Arabidopsis* JMJ proteins as their homologous animal counterpart. Among the five groups of *Arabidopsis* JMJ proteins, four of them (KDM5/JARID1, KDM4/JHDM3/JMJD2, KDM3/JHDM2, and JMJD6) have been implicated as histone demethylases specific for other histone modifications, such as H3K4 and H3K9 (Cho et al, 2012; Hong et al, 2009; Inagaki et al, 2010; Jeong et al, 2009; Lu et al, 2010; Lu et al, 2008; Lu et al, 2011b; Saze et al, 2008; Yang et al, 2012; Yang et al, 2010; Yu et al, 2008a).

However, the group that contains no other known functional protein domains but the catalytic JmjC domain is not as widely studied even in the animal. In *Arabidopsis*, there are three members in this group: JMJ30/AT3G20810,

JMJ31/AT5G19840 and JMJ32/AT3G45880. JMJ30 has been implicated in circadian clock regulation (Jones et al, 2010; Lu et al, 2011c), but no detailed biochemical study was reported. At closer inspection, I found that JMJ30 and JMJ32 contain all the active amino acid residues required for Fe(II) and α-KG-binding (Figure 7)(Klose et al, 2006a). Like the members of the animal JMJD5, JMJ4, L0C339123 sub-group of JMJ proteins (Klose et al, 2006a), the *Arabidopsis* JMJ31 also has a different variant of amino acid for one of its key α-KG-binding residues (serine in place of threonine/tyrosine/phenyalanine) and is thus likely to be enzymatically inactive (Figure 7). Hence, I setup the project to study members of this group of JMJ proteins that contain JmjC domain only, giving more emphasis on JMJ30 and JMJ32.

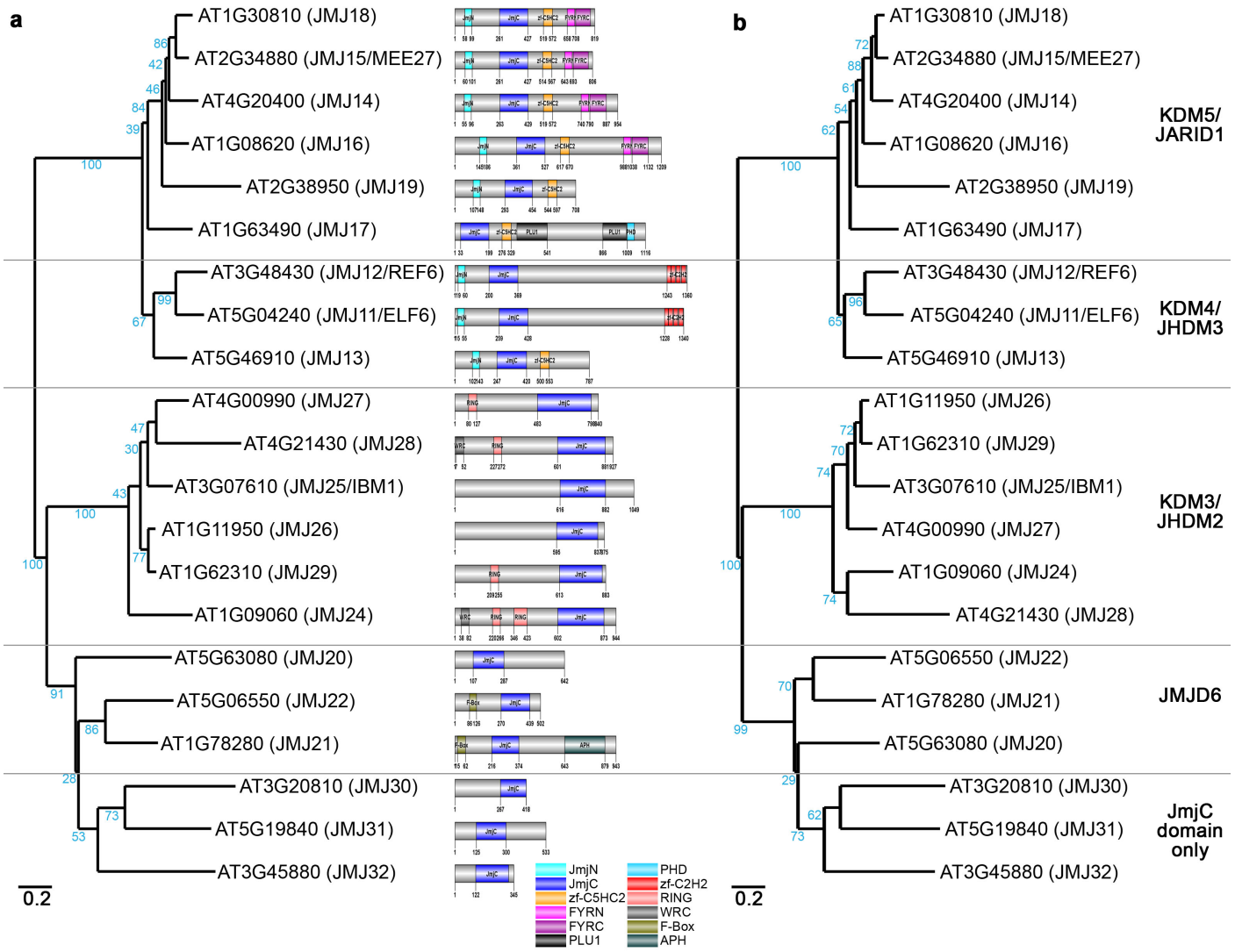

Figure 6. Phylogenetic analysis of the JMJ proteins in the *Arabidopsis* genome.

21 *Arabidopsis* JmjC domain-containing genes can be grouped into 5 groups based on their (**a**) full-length sequence, or (**b**) their JmjC domain sequences only. The two trees differ mainly in the arrangement of the members in the KDM3/JHDM2 group and the position of JMJ20 between the JMJD6 group and JmjC domain only group.

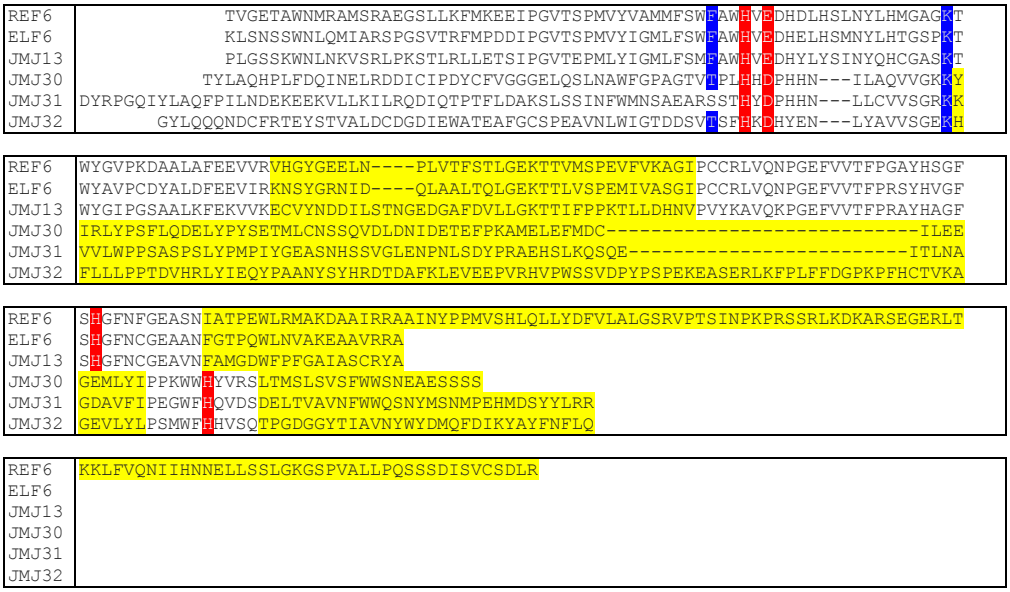

Figure 7. Multiple sequence alignment of the JmjC domains of KDM4/JHDM3/JMJD2 and JmjC-domain only group members.

RELATIVE OF EARLY FLOWERING 6 (REF6), EARLY FLOWERING 6 (ELF6) and JUMONJI 13 (JMJ13) belongs to the KDM4/JHDM3/JMJD2 group while the JmjC-domain only group contains JMJ30, JMJ31 and JMJ32. Fe(II)-binding and α-ketoglutarate-binding residues are marked in red and blue respectively. The variable regions within the JmjC domain are highlighted in yellow. Note that like the members of the animal JMJD5, JMJ4, L0C339123 sub-group of JMJ proteins (Klose et al, 2006a), JMJ31 also has a different variant of amino acid for one of its key α-KG-binding residues (serine in place of threonine/tyrosine/phenyalanine) and is thus likely to be enzymatically inactive. KDM4/JHDM3/JMJD2: JMJ12/REF6 (AT3G48430), JMJ11/ELF6 (AT5G04240), JMJ13 (AT5G46910); JmjC-domain only: JMJ30 (AT3G20810), JMJ31 (AT5G19840), JMJ32 (AT3G45880).

3.3 Loss-of-function mutation of *jmj30* and *jmj32* causes an early-flowering phenotype at elevated temperature

To elucidate the function of this group, I used two previously-described loss-of-function mutants for *JMJ30*: *jmj30-1* (SAIL_811_H12) and *jmj30-2* (GK-454C10)(Jones et al, 2010; Lu et al, 2011c), and isolated one T-DNA insertional mutant for *JMJ32*: *jmj32-1* (SALK_003313), and three T-DNA insertional mutant for JMJ31: *jmj31-1* (SALK_029755), *jmj31-2* (SALK_076996), *jmj31-3* (GK-175C06)(Table 3, Figure 8a). No full-length *JMJ30* mRNA was detected for either allele, and I decided to use *jmj30-2* for subsequent experiments, as it produced no partial fragment (Figure 8b). Partial fragment of *JMJ32* mRNA was still detectable in *jmj32-1*, however, because the T-DNA is inserted at the catalytic JmjC domain, it likely produces a null mutant (Figure 8a,d). The T-DNA mutant of *jmj31* showed varied degree of effect on *JMJ31* expression and transcript integrity. Insertion at exon 14 in *jmj31-1* abolished the expression after the insertion (Figure 8c). The *jmj31-2* and *jmj31-3* mutants, inserted in the promoter and intron 4 respectively, caused an up-regulation of *JMJ31* (Figure 8c). Due to the fact that JMJ31 has an enzymatic inactive variant for its key α-KG-binding amino acids, I crossed the mutant alleles of other two members in the group to produce a *jmj30-2 jmj32-1* double mutant for further studies.

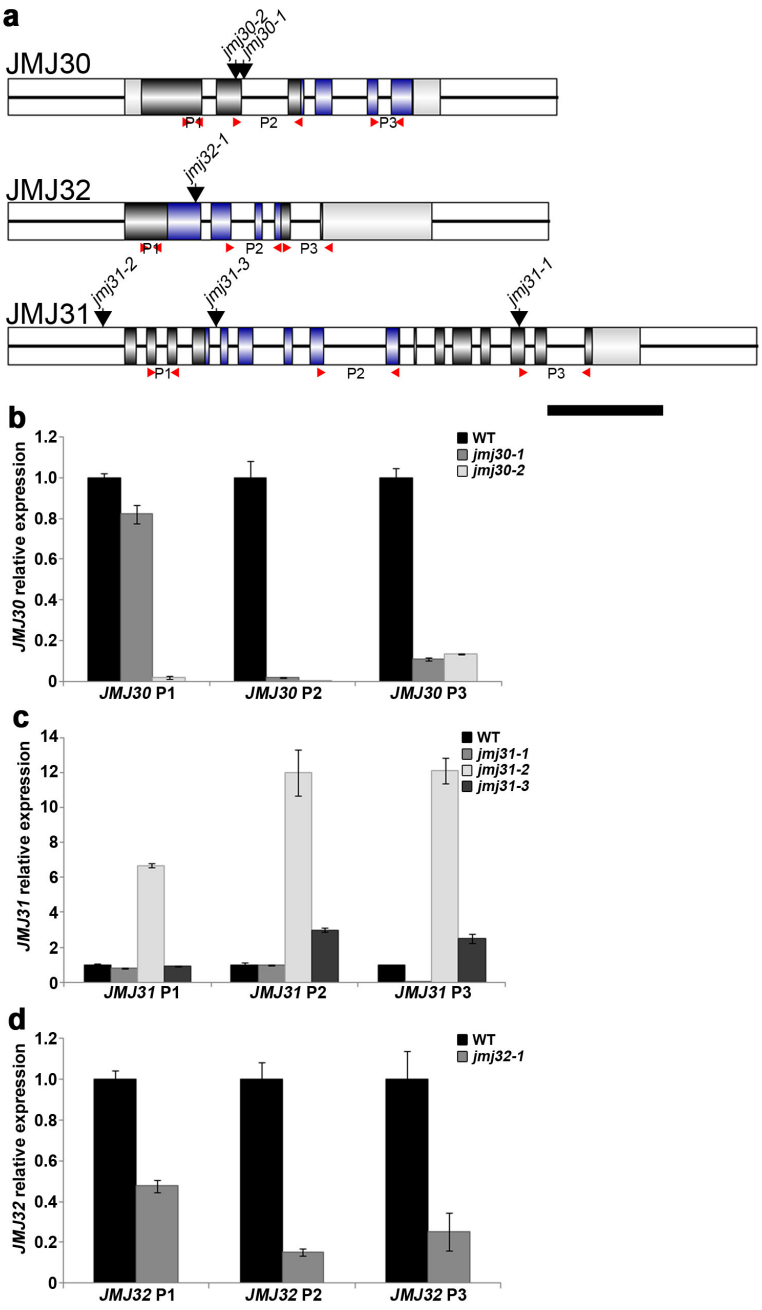

Figure 8. *jmj30-2* and *jmj32-1* produce loss-of-function mutants.

(**a**) Schematic drawing of *JMJ30*, *JMJ32* and *JMJ31* genome structure showing regions amplified by primers used for mRNA expression analysis. Gray boxes indicate the 5'and 3'UTR. Black boxes indicate exons, while blue boxes indicate exons coding for the JmjC domain. White boxes with a line indicate introns. T-DNA insertion mutants are marked by downward pointing arrows above the schematic diagrams, whereas smaller arrowheads below denote regions amplified by primers used for RT-qPCR. Scale bar, 1 kb. (**b**,**c**,**d**) Relative mRNA expression level in 10 DAG seedlings was analyzed by qRT-PCR. Graphs showed expression of (**b**) *JMJ30* in WT, *jmj30-1* and *jmj30-2*, (**c**) *JMJ31* mRNA expression in WT, *jmj31-1*, *jmj31-2* and *jmj31-3*, and (**d**) *JMJ32* mRNA expression in WT and *jmj32-1*. Relative fold changes to WT are presented. Bars indicate s.d. of three biological replicates.

Under the standard growth conditions (22°C LD), neither the single nor the double *jmj30-2 jmj32-1* (herein *jmj30 jmj32*) mutants differed from WT in terms of flowering time, which is similar to the *flc* mutant's lack of a phenotype under standard growth conditions (Figure 4a,b, Figure 9a,b). However, I found that the *jmj30 jmj32* double mutant flowered earlier than the WT when grown under elevated temperatures with the decreased leaf number ratio (29°C/22°C) of 0.52 compared to 0.69 in WT, but no obvious difference in phyllochron length (Figure 9a,b), as was observed in *flc* (Figure 4a,b). I then studied the response of *jmj30 jmj32* to elevated temperature in short days (SD, 8-h light/16-h dark) and observed the enhanced early-flowering phenotype compared to WT grown under the same conditions, with the leaf number ratio (29°C/22°C) of 0.19 for *jmj30 jmj32* and 0.24 for WT (Figure 10a,b).

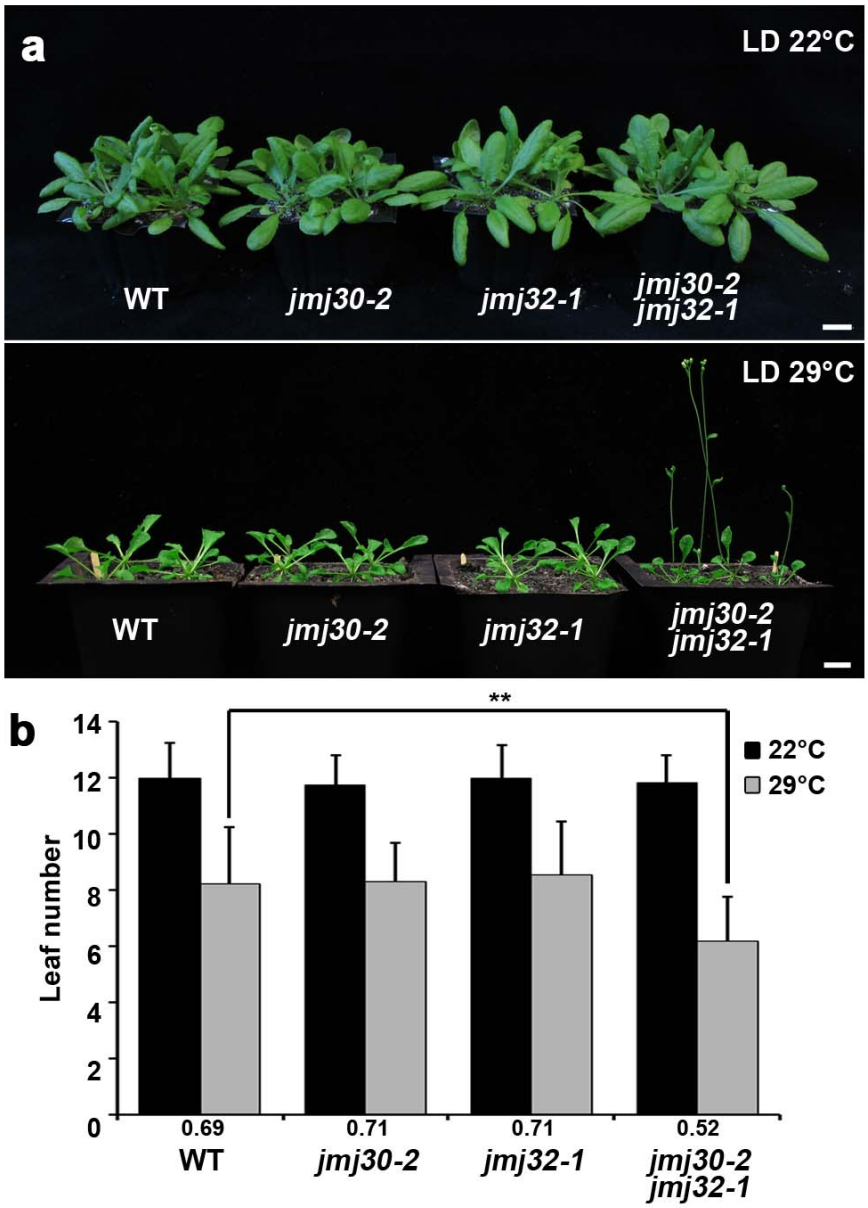

Figure 9. *jmj30 jmj32* loss-of-function mutant accelerates flowering at elevated temperatures.

(**a**) *jmj30-2*, *jmj32-1* and *jmj30-2 jmj32-1* flower at a similar time as WT when grown under LD 22°C conditions, but *jmj30-2 jmj32-1* showed accelerated flowering when grown under LD 29°C conditions. Representative 25-day-old plants (LD 22°C) or 23-day-old plants (LD 29°C) were shown as comparison. Scale bar, 1 cm. (**d**) Total primary rosette leaves before bolting in WT, *jmj30-2*, *jmj32-1* and *jmj30-2 jmj32-1* plants grown under LD 22°C and 29°C conditions were counted (2 independent experiments with 15-20 plants each). Numbers below graph indicate leaf number ratio (29°C/22°C). Bars indicate s.d.; two-tailed Student's *t*-test, **P <0.01.

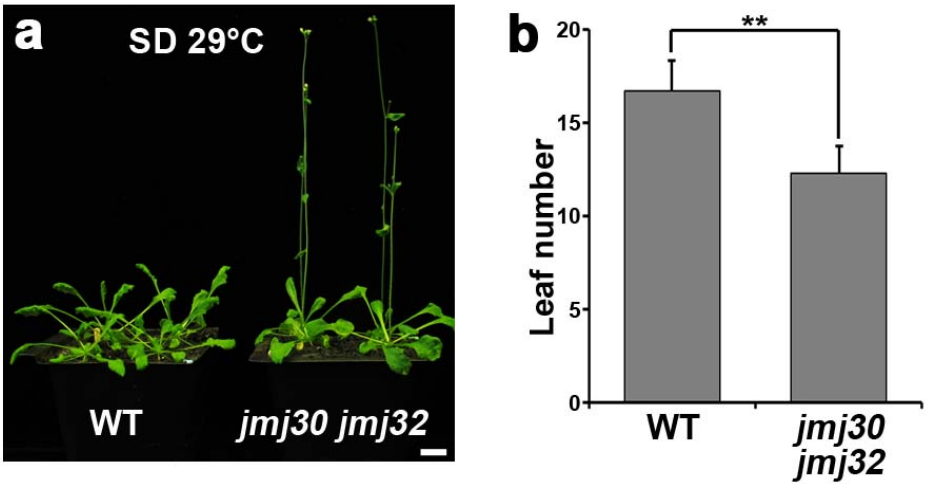

Figure 10. *jmj30 jmj32* double mutant accelerates flowering at higher temperatures under short day conditions.

(**a**) *jmj30 jmj32* double mutant showed early-flowering phenotype when grown under SD 29°C conditions. Representative 40-day-old plants were shown as comparison. Scale bar, 1 cm. (**b**) Total primary rosette leaves before bolting in WT and *jmj30-2 jmj32-1* plants grown under SD 29°C conditions were counted (2 independent experiments with 15-20 plants each). Bars indicate s.d.; two-tailed Student's *t*-test, **P<0.01.

I next proceed to look at the expression profile of the flowering time genes. I collected 5, 9, and 13 DAG seedling samples grown at 29°C LD conditions at the end of the light photoperiod, and analyzed the *FLC* expression by qRT-PCR. The *jmj30 jmj32* double mutant decreased *FLC* expression at all tested time points (Figure 11a). Furthermore, the trend of decreased *FLC* expression at 13 DAG is similar in *jmj30 jmj32* seedlings grown at 29°C (Figure 11a) and WT grown at 22°C (Figure 4c). The other thermosensory mediator *SVP* was not significantly affected (Figure 11b). In contrast, the expression of the florigen *FT* and another floral promoter *SOC1* were increased especially in 13 DAG seedlings of *jmj30 jmj32* relative to WT at 29°C LD (Figure 11c,d). These results align with reports that the FLC-SVP complex represses *FT* in leaves and *SOC1* in both leaves and shoot apical meristems (Searle et al, 2006). *AGL24* and *CO* were not significantly affected in *jmj30 jmj32*, implying that *JMJ30* and *JMJ32* may not affect the photoperiod pathway (Figure 11e,f). In short, the results suggest that *jmj30 jmj32* mutations decrease *FLC* expression at elevated temperature, and this effect appears to up-regulate the floral integrators *FT* and *SOC1*, which are two common targets of FLC.

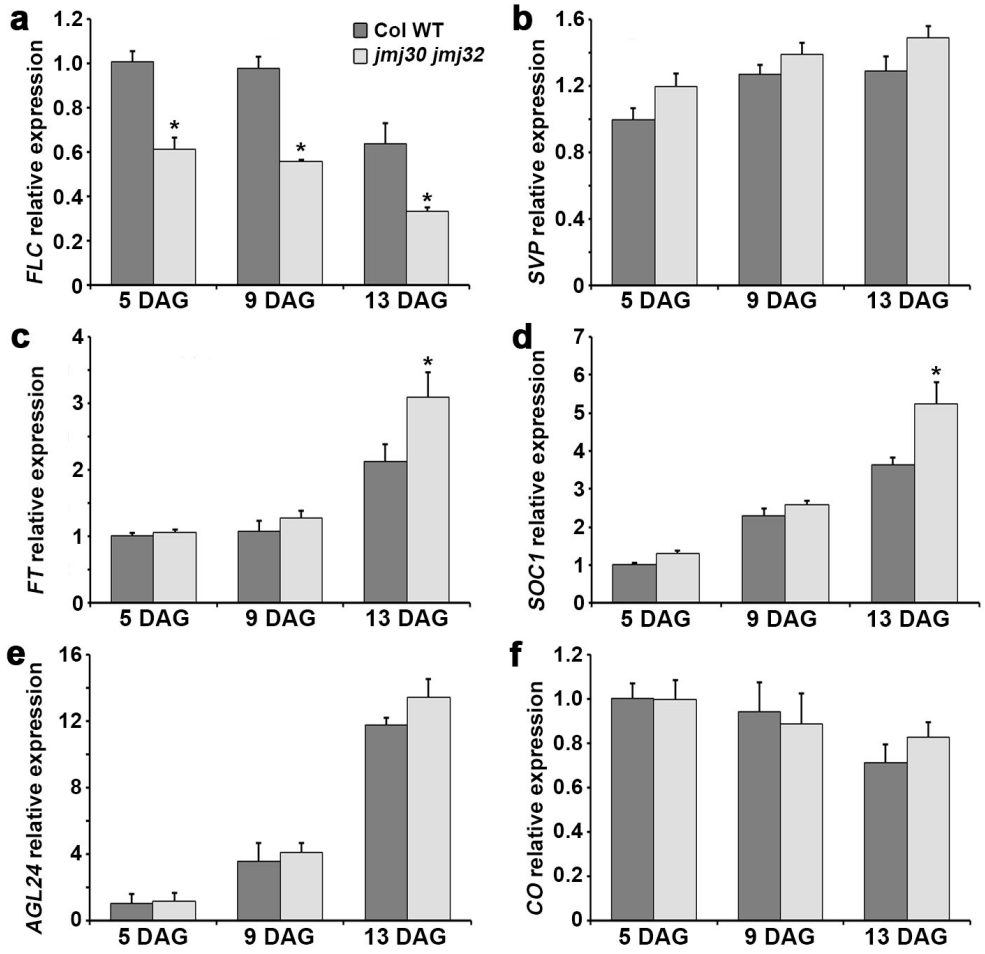

Figure 11. Expression profiles of flowering time genes.

RT-qPCR-based expression profiles of (**a**) *FLC*, (**b**) *SVP*, (**c**) *FT*, (**d**) *SOC1*, (**e**) *AGL24*, and (**f**) *CO* in 5, 9 and 13 DAG seedlings of WT and *jmj30-2 jmj32-1* grown under LD 29°C conditions. Relative fold changes to WT 5 DAG seedlings are presented. Bars indicate s.d. of three biological replicates; two-tailed Student's *t*-test, *P<0.05.

3.4 JMJ30, JMJ31 and JMJ32 are ubiquitously expressed in the nucleus

To reveal the function of JMJ30, JMJ31 and JMJ32, I characterized their spatial expression patterns. Transcript profiling data deposited at the *Arabidopsis* eFP Browser suggest that *JMJ30*, *JMJ31* and *JMJ32* are rather ubiquitously expressed at the rosette leaves, shoot apex and developing flowers (Figure 12a-c)(Winter et al, 2007). To confirm this, I extracted RNA from different tissues of WT plants, and through RT-PCR, I concluded that *JMJ30*, JMJ31 and *JMJ32* were expressed in all tested tissue types, namely, seedlings, roots, rosette leaves, cauline leaves, stems and inflorescences (Figure 13)(Lu et al, 2008). *JMJ30* was highly expressed in leaves, whereas *JMJ31* and *JMJ32* expression showed no appreciable difference across the various tissue types.

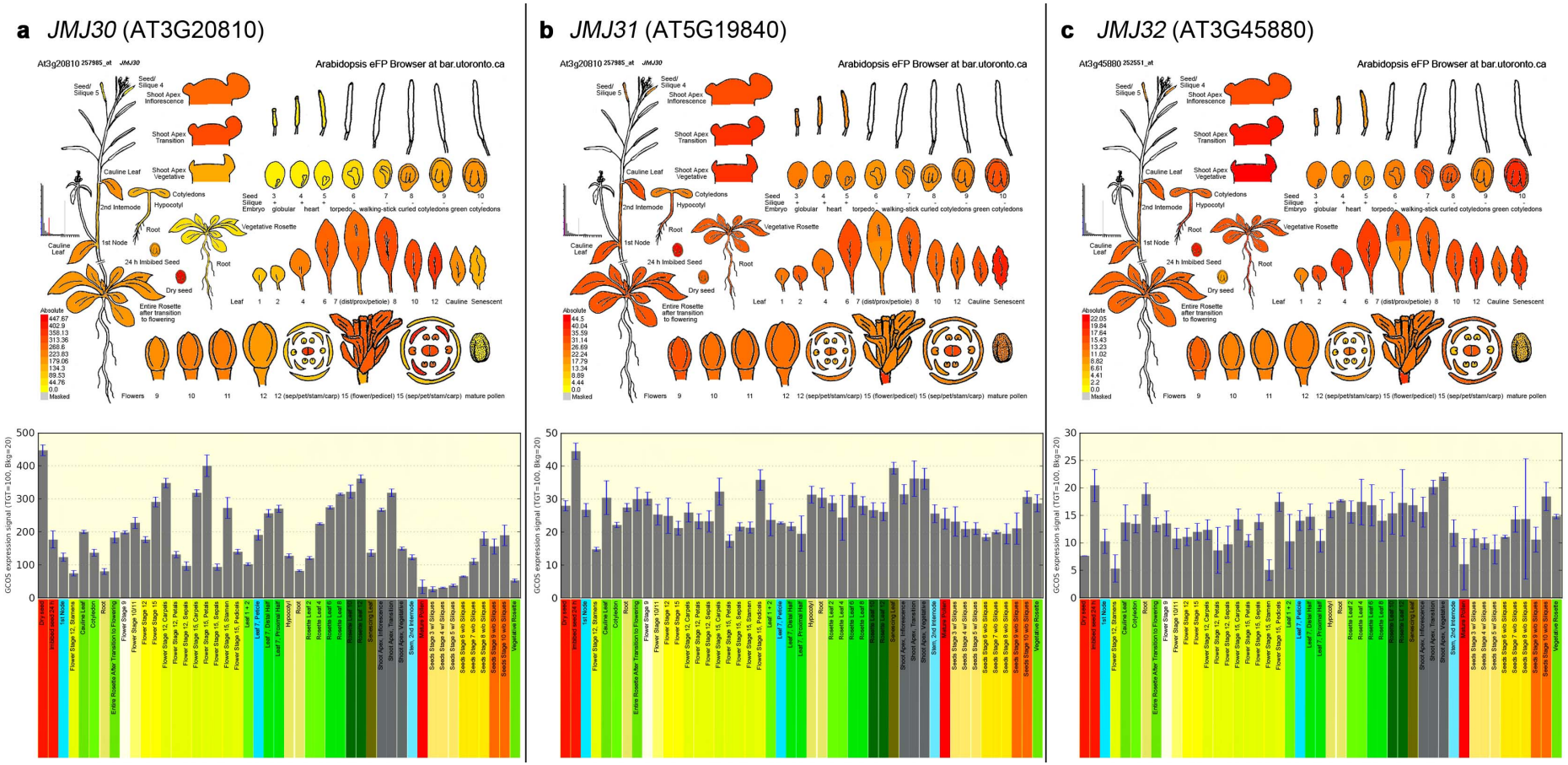

Figure 12. eFP browser view of *JMJ30*, *JMJ31* and *JMJ32* gene expression during *Arabidopsis* development.
The expression pattern analysis of (**a**) *JMJ30*, (**b**) *JMJ31*, and (**c**) *JMJ32* was performed using the *Arabidopsis* eFP browser (http://bar.utoronto.ca/efp/cgi-bin/efpWeb.cgi)(Winter et al, 2007). Data are normalized by the GCOS method.

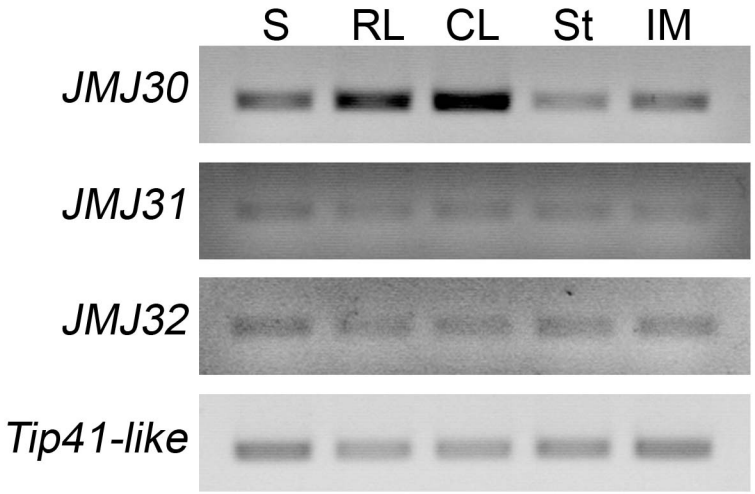

Figure 13. *JMJ30*, *JMJ31* and *JMJ32* mRNA are detected ubiquitously.

Semi quantitative RT-PCR showing spatial expression of JMJ30, JMJ31 and JMJ32 revealed that these *JMJ* genes are ubiquitously expressed. 25 cycles was used to amplify the product. *Tip41-like* was use as internal reference genes (Czechowski et al, 2005). S, Seedling; RL, rosette leaf; CL, cauline leaf; St, stem; IM, inflorescence meristem.

Next, to better understand the spatial distribution of JMJ30, JMJ31 and JMJ32 at the protein level, constructs harboring their upstream promoter and downstream sequences plus the genomic coding sequence (6.1-kb *JMJ30*, 7.5-kb *JMJ31* and 5.3-kb *JMJ32*) fused with the GUS reporter gene were transformed into WT plants (Figure 14a). This genomic fragment of JMJ30, when fused with the short HA epitope tag, was sufficient to rescue the *jmj30 jmj32* early-flowering phenotype at 29 °C LD (Figure 15a,b), indicating that the fragment contains all the *cis*-elements necessary to capture the endogenous expression pattern. Histochemical GUS staining results showed that JMJ proteins were rather ubiquitously expressed, including in the leaves, roots, and inflorescences (Figure 14b). Furthermore, JMJ30 and JMJ32 expression in the vasculature of leaves overlapped with the expression patterns of their putative targets *FLC* (Bastow et al, 2004), *FT* (Yoo et al, 2005) and *SOC1* (Hepworth et al, 2002; Liu et al, 2008a), and FLC is known to directly repress *FT* and *SOC1* in the leaf veins (Searle et al, 2006).

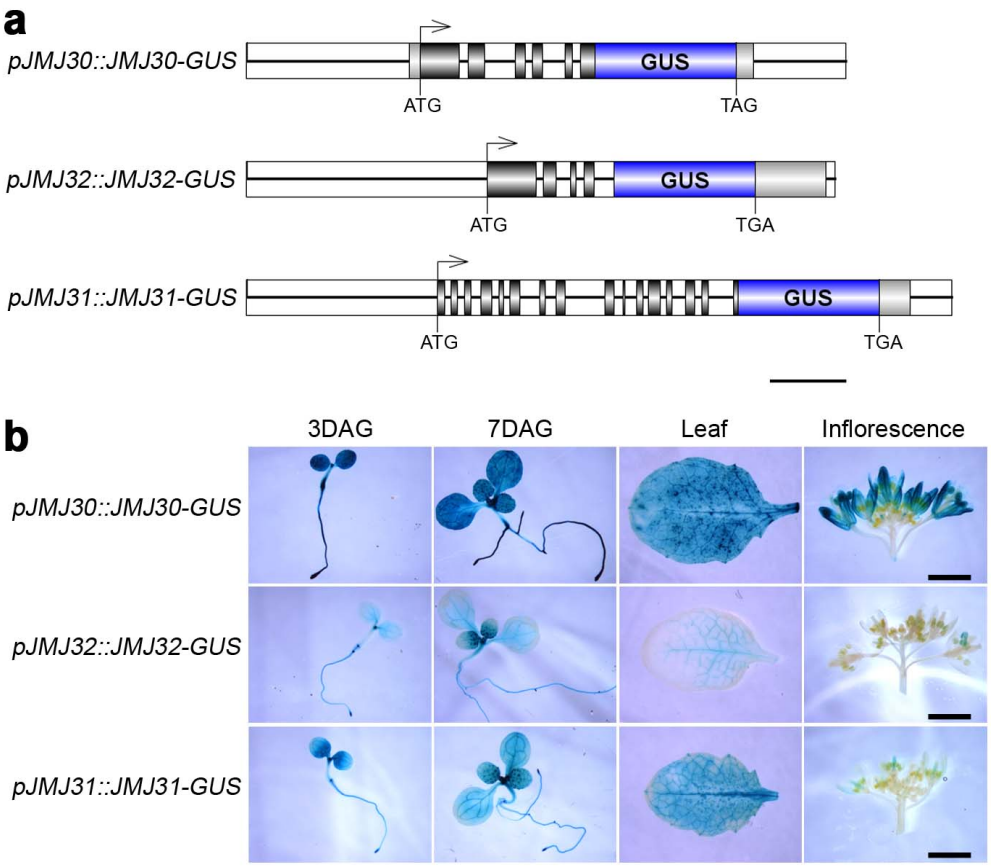

Figure 14. JMJ30, JMJ31 and JMJ32 are expressed ubiquitously across the plant.

(**a**) Schematic drawings of *pJMJ30::JMJ30-GUS*, *pJMJ32::JMJ32-GUS* and *pJMJ31::JMJ31-GUS*. Exons are represented by black boxes, and GUS is represented by blue boxes. Lines indicate promoter, introns and 3' downstream regions. Scale bar, 1 kb. (**b**) Histochemical GUS staining of *pJMJ30::JMJ30-GUS*, *pJMJ32::JMJ32-GUS* and *pJMJ31::JMJ31-GUS* transgenic lines. 3 and 7 DAG seedlings, rosette leaves and inflorescences were stained overnight. Scale bars, 2 mm.

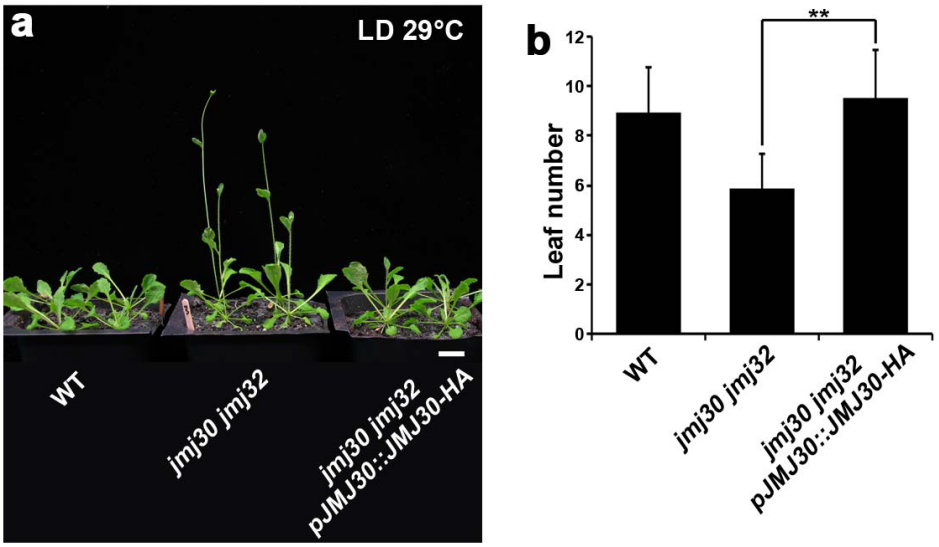

Figure 15. *pJMJ30::JMJ30-HA* complements the *jmj30 jmj32* mutations.

(**a**) Compared to WT, *jmj30 jmj32* showed accelerated flowering when grown under 29 °C LD conditions. However, introduction of an endogenous *pJMJ30* promoter driven JMJ30-HA construct rescued the early-flowering phenotype of *jmj30 jmj32* at 29°C LD. Representative 23-day-old plants were shown as comparison. Scale bar, 1 cm. (**b**) Total primary rosette leaves before bolting in WT, *jmj30 jmj32* and *jmj30 jmj32 pJMJ30::JMJ30-HA* plants grown under 29 °C LD conditions were counted (2 independent experiments with 15-20 plants each). Bars indicate s.d.; two-tailed Student's *t*-test, **P<0.01.

To study the sub-cellular localization of JMJ30, JMJ32, and JMJ31, I transiently over-expressed JMJ-VENUS in tobacco *Nicotiana benthamiana*. I observed that JMJ30, JMJ32, and JMJ31 localized not only to the nucleus but also occasionally to the endoplasmic reticulum and cytoplasm (Figure 16) as reported previously (Lu et al, 2011c), which could be artifacts from the over-expression of the JMJ proteins. I thus generated an endogenous *pJMJ30* promoter-driven JMJ30-HA in *jmj30-2,* which complements the early-flowering phenotype of *jmj30 jmj32* (Figure 15a,b), and performed an immunolocalization assay using anti-HA and anti-H3K27me3 antibodies on its protoplasts. I observed that JMJ30-HA localized primarily to the nucleus, consistent with its role as a histone demethylase, and its expression pattern resembled that of H3K27me3 (Figure 17a,b). Moreover, immunolocalization assay performed using the extracted nuclei from *jmj30-2 pJMJ30::JMJ30-HA* showed that JMJ30-HA localization to the euchromatin but not the DAPI-dense heterochromatic chromocenters, resembling reported localization of H3K27me3 (Lindroth et al, 2004; Mathieu et al, 2005a), and this localization was not affected by the ambient temperature (Figure 17c).

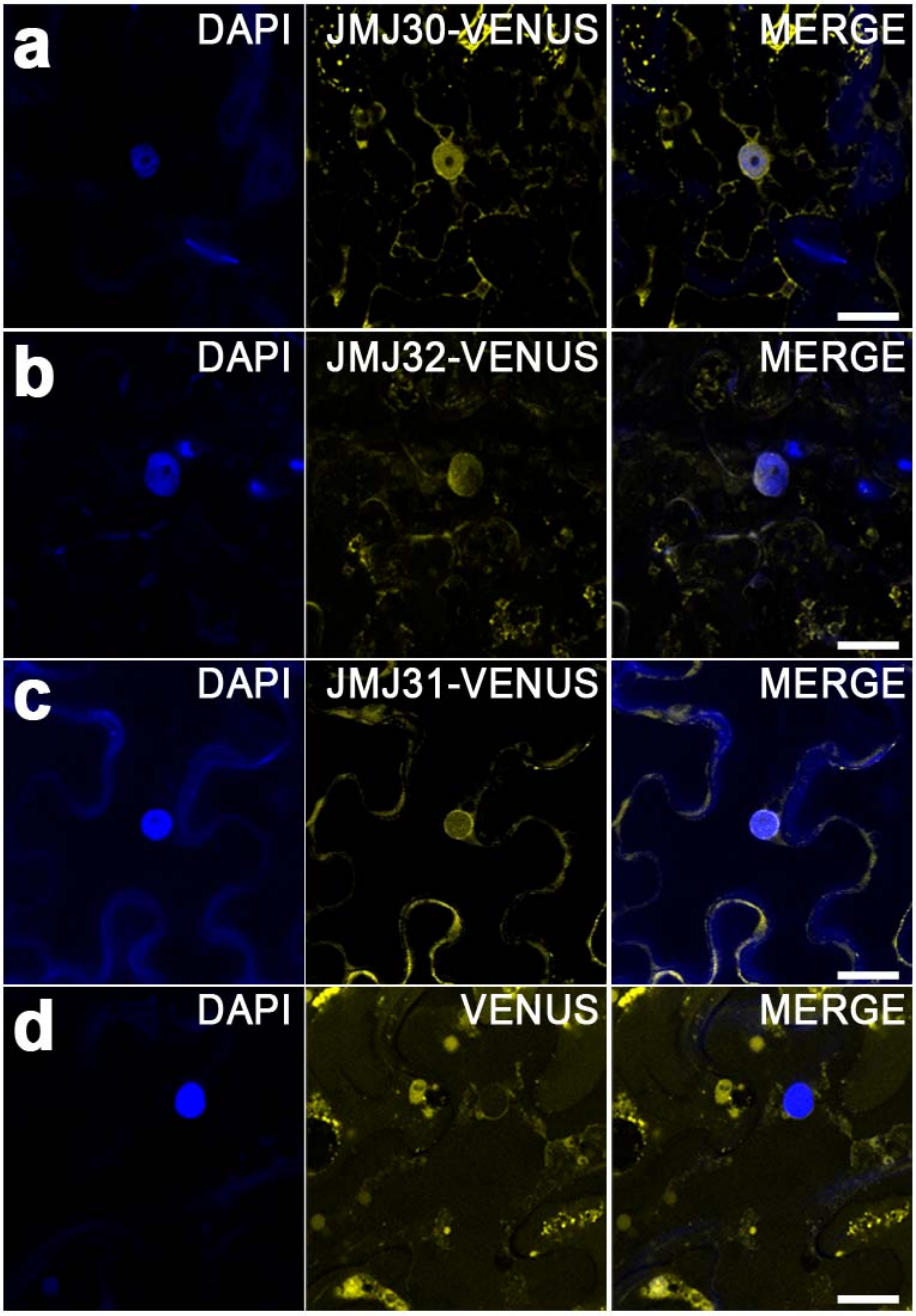

Figure 16. Over-expression of JMJ30, JMJ31, and JMJ32 protein localize to the nucleus in tobacco.

Transient over-expression of (**a**) JMJ30-VENUS, (**b**) JMJ32-VENUS, (**c**) JMJ31-VENUS, and (**d**) VENUS-only in tobacco leaves. JMJ30-, JMJ32-, and JMJ31-VENUS localized not only to the nucleus but also occasionally to the endoplasmic reticulum and cytoplasm. DAPI was used to visualize the chromatin. Scale bar, 25 μm.

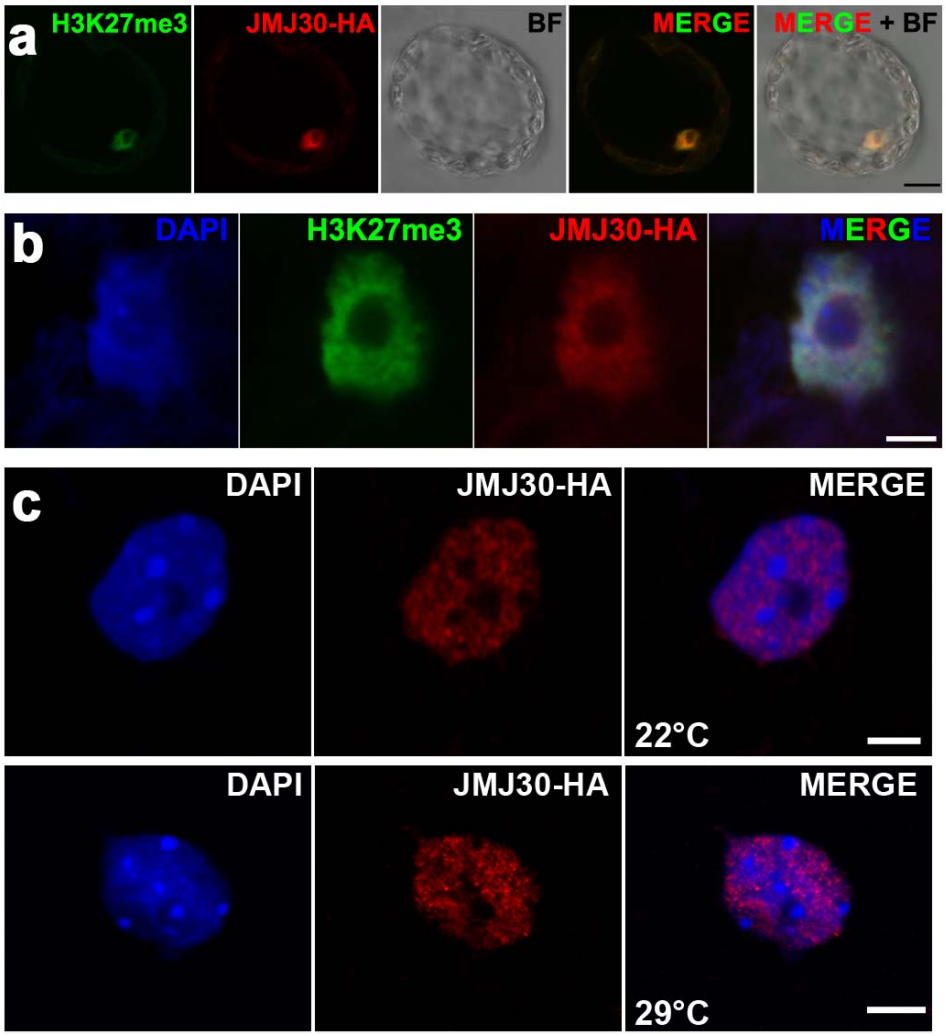

Figure 17. Endogenous *pJMJ30* promoter driven JMJ30 can localize to the nucleus.

(**a**,**b**) Immunolocalization of H3K27me3 and JMJ30-HA in protoplasts generated from *jmj30-2 pJMJ30::JMJ30-HA* transgenic lines. (**a**) JMJ30-HA localization resembles that of H3K27me3 in the nucleus. Scale bar, 10 µm. (**b**) Image shows enlarged view of a nucleus. Scale bar, 2.5 µm. (**c**) Immunolocalization of JMJ30-HA in nuclei extracted from the leaves of *jmj30-2 pJMJ30::JMJ30-HA* transgenic lines grown under LD 22°C and 29°C conditions. Anti-HA antibody and DAPI were used to visualize JMJ30-HA proteins and chromatin, respectively. Scale bar, 5 µm.

3.5 JMJ30 and JMJ32 specifically demethylate H3K27me2/3

Proteins that have the catalytic JmjC domain are known to be histone demethylases (Klose et al, 2006a), and JMJ30-HA localization which resembled the euchromatic histone marks inspired us to study the biochemical function of these histone demethylases. I first determined whether they could demethylate methylated histones *in vitro*. I transiently over-expressed *35S::JMJ30-HA* in tobacco leaves and immunoaffinity-purified the protein using anti-HA agarose beads. Using these purified proteins, an *in vitro* demethylase assay was carried out. I incubated calf thymus histones with JMJ30-HA proteins, together with reported JmjC cofactors Fe(II) ions and α-KG. Indeed, western blotting analyses indicated that JMJ30-HA was able to demethylate oligonucleosomes at H3K27me3 and H3K27me2 but not at H3K27me1 (Figure 18a). Similar *in vitro* demethylase assays were performed using purified JMJ32-HA and JMJ31-HA, however, no clear reduction of the hisone modifications was observed (data not shown).

To investigate the demethylase activity of JMJ30 further, I purified a mutated version of JMJ30-HA (JMJ30H326A-HA), in which one of its conserved Fe(II)-binding histidine residues in the JmjC domain was mutated to alanine. I found that the effect of JMJ30H326A-HA on H3K27me2/3 was completely abolished by the mutation (Figure 18b). To address their substrate specificity, I looked at their ability to demethylate other histone methylation marks. Consistent with the previously reported group-specific characteristics of JMJ proteins, I did not see noticeable demethylation activity for H3K4me2/3, H3K9me2/3 and H3K36me2/3 in the *in vitro* demethylase assay (Figure 18a).

The results indicate that JMJ30 can specifically demethylate H3K27me2/3 *in vitro* and that its activity is dependent on its JmjC domain.

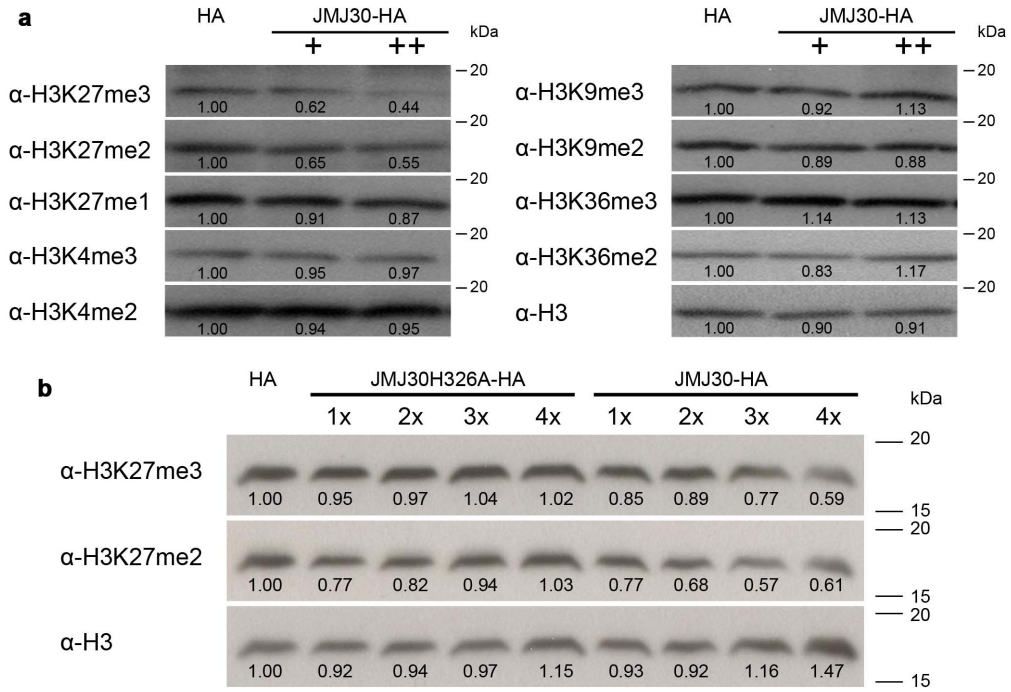

Figure 18. JMJ30 demethylates H3K27me2/3 *in vitro*.

(**a**) Immunoaffinity-purified JMJ30-HA was co-incubated with substrate calf thymus histone and cofactors Fe(II) ions and α-KG at 37°C for 4 hours. Immunoblot analysis of histone demethylase activity of JMJ30 was performed using antibodies indicated to the left. The anti-H3 antibody is used as loading control. (**b**) A mutated version of JMJ30-HA (JMJ30H326A-HA) was unable to demethylate H3K27me2/3 *in vitro* when a conserved Fe(II)-binding histidine residue in the JmjC domain was replaced by alanine. Numbers indicate relative band intensity compared to control reaction (HA) performed using an anti-HA precipitate from WT.

Next, to confirm whether JMJ30 and JMJ32 can exert this demethylase activity in plants, I transiently over-expressed *35S::JMJ30-HA* and *35S::JMJ32-HA*, and their respective mutated versions of *35S::JMJ30H326A-HA* and *35S::JMJ32H174A-HA* in *Arabidopsis* leaf protoplasts. Immunostaining assays were then conducted on the isolated nuclei using anti-H3K27me3 and anti-HA antibodies to observe their demethylase activity *in vivo*. I found that the over-expression of JMJ30-HA reduced H3K27me3 levels, however, over-expression of the mutated JMJ30H326A-HA has no effect on H3K27me3 methylation (Figure 19a,b). Similarly, the H3K27me3 levels were reduced in nuclei over-expressing JMJ32-HA but not in the mutated JMJ32H174A-HA expressing nuclei (Figure 19c,d). Taken together, these results indicate that JMJ30 and JMJ32 function as H3K27me3 demethylases *in vitro* and *in vivo*. Future work of substituting the α-KG-binding tyrosine residue of JMJ30 and JMJ32 with serine (JMJ30T323S and JMJ32T171S), as in JMJ31, might shed light on the effect of this substitution on the enzymatic activity of this group of JMJ proteins.

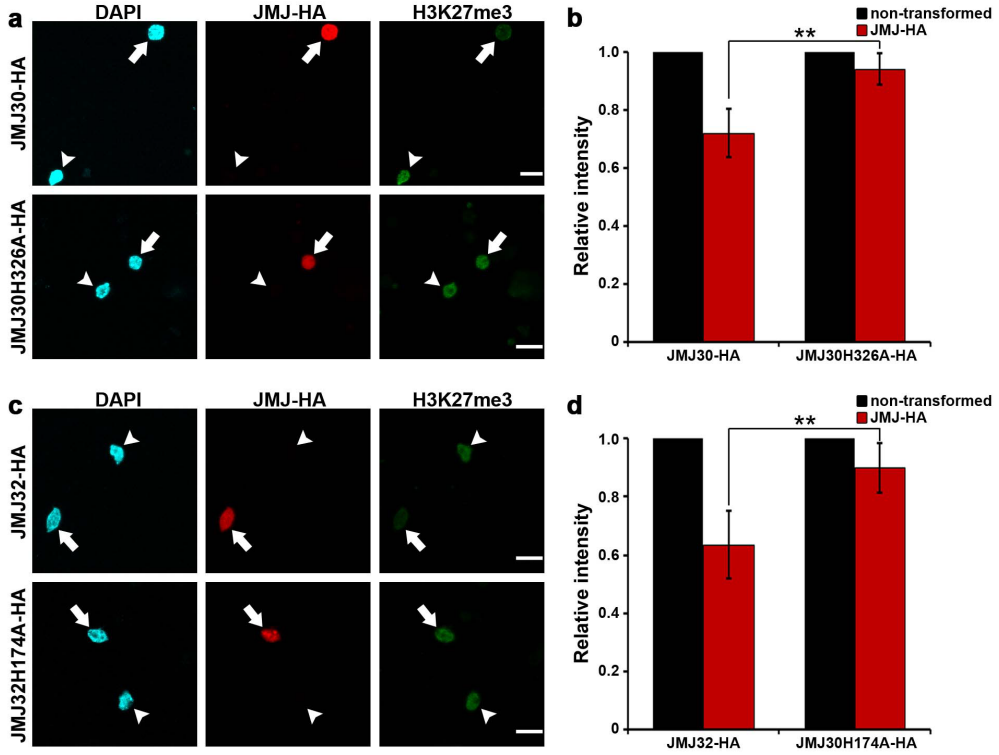

Figure 19. Over-expression of JMJ30 and JMJ32 caused decreased H3K27me3 levels.

Immunostaining of H3K27me3 and JMJ30-HA or JMJ32-HA in nuclei extracted from *Arabidopsis* leaf protoplasts transiently over-expressing (**a**) JMJ30-HA or (**c**) JMJ32-HA or their respective mutated version of JMJ30H326A-HA and JMJ32H174A-HA. Over-expression of JMJ30-HA and JMJ32-HA reduced H3K27me3 levels. However, mutations of the conserved Fe(II)-binding histidine residue in the JmjC domain of JMJ30H326A-HA and JMJ32H174A-HA showed no effect on H3K27me3 demethylation. Anti-HA antibodies, anti-H3K27me3 antibodies and DAPI were used to visualize JMJ30/32-HA proteins, H3K27me3 marks and chromatin, respectively. Arrows indicate transformed nuclei over-expressing the JMJ-HA proteins. Arrowheads indicate control non-transformed nuclei. Scale bar, 10 μm. (**b**,**d**) The intensities of at least 50 pairs of closely-located JMJ-HA-transformed and non-transformed nuclei were analyzed using ImageJ. Data were presented as a relative intensity of transformed/non-transformed nuclei. (**b**) Statistical analysis of **a**. (**d**) Statistical analysis of **c**. Bar indicates s.d.; two-tailed Student's *t*-test, **P<0.01.

3.6 *JMJ30* over-expression delays flowering by up-regulating *FLC*

To further elucidate the function of JMJ30, I over-expressed JMJ30-HA in WT plants and confirmed that *35S::JMJ30-HA* transgenic lines exhibit constitutive over-expression of JMJ30 and late flowering phenotypes at 22°C LD conditions (Figure 20a,b,c,d)(Lu et al, 2011c). To understand the effects of JMJ30 over-expression at a molecular level, I checked the expression profiles of the flowering time genes by qRT-PCR in two independent transgenic lines grown at 22°C under inductive LD conditions. Supporting the phenotypic observations, the floral repressor *FLC* is strongly increased in the *35S::JMJ30-HA* over-expression lines (Figure 21a). I also found that *FT* and *SOC1* are mildly down-regulated (Figure 21a). As *FLC* is the common repressor of the two floral integrators (Searle et al, 2006) and was most significantly affected, the increase in *FLC* expression is likely to be the main reason for the late-flowering phenotype.

Based on the results, I hypothesized that *FLC* is a target of JMJ30. To test whether *FLC* is genetically necessary for JMJ30 functions, I performed a genetic analysis by crossing *35S::JMJ30-HA* with *flc-3*. Introduction of the *flc* mutation largely abolished the late-flowering phenotype of *35S::JMJ30-HA*, and *35S::JMJ30-HA flc-3* flowered at a similar time as *flc-3* or WT plants (Figure 21b,c). Taken together, these results support the notion that *JMJ30* and *FLC* function in the same genetic pathway that regulates flowering time and that FLC functions downstream of the histone demethylase JMJ30.

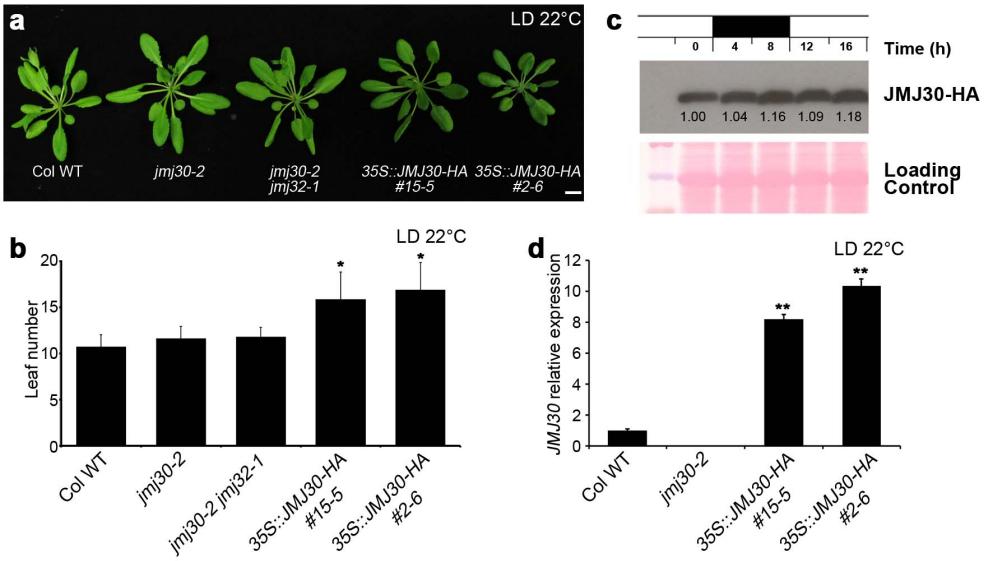

Figure 20. Over-expression of *JMJ30* produces a late-flowering phenotype.

(**a**) *35S::JMJ30-HA* transgenic plants showed a late-flowering phenotype when grown at LD 22°C. Representative 27-day-old plants were shown as comparison. Scale bar, 1 cm. Plants in the genotypes of WT, *jmj30-2, jmj30-2 jmj32-1, 35S::JMJ30-HA line #15-5 and 35S::JMJ30-HA line #2-6* were removed from the soils and aligned to take the photo. (**b**) Total primary rosette leaves before bolting in WT, *jmj30-2*, *jmj30-2 jmj32-1* and *35S::JMJ30-HA* plants grown under LD 22°C conditions were counted (2 independent experiments with 15-20 plants each). Bars indicate s.d.; two-tailed Student's *t*-test, *P<0.05. (**c**) Relative JMJ30-HA protein levels over 16 h examined by western blot using anti-HA-HRP antibody. Total proteins from *35S::JMJ30-HA* seedlings grown under 22°C LD conditions were used. Ponceau Red-stained membrane is shown as a loading control. Numbers indicate relative band intensity compared to 22°C 0h sample. Two biological replicates were performed and one set of the data is shown here. (**d**) Relative expression of *JMJ30* transcripts in WT, *jmj30-2*, and two independent lines of *35S::JMJ30-HA*, analyzed by qRT-PCR. Relative fold changes to WT are presented. Bars indicate s.d. of three biological replicates; two-tailed Student's *t*-test, **P<0.01.

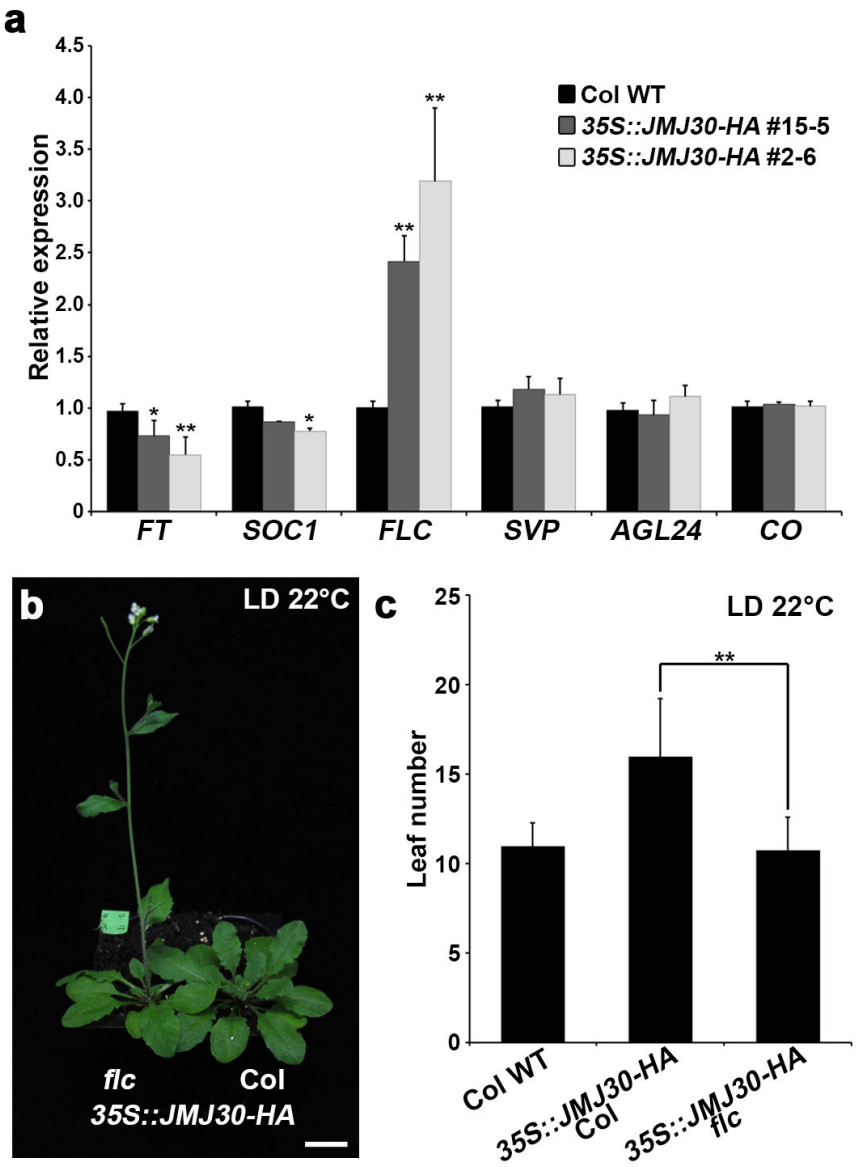

Figure 21. *FLC* is a target of the over-expression of *JMJ30*, which increased expression leads to a delayed flowering phenotype.

(**a**) mRNA expression levels of flowering time genes in WT and two independent lines of *35S::JMJ30-HA*, analyzed by qRT-PCR. Relative fold changes to WT are presented. Bars indicate s.d. of three biological replicates; two-tailed Student's *t*-test, *P<0.05, **P<0.01. (**b**) Introduction of *flc* mutation rescues the late-flowering phenotype of *35S::JMJ30-HA*. Scale bar, 1 cm. (**c**) Total primary rosette leaves before bolting in WT, *35S::JMJ30-HA* and *35S::JMJ30-HA flc* plants grown under LD 22°C conditions were counted (2 independent experiments with 20-50 plants each). Bars indicate s.d.; two-tailed Student's *t*-test, **P <0.01.

3.7 JMJ30 and JMJ32 regulate H3K27me3 at the *FLC* locus

My results suggested that JMJ30 functions as an H3K27me2/3 demethylase *in vitro* (Figure 18a,b) and *in vivo* (Figure 19a,b), and that *FLC* may be a direct target of JMJ30 (Figure 11a, Figure 21a-c). I was interested in verifying whether the increased *FLC* expression in *JMJ30* over-expression lines is similarly reflected in the H3K27 methylation status of the *FLC* locus. ChIP assays were carried out comparing the H3K27me3 levels between WT and the *35S::JMJ30-HA* plants (Figure 22a), and I found that the repressive H3K27me3 levels were decreased at the *FLC* locus in the *35S::JMJ30-HA* lines (Figure 22b), which is consistent with the increased *FLC* expression levels (Figure 21a).

I next measured H3K27me3 enrichment at the *FLC* locus in *jmj30 jmj32* and WT grown under 29°C LD conditions, in which the *jmj30 jmj32* double mutant showed decreased *FLC* expression and accelerated flowering (Figure 9a,b, Figure 11a). Consistent with its expression, I found that the H3K27me3 levels at the *FLC* locus are increased in *jmj30 jmj32* at 29°C (Figure 22c). Taken together, these results indicate that JMJ30 and JMJ32 demethylate H3K27me3 at the *FLC* locus to activate *FLC* expression at elevated temperatures.

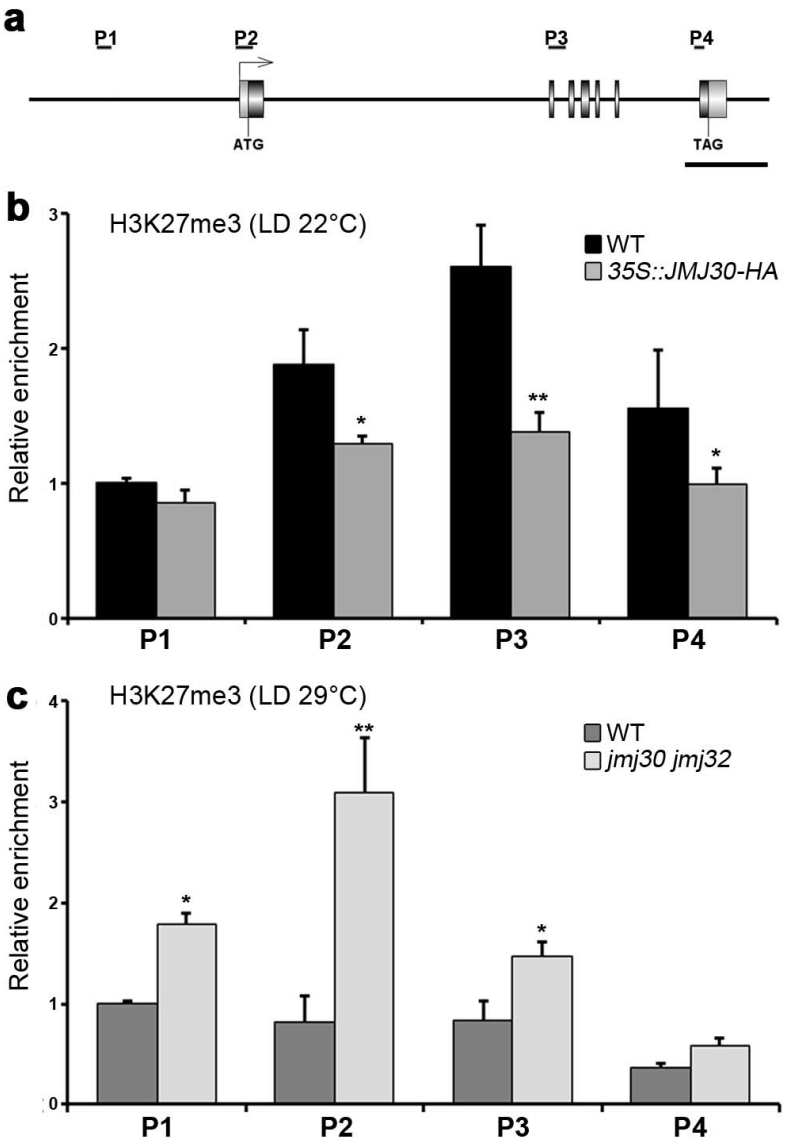

Figure 22. The repressive H3K27me3 on the *FLC* locus is affected by JMJ30 and JMJ32.

(**a**) Schematic drawing of the *FLC* genome structure showing regions amplified by primers used for ChIP analysis. Scale bar, 1 kb. (**b**,**c**) ChIP analysis of H3K27me3 enrichment on the *FLC* locus in (**b**) 8 DAG WT and *35S::JMJ30-HA* seedlings grown under LD 22°C conditions and (**c**) 8 DAG WT and *jmj30 jmj32* seedlings grown under LD 29°C conditions. An anti-H3 antibody was used as a control. Bar indicates s.e.m. of three biological replicates; two-tailed Student's *t*-test, *P<0.05, **P<0.01.

3.8 Prolonged JMJ30 activity directly regulates *FLC* expression

The ability of JMJ30 to affect the H3K27me3 level on *FLC* chromatin leads us to speculate that JMJ30 may directly bind to the *FLC* locus and demethylate the repressive mark. ChIP assays were conducted using the over-expression *35S::JMJ30-HA* transgenic line grown under LD 22°C conditions and the endogenous promoter-driven *pJMJ30::JMJ30-HA jmj30-2* line grown under LD 29°C conditions (Figure 23a). I immunoprecipitated the epitope-tagged JMJ30-HA protein using anti-HA agarose to assess the level of JMJ30-HA binding across the *FLC* chromatin region. Compared with WT plants, I found that JMJ30-HA associates with *FLC* chromatin directly in both lines, with the P2 region near the transcriptional start site showing the highest levels of binding enrichment (Figure 23b,c).

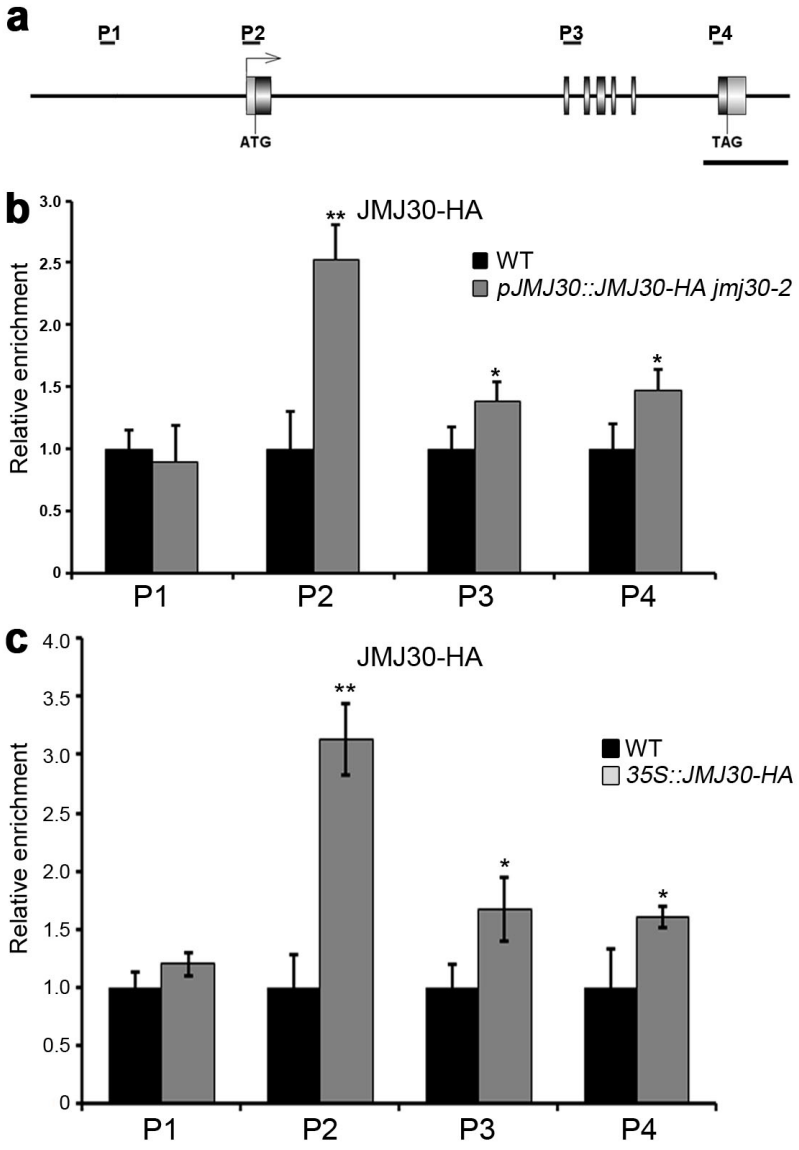

Figure 23. JMJ30 binds the *FLC* locus directly.

(**a**) Schematic drawing of the *FLC* genome structure showing regions amplified by primers used for ChIP analysis. Scale bar, 1 kb. (**b**,**c**) ChIP analysis of JMJ30-HA enrichment at the *FLC* locus in (**b**) 8 DAG WT and *jmj30-2 pJMJ30::JMJ30-HA* seedlings grown under 29°C conditions, and (**c**) 8 DAG *35S::JMJ30-HA* seedlings grown under LD 22°C conditions. JMJ30-HA directly binds near the transcriptional start site of the *FLC* locus. A mouse IgG was used as control. Bar indicates s.e.m. of three biological replicates; two-tailed Student's *t*-test, *P<0.05, **P<0.01.

To further elucidate the mechanism underlying the positive regulation of *FLC* expression at elevated temperatures by JMJ30, I was interested in *JMJ30* mRNA and protein expression and stability at 22°C and 29°C. *JMJ30* mRNA diurnal expression has been previously reported (Jones et al, 2010; Lu et al, 2011c). Taking samples from WT seedlings grown at 22°C and 29°C under LD condition every 4 hours, I found that *JMJ30* expression peaked approximately 4 hours before dark for both conditions, and the peak levels in the *JMJ30* diurnal expression were not significantly affected by the temperature. However, I found that the width of the peak broadened under the 29°C conditions (Figure 24a), which could be due to prolonged expression or increased mRNA stability.

To test if the protein expression of JMJ30 is similarly affected, I did a western blot with total proteins extracted from *jmj30-2 pJMJ30::JMJ30-HA* using an anti-HA-HRP antibody. Under standard growth conditions (22°C LD), the peak of the JMJ30-HA protein accumulation at the beginning of dark was slightly delayed compared to its mRNA expression, and JMJ30-HA was degraded quickly after that (Figure 24b). At 29°C, not only was the JMJ30-HA protein accumulation lengthened, it was also more stable as it persisted much longer than expected based on mRNA expression (Figure 24a,b). To confirm this, I performed a protein stability assay by pre-treating the seedlings with cycloheximide to prevent *de novo* protein synthesis, and adding the proteasome inhibitor MG132 at the end of the light photoperiod. I collected the samples at different time points and found that the rapid degradation of JMJ30-HA degradation at 22°C was inhibited by the addition of the proteasome inhibitor MG132 (Figure 25a), suggesting that the proteasome-

dependent JMJ30-HA degradation is impaired at higher temperatures (Figure 25b). These results suggested that the strongly-prolonged JMJ30 expression at elevated temperatures may allow JMJ30 to bind and demethylate H3K27me3 at the *FLC* locus, thus maintaining a transcriptionally permissive chromatin status.

In order to identify the potential interacting proteins that caused the differences in JMJ30 protein stability, I collected samples from *pJMJ30::JMJ30-HA jmj30-2* plants grown at 22°C and 29°C. I prepared nuclear extracts from the plant samples and immunoprecipitated the JMJ30-HA protein and their interacting partners using anti-HA beads. After washing and purification, the samples were casted into a tube gel, and sent for mass spectrometry analysis. I identified putative F-box protein (AT4G10190) as potential mediator of JMJ30 stability, as this interaction was only found in the samples from 22°C grown plants (Table 7). The dissociation of JMJ30 from this F-box protein may attenuate the Skp-Cullin-F-box (SCF) complex-mediated degradation pathway. However, I also found a putative E3 ubiquitin-protein ligase XBAT35 (AT3G23280) that binds JMJ30 at 29°C (Table 7). Thus, various elements may be used to degrade JMJ30 at different temperature. Interestingly, one component of the PRC1 complex RING1B (AT1G03770) also interacts with JMJ30 in both temperatures (Table 7). The biological meaning of this interaction is unknown, but it suggests crosstalks between PRC1 and PRC2 complexes. These interactions between JMJ30 and other proteins remain to be validated via yeast-2-hybrid or co-immunoprecipitation.

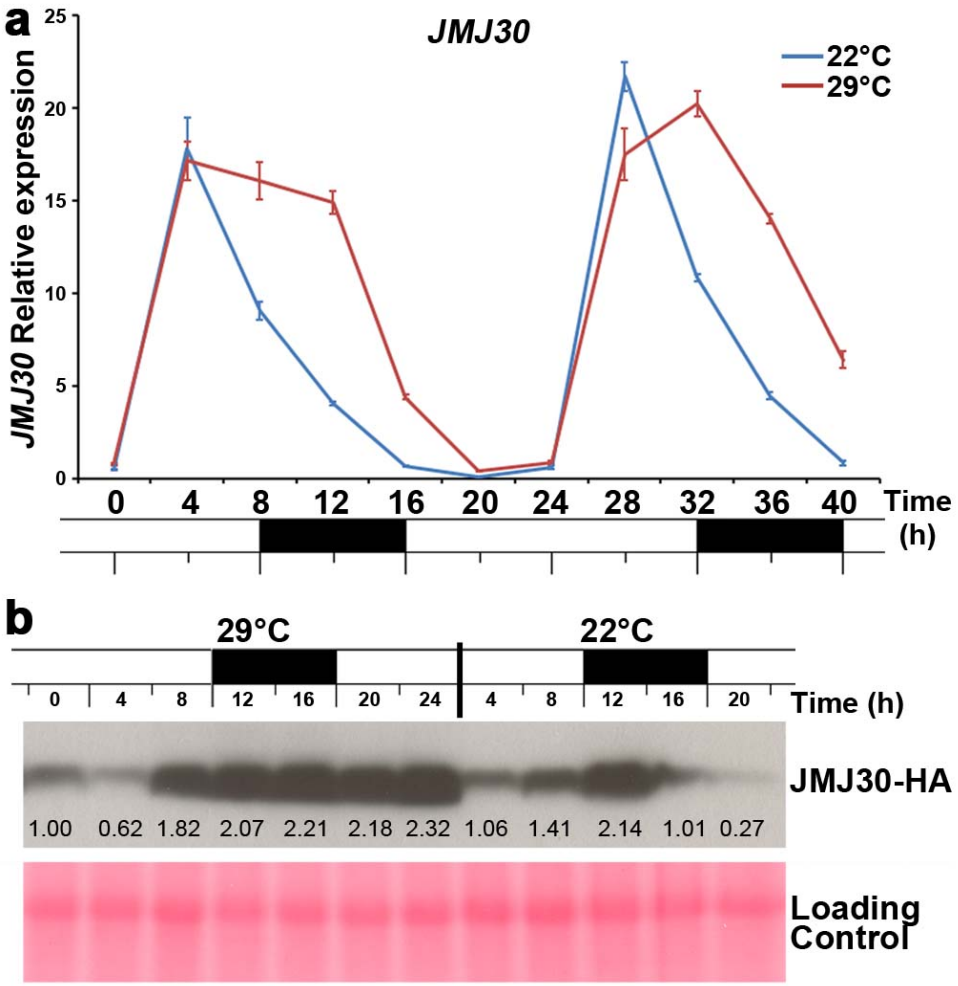

Figure 24. JMJ30 activity is prolonged JMJ30 activity under elevated temperature

(**a**) *JMJ30* mRNA levels in WT seedlings grown under LD 22°C and 29°C conditions, analyzed by qRT-PCR over 40 hours (h). Relative fold changes to 0 h are presented. Bars indicate s.d. of three biological replicates. (**b**) Relative JMJ30-HA protein levels over 24 h examined by western blot using anti-HA-HRP antibody. Total proteins from *jmj30-2 pJMJ30::JMJ30-HA* seedlings grown under LD 22°C and 29°C conditions were used. Ponceau Red-stained membrane is shown as a loading control. Numbers indicate relative band intensity compared to 29°C 0h sample.

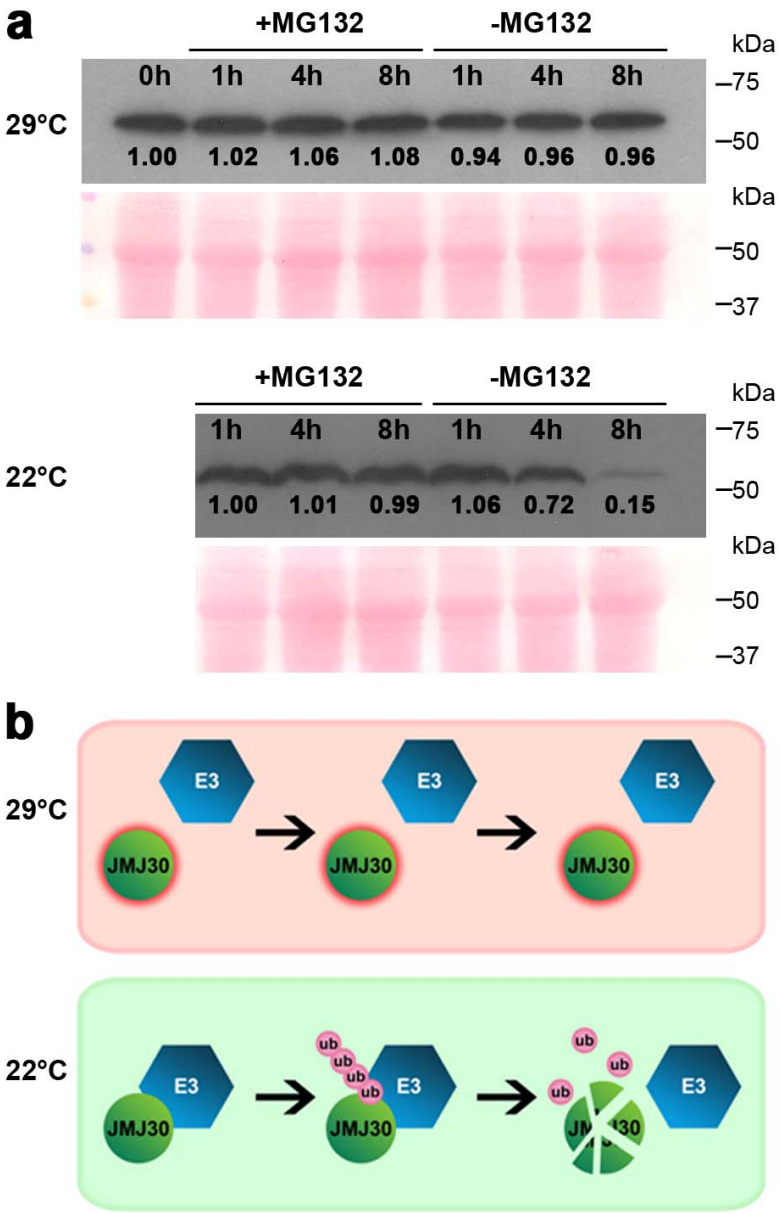

Figure 25. Temperature-dependent stabilization of JMJ30-HA protein.

(**a**) The *jmj30-2 pJMJ30::JMJ30-HA* plants grown at LD 22°C were pre-treated for 30 min with the protein synthesis inhibitor cycloheximide (CHX). After adding the proteasome inhibitor MG132 (+MG132) or DMSO (-MG132) at 0 hours (h) (right before the beginning of dark photoperiod), the plants were transferred to 22°C or 29 °C. Samples were harvested at 1h, 4h, and 8h. JMJ30-HA protein levels were examined by western blot using anti-HA-HRP antibody. Ponceau Red-stained membrane is shown as a loading control. Numbers indicate relative band intensity compared to 29°C 0h or 22°C 1h sample. (**b**) Model of temperature dependent JMJ30 protein stability. At 22°C, JMJ30 may be targeted by E3 ubiquitin ligase, and removed via the 26S proteasome degradation pathway. At 29°C, JMJ30 is shielded from E3 ubiquitin ligase by unknown mechanism and is hence stabilized.

Table 7. Proteins that potentially interact with JMJ30 at 22°C or 29 °C.

Interacting proteins were identified via immunoprecipitation using *jmj30-2 pJMJ30::JMJ30-HA* followed by mass spectrometry. Proteins of interest are highlighted in grey.

Protein ID	AtG number	Protein Name	Name
Immunoprecipitated from *pJMJ30::JMJ30-HA jmj32-2* plants grown in LD 22°C condition			
O04310|JAL34	AT3G16460	Jacalin-related lectin 34	JAL34
P25857|G3PB	AT1G42970	Glyceraldehyde-3-phosphate dehydrogenase GAPB, chloroplastic	GAPB
Q8W4H7|EF1A2	AT1G07930	Elongation factor 1-alpha 2	A2
Q9FMG4|SC35	AT5G64200	Serine/arginine-rich splicing factor SC35	SC35
O65543|PP343	AT4G31070	Pentatricopeptide repeat-containing protein, mitochondrial	PCMP-E7
O82622|FB227	AT4G10190	Putative F-box protein At4g10190	At4g10190
Q8RWG1|Y4139	AT4G31390	Uncharacterized aarF domain-containing protein kinase, chloroplastic	At4g31390
Q8L7W5|SMO11	AT4G12110	Methylsterol monooxygenase 1-1	SMO1-1
Q0WX00|RNG1B	AT1G03770	Putative E3 ubiquitin-protein ligase RING1b	RING1B
Q9C578|RCL1	AT5G22100	Probable RNA 3'-terminal phosphate cyclase-like protein	At5g22100
Immunoprecipitated from *pJMJ30::JMJ30-HA jmj32-2* plants grown in LD 29°C condition			
Q9SI75|EFGC	AT1G62750	Elongation factor G, chloroplastic	CPEFG
O04310|JAL34	AT3G16460	Jacalin-related lectin 34	JAL34
Q9FMG4|SC35	AT5G64200	Serine/arginine-rich splicing factor SC35	SC35
Q8W4H7|EF1A2	AT1G07930	Elongation factor 1-alpha 2	A2
Q0WX00|RNG1B	AT1G03770	Putative E3 ubiquitin-protein ligase RING1b	RING1B
Q9FT72|RQL3	AT4G35740	ATP-dependent DNA helicase Q-like 3	RECQL3
Q940A2|P2C31	AT2G40860	Protein kinase and PP2C-like domain-containing protein	At2g40860
O81024|EKI	AT2G26830	Probable ethanolamine kinase	EMB1187
Q7G8V2|ARR15	AT1G74890	Two-component response regulator ARR15	ARR15
F4JUF8|DIR15	AT4G38700	Dirigent protein 15	DIR15
Q84JX1|PME19	AT1G11590	Probable pectinesterase/pectinesterase inhibitor 19	PME19
Q4FE47|XB35	AT3G23280	Putative E3 ubiquitin-protein ligase XBAT35	XBAT35

3.9 JMJ30-regulated genes are enriched for H3K27me3 targets

To investigate whether *JMJ30* over-expression and *jmj30 jmj32* loss-of-function mutants influence gene transcription at a global level, I performed expression profiling using NimbleGen 12 x 135K arrays. Compared with WT, 469 genes were down-regulated and 657 genes were up-regulated in *jmj30 jmj32* under 29°C LD conditions (Supplementary Data 1, NCBI Gene Expression Omnibus GSE51898). On the other hand, 516 genes were up-regulated and 588 genes were down-regulated in *35S::JMJ30-HA* compared with WT (Supplementary Data 2). The transcriptome analyses suggested that despite only showing flowering phenotypes, the loss-of-function and over-expression of *JMJ30* did affect global expression profiles.

Previous studies identified that at least 25% (27.70% of genes analyzed in our microarray) of the *Arabidopsis* genome is targeted by H3K27me3 (Lafos et al, 2011; Zhang et al, 2007), and my study showed that JMJ30 and JMJ32 are H3K27me3 demethylases. I found that 193 of the 469 (41.15%) total down-regulated genes in *jmj30 jmj32* and 213 of the 516 (41.28%) genes up-regulated in *35S::JMJ30-HA* overlapped with reported H3K27me3-regulated genes (Figure 26a, Supplementary Data 1 and 2)(Lafos et al, 2011; Zhang et al, 2007). Moreover, the genes down-regulated in *jmj30 jmj32* showed enrichment for PcG targets (41.15%, Fisher's exact test, P-value = 3.499×10^{-10}) compared to the up-regulated genes (201 out of 657, 30.59%, Fisher's exact test, P-value = 0.0565). Comparing the gene expression profile of *jmj30 jmj32* mutant (Supplementary Data 1) with another epigenomic profiling of H3K4me2, H3K4me3, H3K27me3 and H3K36me3 (Roudier et al, 2011), I

found that genes down-regulated in *jmj30 jmj32* not only showed enrichment with H3K27me3 targets, but also depletion of H3K4me2-, H3K4me3-, and H3K36me3-regulated genes (Figure 26c,d, Table 8).

Gene ontology analysis of the H3K27me3 targets affected by JMJ30/JMJ32 (shaded in Figure 26a) revealed that, in terms of molecular function, genes involved in transcription factor activity (Fisher's exact test, P-value = 8.899 x 10^{-3}) were more enriched, and there were slight enrichment in transcription, DNA-dependent genes in terms of biological process (Fisher's exact test, P-value = 6.074 x 10^{-2})(Figure 26b). The 40% correlation between reported H3K27me3 targets and our transcriptome profiling suggested that JMJ30/JMJ32-mediated gene regulation positively influences gene expression by demethylating the repressive H3K27me3, thereby contributing to gene de-repression.

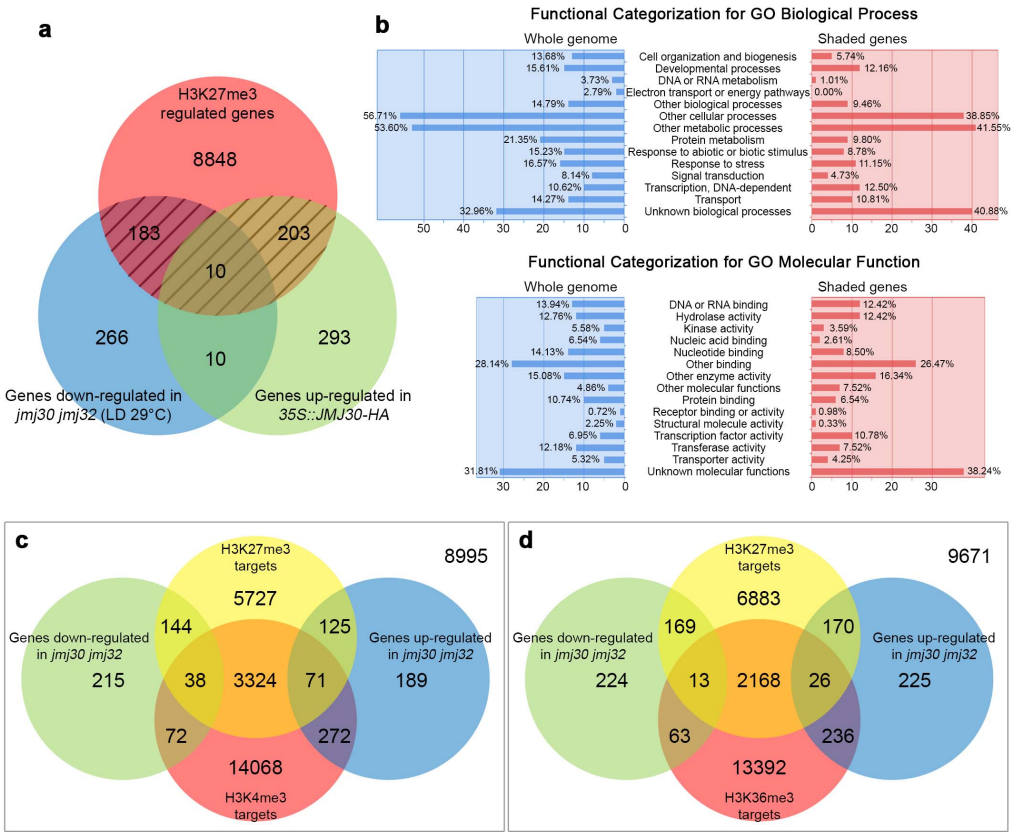

Figure 26. Hundreds of genes are regulated by *JMJ30/JMJ32*.

(**a**) Diagram showing overlap of genes down-regulated in *jmj30 jmj32* grown under LD 29°C conditions, genes up-regulated in *35S::JMJ30-HA* and reported H3K27me3-regulated genes (Lafos et al, 2011; Zhang et al, 2007). Genes showing a 1.5-fold change within a 90% confidence interval were considered to be differentially expressed. (**b**) Functional categorization for Gene Ontology of genes shaded in (**a**). (**c**) Venn diagram showing overlap of genes affected in *jmj30 jmj32* and reported H3K27me3- and H3K4me3-regulated genes (Roudier et al, 2011). (**d**) Venn diagram showing overlap of genes affected in *jmj30 jmj32* and reported H3K27me3- and H3K36me3-regulated genes (Roudier et al, 2011)

Table 8. Enrichment of H3K4me2-, H3K4me3-, H3K27me3-, and H3K36me3-targets in genes affected in the *jmj30 jmj32* mutant.

Gene enrichment and depletion was tested with Fisher's exact test using R. Statistically significant (P<0.01) enrichment were highlighted in green, whereas depletion were highlighted in red. Epigenomic profiles were taken from (Roudier et al, 2011).

	Whole genome	**Down-regulated in *jmj30 jmj32***	**Up-regulated in *jmj30 jmj32***
H3K4me2 target	23212	224	473
Non-H3K4me2 target	10028	245	184
Total	33240	469	657
Percentage	69.83%	47.76%	71.99%
***P*-value (enrichment)**		1.000	0.119
***P*-value (depletion)**		2.20×10^{-16}	0.897

	Whole genome	**Down-regulated in *jmj30 jmj32***	**Up-regulated in *jmj30 jmj32***
H3K4me3 target	17845	110	343
Non-H3K4me3 target	15395	359	314
Total	33240	469	657
Percentage	53.69%	23.45%	52.21%
***P*-value (enrichment)**		1.000	0.790
***P*-value (depletion)**		2.20×10^{-16}	0.233

	Whole genome	**Down-regulated in *jmj30 jmj32***	**Up-regulated in *jmj30 jmj32***
H3K27me3 target	9429	182	196
Non-H3K27me3 target	23811	287	461
Total	33240	469	657
Percentage	28.37%	38.81%	29.83%
***P*-value (enrichment)**		5.94×10^{-7}	0.212
***P*-value (depletion)**		1.000	0.813

	Whole genome	**Down-regulated in *jmj30 jmj32***	**Up-regulated in *jmj30 jmj32***
H3K36me3 target	15898	76	262
Non-H3K36me3 target	17342	393	395
Total	33240	469	657
Percentage	47.83%	16.20%	39.88%
***P*-value (enrichment)**		1.000	1.000
***P*-value (depletion)**		2.20×10^{-16}	2.09×10^{-5}

3.10 Genetic relationship between *JMJ30*/*JMJ32* and *CLF* and *REF6*

Upon uncovering that JMJ30 and JMJ32 may function as H3K27me3 demethylases, I was interested in understanding their genetic relationship with the H3K27me3 HMTases. In *Arabidopsis*, CLF function as the main H3K27me3 HMTase regulating a range of developmental processes (Thorstensen et al, 2011). Since the HMTase and histone demethylase function antagonistically in regulating the dynamism of H3K27me3 deposition, I wondered whether the loss-of-function of the demethylases could rescue the phenotype of the mutant of the H3K27me3 HMTase. I thus crossed *jmj30-2 jmj32-1* mutant into the *clf-28* mutant to observe the phenotype. The *clf jmj30 jmj32* was phenotypically similar to *clf* single mutant in terms of leaf curling (Figure 27a) and flowering time (Figure 27b,c), suggesting that *clf* might be epistatic to *jmj30 jmj32*. Unlike *clf ref6*, *clf jmj30 jmj32* showed no rescue of leaf curling, suggesting that *REF6* and *JMJ30*/*JMJ32* may target different sets of genes during development (Lu et al, 2011a).

Since REF6 is also reported to be an H3K27me3 demethylase, I was interested in knowing if the mutations of all known H3K27me3 demethylases will produce any phenotype (Lu et al, 2011a), as loss-of-function of the H3K27me3 demethylase in animal produces severe phenotypes (Agger et al, 2007; Burgold et al, 2012; Lan et al, 2007; Vandamme et al, 2012). (Note: ELF6 function as an H3K27me3 demethylase was not reported yet at the time of study (Crevillen et al, 2014).) I generated the double and triple mutant of *jmj30-2 jmj32-1* with *ref6-1*. The loss of function of *ref6* causes a late-flowering phenotype and up-regulation of the floral repressor *FLC* (Ko et al,

2010; Lu et al, 2011a). I found that *jmj30* was able to slightly rescue this late flowering phenotype in *ref6 jmj30*, and the rescue is more obvious in *ref6 jmj30 jmj32* (Figure 28a,b). I next look at expression of *FLC* and its downstream target *FT* in the mutants of H3K27me3 demethylases. The difference in *FLC* expression corresponds with the phenotype as I see an up-regulation of *FLC* in *ref6* compared to WT, and this increase in *FLC* is slightly rescued in *ref6 jmj30* and *ref6 jmj30 jmj32* (Figure 28c). The exact opposite was observed for *FT* expression: *FT* was decreased in *ref6*, and mutants of *ref6 jmj30* and *ref6 jmj30 jmj32* increased *FT* expression, thus promoting its flowering (Figure 28d). It is of note that, unlike the null mutation of H3K27me3 demethylase in metazoan, the *ref6-1 jmj30-2 jmj32-1* triple mutant showed no severe developmental defects other than its late-flowering phenotype, suggesting the existence of other H3K27me3 demethylase (Figure 28a,b).

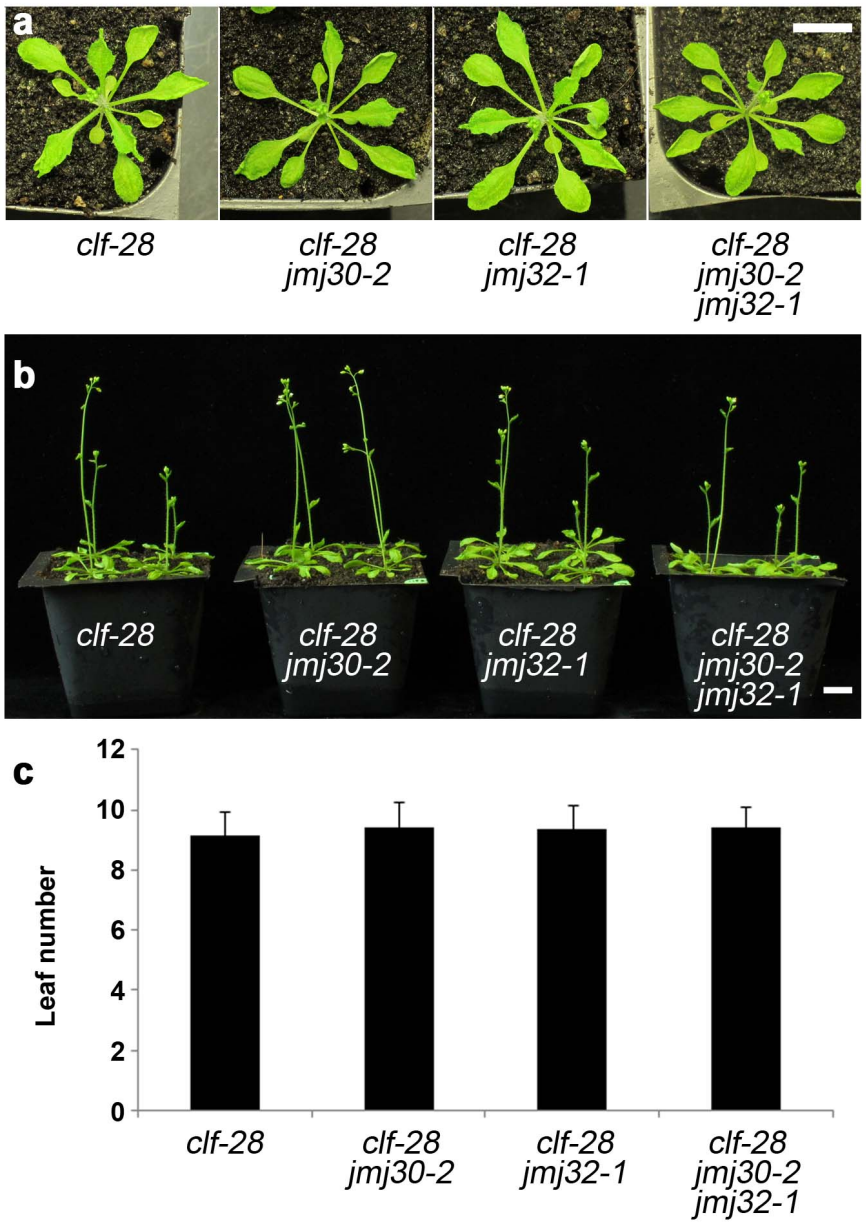

Figure 27. *clf* is epistatic to *jmj30 jmj32*.

The *jmj30 jmj32* mutant did not rescue the *clf* mutation, both in terms of leaf curling and flowering time. (**a**) Top view of *clf*, *clf jmj30*, *clf jmj32*, *clf jmj30 jmj32* plants showing the leaf curling phenotype. (**b**) *clf jmj30*, *clf jmj32* and *clf jmj30 jmj32* flower at a similar time as *clf* when grown under LD 22°C conditions. Scale bar, 1 cm. (**c**) Total primary rosette leaves before bolting in *clf*, *clf jmj30*, *clf jmj32* and *clf jmj30 jmj32* plants grown under LD 22°C conditions were counted (2 independent experiments with 12-16 plants each). Bars indicate s.d.

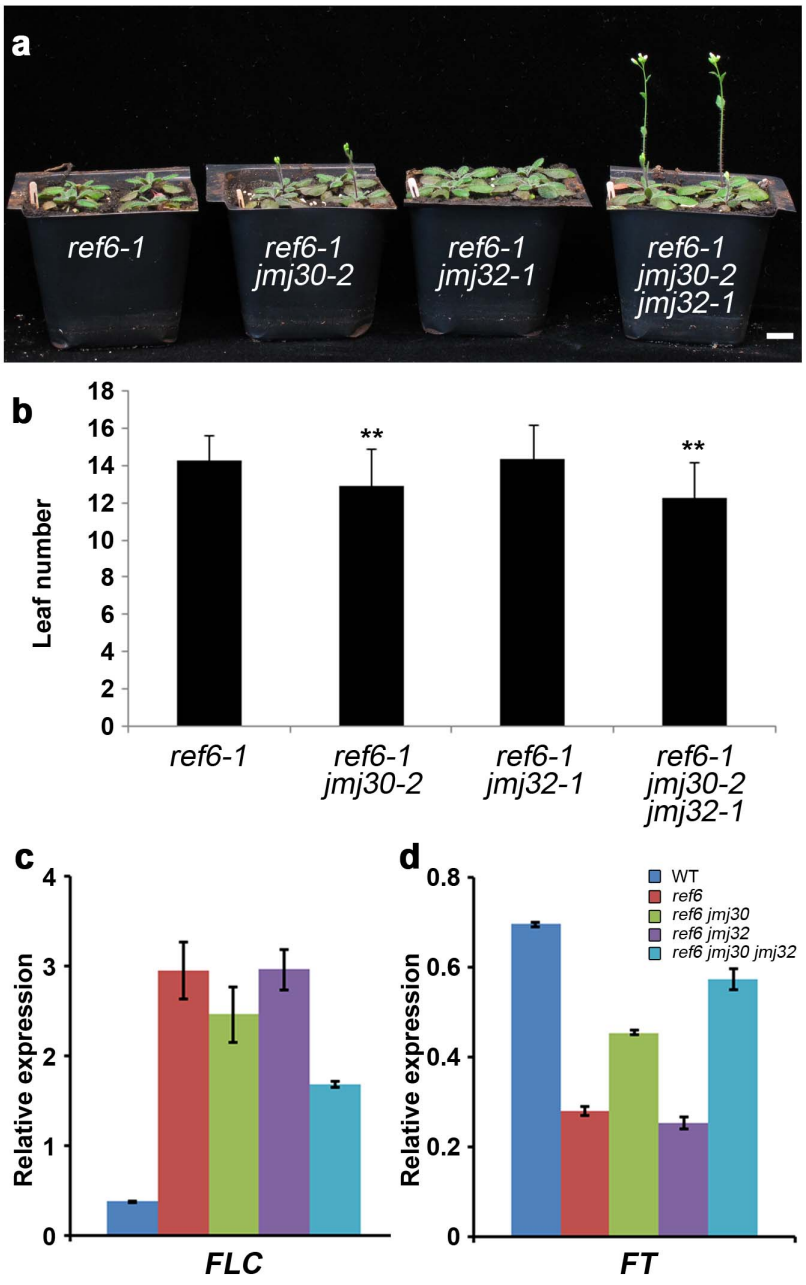

Figure 28. *jmj30 jmj32* slightly rescues the late-flowering phenotype of *ref6*.

(**a**) *ref6 jmj30* and *ref6 jmj30 jmj32* flowered earlier than *ref6* when grown under LD 22°C conditions. Scale bar, 1 cm. (**b**) Total primary rosette leaves before bolting in *ref6*, *ref6 jmj30*, *ref6 jmj32* and *ref6 jmj30 jmj32* plants grown under LD 22°C conditions were counted (2 independent experiments with 12-16 plants each). Bars indicate s.d; two-tailed Student's *t*-test, **P<0.01. Relative mRNA expression of (**c**) *FLC* and (**d**) *FT* analyzed by qRT-PCR in WT, *ref6*, *ref6 jmj30*, *ref6 jmj32* and *ref6 jmj30 jmj32* 13 DAG seedlings grown under 22°C conditions,. Bars indicate s.d. of three technical replicates.

3.11 *JMJ30* and *JMJ32* buffer *FLC* silencing during vernalization

The rapid-cycling Col-0 ecotype has a non-functional *fri* and low expression level of *FLC*, hence it shows an early-flowering phenotype and completes its life cycle in 2-3 months. Previous studies had shown that introgression of a functional allele of *FRI* from the Sf-2 ecotype into Col WT causes a drastic up-regulation of *FLC* and a late-flowering phenotype (Lee et al, 1993; Michaels & Amasino, 1999). The Col WT with *FRI*-Sf2 (herein *FRI*) has to undergo weeks of vernalization to induce PRC2-mediated *FLC* silencing and cause early-flowering upon return to warm conditions.

Under the functional *FRI* background, *FRI jmj30 jmj32* showed only a modest decrease of *FLC* at 3-weeks-after-germination at 29°C LD (Figure 29). A strong transcription activity driven by activators such as *FRI* may negatively affect the deposition of the repressive H3K27me3 marks at the *FLC* locus as previously suggested (Buzas et al, 2011), possibly masking the effect of JMJ30/JMJ32.

Since I identified JMJ30/32 as H3K27me3 histone demethylases, and *FRI*-activated *FLC* is gradually silenced through vernalization with the accumulation of H3K27me3 (Angel et al, 2011), I wonder whether PRC2 and JMJ30/32 may act antagonistically in regulating *FLC* expression, where PRC2 deposits the repressive mark on the *FLC* locus while JMJ30/32 actively removes it. If this genetic interaction happens in a competitive manner, the flowering repressor *FLC* would be more easily repressed in the loss-of-function mutant of the *jmj30 jmj32* histone demethylases. In other words, the *jmj30 jmj32* plants would be sensitized for vernalization. To understand the

genetic interaction of *FRI* and *JMJ30*/*JMJ32*, I crossed *jmj30 jmj32* double mutant into the *FRI* background, and exposed *FRI* and *FRI jmj30 jmj32* to different period of vernalization treatment: non-vernalized (NV), vernalized 2-weeks (V2W), vernalized 4-weeks (V4W), and vernalized 6-weeks (V6W) (Figure 30a,b). Flowering time initially showed no differences between untreated *FRI* and *FRI jmj30 jmj32* (leaf number ratio of *FRI jmj30 jmj32*/*FRI* NV: 0.91). However, V2W- and V4W-treated *FRI jmj30 jmj32* flowered earlier than their *FRI* counterpart, suggesting *FRI jmj30 jmj32* reached the vernalized state faster (leaf number ratio of *FRI jmj30 jmj32*/*FRI* V2W: 0.78; V4W: 0.81). With V6W-treatment, both *FRI* and *FRI jmj30 jmj32* were fully vernalized, hence they showed a similar early flowering phenotype (leaf number ratio of *FRI jmj30 jmj32*/*FRI* V6W: 0.95). These data show that compared to *FRI*, *FRI jmj30 jmj32* is more sensitive to vernalization-induced flowering.

Since *FLC* is the key gene being regulated in the vernalization pathway, I next wonder the difference in flowering time between *FRI* and *FRI jmj30 jmj32* is due to the difference in *FLC* expression. I extracted RNA from seedling samples with different period of exposure to cold, and analyzed the expression of *FLC* in the two genotypes (Figure 31a). Indeed, the difference in *FLC* expression was similarly reflected as in their phenotypic difference. *FLC* expression was similarly high in NV samples. In V2W-treated samples, *FLC* expression level was relatively unchanged in *FRI*, but *FRI jmj30 jmj32* already showed a 20% decrease in *FLC* expression. The expression difference gets smaller at V4W- and V6W-treatments. It is worth noticing that V4W-treated

FRI jmj30 jmj32 already reduced *FLC* level to a comparable level with V6W-treated *FRI*.

FLC silencing during vernalization is due to the gradual increase of the repressive H3K27me3 marks on its locus (Angel et al, 2011). I thus wondered whether this hastened *FLC* repression was due to increased H3K27me3 accumulation. I performed a H3K27me3 ChIP using *FRI* and *FRI jmj30 jmj32* seedlings with either no vernalization (NV), partial vernalization (V2W) or full vernalization (V6W)(Figure 31b). Similar to the *FLC* mRNA expression, low level of H3K27me3 marks were observed initially when both *FRI* and *FRI jmj30 jmj32* were untreated. When the plants were partially vernalized at V2W, I detected higher levels of H3K27me3 enrichment at the *FLC* locus in *FRI jmj30 jmj32* seedlings, explaining the *FLC* mRNA expression differences. With full vernalization, both *FRI* and *FRI jmj30 jmj32* showed high H3K27me3 levels, especially at the transcriptional start site, where JMJ30 was localized (Figure 23b,c). These results suggested that in the absence of the H3K27me3 demethylases JMJ30/JMJ32, *FLC* is more easily silenced by the repressive marks, suggesting that JMJ30/JMJ32 may counter the effect of PRC2 during vernalization to fine-tune the level of suppression.

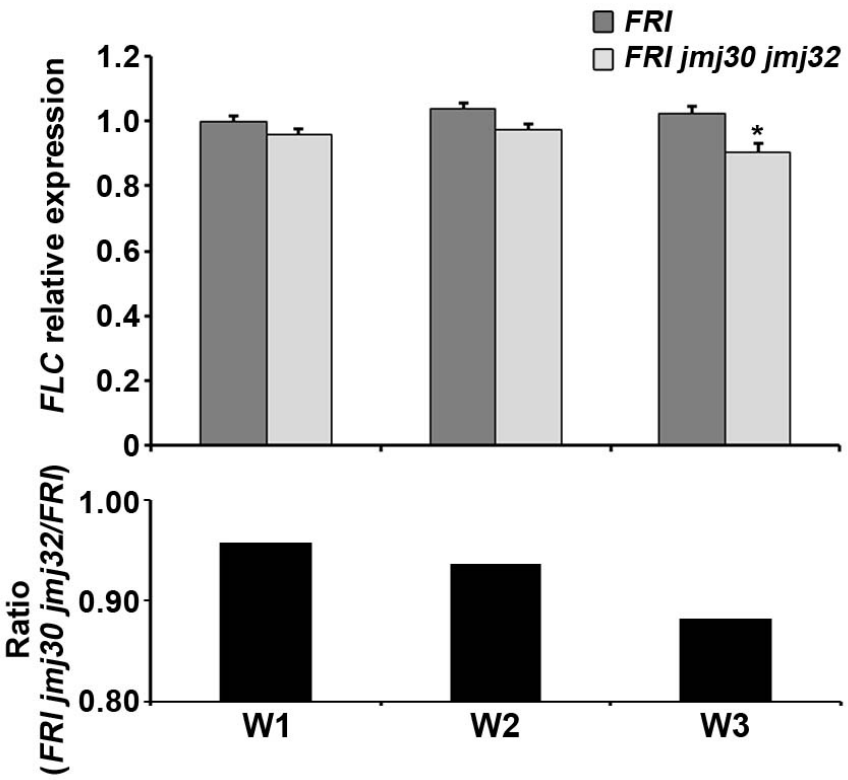

Figure 29. *FRI jmj30 jmj32* showed a modest reduced expression of *FLC* when grown at elevated temperature.

Relative expression of *FLC* analyzed by qRT-PCR in 1-week (W1), 2-week (W2) and 3-week (W3) old seedlings of *FRI* and *FRI jmj30 jmj32* grown at LD 29°C. The *FLC* expression ratio of *FRI jmj30 jmj32*/*FRI* is shown below the graph. Bars indicate s.d. of three biological replicates; two-tailed Student's *t*-test, *P<0.05.

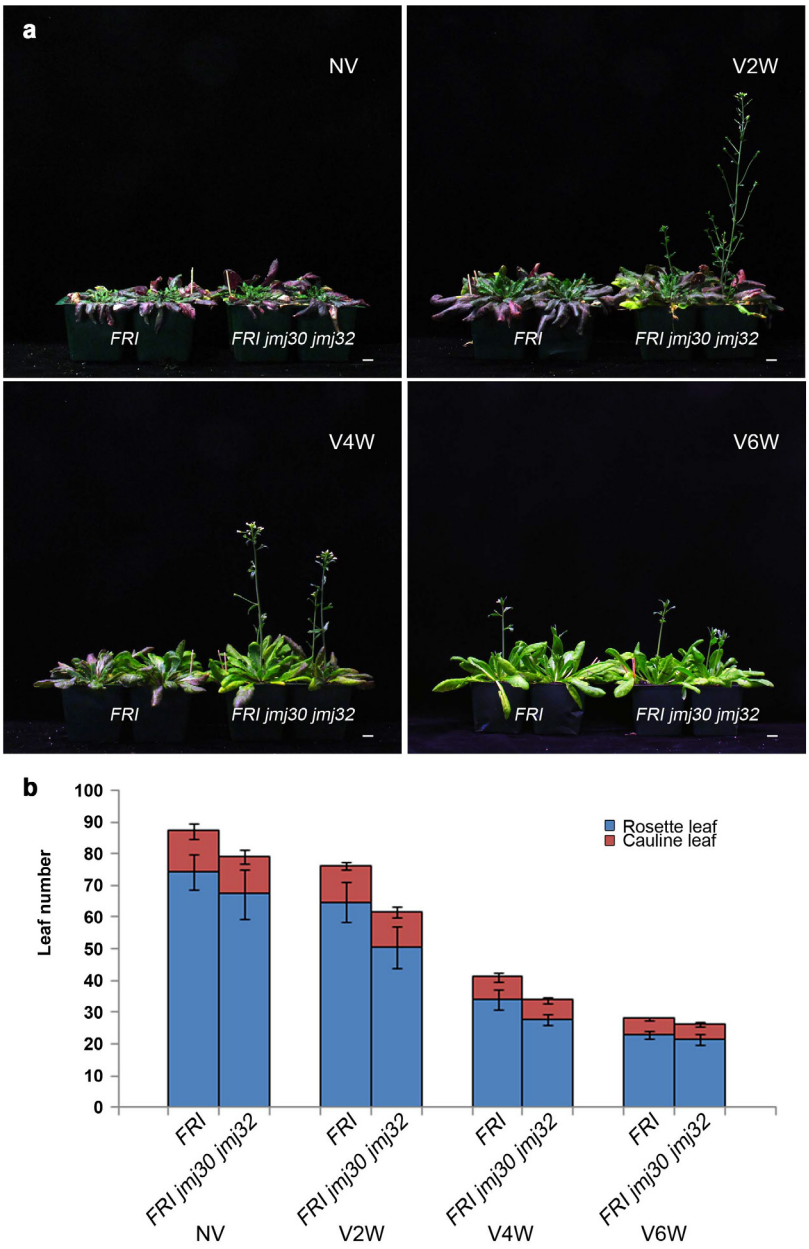

Figure 30. *FRI jmj30 jmj32* is sensitized for vernalization.

(**a**) Primary rosette leaves were counted for *FRI* and *FRI jmj30 jmj32* plants with either no treatment (Non-vernalized, NV) or exposure to different period of vernalization treatment (vernalized 2-weeks, V2W; vernalized 4-weeks, V4W; vernalized 6-weeks, V6W). Flowering time was initially indifferent between untreated *FRI* and *FRI jmj30 jmj32*. However, V2W- and V4W-treated *FRI jmj30 jmj32* flowered earlier than their *FRI* counterpart, suggesting that *FRI jmj30 jmj32* reached the vernalized threshold faster. With V6W-treatment, both *FRI* and *FRI jmj30 jmj32* were fully vernalized, hence they showed indifferent flowering time. (**b**) Total rosette leaves before bolting and cauline leaves in *FRI* and *FRI jmj30 jmj32* plants grown under LD 22°C conditions after vernalization treatment were counted (2 independent experiments with 12 plants each). Bars indicate s.d.

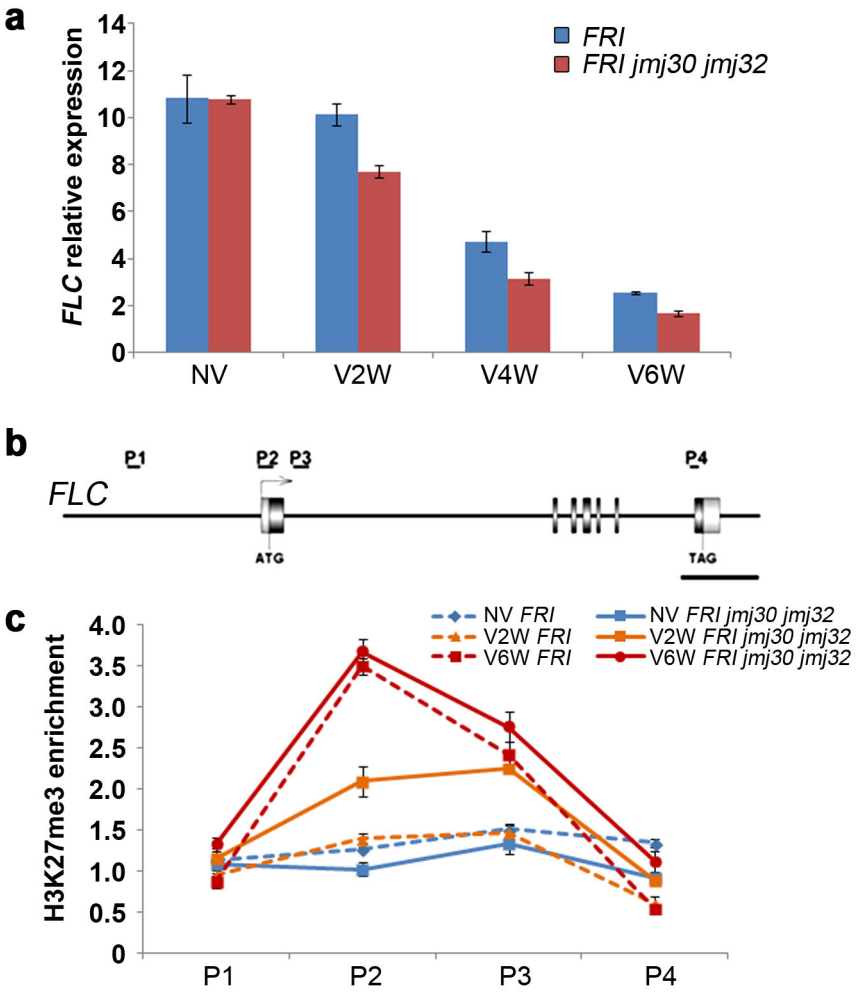

Figure 31. *FLC* vernalization-induced silencing occurs at a faster pace in *FRI jmj30 jmj32*.

(**a**) *FLC* relative expression in *FRI* and *FRI jmj30 jmj32* plants with either no treatment (Non-vernalized, NV) or exposure to different period of vernalization treatment (vernalized 2-weeks, V2W; vernalized 4-weeks, V4W; vernalized 6-weeks, V6W). *FLC* expression was initially indifferent between *FRI* and *FRI jmj30 jmj32*, but showed the largest difference in V2W- and V4W-treated seedlings. (**b**) Schematic drawing of the *FLC* genome structure showing regions amplified by primers used for ChIP analysis. Scale bar, 1 kb. (**c**) ChIP analysis of H3K27me3 enrichment at the *FLC* locus in *FRI* and *FRI jmj30 jmj32* seedlings with no vernalization (NV), partial vernalization (V2W) and full vernalization (V6W). Bar indicates s.d. of three technical replicates.

3.12 Loss of function of *jmj30* and *jmj32* negatively affect the heat tolerance of germinating seedlings

In an initial screen for effect of *jmj30 jmj32* on gene expression, I found that many stress-responsive and stimuli-responsive genes were down-regulated in the double mutant (Table 9). However, no obvious phenotypic difference was observed when *jmj30 jm32* plants were grown at a high ambient temperature environment, besides their early-flowering phenotype (Figure 9a,b).

In a recent set of experiment performed to examine JMJ30/JMJ32 regulation on vernalization and the reversal of vernalization, I found that the germinating seedlings of *FRI jmj30 jmj32* were less tolerant to heat stress treatment (Figure 32a,b). The seeds of *FRI* and *FRI jmj30 jm32* were sterilized and sowed on MS plates. After stratification and vernalization in the dark for 3 weeks, the seeds were exposed to a heat stress temperature of 37°C under LD condition for 3 days or 7 days. The *FRI* and *FRI jmj30 jmj32* plants were then returned to standard growth conditions of 22°C LD after the heat treatment to continue their growth.

I found that mutation of *jmj30 jmj32* did not affect the seed germination as shoot and root elongation can still occur (Figure 32a,b). However, after germination, the *FRI jmj30 jmj32* seedlings showed a higher number of plants with white variegated leaves when treated with 37°C for 3 days (Figure 32a). When plants were treated with 37°C for 7 days, more severe effects was observed as *FRI jmj30 jmj32* showed increased number of plant death with the plantlets ceasing growth and turning white. This observation suggests that

mutation of *jmj30 jmj32* caused reduced heat tolerance in the germinating seedlings.

However, there remained a few unanswered questions in this experiment, e.g. what are the key genes affected in *FRI jmj30 jm32* that give rise to this reduced heat tolerance phenotype, are the genes affected in *FRI jmj30 jm32* regulated by the repressive H3K27me3 marks, is the 3-week vernalization necessary to reproduce the result, and is the functional *FRI* required in this tolerance response. To answer these questions, the experiment will be repeated comparing Col WT with *jmj30 jmj32* and treated with 37°C heat stress temperature without vernalization. Once I confirmed the phenotype and optimum treatment conditions, I will be comparing the mRNA expression profile and genome wide H3K27me3 ChIP of the imbibed and after treatment seeds of WT and *jmj30 jmj32*. These would aid us in understanding the heat tolerance mechanism and isolating genes regulating such heat stress response.

Table 9. Stress-responsive genes down-regulated in *jmj30 jmj32*.

Locus	P value	Fold change	Description
AT1G01060	0.0756	2.060 down	LHY (LATE ELONGATED HYPOCOTYL); DNA binding / transcription factor
AT1G03070	0.0405	1.815 down	glutamate binding
AT1G07890	0.0406	1.635 down	APX1 (ascorbate peroxidase 1); L-ascorbate peroxidase
AT1G11270	0.0219	1.899 down	F-box family protein
AT1G15520	0.0396	2.042 down	PDR12 (PLEIOTROPIC DRUG RESISTANCE 12); ATPase, coupled to transmembrane movement of substances
AT1G16130	0.000956	2.376 down	WAKL2 (wall associated kinase-like 2); kinase
AT1G20900	0.086	2.216 down	ESC (ESCAROLA); double-stranded DNA binding
AT1G22920	0.0624	1.639 down	CSN5A (COP9 SIGNALOSOME 5A)
AT1G55880	0.0862	1.879 down	pyridoxal-5'-phosphate-dependent enzyme, beta family protein
AT1G56540	0.0949	1.515 down	disease resistance protein (TIR-NBS-LRR class), putative
AT1G63750	0.0151	1.590 down	ATP binding / nucleoside-triphosphatase/ nucleotide binding / protein binding
AT1G66950	0.0724	1.608 down	PDR11 (PLEIOTROPIC DRUG RESISTANCE 11); ATPase, coupled to transmembrane movement of substances
AT1G70510	0.0142	1.809 down	KNAT2 (KNOTTED-LIKE FROM ARABIDOPSIS THALIANA 2); transcription factor
AT1G72140	0.00964	4.073 down	proton-dependent oligopeptide transport (POT) family protein
AT1G74660	0.0563	2.671 down	MIF1 (MINI ZINC FINGER 1); DNA binding / transcription factor
AT1G79680	0.0954	1.742 down	wall-associated kinase, putative
AT2G02390	0.0192	2.958 down	ATGSTZ1 (ARABIDOPSIS THALIANA GLUTATHIONE S-TRANSFERASE ZETA 1); catalytic/ glutathione transferase
AT2G18050	0.039	2.454 down	HIS1-3 (HISTONE H1-3); DNA binding / nucleosomal DNA binding
AT2G22880	0.033	1.754 down	VQ motif-containing protein
AT2G30480	0.078	2.357 down	unknown protein
AT2G32140	0.00353	1.740 down	transmembrane receptor
AT2G33740	0.0783	1.562 down	CUTA; copper ion binding
AT2G34500	0.0702	1.658 down	CYP710A1 (cytochrome P450, family 710, subfamily A, polypeptide 1); C-22 sterol desaturase/ oxygen binding
AT2G37770	0.0912	2.659 down	aldo/keto reductase family protein
AT2G38920	0.0469	2.243 down	SPX (SYG1/Pho81/XPR1) domain-containing protein / zinc finger (C3HC4-type RING finger) protein-related
AT2G41070	0.0765	1.544 down	EEL (ENHANCED EM LEVEL); DNA binding / transcription factor
AT2G42720	0.0634	2.138 down	F-box family protein
AT2G45570	0.0129	2.235 down	CYP76C2; electron carrier/ heme binding / iron ion binding / monooxygenase/ oxygen binding
AT2G47890	0.0301	1.714 down	zinc finger (B-box type) family protein
AT3G06550	0.0418	1.831 down	CONTAINS InterPro DOMAIN/s: Cas1p-like (InterPro:IPR012419); BEST Arabidopsis thaliana protein match is: O-acetyltransferase family protein (TAIR:AT2G34410.2);
AT3G06820	0.0559	1.535 down	mov34 family protein
AT3G07650	0.0595	1.563 down	COL9 (CONSTANS-LIKE 9); transcription factor/ zinc ion binding
AT3G13610	0.0425	1.699 down	oxidoreductase, 2OG-Fe(II) oxygenase family protein

AT3G13662	0.00334	1.894 down	CONTAINS InterPro DOMAIN/s: Plant disease resistance response protein (InterPro:IPR004265); BEST Arabidopsis thaliana protein match is: disease resistance-responsive protein-related / dirigent protein-related (TAIR:AT5G49040.1)
AT3G21780	0.0116	1.874 down	UGT71B6 (UDP-glucosyl transferase 71B6); UDP-glycosyltransferase/ abscisic acid glucosyltransferase/ transferase, transferring glycosyl groups
AT3G21890	0.0882	1.530 down	zinc finger (B-box type) family protein
AT3G27660	0.033	1.908 down	OLEO4 (OLEOSIN 4)
AT3G48640	0.00625	1.660 down	unknown protein
AT3G57390	0.00676	2.250 down	AGL18; transcription factor
AT3G59760	0.00325	2.172 down	OASC (O-ACETYLSERINE (THIOL) LYASE ISOFORM C); ATP binding / cysteine synthase
AT3G59845	0.0166	2.250 down	NADP-dependent oxidoreductase, putative
AT3G60010	0.0455	1.595 down	ASK13 (ARABIDOPSIS SKP1-LIKE 13); protein binding / ubiquitin-protein ligase
AT3G63250	0.00947	2.937 down	HMT2 (HOMOCYSTEINE METHYLTRANSFERASE 2); homocysteine S-methyltransferase
AT4G01420	0.0881	1.716 down	CBL5 (CALCINEURIN B-LIKE PROTEIN 5); calcium ion binding
AT4G11030	0.0737	1.518 down	long-chain-fatty-acid--CoA ligase, putative / long-chain acyl-CoA synthetase, putative
AT4G14690	0.00502	2.035 down	ELIP2 (EARLY LIGHT-INDUCIBLE PROTEIN 2); chlorophyll binding
AT4G15400	0.0661	1.509 down	transferase family protein
AT4G15975	0.0225	2.463 down	protein binding / zinc ion binding
AT4G18360	0.0958	2.344 down	(S)-2-hydroxy-acid oxidase, peroxisomal, putative / glycolate oxidase, putative / short chain alpha-hydroxy acid oxidase, putative
AT4G18450	0.0632	1.624 down	ethylene-responsive factor, putative
AT4G20260	0.0554	1.878 down	DREPP plasma membrane polypeptide family protein
AT4G20380	0.0683	1.907 down	zinc finger protein (LSD1)
AT4G21320	0.0461	1.717 down	HSA32 (HEAT-STRESS-ASSOCIATED 32); catalytic
AT4G23493	0.064	3.820 down	unknown protein
AT4G31240	0.0714	1.652 down	CONTAINS InterPro DOMAIN/s: Thioredoxin fold (InterPro:IPR012335), Thioredoxin-like (InterPro:IPR017936), Thioredoxin-like fold (InterPro:IPR012336), C1-like (InterPro:IPR011424); BEST Arabidopsis thaliana protein match is: DC1 domain-containing protein (TAIR:AT1G60420.1);
AT4G33985	0.0571	1.729 down	unknown protein
AT4G35770	0.00587	3.343 down	SEN1 (SENESCENCE 1)
AT5G05490	0.0846	2.360 down	SYN1 (SYNAPTIC 1)
AT5G10040	0.0494	1.864 down	unknown protein
AT5G13820	0.0259	1.669 down	TBP1 (TELOMERIC DNA BINDING PROTEIN 1); DNA binding / double-stranded telomeric DNA binding
AT5G17490	0.0105	3.520 down	RGL3 (RGA-LIKE PROTEIN 3); transcription factor
AT5G18130	0.0374	2.625 down	unknown protein
AT5G24110	0.0312	2.402 down	WRKY30; transcription factor
AT5G27420	0.0476	2.841 down	zinc finger (C3HC4-type RING finger) family protein
AT5G42500	0.0772	2.044 down	disease resistance-responsive family protein
AT5G45090	0.0124	1.726 down	AtPP2-A7 (Phloem protein 2-A7); carbohydrate binding
AT5G47370	0.0133	1.593 down	HAT2; DNA binding / transcription factor/ transcription

			repressor
AT5G51760	0.0641	2.927 down	AHG1 (ABA-hypersensitive germination 1); catalytic/ protein serine/threonine phosphatase
AT5G53680	0.0553	2.830 down	RNA recognition motif (RRM)-containing protein
AT5G59220	0.017	1.906 down	protein phosphatase 2C, putative / PP2C, putative

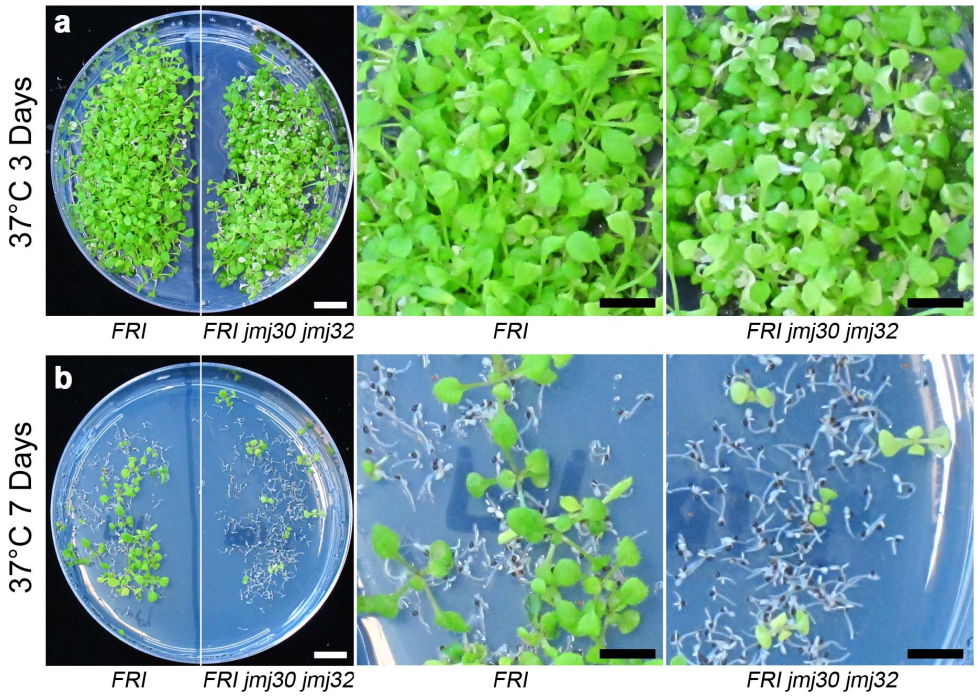

Figure 32. *FRI jmj30 jmj32* shows reduced heat tolerance.

(**a**) *FRI jmj30 jmj32* did not affect seed germination. However, after germination, the *FRI jmj30 jmj32* seedlings showed a higher number of white variegated leaves when treated with 37°C for 3 days. (**b**) A more severe effect was observed when plants were treated with 37°C for 7 days as *FRI jmj30 jmj32* showed increased number of plant death (whitish non-growing seedlings). Seeds were vernalized in the dark for 3 weeks, and treated in 37°C in LD for either 3 days or 7 days, then returned to standard growth conditions of 22°C LD for normal growth. Scale bar, 1cm.

Chapter 4

Discussion

Chapter 4 Discussion

4.1 JMJ30 and JMJ32 regulate thermal induction of flowering

In this study, I revealed that the histone modifiers JMJ30 and JMJ32 demethylate H3K27me3 marks at the *FLC* locus to delay the repression of the floral repressor at elevated temperatures. In the flowering pathways, *FLC* is the central repressor that represses two floral integrators, *FT* and *SOC1*, in *Arabidopsis* (Searle et al, 2006). I showed that JMJ30 specifically demethylates H3K27me2/3 *in vitro* (Figure 18a,b) and *in vivo* (Figure 19). Moreover, *jmj30 jmj32* double mutant showed accelerated flowering when grown under 29°C LD or SD conditions (Figure 9a,b, Figure 10a,b), a temperature below the one used in basal thermo-tolerance experiments (Chen et al, 2006). On the other hand, over-expression of *JMJ30-HA* led to an obvious late-flowering phenotype (Figure20).

The mutation of *fri flc* leads to early-flowering under LD (Figure 4a,b) or SD (Balasubramanian et al, 2006) conditions with increased temperatures, highlighting the role of *FLC* in repressing flowering at elevated temperature. In both *jmj30 jmj32* and *35S::JMJ30-HA* lines, I noticed that *FLC* expression was the most obviously affected (Figure 11a, Figure 21a). The direct binding of JMJ30-HA to the transcriptional start site of the *FLC* locus shows that *FLC* is a direct target of JMJ30 (Figure 23b,c). Moreover, the genetic rescue of the late-flowering phenotype of *JMJ30* overexpression by introducing the *flc* mutation strengthens the notion that JMJ30 functions through *FLC* to help regulate flowering time (Figure 21b,c). My work shows the importance of the balancing act between PcG-mediated histone methylation and JMJ30/JMJ32-

mediated histone demethylation on H3K27 in controlling the expression of genes such as *FLC*.

4.2 Antagonistic function of PRC2 and JMJ30/JMJ32

PRC2 containing EMF2, FIE, MSI1, CLF/SWN are recruited possibly via PRE to deposit the repressive H3K27me3 marks at the region. This results in a repressive chromatin status at the region and silences gene transcription (Figure 33). The H3K27me3 marks may further recruit PRC1 complex to reinforce the repressive state via H2AK119 monoubiquitination. Functioning antagonistically with the CLF-containing HMTase complex, JMJ30/JMJ32-containing histone demethylase complex removes the H3K27me3 mark from the region (Figure 33). Removal of the repressive H3K27me3, together with the deposition of active histone modifications H3K4me3 and H3K36me3 reinstate the permissive chromatin state at the region.

The Trx complex containing the human Mixed Lineage Leukemia (MLL) proteins or their *Drosophila* homologs, Trx and Trithorax related (Trr) is capable of methylating histone H3 on lysine 4 (Kanda et al, 2013). It is shown that the metazoan H3K27me3 demethylase UTX is found in the MLL3- and MLL4-containing Trx complexes (Hong et al, 2007). This forms two positive reinforcing reactions in one complex: on one hand, UTX is removing the repressive H3K27me3 marks; on the other hand, MLL3/MLL4 is depositing active H3K4me3 marks. It is thus interesting to speculate whether a similar scenario may be occurring in *Arabidopsis*, with JMJ30/JMJ32 forming a complex with the COMPASS-like H3K4 methylation complex, or other

chromatin-activating complexes like the PAF1 complex or MRG1/2-HAM1/2 complex.

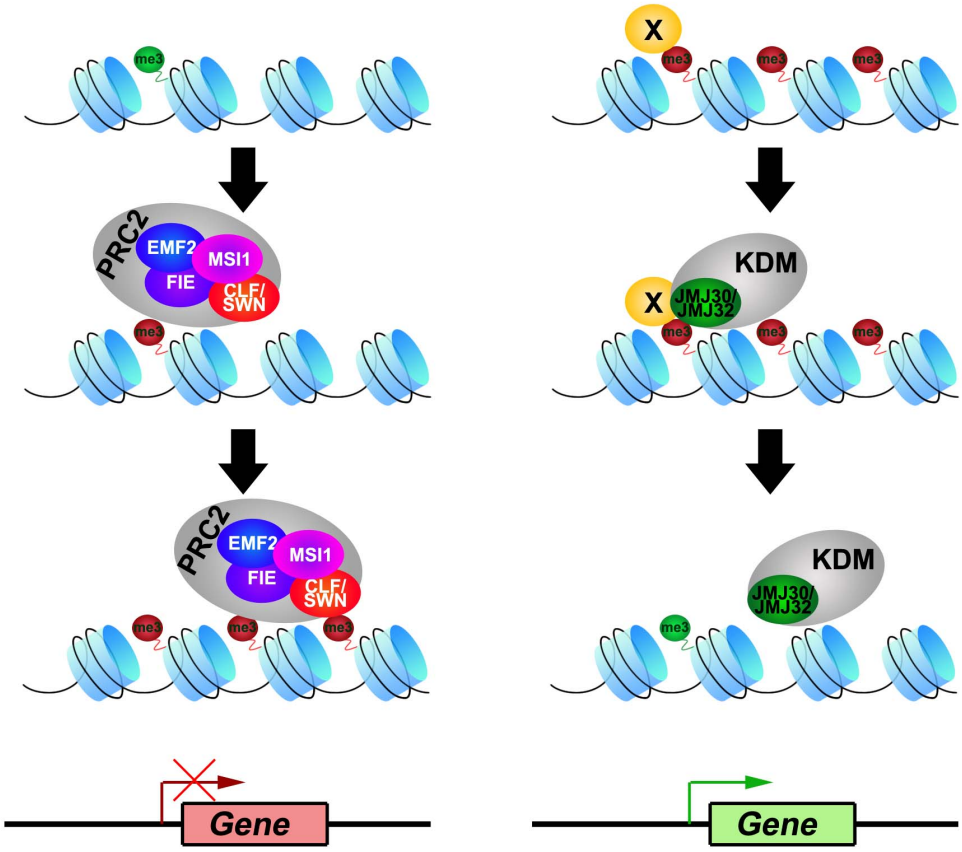

Figure 33. Model of the antagonistic action of PRC2 and JMJ30/JMJ32 on gene regulation.

Chromatin marked with active histone modification H3K4me3/H3K36me3 (green me3 circle) is in a permissive state of transcription. Recruitment of the PRC2 complex occurs possibly via the polycomb repressive element (PRE). PRC2 complex containing core components of EMBRYONIC FLOWER 2 (EMF2), MULTICOPY SUPRESSOR OF IRA 1 (MSI1), FERTILIZATION INDEPENDENT ENDOSPERM (FIE), CURLY LEAF (CLF) or SWINGER (SWN) mediates the deposition and spreading of the repressive histone modification H3K27me3 (red me3 circle) across the region. This results in a repressive chromatin state and silences gene expression at the region. Functioning antagonistically, histone lysine demethylase (KDM) complex containing JMJ30/JMJ3 is recruited by unknown factors (factor X) to its target sites. JMJ30/JMJ32 removes the H3K27me3 marks from the region. Coupled with the deposition of activating histone modifications, genes at the region can resume active transcription.

4.3 Crosstalks between the temperature-sensing and circadian clock regulation

JMJ30 transcript shows diurnal circadian rhythm (Figure 24a)(Jones et al, 2010; Lu et al, 2011c). JMJ30/JMJ32-dependent *FLC* delayed repression at elevated temperatures led us to examine whether the higher activity of JMJ30 is mediated through increased expression levels or a shift in circadian rhythms. I found that *JMJ30* diurnal expression is increased by maintaining the high peak before dropping to start another cycle (Figure 24a) and the protein is further stabilized (Figure 24b, Figure 25a). Although *FLC* itself is not controlled by circadian regulation, I reasoned that the increased accumulation of the JMJ30 protein at a higher temperature can help maintain the *FLC* locus in a transcriptionally permissive state. Our data showed that instability of JMJ30 protein at 22 °C is mediated by proteasomal degradation pathway, which is blocked by the proteasome inhibitor MG132 or when the plants are grown at 29°C (Figure 25a). Thus, the future work includes the searching and confirming the interacting partners of JMJ30 in its temperature-dependent behavior (Table 7).

FLC is also known to mediate the temperature compensation mechanism of the circadian clock at elevated temperatures by lengthening the circadian period, possibly through regulating the expression of an MYB transcription factor *LUX ARRHYTHMO* (*LUX*)(Edwards et al, 2006). During circadian oscillation, the transcriptional feedback loop between the central clock genes *CIRCADIAN CLOCK ASSOCIATED 1* (*CCA1*), *LATE ELONGATED HYPOCOTYL* (*LHY*) and *TIMING OF CAB EXPRESSION 1* (*TOC1*) forms the core oscillator (Nagel & Kay, 2012). Two core clock genes, *CCA1* and

LHY, directly bind and repress *JMJ30* (Lu et al, 2011c), while JMJ30, in turn, promotes the expression of the morning-phased clock genes, *CCA1* and *LHY* (Jones et al, 2010), forming a negative feedback loop similar to the central *CCA1*/*LHY*/*TOC1* oscillation. Taken together, the interactions between *FLC*, *JMJ30*, and the circadian clock genes provide a platform for crosstalk between the flowering pathway and circadian regulation to modulate plant responses to fluctuating temperatures.

4.4 *JMJ30* and *JMJ32* regulate specific H3K27me3-targeted genes

Expression profiling showed that 396 out of thousands of H3K27me3-regulated genes are up-regulated in *35S::JMJ30-HA* and/or down-regulated in *jmj30 jmj32*. The fact that the expression profiles of many H3K27me3-regulated genes are not affected suggests that JMJ30 and JMJ32 may only target a subset of H3K27me3-regulated genes. Because JMJ30 and JMJ32 contain only the catalytic JmjC domain, the activity of these histone modifiers may be dependent on the availability of a recruiter to the target genes.

In animals, the H3K27me3 demethylases are developmentally essential, and loss-of-function mutants of the demethylases usually lead to severe developmental defects and lethality. In mouse, JMJD3 inactivation results in perinatal lethality due to respiratory failure (Burgold et al, 2012) whereas the loss of the zebrafish Utx1 leads to posterior developmental defects (Lan et al, 2007). In *Caenorhabditis elegans*, the *utx-1* loss-of-function mutant leads to sterility and embryonic lethality (Vandamme et al, 2012) whereas loss of the

JMJD3 homologue causes abnormal gonad development (Agger et al, 2007). In *Arabidopsis*, one member of the KDM4/JHDM3/JMJD2 group, *REF6*, has been shown to target the floral inducer *FT* (Lu et al, 2011b). Because *FT* functions downstream of *FLC*, *ref6-1* is supposed to be epistatic to *jmj30-2 jmj32-1*, as was observed in the late-flowering phenotype of *ref6-1 jmj30-2 jmj32-1* (Figure 28a,b). It is of note that the *ref6-1 jmj30-2 jmj32-1* triple mutant showed no severe developmental defects other than its late-flowering phenotype (Figure 28a,b). The lack of phenotype suggests that other H3K27me3 demethylases exist in addition to these JMJ proteins, that the feedback loop to the histone methylation is robust and flexible, or that the developmental plasticity is greater in plants than in animals. It is recently reported that *ELF6* function as another H3K27me3 demethylase in regulating *FLC* resetting (Crevillen et al, 2014). I am in the midst of creating the *elf6 ref6 jmj30 jmj32* quadruple mutant to observe its developmental phenotype. *FRI elf6-5* only shows a mild *FLC* next generation reactivation defect (Crevillen et al, 2014), hence I am also creating the *FRI elf6 jmj30 jmj32* plants to examine their effect on *FLC* resetting. The mutation of *ref6* is omitted from the *FLC* resetting study because it causes an up-regulation of *FLC* instead of decreased *FLC* expression as what is observed in *elf6* or *jmj30 jmj32* (Crevillen et al, 2014).

In addition to the floral integrators, *FT* and *SOC1*, FLC also binds and regulates many stress-responsive genes, such as the cold response genes *C-REPEAT/DRE BINDING FACTOR 1* (*CBF1*) and *CBF3* (Deng et al, 2011), and many genes involved in stress and stimulus response are implicated as

target genes of JMJ30 and JMJ32 (Figure 26b). It would be interesting to further study the roles of *JMJ30*, *JMJ32* and *FLC* in stress responses.

4.5 High temperature-enhanced *FLC* by JMJ30/JMJ32 constitutes a parallel thermosensory pathway

One of the key players in the thermosensory pathway, the repressive H2A.Z occupancy controlling the accessibility of *PIF4*, mediates thermosensory responses by wrapping DNA more tightly at lower temperatures, thus negatively affecting *PIF4*–mediated transcription (Kumar et al, 2012; Kumar & Wigge, 2010). Although the heat-induced up-regulation outcome of the H2A.Z-mediated mechanism fits the *FLC* expression profile, *FLC* does not seem to be a PIF4-regulated target gene (Oh et al, 2012). On the other hand, recent publications showed that SVP, FLC, and different splice variants of FLM form MADS-box heterocomplexes to control flowering time in response to ambient temperature changes (Gu et al, 2013a; Lee et al, 2013a). The SVP-FLM-β complex delays flowering through the transcriptional repression of *FT* and *SOC1* at low temperatures, which is alleviated by the *FLM-δ* dominant-negative at increased temperatures (Lee et al, 2013a). SVP may also form a complex with FLC to repress flowering at elevated temperatures, although this is less likely because SVP is rapidly degraded at elevated temperatures (Lee et al, 2013a). Taken together, my work suggests that JMJ30- and JMJ32-regulated *FLC* expression, in parallel with temperature-responsive H2A.Z nucleosome occupancy (Kumar & Wigge, 2010) and SVP-FLM cold-sensing

pathways (Lee et al, 2013a), may function to balance and coordinate flowering time in response to fluctuating temperatures.

A recent study showed that flowering in chrysanthemum is repressed at elevated temperatures through the down-regulation of one of its floral inducers, *FLOWERING LOCUS T-like 3* (*FTL3*)(Nakano et al, 2013). Together with my results, this finding suggests that the need for a thermosensory balancing mechanism that represses flowering at elevated temperatures may be conserved, although the molecules involved in the process may differ. When plants are grown in an environment with fluctuating temperatures, the interplay between floral inductive and repressive signals plays a key role in determining the optimal flowering time for reproductive success. All in all, this study provides insights into the regulation of flowering time through *FLC* heat-inductive expression, which is partly achieved through the activity of H3K27 demethylases, JMJ30 and JMJ32.

4.6 Substrate specificity of JMJ proteins

JMJ proteins from the same group are implicated to target similar histone modifications (Klose et al, 2006a; Lu et al, 2008). This study showed that although residing in a different group compared to REF6 and ELF6, JMJ30 and JMJ32 also target H3K27me3 marks. JMJ30 and JMJ32 differ from REF6 both in their JmjC domain sequences and their lack of the JmjN domain (Lu et al, 2008). Moreover, the JmjC domains of JMJ30, JMJ32 and REF6 showed considerable diversifications even among members of the same group, except for the highly conserved amino acids close to the Fe(II) and α-KG-binding

residues (Figure 7)(Lu et al, 2008). Such variations within the catalytic domains of JMJ proteins have been reported in human JHDM1 and JMJD2A, both of which carry out H3K36me2 demethylation (Ng et al, 2007). Thus, it is not uncommon for JMJ proteins with diverse variation within the JmjC domain to target the same substrate, as in the case of REF6, JMJ30 and JMJ32 in *Arabidopsis*. Crystal structures of JMJ30, JMJ32, REF6 and their cognate substrate (H3K27me3) may be helpful to verify substrate specificity-determining residues.

REF6 and ELF6 are first suggested to be H3K9me3 demethylase as H3K9me3 levels are obviously increased in at the *TCH4* locus in *elf6* and *ref6* mutants (Yu et al, 2008b). Later, another group reported that H3K4me2/3 and H3K36me2 levels were increased at the *FLC* locus in *ref6* mutant, and showed that purified REF6:6xHis can specifically demethylate H3K4me2/3 and H3K36me2/3 *in vitro*, suggesting that REF6 functions as an H3K4me2/3 and H3K36me2/3 demethylase (Ko et al, 2010). REF6 and ELF6 were homologous to the JHDM3 group from human and mouse which also targets H3K9 and H3K36 methylation, suggesting conservation of substrate specificity among homologs in different species (Klose et al, 2006a). However, recent publication showed that REF6 function as H3K27me2/3-specific demethylase, as *REF6* decreased H3K27me2/3 levels both *in vitro* and *in vivo*, overexpression of *REF6* showed global drastic decrease of H3K27me3 levels, and *ref6* mutant showed H3K27me3 hypermethylation in several hundred endogenous genes (Lu et al, 2011b). ELF6, a homolog of REF6, is also shown to be able to demethylate H3K27me2/3 *in vivo* (Crevillen et al, 2014). Similar to the case in REF6, JMJ30 is also recently reported to be

able to demethylate H3K36me2/3 *in vitro* and increases H3K36me2 levels at the *FT* locus (Yan et al, 2014). These conflicting results among these reports suggest that JMJ proteins might have context-dependent substrate specificity. Indeed, the metazoan JHDM3/JMJD2 group proteins such as JMJD2A show dual substrate specificity for H3K9 and H3K36 methylation, a repressive and activating mark respectively (Klose et al, 2006a).

In *Arabidopsis*, the JmjC-domain only group contains another member JMJ31/AT5G19840, which has a different variant for one of its key α-KG binding amino acid and is likely to be enzymatically inactive (Klose et al, 2006a). Moreover, the analysis of the *jmj31* mutants was not included in this study because single *jmj31* mutants showed no obvious phenotype, and triple mutant of *jmj30 jmj32 jmj31* showed no enhanced phenotype and still flowered at the same time as *jmj30 jmj32* double mutant (data not shown). Intriguingly, the first JMJ protein isolated in mouse, Jarid2/Jumonji, also has the same amino acid substitution (serine in place of threonine/tyrosine/phenyalanine at one of its key α-KG-binding residues)(Takeuchi et al, 1995). The mouse Jarid2/Jumonji protein regulates multiple developmental processes including cardiac, hematopoietic and hepatic development (Mysliwiec et al, 2012). Despite being enzymatically inactive, Jarid2/Jumonji interacts with other histone modifier to transcriptionally regulate its target genes (Mysliwiec et al, 2012; Pasini et al, 2010). Hence, it would be interesting to study the potential function of JMJ31 in modulating chromatin status of genes in *Arabidopsis*.

4.7 Future prospect of JMJ30 and JMJ32

Ours and others' previous data had shown that overexpression of JMJ30 is sufficient to induce a mild late-flowering phenotype in Col by upregulating *FLC* expression (Gan et al, 2014a; Lu et al, 2011c). To control the floral transition, I aim to chemically induce the overexpression of *JMJ30* by utilizing the β-estradiol inducible XVE system (Zuo et al, 2000). By regulating the expression of *FLC*, I would be able to control flowering time and this can be utilized to increase the yield and prevent the loss of crops. When the growth condition is conducive, prolonging the fruit-bearing growth period would increase the final yield. On the other hand, if harsh growth conditions (e.g. droughts, heat waves) are to be expected ahead, inducing flowering and fruiting of crops may prevent unrecoverable losses.

Furthermore, in the agriculture industry, it is empirically known that the effect of vernalization can be reversed by exposing the seeds or plantlets to a short period of high temperature, a process termed devernalization (Gregory & Purvis, 1937; Purvis & Gregory, 1945). The similar phenomenon can be observed in the model organism of *Brassicaceae*, *Arabidopsis*, and a recent paper highlight that *FLC* is involved in this pathway (Perilleux et al, 2013). Reversal of the floral induction is important for certain crop plants that are harvests for their leaves (e.g. cabbage) or roots (e.g. root chicory). The seeds of crop plants are frequently stored at a lower temperature to prevent spoilage, and prolong their lifespan and viability. However this storage temperature will induce the crop plant to flower early when planted, which may not be favorable phenomenon from the agricultural view for crop plants, such as onion sets planted for the bulbs with fleshy leaves, or sugar beets planted for

their fleshy root. Thus, a devernalization treatment would reverse this effect and allow optimum production of crops. Farmers control the timing of flowering of crops by treating the plants under a certain temperature. However, this empirical practice of flowering control is labor-intensive and does not always work as expected. I am hence interested in understanding whether JMJ30/JMJ32 participates in the devernalization process, and develop a molecular-based technology to control flowering time in useful crop plants. To achieve these aspects, it is important to understand the molecular mechanism of flowering, and I believe that JMJ30/JMJ32 would play a role in epigenetically regulating the expression of the key floral repressor *FLC* in these scenarios.

References

Abe M, Kobayashi Y, Yamamoto S, Daimon Y, Yamaguchi A, Ikeda Y, Ichinoki H, Notaguchi M, Goto K, Araki T (2005) FD, a bZIP protein mediating signals from the floral pathway integrator FT at the shoot apex. *Science* **309:** 1052-1056

Achard P, Herr A, Baulcombe DC, Harberd NP (2004) Modulation of floral development by a gibberellin-regulated microRNA. *Development* **131:** 3357-3365

Agger K, Cloos PA, Christensen J, Pasini D, Rose S, Rappsilber J, Issaeva I, Canaani E, Salcini AE, Helin K (2007) UTX and JMJD3 are histone H3K27 demethylases involved in HOX gene regulation and development. *Nature* **449:** 731-734

Angel A, Song J, Dean C, Howard M (2011) A Polycomb-based switch underlying quantitative epigenetic memory. *Nature* **476:** 105-108

Avner P, Heard E (2001) X-chromosome inactivation: counting, choice and initiation. *Nature reviews Genetics* **2:** 59-67

Balasubramanian S, Sureshkumar S, Lempe J, Weigel D (2006) Potent induction of Arabidopsis thaliana flowering by elevated growth temperature. *PLoS genetics* **2:** e106

Bastow R, Mylne JS, Lister C, Lippman Z, Martienssen RA, Dean C (2004) Vernalization requires epigenetic silencing of FLC by histone methylation. *Nature* **427:** 164-167

Baumbusch LO, Thorstensen T, Krauss V, Fischer A, Naumann K, Assalkhou R, Schulz I, Reuter G, Aalen RB (2001) The Arabidopsis thaliana genome contains at least 29 active genes encoding SET domain proteins that can be assigned to four evolutionarily conserved classes. *Nucleic acids research* **29:** 4319-4333

Baurle I, Dean C (2008) Differential interactions of the autonomous pathway RRM proteins and chromatin regulators in the silencing of Arabidopsis targets. *PloS one* **3:** e2733

Berger N, Dubreucq B, Roudier F, Dubos C, Lepiniec L (2011) Transcriptional regulation of Arabidopsis LEAFY COTYLEDON2 involves

RLE, a cis-element that regulates trimethylation of histone H3 at lysine-27. *The Plant cell* **23:** 4065-4078

Berger SL, Kouzarides T, Shiekhattar R, Shilatifard A (2009) An operational definition of epigenetics. *Genes & development* **23:** 781-783

Blazquez MA, Ahn JH, Weigel D (2003) A thermosensory pathway controlling flowering time in Arabidopsis thaliana. *Nat Genet* **33:** 168-171

Bratzel F, López-Torrejón G, Koch M, Del Pozo JC, Calonje M (2010) Keeping Cell Identity in Arabidopsis Requires PRC1 RING-Finger Homologs that Catalyze H2A Monoubiquitination. *Current Biology* **20:** 1853-1859

Burgold T, Voituron N, Caganova M, Tripathi PP, Menuet C, Tusi BK, Spreafico F, Bevengut M, Gestreau C, Buontempo S, Simeone A, Kruidenier L, Natoli G, Casola S, Hilaire G, Testa G (2012) The H3K27 demethylase JMJD3 is required for maintenance of the embryonic respiratory neuronal network, neonatal breathing, and survival. *Cell reports* **2:** 1244-1258

Buzas DM, Robertson M, Finnegan EJ, Helliwell CA (2011) Transcription-dependence of histone H3 lysine 27 trimethylation at the Arabidopsis polycomb target gene FLC. *Plant J* **65:** 872-881

Caicedo AL, Stinchcombe JR, Olsen KM, Schmitt J, Purugganan MD (2004) Epistatic interaction between Arabidopsis FRI and FLC flowering time genes generates a latitudinal cline in a life history trait. *Proceedings of the National Academy of Sciences of the United States of America* **101:** 15670-15675

Calonje M (2014) PRC1 marks the difference in plant PcG repression. *Molecular plant* **7:** 459-471

Capovilla G, Schmid M, Pose D (2015) Control of flowering by ambient temperature. *Journal of experimental botany* **66:** 59-69

Carrozza MJ, Li B, Florens L, Suganuma T, Swanson SK, Lee KK, Shia WJ, Anderson S, Yates J, Washburn MP, Workman JL (2005) Histone H3 methylation by Set2 directs deacetylation of coding regions by Rpd3S to suppress spurious intragenic transcription. *Cell* **123:** 581-592

Chanvivattana Y, Bishopp A, Schubert D, Stock C, Moon YH, Sung ZR, Goodrich J (2004) Interaction of Polycomb-group proteins controlling flowering in Arabidopsis. *Development* **131:** 5263-5276

Chen J, Burke JJ, Velten J, Xin Z (2006) FtsH11 protease plays a critical role in Arabidopsis thermotolerance. *Plant J* **48:** 73-84

Cho JN, Ryu JY, Jeong YM, Park J, Song JJ, Amasino RM, Noh B, Noh YS (2012) Control of seed germination by light-induced histone arginine demethylation activity. *Developmental cell* **22:** 736-748

Chouard P (1960) Vernalization and its Relations to Dormancy. *Annual Review of Plant Physiology* **11:** 191-238

Clough SJ, Bent AF (1998) Floral dip: a simplified method for Agrobacterium-mediated transformation of Arabidopsis thaliana. *Plant J* **16:** 735-743

Corbesier L, Vincent C, Jang S, Fornara F, Fan Q, Searle I, Giakountis A, Farrona S, Gissot L, Turnbull C, Coupland G (2007) FT protein movement contributes to long-distance signaling in floral induction of Arabidopsis. *Science* **316:** 1030-1033

Crevillen P, Yang H, Cui X, Greeff C, Trick M, Qiu Q, Cao X, Dean C (2014) Epigenetic reprogramming that prevents transgenerational inheritance of the vernalized state. *Nature* **515:** 587-590

Cubas P, Vincent C, Coen E (1999) An epigenetic mutation responsible for natural variation in floral symmetry. *Nature* **401:** 157-161

Cuthbert GL, Daujat S, Snowden AW, Erdjument-Bromage H, Hagiwara T, Yamada M, Schneider R, Gregory PD, Tempst P, Bannister AJ, Kouzarides T (2004) Histone deimination antagonizes arginine methylation. *Cell* **118:** 545-553

Czechowski T, Stitt M, Altmann T, Udvardi MK, Scheible WR (2005) Genome-wide identification and testing of superior reference genes for transcript normalization in Arabidopsis. *Plant physiology* **139:** 5-17

De Lucia F, Crevillen P, Jones AM, Greb T, Dean C (2008) A PHD-polycomb repressive complex 2 triggers the epigenetic silencing of FLC during vernalization. *Proceedings of the National Academy of Sciences of the United States of America* **105:** 16831-16836

Deng W, Ying H, Helliwell CA, Taylor JM, Peacock WJ, Dennis ES (2011) FLOWERING LOCUS C (FLC) regulates development pathways throughout

the life cycle of Arabidopsis. *Proceedings of the National Academy of Sciences of the United States of America* **108:** 6680-6685

Dennis ES, Peacock WJ (2007) Epigenetic regulation of flowering. *Curr Opin Plant Biol* **10:** 520-527

Edwards KD, Anderson PE, Hall A, Salathia NS, Locke JC, Lynn JR, Straume M, Smith JQ, Millar AJ (2006) FLOWERING LOCUS C mediates natural variation in the high-temperature response of the Arabidopsis circadian clock. *The Plant cell* **18:** 639-650

Folco HD, Pidoux AL, Urano T, Allshire RC (2008) Heterochromatin and RNAi are required to establish CENP-A chromatin at centromeres. *Science* **319:** 94-97

Gan ES, Huang J, Ito T (2013) Functional roles of histone modification, chromatin remodeling and microRNAs in Arabidopsis flower development. *International review of cell and molecular biology* **305:** 115-161

Gan ES, Xu Y, Wong JY, Geraldine Goh J, Sun B, Wee WY, Huang J, Ito T (2014a) Jumonji demethylases moderate precocious flowering at elevated temperature via regulation of FLC in Arabidopsis. *Nature communications* **5:** 5098

Gan ES, Xu Y, Wong JY, Goh JG, Sun B, Wee WY, Huang J, Ito T (2014b) Jumonji demethylases moderate precocious flowering at elevated temperature via regulation of FLC in Arabidopsis. *Nature communications* **5:** 5098

Gocal GF, Sheldon CC, Gubler F, Moritz T, Bagnall DJ, MacMillan CP, Li SF, Parish RW, Dennis ES, Weigel D, King RW (2001) GAMYB-like genes, flowering, and gibberellin signaling in Arabidopsis. *Plant physiology* **127:** 1682-1693

Goldberg AD, Allis CD, Bernstein E (2007) Epigenetics: a landscape takes shape. *Cell* **128:** 635-638

Goodrich J, Tweedie S (2002) Remembrance of things past: chromatin remodeling in plant development. *Annual review of cell and developmental biology* **18:** 707-746

Gregory FG, Purvis ON (1937) Devernalization of Spring Rye by Anaerobic Conditions and Revernalisation by Low Temperature. *Nature* **140:** 547

Gu X, Jiang D, Yang W, Jacob Y, Michaels SD, He Y (2011) Arabidopsis homologs of retinoblastoma-associated protein 46/48 associate with a histone deacetylase to act redundantly in chromatin silencing. *PLoS genetics* **7:** e1002366

Gu X, Le C, Wang Y, Li Z, Jiang D, He Y (2013a) Arabidopsis FLC clade members form flowering-repressor complexes coordinating responses to endogenous and environmental cues. *Nature communications* **4:** 1947

Gu X, Le C, Wang Y, Li Z, Jiang D, Wang Y, He Y (2013b) Arabidopsis FLC clade members form flowering-repressor complexes coordinating responses to endogenous and environmental cues. *Nature communications* **4:** 1947

Gu X, Wang Y, He Y (2013c) Photoperiodic regulation of flowering time through periodic histone deacetylation of the florigen gene FT. *PLoS Biol* **11:** e1001649

Guccione E, Bassi C, Casadio F, Martinato F, Cesaroni M, Schuchlautz H, Luscher B, Amati B (2007) Methylation of histone H3R2 by PRMT6 and H3K4 by an MLL complex are mutually exclusive. *Nature* **449:** 933-937

Hansen JC, Tse C, Wolffe AP (1998) Structure and function of the core histone N-termini: more than meets the eye. *Biochemistry* **37:** 17637-17641

He Y, Amasino RM (2005) Role of chromatin modification in flowering-time control. *Trends Plant Sci* **10:** 30-35

He Y, Doyle MR, Amasino RM (2004) PAF1-complex-mediated histone methylation of FLOWERING LOCUS C chromatin is required for the vernalization-responsive, winter-annual habit in Arabidopsis. *Genes & development* **18:** 2774-2784

Hellens RP, Edwards EA, Leyland NR, Bean S, Mullineaux PM (2000) pGreen: a versatile and flexible binary Ti vector for Agrobacterium-mediated plant transformation. *Plant molecular biology* **42:** 819-832

Helliwell CA, Robertson M, Finnegan EJ, Buzas DM, Dennis ES (2011) Vernalization-repression of Arabidopsis FLC requires promoter sequences but not antisense transcripts. *PloS one* **6:** e21513

Heo JB, Sung S (2011) Vernalization-mediated epigenetic silencing by a long intronic noncoding RNA. *Science* **331:** 76-79

Hepworth SR, Valverde F, Ravenscroft D, Mouradov A, Coupland G (2002) Antagonistic regulation of flowering-time gene SOC1 by CONSTANS and FLC via separate promoter motifs. *EMBO J* **21:** 4327-4337

Hong EH, Jeong YM, Ryu JY, Amasino RM, Noh B, Noh YS (2009) Temporal and spatial expression patterns of nine Arabidopsis genes encoding Jumonji C-domain proteins. *Mol Cells* **27:** 481-490

Hong S, Cho YW, Yu LR, Yu H, Veenstra TD, Ge K (2007) Identification of JmjC domain-containing UTX and JMJD3 as histone H3 lysine 27 demethylases. *Proceedings of the National Academy of Sciences of the United States of America* **104:** 18439-18444

Hornyik C, Terzi LC, Simpson GG (2010) The spen family protein FPA controls alternative cleavage and polyadenylation of RNA. *Developmental cell* **18:** 203-213

Horton JR, Upadhyay AK, Qi HH, Zhang X, Shi Y, Cheng X (2010) Enzymatic and structural insights for substrate specificity of a family of jumonji histone lysine demethylases. *Nature structural & molecular biology* **17:** 38-43

Hsia DA, Tepper CG, Pochampalli MR, Hsia EY, Izumiya C, Huerta SB, Wright ME, Chen HW, Kung HJ, Izumiya Y (2010) KDM8, a H3K36me2 histone demethylase that acts in the cyclin A1 coding region to regulate cancer cell proliferation. *Proceedings of the National Academy of Sciences of the United States of America* **107:** 9671-9676

Huang S, Litt M, Felsenfeld G (2005a) Methylation of histone H4 by arginine methyltransferase PRMT1 is essential in vivo for many subsequent histone modifications. *Genes & development* **19:** 1885-1893

Huang T, Bohlenius H, Eriksson S, Parcy F, Nilsson O (2005b) The mRNA of the Arabidopsis gene FT moves from leaf to shoot apex and induces flowering. *Science* **309:** 1694-1696

Huang Y, Fang J, Bedford MT, Zhang Y, Xu RM (2006) Recognition of histone H3 lysine-4 methylation by the double tudor domain of JMJD2A. *Science* **312:** 748-751

Ietswaart R, Wu Z, Dean C (2012) Flowering time control: another window to the connection between antisense RNA and chromatin. *Trends in genetics : TIG* **28:** 445-453

Imaizumi T, Schultz TF, Harmon FG, Ho LA, Kay SA (2005) FKF1 F-box protein mediates cyclic degradation of a repressor of CONSTANS in Arabidopsis. *Science* **309:** 293-297

Inagaki S, Miura-Kamio A, Nakamura Y, Lu F, Cui X, Cao X, Kimura H, Saze H, Kakutani T (2010) Autocatalytic differentiation of epigenetic modifications within the Arabidopsis genome. *EMBO J* **29:** 3496-3506

Ito T (2014) Growth and differentiation control in Arabidopsis flower development. *Life Science Leading Author's Review* **3**

Jacob Y, Stroud H, Leblanc C, Feng S, Zhuo L, Caro E, Hassel C, Gutierrez C, Michaels SD, Jacobsen SE (2010) Regulation of heterochromatic DNA replication by histone H3 lysine 27 methyltransferases. *Nature* **466:** 987-991

Jenuwein T, Allis CD (2001) Translating the histone code. *Science* **293:** 1074-1080

Jeong JH, Song HR, Ko JH, Jeong YM, Kwon YE, Seol JH, Amasino RM, Noh B, Noh YS (2009) Repression of FLOWERING LOCUS T chromatin by functionally redundant histone H3 lysine 4 demethylases in Arabidopsis. *PloS one* **4:** e8033

Jiang D, Kong NC, Gu X, Li Z, He Y (2011) Arabidopsis COMPASS-like complexes mediate histone H3 lysine-4 trimethylation to control floral transition and plant development. *PLoS genetics* **7:** e1001330

Jiang D, Wang Y, He Y (2008a) Repression of FLOWERING LOCUS C and FLOWERING LOCUS T by the Arabidopsis Polycomb repressive complex 2 components. *PloS one* **3:** e3404

Jiang D, Wang Y, Wang Y, He Y (2008b) Repression of FLOWERING LOCUS C and FLOWERING LOCUS T by the Arabidopsis Polycomb repressive complex 2 components. *PloS one* **3:** e3404

Jiang D, Yang W, He Y, Amasino RM (2007) Arabidopsis relatives of the human lysine-specific Demethylase1 repress the expression of FWA and FLOWERING LOCUS C and thus promote the floral transition. *The Plant cell* **19:** 2975-2987

Jones MA, Covington MF, DiTacchio L, Vollmers C, Panda S, Harmer SL (2010) Jumonji domain protein JMJD5 functions in both the plant and human

circadian systems. *Proceedings of the National Academy of Sciences of the United States of America* **107:** 21623-21628

Jones MA, Harmer S (2011) JMJD5 Functions in concert with TOC1 in the arabidopsis circadian system. *Plant signaling & behavior* **6:** 445-448

Jones RS, Gelbart WM (1993) The Drosophila Polycomb-group gene Enhancer of zeste contains a region with sequence similarity to trithorax. *Mol Cell Biol* **13:** 6357-6366

Kahn TG, Stenberg P, Pirrotta V, Schwartz YB (2014) Combinatorial interactions are required for the efficient recruitment of pho repressive complex (PhoRC) to polycomb response elements. *PLoS genetics* **10:** e1004495

Kanda H, Nguyen A, Chen L, Okano H, Hariharan IK (2013) The Drosophila ortholog of MLL3 and MLL4, trithorax related, functions as a negative regulator of tissue growth. *Mol Cell Biol* **33:** 1702-1710

Kirmizis A, Santos-Rosa H, Penkett CJ, Singer MA, Vermeulen M, Mann M, Bahler J, Green RD, Kouzarides T (2007) Arginine methylation at histone H3R2 controls deposition of H3K4 trimethylation. *Nature* **449:** 928-932

Klose RJ, Kallin EM, Zhang Y (2006a) JmjC-domain-containing proteins and histone demethylation. *Nature reviews Genetics* **7:** 715-727

Klose RJ, Yamane K, Bae Y, Zhang D, Erdjument-Bromage H, Tempst P, Wong J, Zhang Y (2006b) The transcriptional repressor JHDM3A demethylates trimethyl histone H3 lysine 9 and lysine 36. *Nature* **442:** 312-316

Klose RJ, Zhang Y (2007) Regulation of histone methylation by demethylimination and demethylation. *Nature reviews Molecular cell biology* **8:** 307-318

Ko JH, Mitina I, Tamada Y, Hyun Y, Choi Y, Amasino RM, Noh B, Noh YS (2010) Growth habit determination by the balance of histone methylation activities in Arabidopsis. *EMBO J* **29:** 3208-3215

Koornneef M, Hanhart CJ, van der Veen JH (1991) A genetic and physiological analysis of late flowering mutants in Arabidopsis thaliana. *Molecular & general genetics : MGG* **229:** 57-66

Kotake T, Takada S, Nakahigashi K, Ohto M, Goto K (2003) Arabidopsis TERMINAL FLOWER 2 gene encodes a heterochromatin protein 1 homolog and represses both FLOWERING LOCUS T to regulate flowering time and several floral homeotic genes. *Plant & cell physiology* **44:** 555-564

Ku M, Koche RP, Rheinbay E, Mendenhall EM, Endoh M, Mikkelsen TS, Presser A, Nusbaum C, Xie X, Chi AS, Adli M, Kasif S, Ptaszek LM, Cowan CA, Lander ES, Koseki H, Bernstein BE (2008) Genomewide analysis of PRC1 and PRC2 occupancy identifies two classes of bivalent domains. *PLoS genetics* **4:** e1000242

Kumar SV, Lucyshyn D, Jaeger KE, Alos E, Alvey E, Harberd NP, Wigge PA (2012) Transcription factor PIF4 controls the thermosensory activation of flowering. *Nature* **484:** 242-245

Kumar SV, Wigge PA (2010) H2A.Z-containing nucleosomes mediate the thermosensory response in Arabidopsis. *Cell* **140:** 136-147

Lafos M, Kroll P, Hohenstatt ML, Thorpe FL, Clarenz O, Schubert D (2011) Dynamic regulation of H3K27 trimethylation during Arabidopsis differentiation. *PLoS genetics* **7:** e1002040

Lagarou A, Mohd-Sarip A, Moshkin YM, Chalkley GE, Bezstarosti K, Demmers JA, Verrijzer CP (2008) dKDM2 couples histone H2A ubiquitylation to histone H3 demethylation during Polycomb group silencing. *Genes & development* **22:** 2799-2810

Lan F, Bayliss PE, Rinn JL, Whetstine JR, Wang JK, Chen S, Iwase S, Alpatov R, Issaeva I, Canaani E, Roberts TM, Chang HY, Shi Y (2007) A histone H3 lysine 27 demethylase regulates animal posterior development. *Nature* **449:** 689-694

Lando D, Peet DJ, Gorman JJ, Whelan DA, Whitelaw ML, Bruick RK (2002) FIH-1 is an asparaginyl hydroxylase enzyme that regulates the transcriptional activity of hypoxia-inducible factor. *Genes & development* **16:** 1466-1471

Laubinger S, Marchal V, Le Gourrierec J, Wenkel S, Adrian J, Jang S, Kulajta C, Braun H, Coupland G, Hoecker U (2006) Arabidopsis SPA proteins regulate photoperiodic flowering and interact with the floral inducer CONSTANS to regulate its stability. *Development* **133:** 3213-3222

Lee I, Bleecker A, Amasino R (1993) Analysis of naturally occurring late flowering in Arabidopsis thaliana. *Molecular & general genetics : MGG* **237:** 171-176

Lee JH, Ryu HS, Chung KS, Pose D, Kim S, Schmid M, Ahn JH (2013a) Regulation of Ambient Temperature-Responsive Flowering by MADS-Box Transcription Factor Repressor Complexes. *Science* **342:** 628-632

Lee JH, Ryu HS, Chung KS, Pose D, Kim S, Schmid M, Ahn JH (2013b) Regulation of temperature-responsive flowering by MADS-box transcription factor repressors. *Science* **342:** 628-632

Lee JH, Yoo SJ, Park SH, Hwang I, Lee JS, Ahn JH (2007) Role of SVP in the control of flowering time by ambient temperature in Arabidopsis. *Genes & development* **21:** 397-402

Lee MH, Lee Y, Hwang I (2013c) In vivo localization in Arabidopsis protoplasts and root tissue. *Methods Mol Biol* **1043:** 113-120

Lewis EB (1978) A gene complex controlling segmentation in Drosophila. *Nature* **276:** 565-570

Lewis PH (1949) PC: Polycomb. *Drosophila Information Service* **21:** 69

Li C, Gu M, Shi N, Zhang H, Yang X, Osman T, Liu Y, Wang H, Vatish M, Jackson S, Hong Y (2011a) Mobile FT mRNA contributes to the systemic florigen signalling in floral induction. *Scientific reports* **1:** 73

Li C, Zhang K, Zeng X, Jackson S, Zhou Y, Hong Y (2009) A cis element within flowering locus T mRNA determines its mobility and facilitates trafficking of heterologous viral RNA. *Journal of virology* **83:** 3540-3548

Li D, Liu C, Shen L, Wu Y, Chen H, Robertson M, Helliwell CA, Ito T, Meyerowitz E, Yu H (2008) A repressor complex governs the integration of flowering signals in Arabidopsis. *Developmental cell* **15:** 110-120

Li W, Wang Z, Li J, Yang H, Cui S, Wang X, Ma L (2011b) Overexpression of AtBMI1C, a polycomb group protein gene, accelerates flowering in Arabidopsis. *PloS one* **6:** e21364

Liebman SW, Chernoff YO (2012) Prions in yeast. *Genetics* **191:** 1041-1072

Lindroth AM, Shultis D, Jasencakova Z, Fuchs J, Johnson L, Schubert D, Patnaik D, Pradhan S, Goodrich J, Schubert I, Jenuwein T, Khorasanizadeh S, Jacobsen SE (2004) Dual histone H3 methylation marks at lysines 9 and 27 required for interaction with CHROMOMETHYLASE3. *EMBO J* **23:** 4286-4296

Litt M, Qiu Y, Huang S (2009) Histone arginine methylations: their roles in chromatin dynamics and transcriptional regulation. *Bioscience reports* **29:** 131-141

Liu C, Chen H, Er HL, Soo HM, Kumar PP, Han JH, Liou YC, Yu H (2008a) Direct interaction of AGL24 and SOC1 integrates flowering signals in Arabidopsis. *Development* **135:** 1481-1491

Liu C, Thong Z, Yu H (2009) Coming into bloom: the specification of floral meristems. *Development* **136:** 3379-3391

Liu F, Marquardt S, Lister C, Swiezewski S, Dean C (2010) Targeted 3' processing of antisense transcripts triggers Arabidopsis FLC chromatin silencing. *Science* **327:** 94-97

Liu L, Liu C, Hou X, Xi W, Shen L, Tao Z, Wang Y, Yu H (2012) FTIP1 is an essential regulator required for florigen transport. *PLoS Biol* **10:** e1001313

Liu LJ, Zhang YC, Li QH, Sang Y, Mao J, Lian HL, Wang L, Yang HQ (2008b) COP1-mediated ubiquitination of CONSTANS is implicated in cryptochrome regulation of flowering in Arabidopsis. *The Plant cell* **20:** 292-306

Lu F, Cui X, Zhang S, Jenuwein T, Cao X (2011a) Arabidopsis REF6 is a histone H3 lysine 27 demethylase. *Nat Genet* **43:** 715-719

Lu F, Cui X, Zhang S, Liu C, Cao X (2010) JMJ14 is an H3K4 demethylase regulating flowering time in Arabidopsis. *Cell research* **20:** 387-390

Lu F, Li G, Cui X, Liu C, Wang XJ, Cao X (2008) Comparative analysis of JmjC domain-containing proteins reveals the potential histone demethylases in Arabidopsis and rice. *J Integr Plant Biol* **50:** 886-896

Lu FL, Cui X, Zhang SB, Jenuwein T, Cao XF (2011b) Arabidopsis REF6 is a histone H3 lysine 27 demethylase. *Nat Genet* **43:** 715-U144

Lu KJ, Huang NC, Liu YS, Lu CA, Yu TS (2012) Long-distance movement of Arabidopsis FLOWERING LOCUS T RNA participates in systemic floral regulation. *RNA biology* **9:** 653-662

Lu SX, Knowles SM, Webb CJ, Celaya RB, Cha C, Siu JP, Tobin EM (2011c) The Jumonji C domain-containing protein JMJ30 regulates period length in the Arabidopsis circadian clock. *Plant physiology* **155:** 906-915

Lysak M, Fransz P, Schubert I (2006) Cytogenetic analyses of Arabidopsis. *Methods Mol Biol* **323:** 173-186

Mathieu O, Probst AV, Paszkowski J (2005a) Distinct regulation of histone H3 methylation at lysines 27 and 9 by CpG methylation in Arabidopsis. *EMBO J* **24:** 2783-2791

Mathieu O, Probst AV, Paszkowski J (2005b) Distinct regulation of histone H3 methylation at lysines 27 and 9 by CpG methylation in Arabidopsis. *The EMBO journal* **24:** 2783-2791

Michaels SD, Amasino RM (1999) FLOWERING LOCUS C encodes a novel MADS domain protein that acts as a repressor of flowering. *The Plant cell* **11:** 949-956

Michaels SD, Amasino RM (2001) Loss of FLOWERING LOCUS C activity eliminates the late-flowering phenotype of FRIGIDA and autonomous pathway mutations but not responsiveness to vernalization. *The Plant cell* **13:** 935-941

Moon J, Suh SS, Lee H, Choi KR, Hong CB, Paek NC, Kim SG, Lee I (2003) The SOC1 MADS-box gene integrates vernalization and gibberellin signals for flowering in Arabidopsis. *Plant J* **35:** 613-623

Murray MG, Thompson WF (1980) Rapid isolation of high molecular weight plant DNA. *Nucleic acids research* **8:** 4321-4325

Mutasa-Gottgens E, Hedden P (2009) Gibberellin as a factor in floral regulatory networks. *Journal of experimental botany* **60:** 1979-1989

Mysliwiec MR, Carlson CD, Tietjen J, Hung H, Ansari AZ, Lee Y (2012) Jarid2 (Jumonji, AT rich interactive domain 2) regulates NOTCH1 expression via histone modification in the developing heart. *J Biol Chem* **287:** 1235-1241

Nagel DH, Kay SA (2012) Complexity in the wiring and regulation of plant circadian networks. *Current biology : CB* **22:** R648-657

Nakano Y, Higuchi Y, Sumitomo K, Hisamatsu T (2013) Flowering retardation by high temperature in chrysanthemums: involvement of FLOWERING LOCUS T-like 3 gene repression. *Journal of experimental botany* **64:** 909-920

Ng SS, Kavanagh KL, McDonough MA, Butler D, Pilka ES, Lienard BM, Bray JE, Savitsky P, Gileadi O, von Delft F, Rose NR, Offer J, Scheinost JC, Borowski T, Sundstrom M, Schofield CJ, Oppermann U (2007) Crystal structures of histone demethylase JMJD2A reveal basis for substrate specificity. *Nature* **448:** 87-91

Niu L, Lu F, Pei Y, Liu C, Cao X (2007) Regulation of flowering time by the protein arginine methyltransferase AtPRMT10. *EMBO reports* **8:** 1190-1195

Niu L, Zhang Y, Pei Y, Liu C, Cao X (2008) Redundant requirement for a pair of PROTEIN ARGININE METHYLTRANSFERASE4 homologs for the proper regulation of Arabidopsis flowering time. *Plant physiology* **148:** 490-503

Noh B, Lee SH, Kim HJ, Yi G, Shin EA, Lee M, Jung KJ, Doyle MR, Amasino RM, Noh YS (2004) Divergent roles of a pair of homologous jumonji/zinc-finger-class transcription factor proteins in the regulation of Arabidopsis flowering time. *The Plant cell* **16:** 2601-2613

Oh E, Zhu JY, Wang ZY (2012) Interaction between BZR1 and PIF4 integrates brassinosteroid and environmental responses. *Nature cell biology* **14:** 802-809

Pal S, Vishwanath SN, Erdjument-Bromage H, Tempst P, Sif S (2004) Human SWI/SNF-associated PRMT5 methylates histone H3 arginine 8 and negatively regulates expression of ST7 and NM23 tumor suppressor genes. *Mol Cell Biol* **24:** 9630-9645

Pasini D, Cloos PA, Walfridsson J, Olsson L, Bukowski JP, Johansen JV, Bak M, Tommerup N, Rappsilber J, Helin K (2010) JARID2 regulates binding of the Polycomb repressive complex 2 to target genes in ES cells. *Nature* **464:** 306-310

Patton DA, Schetter AL, Franzmann LH, Nelson K, Ward ER, Meinke DW (1998) An embryo-defective mutant of arabidopsis disrupted in the final step of biotin synthesis. *Plant physiology* **116:** 935-946

Perilleux C, Pieltain A, Jacquemin G, Bouche F, Detry N, D'Aloia M, Thiry L, Aljochim P, Delansnay M, Mathieu AS, Lutts S, Tocquin P (2013) A root chicory MADS box sequence and the Arabidopsis flowering repressor FLC share common features that suggest conserved function in vernalization and de-vernalization responses. *Plant J* **75:** 390-402

Pien S, Grossniklaus U (2007) Polycomb group and trithorax group proteins in Arabidopsis. *Biochim Biophys Acta* **1769:** 375-382

Praveen KS, Fowke LC, King J (1985) An efficient procedure for isolation of nuclei from plant protoplasts. *Protoplasma* **128:** 184-189

Purvis ON, Gregory FG (1945) Devernalization by High Temperature. *Nature* **155:** 113-114

Putterill J, Robson F, Lee K, Simon R, Coupland G (1995) The CONSTANS gene of Arabidopsis promotes flowering and encodes a protein showing similarities to zinc finger transcription factors. *Cell* **80:** 847-857

Rosloski SM, Singh A, Jali SS, Balasubramanian S, Weigel D, Grbic V (2013) Functional analysis of splice variant expression of MADS AFFECTING FLOWERING 2 of Arabidopsis thaliana. *Plant molecular biology* **81:** 57-69

Roudier F, Ahmed I, Berard C, Sarazin A, Mary-Huard T, Cortijo S, Bouyer D, Caillieux E, Duvernois-Berthet E, Al-Shikhley L, Giraut L, Despres B, Drevensek S, Barneche F, Derozier S, Brunaud V, Aubourg S, Schnittger A, Bowler C, Martin-Magniette ML, Robin S, Caboche M, Colot V (2011) Integrative epigenomic mapping defines four main chromatin states in Arabidopsis. *EMBO J* **30:** 1928-1938

Sawa M, Nusinow DA, Kay SA, Imaizumi T (2007) FKF1 and GIGANTEA complex formation is required for day-length measurement in Arabidopsis. *Science* **318:** 261-265

Saze H, Shiraishi A, Miura A, Kakutani T (2008) Control of genic DNA methylation by a jmjC domain-containing protein in Arabidopsis thaliana. *Science* **319:** 462-465

Schmitz RJ, Sung S, Amasino RM (2008) Histone arginine methylation is required for vernalization-induced epigenetic silencing of FLC in winter-annual Arabidopsis thaliana. *Proceedings of the National Academy of Sciences of the United States of America* **105:** 411-416

Schoeftner S, Sengupta AK, Kubicek S, Mechtler K, Spahn L, Koseki H, Jenuwein T, Wutz A (2006) Recruitment of PRC1 function at the initiation of X inactivation independent of PRC2 and silencing. *EMBO J* **25:** 3110-3122

Schubert D, Clarenz O, Goodrich J (2005) Epigenetic control of plant development by Polycomb-group proteins. *Curr Opin Plant Biol* **8:** 553-561

Schuettengruber B, Martinez AM, Iovino N, Cavalli G (2011) Trithorax group proteins: switching genes on and keeping them active. *Nature reviews Molecular cell biology* **12:** 799-814

Schwartz YB, Pirrotta V (2008) Polycomb complexes and epigenetic states. *Curr Opin Cell Biol* **20:** 266-273

Searle I, He Y, Turck F, Vincent C, Fornara F, Krober S, Amasino RA, Coupland G (2006) The transcription factor FLC confers a flowering response to vernalization by repressing meristem competence and systemic signaling in Arabidopsis. *Genes & development* **20:** 898-912

Sengoku T, Yokoyama S (2011) Structural basis for histone H3 Lys 27 demethylation by UTX/KDM6A. *Genes & development* **25:** 2266-2277

Shi Y, Lan F, Matson C, Mulligan P, Whetstine JR, Cole PA, Casero RA, Shi Y (2004) Histone demethylation mediated by the nuclear amine oxidase homolog LSD1. *Cell* **119:** 941-953

Shindo C, Aranzana MJ, Lister C, Baxter C, Nicholls C, Nordborg M, Dean C (2005) Role of FRIGIDA and FLOWERING LOCUS C in determining variation in flowering time of Arabidopsis. *Plant physiology* **138:** 1163-1173

Sing A, Pannell D, Karaiskakis A, Sturgeon K, Djabali M, Ellis J, Lipshitz HD, Cordes SP (2009) A vertebrate Polycomb response element governs segmentation of the posterior hindbrain. *Cell* **138:** 885-897

Soppe WJ, Bentsink L, Koornneef M (1999) The early-flowering mutant efs is involved in the autonomous promotion pathway of Arabidopsis thaliana. *Development* **126:** 4763-4770

Spedaletti V, Polticelli F, Capodaglio V, Schinina ME, Stano P, Federico R, Tavladoraki P (2008) Characterization of a lysine-specific histone demethylase from Arabidopsis thaliana. *Biochemistry* **47:** 4936-4947

Srikanth A, Schmid M (2011) Regulation of flowering time: all roads lead to Rome. *Cell Mol Life Sci* **68:** 2013-2037

Stassen MJ, Bailey D, Nelson S, Chinwalla V, Harte PJ (1995) The Drosophila trithorax proteins contain a novel variant of the nuclear receptor type DNA binding domain and an ancient conserved motif found in other chromosomal proteins. *Mech Dev* **52:** 209-223

Strahl BD, Allis CD (2000) The language of covalent histone modifications. *Nature* **403:** 41-45

Sun B, Looi LS, Guo S, He Z, Gan ES, Huang J, Xu Y, Wee WY, Ito T (2014) Timing mechanism dependent on cell division is invoked by Polycomb eviction in plant stem cells. *Science* **343:** 1248559

Sun B, Xu Y, Ng KH, Ito T (2009) A timing mechanism for stem cell maintenance and differentiation in the Arabidopsis floral meristem. *Genes & development* **23:** 1791-1804

Sung S, Amasino RM (2004) Vernalization in Arabidopsis thaliana is mediated by the PHD finger protein VIN3. *Nature* **427:** 159-164

Sung S, He Y, Eshoo TW, Tamada Y, Johnson L, Nakahigashi K, Goto K, Jacobsen SE, Amasino RM (2006) Epigenetic maintenance of the vernalized state in Arabidopsis thaliana requires LIKE HETEROCHROMATIN PROTEIN 1. *Nat Genet* **38:** 706-710

Swiezewski S, Liu F, Magusin A, Dean C (2009) Cold-induced silencing by long antisense transcripts of an Arabidopsis Polycomb target. *Nature* **462:** 799-802

Takeuchi T, Yamazaki Y, Katoh-Fukui Y, Tsuchiya R, Kondo S, Motoyama J, Higashinakagawa T (1995) Gene trap capture of a novel mouse gene, jumonji, required for neural tube formation. *Genes & development* **9:** 1211-1222

Thines BC, Youn Y, Duarte MI, Harmon FG (2014) The time of day effects of warm temperature on flowering time involve PIF4 and PIF5. *Journal of experimental botany* **65:** 1141-1151

Thorstensen T, Grini PE, Aalen RB (2011) SET domain proteins in plant development. *Biochim Biophys Acta* **1809:** 407-420

Tschiersch B, Hofmann A, Krauss V, Dorn R, Korge G, Reuter G (1994) The protein encoded by the Drosophila position-effect variegation suppressor gene Su(var)3-9 combines domains of antagonistic regulators of homeotic gene complexes. *EMBO J* **13:** 3822-3831

Tsukada Y, Fang J, Erdjument-Bromage H, Warren ME, Borchers CH, Tempst P, Zhang Y (2006) Histone demethylation by a family of JmjC domain-containing proteins. *Nature* **439:** 811-816

Turck F, Roudier F, Farrona S, Martin-Magniette ML, Guillaume E, Buisine N, Gagnot S, Martienssen RA, Coupland G, Colot V (2007) Arabidopsis TFL2/LHP1 specifically associates with genes marked by trimethylation of histone H3 lysine 27. *PLoS genetics* **3:** e86

Vakoc CR, Mandat SA, Olenchock BA, Blobel GA (2005) Histone H3 lysine 9 methylation and HP1gamma are associated with transcription elongation through mammalian chromatin. *Molecular cell* **19:** 381-391

Vandamme J, Lettier G, Sidoli S, Di Schiavi E, Norregaard Jensen O, Salcini AE (2012) The C. elegans H3K27 demethylase UTX-1 is essential for normal development, independent of its enzymatic activity. *PLoS genetics* **8:** e1002647

Waddington CH (1942) The epigenotype. *Endeavour* **1:** 18 - 20

Wang Y, Gu X, Yuan W, Schmitz RJ, He Y (2014) Photoperiodic control of the floral transition through a distinct polycomb repressive complex. *Developmental cell* **28:** 727-736

Wang Y, Wysocka J, Sayegh J, Lee YH, Perlin JR, Leonelli L, Sonbuchner LS, McDonald CH, Cook RG, Dou Y, Roeder RG, Clarke S, Stallcup MR, Allis CD, Coonrod SA (2004) Human PAD4 regulates histone arginine methylation levels via demethylimination. *Science* **306:** 279-283

Whetstine JR, Nottke A, Lan F, Huarte M, Smolikov S, Chen Z, Spooner E, Li E, Zhang G, Colaiacovo M, Shi Y (2006) Reversal of histone lysine trimethylation by the JMJD2 family of histone demethylases. *Cell* **125:** 467-481

Winter D, Vinegar B, Nahal H, Ammar R, Wilson GV, Provart NJ (2007) An "Electronic Fluorescent Pictograph" browser for exploring and analyzing large-scale biological data sets. *PloS one* **2:** e718

Woo CJ, Kharchenko PV, Daheron L, Park PJ, Kingston RE (2010) A region of the human HOXD cluster that confers polycomb-group responsiveness. *Cell* **140:** 99-110

Wood CC, Robertson M, Tanner G, Peacock WJ, Dennis ES, Helliwell CA (2006) The Arabidopsis thaliana vernalization response requires a polycomb-like protein complex that also includes VERNALIZATION INSENSITIVE 3. *Proceedings of the National Academy of Sciences of the United States of America* **103:** 14631-14636

Wu TY, Juan YT, Hsu YH, Wu SH, Liao HT, Fung RW, Charng YY (2013) Interplay between heat shock proteins HSP101 and HSA32 prolongs heat acclimation memory posttranscriptionally in Arabidopsis. *Plant physiology* **161:** 2075-2084

Xu Y, Gan ES, Zhou J, Wee WY, Zhang X, Ito T (2014) Arabidopsis MRG domain proteins bridge two histone modifications to elevate expression of flowering genes. *Nucleic acids research* **42:** 10960-10974

Xu Y, Wang Y, Stroud H, Gu X, Sun B, Gan ES, Ng KH, Jacobsen SE, He Y, Ito T (2013) A matrix protein silences transposons and repeats through interaction with retinoblastoma-associated proteins. *Current biology : CB* **23:** 345-350

Yan D, Zhang Y, Niu L, Yuan Y, Cao X (2007) Identification and characterization of two closely related histone H4 arginine 3 methyltransferases in Arabidopsis thaliana. *The Biochemical journal* **408:** 113-121

Yan Y, Shen L, Chen Y, Bao S, Thong Z, Yu H (2014) A MYB-domain protein EFM mediates flowering responses to environmental cues in Arabidopsis. *Developmental cell* **30:** 437-448

Yang C, Bratzel F, Hohmann N, Koch M, Turck F, Calonje M (2013) VAL- and AtBMI1-mediated H2Aub initiate the switch from embryonic to postgerminative growth in Arabidopsis. *Current biology : CB* **23:** 1324-1329

Yang H, Han Z, Cao Y, Fan D, Li H, Mo H, Feng Y, Liu L, Wang Z, Yue Y, Cui S, Chen S, Chai J, Ma L (2012) A companion cell-dominant and

developmentally regulated H3K4 demethylase controls flowering time in Arabidopsis via the repression of FLC expression. *PLoS genetics* **8:** e1002664

Yang W, Jiang D, Jiang J, He Y (2010) A plant-specific histone H3 lysine 4 demethylase represses the floral transition in Arabidopsis. *Plant J* **62:** 663-673

Yoo SK, Chung KS, Kim J, Lee JH, Hong SM, Yoo SJ, Yoo SY, Lee JS, Ahn JH (2005) CONSTANS activates SUPPRESSOR OF OVEREXPRESSION OF CONSTANS 1 through FLOWERING LOCUS T to promote flowering in Arabidopsis. *Plant physiology* **139:** 770-778

Yu X, Li L, Guo M, Chory J, Yin Y (2008a) Modulation of brassinosteroid-regulated gene expression by Jumonji domain-containing proteins ELF6 and REF6 in Arabidopsis. *Proceedings of the National Academy of Sciences of the United States of America* **105:** 7618-7623

Yu X, Li L, Li L, Guo M, Chory J, Yin Y (2008b) Modulation of brassinosteroid-regulated gene expression by Jumonji domain-containing proteins ELF6 and REF6 in Arabidopsis. *Proceedings of the National Academy of Sciences of the United States of America* **105:** 7618-7623

Zhang H, van Nocker S (2002) The VERNALIZATION INDEPENDENCE 4 gene encodes a novel regulator of FLOWERING LOCUS C. *Plant J* **31:** 663-673

Zhang X, Clarenz O, Cokus S, Bernatavichute YV, Pellegrini M, Goodrich J, Jacobsen SE (2007) Whole-genome analysis of histone H3 lysine 27 trimethylation in Arabidopsis. *PLoS Biol* **5:** e129

Zhen Y, Dhakal P, Ungerer MC (2011) Fitness benefits and costs of cold acclimation in Arabidopsis thaliana. *The American naturalist* **178:** 44-52

Zheng B, Chen X (2011) Dynamics of histone H3 lysine 27 trimethylation in plant development. *Curr Opin Plant Biol* **14:** 123-129

Zuo J, Niu QW, Chua NH (2000) Technical advance: An estrogen receptor-based transactivator XVE mediates highly inducible gene expression in transgenic plants. *Plant J* **24:** 265-273

Appendix

List of publications

List of publications published during the course of study (in reverse chronological order). A major portion of the results presented in this thesis is published in the research paper marked with (***) below.

- Eng-Seng Gan, Yifeng Xu, Toshiro Ito. (2015) Dynamics of H3K27me3 methylation and demethylation in plant development. *Plant Signaling & Behavior*, in press.
- Siyi Guo, Bo Sun, Liang-Sheng Looi, Yifeng Xu, Eng-Seng Gan, Jiangbo Huang, Toshiro Ito. (2015) Co-ordination of flower development through epigenetic regulation in two model species: rice and Arabidopsis. *Plant and Cell Physiology*, pii: pcv037.
- ***Eng-Seng Gan, Yifeng Xu, Jie-Yun Wong, Jessamine Geraldine Goh, Bo Sun, Wan-Yi Wee, Jiangbo Huang, Toshiro Ito. (2014) Jumonji demethylases moderate precocious flowering at elevated temperature via regulation of FLC in Arabidopsis. *Nature Communications* **5**, 5098.
- Yifeng Xu, Eng-Seng Gan, Jie Zhou, Wan-Yi Wee, Xiaoyu Zhang, Toshiro Ito. (2014) Arabidopsis MRG domain proteins bridge two histone modifications to elevate expression of flowering genes. *Nucleic Acids Research* **42**, 10960-74.
- Bo Sun, Liang-Sheng Looi, Siyi Guo, Zemiao He, Eng-Seng Gan, Jiangbo Huang, Yifeng Xu, Wan-Yi Wee, Toshiro Ito. (2014) Timing mechanism dependent on cell division is invoked by Polycomb eviction in plant stem cells. *Science* **343**, 1248559.
- Yifeng Xu, Eng-Seng Gan, Toshiro Ito. (2014) Misexpression approaches for the manipulation of flower development. *Methods in molecular biology* **1110**, 383-99.

- Eng-Seng Gan, Jiangbo Huang, Toshiro Ito. (2013) Functional roles of histone modification, chromatin remodeling and microRNAs in arabidopsis flower development. *International Review of Cell and Molecular Biology* **305**, 115-161.

- Yifeng Xu, Eng-Seng Gan, Yuehui He, Toshiro Ito. (2013) Flowering and genome integrity control by a nuclear matrix protein in Arabidopsis. *Nucleus* **4**, 274-6.

- Yifeng Xu, Eng-Seng Gan, Toshiro Ito. (2013) The AT-hook/PPC domain protein TEK negatively regulates floral repressors including MAF4 and MAF5. *Plant Signaling & Behavior* **8**, e25006.

- Yifeng Xu, Yizhong Wang, Hume Stroud, Xiaofeng Gu, Bo Sun, Eng-Seng Gan, Kian Hong Ng, Steven E. Jacobsen, Yuehui He, Toshiro Ito. (2013) A matrix protein silences transposons and repeats through interaction with retinoblastoma-associated proteins. *Current Biology* **23**, 345-350.

Supplementary Data 1. Genes affected in *jmj30-2 jmj32-1* compared to WT grown under LD 29°C conditions.

Gene ID	P-value	Fold change compared to Col WT	DESCRIPTION
AT1G01305	0.0175	1.580 down	unknown protein
AT1G02070	0.0964	2.025 down	unknown protein
AT1G05420	0.0379	1.631 down	OFP12 (OVATE FAMILY PROTEIN 12)
AT1G05930	0.0927	1.538 down	DNA binding
AT1G10095	0.0206	1.923 down	protein prenyltransferase
AT1G10990	0.0355	1.775 down	unknown protein
AT1G11030	0.0333	1.571 down	pre-tRNA
AT1G11630	0.0196	1.619 down	pentatricopeptide (PPR) repeat-containing protein
AT1G12030	0.0497	2.402 down	unknown protein
AT1G13608	0.0411	3.254 down	Encodes a defensin-like (DEFL) family protein.
AT1G13660	0.0752	2.166 down	transposable element gene
AT1G13860	0.0505	1.645 down	dehydration-responsive protein-related
AT1G15415	0.059	1.793 down	The protein encoded by this gene was identified as a part of pollen proteome by mass spec analysis. It has weak homology to LEA (late embryo abundant) proteins.
AT1G15480	0.0968	1.541 down	DNA binding
AT1G16160	0.0678	1.797 down	WAKL5 (wall associated kinase-like 5); kinase
AT1G17277	0.0425	1.584 down	transposable element gene
AT1G17770	0.0373	1.721 down	SUVH7 (SU(VAR)3-9 HOMOLOG 7); DNA binding / histone-lysine N-methyltransferase/ zinc ion binding
AT1G18510	0.0162	1.527 down	TET16 (TETRASPANIN 16)
AT1G18860	0.0265	1.725 down	WRKY61; transcription factor
AT1G18930	0.0454	1.981 down	transposable element gene
AT1G21360	0.0584	1.563 down	GLTP2 (glycolipid transfer protein 2); glycolipid binding / glycolipid transporter
AT1G21528	0.0621	2.238 down	unknown protein
AT1G21890	0.0706	1.554 down	nodulin MtN21 family protein
AT1G22130	0.0635	1.506 down	AGL104 (AGAMOUS-LIKE 104); DNA binding / transcription factor
AT1G22150	0.0661	1.658 down	SULTR1;3; sulfate transmembrane transporter
AT1G22240	0.0611	1.938 down	APUM8 (Arabidopsis Pumilio 8); RNA binding / binding
AT1G22690	0.0318	1.760 down	gibberellin-responsive protein, putative
AT1G23020	0.0549	2.319 down	FRO3; ferric-chelate reductase
AT1G23510	0.0888	1.526 down	unknown protein
AT1G24250	0.0628	2.123 down	paired amphipathic helix repeat-containing protein
AT1G24320	0.039	1.613 down	alpha-glucosidase, putative
AT1G24967	0.0424	1.663 down	transposable element gene
AT1G25422	0.0264	1.683 down	unknown protein
AT1G26420	0.0127	1.826 down	FAD-binding domain-containing protein
AT1G26900	0.0163	1.539 down	pentatricopeptide (PPR) repeat-containing protein
AT1G27080	0.0434	1.695 down	NRT1.6 (NITRATE TRANSPORTER 1.6); low affinity nitrate transmembrane transporter/ transporter
AT1G27790	0.00527	2.003 down	transposable element gene
AT1G28327	0.0549	2.695 down	BEST Arabidopsis thaliana protein match is: RING1B (RING 1B); protein binding / zinc ion binding (TAIR:AT1G03770.1); Has 20 Blast hits to 20 proteins in 5 species: Archae - 0; Bacteria - 0; Metazoa - 0; Fungi - 0; Plants - 20; Viruses - 0; Other Eukaryotes - 0 (source: NCBI BLink).
AT1G28465	0.000507	1.571 down	transposable element gene
AT1G29160	0.0806	1.506 down	Dof-type zinc finger domain-containing protein
AT1G29390	0.0209	1.890 down	COR314-TM2
AT1G29465	0.0357	1.994 down	unknown protein
AT1G30475	0.0789	1.684 down	BEST Arabidopsis thaliana protein match is: emb1303 (embryo defective 1303) (TAIR:AT1G56200.1); Has 15 Blast hits to 15 proteins in 2 species: Archae - 0; Bacteria - 0; Metazoa - 0; Fungi - 0; Plants - 15; Viruses - 0; Other Eukaryotes - 0 (source: NCBI BLink).
AT1G30560	0.0749	1.668 down	transporter, putative
AT1G32390	0.0666	1.568 down	transposable element gene
AT1G32880	0.0999	1.506 down	importin alpha-1 subunit, putative
AT1G32910	0.0293	1.618 down	transferase family protein
AT1G33760	0.0195	1.504 down	AP2 domain-containing transcription factor, putative
AT1G36520	0.0379	2.174 down	transposable element gene
AT1G37160	0.0516	1.709 down	transposable element gene
AT1G37867	0.0794	1.848 down	transposable element gene
AT1G37933	0.039	1.521 down	transposable element gene
AT1G38280	0.0927	1.594 down	transposable element gene
AT1G39830	0.0787	1.799 down	transposable element gene
AT1G40093	0.071	1.933 down	transposable element gene
AT1G40115	0.0259	1.545 down	transposable element gene
AT1G41720	0.0269	1.528 down	transposable element gene
AT1G41855	0.0937	1.900 down	transposable element gene
AT1G42220	0.0592	1.751 down	transposable element gene
AT1G42360	0.00626	2.276 down	transposable element gene
AT1G42393	0.042	1.551 down	transposable element gene
AT1G42590	0.0435	2.076 down	transposable element gene
AT1G42605	0.0528	2.480 down	transposable element gene
AT1G43020	0.0902	1.584 down	unknown protein
AT1G43590	0.0272	2.464 down	transposable element gene

AT1G44224	0.0458	1.697 down	Encodes a ECA1 gametogenesis related family protein
AT1G44414	0.023	2.209 down	unknown protein
AT1G44478	0.0494	1.777 down	BEST Arabidopsis thaliana protein match is: CYP59 (CYCLOPHILIN 59); RNA binding / nucleic acid binding / peptidyl-prolyl cis-trans isomerase (TAIR:AT1G53720.1); Has 293 Blast hits to 276 proteins in 65 species: Archae - 0; Bacteria - 0; Metazoa - 216; Fungi - 11; Plants - 38; Viruses - 0; Other Eukaryotes - 28 (source: NCBI BLink).
AT1G44608	0.0598	1.865 down	unknown protein
AT1G44840	0.083	1.954 down	transposable element gene
AT1G48130	0.048	1.942 down	ATPER1; antioxidant/ thioredoxin peroxidase
AT1G48190	0.033	1.677 down	CONTAINS InterPro DOMAIN/s: Galactose oxidase/kelch, beta-propeller (InterPro:IPR011043), Kelch repeat type 2 (InterPro:IPR011498), Kelch-type beta propeller (InterPro:IPR015915); BEST Arabidopsis thaliana protein match is: kelch repeat-containing F-box family protein (TAIR:AT4G39590.1); Has 89 Blast hits to 89 proteins in 2 species: Archae - 0; Bacteria - 0; Metazoa - 0; Fungi - 0; Plants - 89; Viruses - 0; Other Eukaryotes - 0 (source: NCBI BLink).
AT1G49005	0.0516	2.635 down	CLE11 (CLAVATA3/ESR-RELATED 11); protein binding / receptor binding
AT1G51240	0.0936	1.714 down	CONTAINS InterPro DOMAIN/s: Plant self-incompatibility S1 (InterPro:IPR010264); BEST Arabidopsis thaliana protein match is: unknown protein (TAIR:AT1G51250.1); Has 16 Blast hits to 16 proteins in 1 species: Archae - 0; Bacteria - 0; Metazoa - 0; Fungi - 0; Plants - 16; Viruses - 0; Other Eukaryotes - 0 (source: NCBI BLink).
AT1G51860	0.0688	1.643 down	leucine-rich repeat protein kinase, putative
AT1G51913	0.0809	1.630 down	unknown protein
AT1G52820	0.0483	1.850 down	2-oxoglutarate-dependent dioxygenase, putative
AT1G53820	0.0823	1.553 down	zinc finger (C3HC4-type RING finger) family protein
AT1G54200	0.0897	1.594 down	unknown protein
AT1G54560	0.0204	2.692 down	XIE; motor/ protein binding
AT1G55790	0.056	1.603 down	ATP binding / nucleotide binding / phenylalanine-tRNA ligase
AT1G56730	0.0854	1.865 down	pre-tRNA
AT1G56850	0.021	1.829 down	pre-tRNA
AT1G57650	0.0838	1.711 down	CONTAINS InterPro DOMAIN/s: Leucine-rich repeat 3 (InterPro:IPR011713); BEST Arabidopsis thaliana protein match is: disease resistance protein (TIR-NBS-LRR class), putative (TAIR:AT2G14080.1); Has 9494 Blast hits to 5230 proteins in 243 species: Archae - 14; Bacteria - 521; Metazoa - 749; Fungi - 25; Plants - 7706; Viruses - 8; Other Eukaryotes - 471 (source: NCBI BLink).
AT1G57690	0.00331	1.528 down	F-box family protein
AT1G58310	0.0194	2.145 down	F-box family protein
AT1G62035	0.0399	1.566 down	MIR171C; miRNA
AT1G62214	0.0224	1.563 down	unknown pseudogene
AT1G63550	0.0679	1.753 down	CONTAINS InterPro DOMAIN/s: Protein of unknown function DUF26 (InterPro:IPR002902); BEST Arabidopsis thaliana protein match is: receptor-like protein kinase-related (TAIR:AT1G63570.1); Has 4939 Blast hits to 2168 proteins in 204 species: Archae - 8; Bacteria - 183; Metazoa - 580; Fungi - 134; Plants - 2707; Viruses - 661; Other Eukaryotes - 666 (source: NCBI BLink).
AT1G65090	0.0348	2.374 down	unknown protein
AT1G65385	0.0961	1.514 down	pseudogene, putative serpin, blastp match of 51% identity and 9.6e-61 P-value to GP
AT1G65483	0.0237	1.972 down	unknown protein
AT1G65780	0.0251	1.575 down	tRNA-splicing endonuclease positive effector-related
AT1G66270	0.0535	1.717 down	BGLU21; catalytic/ cation binding / hydrolase, hydrolyzing O-glycosyl compounds
AT1G66930	0.0384	1.581 down	serine/threonine protein kinase family protein
AT1G68290	0.0613	1.922 down	ENDO 2 (endonuclease 2); T/G mismatch-specific endonuclease/ endonuclease/ nucleic acid binding / single-stranded DNA specific endodeoxyribonuclease
AT1G69110	0.0929	2.445 down	pseudogene, 40S ribosomal protein S20
AT1G70895	0.093	1.901 down	CLE17 (CLAVATA3/ESR-RELATED 17); protein binding / receptor binding
AT1G72100	0.0371	1.549 down	late embryogenesis abundant domain-containing protein / LEA domain-containing protein
AT1G72416	0.0141	1.517 down	heat shock protein binding
AT1G72430	0.088	1.565 down	auxin-responsive protein-related
AT1G73130	0.0846	1.654 down	unknown protein
AT1G73780	0.0539	1.954 down	protease inhibitor/seed storage/lipid transfer protein (LTP) family protein
AT1G75470	0.0241	2.004 down	ATPUP15; purine transmembrane transporter
AT1G75550	0.0972	1.580 down	glycine-rich protein
AT1G75590	0.0583	1.899 down	auxin-responsive family protein
AT1G75790	0.0575	2.225 down	sks18 (SKU5 Similar 18); copper ion binding / pectinesterase
AT1G75960	0.00123	2.097 down	AMP-binding protein, putative
AT1G76500	0.0464	2.073 down	SOB3 (SUPPRESSOR OF PHYB-4#3); DNA binding
AT1G78600	0.0343	1.564 down	LZF1 (LIGHT-REGULATED ZINC FINGER PROTEIN 1); transcription factor/ zinc ion binding
AT1G79075	0.0441	1.714 down	other RNA
AT1G80740	0.00926	1.589 down	CMT1 (CHROMOMETHYLASE 1); DNA binding / chromatin binding
AT2G03320	0.1	1.742 down	unknown protein
AT2G03600	0.0474	1.794 down	ATUPS3 (Arabidopsis thaliana ureide permease 3)
AT2G03950	0.0624	1.730 down	transposable element gene
AT2G04670	0.0322	1.891 down	transposable element gene
AT2G04852	0.0476	1.853 down	Potential natural antisense gene, locus overlaps with AT2G04850
AT2G05350	0.0552	1.523 down	unknown protein
AT2G05915	0.0695	21.000 down	unknown protein
AT2G06420	0.0836	1.785 down	unknown protein
AT2G06630	0.0972	1.572 down	transposable element gene
AT2G06845	0.000383	18.667 down	beta-galactosidase
AT2G07694	0.0222	1.619 down	transposable element gene
AT2G10070	0.042	1.511 down	transposable element gene
AT2G10836	0.0802	1.509 down	transposable element gene
AT2G11570	0.0144	1.543 down	unknown protein

AT2G11680	0.0641	1.504 down	transposable element gene
AT2G12130	0.0946	1.626 down	transposable element gene
AT2G12150	0.0941	1.944 down	transposable element gene
AT2G13160	0.00458	1.564 down	transposable element gene
AT2G13400	0.0302	1.638 down	transposable element gene
AT2G13865	0.06	2.072 down	transposable element gene
AT2G14200	0.0222	1.815 down	transposable element gene
AT2G14245	0.0803	1.818 down	transposable element gene
AT2G14500	0.0163	1.669 down	F-box family protein
AT2G14590	0.0978	1.671 down	transposable element gene
AT2G14730	0.0713	1.572 down	transposable element gene
AT2G14790	0.0311	1.518 down	transposable element gene
AT2G14830	0.0798	1.675 down	unknown protein
AT2G15460	0.0407	1.905 down	glycoside hydrolase family 28 protein / polygalacturonase (pectinase) family protein
AT2G16520	0.0851	1.538 down	BEST Arabidopsis thaliana protein match is: zinc finger (C3HC4-type RING finger) family protein (TAIR:AT3G45570.1); Has 44 Blast hits to 41 proteins in 1 species: Archae - 0; Bacteria - 0; Metazoa - 0; Fungi - 0; Plants - 44; Viruses - 0; Other Eukaryotes - 0 (source: NCBI BLink).
AT2G17556	0.00503	2.142 down	unknown protein
AT2G18196	0.0745	1.730 down	metal ion binding
AT2G18270	0.015	1.552 down	unknown protein
AT2G19960	0.0182	1.753 down	hAT dimerisation domain-containing protein / transposase-related
AT2G20298	0.0674	1.726 down	pseudogene of exonuclease family protein
AT2G21720	0.0314	1.531 down	unknown protein
AT2G22121	0.061	1.687 down	LCR35 (Low-molecular-weight cysteine-rich 35)
AT2G22380	0.0884	2.363 down	pre-tRNA
AT2G23190	0.0419	1.527 down	CYP81D7; electron carrier/ heme binding / iron ion binding / monooxygenase/ oxygen binding
AT2G23490	0.0183	1.728 down	transposable element gene
AT2G23570	0.00917	1.633 down	MES19 (METHYL ESTERASE 19); hydrolase
AT2G23590	0.0037	1.671 down	MES8 (METHYL ESTERASE 8); hydrolase/ hydrolase, acting on ester bonds
AT2G23710	0.0988	1.876 down	transposable element gene
AT2G23834	0.0271	1.576 down	unknown protein
AT2G24950	0.0615	1.916 down	unknown protein
AT2G25370	0.0691	1.582 down	zinc finger protein-related
AT2G25482	0.0905	2.406 down	Encodes a ECA1 gametogenesis related family protein
AT2G26050	0.0149	1.633 down	zinc ion binding
AT2G26882	0.0454	1.996 down	other RNA
AT2G26940	0.0969	1.576 down	zinc finger (C2H2 type) family protein
AT2G29628	0.072	1.642 down	unknown protein
AT2G29800	0.014	1.912 down	kelch repeat-containing F-box family protein
AT2G29830	0.0154	2.328 down	kelch repeat-containing F-box family protein
AT2G30750	0.013	2.106 down	CYP71A12 (cytochrome P450, family 71, subfamily A, polypeptide 12); electron carrier/ heme binding / iron ion binding / monooxygenase/ oxygen binding
AT2G31590	0.0351	1.539 down	unknown protein
AT2G32740	0.0838	1.873 down	exostosin family protein
AT2G32750	0.0258	1.610 down	exostosin family protein
AT2G33090	0.0302	1.644 down	CONTAINS InterPro DOMAIN/s: TFIIS N-terminal (InterPro:IPR017923), Transcription elongation factor, TFIIS/CRSP70, N-terminal, sub-type (InterPro:IPR003617); BEST Arabidopsis thaliana protein match is: unknown protein (TAIR:AT2G33300.1); Has 40 Blast hits to 40 proteins in 10 species: Archae - 0; Bacteria - 3; Metazoa - 0; Fungi - 0; Plants - 36; Viruses - 0; Other Eukaryotes - 1 (source: NCBI BLink).
AT2G33190	0.0657	1.524 down	F-box family protein
AT2G36540	0.0616	2.118 down	NLI interacting factor (NIF) family protein
AT2G38300	0.0394	1.624 down	DNA binding / transcription factor
AT2G38310	0.0611	1.581 down	unknown protein
AT2G39110	0.00928	1.726 down	protein kinase, putative
AT2G39410	0.0397	1.710 down	hydrolase, alpha/beta fold family protein
AT2G40330	0.0999	1.662 down	Bet v I allergen family protein
AT2G41240	0.0531	16.797 down	BHLH100 (BASIC HELIX-LOOP-HELIX PROTEIN 100); DNA binding / transcription factor
AT2G44970	0.00403	2.659 down	lipase-related
AT2G47040	0.0802	1.500 down	VGD1 (VANGUARD1); enzyme inhibitor/ pectinesterase
AT3G01325	0.0637	1.509 down	Expressed protein
AT3G01360	0.0535	1.828 down	unknown protein
AT3G03080	0.0554	1.708 down	NADP-dependent oxidoreductase, putative
AT3G04200	0.0137	1.912 down	germin-like protein, putative
AT3G04440	0.0121	1.530 down	unknown protein
AT3G05480	0.0469	1.562 down	RAD9
AT3G06040	0.00639	2.136 down	ribosomal protein L12 family protein
AT3G06090	0.0259	1.847 down	unknown protein
AT3G06990	0.0821	1.699 down	DC1 domain-containing protein
AT3G07115	0.0898	1.926 down	pre-tRNA
AT3G10430	0.0444	1.996 down	F-box family protein
AT3G11980	0.0541	1.644 down	MS2 (MALE STERILITY 2); fatty acyl-CoA reductase (alcohol-forming)/ oxidoreductase, acting on the CH-CH group of donors, NAD or NADP as acceptor
AT3G12510	0.093	1.539 down	unknown protein
AT3G13260	0.0742	1.545 down	transposable element gene
AT3G13855	0.0518	1.575 down	U6-26; snRNA
AT3G14431	0.031	2.072 down	unknown protein
AT3G15440	0.029	1.584 down	BEST Arabidopsis thaliana protein match is: zinc finger (C3HC4-type RING finger) family protein (TAIR:AT3G15740.1); Has 6 Blast hits to 6 proteins in 1 species: Archae - 0; Bacteria

			- 0; Metazoa - 0; Fungi - 0; Plants - 6; Viruses - 0; Other Eukaryotes - 0 (source: NCBI BLink).
AT3G16050	0.0203	1.517 down	A37; protein heterodimerization
AT3G16430	0.00608	1.651 down	JAL31 (JACALIN-RELATED LECTIN 31); copper ion binding
AT3G16880	0.0524	1.820 down	F-box protein-related
AT3G16895	0.0906	1.690 down	Encodes a defensin-like (DEFL) family protein.
AT3G18930	0.0469	1.818 down	zinc finger (C3HC4-type RING finger) family protein
AT3G19430	0.0723	2.021 down	late embryogenesis abundant protein-related / LEA protein-related
AT3G20220	0.0324	1.649 down	auxin-responsive protein, putative
AT3G20810	0.00165	86.824 down	transcription factor jumonji (jmjC) domain-containing protein
AT3G22730	0.0667	2.115 down	F-box family protein
AT3G23171	0.0438	1.667 down	unknown protein
AT3G23720	0.0183	1.631 down	transposable element gene
AT3G25090	0.00324	2.388 down	F-box family protein-related
AT3G25420	0.0774	1.922 down	scpl21 (serine carboxypeptidase-like 21); serine-type carboxypeptidase
AT3G25440	0.0627	1.566 down	RNA binding
AT3G25750	0.0358	1.627 down	F-box family protein
AT3G26860	0.0355	1.518 down	CONTAINS InterPro DOMAIN/s: Plant self-incompatibility S1 (InterPro:IPR010264); BEST Arabidopsis thaliana protein match is: unknown protein (TAIR:AT3G27331.1); Has 21 Blast hits to 21 proteins in 1 species: Archae - 0; Bacteria - 0; Metazoa - 0; Fungi - 0; Plants - 21; Viruses - 0; Other Eukaryotes - 0 (source: NCBI BLink).
AT3G27140	0.0178	2.220 down	protein phosphatase 2C, putative / PP2C, putative
AT3G28020	0.0603	1.523 down	BEST Arabidopsis thaliana protein match is: ATP binding / DNA binding (TAIR:AT3G48770.1); Has 26 Blast hits to 21 proteins in 4 species: Archae - 0; Bacteria - 0; Metazoa - 0; Fungi - 0; Plants - 26; Viruses - 0; Other Eukaryotes - 0 (source: NCBI BLink).
AT3G28150	0.0406	1.763 down	unknown protein
AT3G28321	0.0445	1.593 down	unknown protein
AT3G28890	0.064	1.665 down	AtRLP43 (Receptor Like Protein 43); kinase/ protein binding
AT3G28958	0.000211	1.697 down	plastocyanin-like domain-containing protein
AT3G29545	0.0247	2.751 down	transposable element gene
AT3G29600	0.013	2.297 down	transposable element gene
AT3G29820	0.0523	1.931 down	transposable element gene
AT3G30393	0.0777	1.765 down	transposable element gene
AT3G30580	0.0537	1.593 down	unknown protein
AT3G30670	0.0244	1.549 down	transposable element gene
AT3G30770	0.0563	1.728 down	ATP binding / aminoacyl-tRNA ligase/ nucleotide binding
AT3G31068	0.0753	3.352 down	unknown protein
AT3G31375	0.0602	1.968 down	transposable element gene
AT3G32080	0.0712	1.596 down	transposable element gene
AT3G32387	0.0791	1.592 down	pseudogene, putative clpB heat shock protein, blastp match of 63% identity and 5.8e-148 P-value to GP
AT3G32391	0.0497	1.701 down	transposable element gene
AT3G32896	0.0539	1.806 down	unknown protein
AT3G32903	0.00783	1.638 down	transposable element gene
AT3G32912	0.0636	1.842 down	transposable element gene
AT3G32925	0.0978	2.493 down	transposable element gene
AT3G33066	0.0175	1.530 down	transposable element gene
AT3G33565	0.05	1.630 down	transposable element gene
AT3G42115	0.00812	1.521 down	transposable element gene
AT3G42410	0.0287	1.541 down	transposable element gene
AT3G42440	0.0625	1.680 down	transposable element gene
AT3G42530	0.0772	1.577 down	transposable element gene
AT3G43150	0.0226	1.852 down	unknown protein
AT3G43154	0.0424	1.861 down	transposable element gene
AT3G43357	0.0469	1.697 down	transposable element gene
AT3G43360	0.035	3.538 down	transposable element gene
AT3G43444	0.0585	1.779 down	transposable element gene
AT3G43447	0.00218	1.551 down	transposable element gene
AT3G43485	0.0241	2.318 down	transposable element gene
AT3G43546	0.0858	1.528 down	transposable element gene
AT3G44115	0.085	1.796 down	unknown protein
AT3G44250	0.00843	2.186 down	CYP71B38; electron carrier/ heme binding / iron ion binding / monooxygenase/ oxygen binding
AT3G44390	0.0967	1.525 down	transposable element gene
AT3G44440	0.097	1.510 down	unknown protein
AT3G44704	0.0771	1.610 down	unknown protein
AT3G46310	0.0433	1.744 down	unknown protein
AT3G46380	0.0605	1.756 down	unknown protein
AT3G49700	0.0157	1.903 down	ACS9 (1-AMINOCYCLOPROPANE-1-CARBOXYLATE SYNTHASE 9); 1-aminocyclopropane-1-carboxylate synthase
AT3G50010	0.0465	2.991 down	DC1 domain-containing protein
AT3G51370	0.064	1.539 down	protein phosphatase 2C, putative / PP2C, putative
AT3G53015	0.0183	1.600 down	MIR771a; miRNA
AT3G53232	0.091	2.061 down	RTFL1 (ROTUNDIFOLIA LIKE 1)
AT3G53294	0.0346	1.738 down	unknown protein
AT3G53330	0.0849	1.764 down	plastocyanin-like domain-containing protein
AT3G55300	0.062	1.531 down	transposable element gene
AT3G55590	0.0752	1.649 down	GDP-mannose pyrophosphorylase, putative
AT3G56530	0.0838	1.658 down	anac064 (Arabidopsis NAC domain containing protein 64); transcription factor
AT3G56970	0.0347	7.358 down	BHLH038; DNA binding / transcription factor

AT3G56980	0.0205	8.315 down	BHLH039; DNA binding / transcription factor
AT3G57958	0.0603	2.239 down	unknown protein
AT3G58620	0.0557	1.573 down	TTL4 (Tetratricopetide-repeat Thioredoxin-Like 4); binding
AT3G58877	0.0611	1.670 down	unknown protein
AT3G59130	0.0498	1.545 down	CONTAINS InterPro DOMAIN/s: DC1 (InterPro:IPR004146), C1-like (InterPro:IPR011424); BEST Arabidopsis thaliana protein match is: DC1 domain-containing protein (TAIR:AT3G59120.1); Has 842 Blast hits to 430 proteins in 13 species: Archae - 0; Bacteria - 0; Metazoa - 3; Fungi - 0; Plants - 833; Viruses - 0; Other Eukaryotes - 6 (source: NCBI BLink).
AT3G61340	0.0538	1.907 down	F-box family protein
AT3G61829	0.0213	1.944 down	unknown protein
AT3G61930	0.0747	1.741 down	unknown protein
AT3G62150	0.00469	1.828 down	PGP21 (P-GLYCOPROTEIN 21); ATPase, coupled to transmembrane movement of substances
AT4G00460	0.0189	1.561 down	Rho guanyl-nucleotide exchange factor
AT4G02690	0.00667	1.952 down	glutamate binding
AT4G03050	0.0758	1.548 down	AOP3; iron ion binding / oxidoreductase
AT4G03823	0.0338	1.558 down	pseudogene of unknown protein
AT4G03826	0.0786	1.805 down	transposable element gene
AT4G04105	0.0245	2.329 down	transposable element gene
AT4G05350	0.0423	1.561 down	zinc finger (C3HC4-type RING finger) family protein
AT4G05575	0.0173	1.594 down	Pseudogene of AT5G30520; unknown protein
AT4G06530	0.0414	1.754 down	transposable element gene
AT4G06546	0.0152	2.093 down	transposable element gene
AT4G06560	0.0295	1.535 down	transposable element gene
AT4G06614	0.0493	1.653 down	transposable element gene
AT4G06672	0.00609	1.986 down	transposable element gene
AT4G06692	0.0296	1.938 down	transposable element gene
AT4G06700	0.047	1.623 down	transposable element gene
AT4G06726	0.0425	1.550 down	transposable element gene
AT4G06734	0.00584	1.575 down	transposable element gene
AT4G06752	0.0203	3.128 down	transposable element gene
AT4G07494	0.0223	1.704 down	transposable element gene
AT4G07522	0.0707	1.555 down	transposable element gene
AT4G07896	0.0125	2.134 down	transposable element gene
AT4G08054	0.0945	1.635 down	transposable element gene
AT4G08078	0.085	1.605 down	transposable element gene
AT4G08275	0.0224	1.736 down	transposable element gene
AT4G08405	0.0945	1.608 down	transposable element gene
AT4G09280	0.0749	1.544 down	transposable element gene
AT4G10720	0.0304	3.274 down	ankyrin repeat family protein
AT4G11470	0.019	1.817 down	protein kinase family protein
AT4G12160	0.0616	1.751 down	pseudogene, 40S ribosomal protein S9 (RPS9A), ribosomal protein S9.e - slime mold,PIR1:R3DO24; blastp match of 56% identity and 7.2e-09 P-value to SP
AT4G12360	0.00726	1.603 down	protease inhibitor/seed storage/lipid transfer protein (LTP) family protein
AT4G13390	0.0491	1.734 down	proline-rich extensin-like family protein
AT4G13860	0.1	2.514 down	glycine-rich RNA-binding protein, putative
AT4G16230	0.0777	2.182 down	carboxylesterase/ hydrolase, acting on ester bonds
AT4G17453	0.0919	1.684 down	unknown protein
AT4G18690	0.0895	1.682 down	unknown protein
AT4G19280	0.00198	1.789 down	transposable element gene
AT4G19820	0.00616	1.571 down	glycosyl hydrolase family 18 protein
AT4G20220	0.0837	2.324 down	CONTAINS InterPro DOMAIN/s: Reverse transcriptase, RNA-dependent DNA polymerase (InterPro:IPR013103); Has 58 Blast hits to 58 proteins in 7 species: Archae - 0; Bacteria - 0; Metazoa - 0; Fungi - 0; Plants - 58; Viruses - 0; Other Eukaryotes - 0 (source: NCBI BLink).
AT4G20235	0.053	1.748 down	CYP71A28; electron carrier/ heme binding / iron ion binding / monooxygenase
AT4G20440	0.0494	1.783 down	smB (small nuclear ribonucleoprotein associated protein B)
AT4G20650	0.0821	1.605 down	CONTAINS InterPro DOMAIN/s: Protein of unknown function DUF26 (InterPro:IPR002902), Protein of unknown function DUF1204 (InterPro:IPR009596); BEST Arabidopsis thaliana protein match is: receptor-like protein kinase-related (TAIR:AT4G20640.1); Has 882 Blast hits to 868 proteins in 42 species: Archae - 2; Bacteria - 18; Metazoa - 43; Fungi - 4; Plants - 811; Viruses - 0; Other Eukaryotes - 4 (source: NCBI BLink).
AT4G20900	0.0167	1.947 down	MS5 (MALE-STERILE 5)
AT4G21200	0.0317	1.941 down	GA2OX8 (GIBBERELLIN 2-OXIDASE 8); gibberellin 2-beta-dioxygenase
AT4G21590	0.0597	1.540 down	ENDO3 (endonuclease 3); T/G mismatch-specific endonuclease/ endonuclease/ nucleic acid binding / single-stranded DNA specific endodeoxyribonuclease
AT4G22020	0.00446	1.769 down	pseudogene, hypothetical protein, similar to uncharacterized glycine-rich protein (GI:7269047)
AT4G22635	0.0165	2.670 down	pre-tRNA
AT4G23310	0.0995	2.952 down	receptor-like protein kinase, putative
AT4G25530	0.028	2.115 down	FWA; DNA binding / protein binding / protein homodimerization/ transcription factor
AT4G27120	0.0234	1.686 down	unknown protein
AT4G27550	0.019	1.765 down	ATTPS4; alpha,alpha-trehalose-phosphate synthase (UDP-forming)/ transferase, transferring glycosyl groups
AT4G27765	0.0248	1.562 down	MIR828a; miRNA
AT4G28840	0.0229	1.736 down	unknown protein
AT4G29460	0.0574	1.547 down	phospholipase A2 gamma, secretory low molecular weight
AT4G29610	0.0729	1.788 down	cytidine deaminase, putative / cytidine aminohydrolase, putative
AT4G29930	0.0311	1.799 down	basic helix-loop-helix (bHLH) family protein
AT4G30050	0.0199	2.057 down	unknown protein
AT4G30170	0.0299	2.890 down	peroxidase, putative

AT4G30662	0.0039	1.577 down	unknown protein
AT4G31320	0.0475	1.531 down	auxin-responsive protein, putative / small auxin up RNA (SAUR_C)
AT4G31630	0.0255	2.433 down	transcriptional factor B3 family protein
AT4G33610	0.0857	1.664 down	glycine-rich protein
AT4G33860	0.0997	1.751 down	glycosyl hydrolase family 10 protein
AT4G34412	0.0975	1.531 down	CONTAINS InterPro DOMAIN/s: Kinase binding protein CGI-121 (InterPro:IPR013926); Has 194 Blast hits to 194 proteins in 96 species: Archae - 0; Bacteria - 4; Metazoa - 78; Fungi - 77; Plants - 19; Viruses - 0; Other Eukaryotes - 16 (source: NCBI BLink).
AT4G34970	0.085	2.898 down	ADF9 (ACTIN DEPOLYMERIZING FACTOR 9); actin binding
AT4G35210	0.0239	1.579 down	unknown protein
AT4G35710	0.0555	1.692 down	unknown protein
AT4G35840	0.0677	1.778 down	zinc finger (C3HC4-type RING finger) family protein
AT4G38700	0.0874	1.802 down	disease resistance-responsive family protein
AT4G39020	0.0868	1.918 down	SH3 domain-containing protein
AT4G39260	0.0432	1.858 down	GR-RBP8; RNA binding / nucleic acid binding / nucleotide binding
AT4G39320	0.00891	1.691 down	microtubule-associated protein-related
AT4G39364	0.0727	1.531 down	snoRNA
AT4G39530	0.00425	1.688 down	pentatricopeptide (PPR) repeat-containing protein
AT4G39865	0.0684	1.500 down	pre-tRNA
AT5G01040	0.0944	1.667 down	LAC8 (laccase 8); laccase
AT5G02930	0.0386	1.504 down	F-box family protein
AT5G03240	0.00783	1.570 down	UBQ3 (POLYUBIQUITIN 3); protein binding
AT5G03400	0.0187	1.572 down	unknown protein
AT5G03580	0.094	1.634 down	polyadenylate-binding protein, putative / PABP, putative
AT5G03750	0.0651	1.703 down	BEST Arabidopsis thaliana protein match is: zinc finger (C3HC4-type RING finger) family protein (TAIR:AT5G03450.1); Has 23 Blast hits to 20 proteins in 7 species: Archae - 0; Bacteria - 0; Metazoa - 2; Fungi - 0; Plants - 20; Viruses - 0; Other Eukaryotes - 1 (source: NCBI BLink).
AT5G03980	0.0646	3.293 down	GDSL-motif lipase/hydrolase family protein
AT5G03990	0.0735	1.760 down	unknown protein
AT5G04500	0.0122	1.680 down	glycosyltransferase family protein 47
AT5G05250	0.0383	1.656 down	unknown protein
AT5G05320	0.096	1.580 down	monooxygenase, putative (MO3)
AT5G05490	0.0579	2.071 down	SYN1 (SYNAPTIC 1)
AT5G07560	0.0994	1.610 down	GRP20 (GLYCINE-RICH PROTEIN 20); lipid binding / nutrient reservoir
AT5G07570	0.0644	2.928 down	glycine/proline-rich protein
AT5G07780	0.0311	3.308 down	formin homology 2 domain-containing protein / FH2 domain-containing protein
AT5G08315	0.00745	1.647 down	Encodes a defensin-like (DEFL) family protein.
AT5G09280	0.0822	3.486 down	pectate lyase family protein
AT5G09360	0.0293	2.051 down	LAC14 (laccase 14); laccase
AT5G09480	0.0521	1.782 down	hydroxyproline-rich glycoprotein family protein
AT5G09940	0.0662	1.950 down	unknown protein
AT5G10140	0.0708	3.000 down	FLC (FLOWERING LOCUS C); specific transcriptional repressor/ transcription factor
AT5G10770	0.0909	1.750 down	chloroplast nucleoid DNA-binding protein, putative
AT5G14070	0.0000825	1.605 down	ROXY2; electron carrier/ protein disulfide oxidoreductase
AT5G14130	0.0339	2.473 down	peroxidase, putative
AT5G14160	0.00323	2.357 down	F-box family protein
AT5G14920	0.0904	1.511 down	gibberellin-regulated family protein
AT5G15210	0.0867	1.570 down	ATHB30 (ARABIDOPSIS THALIANA HOMEOBOX PROTEIN 30); DNA binding / transcription factor
AT5G16190	0.0633	1.643 down	ATCSLA11; cellulose synthase/ transferase, transferring glycosyl groups
AT5G17430	0.0591	1.787 down	BBM (BABY BOOM); DNA binding / transcription factor
AT5G18340	0.0107	2.510 down	U-box domain-containing protein
AT5G19080	0.0201	1.512 down	zinc finger (C3HC4-type RING finger) family protein
AT5G20240	0.0383	2.055 down	PI (PISTILLATA); DNA binding / transcription factor
AT5G20400	0.0485	1.694 down	oxidoreductase, 2OG-Fe(II) oxygenase family protein
AT5G22600	0.0258	2.057 down	CONTAINS InterPro DOMAIN/s: FBD (InterPro:IPR013596), FBD-like (InterPro:IPR006566), Leucine-rich repeat 2 (InterPro:IPR013101); BEST Arabidopsis thaliana protein match is: F-box family protein (TAIR:AT5G22610.1); Has 491 Blast hits to 482 proteins in 9 species: Archae - 0; Bacteria - 0; Metazoa - 0; Fungi - 8; Plants - 483; Viruses - 0; Other Eukaryotes - 0 (source: NCBI BLink).
AT5G26236	0.0142	2.001 down	transposable element gene
AT5G26280	0.00804	1.872 down	meprin and TRAF homology domain-containing protein / MATH domain-containing protein
AT5G26590	0.0343	1.840 down	transposable element gene
AT5G27140	0.0736	1.508 down	SAR DNA-binding protein, putative
AT5G27345	0.0688	1.608 down	transposable element gene
AT5G27810	0.0919	1.516 down	sequence-specific DNA binding / transcription factor
AT5G28235	0.0116	2.343 down	Ulp1 protease family protein
AT5G28250	0.0399	1.548 down	transposable element gene
AT5G28615	0.0751	1.636 down	CONTAINS InterPro DOMAIN/s: RNA-directed DNA polymerase (reverse transcriptase), related (InterPro:IPR015706); BEST Arabidopsis thaliana protein match is: unknown protein (TAIR:AT4G04650.1); Has 77 Blast hits to 77 proteins in 7 species: Archae - 0; Bacteria - 0; Metazoa - 0; Fungi - 0; Plants - 77; Viruses - 0; Other Eukaryotes - 0 (source: NCBI BLink).
AT5G28644	0.0982	2.497 down	transposable element gene
AT5G30762	0.0973	1.921 down	transposable element gene
AT5G32002	0.0105	2.375 down	transposable element gene
AT5G32035	0.00692	1.535 down	transposable element gene
AT5G32161	0.0508	2.180 down	transposable element gene
AT5G32306	0.032	2.170 down	transposable element gene
AT5G32312	0.000905	2.872 down	transposable element gene

AT5G32473	0.0534	2.366 down	transposable element gene
AT5G32517	0.0791	2.192 down	transposable element gene
AT5G32726	0.0839	1.893 down	transposable element gene
AT5G33000	0.0998	1.788 down	transposable element gene
AT5G33232	0.0179	1.676 down	transposable element gene
AT5G33285	0.0112	1.638 down	transposable element gene
AT5G33315	0.0523	1.826 down	transposable element gene
AT5G33715	0.0267	1.663 down	transposable element gene
AT5G33898	0.0436	1.528 down	unknown protein
AT5G34480	0.091	1.868 down	transposable element gene
AT5G34836	0.0624	2.067 down	transposable element gene
AT5G34843	0.0246	1.560 down	transposable element gene
AT5G35604	0.00109	1.663 down	BEST Arabidopsis thaliana protein match is: myosin heavy chain-related (TAIR:AT5G32590.1); Has 34 Blast hits to 33 proteins in 13 species: Archae - 0; Bacteria - 0; Metazoa - 10; Fungi - 1; Plants - 19; Viruses - 0; Other Eukaryotes - 4 (source: NCBI BLink).
AT5G35777	0.0204	1.999 down	transposable element gene
AT5G35791	0.000721	2.409 down	transposable element gene
AT5G35912	0.0718	1.665 down	transposable element gene
AT5G35950	0.0859	1.665 down	jacalin lectin family protein
AT5G36030	0.0654	1.702 down	transposable element gene
AT5G36900	0.0749	1.814 down	unknown protein
AT5G37120	0.0521	1.734 down	transposable element gene
AT5G38120	0.0807	1.584 down	4-coumarate--CoA ligase family protein / 4-coumaroyl-CoA synthase family protein
AT5G38192	0.0779	1.898 down	transposable element gene
AT5G38390	0.0736	1.988 down	F-box family protein
AT5G38920	0.076	1.671 down	nucleic acid binding / ribonuclease H
AT5G40490	0.0448	1.847 down	RNA recognition motif (RRM)-containing protein
AT5G41505	0.0833	1.962 down	transposable element gene
AT5G42840	0.0689	2.508 down	DC1 domain-containing protein
AT5G43280	0.0954	1.561 down	ATDCI1 (DELTA(3,5),DELTA(2,4)-DIENOYL-COA ISOMERASE 1); delta3,5-delta2,4-dienoyl-CoA isomerase/ enoyl-CoA hydratase
AT5G44840	0.0685	1.695 down	glycoside hydrolase family 28 protein / polygalacturonase (pectinase) family protein
AT5G45570	0.00142	1.958 down	Ulp1 protease family protein
AT5G45820	0.04	3.384 down	CIPK20 (CBL-INTERACTING PROTEIN KINASE 20); kinase/ protein serine/threonine kinase
AT5G45880	0.0551	1.512 down	pollen Ole e 1 allergen and extensin family protein
AT5G47350	0.0927	2.134 down	palmitoyl protein thioesterase family protein
AT5G47455	0.0316	1.661 down	unknown protein
AT5G47600	0.05	2.185 down	heat shock protein-related
AT5G48280	0.0839	1.818 down	unknown protein
AT5G48330	0.0765	1.509 down	regulator of chromosome condensation (RCC1) family protein
AT5G48720	0.0159	1.921 down	XRI1 (X-RAY INDUCED TRANSCRIPT 1)
AT5G49138	0.0179	1.714 down	other RNA
AT5G49490	0.0658	1.560 down	AGL83 (AGAMOUS-LIKE 83); DNA binding / transcription factor
AT5G49743	0.0119	1.533 down	transposable element gene
AT5G50720	0.077	1.893 down	ATHVA22E
AT5G50790	0.00362	3.246 down	nodulin MtN3 family protein
AT5G51410	0.00529	1.587 down	LUC7 N_terminus domain-containing protein
AT5G52360	0.0201	1.512 down	ADF10 (ACTIN DEPOLYMERIZING FACTOR 10); actin binding
AT5G52605	0.00892	1.751 down	Encodes a defensin-like (DEFL) family protein.
AT5G53450	0.000176	1.669 down	ORG1 (OBP3-responsive gene 1); ATP binding / kinase/ protein kinase
AT5G53910	0.0468	1.929 down	(S)-2-hydroxy-acid oxidase, peroxisomal, putative / glycolate oxidase, putative / short chain alpha-hydroxy acid oxidase, putative
AT5G54062	0.0168	1.837 down	unknown protein
AT5G54320	0.0565	2.169 down	unknown protein
AT5G56050	0.0831	3.015 down	CONTAINS InterPro DOMAIN/s: Harpin-induced 1 (InterPro:IPR010847); BEST Arabidopsis thaliana protein match is: unknown protein (TAIR:AT4G26490.1); Has 322 Blast hits to 322 proteins in 28 species: Archae - 0; Bacteria - 8; Metazoa - 10; Fungi - 1; Plants - 299; Viruses - 2; Other Eukaryotes - 2 (source: NCBI BLink).
AT5G56110	0.0111	1.730 down	ATMYB103 (ARABIDOPSIS THALIANA MYB DOMAIN PROTEIN 103); DNA binding / transcription factor
AT5G57620	0.0818	1.652 down	MYB36 (myb domain protein 36); DNA binding / transcription factor
AT5G59190	0.00965	1.671 down	subtilase family protein
AT5G59200	0.0623	1.806 down	pentatricopeptide (PPR) repeat-containing protein
AT5G59680	0.0326	1.675 down	leucine-rich repeat protein kinase, putative
AT5G60460	0.0976	1.621 down	sec61beta family protein
AT5G60590	0.0379	1.715 down	yrdC protein-related
AT5G60615	0.0624	2.564 down	Encodes a defensin-like (DEFL) family protein.
AT5G61730	0.0235	1.530 down	ATATH11; ATPase, coupled to transmembrane movement of substances / transporter
AT5G62080	0.0996	1.794 down	protease inhibitor/seed storage/lipid transfer protein (LTP) family protein
AT5G62320	0.0429	1.782 down	ATMYB99 (MYB DOMAIN PROTEIN 99); DNA binding / transcription factor
AT5G62360	0.0602	1.921 down	invertase/pectin methylesterase inhibitor family protein
AT5G62430	0.086	1.713 down	CDF1 (CYCLING DOF FACTOR 1); DNA binding / protein binding / transcription factor
AT5G63600	0.0399	1.537 down	FLS5 (FLAVONOL SYNTHASE 5); flavonol synthase
AT5G64401	0.0577	1.974 down	unknown protein
AT5G65130	0.0404	2.366 down	AP2 domain-containing transcription factor, putative
AT5G66260	0.0966	1.825 down	auxin-responsive protein, putative
AT5G66985	0.0362	2.501 down	unknown protein
AT5G67245	0.0792	1.760 down	unknown protein
AT1G01020	0.037	1.790 up	ARV1
AT1G01200	0.0611	1.709 up	ATRABA3 (ARABIDOPSIS RAB GTPASE HOMOLOG A3); GTP binding

AT1G01540	0.0226	1.718 up	protein kinase family protein
AT1G02380	0.0784	1.513 up	unknown protein
AT1G02450	0.00847	1.602 up	NIMIN1 (NIM1-INTERACTING 1); protein binding
AT1G02880	0.0177	1.668 up	TPK1 (THIAMIN PYROPHOSPHOKINASE1); thiamin diphosphokinase
AT1G02965	0.0186	1.558 up	unknown protein
AT1G03106	0.0142	1.555 up	unknown protein
AT1G03180	0.0317	2.237 up	unknown protein
AT1G04220	0.0685	2.217 up	KCS2 (3-KETOACYL-COA SYNTHASE 2); fatty acid elongase
AT1G04550	0.0689	1.772 up	IAA12 (AUXIN-INDUCED PROTEIN 12); transcription factor/ transcription repressor
AT1G04640	0.0242	1.806 up	LIP2 (LIPOYLTRANSFERASE 2); lipoyltransferase
AT1G05136	0.0827	1.512 up	unknown protein
AT1G05291	0.0193	2.208 up	unknown protein
AT1G06310	0.0439	2.375 up	ACX6 (ACYL-COA OXIDASE 6); FAD binding / acyl-CoA dehydrogenase/ acyl-CoA oxidase/ electron carrier/ oxidoreductase/ oxidoreductase, acting on the CH-CH group of donors
AT1G06640	0.00686	2.821 up	2-oxoglutarate-dependent dioxygenase, putative
AT1G06645	0.0566	1.636 up	oxidoreductase
AT1G07410	0.0273	1.595 up	ATRABA2B (ARABIDOPSIS RAB GTPASE HOMOLOG A2B); GTP binding / GTPase/ protein binding
AT1G07710	0.0553	2.650 up	ankyrin repeat family protein
AT1G07745	0.0773	1.584 up	RAD51D (ARABIDOPSIS HOMOLOG OF RAD51 D); ATP binding / DNA binding / DNA-dependent ATPase
AT1G07840	0.0192	1.940 up	leucine zipper factor-related
AT1G08860	0.0749	1.628 up	BON3 (BONZAI 3); calcium-dependent phospholipid binding
AT1G08970	0.0585	2.157 up	NF-YC9 (NUCLEAR FACTOR Y, SUBUNIT C9); DNA binding / transcription factor
AT1G10417	0.0473	1.946 up	Encodes protein with unknown function whose expression is repressed by inoculation with Agrobacterium tumerifaciens.
AT1G10640	0.0898	1.598 up	polygalacturonase
AT1G10657	0.063	4.090 up	unknown protein
AT1G10740	0.0649	1.901 up	unknown protein
AT1G11250	0.0921	1.717 up	SYP125 (SYNTAXIN OF PLANTS 125); SNAP receptor
AT1G11640	0.0879	1.914 up	pre-tRNA
AT1G11980	0.0732	1.638 up	RUB3 (UBIQUITIN-RELATED PROTEIN 3)
AT1G12170	0.1	1.594 up	F-box family protein
AT1G12520	0.0132	2.419 up	ATCCS (COPPER CHAPERONE FOR SOD1); superoxide dismutase/ superoxide dismutase copper chaperone
AT1G12938	0.007	1.787 up	unknown protein
AT1G13130	0.0869	1.553 up	glycosyl hydrolase family 5 protein / cellulase family protein
AT1G13520	0.051	2.310 up	unknown protein
AT1G13580	0.0615	1.668 up	LAG13 (LAG1 LONGEVITY ASSURANCE HOMOLOG 3)
AT1G14260	0.0373	1.855 up	zinc finger (C3HC4-type RING finger) family protein
AT1G14820	0.0309	1.949 up	SEC14 cytosolic factor family protein / phosphoglyceride transfer family protein
AT1G15080	0.0113	1.745 up	LPP2 (LIPID PHOSPHATE PHOSPHATASE 2); acid phosphatase/ phosphatidate phosphatase
AT1G15180	0.025	1.573 up	MATE efflux family protein
AT1G15220	0.00744	1.535 up	CCMH; oxidoreductase
AT1G15430	0.0118	2.036 up	CONTAINS InterPro DOMAIN/s: Protein of unknown function DUF1644 (InterPro:IPR012866); BEST Arabidopsis thaliana protein match is: zinc ion binding (TAIR:AT1G80220.1); Has 144 Blast hits to 135 proteins in 7 species: Archae - 0; Bacteria - 0; Metazoa - 0; Fungi - 0; Plants - 144; Viruses - 0; Other Eukaryotes - 0 (source: NCBI BLink).
AT1G15550	0.0289	3.259 up	GA3OX1 (GIBBERELLIN 3-OXIDASE 1); gibberellin 3-beta-dioxygenase/ transcription factor binding
AT1G16220	0.0961	1.951 up	protein phosphatase 2C family protein / PP2C family protein
AT1G16540	0.0297	1.929 up	ABA3 (ABA DEFICIENT 3); Mo-molybdopterin cofactor sulfurase/ selenocysteine lyase
AT1G17145	0.036	1.637 up	protein binding / zinc ion binding
AT1G17260	0.00405	2.124 up	AHA10 (Autoinhibited H(+)-ATPase isoform 10); ATPase/ ATPase, coupled to transmembrane movement of ions, phosphorylative mechanism / cation-transporting ATPase
AT1G17890	0.0161	2.660 up	GER2; binding / catalytic/ coenzyme binding
AT1G17910	0.0527	1.525 up	wall-associated kinase, putative
AT1G18200	0.0988	1.724 up	AtRABA6b (Arabidopsis Rab GTPase homolog A6b); GTP binding / GTPase/ protein binding
AT1G18735	0.0652	2.262 up	other RNA
AT1G19640	0.0818	1.971 up	JMT (JASMONIC ACID CARBOXYL METHYLTRANSFERASE); jasmonate O-methyltransferase
AT1G20590	0.0618	2.187 up	cyclin, putative
AT1G21010	0.0312	1.652 up	unknown protein
AT1G21070	0.0108	1.620 up	transporter-related
AT1G21925	0.0792	2.329 up	Encodes a Plant thionin family protein
AT1G22230	0.0391	1.919 up	unknown protein
AT1G24070	0.0534	2.345 up	ATCSLA10; cellulose synthase/ transferase, transferring glycosyl groups
AT1G24280	0.0795	1.651 up	G6PD3 (GLUCOSE-6-PHOSPHATE DEHYDROGENASE 3); glucose-6-phosphate dehydrogenase
AT1G24470	0.0854	2.472 up	short-chain dehydrogenase/reductase (SDR) family protein
AT1G24640	0.0847	1.707 up	transposable element gene
AT1G25560	0.0162	1.804 up	TEM1 (TEMPRANILLO 1); transcription factor
AT1G26300	0.0819	1.788 up	BSD domain-containing protein
AT1G26320	0.0416	1.720 up	NADP-dependent oxidoreductase, putative
AT1G27300	0.0579	1.658 up	unknown protein
AT1G27740	0.0289	1.632 up	basic helix-loop-helix (bHLH) family protein
AT1G28307	0.0152	1.792 up	unknown protein
AT1G28700	0.0699	1.941 up	unknown protein
AT1G29120	0.0357	2.376 up	unknown protein
AT1G29170	0.00907	2.019 up	WAVE2
AT1G29580	0.0543	1.848 up	unknown protein
AT1G29790	0.0411	1.531 up	BEST Arabidopsis thaliana protein match is: methyltransferase (TAIR:AT5G40830.2); Has 127

			Blast hits to 127 proteins in 12 species: Archae - 0; Bacteria - 0; Metazoa - 0; Fungi - 0; Plants - 127; Viruses - 0; Other Eukaryotes - 0 (source: NCBI BLink).
AT1G30100	0.0646	1.734 up	NCED5 (NINE-CIS-EPOXYCAROTENOID DIOXYGENASE 5); 9-cis-epoxycarotenoid dioxygenase
AT1G30110	0.0397	1.676 up	ATNUDX25 (ARABIDOPSIS THALIANA NUDIX HYDROLASE HOMOLOG 25); bis(5'-nucleosyl)-tetraphosphatase (asymmetrical)
AT1G32337	0.0386	1.578 up	unknown protein
AT1G32585	0.0448	1.539 up	VQ motif-containing protein-related
AT1G33160	0.0216	1.734 up	pseudogene, similar to actin, blastp match of 74% identity and 8.3e-48 P-value to GP
AT1G34690	0.0899	2.121 up	pseudogene, putative maturase, blastp match of 75% identity and 2.2e-25 P-value to SP
AT1G34842	0.0499	2.388 up	transposable element gene
AT1G35170	0.0325	1.658 up	CONTAINS InterPro DOMAIN/s: TRAM, LAG1 and CLN8 homology (InterPro:IPR006634); BEST Arabidopsis thaliana protein match is: unknown protein (TAIR:AT1G35180.1); Has 92 Blast hits to 92 proteins in 36 species: Archae - 0; Bacteria - 0; Metazoa - 40; Fungi - 2; Plants - 25; Viruses - 0; Other Eukaryotes - 25 (source: NCBI BLink).
AT1G35240	0.0541	1.758 up	ARF20 (AUXIN RESPONSE FACTOR 20); transcription factor
AT1G35270	0.0404	2.177 up	pseudogene, hypothetical protein
AT1G36220	0.0381	1.529 up	pseudogene, seryl-tRNA synthetase, similar to GI:3319776 from (Zea mays); blastp match of 70% identity and 1.6e-30 P-value to SP
AT1G36763	0.0926	1.603 up	transposable element gene
AT1G36840	0.0000464	1.543 up	transposable element gene
AT1G37050	0.0297	1.504 up	transposable element gene
AT1G37150	0.00798	1.506 up	HCS2 (holocarboxylase synthetase 2); biotin-[acetyl-CoA-carboxylase] ligase/ catalytic
AT1G37200	0.0263	1.664 up	transposable element gene
AT1G37735	0.0147	1.557 up	transposable element gene
AT1G38440	0.0669	1.734 up	transposable element gene
AT1G39511	0.0829	1.553 up	transposable element gene
AT1G42480	0.00542	2.583 up	unknown protein
AT1G42695	0.0434	1.541 up	transposable element gene
AT1G43666	0.0705	2.039 up	lipid transfer protein-related
AT1G44446	0.0959	1.872 up	CH1 (CHLORINA 1); chlorophyllide a oxygenase
AT1G44940	0.0404	1.585 up	unknown protein
AT1G47290	0.0839	1.590 up	AT3BETAHSD/D1 (3BETA-HYDROXYSTEROID-DEHYDROGENASE/DECARBOXYLASE ISOFORM 1); 3-beta-hydroxy-delta5-steroid dehydrogenase/ sterol-4-alpha-carboxylate 3-dehydrogenase (decarboxylating)
AT1G47606	0.0882	1.568 up	transposable element gene
AT1G48520	0.0611	2.289 up	GATB (GLU-ADT SUBUNIT B); carbon-nitrogen ligase, with glutamine as amido-N-donor / glutaminyl-tRNA synthase (glutamine-hydrolyzing)/ ligase
AT1G48610	0.0211	3.526 up	AT hook motif-containing protein
AT1G48860	0.0934	1.663 up	3-phosphoshikimate 1-carboxyvinyltransferase, putative / 5-enolpyruvylshikimate-3-phosphate, putative / EPSP synthase, putative
AT1G49860	0.077	1.678 up	ATGSTF14; glutathione transferase
AT1G50020	0.054	1.620 up	unknown protein
AT1G50050	0.0445	1.738 up	pathogenesis-related protein, putative
AT1G50310	0.0316	2.214 up	STP9 (SUGAR TRANSPORTER 9); carbohydrate transmembrane transporter/ sugar:hydrogen symporter
AT1G50550	0.0329	1.675 up	a cytochrome P450 pseudogene
AT1G50650	0.032	1.566 up	stigma-specific Stig1 family protein
AT1G51480	0.0273	2.078 up	disease resistance protein (CC-NBS-LRR class), putative
AT1G52240	0.0573	1.752 up	ROPGEF11 (RHO GUANYL-NUCLEOTIDE EXCHANGE FACTOR 11); Rho guanyl-nucleotide exchange factor
AT1G52790	0.0454	1.640 up	oxidoreductase, 2OG-Fe(II) oxygenase family protein
AT1G54970	0.00132	1.627 up	ATPRP1 (PROLINE-RICH PROTEIN 1); structural constituent of cell wall
AT1G55420	0.00919	2.274 up	EDA11 (embryo sac development arrest 11); protein binding / zinc ion binding
AT1G55770	0.0446	1.690 up	invertase/pectin methylesterase inhibitor family protein
AT1G58050	0.0942	1.549 up	helicase domain-containing protein
AT1G58280	0.0875	1.662 up	CONTAINS InterPro DOMAIN/s: Phosphoglycerate mutase (InterPro:IPR013078); BEST Arabidopsis thaliana protein match is: unknown protein (TAIR:AT5G64460.6); Has 337 Blast hits to 337 proteins in 68 species: Archae - 0; Bacteria - 4; Metazoa - 0; Fungi - 175; Plants - 69; Viruses - 0; Other Eukaryotes - 89 (source: NCBI BLink).
AT1G59590	0.0363	2.104 up	ZCF37
AT1G59830	0.0801	1.504 up	PP2A-1; protein serine/threonine phosphatase
AT1G59980	0.021	2.019 up	ARL2 (ARG1-LIKE 2); heat shock protein binding / unfolded protein binding
AT1G60120	0.0734	1.537 up	transposable element gene
AT1G60989	0.0274	1.607 up	SCRL7 (SCR-Like 7)
AT1G61150	0.0533	1.502 up	CONTAINS InterPro DOMAIN/s: CTLH, C-terminal to LisH motif (InterPro:IPR006595), CT11-RanBPM (InterPro:IPR013144); BEST Arabidopsis thaliana protein match is: unknown protein (TAIR:AT4G09300.1); Has 486 Blast hits to 476 proteins in 122 species: Archae - 0; Bacteria - 4; Metazoa - 235; Fungi - 76; Plants - 132; Viruses - 0; Other Eukaryotes - 39 (source: NCBI BLink).
AT1G61520	0.0416	1.734 up	LHCA3; chlorophyll binding
AT1G61660	0.0323	1.648 up	basic helix-loop-helix (bHLH) family protein
AT1G62305	0.0278	1.542 up	unknown protein
AT1G62840	0.096	1.589 up	unknown protein
AT1G63390	0.0587	1.943 up	flavin-containing monooxygenase-related / FMO-related
AT1G63600	0.00499	1.803 up	protein kinase-related
AT1G63860	0.0957	2.237 up	ATP binding / protein binding / transmembrane receptor
AT1G64380	0.03	2.310 up	AP2 domain-containing transcription factor, putative
AT1G64930	0.0228	1.650 up	CYP89A7; electron carrier/ heme binding / iron ion binding / monooxygenase/ oxygen binding
AT1G65060	0.0662	1.926 up	4CL3; 4-coumarate-CoA ligase

AT1G65585	0.0924	1.655 up	pseudogene, similar to oj9911130.20, blastp match of 25% identity and 8.9e-08 P-value to GP
AT1G66090	0.0602	2.488 up	disease resistance protein (TIR-NBS class), putative
AT1G66230	0.0182	1.602 up	MYB20 (myb domain protein 20); DNA binding / transcription factor
AT1G66830	0.0576	2.406 up	leucine-rich repeat transmembrane protein kinase, putative
AT1G66852	0.0391	1.630 up	CONTAINS InterPro DOMAIN/s: X8 (InterPro:IPR012946); BEST Arabidopsis thaliana protein match is: glycosyl hydrolase family protein 17 (TAIR:AT1G66870.1); Has 719 Blast hits to 683 proteins in 29 species: Archae - 0; Bacteria - 0; Metazoa - 0; Fungi - 0; Plants - 719; Viruses - 0; Other Eukaryotes - 0 (source: NCBI BLink).
AT1G68020	0.0842	1.956 up	ATTPS6; alpha,alpha-trehalose-phosphate synthase (UDP-forming)/ transferase, transferring glycosyl groups / trehalose-phosphatase
AT1G69260	0.0239	1.918 up	AFP1 (ABI FIVE BINDING PROTEIN)
AT1G69610	0.0584	1.534 up	structural constituent of ribosome
AT1G70000	0.0825	1.509 up	DNA-binding family protein
AT1G70480	0.0152	1.934 up	unknown protein
AT1G70800	0.0216	1.986 up	C2 domain-containing protein
AT1G71015	0.0618	1.594 up	unknown protein
AT1G72960	0.0431	1.806 up	root hair defective 3 GTP-binding (RHD3) family protein
AT1G73000	0.0785	1.932 up	BEST Arabidopsis thaliana protein match is: Bet v I allergen family protein (TAIR:AT2G26040.1); Has 178 Blast hits to 178 proteins in 18 species: Archae - 0; Bacteria - 0; Metazoa - 0; Fungi - 0; Plants - 178; Viruses - 0; Other Eukaryotes - 0 (source: NCBI BLink).
AT1G74010	0.0186	1.917 up	strictosidine synthase family protein
AT1G74930	0.0944	2.614 up	ORA47; DNA binding / transcription factor
AT1G76650	0.00314	2.063 up	calcium-binding EF hand family protein
AT1G77090	0.00391	1.589 up	thylakoid lumenal 29.8 kDa protein
AT1G77410	0.0323	1.530 up	BGAL16 (beta-galactosidase 16); beta-galactosidase/ catalytic/ cation binding / sugar binding
AT1G77950	0.0876	1.571 up	AGL67 (AGAMOUS-LIKE 67); transcription factor
AT1G78200	0.0386	1.757 up	protein phosphatase 2C, putative / PP2C, putative
AT1G78290	0.0783	2.292 up	serine/threonine protein kinase, putative
AT1G78480	0.0509	1.559 up	prenyltransferase/squalene oxidase repeat-containing protein
AT1G80210	0.000975	3.627 up	CONTAINS InterPro DOMAIN/s: Mov34/MPN/PAD-1 (InterPro:IPR000555); BEST Arabidopsis thaliana protein match is: mov34 family protein (TAIR:AT3G06820.2); Has 803 Blast hits to 722 proteins in 170 species: Archae - 0; Bacteria - 3; Metazoa - 437; Fungi - 151; Plants - 118; Viruses - 0; Other Eukaryotes - 94 (source: NCBI BLink).
AT1G80555	0.0341	2.156 up	3-isopropylmalate dehydrogenase/ oxidoreductase, acting on the CH-OH group of donors, NAD or NADP as acceptor
AT2G01810	0.0658	1.545 up	PHD finger family protein
AT2G01830	0.0666	1.575 up	WOL (WOODEN LEG); cytokinin receptor/ osmosensor/ phosphoprotein phosphatase/ protein histidine kinase
AT2G01900	0.0146	1.743 up	endonuclease/exonuclease/phosphatase family protein
AT2G03280	0.0751	2.372 up	unknown protein
AT2G03410	0.0194	1.511 up	Mo25 family protein
AT2G03730	0.0917	1.641 up	ACR5; amino acid binding
AT2G04039	0.0247	1.512 up	unknown protein
AT2G04120	0.0835	1.556 up	pseudogene, RAS-related GTP binding protein, blastp match of 80% identity and 5.7e-32 P-value to SP
AT2G04270	0.000508	3.800 up	RNEE/G (RNASE E/G-LIKE); endoribonuclease
AT2G04650	0.00633	1.652 up	ADP-glucose pyrophosphorylase family protein
AT2G05690	0.0287	1.701 up	transposable element gene
AT2G06910	0.047	1.786 up	transposable element gene
AT2G06980	0.0205	2.068 up	transposable element gene
AT2G07290	0.067	1.502 up	unknown protein
AT2G10560	0.0492	1.538 up	unknown protein
AT2G10830	0.0304	1.533 up	transposable element gene
AT2G11780	0.0082	2.353 up	transposable element gene
AT2G11980	0.0575	1.567 up	transposable element gene
AT2G12385	0.0497	1.835 up	transposable element gene
AT2G13190	0.0257	1.609 up	transposable element gene
AT2G13530	0.0375	2.439 up	transposable element gene
AT2G14340	0.0726	1.568 up	transposable element gene
AT2G14640	0.0302	1.575 up	transposable element gene
AT2G15870	0.0472	1.577 up	transposable element gene
AT2G16060	0.0426	1.913 up	AHB1 (ARABIDOPSIS HEMOGLOBIN 1); oxygen binding / oxygen transporter
AT2G16370	0.0616	1.506 up	THY-1 (THYMIDYLATE SYNTHASE 1); dihydrofolate reductase/ thymidylate synthase
AT2G16790	0.0728	1.777 up	shikimate kinase family protein
AT2G16890	0.0464	1.944 up	UDP-glucoronosyl/UDP-glucosyl transferase family protein
AT2G17550	0.0646	1.611 up	unknown protein
AT2G18410	0.028	1.580 up	unknown protein
AT2G19060	0.0347	1.706 up	GDSL-motif lipase/hydrolase family protein
AT2G19530	0.052	1.829 up	unknown protein
AT2G21655	0.066	1.541 up	unknown protein
AT2G21940	0.0963	1.846 up	shikimate kinase, putative
AT2G22200	0.00307	2.169 up	AP2 domain-containing transcription factor
AT2G23000	0.0414	1.762 up	scpl10 (serine carboxypeptidase-like 10); serine-type carboxypeptidase
AT2G23755	0.0502	1.723 up	unknown protein
AT2G23990	0.0956	1.540 up	plastocyanin-like domain-containing protein
AT2G24070	0.0139	2.065 up	unknown protein
AT2G24600	0.0319	2.072 up	ankyrin repeat family protein
AT2G25600	0.0724	2.476 up	SPIK (Shaker Pollen Inward K+ channel); cyclic nucleotide binding / inward rectifier potassium channel/ potassium channel

AT2G25710	0.0781	1.904 up	HCS1 (HOLOCARBOXYLASE SYNTHASE); biotin-[acetyl-CoA-carboxylase] ligase/ catalytic
AT2G26190	0.0621	1.500 up	calmodulin-binding family protein
AT2G26820	0.0491	1.720 up	ATPP2-A3 (Phloem protein 2-A3); carbohydrate binding
AT2G27280	0.00891	1.756 up	unknown protein
AT2G27550	0.0643	2.613 up	ATC (ARABIDOPSIS THALIANA CENTRORADIALIS); phosphatidylethanolamine binding
AT2G28210	0.0646	2.357 up	ATACA2 (ALPHA CARBONIC ANHYDRASE 2); carbonate dehydratase/ zinc ion binding
AT2G28400	0.0536	2.333 up	unknown protein
AT2G28700	0.048	2.153 up	AGL46 (AGAMOUS-LIKE 46); DNA binding / transcription factor
AT2G28800	0.0486	2.121 up	ALB3 (ALBINO 3); P-P-bond-hydrolysis-driven protein transmembrane transporter
AT2G28940	0.0769	1.885 up	protein kinase family protein
AT2G30120	0.0373	1.884 up	unknown protein
AT2G30880	0.0022	6.471 up	pleckstrin homology (PH) domain-containing protein
AT2G31220	0.0544	1.656 up	basic helix-loop-helix (bHLH) family protein
AT2G31430	0.0638	1.980 up	invertase/pectin methylesterase inhibitor family protein
AT2G32530	0.0342	2.032 up	ATCSLB03; cellulose synthase/ transferase/ transferase, transferring glycosyl groups
AT2G32610	0.0437	1.917 up	ATCSLB01; cellulose synthase/ transferase/ transferase, transferring glycosyl groups
AT2G33380	0.0295	2.084 up	RD20 (RESPONSIVE TO DESSICATION 20); calcium ion binding
AT2G33460	0.0772	1.916 up	RIC1 (ROP-INTERACTIVE CRIB MOTIF-CONTAINING PROTEIN 1); protein binding
AT2G33470	0.0558	1.514 up	GLTP1 (glycolipid transfer protein 1); glycolipid binding / glycolipid transporter
AT2G33705	0.0151	1.621 up	F-box family protein
AT2G34260	0.0855	2.245 up	transducin family protein / WD-40 repeat family protein
AT2G34310	0.0395	1.748 up	unknown protein
AT2G34740	0.0636	1.635 up	catalytic/ protein serine/threonine phosphatase
AT2G34840	0.0375	1.517 up	coatomer protein epsilon subunit family protein / COPE family protein
AT2G35200	0.0903	1.520 up	unknown protein
AT2G35640	0.0534	2.377 up	hydroxyproline-rich glycoprotein family protein
AT2G35710	0.0663	1.723 up	glycogenin glucosyltransferase (glycogenin)-related
AT2G36040	0.0838	2.138 up	transposable element gene
AT2G36571	0.00352	1.603 up	unknown protein
AT2G36680	0.0307	1.629 up	CONTAINS InterPro DOMAIN/s: Modifier of rudimentary, Modr (InterPro:IPR009851); BEST Arabidopsis thaliana protein match is: VPS37-1 (TAIR:AT3G53120.1); Has 46 Blast hits to 46 proteins in 14 species: Archae - 0; Bacteria - 0; Metazoa - 7; Fungi - 0; Plants - 35; Viruses - 0; Other Eukaryotes - 4 (source: NCBI BLink).
AT2G36724	0.0967	1.717 up	unknown protein
AT2G37040	0.0926	1.706 up	pal1 (Phe ammonia lyase 1); phenylalanine ammonia-lyase
AT2G38020	0.00796	2.244 up	VCL1 (VACUOLELESS 1)
AT2G38890	0.099	1.691 up	unknown protein
AT2G39450	0.0906	1.511 up	MTP11; cation transmembrane transporter/ manganese ion transmembrane transporter/ manganese:hydrogen antiporter
AT2G39690	0.0322	1.807 up	unknown protein
AT2G39920	0.0751	1.738 up	acid phosphatase class B family protein
AT2G40020	0.034	2.384 up	CONTAINS InterPro DOMAIN/s: WIYLD domain (InterPro:IPR018848); BEST Arabidopsis thaliana protein match is: unknown protein (TAIR:AT1G45248.5); Has 87 Blast hits to 75 proteins in 21 species: Archae - 0; Bacteria - 2; Metazoa - 42; Fungi - 0; Plants - 28; Viruses - 0; Other Eukaryotes - 15 (source: NCBI BLink).
AT2G40150	0.0779	1.950 up	CONTAINS InterPro DOMAIN/s: Protein of unknown function DUF231, plant (InterPro:IPR004253); BEST Arabidopsis thaliana protein match is: ESK1 (ESKIMO 1) (TAIR:AT3G55990.1); Has 712 Blast hits to 693 proteins in 16 species: Archae - 0; Bacteria - 0; Metazoa - 0; Fungi - 0; Plants - 712; Viruses - 0; Other Eukaryotes - 0 (source: NCBI BLink).
AT2G41000	0.0423	1.607 up	heat shock protein binding
AT2G41100	0.0867	4.463 up	TCH3 (TOUCH 3); calcium ion binding
AT2G41600	0.0822	2.549 up	CONTAINS InterPro DOMAIN/s: Mitochondrial glycoprotein (InterPro:IPR003428); Has 20 Blast hits to 20 proteins in 3 species: Archae - 0; Bacteria - 0; Metazoa - 0; Fungi - 0; Plants - 20; Viruses - 0; Other Eukaryotes - 0 (source: NCBI BLink).
AT2G43430	0.0911	2.222 up	GLX2-1 (GLYOXALASE 2-1); hydroxyacylglutathione hydrolase
AT2G43760	0.0389	1.992 up	molybdopterin biosynthesis MoaE family protein
AT2G44120	0.0225	1.895 up	60S ribosomal protein L7 (RPL7C)
AT2G44280	0.0109	1.788 up	unknown protein
AT2G45010	0.0482	2.189 up	unknown protein
AT2G45380	0.0456	1.968 up	BEST Arabidopsis thaliana protein match is: glycine-rich protein (TAIR:AT4G22740.2); Has 48 Blast hits to 48 proteins in 15 species: Archae - 0; Bacteria - 0; Metazoa - 14; Fungi - 0; Plants - 28; Viruses - 0; Other Eukaryotes - 6 (source: NCBI BLink).
AT2G45570	0.0712	1.697 up	CYP76C2; electron carrier/ heme binding / iron ion binding / monooxygenase/ oxygen binding
AT2G45760	0.0377	1.523 up	BAP2 (BON ASSOCIATION PROTEIN 2)
AT2G45950	0.0991	2.165 up	ASK20 (ARABIDOPSIS SKP1-LIKE 20); protein binding / ubiquitin-protein ligase
AT2G46130	0.0608	1.617 up	WRKY43; transcription factor
AT2G46280	0.0809	2.755 up	TRIP-1 (TGF-BETA RECEPTOR INTERACTING PROTEIN 1); nucleotide binding / protein binding
AT2G46460	0.0349	1.693 up	nucleic acid binding
AT3G01260	0.0443	1.700 up	aldose 1-epimerase/ carbohydrate binding / catalytic/ isomerase
AT3G01320	0.021	1.570 up	SNL1 (SIN3-LIKE 1)
AT3G01480	0.0452	2.230 up	CYP38 (cyclophilin 38); peptidyl-prolyl cis-trans isomerase
AT3G01830	0.047	1.511 up	calmodulin-related protein, putative
AT3G03341	0.0748	2.584 up	unknown protein
AT3G04120	0.0475	1.511 up	GAPC1 (GLYCERALDEHYDE-3-PHOSPHATE DEHYDROGENASE C SUBUNIT 1); glyceraldehyde-3-phosphate dehydrogenase (phosphorylating)/ glyceraldehyde-3-phosphate dehydrogenase
AT3G04545	0.0219	1.566 up	Encodes a defensin-like (DEFL) family protein.
AT3G04997	0.0887	1.565 up	unknown protein
AT3G05936	0.0451	2.198 up	unknown protein

AT3G06080	0.0257	2.320 up	unknown protein
AT3G06330	0.0444	1.501 up	zinc finger (C3HC4-type RING finger) family protein
AT3G06630	0.0113	1.606 up	protein kinase family protein
AT3G08870	0.0918	1.578 up	lectin protein kinase, putative
AT3G09870	0.0648	1.704 up	auxin-responsive family protein
AT3G10420	0.0862	2.063 up	sporulation protein-related
AT3G10930	0.00927	2.345 up	unknown protein
AT3G11220	0.0426	1.893 up	Paxneb protein-related
AT3G11470	0.00975	1.858 up	4'-phosphopantetheinyl transferase family protein
AT3G12100	0.0476	2.602 up	cation efflux family protein / metal tolerance protein, putative
AT3G12190	0.0142	1.682 up	BEST Arabidopsis thaliana protein match is: protein transport protein-related (TAIR:AT5G27220.1); Has 37020 Blast hits to 20334 proteins in 1003 species: Archae - 493; Bacteria - 2404; Metazoa - 19960; Fungi - 1962; Plants - 927; Viruses - 159; Other Eukaryotes - 11115 (source: NCBI BLink).
AT3G12835	0.0299	2.165 up	unknown protein
AT3G13650	0.079	2.043 up	disease resistance response
AT3G13784	0.0456	1.933 up	AtcwINV5 (Arabidopsis thaliana cell wall invertase 5); hydrolase, hydrolyzing O-glycosyl compounds
AT3G13790	0.088	1.674 up	ATBFRUCT1; beta-fructofuranosidase/ hydrolase, hydrolyzing O-glycosyl compounds
AT3G14150	0.00412	1.513 up	(S)-2-hydroxy-acid oxidase, peroxisomal, putative / glycolate oxidase, putative / short chain alpha-hydroxy acid oxidase, putative
AT3G14440	0.0916	2.301 up	NCED3 (NINE-CIS-EPOXYCAROTENOID DIOXYGENASE 3); 9-cis-epoxycarotenoid dioxygenase
AT3G15358	0.000188	1.616 up	unknown protein
AT3G15518	0.0476	1.728 up	unknown protein
AT3G15630	0.0665	2.064 up	unknown protein
AT3G16700	0.0985	1.530 up	fumarylacetoacetate hydrolase family protein
AT3G17609	0.0281	1.651 up	HYH (HY5-HOMOLOG); DNA binding / transcription factor
AT3G18540	0.00855	2.295 up	unknown protein
AT3G18570	0.0444	2.060 up	glycine-rich protein / oleosin
AT3G19000	0.0942	1.926 up	oxidoreductase, 2OG-Fe(II) oxygenase family protein
AT3G19323	0.07	1.962 up	pseudogene of poly(A) binding protein
AT3G20590	0.0835	1.529 up	non-race specific disease resistance protein, putative
AT3G21465	0.0631	2.692 up	unknown protein
AT3G21620	0.0953	1.612 up	early-responsive to dehydration protein-related / ERD protein-related
AT3G21700	0.0617	1.530 up	SGP2; GTP binding
AT3G22723	0.0267	1.571 up	unknown protein
AT3G23240	0.0508	1.508 up	ERF1 (ETHYLENE RESPONSE FACTOR 1); DNA binding / transcription activator/ transcription factor
AT3G24300	0.0385	1.718 up	AMT1;3 (AMMONIUM TRANSPORTER 1;3); ammonium transmembrane transporter
AT3G24982	0.0131	1.603 up	protein binding
AT3G25180	0.0329	2.019 up	CYP82G1; electron carrier/ heme binding / iron ion binding / monooxygenase/ oxygen binding
AT3G25233	0.031	1.620 up	unknown protein
AT3G25460	0.0625	1.548 up	F-box family protein
AT3G25880	0.0879	2.164 up	auxin-resistance protein, putative
AT3G26790	0.0376	1.622 up	FUS3 (FUSCA 3); DNA binding / transcription activator/ transcription factor
AT3G26813	0.0994	1.748 up	MIR169J; miRNA
AT3G26960	0.0706	1.654 up	unknown protein
AT3G27420	0.00209	1.785 up	unknown protein
AT3G28070	0.0627	1.675 up	nodulin MtN21 family protein
AT3G28340	0.0766	1.902 up	GATL10 (Galacturonosyltransferase-like 10); polygalacturonate 4-alpha-galacturonosyltransferase/ transferase, transferring hexosyl groups
AT3G28899	0.00358	17.369 up	unknown protein
AT3G28915	0.0508	1.567 up	transposable element gene
AT3G29000	0.0745	1.546 up	calcium-binding EF hand family protein
AT3G29575	0.0629	1.560 up	AFP3 (ABI FIVE BINDING PROTEIN 3)
AT3G30803	0.053	1.840 up	transposable element gene
AT3G30844	0.0987	1.565 up	transposable element gene
AT3G31442	0.0861	1.817 up	transposable element gene
AT3G32160	0.0462	1.573 up	unknown protein
AT3G32340	0.049	1.593 up	transposable element gene
AT3G33076	0.0144	8.803 up	transposable element gene
AT3G33530	0.0498	1.560 up	transducin family protein / WD-40 repeat family protein
AT3G42383	0.0337	1.983 up	transposable element gene
AT3G42970	0.0707	1.523 up	unknown protein
AT3G43205	0.0146	1.666 up	transposable element gene
AT3G43291	0.0523	1.775 up	unknown protein
AT3G43586	0.0862	1.629 up	transposable element gene
AT3G43620	0.0399	1.778 up	transposable element gene
AT3G44960	0.0835	1.575 up	unknown protein
AT3G45050	0.0845	2.099 up	unknown protein
AT3G45380	0.029	1.802 up	transposable element gene
AT3G45790	0.0232	1.737 up	protein kinase-related
AT3G46370	0.0115	2.893 up	leucine-rich repeat protein kinase, putative
AT3G47510	0.0625	1.837 up	unknown protein
AT3G47790	0.0567	1.602 up	ATATH7; ATPase, coupled to transmembrane movement of substances / transporter
AT3G47810	0.00646	2.766 up	MAG1 (MAIGO 1); hydrolase/ protein serine/threonine phosphatase
AT3G47990	0.00407	1.619 up	zinc finger (C3HC4-type RING finger) family protein
AT3G48360	0.097	4.065 up	BT2 (BTB AND TAZ DOMAIN PROTEIN 2); protein binding / transcription factor/ transcription regulator
AT3G48526	0.0302	1.782 up	transposable element gene

AT3G48840	0.0679	1.502 up	nucleic acid binding / nucleotide binding
AT3G49070	0.084	1.808 up	unknown protein
AT3G49430	0.0509	2.390 up	SRp34a (Ser/Arg-rich protein 34a); RNA binding / nucleic acid binding / nucleotide binding
AT3G49940	0.0412	1.503 up	LBD38 (LOB DOMAIN-CONTAINING PROTEIN 38)
AT3G50380	0.0427	1.537 up	CONTAINS InterPro DOMAIN/s: Vacuolar protein sorting-associated protein (InterPro:IPR009543); Has 239 Blast hits to 235 proteins in 73 species: Archae - 0; Bacteria - 0; Metazoa - 130; Fungi - 71; Plants - 23; Viruses - 0; Other Eukaryotes - 15 (source: NCBI BLink).
AT3G50808	0.0709	1.528 up	unknown protein
AT3G52060	0.0611	2.575 up	unknown protein
AT3G52072	0.00921	1.559 up	other RNA
AT3G52390	0.03	1.597 up	tatD-related deoxyribonuclease family protein
AT3G52950	0.0304	1.563 up	CBS domain-containing protein / octicosapeptide/Phox/Bemp1 (PB1) domain-containing protein
AT3G53200	0.0705	1.940 up	AtMYB27 (myb domain protein 27); DNA binding / transcription factor
AT3G53640	0.0391	1.787 up	protein kinase family protein
AT3G54710	0.0896	1.924 up	CDT1B (ARABIDOPSIS HOMOLOG OF YEAST CDT1 BARABIDOPSIS HOMOLOG OF YEAST CDT1 B); cyclin-dependent protein kinase
AT3G55140	0.0266	4.453 up	pectate lyase family protein
AT3G55400	0.00321	4.530 up	OVA1 (OVULE ABORTION 1); ATP binding / aminoacyl-tRNA ligase/ methionine-tRNA ligase/ nucleotide binding
AT3G55480	0.0608	1.708 up	adaptin family protein
AT3G56275	0.0456	1.989 up	pseudogene of unknown protein
AT3G56400	0.0185	1.609 up	WRKY70; transcription factor/ transcription repressor
AT3G57072	0.0696	1.645 up	unknown protein
AT3G57380	0.0892	2.053 up	transferase, transferring glycosyl groups
AT3G57930	0.0594	1.910 up	unknown protein
AT3G58480	0.00839	2.123 up	calmodulin-binding family protein
AT3G58740	0.0409	1.571 up	CSY1 (CITRATE SYNTHASE 1); citrate (SI)-synthase/ transferase, transferring acyl groups, acyl groups converted into alkyl on transfer
AT3G59310	0.0449	1.684 up	unknown protein
AT3G59710	0.0983	1.729 up	short-chain dehydrogenase/reductase (SDR) family protein
AT3G59880	0.0996	1.711 up	unknown protein
AT3G59890	0.0748	1.510 up	dihydrodipicolinate reductase family protein
AT3G60090	0.0144	1.659 up	VQ motif-containing protein
AT3G61415	0.0391	1.610 up	ASK21 (ARABIDOPSIS SKP1-LIKE 21); protein binding / ubiquitin-protein ligase
AT3G62070	0.0743	1.716 up	unknown protein
AT3G62210	0.0254	1.828 up	EDA32 (embryo sac development arrest 32)
AT3G62620	0.0766	1.668 up	sucrose-phosphatase-related
AT3G62820	0.0204	1.644 up	invertase/pectin methylesterase inhibitor family protein
AT3G63020	0.00864	1.795 up	unknown protein
AT4G00070	0.0364	1.623 up	CONTAINS InterPro DOMAIN/s: Zinc finger, RING/FYVE/PHD-type (InterPro:IPR013083); BEST Arabidopsis thaliana protein match is: zinc finger protein-related (TAIR:AT1G36950.1); Has 412 Blast hits to 412 proteins in 58 species: Archae - 0; Bacteria - 0; Metazoa - 32; Fungi - 25; Plants - 277; Viruses - 0; Other Eukaryotes - 78 (source: NCBI BLink).
AT4G00355	0.00573	1.870 up	unknown protein
AT4G00770	0.0466	1.541 up	unknown protein
AT4G01190	0.0209	2.196 up	ATPIPK10 (Arabidopsis phosphatidylinositol phosphate kinase 10); 1-phosphatidylinositol-4-phosphate 5-kinase
AT4G01650	0.0987	1.549 up	CONTAINS InterPro DOMAIN/s: Streptomyces cyclase/dehydrase (InterPro:IPR005031); BEST Arabidopsis thaliana protein match is: unknown protein (TAIR:AT5G08720.1); Has 322 Blast hits to 309 proteins in 56 species: Archae - 0; Bacteria - 121; Metazoa - 0; Fungi - 0; Plants - 46; Viruses - 0; Other Eukaryotes - 155 (source: NCBI BLink).
AT4G01980	0.0662	2.166 up	transposable element gene
AT4G03590	0.0661	1.512 up	CONTAINS InterPro DOMAIN/s: Cystatin-related, plant (InterPro:IPR006525); BEST Arabidopsis thaliana protein match is: unknown protein (TAIR:AT4G03570.1); Has 69 Blast hits to 67 proteins in 21 species: Archae - 0; Bacteria - 1; Metazoa - 12; Fungi - 14; Plants - 26; Viruses - 1; Other Eukaryotes - 15 (source: NCBI BLink).
AT4G04130	0.0819	1.577 up	transposable element gene
AT4G06504	0.00756	1.856 up	transposable element gene
AT4G06538	0.00211	1.566 up	transposable element gene
AT4G06545	0.0755	1.504 up	transposable element gene
AT4G06567	0.0326	1.507 up	transposable element gene
AT4G06585	0.0249	1.541 up	transposable element gene
AT4G06650	0.00492	1.653 up	transposable element gene
AT4G06652	0.0656	1.642 up	transposable element gene
AT4G06666	0.0912	1.531 up	transposable element gene
AT4G07496	0.00334	1.959 up	transposable element gene
AT4G07521	0.0959	1.543 up	transposable element gene
AT4G08300	0.0953	2.558 up	nodulin MtN21 family protein
AT4G08872	0.0608	1.619 up	transposable element gene
AT4G09000	0.00835	2.464 up	14-3-3-like protein GF14 chi / general regulatory factor 1 (GRF1)
AT4G09468	0.0726	1.705 up	Pseudogene of AT1G16740; ribosomal protein L20 family protein
AT4G09800	0.0245	1.575 up	RPS18C (S18 RIBOSOMAL PROTEIN); RNA binding / nucleic acid binding / structural constituent of ribosome
AT4G09970	0.035	2.355 up	unknown protein
AT4G10170	0.0717	1.505 up	synaptobrevin-related family protein
AT4G10350	0.0291	1.617 up	ANAC070 (Arabidopsis NAC domain containing protein 70); transcription factor
AT4G10430	0.0397	1.521 up	CONTAINS InterPro DOMAIN/s: TMPIT-like (InterPro:IPR012926); BEST Arabidopsis thaliana

			protein match is: unknown protein (TAIR:AT1G33230.1); Has 196 Blast hits to 196 proteins in 60 species: Archae - 0; Bacteria - 0; Metazoa - 146; Fungi - 0; Plants - 40; Viruses - 0; Other Eukaryotes - 10 (source: NCBI BLink).
AT4G10440	0.0112	1.585 up	dehydration-responsive family protein
AT4G10507	0.0765	1.516 up	other RNA
AT4G10520	0.00351	1.872 up	subtilase family protein
AT4G10530	0.0774	1.578 up	subtilase family protein
AT4G10860	0.0181	1.622 up	unknown protein
AT4G11000	0.0332	1.709 up	ankyrin repeat family protein
AT4G11280	0.0869	3.348 up	ACS6 (1-AMINOCYCLOPROPANE-1-CARBOXYLIC ACID (ACC) SYNTHASE 6); 1-aminocyclopropane-1-carboxylate synthase
AT4G11370	0.0746	2.122 up	RHA1A; protein binding / zinc ion binding
AT4G11500	0.052	2.035 up	pseudogene, similar to putative receptor-like serine-threonine protein kinase, blastp match of 59% identity and 6.5e-66 P-value to GP
AT4G12100	0.0632	1.690 up	ubiquitin protein ligase binding
AT4G12180	0.00978	1.595 up	transposable element gene
AT4G12410	0.0587	1.623 up	auxin-responsive family protein
AT4G13493	0.0808	2.864 up	MIR850a; miRNA
AT4G13800	0.0536	2.213 up	permease-related
AT4G14226	0.0905	1.614 up	unknown protein
AT4G14310	0.0955	3.428 up	CONTAINS InterPro DOMAIN/s: WD40 repeat-like (InterPro:IPR011046); Has 1571 Blast hits to 1320 proteins in 206 species: Archae - 6; Bacteria - 142; Metazoa - 581; Fungi - 102; Plants - 66; Viruses - 5; Other Eukaryotes - 669 (source: NCBI BLink).
AT4G14480	0.0133	1.521 up	protein kinase family protein
AT4G14970	0.00503	1.662 up	unknown protein
AT4G15030	0.0474	1.719 up	unknown protein
AT4G15215	0.00761	2.574 up	PDR13; ATP binding / ATPase/ nucleoside-triphosphatase/ nucleotide binding
AT4G15250	0.0098	1.736 up	zinc finger (B-box type) family protein
AT4G15480	0.00854	1.853 up	UGT84A1; UDP-glycosyltransferase/ sinapate 1-glucosyltransferase/ transferase, transferring glycosyl groups
AT4G17420	0.0812	3.263 up	CONTAINS InterPro DOMAIN/s: Protein of unknown function DUF124 (InterPro:IPR002838), Tryptophan RNA-binding attenuator protein-like (InterPro:IPR016031); BEST Arabidopsis thaliana protein match is: unknown protein (TAIR:AT5G47420.1).
AT4G17800	0.054	1.670 up	DNA-binding protein-related
AT4G18090	0.0454	1.703 up	unknown protein
AT4G18422	0.0414	1.530 up	unknown protein
AT4G18990	0.0947	2.202 up	xyloglucan:xyloglucosyl transferase, putative / xyloglucan endotransglycosylase, putative / endo-xyloglucan transferase, putative
AT4G19230	0.0183	1.582 up	CYP707A1; (+)-abscisic acid 8'-hydroxylase/ oxygen binding
AT4G19452	0.0411	2.444 up	pseudogene of F-box family protein
AT4G19645	0.0729	1.542 up	CONTAINS InterPro DOMAIN/s: TRAM, LAG1 and CLN8 homology (InterPro:IPR006634); BEST Arabidopsis thaliana protein match is: unknown protein (TAIR:AT1G31300.2); Has 401 Blast hits to 401 proteins in 98 species: Archae - 0; Bacteria - 0; Metazoa - 186; Fungi - 102; Plants - 84; Viruses - 0; Other Eukaryotes - 29 (source: NCBI BLink).
AT4G20040	0.00857	1.586 up	CONTAINS InterPro DOMAIN/s: Pectin lyase fold/virulence factor (InterPro:IPR011050), Parallel beta-helix repeat (InterPro:IPR006626); BEST Arabidopsis thaliana protein match is: QRT3 (QUARTET 3); polygalacturonase (TAIR:AT4G20050.2); Has 90 Blast hits to 90 proteins in 38 species: Archae - 0; Bacteria - 51; Metazoa - 0; Fungi - 0; Plants - 28; Viruses - 0; Other Eukaryotes - 11 (source: NCBI BLink).
AT4G20200	0.0185	1.841 up	terpene synthase/cyclase family protein
AT4G21690	0.0676	2.218 up	GA3OX3 (GIBBERELLIN 3-OXIDASE 3); iron ion binding / oxidoreductase
AT4G21730	0.0598	1.539 up	pseudogene of N-ethylmaleimide sensitive factor (NSF)
AT4G22070	0.0389	1.684 up	WRKY31; transcription factor
AT4G22590	0.0626	1.590 up	trehalose-6-phosphate phosphatase, putative
AT4G22620	0.0945	2.316 up	auxin-responsive family protein
AT4G22950	0.0608	1.513 up	AGL19 (AGAMOUS-LIKE 19); transcription factor
AT4G23970	0.0988	1.772 up	unknown protein
AT4G24150	0.016	2.053 up	AtGRF8 (GROWTH-REGULATING FACTOR 8); transcription activator
AT4G24652	0.0433	1.612 up	Pseudogene of AT4G20330; transcription initiation factor-related
AT4G25450	0.00676	2.223 up	ATNAP8; ATPase, coupled to transmembrane movement of substances / transporter
AT4G26820	0.0621	1.873 up	CONTAINS InterPro DOMAIN/s: Harpin-induced 1 (InterPro:IPR010847); Has 2 Blast hits to 2 proteins in 1 species: Archae - 0; Bacteria - 0; Metazoa - 0; Fungi - 0; Plants - 2; Viruses - 0; Other Eukaryotes - 0 (source: NCBI BLink).
AT4G27430	0.0426	1.905 up	CIP7 (COP1-INTERACTING PROTEIN 7); transcription activator
AT4G27440	0.0646	1.547 up	PORB (PROTOCHLOROPHYLLIDE OXIDOREDUCTASE B); oxidoreductase/ protochlorophyllide reductase
AT4G27657	0.0475	1.679 up	unknown protein
AT4G28365	0.0145	1.517 up	plastocyanin-like domain-containing protein
AT4G28830	0.0397	1.601 up	methyltransferase/ nucleic acid binding
AT4G28890	0.0694	1.784 up	protein binding / ubiquitin-protein ligase/ zinc ion binding
AT4G29050	0.0718	2.012 up	lectin protein kinase family protein
AT4G29540	0.0499	1.510 up	bacterial transferase hexapeptide repeat-containing protein
AT4G29905	0.044	1.969 up	unknown protein
AT4G30074	0.0976	1.828 up	LCR19 (Low-molecular-weight cysteine-rich 19)
AT4G30993	0.0586	1.668 up	unknown protein
AT4G31150	0.0903	1.740 up	endonuclease V family protein
AT4G31620	0.0459	1.631 up	transcriptional factor B3 family protein
AT4G31640	0.0297	2.780 up	transcriptional factor B3 family protein
AT4G31660	0.089	1.538 up	transcriptional factor B3 family protein
AT4G32220	0.0316	2.170 up	transposable element gene

AT4G32370	0.0149	1.565 up	glycoside hydrolase family 28 protein / polygalacturonase (pectinase) family protein
AT4G32530	0.046	4.822 up	vacuolar ATP synthase, putative / V-ATPase, putative
AT4G32580	0.000116	1.514 up	thioredoxin family protein
AT4G32630	0.0538	1.898 up	ARF GTPase activator/ zinc ion binding
AT4G32870	0.0871	1.963 up	unknown protein
AT4G33050	0.0106	1.787 up	EDA39 (embryo sac development arrest 39); calmodulin binding
AT4G33130	0.0665	2.003 up	unknown protein
AT4G33510	0.0505	3.868 up	DHS2 (3-deoxy-d-arabino-heptulosonate 7-phosphate synthase); 3-deoxy-7-phosphoheptulonate synthase
AT4G33925	0.0472	1.578 up	unknown protein
AT4G34000	0.0958	1.858 up	ABF3 (ABSCISIC ACID RESPONSIVE ELEMENTS-BINDING FACTOR 3); DNA binding / protein binding / transcription activator/ transcription factor
AT4G35090	0.0488	3.063 up	CAT2 (CATALASE 2); catalase
AT4G35620	0.0522	2.971 up	CYCB2;2 (Cyclin B2;2); cyclin-dependent protein kinase regulator
AT4G36540	0.0674	1.752 up	BEE2 (BR Enhanced Expression 2); DNA binding / transcription factor
AT4G36770	0.00488	1.698 up	UDP-glycosyltransferase/ transferase, transferring glycosyl groups
AT4G36850	0.0668	1.624 up	CONTAINS InterPro DOMAIN/s: Cystinosin/ERS1p repeat (InterPro:IPR006603); BEST Arabidopsis thaliana protein match is: PQ-loop repeat family protein / transmembrane family protein (TAIR:AT2G41050.1); Has 599 Blast hits to 441 proteins in 106 species: Archae - 0; Bacteria - 0; Metazoa - 197; Fungi - 311; Plants - 38; Viruses - 0; Other Eukaryotes - 53 (source: NCBI BLink).
AT4G37240	0.0985	1.884 up	unknown protein
AT4G37550	0.0617	3.210 up	formamidase, putative / formamide amidohydrolase, putative
AT4G37620	0.0909	1.619 up	transposable element gene
AT4G37630	0.0593	2.870 up	CYCD5;1 (cyclin d5;1); cyclin-dependent protein kinase
AT4G37682	0.0587	3.222 up	CONTAINS InterPro DOMAIN/s: Protein of unknown function DUF1399 (InterPro:IPR009836); BEST Arabidopsis thaliana protein match is: glycine-rich protein (TAIR:AT4G37900.1); Has 19 Blast hits to 19 proteins in 6 species: Archae - 0; Bacteria - 0; Metazoa - 0; Fungi - 0; Plants - 19; Viruses - 0; Other Eukaryotes - 0 (source: NCBI BLink).
AT4G37790	0.0441	1.754 up	HAT22; transcription factor
AT4G38340	0.0307	2.192 up	RWP-RK domain-containing protein
AT4G38590	0.0128	1.814 up	glycosyl hydrolase family 35 protein
AT4G39360	0.0596	2.014 up	unknown protein
AT4G39750	0.0654	1.945 up	F-box family protein-related
AT4G40090	0.0282	1.941 up	AGP3 (arabinogalactan-protein 3)
AT5G01300	0.0292	1.753 up	phosphatidylethanolamine-binding family protein
AT5G01490	0.0221	1.682 up	CAX4 (CATION EXCHANGER 4); calcium:cation antiporter/ calcium:hydrogen antiporter/ cation:cation antiporter
AT5G01650	0.0423	1.681 up	macrophage migration inhibitory factor family protein / MIF family protein
AT5G02780	0.00933	1.529 up	In2-1 protein, putative
AT5G03890	0.0698	1.659 up	unknown protein
AT5G04730	0.0131	1.780 up	unknown protein
AT5G04830	0.0458	1.832 up	unknown protein
AT5G04980	0.0951	1.560 up	endonuclease/exonuclease/phosphatase family protein
AT5G05050	0.0452	1.504 up	peptidase C1A papain family protein
AT5G05280	0.0973	1.659 up	zinc finger (C3HC4-type RING finger) family protein
AT5G06530	0.0641	1.543 up	ABC transporter family protein
AT5G07100	0.0921	1.853 up	WRKY26; transcription factor
AT5G07530	0.0376	1.527 up	GRP17 (GLYCINE RICH PROTEIN 17); lipid binding
AT5G08150	0.0776	1.746 up	unknown protein
AT5G08320	0.0202	1.712 up	unknown protein
AT5G08360	0.0296	2.426 up	unknown protein
AT5G08370	0.0922	1.784 up	AtAGAL2 (Arabidopsis thaliana ALPHA-GALACTOSIDASE 2); alpha-galactosidase/ catalytic/ hydrolase, hydrolyzing O-glycosyl compounds
AT5G09240	0.0694	2.230 up	transcriptional coactivator p15 (PC4) family protein
AT5G09345	0.084	2.047 up	pre-tRNA
AT5G09720	0.00382	1.752 up	metal ion transmembrane transporter
AT5G09930	0.0626	1.524 up	ATGCN2; transporter
AT5G10000	0.0179	1.731 up	ATFD4 (ferredoxin 4); 2 iron, 2 sulfur cluster binding / electron carrier/ iron-sulfur cluster binding
AT5G10060	0.0157	1.675 up	CONTAINS InterPro DOMAIN/s: Protein of unknown function DUF618 (InterPro:IPR006903), Regulation of nuclear pre-mRNA protein (InterPro:IPR006569), ENTH/VHS (InterPro:IPR008942); BEST Arabidopsis thaliana protein match is: unknown protein (TAIR:AT5G65180.1); Has 4531 Blast hits to 4161 proteins in 412 species: Archae - 14; Bacteria - 404; Metazoa - 1999; Fungi - 666; Plants - 262; Viruses - 36; Other Eukaryotes - 1150 (source: NCBI BLink).
AT5G10320	0.0297	1.569 up	unknown protein
AT5G11860	0.0827	2.821 up	NLI interacting factor (NIF) family protein
AT5G11940	0.0691	1.934 up	subtilase family protein
AT5G12040	0.0869	1.738 up	carbon-nitrogen hydrolase family protein
AT5G12150	0.00658	1.504 up	pleckstrin homology (PH) domain-containing protein / RhoGAP domain-containing protein
AT5G13080	0.069	2.178 up	WRKY75; transcription factor
AT5G13130	0.0181	1.774 up	ATP binding
AT5G13250	0.0128	1.616 up	unknown protein
AT5G13920	0.00593	1.791 up	zinc knuckle (CCHC-type) family protein
AT5G14010	0.0911	1.714 up	zinc finger (C2H2 type) family protein
AT5G14250	0.084	2.139 up	COP13 (CONSTITUTIVE PHOTOMORPHOGENIC 13); protein binding
AT5G14380	0.0434	1.822 up	AGP6 (Arabinogalactan proteins 6)
AT5G15190	0.0223	1.761 up	unknown protein
AT5G15610	0.0241	4.720 up	proteasome family protein

AT5G15860	0.0444	1.619 up	ATPCME (PRENYLCYSTEINE METHYLESTERASE); prenylcysteine methylesterase
AT5G15890	0.0927	1.890 up	unknown protein
AT5G15990	0.0157	2.195 up	transposable element gene
AT5G16160	0.0662	1.934 up	unknown protein
AT5G16180	0.0205	1.525 up	CRS1 (ARABIDOPSIS ORTHOLOG OF MAIZE CHLOROPLAST SPLICING FACTOR CRS1); RNA splicing factor, transesterification mechanism
AT5G16310	0.0288	1.594 up	UCH1; ubiquitin thiolesterase
AT5G16390	0.0912	1.923 up	CAC1 (CHLOROPLASTIC ACETYLCOENZYME A CARBOXYLASE 1); acetyl-CoA carboxylase/ biotin binding
AT5G16490	0.0216	1.716 up	RIC4 (ROP-INTERACTIVE CRIB MOTIF-CONTAINING PROTEIN 4); protein binding
AT5G16700	0.0538	1.971 up	glycosyl hydrolase family 5 protein / cellulase family protein
AT5G16770	0.0906	1.652 up	AtMYB9 (myb domain protein 9); DNA binding / transcription factor
AT5G16820	0.00233	1.551 up	HSF3 (HEAT SHOCK FACTOR 3); DNA binding / transcription factor
AT5G17010	0.059	1.836 up	sugar transporter family protein
AT5G17810	0.0804	2.121 up	WOX12 (WUSCHEL related homeobox 12); DNA binding / transcription factor
AT5G18090	0.0113	1.721 up	transcriptional factor B3 family protein
AT5G19500	0.0207	1.611 up	tryptophan/tyrosine permease family protein
AT5G19790	0.00861	1.773 up	RAP2.11 (related to AP2 11); DNA binding / transcription factor
AT5G20780	0.0637	1.700 up	transposable element gene
AT5G21940	0.0675	2.296 up	unknown protein
AT5G22150	0.0182	2.215 up	unknown protein
AT5G22170	0.0497	1.787 up	unknown protein
AT5G22390	0.0858	2.016 up	unknown protein
AT5G22960	0.0623	1.504 up	serine carboxypeptidase S10 family protein
AT5G23990	0.0702	1.664 up	FRO5 (FERRIC REDUCTION OXIDASE 5); ferric-chelate reductase
AT5G24090	0.00145	1.544 up	acidic endochitinase (CHIB1)
AT5G24630	0.0189	2.585 up	BIN4 (brassinosteroid-insensitive4); double-stranded DNA binding
AT5G26200	0.0103	1.869 up	mitochondrial substrate carrier family protein
AT5G26920	0.014	2.179 up	CBP60G (CAM-BINDING PROTEIN 60-LIKE.G); calmodulin binding
AT5G27420	0.0022	1.800 up	zinc finger (C3HC4-type RING finger) family protein
AT5G27845	0.018	2.622 up	transposable element gene
AT5G27927	0.048	1.709 up	transposable element gene
AT5G28110	0.0539	1.922 up	transposable element gene
AT5G28335	0.00733	9.507 up	transposable element gene
AT5G28570	0.0828	1.918 up	transposable element gene
AT5G28660	0.0181	1.683 up	CONTAINS InterPro DOMAIN/s: Six-bladed beta-propeller, TolB-like (InterPro:IPR011042); BEST Arabidopsis thaliana protein match is: unknown protein (TAIR:AT2G47370.1); Has 39 Blast hits to 39 proteins in 10 species: Archae - 0; Bacteria - 2; Metazoa - 0; Fungi - 0; Plants - 37; Viruses - 0; Other Eukaryotes - 0 (source: NCBI BLink).
AT5G28880	0.0539	1.675 up	transposable element gene
AT5G28885	0.094	1.574 up	unknown protein
AT5G29046	0.0536	1.862 up	transposable element gene
AT5G29050	0.0429	1.718 up	unknown protein
AT5G29100	0.0579	1.553 up	transposable element gene
AT5G30852	0.0923	2.258 up	transposable element gene
AT5G32510	0.0738	2.210 up	transposable element gene
AT5G32519	0.0988	1.546 up	transposable element gene
AT5G32900	0.0226	2.130 up	transposable element gene
AT5G34266	0.00535	1.557 up	transposable element gene
AT5G34810	0.0179	2.574 up	transposable element gene
AT5G34846	0.055	1.535 up	transposable element gene
AT5G34866	0.0999	1.618 up	transposable element gene
AT5G35048	0.099	2.112 up	transposable element gene
AT5G35918	0.0357	1.605 up	transposable element gene
AT5G36050	0.0173	2.228 up	transposable element gene
AT5G36100	0.0854	1.751 up	unknown protein
AT5G36500	0.0543	1.781 up	Encodes a ECA1 gametogenesis related family protein
AT5G36870	0.0256	1.745 up	ATGSL09 (glucan synthase-like 9); 1,3-beta-glucan synthase
AT5G36920	0.0925	2.077 up	unknown protein
AT5G37240	0.0741	1.736 up	unknown protein
AT5G37300	0.0581	1.791 up	WSD1; diacylglycerol O-acyltransferase/ long-chain-alcohol O-fatty-acyltransferase
AT5G37450	0.084	2.144 up	leucine-rich repeat transmembrane protein kinase, putative
AT5G37780	0.0904	1.941 up	CAM1 (CALMODULIN 1); calcium ion binding
AT5G38380	0.0347	3.483 up	unknown protein
AT5G38510	0.00384	1.960 up	rhomboid family protein
AT5G38895	0.0678	1.653 up	zinc finger (C3HC4-type RING finger) family protein
AT5G39090	0.0258	1.739 up	transferase family protein
AT5G39270	0.0491	2.038 up	ATEXPA22 (ARABIDOPSIS THALIANA EXPANSIN A22)
AT5G39310	0.0801	1.879 up	ATEXPA24 (ARABIDOPSIS THALIANA EXPANSIN A24)
AT5G40540	0.00338	1.522 up	protein kinase, putative
AT5G40855	0.035	3.891 up	unknown protein
AT5G41070	0.0488	2.194 up	DRB5 (DSRNA-BINDING PROTEIN 5); double-stranded RNA binding
AT5G41310	0.0371	2.485 up	kinesin motor protein-related
AT5G41510	0.0285	1.506 up	F-box family protein
AT5G41740	0.0326	1.566 up	disease resistance protein (TIR-NBS-LRR class), putative
AT5G41910	0.0344	2.151 up	RNA polymerase II mediator complex protein-related
AT5G42040	0.0139	2.023 up	RPN12b (Regulatory Particle Non-ATPase 12b); peptidase
AT5G42504	0.0574	1.565 up	unknown protein
AT5G42510	0.053	1.521 up	disease resistance-responsive family protein
AT5G43196	0.0309	1.931 up	Pseudogene of AT5G43210; endo/excinuclease amino terminal domain-containing protein

AT5G43380	0.0693	1.722 up	TOPP6; protein serine/threonine phosphatase
AT5G43440	0.0992	1.767 up	2-oxoglutarate-dependent dioxygenase, putative
AT5G43860	0.0914	1.885 up	ATCLH2; chlorophyllase
AT5G44350	0.0714	1.760 up	ethylene-responsive nuclear protein -related
AT5G45307	0.0475	1.543 up	MIR168/MIR168B; miRNA
AT5G45320	0.0334	1.606 up	CONTAINS InterPro DOMAIN/s: Harpin-induced 1 (InterPro:IPR010847); BEST Arabidopsis thaliana protein match is: unknown protein (TAIR:AT3G26350.1); Has 162 Blast hits to 162 proteins in 10 species: Archae - 0; Bacteria - 0; Metazoa - 0; Fungi - 0; Plants - 162; Viruses - 0; Other Eukaryotes - 0 (source: NCBI BLink).
AT5G45710	0.0457	1.679 up	RHA1 (ROOT HANDEDNESS 1); DNA binding / transcription factor
AT5G46040	0.0283	1.778 up	proton-dependent oligopeptide transport (POT) family protein
AT5G47225	0.062	1.880 up	transposable element gene
AT5G47320	0.0451	1.662 up	RPS19 (RIBOSOMAL PROTEIN S19); RNA binding
AT5G47530	0.0293	1.807 up	auxin-responsive protein, putative
AT5G49010	0.0109	2.469 up	SLD5 (SYNTHETIC LETHALITY WITH DPB11-1 5)
AT5G49120	0.0364	2.842 up	senescence-associated protein-related
AT5G49380	0.0581	1.890 up	CONTAINS InterPro DOMAIN/s: Protein of unknown function DUF625 (InterPro:IPR006887); BEST Arabidopsis thaliana protein match is: binding (TAIR:AT3G06670.1); Has 367 Blast hits to 367 proteins in 124 species: Archae - 0; Bacteria - 0; Metazoa - 206; Fungi - 89; Plants - 34; Viruses - 0; Other Eukaryotes - 38 (source: NCBI BLink).
AT5G49470	0.0329	1.522 up	protein kinase family protein
AT5G49750	0.0294	1.805 up	leucine-rich repeat family protein
AT5G50200	0.0476	1.778 up	WR3 (WOUND-RESPONSIVE 3); nitrate transmembrane transporter
AT5G51250	0.0868	1.639 up	kelch repeat-containing F-box family protein
AT5G51480	0.0057	1.596 up	SKS2 (SKU5 SIMILAR 2); copper ion binding / oxidoreductase
AT5G52340	0.0304	2.064 up	ATEXO70A2 (exocyst subunit EXO70 family protein A2); protein binding
AT5G53050	0.0731	1.882 up	hydrolase, alpha/beta fold family protein
AT5G53760	0.0364	1.605 up	MLO11 (MILDEW RESISTANCE LOCUS O 11); calmodulin binding
AT5G53980	0.0991	2.442 up	ATHB52 (ARABIDOPSIS THALIANA HOMEOBOX PROTEIN 52); transcription factor
AT5G54020	0.0156	1.817 up	zinc ion binding
AT5G54140	0.0369	1.516 up	ILL3; IAA-amino acid conjugate hydrolase/ metallopeptidase
AT5G54560	0.0899	1.719 up	unknown protein
AT5G54570	0.0688	1.791 up	BGLU41 (BETA GLUCOSIDASE 41); catalytic/ cation binding / hydrolase, hydrolyzing O-glycosyl compounds
AT5G54950	0.0971	1.796 up	aconitate hydratase-related / citrate hydro-lyase-related / aconitase-related
AT5G56970	0.0761	1.903 up	CKX3 (CYTOKININ OXIDASE 3); amine oxidase/ cytokinin dehydrogenase
AT5G57220	0.0395	2.308 up	CYP81F2; electron carrier/ heme binding / iron ion binding / monooxygenase/ oxygen binding
AT5G57340	0.0567	2.889 up	unknown protein
AT5G57655	0.0986	3.350 up	xylose isomerase family protein
AT5G57860	0.0905	1.749 up	ubiquitin family protein
AT5G58003	0.0672	1.592 up	CPL4 (C-TERMINAL DOMAIN PHOSPHATASE-LIKE 4); phosphoprotein phosphatase
AT5G58980	0.00364	1.550 up	ceramidase family protein
AT5G59160	0.0905	1.505 up	TOPP2; protein serine/threonine phosphatase
AT5G59170	0.0579	1.548 up	proline-rich family protein
AT5G60400	0.00935	1.780 up	unknown protein
AT5G60440	0.0847	2.309 up	AGL62 (Agamous-like 62); DNA binding / transcription factor
AT5G60680	0.044	2.730 up	unknown protein
AT5G61110	0.0153	1.664 up	protein binding / zinc ion binding
AT5G61340	0.0688	1.605 up	unknown protein
AT5G61440	0.0917	2.297 up	ACHT5 (ATYPICAL CYS HIS RICH THIOREDOXIN 5)
AT5G61450	0.0411	1.711 up	2-phosphoglycerate kinase-related
AT5G61630	0.0253	1.922 up	unknown protein
AT5G61830	0.0129	1.643 up	short-chain dehydrogenase/reductase (SDR) family protein
AT5G62162	0.0252	1.819 up	MIR399C; miRNA
AT5G62210	0.0952	2.914 up	embryo-specific protein-related
AT5G62230	0.0978	1.631 up	ERL1 (ERECTA-LIKE 1); kinase
AT5G62480	0.0796	2.126 up	ATGSTU9 (ARABIDOPSIS THALIANA GLUTATHIONE S-TRANSFERASE TAU 9); glutathione transferase
AT5G62490	0.0435	2.031 up	ATHVA22B
AT5G62720	0.0981	2.505 up	integral membrane HPP family protein
AT5G63065	0.00896	1.757 up	Encodes a Plant thionin family protein
AT5G63080	0.0322	2.459 up	transcription factor jumonji (jmjC) domain-containing protein
AT5G63580	0.087	2.625 up	FLS2 (FLAVONOL SYNTHASE 2); flavonol synthase
AT5G63870	0.0289	1.726 up	PP7 (SERINE/THREONINE PHOSPHATASE 7); protein serine/threonine phosphatase
AT5G65070	0.03	1.953 up	MAF4 (MADS AFFECTING FLOWERING 4); transcription factor
AT5G66070	0.0748	2.276 up	zinc finger (C3HC4-type RING finger) family protein
AT5G66150	0.0741	1.749 up	glycosyl hydrolase family 38 protein
AT5G66160	0.0166	2.675 up	JR700; peptidase/ protein binding / zinc ion binding
AT5G66170	0.0194	1.638 up	CONTAINS InterPro DOMAIN/s: Rhodanese-like (InterPro:IPR001763); BEST Arabidopsis thaliana protein match is: unknown protein (TAIR:AT2G17850.1); Has 126 Blast hits to 126 proteins in 29 species: Archae - 2; Bacteria - 25; Metazoa - 0; Fungi - 0; Plants - 89; Viruses - 0; Other Eukaryotes - 10 (source: NCBI BLink).
AT5G66210	0.0984	5.883 up	CPK28; ATP binding / calcium ion binding / calmodulin-dependent protein kinase/ protein kinase/ protein serine/threonine kinase/ protein tyrosine kinase
AT5G66455	0.0308	1.585 up	pseudogene of pentatricopeptide (PPR) repeat-containing protein
AT5G66510	0.0461	1.966 up	GAMMA CA3 (GAMMA CARBONIC ANHYDRASE 3); carbonate dehydratase
AT5G66558	0.0758	2.045 up	other RNA
AT5G66930	0.0089	1.556 up	unknown protein
AT5G67520	0.059	1.953 up	adenylylsulfate kinase, putative

Supplementary Data 2. Genes affected in *35S::JMJ30-HA* compared to WT grown under LD 22°C conditions.

Gene ID	P-value	Fold change compared to Col WT	DESCRIPTION
AT1G01180	0.0171	2.063 down	unknown protein
AT1G02405	0.0942	2.350 down	proline-rich family protein
AT1G02590	0.0108	3.770 down	aldehyde oxidase, putative
AT1G03490	0.0208	1.536 down	ANAC006 (Arabidopsis NAC domain containing protein 6); transcription factor
AT1G03510	0.0327	1.906 down	pentatricopeptide (PPR) repeat-containing protein
AT1G03850	0.0513	1.625 down	glutaredoxin family protein
AT1G04490	0.039	2.443 down	unknown protein
AT1G04550	0.0539	1.952 down	IAA12 (AUXIN-INDUCED PROTEIN 12); transcription factor/ transcription repressor
AT1G05040	0.0888	1.998 down	unknown protein
AT1G05280	0.0708	1.729 down	fringe-related protein
AT1G06280	0.0482	1.563 down	LBD2 (LOB DOMAIN-CONTAINING PROTEIN 2)
AT1G07410	0.0743	2.133 down	ATRABA2B (ARABIDOPSIS RAB GTPASE HOMOLOG A2B); GTP binding / GTPase/ protein binding
AT1G07800	0.0106	1.557 down	transposable element gene
AT1G07890	0.0936	1.597 down	APX1 (ascorbate peroxidase 1); L-ascorbate peroxidase
AT1G07900	0.0184	1.947 down	LBD1 (LOB DOMAIN-CONTAINING PROTEIN 1)
AT1G08170	0.094	2.019 down	histone H2B family protein
AT1G08340	0.0195	1.720 down	rac GTPase activating protein, putative
AT1G09090	0.0264	1.723 down	ATRBOHB (respiratory burst oxidase homolog B); FAD binding / calcium ion binding / electron carrier/ iron ion binding / oxidoreductase/ oxidoreductase, acting on NADH or NADPH, with oxygen as acceptor / peroxidase
AT1G09486	0.00997	1.806 down	pseudogene, 60S ribosomal protein L21 (RPL21B), temporary automated functional assignment; blastp match of 67% identity and 2.0e-52 P-value to GP
AT1G10095	0.0285	2.442 down	protein prenyltransferase
AT1G11150	0.0125	1.520 down	transposable element gene
AT1G13370	0.0461	2.383 down	histone H3, putative
AT1G13890	0.068	2.148 down	SNAP30 (SOLUBLE N-ETHYLMALEIMIDE-SENSITIVE FACTOR ADAPTOR PROTEIN 30); SNAP receptor
AT1G14420	0.0593	2.229 down	AT59; lyase/ pectate lyase
AT1G14750	0.0415	1.620 down	SDS (SOLO DANCERS); cyclin-dependent protein kinase
AT1G15045	0.0727	2.356 down	hypothetical protein
AT1G15850	0.0311	1.792 down	transducin family protein / WD-40 repeat family protein
AT1G16140	0.0678	1.700 down	pseudogene similar to wall-associated kinase protein family
AT1G17350	0.0196	1.897 down	auxin-induced-related / indole-3-acetic acid induced-related
AT1G17400	0.0627	1.874 down	unknown protein
AT1G18735	0.0717	1.583 down	other RNA
AT1G20065	0.000536	1.672 down	other RNA
AT1G20515	0.0359	2.666 down	other RNA
AT1G20925	0.0669	2.185 down	auxin efflux carrier family protein
AT1G21390	0.00585	1.657 down	emb2170 (embryo defective 2170)
AT1G21860	0.0709	1.931 down	sks7 (SKU5 Similar 7); copper ion binding / oxidoreductase
AT1G22460	0.0626	2.732 down	unknown protein
AT1G22560	0.0628	1.509 down	transposable element gene
AT1G22590	0.072	1.677 down	MADS-box family protein
AT1G22980	0.0446	1.768 down	unknown protein
AT1G23610	0.0702	1.676 down	unknown protein
AT1G23670	0.0324	1.787 down	unknown protein
AT1G24212	0.0674	1.687 down	pseudogene of paired amphipathic helix repeat-containing protein
AT1G24370	0.0847	1.710 down	transposable element gene
AT1G25988	0.0324	1.529 down	CONTAINS InterPro DOMAIN/s: Protein of unknown function DUF572 (InterPro:IPR007590); BEST Arabidopsis thaliana protein match is: cell cycle control protein-related (TAIR:AT1G25682.1); Has 129 Blast hits to 129 proteins in 52 species: Archae - 0; Bacteria - 0; Metazoa - 92; Fungi - 7; Plants - 26; Viruses - 0; Other Eukaryotes - 4 (source: NCBI BLink).
AT1G26990	0.0446	2.323 down	transposable element gene
AT1G28020	0.0206	1.962 down	pentatricopeptide (PPR) repeat-containing protein
AT1G29080	0.0435	1.664 down	peptidase C1A papain family protein
AT1G29420	0.0334	2.245 down	CONTAINS InterPro DOMAIN/s: Auxin responsive SAUR protein (InterPro:IPR003676); BEST Arabidopsis thaliana protein match is: SAUR68 (SMALL AUXIN UPREGULATED 68) (TAIR:AT1G29510.1); Has 372 Blast hits to 362 proteins in 16 species: Archae - 0; Bacteria - 0; Metazoa - 0; Fungi - 0; Plants - 372; Viruses - 0; Other Eukaryotes - 0 (source: NCBI BLink).
AT1G29650	0.0271	2.573 down	transposable element gene
AT1G30030	0.063	1.980 down	transposable element gene
AT1G31140	0.0871	1.647 down	agl63 (AGAMOUS-LIKE 63); DNA binding / transcription factor
AT1G31520	0.016	1.549 down	unknown protein
AT1G32400	0.0504	2.664 down	TOM2A (TOBAMOVIRUS MULTIPLICATION 2A); protein binding
AT1G32992	0.00168	1.824 down	MIR856a; miRNA
AT1G33160	0.0537	2.098 down	pseudogene, similar to actin, blastp match of 74% identity and 8.3e-48 P-value to GP
AT1G33380	0.0285	1.672 down	transposable element gene
AT1G33430	0.00653	2.119 down	galactosyltransferase family protein
AT1G33500	0.035	4.364 down	BEST Arabidopsis thaliana protein match is: kinase interacting family protein (TAIR:AT3G22790.1); Has 3639 Blast hits to 2952 proteins in 364 species: Archae - 50; Bacteria - 374; Metazoa - 1667; Fungi - 244; Plants - 133; Viruses - 6; Other

			Eukaryotes - 1165 (source: NCBI BLink).
AT1G33720	0.046	1.597 down	CYP76C6; electron carrier/ heme binding / iron ion binding / monooxygenase/ oxygen binding
AT1G34095	0.0284	2.274 down	unknown protein
AT1G34480	0.0529	1.994 down	DC1 domain-containing protein
AT1G34650	0.0832	1.505 down	HDG10 (HOMEODOMAIN GLABROUS 10); DNA binding / transcription factor
AT1G35090	0.0293	1.865 down	transposable element gene
AT1G35170	0.0262	1.832 down	CONTAINS InterPro DOMAIN/s: TRAM, LAG1 and CLN8 homology (InterPro:IPR006634); BEST Arabidopsis thaliana protein match is: unknown protein (TAIR:AT1G35180.1); Has 92 Blast hits to 92 proteins in 36 species: Archae - 0; Bacteria - 0; Metazoa - 40; Fungi - 2; Plants - 25; Viruses - 0; Other Eukaryotes - 25 (source: NCBI BLink).
AT1G35690	0.0628	1.531 down	transposable element gene
AT1G36185	0.037	1.594 down	transposable element gene
AT1G36650	0.0292	1.693 down	transposable element gene
AT1G37045	0.0945	1.552 down	transposable element gene
AT1G37471	0.0614	1.825 down	transposable element gene
AT1G38300	0.0512	1.500 down	transposable element gene
AT1G38416	0.0873	2.759 down	transposable element gene
AT1G41896	0.0501	3.098 down	transposable element gene
AT1G42003	0.00986	1.929 down	transposable element gene
AT1G42390	0.0647	1.629 down	transposable element gene
AT1G42480	0.0495	1.754 down	unknown protein
AT1G42700	0.0641	1.917 down	unknown protein
AT1G44045	0.0111	1.614 down	transposable element gene
AT1G44608	0.0629	1.542 down	unknown protein
AT1G44870	0.013	1.671 down	transposable element gene
AT1G45243	0.09	1.694 down	DC1 domain-containing protein
AT1G45248	0.0187	1.788 down	CONTAINS InterPro DOMAIN/s: WIYLD domain (InterPro:IPR018848); BEST Arabidopsis thaliana protein match is: unknown protein (TAIR:AT2G40020.3).
AT1G47625	0.0138	1.855 down	pseudogene of seven transmembrane domain protein
AT1G47915	0.0522	1.517 down	F-box family protein
AT1G48145	0.0303	1.606 down	unknown protein
AT1G48680	0.0192	1.542 down	transposable element gene
AT1G48760	0.056	1.815 down	delta-ADR (delta-adaptin); binding / clathrin binding / protein binding / protein transporter
AT1G48980	0.0473	2.310 down	oxidoreductase
AT1G49150	0.0114	3.020 down	unknown protein
AT1G49435	0.011	1.975 down	LCR16 (Low-molecular-weight cysteine-rich 16)
AT1G49440	0.0328	2.893 down	transposable element gene
AT1G50020	0.00606	57.229 down	unknown protein
AT1G50210	0.0582	1.711 down	pseudogene, similar to NBS-LRR protein, blastp match of 61% identity and 8.2e-06 P-value to GP
AT1G50325	0.029	1.985 down	enzyme inhibitor/ pectinesterase
AT1G51680	0.0728	1.808 down	4CL1 (4-COUMARATE:COA LIGASE 1); 4-coumarate-CoA ligase
AT1G51780	0.0415	1.809 down	ILL5; IAA-amino acid conjugate hydrolase/ metallopeptidase
AT1G51830	0.0621	2.455 down	ATP binding / kinase/ protein serine/threonine kinase
AT1G51930	0.0353	1.627 down	zinc finger (C3HC4-type RING finger) family protein
AT1G52010	0.0255	2.000 down	transposable element gene
AT1G52085	0.00359	1.549 down	pseudogene, similar to jasmonate inducible protein, blastp match of 51% identity and 1.1e-11 P-value to GP
AT1G52650	0.062	2.477 down	CONTAINS InterPro DOMAIN/s: Cyclin-like F-box (InterPro:IPR001810), FBD-like (InterPro:IPR006566); BEST Arabidopsis thaliana protein match is: F-box family protein (TAIR:AT4G13960.1); Has 1151 Blast hits to 1117 proteins in 9 species: Archae - 0; Bacteria - 0; Metazoa - 1; Fungi - 0; Plants - 1150; Viruses - 0; Other Eukaryotes - 0 (source: NCBI BLink).
AT1G54860	0.0557	2.381 down	unknown protein
AT1G55230	0.0305	2.235 down	unknown protein
AT1G55410	0.0432	2.065 down	pseudogene, CHP-rich zinc finger protein, putative, similar to putative CHP-rich zinc finger protein GB:CAB77744 GI:7268217 from (Arabidopsis thaliana)
AT1G57800	0.0326	2.427 down	VIM5 (VARIANT IN METHYLATION 5); protein binding / zinc ion binding
AT1G58460	0.0327	1.793 down	unknown protein
AT1G58766	0.0468	1.507 down	BEST Arabidopsis thaliana protein match is: transcription factor-related (TAIR:AT1G59453.1); Has 32 Blast hits to 28 proteins in 7 species: Archae - 0; Bacteria - 0; Metazoa - 7; Fungi - 0; Plants - 25; Viruses - 0; Other Eukaryotes - 0 (source: NCBI BLink).
AT1G61650	0.0182	3.269 down	pseudogene, similar to chromomethylase-like protein, blastp match of 45% identity and 3.0e-24 P-value to GP
AT1G61688	0.0815	1.905 down	Encodes a defensin-like (DEFL) family protein.
AT1G62230	0.0417	2.048 down	transposable element gene
AT1G62770	0.0695	1.581 down	invertase/pectin methylesterase inhibitor family protein
AT1G62880	0.0181	1.558 down	cornichon family protein
AT1G63280	0.0377	1.750 down	serpin-related / serine protease inhibitor-related
AT1G63910	0.0253	3.432 down	AtMYB103 (myb domain protein 103); DNA binding / transcription activator/ transcription factor
AT1G65330	0.0744	2.152 down	PHE1 (PHERES1); DNA binding / transcription factor
AT1G65585	0.0833	1.740 down	pseudogene, similar to oj991113_30.20, blastp match of 25% identity and 8.9e-08 P-value to GP
AT1G66290	0.0303	2.384 down	F-box family protein
AT1G66470	0.00419	1.649 down	basic helix-loop-helix (bHLH) family protein
AT1G67710	0.00522	1.687 down	ARR11 (RESPONSE REGULATOR 11); transcription factor/ two-component response regulator
AT1G68800	0.00866	2.172 down	TCP12 (TCP DOMAIN PROTEIN 12); transcription factor

AT1G69150	0.0374	2.067 down	DC1 domain-containing protein
AT1G69720	0.0661	2.503 down	ho3 (HEME OXYGENASE 3); heme oxygenase (decyclizing)
AT1G70581	0.065	2.545 down	other RNA
AT1G70680	0.0985	1.955 down	caleosin-related family protein
AT1G71691	0.0161	1.673 down	GDSL-motif lipase/hydrolase family protein
AT1G72660	0.0665	1.827 down	developmentally regulated GTP-binding protein, putative
AT1G75590	0.0807	1.618 down	auxin-responsive family protein
AT1G76250	0.0816	2.077 down	unknown protein
AT1G77530	0.0734	2.009 down	O-methyltransferase family 2 protein
AT1G80160	0.00641	1.958 down	lactoylglutathione lyase family protein / glyoxalase I family protein
AT1G80580	0.0173	1.744 down	ethylene-responsive element-binding family protein
AT1G80940	0.0968	2.387 down	unknown protein
AT1G80960	0.0158	1.782 down	F-box protein-related
AT2G01800	0.0946	1.883 down	COP1-interacting protein-related
AT2G02140	0.02	1.568 down	LCR72 (LOW-MOLECULAR-WEIGHT CYSTEINE-RICH 72); peptidase inhibitor
AT2G04045	0.0113	2.096 down	Encodes a defensin-like (DEFL) family protein.
AT2G04063	0.0498	1.711 down	glycine-rich protein
AT2G04420	0.0712	3.159 down	nucleic acid binding
AT2G04495	0.0534	1.787 down	unknown protein
AT2G04910	0.0466	1.556 down	glycosyl hydrolase family protein 17
AT2G05190	0.0244	2.374 down	pseudogene, cytochrome P450 -related, blastp match of 34% identity and 2.0e-07 P-value to SP
AT2G05300	0.0948	2.632 down	pseudogene of the F-box protein family
AT2G05450	0.0758	1.799 down	transposable element gene
AT2G05642	0.00939	1.630 down	CONTAINS InterPro DOMAIN/s: Nucleic acid-binding, OB-fold (InterPro:IPR012340), Nucleic acid-binding, OB-fold-like (InterPro:IPR016027), Protein of unknown function DUF223, Arabidopsis thaliana (InterPro:IPR003871); BEST Arabidopsis thaliana protein match is: replication protein-related (TAIR:AT1G52950.1); Has 317 Blast hits to 292 proteins in 67 species: Archae - 0; Bacteria - 13; Metazoa - 20; Fungi - 36; Plants - 193; Viruses - 0; Other Eukaryotes - 55 (source: NCBI BLink).
AT2G05750	0.0892	1.675 down	transposable element gene
AT2G05753	0.0248	2.773 down	unknown protein
AT2G06700	0.0164	3.169 down	transposable element gene
AT2G06800	0.0553	1.708 down	transposable element gene
AT2G06983	0.0958	1.676 down	SCRL16 (SCR-Like 16)
AT2G07483	0.0837	2.520 down	transposable element gene
AT2G09830	0.0294	3.224 down	transposable element gene
AT2G09850	0.0206	2.231 down	transposable element gene
AT2G10040	0.0818	2.244 down	transposable element gene
AT2G10270	0.0559	1.585 down	transposable element gene
AT2G10440	0.0397	1.853 down	unknown protein
AT2G11020	0.0684	2.564 down	transposable element gene
AT2G11345	0.0475	1.815 down	transposable element gene
AT2G11390	0.0459	1.929 down	transposable element gene
AT2G12290	0.0583	1.880 down	BEST Arabidopsis thaliana protein match is: RING; protein binding / zinc ion binding (TAIR:AT4G19700.1); Has 39 Blast hits to 39 proteins in 8 species: Archae - 0; Bacteria - 0; Metazoa - 0; Fungi - 0; Plants - 39; Viruses - 0; Other Eukaryotes - 0 (source: NCBI BLink).
AT2G12920	0.0155	2.143 down	transposable element gene
AT2G13295	0.0105	2.763 down	Encodes a Protease inhibitor/seed storage/LTP family protein
AT2G13410	0.0863	1.530 down	pseudogene of unknown protein
AT2G14090	0.0424	1.605 down	pseudogene, expressed protein
AT2G14247	0.00433	2.155 down	Expressed protein
AT2G14335	0.0566	2.028 down	transposable element gene
AT2G15325	0.0152	1.500 down	protease inhibitor/seed storage/lipid transfer protein (LTP) family protein
AT2G15815	0.0261	2.313 down	transposable element gene
AT2G16190	0.0966	1.642 down	BEST Arabidopsis thaliana protein match is: hydroxyproline-rich glycoprotein family protein (TAIR:AT1G49330.1); Has 39 Blast hits to 39 proteins in 16 species: Archae - 0; Bacteria - 0; Metazoa - 5; Fungi - 5; Plants - 27; Viruses - 0; Other Eukaryotes - 2 (source: NCBI BLink).
AT2G16230	0.0549	1.977 down	catalytic/ cation binding / hydrolase, hydrolyzing O-glycosyl compounds
AT2G16760	0.0369	2.436 down	CONTAINS InterPro DOMAIN/s: Six-bladed beta-propeller, TolB-like (InterPro:IPR011042); BEST Arabidopsis thaliana protein match is: unknown protein (TAIR:AT2G47370.1); Has 78 Blast hits to 78 proteins in 24 species: Archae - 0; Bacteria - 32; Metazoa - 0; Fungi - 0; Plants - 42; Viruses - 0; Other Eukaryotes - 4 (source: NCBI BLink).
AT2G16980	0.0726	1.637 down	tetracycline transporter
AT2G18196	0.0243	1.908 down	metal ion binding
AT2G19000	0.0508	1.694 down	BEST Arabidopsis thaliana protein match is: glycine-rich protein (TAIR:AT4G21620.1); Has 49 Blast hits to 49 proteins in 7 species: Archae - 0; Bacteria - 0; Metazoa - 2; Fungi - 0; Plants - 47; Viruses - 0; Other Eukaryotes - 0 (source: NCBI BLink).
AT2G19200	0.0227	2.413 down	unknown protein
AT2G19840	0.00357	1.808 down	transposable element gene
AT2G20630	0.0639	1.882 down	protein phosphatase 2C, putative / PP2C, putative
AT2G21610	0.0782	1.755 down	pectinesterase family protein
AT2G22280	0.0508	4.599 down	pre-tRNA
AT2G22460	0.0153	1.643 down	unknown protein
AT2G23400	0.0111	3.177 down	dehydrodolichyl diphosphate synthase, putative / DEDOL-PP synthase, putative
AT2G24625	0.0975	1.674 down	Encodes a defensin-like (DEFL) family protein.
AT2G24696	0.0808	2.154 down	DNA binding
AT2G24800	0.0795	1.582 down	peroxidase, putative

AT2G25295	0.0378	1.590 down	LCR81 (Low-molecular-weight cysteine-rich 81)
AT2G26320	0.0397	2.342 down	AGL33 (AGAMOUS-LIKE 33); DNA binding / transcription factor
AT2G27550	0.00273	2.199 down	ATC (ARABIDOPSIS THALIANA CENTRORADIALIS); phosphatidylethanolamine binding
AT2G28460	0.0208	2.338 down	protein binding / zinc ion binding
AT2G28690	0.0597	1.809 down	unknown protein
AT2G29610	0.0489	2.659 down	pseudogene of the F-box protein family, contains Pfam profile PF00646: F-box domain
AT2G31081	0.0534	1.782 down	CLE4 (CLAVATA3/ESR-RELATED 4); protein binding / receptor binding
AT2G31500	0.0648	2.235 down	CPK24; ATP binding / calcium ion binding / calmodulin-dependent protein kinase/ kinase/ protein kinase/ protein serine/threonine kinase
AT2G32050	0.0845	1.575 down	cell cycle control protein-related
AT2G32170	0.0185	1.979 down	CONTAINS InterPro DOMAIN/s: N2227-like (InterPro:IPR012901); BEST Arabidopsis thaliana protein match is: unknown protein (TAIR:AT2G32160.3).
AT2G32310	0.0168	2.598 down	unknown protein
AT2G32470	0.00126	1.643 down	F-box family protein-related
AT2G33350	0.0838	2.058 down	CONTAINS InterPro DOMAIN/s: CCT domain (InterPro:IPR010402); BEST Arabidopsis thaliana protein match is: zinc finger CONSTANS-related (TAIR:AT1G04500.1); Has 7688 Blast hits to 4734 proteins in 129 species: Archae - 8; Bacteria - 25; Metazoa - 148; Fungi - 118; Plants - 919; Viruses - 0; Other Eukaryotes - 6470 (source: NCBI BLink).
AT2G33520	0.0625	1.537 down	BEST Arabidopsis thaliana protein match is: proline-rich family protein (TAIR:AT1G12810.1); Has 48 Blast hits to 48 proteins in 15 species: Archae - 0; Bacteria - 0; Metazoa - 7; Fungi - 2; Plants - 39; Viruses - 0; Other Eukaryotes - 0 (source: NCBI BLink).
AT2G34440	0.1	2.526 down	AGL29 (AGAMOUS-LIKE 29); transcription factor
AT2G34990	0.0158	1.599 down	zinc finger (C3HC4-type RING finger) family protein
AT2G35080	0.0189	1.658 down	ATP binding / aminoacyl-tRNA ligase/ nucleotide binding
AT2G35384	0.0553	2.106 down	snoRNA
AT2G37140	0.0154	1.635 down	terpene synthase/cyclase-related
AT2G37740	0.0209	2.276 down	ZFP10 (ZINC-FINGER PROTEIN 10); nucleic acid binding / transcription factor/ zinc ion binding
AT2G38220	0.0506	2.428 down	protein binding / zinc ion binding
AT2G38823	0.0437	2.235 down	unknown protein
AT2G39370	0.0128	1.726 down	unknown protein
AT2G39520	0.0686	1.973 down	unknown protein
AT2G41240	0.0219	1.621 down	BHLH100 (BASIC HELIX-LOOP-HELIX PROTEIN 100); DNA binding / transcription factor
AT2G41780	0.0129	1.849 down	unknown protein
AT2G43220	0.0991	1.864 down	DC1 domain-containing protein
AT2G43610	0.0549	1.544 down	glycoside hydrolase family 19 protein
AT2G43660	0.0127	1.896 down	glycosyl hydrolase family protein 17
AT2G43730	0.0834	1.587 down	lectin-related
AT2G44195	0.0579	1.890 down	unknown protein
AT2G46230	0.0967	2.131 down	CONTAINS InterPro DOMAIN/s: Protein of unknown function DUF652 (InterPro:IPR006984), Nucleotide binding protein, PINc (InterPro:IPR006596); BEST Arabidopsis thaliana protein match is: unknown protein (TAIR:AT1G26530.1); Has 441 Blast hits to 441 proteins in 161 species: Archae - 15; Bacteria - 0; Metazoa - 185; Fungi - 119; Plants - 49; Viruses - 0; Other Eukaryotes - 73 (source: NCBI BLink).
AT2G46590	0.0494	1.616 down	DAG2 (DOF AFFECTING GERMINATION 2); DNA binding / transcription factor
AT2G47570	0.0831	1.581 down	60S ribosomal protein L18 (RPL18A)
AT2G47890	0.063	2.633 down	zinc finger (B-box type) family protein
AT3G01331	0.0218	2.439 down	Encodes a ECA1 gametogenesis related family protein
AT3G01760	0.0871	2.071 down	lysine and histidine specific transporter, putative
AT3G02100	0.0977	2.056 down	UDP-glucoronosyl/UDP-glucosyl transferase family protein
AT3G02440	0.0169	2.181 down	unknown protein
AT3G02610	0.00931	1.505 down	acyl-[acyl-carrier-protein] desaturase/ oxidoreductase/ transition metal ion binding
AT3G02810	0.0642	2.471 down	protein kinase family protein
AT3G02860	0.0224	1.925 down	zinc ion binding
AT3G03240	0.0086	2.646 down	esterase/lipase/thioesterase family protein
AT3G04060	0.0487	2.073 down	anac046 (Arabidopsis NAC domain containing protein 46); transcription factor
AT3G05770	0.00381	1.889 down	unknown protein
AT3G05936	0.0782	1.849 down	unknown protein
AT3G05960	0.064	2.150 down	STP6 (SUGAR TRANSPORTER 6); carbohydrate transmembrane transporter/ monosaccharide transmembrane transporter/ sugar:hydrogen symporter
AT3G06230	0.0743	2.007 down	ATMKK8; MAP kinase kinase/ kinase
AT3G06545	0.0363	1.830 down	unknown protein
AT3G08762	0.0408	1.702 down	unknown protein
AT3G09120	0.0976	2.028 down	unknown protein
AT3G09220	0.025	1.930 down	LAC7 (laccase 7); laccase
AT3G09350	0.0326	1.919 down	armadillo/beta-catenin repeat family protein
AT3G10890	0.0834	1.671 down	(1-4)-beta-mannan endohydrolase, putative
AT3G11010	0.0464	1.523 down	AtRLP34 (Receptor Like Protein 34); kinase/ protein binding
AT3G11750	0.0587	1.903 down	dihydroneopterin aldolase, putative
AT3G12981	0.0894	3.061 down	pseudogene of F-box family protein
AT3G13229	0.0604	1.670 down	unknown protein
AT3G13590	0.00788	1.648 down	DC1 domain-containing protein
AT3G13782	0.0273	1.604 down	NAP1;4 (NUCLEOSOME ASSEMBLY PROTEIN1;4); DNA binding / chromatin binding
AT3G13890	0.0472	1.686 down	ATMYB26 (MYB DOMAIN PROTEIN 26); DNA binding / transcription factor
AT3G14370	0.0356	1.821 down	WAG2; kinase/ protein serine/threonine kinase
AT3G14735	0.0818	2.927 down	U6-1; snRNA
AT3G14770	0.0389	1.520 down	nodulin MtN3 family protein
AT3G14780	0.0403	2.436 down	BEST Arabidopsis thaliana protein match is: ATGSL04 (glucan synthase-like 4); 1,3-beta-glucan synthase/ transferase, transferring glycosyl groups (TAIR:AT3G14570.1); Has 209 Blast hits to 205 proteins in 37 species: Archae - 2; Bacteria - 7; Metazoa - 14; Fungi - 6; Plants - 83; Viruses - 2; Other Eukaryotes - 95 (source: NCBI BLink).

AT3G15605	0.00239	1.841 down	nucleic acid binding
AT3G15870	0.0894	2.120 down	oxidoreductase
AT3G16020	0.0418	2.458 down	phospholipase C
AT3G16450	0.0488	2.809 down	jacalin lectin family protein
AT3G16580	0.0662	1.676 down	F-box family protein
AT3G17200	0.0647	1.626 down	transposable element gene
AT3G18730	0.0283	1.510 down	TSK (TONSOKU); protein binding
AT3G18810	0.0329	1.664 down	protein kinase family protein
AT3G19310	0.0399	3.389 down	phospholipase C/ phosphoric diester hydrolase
AT3G19350	0.0127	1.840 down	MPC (MATERNALLY EXPRESSED PAB C-TERMINAL); poly(A) binding
AT3G19530	0.0142	2.117 down	unknown protein
AT3G20140	0.0114	2.465 down	CYP705A23; electron carrier/ heme binding / iron ion binding / monooxygenase/ oxygen binding
AT3G20190	0.0526	2.133 down	leucine-rich repeat transmembrane protein kinase, putative
AT3G20810	0.0528	1.571 down	transcription factor jumonji (jmjC) domain-containing protein
AT3G20935	0.011	1.737 down	CYP705A28; electron carrier/ heme binding / iron ion binding / monooxygenase
AT3G21120	0.039	2.613 down	F-box family protein
AT3G21380	0.0631	1.541 down	CONTAINS InterPro DOMAIN/s: Mannose-binding lectin (InterPro:IPR001229); BEST Arabidopsis thaliana protein match is: MBP1 (MYROSINASE-BINDING PROTEIN 1); protein binding (TAIR:AT1G52040.1); Has 1279 Blast hits to 507 proteins in 33 species: Archae - 0; Bacteria - 0; Metazoa - 0; Fungi - 0; Plants - 1276; Viruses - 0; Other Eukaryotes - 3 (source: NCBI BLink).
AT3G22057	0.0217	1.761 down	BEST Arabidopsis thaliana protein match is: receptor-like protein kinase-related (TAIR:AT3G22050.1).
AT3G22510	0.08	1.608 down	unknown protein
AT3G22910	0.0553	4.078 down	calcium-transporting ATPase, plasma membrane-type, putative / Ca(2+)-ATPase, putative (ACA13)
AT3G23190	0.0539	1.824 down	lesion inducing protein-related
AT3G23633	0.0942	1.996 down	CONTAINS InterPro DOMAIN/s: F-box associated (InterPro:IPR006527); BEST Arabidopsis thaliana protein match is: F-box family protein (FBX9) (TAIR:AT2G04920.1).
AT3G24780	0.0579	1.729 down	CONTAINS InterPro DOMAIN/s: Uncharacterized conserved protein UCP015417, vWA (InterPro:IPR011205), von Willebrand factor, type A (InterPro:IPR002035); BEST Arabidopsis thaliana protein match is: unknown protein (TAIR:AT5G13210.1); Has 276 Blast hits to 231 proteins in 34 species: Archae - 0; Bacteria - 26; Metazoa - 5; Fungi - 23; Plants - 46; Viruses - 15; Other Eukaryotes - 161 (source: NCBI BLink).
AT3G25050	0.0269	1.785 down	XTH3 (XYLOGLUCAN ENDOTRANSGLUCOSYLASE/HYDROLASE 3); hydrolase, acting on glycosyl bonds / xyloglucan:xyloglucosyl transferase
AT3G25080	0.0951	1.998 down	unknown protein
AT3G25180	0.0136	1.929 down	CYP82G1; electron carrier/ heme binding / iron ion binding / monooxygenase/ oxygen binding
AT3G25233	0.0941	1.878 down	unknown protein
AT3G25265	0.0789	1.536 down	LCR4 (Low-molecular-weight cysteine-rich 4)
AT3G26220	0.0118	1.699 down	CYP71B3; electron carrier/ heme binding / iron ion binding / monooxygenase/ oxygen binding
AT3G26250	0.0667	1.859 down	DC1 domain-containing protein
AT3G26260	0.0673	1.534 down	transposable element gene
AT3G27327	0.0241	1.635 down	transposable element gene
AT3G27328	0.0744	2.046 down	unknown protein
AT3G27380	0.0959	2.027 down	SDH2-1; electron carrier/ succinate dehydrogenase
AT3G28170	0.0306	2.208 down	unknown protein
AT3G28674	0.0653	1.517 down	unknown protein
AT3G28830	0.0224	2.102 down	unknown protein
AT3G28880	0.00546	2.279 down	protein binding
AT3G28990	0.00419	1.640 down	unknown protein
AT3G29431	0.0308	1.616 down	unknown protein
AT3G29460	0.0213	1.849 down	transposable element gene
AT3G29781	0.0331	1.600 down	transposable element gene
AT3G29796	0.0675	2.668 down	unknown protein
AT3G29797	0.077	1.767 down	Encodes a ECA1 gametogenesis related family protein
AT3G30380	0.0481	2.936 down	CONTAINS InterPro DOMAIN/s: Alpha/beta hydrolase fold-1 (InterPro:IPR000073); BEST Arabidopsis thaliana protein match is: unknown protein (TAIR:AT3G01690.1); Has 3127 Blast hits to 3124 proteins in 513 species: Archae - 3; Bacteria - 775; Metazoa - 627; Fungi - 135; Plants - 158; Viruses - 6; Other Eukaryotes - 1423 (source: NCBI BLink).
AT3G30705	0.0916	1.717 down	unknown protein
AT3G30770	0.0295	2.111 down	ATP binding / aminoacyl-tRNA ligase/ nucleotide binding
AT3G30848	0.0531	1.593 down	transposable element gene
AT3G30867	0.0654	2.114 down	pseudogene, putative SNF8 protein homolog, similar to SNF8 protein homolog GB:T04827 GI:7488343 from (Arabidopsis thaliana); blastp match of 70% identity and 4.2e-25 P-value to GP
AT3G31380	0.0181	1.565 down	transposable element gene
AT3G31430	0.0566	1.692 down	unknown protein
AT3G31905	0.0359	1.576 down	transposable element gene
AT3G32021	0.00924	1.541 down	transposable element gene
AT3G33163	0.0254	1.949 down	transposable element gene
AT3G33448	0.0839	1.947 down	transposable element gene
AT3G33545	0.00852	1.905 down	transposable element gene
AT3G33572	0.0802	1.830 down	transposable element gene
AT3G36659	0.0405	1.692 down	invertase/pectin methylesterase inhibitor family protein
AT3G42110	0.0225	1.788 down	transposable element gene
AT3G42140	0.0457	2.368 down	nucleic acid binding / zinc ion binding
AT3G42230	0.0776	1.979 down	transposable element gene

AT3G42290	0.0661	1.518 down	transposable element gene
AT3G42440	0.0503	1.816 down	transposable element gene
AT3G43420	0.036	2.313 down	unknown protein
AT3G43430	0.0497	1.923 down	zinc finger (C3HC4-type RING finger) family protein
AT3G43500	0.0855	1.558 down	unknown protein
AT3G44130	0.0543	3.136 down	F-box family protein
AT3G44425	0.0602	1.665 down	transposable element gene
AT3G44516	0.0252	1.659 down	Pseudogene of AT1G31990; unknown protein
AT3G46310	0.0331	2.423 down	unknown protein
AT3G46616	0.038	1.713 down	unknown protein
AT3G47180	0.0712	1.567 down	zinc finger (C3HC4-type RING finger) family protein
AT3G47280	0.0583	1.590 down	transposable element gene
AT3G48480	0.0228	1.634 down	cysteine-type peptidase
AT3G48940	0.013	1.531 down	remorin family protein
AT3G49630	0.0812	1.656 down	2-oxoacid-dependent oxidase, putative
AT3G50570	0.0807	1.535 down	hydroxyproline-rich glycoprotein family protein
AT3G51200	0.00994	2.017 down	auxin-responsive family protein
AT3G52020	0.0917	2.751 down	scpl39 (serine carboxypeptidase-like 39); serine-type carboxypeptidase
AT3G52705	0.0513	1.603 down	transposable element gene
AT3G53294	0.075	1.658 down	unknown protein
AT3G55540	0.0511	2.007 down	nuclear transport factor 2 (NTF2) family protein
AT3G55672	0.038	2.491 down	CONTAINS InterPro DOMAIN/s: Plant self-incompatibility S1 (InterPro:IPR010264); BEST Arabidopsis thaliana protein match is: unknown protein (TAIR:AT3G55665.1); Has 80 Blast hits to 77 proteins in 7 species: Archae - 0; Bacteria - 0; Metazoa - 0; Fungi - 0; Plants - 80; Viruses - 0; Other Eukaryotes - 0 (source: NCBI BLink).
AT3G55930	0.0725	1.591 down	RNA splicing factor-related
AT3G57130	0.0432	2.424 down	BOP1 (BLADE ON PETIOLE 1); protein binding
AT3G57250	0.00221	2.212 down	emsy N terminus domain-containing protein / ENT domain-containing protein
AT3G57690	0.0872	1.697 down	AGP23 (ARABINOGALACTAN-PROTEIN 23)
AT3G58070	0.0599	1.807 down	GIS (GLABROUS INFLORESCENCE STEMS); nucleic acid binding / transcription factor/ zinc ion binding
AT3G58210	0.078	1.801 down	meprin and TRAF homology domain-containing protein / MATH domain-containing protein
AT3G59590	0.0831	1.621 down	jacalin lectin family protein
AT3G59710	0.0396	2.079 down	short-chain dehydrogenase/reductase (SDR) family protein
AT3G59740	0.0744	1.673 down	receptor lectin kinase 3 (lecRK3)
AT3G59850	0.0913	1.759 down	polygalacturonase, putative / pectinase, putative
AT3G60286	0.0912	1.562 down	unknown protein
AT3G61660	0.00426	2.195 down	unknown protein
AT3G61900	0.0246	3.133 down	auxin-responsive family protein
AT3G62020	0.00645	1.895 down	GLP10 (GERMIN-LIKE PROTEIN 10); manganese ion binding / nutrient reservoir
AT3G62030	0.0406	1.855 down	peptidyl-prolyl cis-trans isomerase, chloroplast / cyclophilin / rotamase / cyclosporin A-binding protein (ROC4)
AT3G62280	0.0903	1.687 down	carboxylesterase/ hydrolase, acting on ester bonds
AT3G63052	0.0506	1.682 down	unknown protein
AT3G63088	0.0395	2.651 down	RTFL14 (ROTUNDIFOLIA LIKE 14)
AT4G00236	0.0641	1.947 down	pseudogene, similar to leaf senescence-associated receptor-like protein kinase, blastp match of 56% identity and 4.7e-52 P-value to GP
AT4G00390	0.0866	1.696 down	transcription regulator
AT4G01220	0.0921	1.556 down	CONTAINS InterPro DOMAIN/s: Reticulon (InterPro:IPR003388); BEST Arabidopsis thaliana protein match is: RGXT1 (rhamnogalacturonan xylosyltransferase 1); UDP-xylosyltransferase (TAIR:AT4G01770.1); Has 153 Blast hits to 150 proteins in 16 species: Archae - 0; Bacteria - 0; Metazoa - 0; Fungi - 0; Plants - 142; Viruses - 0; Other Eukaryotes - 11 (source: NCBI BLink).
AT4G01533	0.00963	2.876 down	other RNA
AT4G01680	0.0924	1.776 down	MYB55 (myb domain protein 55); DNA binding / transcription factor
AT4G02180	0.0908	2.890 down	DC1 domain-containing protein
AT4G03113	0.00184	2.510 down	unknown protein
AT4G03438	0.0395	1.818 down	MIR447C; miRNA
AT4G03580	0.0259	1.960 down	BEST Arabidopsis thaliana protein match is: cathepsin-related (TAIR:AT5G17080.1); Has 215 Blast hits to 146 proteins in 28 species: Archae - 0; Bacteria - 11; Metazoa - 101; Fungi - 14; Plants - 5; Viruses - 0; Other Eukaryotes - 84 (source: NCBI BLink).
AT4G03630	0.0436	1.955 down	root nodule development protein-related
AT4G03680	0.099	1.523 down	transposable element gene
AT4G03745	0.0276	1.528 down	transposable element gene
AT4G04010	0.0456	1.510 down	transposable element gene
AT4G04270	0.0616	1.550 down	transposable element gene
AT4G04480	0.0175	2.427 down	BEST Arabidopsis thaliana protein match is: F-box family protein (TAIR:AT4G22030.1); Has 51 Blast hits to 51 proteins in 4 species: Archae - 0; Bacteria - 0; Metazoa - 0; Fungi - 0; Plants - 51; Viruses - 0; Other Eukaryotes - 0 (source: NCBI BLink).
AT4G04710	0.0421	1.738 down	CPK22; ATP binding / calcium ion binding / calmodulin-dependent protein kinase/ kinase/ protein kinase/ protein serine/threonine kinase
AT4G05310	0.0516	1.632 down	ubiquitin family protein
AT4G05630	0.024	1.836 down	unknown protein
AT4G06500	0.0732	1.930 down	transposable element gene
AT4G06548	0.086	1.542 down	transposable element gene
AT4G06554	0.0186	3.237 down	transposable element gene
AT4G06570	0.0338	2.410 down	transposable element gene
AT4G06591	0.0449	2.046 down	transposable element gene
AT4G07495	0.0417	1.577 down	transposable element gene
AT4G07528	0.0906	2.206 down	transposable element gene
AT4G07843	0.0388	1.757 down	transposable element gene

AT4G07936	0.0811	1.700 down	transposable element gene
AT4G08028	0.0698	2.517 down	Encodes a defensin-like (DEFL) family protein.
AT4G08053	0.0379	1.763 down	transposable element gene
AT4G08094	0.0274	1.622 down	transposable element gene
AT4G08097	0.023	1.556 down	unknown protein
AT4G08550	0.00926	1.909 down	electron carrier/ protein disulfide oxidoreductase
AT4G08602	0.0128	1.747 down	transposable element gene
AT4G08876	0.0853	1.548 down	pyrophosphate--fructose-6-phosphate 1-phosphotransferase-related / pyrophosphate-dependent 6-phosphofructose-1-kinase-related
AT4G09984	0.00865	1.691 down	LCR34 (Low-molecular-weight cysteine-rich 34)
AT4G10150	0.00911	2.236 down	zinc finger (C3HC4-type RING finger) family protein
AT4G10430	0.0406	2.949 down	CONTAINS InterPro DOMAIN/s: TMPIT-like (InterPro:IPR012926); BEST Arabidopsis thaliana protein match is: unknown protein (TAIR:AT1G33230.1); Has 196 Blast hits to 196 proteins in 60 species: Archae - 0; Bacteria - 0; Metazoa - 146; Fungi - 0; Plants - 40; Viruses - 0; Other Eukaryotes - 10 (source: NCBI BLink).
AT4G10490	0.033	2.379 down	oxidoreductase, 2OG-Fe(II) oxygenase family protein
AT4G11350	0.0712	3.313 down	transferase, transferring glycosyl groups
AT4G11375	0.0344	3.630 down	transposable element gene
AT4G11521	0.0424	2.315 down	CONTAINS InterPro DOMAIN/s: Protein of unknown function DUF26 (InterPro:IPR002902); BEST Arabidopsis thaliana protein match is: kinase (TAIR:AT4G11530.1).
AT4G11770	0.00654	3.719 down	kelch repeat-containing F-box family protein
AT4G11910	0.0626	1.955 down	BEST Arabidopsis thaliana protein match is: NYE1 (NON-YELLOWING 1) (TAIR:AT4G22920.1); Has 130 Blast hits to 128 proteins in 45 species: Archae - 0; Bacteria - 50; Metazoa - 0; Fungi - 0; Plants - 78; Viruses - 0; Other Eukaryotes - 2 (source: NCBI BLink).
AT4G12100	0.0528	1.764 down	ubiquitin protein ligase binding
AT4G12440	0.0936	2.037 down	adenine phosphoribosyltransferase, putative
AT4G12580	0.0517	1.566 down	unknown protein
AT4G12930	0.0107	2.385 down	unknown protein
AT4G13080	0.0106	2.204 down	xyloglucan:xyloglucosyl transferase, putative / xyloglucan endotransglycosylase, putative / endo-xyloglucan transferase, putative
AT4G13110	0.0121	2.017 down	BSD domain-containing protein
AT4G14170	0.0975	1.585 down	pentatricopeptide (PPR) repeat-containing protein
AT4G14548	0.0813	2.082 down	other RNA
AT4G14630	0.0546	1.923 down	GLP9 (GERMIN-LIKE PROTEIN 9); manganese ion binding / nutrient reservoir
AT4G15060	0.0541	1.603 down	F-box protein-related
AT4G15242	0.059	2.287 down	other RNA
AT4G15715	0.00775	1.889 down	CONTAINS InterPro DOMAIN/s: Cystatin-related, plant (InterPro:IPR006525); BEST Arabidopsis thaliana protein match is: unknown protein (TAIR:AT5G56920.1); Has 26 Blast hits to 26 proteins in 2 species: Archae - 0; Bacteria - 0; Metazoa - 0; Fungi - 0; Plants - 26; Viruses - 0; Other Eukaryotes - 0 (source: NCBI BLink).
AT4G15735	0.0938	1.728 down	SCRL10 (SCR-Like 10)
AT4G16024	0.0504	2.059 down	unknown protein
AT4G17788	0.00481	2.232 down	MIR160/MIR160B; miRNA
AT4G18000	0.00726	1.687 down	unknown protein
AT4G18110	0.0933	1.685 down	zinc finger (C3HC4-type RING finger) family protein
AT4G18620	0.0275	2.270 down	BEST Arabidopsis thaliana protein match is: Bet v I allergen family protein (TAIR:AT5G45870.1); Has 190 Blast hits to 190 proteins in 20 species: Archae - 0; Bacteria - 0; Metazoa - 12; Fungi - 0; Plants - 178; Viruses - 0; Other Eukaryotes - 0 (source: NCBI BLink).
AT4G19340	0.0918	1.838 down	BEST Arabidopsis thaliana protein match is: kelch repeat-containing protein (TAIR:AT4G19260.1); Has 204 Blast hits to 159 proteins in 69 species: Archae - 0; Bacteria - 0; Metazoa - 46; Fungi - 53; Plants - 67; Viruses - 0; Other Eukaryotes - 38 (source: NCBI BLink).
AT4G19910	0.00121	2.210 down	Toll-Interleukin-Resistance (TIR) domain-containing protein
AT4G20490	0.0481	1.927 down	transposable element gene
AT4G22066	0.0112	1.781 down	Pseudogene of AT5G66830; F-box family protein
AT4G22180	0.033	1.583 down	F-box family protein
AT4G23432	0.0218	1.749 down	unknown protein
AT4G23780	0.0228	1.809 down	unknown protein
AT4G24026	0.0712	2.329 down	unknown protein
AT4G25330	0.0385	1.855 down	unknown protein
AT4G26780	0.0589	1.930 down	AR192; adenyl-nucleotide exchange factor/ chaperone binding / protein binding / protein homodimerization
AT4G27150	0.051	2.016 down	2S seed storage protein 2 / 2S albumin storage protein / NWMU2-2S albumin 2
AT4G27480	0.0651	1.818 down	glycosyltransferase family 14 protein / core-2/I-branching enzyme family protein
AT4G27850	0.0647	2.954 down	proline-rich family protein
AT4G27970	0.0886	2.413 down	SLAH2 (SLAC1 HOMOLOGUE 2); transporter
AT4G28720	0.0909	2.087 down	flavin-containing monooxygenase family protein / FMO family protein
AT4G29276	0.0104	2.593 down	Pseudogene of AT4G29270; acid phosphatase class B family protein
AT4G29740	0.075	1.537 down	CKX4 (CYTOKININ OXIDASE 4); amine oxidase/ cytokinin dehydrogenase
AT4G30067	0.00209	2.221 down	LCR63 (Low-molecular-weight cysteine-rich 63)
AT4G30290	0.0636	1.918 down	XTH19 (XYLOGLUCAN ENDOTRANSGLUCOSYLASE/HYDROLASE 19); hydrolase, acting on glycosyl bonds / hydrolase, hydrolyzing O-glycosyl compounds / xyloglucan:xyloglucosyl transferase
AT4G30430	0.0285	2.524 down	TET9 (TETRASPANIN9)
AT4G31570	0.0682	4.731 down	unknown protein
AT4G31620	0.00967	2.517 down	transcriptional factor B3 family protein
AT4G31660	0.00543	2.650 down	transcriptional factor B3 family protein
AT4G32030	0.0577	2.799 down	unknown protein

AT4G32280	0.0627	1.717 down	IAA29 (INDOLE-3-ACETIC ACID INDUCIBLE 29); transcription factor
AT4G32560	0.0611	2.690 down	paramyosin-related
AT4G35589	0.054	1.780 down	unknown protein
AT4G35655	0.035	1.637 down	CONTAINS InterPro DOMAIN/s: Defence response, Rin4 (InterPro:IPR008700); BEST Arabidopsis thaliana protein match is: nitrate-responsive NOI protein, putative (TAIR:AT2G17660.1); Has 135 Blast hits to 134 proteins in 12 species: Archae - 0; Bacteria - 0; Metazoa - 0; Fungi - 0; Plants - 135; Viruses - 0; Other Eukaryotes - 0 (source: NCBI BLink).
AT4G36560	0.072	2.259 down	unknown protein
AT4G36820	0.0892	3.171 down	unknown protein
AT4G37620	0.0324	1.659 down	transposable element gene
AT4G37770	0.0892	2.138 down	ACS8; 1-aminocyclopropane-1-carboxylate synthase
AT4G37860	0.0102	3.611 down	CONTAINS InterPro DOMAIN/s: Chromatin SPT2 (InterPro:IPR013256); BEST Arabidopsis thaliana protein match is: unknown protein (TAIR:AT2G22720.3); Has 543 Blast hits to 488 proteins in 97 species: Archae - 0; Bacteria - 20; Metazoa - 186; Fungi - 63; Plants - 52; Viruses - 1; Other Eukaryotes - 221 (source: NCBI BLink).
AT4G38090	0.0807	1.947 down	unknown protein
AT4G39590	0.054	2.539 down	kelch repeat-containing F-box family protein
AT5G01140	0.0638	2.017 down	unknown protein
AT5G01520	0.034	2.413 down	zinc finger (C3HC4-type RING finger) family protein
AT5G02420	0.0427	1.683 down	unknown protein
AT5G02640	0.0753	1.807 down	unknown protein
AT5G02730	0.0469	2.438 down	allergen V5/Tpx-1-related family protein
AT5G04350	0.0946	2.712 down	self-incompatibility protein-related
AT5G05150	0.0127	1.524 down	AtATG18e
AT5G06070	0.000351	4.327 down	RBE (RABBIT EARS); nucleic acid binding / transcription factor/ zinc ion binding
AT5G06270	0.0424	2.125 down	unknown protein
AT5G06420	0.0649	3.127 down	zinc finger (CCCH-type/C3HC4-type RING finger) family protein
AT5G07650	0.0581	2.521 down	formin homology 2 domain-containing protein / FH2 domain-containing protein
AT5G08480	0.0704	1.507 down	VQ motif-containing protein
AT5G09270	0.0285	2.936 down	unknown protein
AT5G09990	0.0822	1.743 down	PROPEP5 (Elicitor peptide 5 precursor)
AT5G10770	0.0541	2.011 down	chloroplast nucleoid DNA-binding protein, putative
AT5G12085	0.0121	2.115 down	transposable element gene
AT5G13670	0.00813	2.562 down	nodulin MtN21 family protein
AT5G13910	0.0926	2.521 down	LEP (LEAFY PETIOLE); DNA binding / transcription factor
AT5G14750	0.0275	2.346 down	ATMYB66 (MYB DOMAIN PROTEIN 66); DNA binding / protein binding / transcription factor/ transcription regulator
AT5G15190	0.0235	1.846 down	unknown protein
AT5G15265	0.00469	2.339 down	unknown protein
AT5G15500	0.0858	3.416 down	ankyrin repeat family protein
AT5G16490	0.00177	1.553 down	RIC4 (ROP-INTERACTIVE CRIB MOTIF-CONTAINING PROTEIN 4); protein binding
AT5G17320	0.0638	1.939 down	HDG9 (HOMEODOMAIN GLABROUS 9); DNA binding / sequence-specific DNA binding / transcription factor
AT5G17750	0.0617	1.653 down	AAA-type ATPase family protein
AT5G18220	0.0672	2.746 down	glycosyl hydrolase family 17 protein
AT5G18870	0.0562	2.505 down	inosine-uridine preferring nucleoside hydrolase-related
AT5G19473	0.0566	1.646 down	CONTAINS InterPro DOMAIN/s: Defence response, Rin4 (InterPro:IPR008700); BEST Arabidopsis thaliana protein match is: unknown protein (TAIR:AT5G09960.1); Has 39 Blast hits to 39 proteins in 9 species: Archae - 0; Bacteria - 0; Metazoa - 0; Fungi - 0; Plants - 39; Viruses - 0; Other Eukaryotes - 0 (source: NCBI BLink).
AT5G19490	0.00189	2.474 down	DNA binding / sequence-specific DNA binding
AT5G19530	0.0898	2.056 down	ACL5 (ACAULIS 5); spermine synthase/ thermospermine synthase
AT5G22200	0.0653	4.378 down	harpin-induced family protein / HIN1 family protein / harpin-responsive family protein
AT5G22420	0.0655	1.688 down	FAR7 (FATTY ACID REDUCTASE 7); binding / catalytic/ oxidoreductase, acting on the CH-CH group of donors
AT5G22960	0.0568	1.717 down	serine carboxypeptidase S10 family protein
AT5G23260	0.0801	2.415 down	TT16 (TRANSPARENT TESTA16); transcription factor
AT5G23870	0.0485	3.195 down	pectinacetylesterase family protein
AT5G24790	0.0434	1.648 down	unknown protein
AT5G24860	0.0962	1.663 down	FPF1 (FLOWERING PROMOTING FACTOR 1)
AT5G26610	0.0828	3.258 down	D111/G-patch domain-containing protein
AT5G26742	0.0314	1.931 down	emb1138 (embryo defective 1138); ATP binding / ATP-dependent helicase/ RNA binding / helicase/ nucleic acid binding / zinc ion binding
AT5G26840	0.0691	1.683 down	unknown protein
AT5G28335	0.0991	4.154 down	transposable element gene
AT5G28630	0.0176	2.144 down	glycine-rich protein
AT5G28637	0.0989	1.907 down	transposable element gene
AT5G28680	0.0251	2.157 down	protein kinase family protein
AT5G28710	0.0536	1.920 down	transposable element gene
AT5G28940	0.0827	2.445 down	transposable element gene
AT5G29030	0.0472	1.711 down	pseudogene, hypothetical protein
AT5G29708	0.015	1.886 down	transposable element gene
AT5G30207	0.0748	2.039 down	transposable element gene
AT5G30218	0.0229	2.766 down	transposable element gene
AT5G30390	0.0642	1.834 down	transposable element gene
AT5G30545	0.0962	1.646 down	transposable element gene
AT5G30942	0.0972	1.831 down	transposable element gene
AT5G31536	0.00995	1.685 down	transposable element gene
AT5G32070	0.0202	1.733 down	transposable element gene
AT5G32619	0.022	2.521 down	Encodes a defensin-like (DEFL) family protein.

AT5G32678	0.0661	2.532 down	transposable element gene
AT5G33391	0.0724	3.310 down	transposable element gene
AT5G33406	0.0762	2.228 down	protein dimerization
AT5G34869	0.0227	2.038 down	unknown protein
AT5G35120	0.0249	2.055 down	unknown protein
AT5G35240	0.0155	3.554 down	transposable element gene
AT5G35331	0.00537	1.830 down	transposable element gene
AT5G35470	0.0365	3.019 down	unknown protein
AT5G36228	0.00211	2.195 down	nucleic acid binding / zinc ion binding
AT5G36860	0.0222	1.690 down	transposable element gene
AT5G36870	0.0143	2.075 down	ATGSL09 (glucan synthase-like 9); 1,3-beta-glucan synthase
AT5G37000	0.0613	1.508 down	exostosin family protein
AT5G37150	0.0326	1.685 down	BEST Arabidopsis thaliana protein match is: tRNA-splicing endonuclease positive effector-related (TAIR:AT5G52090.1); Has 4236 Blast hits to 3442 proteins in 554 species: Archae - 133; Bacteria - 787; Metazoa - 1285; Fungi - 856; Plants - 359; Viruses - 41; Other Eukaryotes - 775 (source: NCBI BLink).
AT5G37445	0.04	2.069 down	pseudogene, similar to Similar to splicing factor 3a, subunit 2, 66kDa, blastp match of 60% identity and 1.2e-63 P-value to GP
AT5G37474	0.000125	1.569 down	Encodes a defensin-like (DEFL) family protein.
AT5G37650	0.078	1.607 down	unknown protein
AT5G37750	0.0245	1.740 down	heat shock protein binding / unfolded protein binding
AT5G38030	0.00793	2.541 down	MATE efflux family protein
AT5G38100	0.0728	3.358 down	methyltransferase-related
AT5G38386	0.0532	2.171 down	F-box family protein
AT5G38960	0.0259	2.640 down	germin-like protein, putative
AT5G39330	0.0502	2.925 down	unknown protein
AT5G39581	0.0053	2.049 down	unknown protein
AT5G39660	0.0529	2.081 down	CDF2 (CYCLING DOF FACTOR 2); DNA binding / protein binding / transcription factor
AT5G39700	0.0988	1.799 down	MYB89 (myb domain protein 89); DNA binding / transcription factor
AT5G39750	0.0544	1.986 down	AGL81 (AGAMOUS-LIKE 81); transcription factor
AT5G39820	0.0519	1.656 down	anac094 (Arabidopsis NAC domain containing protein 94); transcription factor
AT5G39890	0.0903	3.885 down	unknown protein
AT5G39920	0.00882	1.780 down	CONTAINS InterPro DOMAIN/s: Pre-mRNA cleavage complex II Clp1 (InterPro:IPR010655); BEST Arabidopsis thaliana protein match is: CLPS5 (CLP1-SIMILAR PROTEIN 5) (TAIR:AT5G39930.1); Has 8 Blast hits to 8 proteins in 4 species: Archae - 0; Bacteria - 0; Metazoa - 0; Fungi - 0; Plants - 8; Viruses - 0; Other Eukaryotes - 0 (source: NCBI BLink).
AT5G40040	0.0924	2.221 down	60S acidic ribosomal protein P2 (RPP2E)
AT5G40820	0.0888	1.849 down	ATRAD3; binding / inositol or phosphatidylinositol kinase/ phosphotransferase, alcohol group as acceptor / protein serine/threonine kinase
AT5G41265	0.0851	2.519 down	pre-tRNA
AT5G41835	0.0866	1.521 down	transposable element gene
AT5G42504	0.0776	1.548 down	unknown protein
AT5G42510	0.0817	3.407 down	disease resistance-responsive family protein
AT5G43000	0.0672	1.980 down	unknown protein
AT5G43340	0.0393	2.220 down	PHT6; carbohydrate transmembrane transporter/ inorganic phosphate transmembrane transporter/ phosphate transmembrane transporter/ sugar:hydrogen symporter
AT5G43513	0.0366	2.765 down	Encodes a defensin-like (DEFL) family protein.
AT5G43725	0.0822	1.980 down	other RNA
AT5G44220	0.00238	4.371 down	F-box family protein
AT5G44280	0.0313	2.662 down	RING1A (RING 1A); protein binding / zinc ion binding
AT5G44310	0.00802	2.508 down	late embryogenesis abundant domain-containing protein / LEA domain-containing protein
AT5G45113	0.0477	10.751 down	mitochondrial transcription termination factor-related / mTERF-related
AT5G45116	0.055	1.570 down	transposable element gene
AT5G45210	0.025	2.478 down	disease resistance protein (TIR-NBS-LRR class), putative
AT5G45905	0.0808	1.609 down	Encodes a defensin-like (DEFL) family protein.
AT5G46115	0.0587	1.665 down	unknown protein
AT5G46610	0.0626	2.992 down	unknown protein
AT5G46795	0.0341	1.554 down	MSP2 (microspore-specific promoter 2)
AT5G46871	0.0869	3.703 down	Encodes a defensin-like (DEFL) family protein.
AT5G48070	0.098	2.322 down	XTH20 (XYLOGLUCAN ENDOTRANSGLUCOSYLASE/HYDROLASE 20); hydrolase, acting on glycosyl bonds / hydrolase, hydrolyzing O-glycosyl compounds / xyloglucan:xyloglucosyl transferase
AT5G48200	0.0543	1.580 down	unknown protein
AT5G48400	0.0682	1.756 down	ATGLR1.2; intracellular ligand-gated ion channel
AT5G48860	0.0163	2.237 down	unknown protein
AT5G48980	0.0392	2.421 down	kelch repeat-containing F-box family protein
AT5G49130	0.0431	2.125 down	MATE efflux family protein
AT5G49360	0.0271	1.529 down	BXL1 (BETA-XYLOSIDASE 1); hydrolase, hydrolyzing O-glycosyl compounds
AT5G49850	0.0742	1.811 down	jacalin lectin family protein
AT5G50300	0.0206	2.088 down	xanthine/uracil/vitamin C permease family protein
AT5G50500	0.0838	1.584 down	unknown protein
AT5G50790	0.097	3.175 down	nodulin MtN3 family protein
AT5G51210	0.031	1.882 down	OLEO3 (OLEOSIN3)
AT5G51490	0.0473	1.814 down	pectinesterase family protein
AT5G52170	0.0689	1.783 down	HDG7 (HOMEODOMAIN GLABROUS 7); DNA binding / sequence-specific DNA binding / transcription factor
AT5G52720	0.0267	2.460 down	metal ion binding
AT5G52770	0.0348	2.321 down	heavy-metal-associated protein-related
AT5G52965	0.00452	3.378 down	unknown protein
AT5G53520	0.0227	1.845 down	ATOPT8 (ARABIDOPSIS THALIANA OLIGOPEPTIDE TRANSPORTER 8); oligopeptide transporter

AT5G54140	0.0454	1.744 down	ILL3; IAA-amino acid conjugate hydrolase/ metallopeptidase
AT5G55970	0.0409	1.753 down	zinc finger (C3HC4-type RING finger) family protein
AT5G56747	0.0425	2.842 down	transposable element gene
AT5G57535	0.0191	2.877 down	unknown protein
AT5G57747	0.012	1.648 down	unknown protein
AT5G59200	0.0615	1.520 down	pentatricopeptide (PPR) repeat-containing protein
AT5G60805	0.0307	1.716 down	Encodes a defensin-like (DEFL) family protein.
AT5G61090	0.0267	2.761 down	nucleic acid binding
AT5G61550	0.0827	2.526 down	protein kinase family protein
AT5G62150	0.00691	1.513 down	peptidoglycan-binding LysM domain-containing protein
AT5G62480	0.0762	3.170 down	ATGSTU9 (ARABIDOPSIS THALIANA GLUTATHIONE S-TRANSFERASE TAU 9); glutathione transferase
AT5G63150	0.0503	1.660 down	unknown protein
AT5G64735	0.00454	4.546 down	pre-tRNA
AT5G64910	0.00745	2.287 down	unknown protein
AT5G65158	0.0278	2.755 down	CONTAINS InterPro DOMAIN/s: Lipoxygenase, LH2 (InterPro:IPR001024), Lipase/lipooxygenase, PLAT/LH2 (InterPro:IPR008976); BEST Arabidopsis thaliana protein match is: lipid-associated family protein (TAIR:AT2G22170.1); Has 83 Blast hits to 83 proteins in 14 species: Archae - 0; Bacteria - 0; Metazoa - 4; Fungi - 0; Plants - 79; Viruses - 0; Other Eukaryotes - 0 (source: NCBI BLink).
AT5G66660	0.0255	1.614 down	unknown protein
AT5G66740	0.0814	3.693 down	unknown protein
AT5G67120	0.094	1.725 down	zinc finger (C3HC4-type RING finger) family protein
AT5G67620	0.0017	1.696 down	unknown protein
AT1G01640	0.0232	1.732 up	speckle-type POZ protein-related
AT1G02136	0.0748	1.909 up	pseudogene of phagocytosis and cell motility protein
AT1G02550	0.0833	1.735 up	invertase/pectin methylesterase inhibitor family protein
AT1G03720	0.0801	2.752 up	cathepsin-related
AT1G03890	0.0576	1.723 up	cupin family protein
AT1G03920	0.0202	1.890 up	protein kinase, putative
AT1G04470	0.0638	1.710 up	CONTAINS InterPro DOMAIN/s: Munc13 homology 1 (InterPro:IPR014770), Protein of unknown function DUF810 (InterPro:IPR008528), Munc13 homology 2 (InterPro:IPR014772); BEST Arabidopsis thaliana protein match is: unknown protein (TAIR:AT2G33420.1); Has 116 Blast hits to 109 proteins in 23 species: Archae - 0; Bacteria - 1; Metazoa - 4; Fungi - 4; Plants - 95; Viruses - 0; Other Eukaryotes - 12 (source: NCBI BLink).
AT1G04960	0.0525	1.916 up	CONTAINS InterPro DOMAIN/s: Protein of unknown function DUF1664 (InterPro:IPR012458); BEST Arabidopsis thaliana protein match is: bZIP family transcription factor (TAIR:AT1G27000.1); Has 95 Blast hits to 94 proteins in 14 species: Archae - 0; Bacteria - 4; Metazoa - 0; Fungi - 0; Plants - 89; Viruses - 0; Other Eukaryotes - 2 (source: NCBI BLink).
AT1G05700	0.0582	1.898 up	leucine-rich repeat protein kinase, putative
AT1G05800	0.0978	1.925 up	DGL (DONGLE); triacylglycerol lipase
AT1G06610	0.0366	1.959 up	pre-tRNA
AT1G07745	0.0497	1.809 up	RAD51D (ARABIDOPSIS HOMOLOG OF RAD51 D); ATP binding / DNA binding / DNA-dependent ATPase
AT1G08870	0.089	2.210 up	pre-tRNA
AT1G09930	0.00196	2.369 up	ATOPT2; oligopeptide transporter
AT1G10155	0.0443	1.551 up	ATPP2-A10 (PHLOEM PROTEIN 2-A10)
AT1G10220	0.02	2.061 up	BEST Arabidopsis thaliana protein match is: ZCF37 (TAIR:AT1G59590.1); Has 30 Blast hits to 30 proteins in 10 species: Archae - 0; Bacteria - 2; Metazoa - 6; Fungi - 0; Plants - 15; Viruses - 0; Other Eukaryotes - 7 (source: NCBI BLink).
AT1G12180	0.095	1.563 up	BEST Arabidopsis thaliana protein match is: heat shock protein-related (TAIR:AT5G47600.1); Has 5 Blast hits to 5 proteins in 2 species: Archae - 0; Bacteria - 0; Metazoa - 0; Fungi - 0; Plants - 5; Viruses - 0; Other Eukaryotes - 0 (source: NCBI BLink).
AT1G13010	0.033	2.170 up	pre-tRNA
AT1G14780	0.058	2.793 up	CONTAINS InterPro DOMAIN/s: Membrane attack complex component/perforin/complement C9 (InterPro:IPR001862); BEST Arabidopsis thaliana protein match is: unknown protein (TAIR:AT4G24290.2); Has 119 Blast hits to 118 proteins in 17 species: Archae - 0; Bacteria - 0; Metazoa - 14; Fungi - 0; Plants - 105; Viruses - 0; Other Eukaryotes - 0 (source: NCBI BLink).
AT1G15540	0.0489	2.371 up	oxidoreductase, 2OG-Fe(II) oxygenase family protein
AT1G15560	0.0477	1.859 up	transposable element gene
AT1G16160	0.0251	2.495 up	WAKL5 (wall associated kinase-like 5); kinase
AT1G18410	0.0196	2.304 up	kinesin motor protein-related
AT1G18486	0.0481	1.902 up	unknown protein
AT1G19190	0.0856	1.995 up	hydrolase
AT1G19392	0.0492	2.706 up	transposable element gene
AT1G19610	0.0333	2.047 up	PDF1.4
AT1G19830	0.00855	1.925 up	auxin-responsive protein, putative
AT1G20060	0.0163	1.642 up	ATP binding / microtubule motor
AT1G21470	0.00484	1.782 up	BEST Arabidopsis thaliana protein match is: CLPC1; ATP binding / ATP-dependent peptidase/ ATPase (TAIR:AT5G50920.1).
AT1G21940	0.0747	2.306 up	unknown protein
AT1G23110	0.000495	1.790 up	unknown protein
AT1G23510	0.00523	2.379 up	unknown protein
AT1G25886	0.00294	1.640 up	transposable element gene
AT1G26600	0.0205	2.239 up	CLE9 (CLAVATA3/ESR-RELATED 9); protein binding / receptor binding
AT1G26710	0.0238	1.526 up	unknown protein
AT1G26880	0.0591	1.678 up	60S ribosomal protein L34 (RPL34A)
AT1G27260	0.0139	2.781 up	paired amphipathic helix repeat-containing protein

AT1G27610	0.0599	1.984 up	unknown protein
AT1G27695	0.0405	1.864 up	glycine-rich protein
AT1G28281	0.0613	1.755 up	unknown protein
AT1G28620	0.000769	1.612 up	pseudogene, lipase, similar to lipase Arab-1 GB:S68410 GI:2129636 (Arabidopsis thaliana); blastp match of 44% identity and 1.2e-48 P-value to GP
AT1G29040	0.0794	1.530 up	unknown protein
AT1G29390	0.0711	1.776 up	COR314-TM2
AT1G30550	0.0056	1.625 up	BEST Arabidopsis thaliana protein match is: WW domain-containing protein (TAIR:AT1G45231.2).
AT1G30560	0.0039	1.982 up	transporter, putative
AT1G30980	0.0503	1.589 up	transposable element gene
AT1G32430	0.0323	3.124 up	F-box family protein
AT1G32505	0.0529	1.651 up	transposable element gene
AT1G32585	0.0983	1.792 up	VQ motif-containing protein-related
AT1G32830	0.0539	2.020 up	transposable element gene
AT1G33000	0.0123	1.859 up	transposable element gene
AT1G33010	0.0124	1.918 up	F-box family protein
AT1G33080	0.076	1.651 up	MATE efflux family protein
AT1G34280	0.0256	2.117 up	unknown protein
AT1G35150	0.0212	1.515 up	BEST Arabidopsis thaliana protein match is: hAT dimerisation domain-containing protein / transposase-related (TAIR:AT2G06500.1); Has 212 Blast hits to 190 proteins in 23 species: Archae - 0; Bacteria - 0; Metazoa - 116; Fungi - 0; Plants - 96; Viruses - 0; Other Eukaryotes - 0 (source: NCBI BLink).
AT1G35280	0.0979	1.624 up	transposable element gene
AT1G35405	0.0288	2.278 up	transposable element gene
AT1G35860	0.0475	2.240 up	TOC75-I (translocon outer membrane complex 75-I)
AT1G36020	0.074	2.024 up	BEST Arabidopsis thaliana protein match is: DEAD/DEAH box helicase, putative (TAIR:AT1G35530.1); Has 5 Blast hits to 5 proteins in 2 species: Archae - 0; Bacteria - 0; Metazoa - 0; Fungi - 0; Plants - 5; Viruses - 0; Other Eukaryotes - 0 (source: NCBI BLink).
AT1G36420	0.0932	1.874 up	transposable element gene
AT1G37170	0.0147	1.784 up	transposable element gene
AT1G37537	0.0302	2.134 up	transposable element gene
AT1G38430	0.0697	1.866 up	transposable element gene
AT1G39510	0.0674	1.536 up	transposable element gene
AT1G39990	0.0787	3.263 up	transposable element gene
AT1G41660	0.0815	2.233 up	transposable element gene
AT1G41726	0.0172	3.316 up	transposable element gene
AT1G41930	0.0521	2.202 up	transposable element gene
AT1G42360	0.0313	2.146 up	transposable element gene
AT1G42500	0.0347	1.511 up	transposable element gene
AT1G43150	0.0131	2.028 up	transposable element gene
AT1G43740	0.0427	2.161 up	transposable element gene
AT1G43845	0.0396	2.465 up	transposable element gene
AT1G44990	0.074	2.429 up	unknown protein
AT1G48400	0.00609	2.545 up	F-box family protein
AT1G50055	0.031	1.731 up	TAS1B; other RNA
AT1G50470	0.00937	1.665 up	CONTAINS InterPro DOMAIN/s: F-box associated (InterPro:IPR006527); BEST Arabidopsis thaliana protein match is: F-box family protein (TAIR:AT3G17560.1); Has 143 Blast hits to 143 proteins in 1 species: Archae - 0; Bacteria - 0; Metazoa - 0; Fungi - 0; Plants - 143; Viruses - 0; Other Eukaryotes - 0 (source: NCBI BLink).
AT1G50735	0.00739	1.920 up	transposable element gene
AT1G50770	0.0656	1.618 up	unknown protein
AT1G50790	0.0879	1.590 up	unknown protein
AT1G51750	0.0392	2.562 up	transposable element gene
AT1G52191	0.0934	2.038 up	BEST Arabidopsis thaliana protein match is: thioesterase family protein (TAIR:AT3G16175.1); Has 195 Blast hits to 195 proteins in 51 species: Archae - 0; Bacteria - 0; Metazoa - 66; Fungi - 28; Plants - 97; Viruses - 0; Other Eukaryotes - 4 (source: NCBI BLink).
AT1G53708	0.00978	1.733 up	RTFL9 (ROTUNDIFOLIA LIKE 9)
AT1G54095	0.000524	1.926 up	unknown protein
AT1G55045	0.0322	1.564 up	unknown protein
AT1G55440	0.094	1.984 up	DC1 domain-containing protein
AT1G55780	0.0151	1.566 up	metal ion binding
AT1G56250	0.00361	2.292 up	AtPP2-B14 (Phloem protein 2-B14); carbohydrate binding
AT1G56380	0.0197	1.937 up	mitochondrial transcription termination factor family protein / mTERF family protein
AT1G56470	0.0101	2.662 up	pseudogene, disease resistance protein (fragment), blastp match of 58% identity and 1.1e-16 P-value to GP
AT1G57450	0.0166	1.776 up	pre-tRNA
AT1G57570	0.0282	1.927 up	jacalin lectin family protein
AT1G57750	0.0682	2.492 up	CYP96A15 (CYTOCHROME P450 96 A1); midchain alkane hydroxylase/ oxygen binding
AT1G57943	0.0957	1.875 up	ATPUP17; purine transmembrane transporter
AT1G59077	0.0454	1.677 up	BEST Arabidopsis thaliana protein match is: transcription factor-related (TAIR:AT1G59453.1); Has 32 Blast hits to 28 proteins in 7 species: Archae - 0; Bacteria - 0; Metazoa - 7; Fungi - 0; Plants - 25; Viruses - 0; Other Eukaryotes - 0 (source: NCBI BLink).
AT1G59630	0.00141	2.772 up	F-box family protein-related
AT1G60310	0.0207	1.750 up	transposable element gene
AT1G60410	0.0481	1.821 up	F-box family protein
AT1G62490	0.0852	1.720 up	mitochondrial transcription termination factor-related / mTERF-related
AT1G62530	0.0882	1.510 up	unknown protein
AT1G63200	0.0714	2.553 up	CONTAINS InterPro DOMAIN/s: Cystatin-related, plant (InterPro:IPR006525); BEST

			Arabidopsis thaliana protein match is: unknown protein (TAIR:AT1G63190.1); Has 34 Blast hits to 34 proteins in 1 species: Archae - 0; Bacteria - 0; Metazoa - 0; Fungi - 0; Plants - 34; Viruses - 0; Other Eukaryotes - 0 (source: NCBI BLink).
AT1G64260	0.00138	2.564 up	zinc finger protein-related
AT1G64295	0.0387	1.662 up	F-box family protein-related
AT1G64410	0.0882	2.073 up	transposable element gene
AT1G64730	0.00389	1.889 up	pseudogene, putative NADH dehydrogenase subunit F, blastp match of 68% identity and 5.3e-08 P-value to GP
AT1G65090	0.0448	2.135 up	unknown protein
AT1G66690	0.00229	1.876 up	S-adenosyl-L-methionine:carboxyl methyltransferase family protein
AT1G67020	0.03	1.699 up	CONTAINS InterPro DOMAIN/s: Retrotransposon gag protein (InterPro:IPR005162); Has 53 Blast hits to 53 proteins in 6 species: Archae - 0; Bacteria - 0; Metazoa - 0; Fungi - 0; Plants - 53; Viruses - 0; Other Eukaryotes - 0 (source: NCBI BLink).
AT1G67820	0.00395	1.563 up	protein phosphatase 2C, putative / PP2C, putative
AT1G67875	0.000634	1.794 up	unknown protein
AT1G68150	0.0849	1.691 up	WRKY9; transcription factor
AT1G69526	0.00676	2.092 up	UbiE/COQ5 methyltransferase family protein
AT1G70010	0.00293	1.551 up	transposable element gene
AT1G70030	0.0317	1.587 up	paired amphipathic helix repeat-containing protein
AT1G70400	0.0525	2.441 up	CONTAINS InterPro DOMAIN/s: NOSIC (InterPro:IPR012976); BEST Arabidopsis thaliana protein match is: emb1220 (embryo defective 1220) (TAIR:AT1G60170.1).
AT1G74400	0.0329	1.634 up	pentatricopeptide (PPR) repeat-containing protein
AT1G75080	0.0605	2.098 up	BZR1 (BRASSINAZOLE-RESISTANT 1); DNA binding / transcription regulator/ transcription repressor
AT1G75610	0.0305	1.936 up	pseudogene, histone H3, identical to histone H3.2 from Medicago sativa GB:AAB36495 GI:488571, Histone H3.2, minor Lolium temulentum SP
AT1G75920	0.0707	1.809 up	family II extracellular lipase 5 (EXL5)
AT1G77520	0.0848	2.323 up	O-methyltransferase family 2 protein
AT1G78400	0.0394	1.679 up	glycoside hydrolase family 28 protein / polygalacturonase (pectinase) family protein
AT1G78720	0.0391	2.846 up	protein transport protein sec61, putative
AT1G80100	0.0153	1.918 up	AHP6 (ARABIDOPSIS HISTIDINE PHOSPHOTRANSFER PROTEIN 6); histidine phosphotransfer kinase/ transferase, transferring phosphorus-containing groups
AT2G01200	0.0123	1.968 up	IAA32 (INDOLE-3-ACETIC ACID INDUCIBLE 32); transcription factor
AT2G01960	0.0288	2.414 up	TET14 (TETRASPANIN14)
AT2G02147	0.000623	2.153 up	LCR73 (Low-molecular-weight cysteine-rich 73)
AT2G02550	0.00271	2.876 up	nuclease
AT2G02720	0.0416	2.584 up	pectate lyase family protein
AT2G03060	0.0251	1.743 up	DNA binding / transcription factor
AT2G03370	0.0843	1.770 up	transferase, transferring glycosyl groups
AT2G03480	0.031	1.544 up	dehydration-responsive protein-related
AT2G04090	0.00724	2.846 up	MATE efflux family protein
AT2G05010	0.0444	2.636 up	transposable element gene
AT2G05020	0.0763	2.429 up	transposable element gene
AT2G05082	0.0744	1.969 up	transposable element gene
AT2G05290	0.049	1.689 up	transposable element gene
AT2G05752	0.0381	1.728 up	unknown protein
AT2G06330	0.0725	1.614 up	transposable element gene
AT2G06440	0.00838	2.710 up	transposable element gene
AT2G06620	0.0286	3.017 up	transposable element gene
AT2G06750	0.0922	2.585 up	transposable element gene
AT2G07090	0.0578	2.585 up	transposable element gene
AT2G07160	0.0573	1.738 up	transposable element gene
AT2G07550	0.0171	2.185 up	transposable element gene
AT2G07663	0.0727	1.706 up	Pseudogene of AT2G07776
AT2G07687	0.0971	1.755 up	cytochrome c oxidase subunit 3
AT2G10223	0.0826	3.347 up	transposable element gene
AT2G10420	0.0799	2.415 up	transposable element gene
AT2G10480	0.00694	4.423 up	transposable element gene
AT2G10680	0.0242	3.436 up	transposable element gene
AT2G10980	0.0219	2.013 up	transposable element gene
AT2G11135	0.047	1.768 up	transposable element gene
AT2G11190	0.0175	1.651 up	transposable element gene
AT2G11775	0.00752	2.276 up	transposable element gene
AT2G11980	0.0262	1.960 up	transposable element gene
AT2G12060	0.0776	1.543 up	transposable element gene
AT2G12320	0.071	2.444 up	transposable element gene
AT2G12410	0.0292	1.832 up	transposable element gene
AT2G13125	0.0141	1.530 up	unknown protein
AT2G13363	0.00875	1.696 up	unknown protein
AT2G14200	0.0807	1.995 up	transposable element gene
AT2G14430	0.0767	1.714 up	transposable element gene
AT2G14780	0.0376	2.597 up	transposable element gene
AT2G14793	0.0707	1.761 up	transposable element gene
AT2G15045	0.0137	1.895 up	transposable element gene
AT2G15150	0.0393	2.093 up	transposable element gene
AT2G16365	0.0518	1.670 up	F-box family protein
AT2G16820	0.0602	1.749 up	transposable element gene
AT2G17055	0.0655	1.553 up	disease resistance protein-related
AT2G18070	0.00652	2.023 up	unknown protein
AT2G18920	0.0446	1.581 up	unknown protein
AT2G19045	0.0376	2.565 up	RALFL13 (RALF-LIKE 13); signal transducer

AT2G20208	0.0253	1.909 up	LCR60 (Low-molecular-weight cysteine-rich 60)
AT2G20510	0.0119	2.363 up	ATTIM44-1; protein-transmembrane transporting ATPase
AT2G20605	0.0193	3.274 up	Encodes a Plant thionin family protein
AT2G20660	0.0793	2.092 up	RALFL14 (ralf-like 14); signal transducer
AT2G21420	0.0482	1.585 up	zinc finger protein-related
AT2G21727	0.0905	1.559 up	Encodes a ECA1 gametogenesis related family protein
AT2G22805	0.0309	1.691 up	Encodes a defensin-like (DEFL) family protein.
AT2G23300	0.0292	1.550 up	leucine-rich repeat transmembrane protein kinase, putative
AT2G24320	0.0627	1.681 up	unknown protein
AT2G24560	0.0951	1.644 up	carboxylesterase/ hydrolase, acting on ester bonds
AT2G24660	0.0188	2.394 up	transposable element gene
AT2G24890	0.00383	1.953 up	transposable element gene
AT2G25460	0.0644	1.512 up	CONTAINS InterPro DOMAIN/s: C2 calcium-dependent membrane targeting (InterPro:IPR000008); BEST Arabidopsis thaliana protein match is: unknown protein (TAIR:AT5G04860.1); Has 53 Blast hits to 36 proteins in 5 species: Archae - 0; Bacteria - 0; Metazoa - 0; Fungi - 0; Plants - 53; Viruses - 0; Other Eukaryotes - 0 (source: NCBI BLink).
AT2G25980	0.0429	2.158 up	jacalin lectin family protein
AT2G26820	0.0742	1.682 up	ATPP2-A3 (Phloem protein 2-A3); carbohydrate binding
AT2G27410	0.0725	1.875 up	unknown protein
AT2G28725	0.0446	1.969 up	unknown protein
AT2G28860	0.0422	1.821 up	CYP710A4 (cytochrome P450, family 710, subfamily A, polypeptide 4); electron carrier/ heme binding / iron ion binding / monooxygenase/ oxygen binding
AT2G29125	0.0432	1.772 up	RTFL2 (ROTUNDIFOLIA LIKE 2)
AT2G29470	0.0144	2.853 up	ATGSTU3 (ARABIDOPSIS THALIANA GLUTATHIONE S-TRANSFERASE TAU 3); glutathione transferase
AT2G29930	0.0776	2.628 up	F-box family protein
AT2G30370	0.0367	1.513 up	allergen-related
AT2G30850	0.00319	1.691 up	pre-tRNA
AT2G31160	0.0438	1.787 up	LSH3 (LIGHT SENSITIVE HYPOCOTYLS 3)
AT2G33240	0.0274	1.587 up	XID; motor/ protein binding
AT2G33585	0.0246	1.552 up	unknown protein
AT2G34330	0.0687	1.517 up	unknown protein
AT2G35658	0.071	2.455 up	unknown protein
AT2G35710	0.0198	2.121 up	glycogenin glucosyltransferase (glycogenin)-related
AT2G36920	0.0468	1.643 up	unknown protein
AT2G38900	0.044	1.864 up	serine protease inhibitor, potato inhibitor I-type family protein
AT2G39760	0.00122	3.214 up	BPM3; protein binding
AT2G40560	0.0394	1.652 up	protein kinase family protein
AT2G40740	0.0295	3.727 up	WRKY55; transcription factor
AT2G41451	0.000999	21.172 up	unknown protein
AT2G41460	0.0182	1.514 up	ARP; DNA-(apurinic or apyrimidinic site) lyase
AT2G43690	0.084	1.614 up	lectin protein kinase, putative
AT2G43960	0.00816	2.047 up	SWAP (Suppressor-of-White-APricot)/surp domain-containing protein
AT2G45320	0.0798	1.671 up	unknown protein
AT2G45760	0.0192	2.335 up	BAP2 (BON ASSOCIATION PROTEIN 2)
AT2G46270	0.0512	1.842 up	GBF3 (G-BOX BINDING FACTOR 3); sequence-specific DNA binding / transcription factor
AT2G46750	0.0402	1.733 up	FAD-binding domain-containing protein
AT2G48090	0.0681	1.522 up	unknown protein
AT3G02310	0.0775	2.412 up	SEP2 (SEPALLATA 2); DNA binding / protein binding / transcription factor
AT3G02480	0.00874	1.843 up	ABA-responsive protein-related
AT3G03456	0.0996	1.657 up	unknown protein
AT3G03860	0.0657	1.545 up	ATAPRL5 (APR-like 5)
AT3G04390	0.00814	1.675 up	xanthine dehydrogenase family protein
AT3G05155	0.0502	2.069 up	sugar transporter, putative
AT3G07900	0.0342	3.098 up	unknown protein
AT3G08700	0.0852	1.878 up	UBC12 (ubiquitin-conjugating enzyme 12); small conjugating protein ligase/ ubiquitin-protein ligase
AT3G08780	0.0606	2.363 up	unknown protein
AT3G09110	0.0991	2.442 up	unknown protein
AT3G10400	0.0367	1.747 up	RNA recognition motif (RRM)-containing protein
AT3G10510	0.0874	2.819 up	kelch repeat-containing F-box family protein
AT3G11165	0.0801	2.171 up	unknown protein
AT3G12240	0.05	2.328 up	SCPL15 (serine carboxypeptidase-like 15); serine-type carboxypeptidase
AT3G13686	0.0182	2.096 up	unknown protein
AT3G15351	0.0547	2.689 up	unknown protein
AT3G18010	0.0645	1.580 up	WOX1 (WUSCHEL related homeobox 1); transcription factor
AT3G18340	0.0224	1.805 up	F-box family protein
AT3G18460	0.091	1.638 up	unknown protein
AT3G19045	0.0552	1.671 up	transposable element gene
AT3G19560	0.0105	2.145 up	F-box family protein
AT3G20760	0.0893	2.798 up	CONTAINS InterPro DOMAIN/s: Nse4 (InterPro:IPR014854); BEST Arabidopsis thaliana protein match is: unknown protein (TAIR:AT1G51130.1); Has 190 Blast hits to 190 proteins in 77 species: Archae - 0; Bacteria - 4; Metazoa - 67; Fungi - 72; Plants - 37; Viruses - 0; Other Eukaryotes - 10 (source: NCBI BLink).
AT3G21240	0.0577	1.570 up	4CL2 (4-COUMARATE:COA LIGASE 2); 4-coumarate-CoA ligase
AT3G21890	0.0211	1.822 up	zinc finger (B-box type) family protein
AT3G22090	0.0525	3.061 up	unknown protein
AT3G23637	0.0852	2.213 up	DVL21 (DEVIL 21)
AT3G24690	0.0768	1.841 up	BEST Arabidopsis thaliana protein match is: glycine-rich protein (TAIR:AT1G27090.1); Has 28 Blast hits to 27 proteins in 8 species: Archae - 0; Bacteria - 2; Metazoa - 0; Fungi - 0; Plants

			- 24; Viruses - 0; Other Eukaryotes - 2 (source: NCBI BLink).
AT3G25730	0.0142	1.878 up	AP2 domain-containing transcription factor, putative
AT3G26120	0.089	2.118 up	TEL1 (TERMINAL EAR1-LIKE 1); RNA binding / nucleic acid binding / nucleotide binding
AT3G26960	0.0392	1.599 up	unknown protein
AT3G27070	0.0631	1.852 up	TOM20-1 (translocase outer membrane 20-1); P-P-bond-hydrolysis-driven protein transmembrane transporter
AT3G28110	0.0658	1.828 up	transposable element gene
AT3G28510	0.0512	1.649 up	AAA-type ATPase family protein
AT3G29152	0.0121	1.552 up	Encodes a Protease inhibitor/seed storage/LTP family protein
AT3G29620	0.00257	1.582 up	transposable element gene
AT3G29740	0.04	1.910 up	protein binding
AT3G30665	0.00334	1.870 up	transposable element gene
AT3G30820	0.0998	1.778 up	unknown protein
AT3G31377	0.0656	2.180 up	transposable element gene
AT3G31900	0.0782	1.683 up	unknown protein
AT3G32047	0.0922	1.548 up	electron carrier/ heme binding / iron ion binding / monooxygenase
AT3G32080	0.0699	2.190 up	transposable element gene
AT3G32091	0.0864	1.627 up	transposable element gene
AT3G32220	0.0529	3.190 up	transposable element gene
AT3G32925	0.0974	1.650 up	transposable element gene
AT3G33035	0.054	2.835 up	transposable element gene
AT3G33166	0.0277	1.701 up	transposable element gene
AT3G33172	0.0309	1.910 up	transposable element gene
AT3G33230	0.0942	1.506 up	transposable element gene
AT3G42120	0.0837	1.665 up	transposable element gene
AT3G42260	0.021	2.832 up	transposable element gene
AT3G42545	0.00635	1.928 up	transposable element gene
AT3G42713	0.0944	1.927 up	transposable element gene
AT3G42760	0.0566	2.887 up	transposable element gene
AT3G42780	0.0316	1.597 up	unknown protein
AT3G42798	0.0687	2.369 up	transposable element gene
AT3G43141	0.0302	1.904 up	transposable element gene
AT3G43431	0.0171	1.608 up	unknown protein
AT3G43460	0.0142	2.012 up	transposable element gene
AT3G43530	0.0115	1.552 up	transposable element gene
AT3G43623	0.0695	1.780 up	unknown protein
AT3G43880	0.0838	1.935 up	unknown protein
AT3G44115	0.00942	1.873 up	unknown protein
AT3G45790	0.0671	1.534 up	protein kinase-related
AT3G45880	0.0706	2.354 up	CONTAINS InterPro DOMAIN/s: Transcription factor jumonji/aspartyl beta-hydroxylase (InterPro:IPR003347); BEST Arabidopsis thaliana protein match is: transcription factor jumonji (jmjC) domain-containing protein (TAIR:AT5G19840.1); Has 836 Blast hits to 833 proteins in 185 species: Archae - 0; Bacteria - 185; Metazoa - 390; Fungi - 96; Plants - 69; Viruses - 0; Other Eukaryotes - 96 (source: NCBI BLink).
AT3G46487	0.00162	2.239 up	transposable element gene
AT3G46570	0.0929	1.946 up	glycosyl hydrolase family 17 protein
AT3G47050	0.0749	1.954 up	glycosyl hydrolase family 3 protein
AT3G47190	0.0257	1.591 up	oxidoreductase, 2OG-Fe(II) oxygenase family protein
AT3G47660	0.00386	1.507 up	Ran GTPase binding / chromatin binding / zinc ion binding
AT3G48010	0.0756	1.758 up	ATCNGC16; calmodulin binding / cyclic nucleotide binding / ion channel
AT3G48770	0.0044	1.818 up	ATP binding / DNA binding
AT3G49270	0.0263	1.690 up	unknown protein
AT3G49330	0.015	1.847 up	invertase/pectin methylesterase inhibitor family protein
AT3G50170	0.00446	2.538 up	unknown protein
AT3G50290	0.0855	1.641 up	transferase, transferring acyl groups other than amino-acyl groups
AT3G50301	0.0528	1.651 up	Pseudogene of AT1G49230; zinc finger (C3HC4-type RING finger) family protein
AT3G50330	0.00313	1.743 up	HEC2 (HECATE 2); DNA binding / transcription factor
AT3G51570	0.0904	1.908 up	disease resistance protein (TIR-NBS-LRR class), putative
AT3G53403	0.0773	1.831 up	Pseudogene of AT3G53410; zinc finger (C3HC4-type RING finger) family protein
AT3G54040	0.0547	1.810 up	photoassimilate-responsive protein-related
AT3G54310	0.062	1.725 up	unknown protein
AT3G54530	0.0214	1.921 up	unknown protein
AT3G55780	0.069	1.660 up	glycosyl hydrolase family 17 protein
AT3G56610	0.0117	2.292 up	unknown protein
AT3G57820	0.0854	1.901 up	60S ribosomal protein L21 (RPL21F), pseudogene, 60S RIBOSOMAL PROTEIN L21 - Arabidopsis thaliana, SWISSPROT:RL21_ARATH; blastp match of 75% identity and 2.5e-15 P-value to GP
AT3G58400	0.057	2.228 up	meprin and TRAF homology domain-containing protein / MATH domain-containing protein
AT3G59415	0.0854	2.322 up	pre-tRNA
AT3G59750	0.0259	1.562 up	receptor lectin kinase, putative
AT3G60020	0.00842	1.564 up	ASK5 (ARABIDOPSIS SKP1-LIKE 5); protein binding / ubiquitin-protein ligase
AT3G61410	0.0769	2.087 up	BEST Arabidopsis thaliana protein match is: protein kinase family protein / U-box domain-containing protein (TAIR:AT2G45910.1); Has 146 Blast hits to 144 proteins in 9 species: Archae - 0; Bacteria - 0; Metazoa - 13; Fungi - 0; Plants - 132; Viruses - 0; Other Eukaryotes - 1 (source: NCBI BLink).
AT3G62245	0.0992	1.673 up	pre-tRNA
AT3G63350	0.0912	1.889 up	AT-HSFA7B; DNA binding / transcription factor
AT4G00114	0.00319	1.666 up	pseudogene of transketolase
AT4G02190	0.0666	1.912 up	DC1 domain-containing protein
AT4G02312	0.0166	2.160 up	transposable element gene
AT4G02314	0.0724	1.578 up	transposable element gene

AT4G03050	0.0355	2.389 up	AOP3; iron ion binding / oxidoreductase
AT4G03376	0.0987	1.671 up	Pseudogene of AT1G56420
AT4G03520	0.0158	2.437 up	ATHM2; enzyme activator
AT4G03825	0.0399	2.722 up	transposable element gene
AT4G03914	0.0691	1.506 up	Pseudogene of AT5G30520; unknown protein
AT4G04030	0.0399	1.617 up	OFP9 (ARABIDOPSIS THALIANA OVATE FAMILY PROTEIN 9)
AT4G04155	0.0138	1.617 up	transposable element gene
AT4G04223	0.075	1.803 up	other RNA
AT4G04405	0.00827	2.114 up	transposable element gene
AT4G04620	0.0772	1.754 up	ATG8B (autophagy 8b); microtubule binding
AT4G04693	0.0471	1.808 up	pseudogene, hypothetical protein
AT4G04820	0.0916	1.500 up	transposable element gene
AT4G05250	0.0191	1.923 up	ubiquitin family protein
AT4G05360	0.0489	2.344 up	zinc knuckle (CCHC-type) family protein
AT4G05502	0.0896	1.653 up	transposable element gene
AT4G06482	0.012	1.554 up	transposable element gene
AT4G06511	0.0547	1.977 up	transposable element gene
AT4G06583	0.0994	1.784 up	unknown protein
AT4G06606	0.0293	2.335 up	transposable element gene
AT4G07339	0.0346	1.693 up	transposable element gene
AT4G07380	0.0466	1.720 up	unknown protein
AT4G07440	0.0433	1.971 up	transposable element gene
AT4G07456	0.052	3.024 up	transposable element gene
AT4G07458	0.0912	3.876 up	transposable element gene
AT4G07521	0.0494	1.738 up	transposable element gene
AT4G07540	0.0685	2.069 up	transposable element gene
AT4G07664	0.0725	1.569 up	transposable element gene
AT4G07742	0.0162	1.993 up	transposable element gene
AT4G07915	0.0461	1.635 up	transposable element gene
AT4G08054	0.0702	2.421 up	transposable element gene
AT4G08071	0.0903	2.079 up	pseudogene, hypothetical protein
AT4G08092	0.0721	1.652 up	transposable element gene
AT4G08655	0.00159	2.644 up	transposable element gene
AT4G08800	0.0153	1.653 up	protein kinase, putative
AT4G09190	0.0552	1.792 up	F-box family protein
AT4G09470	0.0542	2.282 up	Encodes a ECA1 gametogenesis related family protein [pseudogene]
AT4G09660	0.0888	1.989 up	CONTAINS InterPro DOMAIN/s: Zinc finger, TTF-type (InterPro:IPR006580); BEST Arabidopsis thaliana protein match is: hAT dimerisation domain-containing protein (TAIR:AT1G19260.1); Has 372 Blast hits to 344 proteins in 29 species: Archae - 0; Bacteria - 0; Metazoa - 216; Fungi - 0; Plants - 156; Viruses - 0; Other Eukaryotes - 0 (source: NCBI BLink).
AT4G09740	0.0608	1.983 up	AtGH9B14 (Arabidopsis thaliana glycosyl hydrolase 9B14); catalytic/ hydrolase, hydrolyzing O-glycosyl compounds
AT4G10020	0.051	1.923 up	AtHSD5 (hydroxysteroid dehydrogenase 5); binding / catalytic/ oxidoreductase
AT4G10115	0.0897	1.506 up	SCRL20 (SCR-Like 20)
AT4G10270	0.0179	2.068 up	wound-responsive family protein
AT4G12080	0.0814	1.535 up	DNA-binding family protein
AT4G12210	0.0909	2.061 up	zinc finger (C3HC4-type RING finger) family protein
AT4G12220	0.0171	2.317 up	BEST Arabidopsis thaliana protein match is: zinc finger (C3HC4-type RING finger) family protein (TAIR:AT4G12210.1); Has 18 Blast hits to 15 proteins in 1 species: Archae - 0; Bacteria - 0; Metazoa - 0; Fungi - 0; Plants - 18; Viruses - 0; Other Eukaryotes - 0 (source: NCBI BLink).
AT4G12260	0.0251	2.035 up	transposable element gene
AT4G12825	0.0287	1.804 up	Encodes a Protease inhibitor/seed storage/LTP family protein
AT4G13130	0.0567	1.507 up	DC1 domain-containing protein
AT4G13215	0.0554	2.017 up	pseudogene, leucine-rich repeat transmembrane protein kinase -related, similar to leucine-rich repeat transmembrane protein kinase, putative; blastp match of 44% identity and 2.7e-12 P-value to GP
AT4G13570	0.0643	2.078 up	HTA4; DNA binding
AT4G14360	0.0858	1.918 up	dehydration-responsive protein-related
AT4G14450	0.0952	1.572 up	unknown protein
AT4G16050	0.0383	2.125 up	unknown protein
AT4G16090	0.00448	1.765 up	unknown protein
AT4G17850	0.0247	1.618 up	BEST Arabidopsis thaliana protein match is: PHD finger family protein (TAIR:AT5G16680.1); Has 121 Blast hits to 116 proteins in 30 species: Archae - 0; Bacteria - 0; Metazoa - 55; Fungi - 4; Plants - 57; Viruses - 0; Other Eukaryotes - 5 (source: NCBI BLink).
AT4G19940	0.0377	2.235 up	F-box family protein
AT4G20970	0.0245	3.143 up	basic helix-loop-helix (bHLH) family protein
AT4G24340	0.028	2.684 up	phosphorylase family protein
AT4G24890	0.0491	1.764 up	PAP24 (PURPLE ACID PHOSPHATASE 24); acid phosphatase/ protein serine/threonine phosphatase
AT4G25433	0.0994	2.410 up	peptidoglycan-binding LysM domain-containing protein
AT4G25850	0.0929	2.606 up	ORP4B (OSBP(OXYSTEROL BINDING PROTEIN)-RELATED PROTEIN 4B); oxysterol binding
AT4G26250	0.029	1.751 up	AtGolS6 (Arabidopsis thaliana galactinol synthase 6); transferase, transferring glycosyl groups / transferase, transferring hexosyl groups
AT4G27590	0.0279	2.183 up	copper-binding protein-related
AT4G28390	0.0438	1.628 up	AAC3 (ADP/ATP CARRIER 3); ATP:ADP antiporter/ binding
AT4G28410	0.065	2.954 up	aminotransferase-related
AT4G28485	0.0701	1.787 up	unknown protein
AT4G30064	0.0468	2.359 up	LCR61 (Low-molecular-weight cysteine-rich 61)

AT4G31330	0.0822	2.517 up	unknown protein
AT4G31860	0.0113	2.896 up	protein phosphatase 2C, putative / PP2C, putative
AT4G33860	0.00181	1.941 up	glycosyl hydrolase family 10 protein
AT4G34440	0.0611	1.706 up	protein kinase family protein
AT4G36160	0.0692	1.770 up	ANAC076 (ARABIDOPSIS NAC DOMAIN CONTAINING PROTEIN 76); transcription factor
AT4G36925	0.00084	4.558 up	unknown protein
AT4G37630	0.0215	2.174 up	CYCD5;1 (cyclin d5;1); cyclin-dependent protein kinase
AT4G37840	0.0763	2.071 up	HKL3 (HEXOKINASE-LIKE 3); ATP binding / fructokinase/ glucokinase/ hexokinase
AT4G37940	0.0175	1.754 up	AGL21; transcription factor
AT4G39410	0.0754	2.067 up	WRKY13; transcription factor
AT4G39770	0.0172	1.608 up	trehalose-6-phosphate phosphatase, putative
AT5G01280	0.0158	1.550 up	BEST Arabidopsis thaliana protein match is: proline-rich family protein (TAIR:AT3G09000.1); Has 40332 Blast hits to 19265 proteins in 905 species: Archae - 97; Bacteria - 3595; Metazoa - 17370; Fungi - 8276; Plants - 837; Viruses - 1209; Other Eukaryotes - 8948 (source: NCBI BLink).
AT5G01380	0.0667	1.733 up	transcription factor
AT5G01715	0.0863	2.206 up	pseudogene, antisense mRNA to gene At5g01720, blastp match of 29% identity and 3.2e-13 P-value to GP
AT5G02000	0.0547	1.591 up	unknown protein
AT5G02815	0.0267	1.526 up	pre-tRNA
AT5G03600	0.0542	3.235 up	GDSL-motif lipase/hydrolase family protein
AT5G04010	0.0739	2.293 up	unknown protein
AT5G04390	0.0287	2.556 up	zinc finger (C2H2 type) family protein
AT5G05260	0.054	1.965 up	CYP79A2 (CYTOCHROME P450 79A2); oxidoreductase, acting on paired donors, with incorporation or reduction of molecular oxygen, NADH or NADPH as one donor, and incorporation of one atom of oxygen / oxygen binding
AT5G05490	0.00698	1.767 up	SYN1 (SYNAPTIC 1)
AT5G06630	0.0554	1.615 up	proline-rich extensin-like family protein
AT5G07450	0.0669	2.758 up	CYCP4;3 (cyclin p4;3); cyclin-dependent protein kinase
AT5G07460	0.0241	1.606 up	PMSR2 (PEPTIDEMETHIONINE SULFOXIDE REDUCTASE 2); oxidoreductase, acting on sulfur group of donors, disulfide as acceptor / peptide-methionine-(S)-S-oxide reductase
AT5G09250	0.000857	2.841 up	KIWI; DNA binding / protein binding / transcription coactivator
AT5G09360	0.0778	1.617 up	LAC14 (laccase 14); laccase
AT5G09480	0.0532	3.422 up	hydroxyproline-rich glycoprotein family protein
AT5G10140	0.0293	2.867 up	FLC (FLOWERING LOCUS C); specific transcriptional repressor/ transcription factor
AT5G11320	0.0247	2.928 up	YUC4 (YUCCA4); monooxygenase/ oxidoreductase
AT5G12910	0.0618	1.564 up	histone H3, putative
AT5G13350	0.0902	1.721 up	auxin-responsive GH3 family protein
AT5G13900	0.087	1.605 up	protease inhibitor/seed storage/lipid transfer protein (LTP) family protein
AT5G14020	0.094	1.869 up	CONTAINS InterPro DOMAIN/s: BRO1 (InterPro:IPR004328); BEST Arabidopsis thaliana protein match is: unknown protein (TAIR:AT1G73390.3); Has 53 Blast hits to 53 proteins in 7 species: Archae - 0; Bacteria - 0; Metazoa - 0; Fungi - 0; Plants - 53; Viruses - 0; Other Eukaryotes - 0 (source: NCBI BLink).
AT5G14160	0.0388	1.896 up	F-box family protein
AT5G14380	0.0512	2.259 up	AGP6 (Arabinogalactan proteins 6)
AT5G15250	0.0582	2.859 up	FTSH6 (FTSH PROTEASE 6); ATP-dependent peptidase/ ATPase/ metallopeptidase/ peptidase/ zinc ion binding
AT5G16430	0.0863	1.546 up	BEST Arabidopsis thaliana protein match is: DC1 domain-containing protein (TAIR:AT5G45730.1); Has 140 Blast hits to 105 proteins in 3 species: Archae - 0; Bacteria - 0; Metazoa - 0; Fungi - 0; Plants - 140; Viruses - 0; Other Eukaryotes - 0 (source: NCBI BLink).
AT5G18360	0.0887	3.103 up	disease resistance protein (TIR-NBS-LRR class), putative
AT5G18910	0.0413	1.547 up	protein kinase family protein
AT5G22720	0.0295	2.220 up	F-box family protein
AT5G23460	0.0825	1.563 up	unknown protein
AT5G23908	0.0331	1.716 up	unknown protein
AT5G24240	0.00357	177.327 up	phosphatidylinositol 3- and 4-kinase family protein / ubiquitin family protein
AT5G24880	0.0245	3.942 up	BEST Arabidopsis thaliana protein match is: calmodulin-binding protein-related (TAIR:AT5G10660.1); Has 195834 Blast hits to 92446 proteins in 2480 species: Archae - 1007; Bacteria - 19200; Metazoa - 85171; Fungi - 18359; Plants - 7291; Viruses - 1072; Other Eukaryotes - 63734 (source: NCBI BLink).
AT5G24900	0.0221	2.561 up	CYP714A2; electron carrier/ heme binding / iron ion binding / monooxygenase/ oxygen binding
AT5G25920	0.0133	2.257 up	BEST Arabidopsis thaliana protein match is: ATP binding / aminoacyl-tRNA ligase/ aspartic-type endopeptidase/ nucleotide binding (TAIR:AT3G29750.1); Has 3 Blast hits to 2 proteins in 1 species: Archae - 0; Bacteria - 0; Metazoa - 0; Fungi - 0; Plants - 3; Viruses - 0; Other Eukaryotes - 0 (source: NCBI BLink).
AT5G26050	0.0358	1.935 up	CONTAINS InterPro DOMAIN/s: Plant self-incompatibility S1 (InterPro:IPR010264); BEST Arabidopsis thaliana protein match is: unknown protein (TAIR:AT5G11820.1); Has 12 Blast hits to 11 proteins in 1 species: Archae - 0; Bacteria - 0; Metazoa - 0; Fungi - 0; Plants - 12; Viruses - 0; Other Eukaryotes - 0 (source: NCBI BLink).
AT5G26146	0.0631	1.803 up	other RNA
AT5G26642	0.00841	2.102 up	transposable element gene
AT5G26770	0.0585	2.657 up	unknown protein
AT5G26805	0.0319	2.491 up	unknown protein
AT5G27050	0.00786	2.269 up	AGL101; transcription factor
AT5G28076	0.0109	2.239 up	transposable element gene
AT5G28210	0.0806	1.564 up	mRNA capping enzyme family protein
AT5G28550	0.0487	1.517 up	BEST Arabidopsis thaliana protein match is: AESP (ARABIDOPSIS HOMOLOG OF SEPARASE); peptidase (TAIR:AT4G22970.1); Has 7 Blast hits to 7 proteins in 4 species: Archae - 0; Bacteria - 0; Metazoa - 0; Fungi - 0; Plants - 7; Viruses - 0; Other Eukaryotes - 0

			(source: NCBI BLink).
AT5G28605	0.0115	1.944 up	transposable element gene
AT5G28690	0.00596	3.196 up	unknown protein
AT5G28823	0.0743	2.133 up	BEST Arabidopsis thaliana protein match is: zinc knuckle (CCHC-type) family protein (TAIR:AT2G07760.1); Has 99 Blast hits to 71 proteins in 22 species: Archae - 0; Bacteria - 18; Metazoa - 2; Fungi - 56; Plants - 20; Viruses - 0; Other Eukaryotes - 3 (source: NCBI BLink).
AT5G28890	0.0928	1.560 up	transposable element gene
AT5G28892	0.0571	1.641 up	transposable element gene
AT5G28894	0.0942	2.693 up	transposable element gene
AT5G29032	0.0527	2.025 up	transposable element gene
AT5G29046	0.079	1.677 up	transposable element gene
AT5G29560	0.0402	1.679 up	calcium ion binding
AT5G29565	0.0541	1.598 up	transposable element gene
AT5G29646	0.0459	1.921 up	transposable element gene
AT5G30123	0.0761	3.214 up	transposable element gene
AT5G30276	0.0955	2.156 up	transposable element gene
AT5G30721	0.0827	1.517 up	transposable element gene
AT5G31804	0.0712	1.799 up	transposable element gene
AT5G32089	0.0325	3.354 up	transposable element gene
AT5G32475	0.0179	2.176 up	transposable element gene
AT5G32484	0.0262	1.678 up	transposable element gene
AT5G32605	0.00952	1.954 up	transposable element gene
AT5G32613	0.0381	3.295 up	zinc knuckle (CCHC-type) family protein
AT5G32775	0.0126	1.636 up	transposable element gene
AT5G33258	0.0826	1.662 up	pseudogene, hypothetical protein
AT5G34696	0.0918	2.111 up	transposable element gene
AT5G34870	0.0892	1.503 up	zinc knuckle (CCHC-type) family protein
AT5G34885	0.0139	1.660 up	unknown protein
AT5G35354	0.0149	1.645 up	transposable element gene
AT5G35650	0.0469	1.902 up	transposable element gene
AT5G35680	0.0789	1.571 up	eukaryotic translation initiation factor 1A, putative / eIF-1A, putative / eIF-4C, putative
AT5G35770	0.0967	3.042 up	SAP (STERILE APETALA); transcription factor/ transcription regulator
AT5G35796	0.0152	2.208 up	pseudogene, similar to Putative protein kinase, blastp match of 29% identity and 1.6e-16 P-value to GP
AT5G36540	0.0357	1.947 up	Encodes a ECA1 gametogenesis related family protein
AT5G36659	0.0111	4.156 up	Encodes a ECA1 gametogenesis related family protein
AT5G36905	0.0608	3.069 up	transposable element gene
AT5G37050	0.0944	2.098 up	BEST Arabidopsis thaliana protein match is: SNX2a (SORTING NEXIN 2a); phosphoinositide binding (TAIR:AT5G58440.1); Has 23 Blast hits to 19 proteins in 5 species: Archae - 0; Bacteria - 0; Metazoa - 0; Fungi - 0; Plants - 23; Viruses - 0; Other Eukaryotes - 0 (source: NCBI BLink).
AT5G37090	0.0714	2.487 up	transposable element gene
AT5G37490	0.0971	1.660 up	U-box domain-containing protein
AT5G38314	0.06	2.110 up	unknown protein
AT5G38390	0.00987	1.605 up	F-box family protein
AT5G38940	0.0593	1.828 up	manganese ion binding / nutrient reservoir
AT5G39030	0.0509	1.627 up	protein kinase family protein
AT5G39120	0.0318	2.644 up	germin-like protein, putative
AT5G39693	0.0675	1.960 up	MIR869a; miRNA
AT5G40260	0.0425	1.852 up	nodulin MtN3 family protein
AT5G40320	0.0752	2.385 up	DC1 domain-containing protein
AT5G40595	0.0777	1.756 up	unknown protein
AT5G43980	0.0229	2.585 up	PDLP1 (PLASMODESMATA-LOCATED PROTEIN 1)
AT5G44313	0.0164	4.027 up	transposable element gene
AT5G46380	0.0778	1.728 up	unknown protein
AT5G46650	0.0262	2.357 up	zinc finger (C3HC4-type RING finger) family protein
AT5G46960	0.0326	1.569 up	invertase/pectin methylesterase inhibitor family protein
AT5G46980	0.0147	2.027 up	invertase/pectin methylesterase inhibitor family protein
AT5G47950	0.0555	1.621 up	transferase family protein
AT5G48140	0.0356	1.824 up	polygalacturonase, putative / pectinase, putative
AT5G48550	0.0429	1.622 up	F-box family protein-related
AT5G48605	0.0271	1.673 up	Encodes a defensin-like (DEFL) family protein.
AT5G49080	0.0627	2.130 up	transposable element gene
AT5G49520	0.0454	1.880 up	WRKY48; transcription factor
AT5G49860	0.00755	1.804 up	jacalin lectin family protein
AT5G50470	0.0899	1.926 up	NF-YC7 (NUCLEAR FACTOR Y, SUBUNIT C7); DNA binding / transcription factor
AT5G51090	0.0333	2.873 up	unknown protein
AT5G52160	0.0261	2.987 up	protease inhibitor/seed storage/lipid transfer protein (LTP) family protein
AT5G52355	0.0552	3.441 up	pre-tRNA
AT5G53710	0.0782	1.602 up	unknown protein
AT5G54190	0.0284	1.893 up	PORA; oxidoreductase/ protochlorophyllide reductase
AT5G54230	0.0655	2.953 up	MYB49 (myb domain protein 49); transcription factor
AT5G54745	0.0142	1.598 up	DegP protease family
AT5G55980	0.0347	3.581 up	serine-rich protein-related
AT5G56770	0.084	2.691 up	unknown protein
AT5G56840	0.0296	2.588 up	DNA-binding family protein
AT5G58010	0.0257	1.888 up	basic helix-loop-helix (bHLH) family protein
AT5G58770	0.0462	1.781 up	dehydrodolichyl diphosphate synthase, putative / DEDOL-PP synthase, putative
AT5G59040	0.0205	4.521 up	COPT3; copper ion transmembrane transporter/ high affinity copper ion transmembrane transporter

AT5G60530	0.0832	1.559 up	late embryogenesis abundant protein-related / LEA protein-related
AT5G61630	0.0647	2.209 up	unknown protein
AT5G62100	0.0573	1.788 up	ATBAG2 (ARABIDOPSIS THALIANA BCL-2-ASSOCIATED ATHANOGENE 2)
AT5G62490	0.0615	2.623 up	ATHVA22B
AT5G63595	0.0606	1.853 up	FLS4 (FLAVONOL SYNTHASE 4); flavonol synthase/ oxidoreductase
AT5G63750	0.0881	4.360 up	IBR domain-containing protein
AT5G64510	0.0668	2.250 up	unknown protein
AT5G64990	0.0878	2.806 up	AtRABH1a (Arabidopsis Rab GTPase homolog H1a); GTP binding
AT5G65340	0.097	1.929 up	unknown protein
AT5G66985	0.00323	2.670 up	unknown protein

nature COMMUNICATIONS

ARTICLE

Received 21 Feb 2014 | Accepted 27 Aug 2014 | Published 30 Sep 2014

DOI: 10.1038/ncomms6098

Jumonji demethylases moderate precocious flowering at elevated temperature via regulation of *FLC* in *Arabidopsis*

Eng-Seng Gan[1,2], Yifeng Xu[1], Jie-Yun Wong[1], Jessamine Geraldine Goh[1,†], Bo Sun[1], Wan-Yi Wee[1], Jiangbo Huang[1,2] & Toshiro Ito[1,2]

As sessile organisms, plants have evolved multiple mechanisms to respond to environmental changes to improve survival. *Arabidopsis* plants show accelerated flowering at increased temperatures. Here we show that Jumonji-C domain-containing protein JMJ30 directly binds to the flowering-repressor *FLOWERING LOCUS C* (*FLC*) locus and removes the repressive histone modification H3 lysine 27 trimethylation (H3K27me3). At elevated temperatures, the *JMJ30* RNA and protein are stabilized, and *FLC* expression is maintained at high levels to prevent extreme precocious flowering. The double mutant of *JMJ30* and its homologue *JMJ32*, grown at elevated temperatures, exhibits an early-flowering phenotype similar to the *flc* mutant, which is associated with increased H3K27me3 levels at the *FLC* locus and decreased *FLC* expression. Furthermore, ectopic expression of *JMJ30* causes an *FLC*-dependent late-flowering phenotype. Taken together, JMJ30/JMJ32-mediated histone demethylation at the *FLC* locus constitutes a balancing mechanism in flowering control at warm temperatures to prevent premature early flowering.

[1] Temasek Life Sciences Laboratory (TLL), 1 Research Link, National University of Singapore, Singapore 117604, Singapore. [2] Department of Biological Sciences, Faculty of Science, National University of Singapore, 10 Science Drive 4, Singapore 117543, Singapore. † Present address: Division of Infectious Diseases, Department of Medicine, National University Health System (NUHS), 5 Lower Kent Ridge Road, Singapore 119074, Singapore. Correspondence and requests for materials should be addressed to T.I. (email: itot@tll.org.sg).

Unlike animals, plants are sessile organisms that stay in the same location throughout their life cycle and are continually exposed to fluctuating ambient conditions, thus highlighting the importance of rapid adaptation to increase the odds of survival. Plants have evolved a myriad of mechanisms to perceive environmental conditions and respond to these changes, as deviations from normal growth conditions could stress the plants and have severe effects on their growth and development. The inevitable changes to the global climate represent an emerging threat, as many plants are highly sensitive to temperature fluctuations[1]. A slight increase or decrease in ambient temperature could affect the growth rate, organ maturation and function, and flowering transition[2,3].

Under normal growth conditions, upon reaching a certain developmental stage and perceiving the right environmental cues, plants would undergo a floral transition. In *Arabidopsis*, this switch from a vegetative to a reproductive phase is controlled by four pathways, and all inputs congregate on a few key floral regulators: the floral repressor *FLOWERING LOCUS C* (*FLC*), which acts upstream and represses the downstream floral inducers *FLOWERING LOCUS T* (*FT*) and *SUPPRESSOR OF OVEREXPRESSION OF CONSTANS 1* (*SOC1*)[4–7]. In addition, recent findings have revealed a few players involved in a fifth flowering pathway that is responsive to ambient temperature changes and has been called the thermosensory pathway. Elevated ambient temperatures accelerate flowering by reducing the repressive H2A.Z nucleosome occupancy at the *FT* locus, which then allows the transcription factor PHYTOCHROME INTERACTING FACTOR 4 (PIF4) to bind and activate *FT*[8,9]. On the other hand, the MADS-box heterocomplex containing SHORT VEGETATIVE PHASE (SVP) and a temperature-dependent isoform of FLOWERING LOCUS M (FLM) represses flowering at lower temperatures[10–14]. The floral repressor *FLC* was also shown to delay flowering during short exposures to non-freezing cold temperatures[15]. These findings suggest the interplay of multiple thermosensory mechanisms in controlling flowering in response to ambient temperature fluctuations.

Considering how the important 'decision' of the vegetative-reproductive phase change centres on just a few genes, it is not surprising that in addition to regulation by transcription factors, many chromatin remodelling mechanisms have evolved to tightly control the expression of these genes. Accelerated flowering by vernalization treatment involves the epigenetic silencing of *FLC* through the Polycomb Group (PcG)-mediated gradual deposition of the trimethylation of lysine 27 of histone H3 (H3K27me3)[16]. Even when plants are grown under normal non-vernalized conditions, the PRC2-like complex containing CURLY LEAF, EMBRYONIC FLOWER 2 and FERTILIZATION-INDEPENDENT ENDOSPERM represses *FLC* expression during vegetative development[17]. In addition to H3K27me3, *FLC* expression is also regulated by repressive H3K9me2 marks, activating H3K4me3/H3K36me3 marks, and histone acetylation[5,18,19]. These crosstalks of histone marks at the locus depend on the interplay between histone methyltransferases and histone demethylases[20,21].

There are two known classes of histone demethylases, and only the Jumonji-C (JmjC) domain-containing proteins have the ability to demethylate trimethylated histones. There are 21 *JUMONJI* (*JMJ*) genes in *Arabidopsis*, which can be categorized into five groups, namely the KDM5/JARID1, KDM4/JHDM3/JMJD2, KDM3/JHDM2, JMJD6 and JmjC domain-only group, based on their JmjC domain sequences and domain architectures[22,23]. Members from the same group show similar target specificity for histone modifications[24–32]. One of the histone modifications, the repressive PcG-mediated H3K27me3, plays a key role in gene repression and developmental regulation, and is actively and dynamically deposited and removed in plants[33]. However, although the demethylases for H3K27me3, UTX and JMJD3 were found years ago in animals[34], there is no *Arabidopsis* homologue in the same KDM6/JMJD3 group. Only recently, members from the KDM4/JHDM3/JMJD2 group, RELATIVE OF EARLY FLOWERING 6 (REF6) in *Arabidopsis* and JMJ705 in rice, were reported as H3K27me3 demethylases[29,35].

Early flowering at high temperatures mediated by the thermosensory pathways is considered to be an adaptive trait to maximize the reproductive success. However, flowering too early without sufficient vegetative growth may risk not having enough nutrients and resources to support seed maturation. Here we show that JMJ30/AT3G20810 and JMJ32/AT3G45880, two members of the JmjC domain-only group of JMJ proteins, function as H3K27 demethylases and regulate *FLC* expression in *Arabidopsis*. Our results suggest that JMJ30/JMJ32-mediated *FLC* regulation may constitute a balancing mechanism that controls flowering time to ensure reproductive success at elevated temperatures.

Results

***FLC* prevents precocious flowering at elevated temperatures.** The flowering time of the *flc-3* null mutant is indistinguishable from Columbia wild-type (WT) plants when grown at 22 °C under long day (LD, 16-h light/8-h dark) conditions (Fig. 1a,b)[36,37]. However, when grown at 29 °C LD conditions, *flc-3* plants flowered earlier than WT plants with the leaf number ratio (29 °C/22 °C) of 0.51 for *flc-3* and 0.69 for WT (Fig. 1a,b), suggesting that *FLC* contributes to preventing precocious flowering at elevated temperatures[38]. Although *FLC* expression is low in WT plants that lack a functional *FRIGIDA* (*FRI*)[38], expression analyses are still able to detect basal *FLC* expression, which gradually decreases during vegetative development (Fig. 1c)[27]. To determine whether *FLC* temporal expression level is affected by elevated temperatures, we analysed *FLC* expression in plants grown at 22 °C and 29 °C under LD conditions at 5, 9 and 13 days-after-germination (DAG) before the plants undergo the bolting process. We observed that after shifting to 29 °C at 3 DAG, *FLC* expression was initially comparable between plants grown at 22 °C and 29 °C at 5 DAG (Fig. 1c). *FLC* expression decreases gradually at 9 and 13 DAG in plants grown under both the 22 °C and 29 °C conditions, but this *FLC* downregulation is significantly attenuated in plants grown at 29 °C (Fig. 1c). This result showed that *FLC* repression during vegetative development is delayed during growth at elevated temperatures.

We wondered whether this delayed repression is regulated at the chromatin level. As *FLC* reduction during the developmental switch from vegetative to reproductive phase is known to be regulated by the repressive H3K27me3 (refs 16,17), we performed chromatin immunoprecipitation (ChIP) assays to assess the level of H3K27me3 at the *FLC* locus at 8 DAG, which is on the brink of floral transition occurring at 9 DAG[39] (Fig. 1d,e). Compared with WT plants grown under 22 °C LD conditions, WT plants grown at 29 °C showed reduced H3K27me3 enrichment at the *FLC* locus (Fig. 1e). This finding indicates that delayed *FLC* repression at elevated temperatures is associated with the reduction of the repressive H3K27me3 at the *FLC* locus. Taken together, these results suggest that H3K27me3-associated histone modifiers may participate in the thermosensory pathway by regulating *FLC* expression at elevated temperatures to control flowering in moderation.

Mutation of *jmj30* and *jmj32* promotes flowering at 29 °C. The lower levels of H3K27me3 at the *FLC* locus at elevated

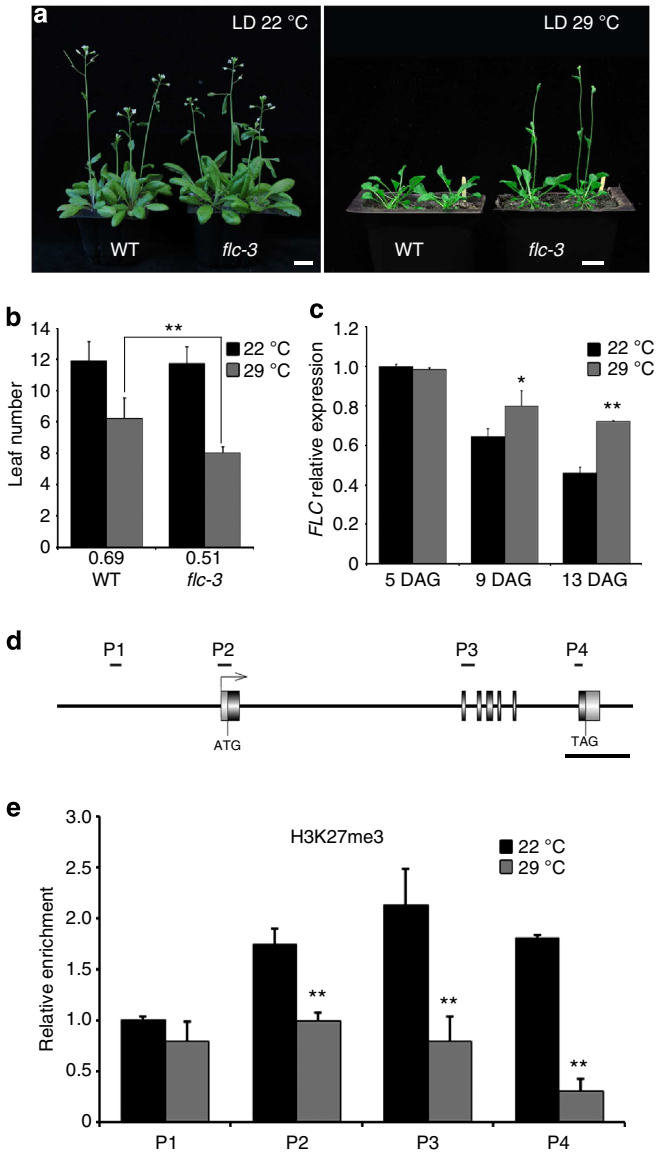

Figure 1 | *FLC* is a suppressor of thermal induction of flowering. (**a**) *flc-3* flowers at a similar time as WT when grown in LD 22 °C, but flowering is accelerated in *flc-3* when grown under LD 29 °C conditions. Representative 30-day-old plants (LD 22 °C) or 23-day-old plants (LD 29 °C) are shown for comparison. Scale bar, 1 cm. (**b**) Total primary rosette leaves before bolting in WT and *flc-3* plants grown under LD 22 °C and 29 °C conditions were counted (two independent experiments with 15–20 plants each). Numbers below graph indicate leaf number ratio (29 °C/22 °C). Bars indicate standard deviation (s.d.); two-tailed Student's *t*-test, $^{**}P<0.01$. (**c**) *FLC* mRNA levels in 5, 9 and 13 DAG seedlings grown under LD 22 °C and 29 °C conditions. Relative fold changes to 5 DAG seedlings grown under 22 °C conditions are presented. Bars indicate s.d. of three biological replicates; two-tailed Student's *t*-test, $^{*}P<0.05$, $^{**}P<0.01$. (**d**) Schematic drawing of the *FLC* genome structure showing regions amplified by primers used for ChIP analysis. Scale bar, 1 kb. (**e**) ChIP analysis of H3K27me3 enrichment at the *FLC* locus in 8 DAG WT seedlings grown under LD 22 °C and 29 °C conditions. An anti-H3 antibody was used as a control. Bar indicates standard error of the mean (s.e.m.) of three biological replicates; two-tailed Student's *t*-test, $^{**}P<0.01$.

temperatures and the increased level of *FLC* expression led us to conjecture that the effect may be maintained through the action of H3K27me3 demethylases. However, *FLC* expression is upregulated rather than downregulated in the loss-of-function mutant of the only known *Arabidopsis* H3K27me3 demethylase, *REF6* (refs 29,40). Hence, we reasoned that there might be other JMJ proteins that may remove the H3K27me3 repressive marks at the *FLC* locus.

Among the five groups of *Arabidopsis* JMJ proteins, four of them (KDM5/JARID1, KDM4/JHDM3/JMJD2, KDM3/JHDM2 and JMJD6) have been implicated as histone demethylases specific for other histone modifications, such as H3K4 and H3K9 (refs 22–32). Little is known about the enzymatic function of the JmjC domain-only group that contains no other known functional protein domains but the catalytic JmjC domain, except their role in circadian regulation[41,42]. To elucidate the function of this group, we used two previously described loss-of-function mutants for *JMJ30*: *jmj30-1* (SAIL_811_H12) and *jmj30-2* (GK-454C10)[41,42], and isolated one T-DNA insertional mutant for *JMJ32*: *jmj32-1* (SALK_003313; Fig. 2a). No full-length *JMJ30* mRNA was detected for either allele, and we decided to use *jmj30-2* for subsequent experiments, as it produced no partial fragments (Fig. 2b, Supplementary Fig. 1a,b). No full-length *JMJ32* mRNA was detected in *jmj32-1*, but partial fragments were still detectable (Fig. 2b, Supplementary Fig. 1a,c). However, because the T-DNA is inserted at the catalytic JmjC domain in *jmj32-1* (Fig. 2a), it likely produces a null mutant. Under the standard growth conditions (22 °C LD), neither the single nor the double *jmj30-2 jmj32-1* (herein *jmj30 jmj32*) mutants differed from WT in terms of flowering time, which is similar to the *flc* mutant's lack of a phenotype under standard growth conditions (Figs 1a,b and 2c,d). However, we found that the *jmj30 jmj32* double mutant flowered earlier than the WT when grown under elevated temperatures with the decreased leaf number ratio (29 °C/22 °C) of 0.52 compared with 0.69 in WT, but no obvious difference in phyllochron length (Fig. 2c,d), as was observed in *flc* (Fig. 1a,b). We then studied the response of *jmj30 jmj32* to elevated temperature in short days (SDs, 8-h light/16-h dark) and observed the enhanced early-flowering phenotype compared with WT grown under the same conditions, with the leaf number ratio (29 °C/22 °C) of 0.19 for *jmj30 jmj32* and 0.24 for WT (Supplementary Fig. 2a,b).

We next proceed to look at the expression profile of the flowering time genes. We collected 5, 9 and 13 DAG seedling samples grown at 29 °C LD conditions at the end of the light photoperiod. The *jmj30 jmj32* double mutant decreased *FLC* expression at all tested time points (Fig. 3a). Furthermore, the trend of decreased *FLC* expression at 13 DAG is similar in *jmj30 jmj32* seedlings grown at 29 °C (Fig. 3a) and WT grown at 22 °C (Fig. 1c). The other thermosensory mediator *SVP* was not significantly affected (Fig. 3b). In contrast, the expression of the florigen *FT* and another floral promoter *SOC1* were increased especially in 13 DAG seedlings of *jmj30 jmj32* relative to WT at 29 °C LD (Fig. 3c,d). These results align with reports that the FLC-SVP complex represses *FT* in leaves and *SOC1* in both leaves and shoot apical meristems[43]. *AGAMOUS-LIKE 24* (*AGL24*) and *CONSTANS* (*CO*) were not significantly affected in *jmj30 jmj32* (Fig. 3e,f). In short, the results suggest that *jmj30 jmj32* mutations decrease *FLC* expression at elevated temperatures, and this effect appears to upregulate the floral integrators *FT* and *SOC1*, which are two common targets of FLC.

Characterization of JMJ30 and JMJ32. To further reveal the function of JMJ30 and JMJ32, we characterized their spatial expression patterns. Transcript profiling data deposited at the *Arabidopsis* eFP Browser suggest that *JMJ30* and *JMJ32* are rather ubiquitously expressed at the rosette leaves, shoot apex and developing flowers (Supplementary Fig. 3a,b)[44]. To confirm this,

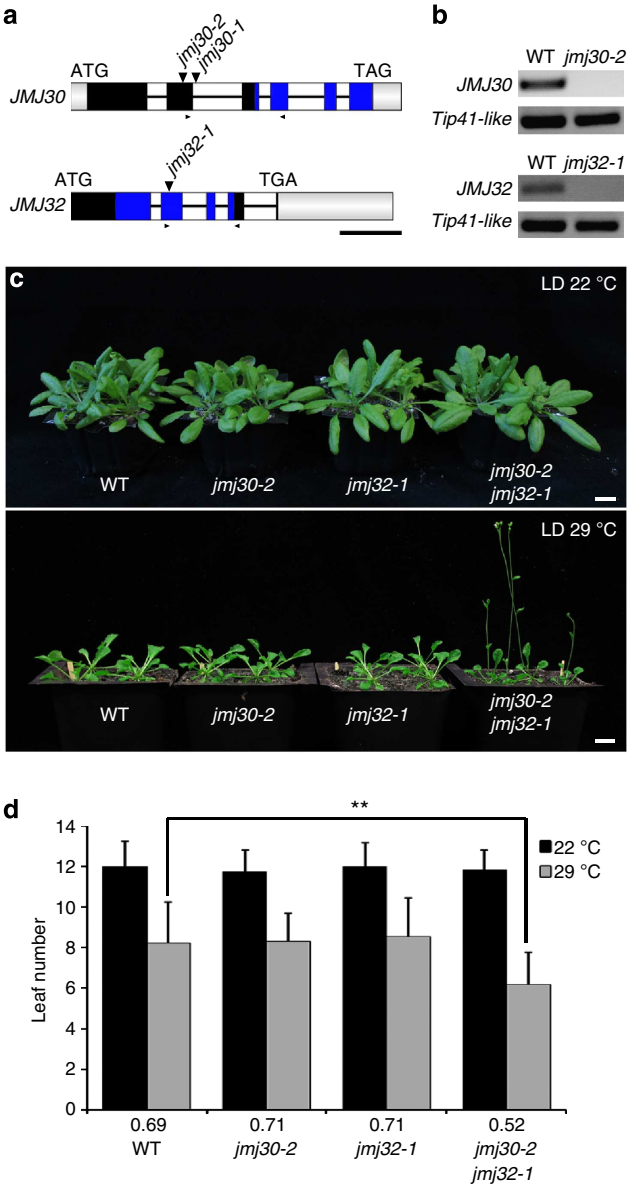

Figure 2 | *jmj30 jmj32* loss-of-function mutant accelerates flowering at elevated temperatures. (**a**) Schematic drawings of *JMJ30* and *JMJ32* genomic structures. Grey boxes indicate the 5′and 3′ untranslated region (UTR). Black boxes indicate exons, whereas blue boxes indicate exons coding for the JmjC domain. White boxes with a line indicate introns. T-DNA insertion sites are marked by downward pointing arrowheads above the schematic diagrams, whereas smaller arrowheads show primers used for RT–PCR. Scale bar, 500 bp. (**b**) RT–PCR of *JMJ30* and *JMJ32* in WT, *jmj30-2* and *jmj32-1*. *Tip-41 like* is shown as an internal control. (**c**) *jmj30-2*, *jmj32-1* and *jmj30-2 jmj32-1* flower at a similar time as WT when grown under LD 22 °C conditions, but *jmj30-2 jmj32-1* showed accelerated flowering when grown under LD 29 °C conditions. Representative 25-day-old plants (LD 22 °C) or 23-day-old plants (LD 29 °C) were shown as comparison. Scale bar, 1 cm. (**d**) Total primary rosette leaves before bolting in WT, *jmj30-2*, *jmj32-1* and *jmj30-2 jmj32-1* plants grown under LD 22 °C and 29 °C conditions were counted (two independent experiments with 15–20 plants each). Numbers below graph indicate leaf number ratio (29 °C/22 °C). Bars indicate s.d.; two-tailed Student's *t*-test, $^{**}P<0.01$.

we extracted RNA from different tissues of WT plants, and by reverse transcription–PCR (RT–PCR), we concluded that *JMJ30* and *JMJ32* were expressed in all tested tissue types, namely, seedlings, roots, rosette leaves, cauline leaves, stems and inflorescences (Supplementary Fig. 4a)[22]. *JMJ30* was highly expressed in leaves, whereas *JMJ32* expression showed no appreciable difference across the various tissue types.

Next, to better understand the spatial distribution of JMJ30 and JMJ32 at the protein level, constructs harbouring their upstream promoter and downstream sequences plus the genomic coding sequence (6.1-kb JMJ30 and 5.3-kb JMJ32) fused with the β-glucuronidase (GUS) reporter gene were transformed into WT plants (Fig. 4a). This genomic fragment of JMJ30, when fused with the short haemagglutinin (HA) epitope tag, was sufficient to rescue the *jmj30 jmj32* early-flowering phenotype at 29 °C LD (Supplementary Fig. 5a,b), indicating that the fragment contains all the *cis*-elements necessary to capture the endogenous expression pattern. Histochemical GUS staining results showed that JMJ proteins were rather ubiquitously expressed, including in the leaves, roots and inflorescences (Fig. 4b,c). Furthermore, JMJ30 and JMJ32 expression in the vasculature of leaves overlapped with the expression patterns of their putative targets *FLC*[45], *FT*[46] and *SOC1* (refs 47,48), and FLC is known to directly repress *FT* and *SOC1* in the leaf veins[43].

To study the sub-cellular localization of JMJ30 and JMJ32, we transiently overexpressed JMJ-VENUS in tobacco *Nicotiana benthamiana*. We observed that JMJ30 and JMJ32 localized not only to the nucleus but also occasionally to the endoplasmic reticulum and cytoplasm (Supplementary Fig. 4b) as reported previously[41], which could be artefacts from the overexpression of the JMJ proteins. We thus generated an endogenous *pJMJ30* promoter-driven JMJ30-HA in *jmj30-2,* which complements the early-flowering phenotype of *jmj30 jmj32* (Supplementary Fig. 5a,b), and performed an immunolocalization assay using anti-HA and anti-H3K27me3 antibodies on its protoplasts. We observed that JMJ30-HA localized primarily to the nucleus, consistent with its role as a histone demethylase, and its expression pattern resembled that of H3K27me3 (Fig. 4d,e). Moreover, immunolocalization assay performed using the extracted nuclei from *jmj30-2 pJMJ30::JMJ30-HA* showed that JMJ30-HA localization to the euchromatin but not to the 4′,6-diamidino-2-phenylindole (DAPI)-dense heterochromatic chromocentres, resembling reported localization of H3K27me3 (refs 49,50), and this localization was not affected by the ambient temperature (Supplementary Fig. 4c).

JMJ30 and JMJ32 specifically demethylate H3K27me2/3. Proteins that have the catalytic JmjC domain are known to be histone demethylases[51], and JMJ30-HA localization that resembled the euchromatic histone marks inspired us to study the biochemical function of these histone demethylases. We first determined whether they could demethylate methylated histones *in vitro*. We transiently overexpressed *35S::JMJ30-HA* in tobacco leaves and immunoaffinity-purified the protein using anti-HA agarose beads. Using these purified proteins, an *in vitro* demethylase assay was carried out. We incubated calf thymus histones with JMJ30-HA proteins, together with reported JmjC cofactors Fe(II) ions and α-ketoglutarate (α-KG). Indeed, western blotting analyses indicated that JMJ30-HA was able to demethylate oligonucleosomes at H3K27me3 and H3K27me2 but not at H3K27me1 (Fig. 5a).

To investigate the demethylase activity of JMJ30 further, we purified a mutated version of JMJ30-HA (JMJ30H326A-HA), in which one of its conserved Fe(II)-binding histidine residues in the JmjC domain was mutated to alanine. We found that the effect of JMJ30H326A-HA on H3K27me2/3 was completely abolished by the mutation (Fig. 5b). To address their substrate specificity, we looked at their ability to demethylate other histone methylation

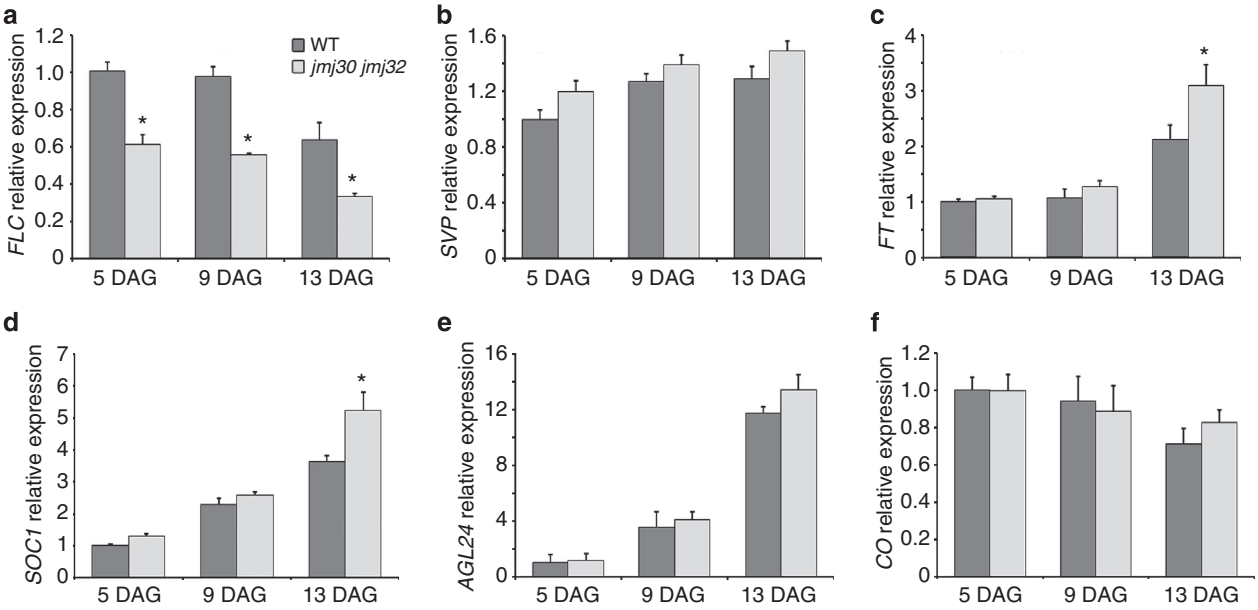

Figure 3 | Expression profiles of flowering time genes. (**a**–**f**) RT–qPCR-based expression profiles of (**a**) *FLC*, (**b**) *SVP*, (**c**) *FT*, (**d**) *SOC1*, (**e**) *AGL24* and (**f**) *CO* in 5, 9 and 13 DAG seedlings of WT and *jmj30-2 jmj32-1* grown under LD 29 °C conditions. Relative fold changes to WT 5 DAG seedlings are presented. Bars indicate s.d. of three biological replicates; two-tailed Student's *t*-test, $^{*}P<0.05$.

marks. Consistent with the previously reported group-specific characteristics of JMJ proteins, we did not see noticeable demethylation activity for H3K4me2/3, H3K9me2/3 and H3K36me2/3 in the *in vitro* demethylase assay (Fig. 5a). The results indicate that JMJ30 can specifically demethylate H3K27me2/3 *in vitro* and that its activity is dependent on its JmjC domain.

Next, to confirm whether JMJ30 and JMJ32 can exert this demethylase activity in plants, we transiently overexpressed *35S::JMJ30-HA* and *35S::JMJ32-HA*, and their respective mutated versions of *35S::JMJ30H326A-HA* and *35S::JMJ32H174A-HA* in *Arabidopsis* leaf protoplasts. Immunostaining assays were then conducted on the isolated nuclei using anti-H3K27me3 and anti-HA antibodies to observe their demethylase activity *in vivo*. We found that the overexpression of JMJ30-HA reduced H3K27me3 levels, however, overexpression of the mutated JMJ30H326A-HA has no effect on H3K27me3 methylation (Supplementary Fig. 6a,b). Similarly, the H3K27me3 levels were reduced in nuclei overexpressing JMJ32-HA but not in the mutated JMJ32H174A-HA-expressing nuclei (Supplementary Fig. 6c,d). Taken together, these results indicate that JMJ30 and JMJ32 function as H3K27me3 demethylases.

***JMJ30* overexpression delays flowering by upregulating *FLC*.** To further elucidate the function of JMJ30, we overexpressed JMJ30-HA in WT plants and confirmed that *35S::JMJ30-HA* transgenic lines exhibit constitutive overexpression of JMJ30 and late-flowering phenotypes at 22 °C LD conditions (Supplementary Fig. 7a–d)[41]. To understand the effects of JMJ30 overexpression at a molecular level, we checked the expression profiles of the flowering time genes in two independent transgenic lines grown at 22 °C under inductive LD conditions. Supporting the phenotypic observations, the floral repressor *FLC* is strongly increased in the *35S::JMJ30-HA* overexpression lines (Fig. 6a). We also found that *FT* and *SOC1* are mildly downregulated (Fig. 6a). As FLC is the common repressor of the two floral integrators[43] and was most significantly affected, the increase in *FLC* expression is likely to be the main reason for the late-flowering phenotype.

Based on the results, we hypothesized that *FLC* is a target of JMJ30. To test whether *FLC* is genetically necessary for JMJ30 functions, we performed a genetic analysis by crossing *35S::JMJ30-HA* with *flc-3*. Introduction of the *flc* mutation largely abolished the late-flowering phenotype of *35S::JMJ30-HA*, and *35S::JMJ30-HA flc-3* flowered at a similar time as *flc-3* or WT plants (Fig. 6b,c). Taken together, these results support the notion that *JMJ30* and *FLC* function in the same genetic pathway that regulates flowering time and that FLC functions downstream of the histone demethylase JMJ30.

JMJ30 and JMJ32 regulate H3K27me3 at the *FLC* locus. Our results suggested that JMJ30 functions as an H3K27me2/3 demethylase *in vitro* (Fig. 5a,b) and *in vivo* (Supplementary Fig. 6a,b), and that *FLC* may be a direct target of JMJ30 (Figs 3a and 6a–c). We were interested in verifying whether the increased *FLC* expression in *JMJ30* overexpression lines is similarly reflected in the H3K27 methylation status of the *FLC* locus. ChIP assays were carried out comparing the H3K27me3 levels between WT and our *35S::JMJ30-HA* plants, and we found that the repressive H3K27me3 levels were decreased at the *FLC* locus in the *35S::JMJ30-HA* lines (Fig. 7a), which is consistent with the increased *FLC* expression levels (Fig. 6a).

We next measured H3K27me3 enrichment at the *FLC* locus in *jmj30 jmj32* and WT grown under 29 °C LD conditions, in which the *jmj30 jmj32* double mutant showed decreased *FLC* expression and accelerated flowering (Figs 2c,d and 3a). Consistent with its expression, we found that the H3K27me3 levels at the *FLC* locus are increased in *jmj30 jmj32* at 29 °C (Fig. 7b). Taken together, these results indicate that JMJ30 and JMJ32 demethylate H3K27me3 at the *FLC* locus to activate *FLC* expression at elevated temperatures.

Prolonged JMJ30 activity directly regulates *FLC* expression. The ability of JMJ30 to affect the H3K27me3 level on *FLC* chromatin leads us to speculate that JMJ30 may directly bind to the *FLC* locus and demethylate the repressive mark. ChIP assays were conducted using the overexpression *35S::JMJ30-HA*

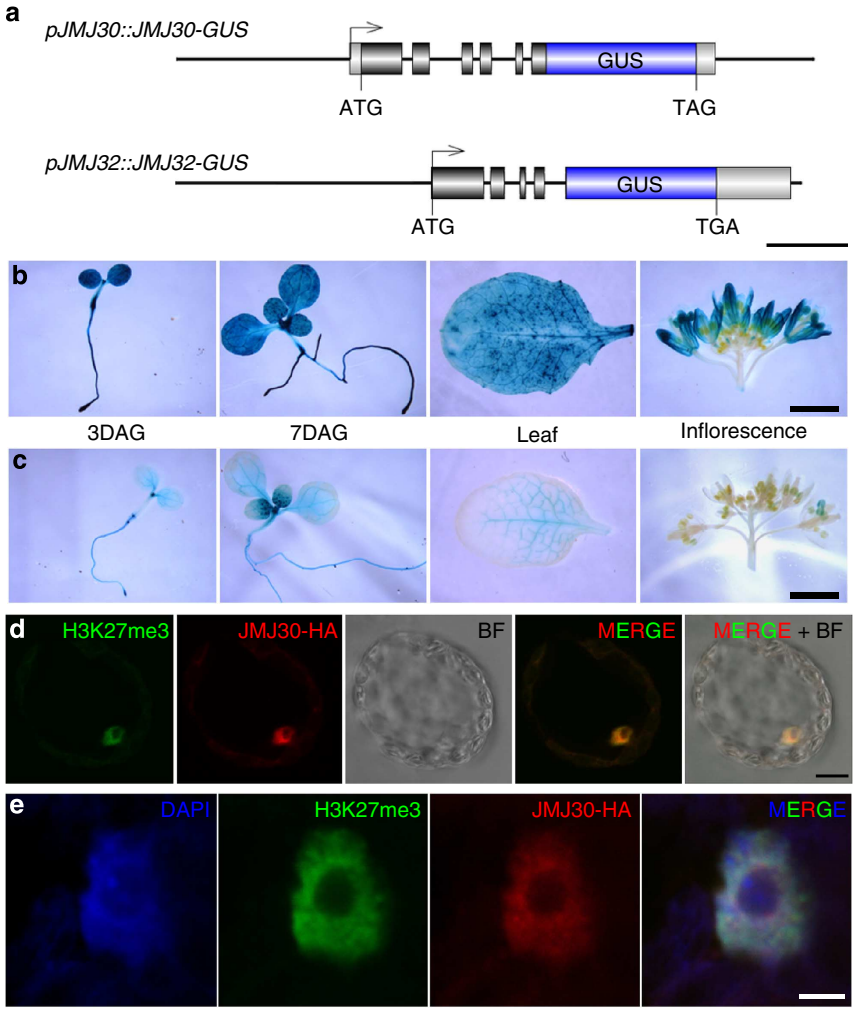

Figure 4 | Spatial expression patterns of JMJ30 and JMJ32. (**a**) Schematic drawings of *pJMJ30::JMJ30-GUS* and *pJMJ32::JMJ32-GUS*. Exons are represented by black boxes, and GUS is represented by blue boxes. Lines indicate promoter, introns and 3′ downstream regions. Scale bar, 1 kb. (**b**,**c**) Histochemical GUS staining of (**b**) *pJMJ30::JMJ30-GUS* and (**c**) *pJMJ32::JMJ32-GUS* transgenic lines. 3 and 7 DAG seedlings, rosette leaves and inflorescences were stained overnight. Scale bars, 2 mm. (**d**,**e**) Immunolocalization of H3K27me3 and JMJ30-HA in protoplasts generated from *jmj30-2 pJMJ30::JMJ30-HA* transgenic lines. (**d**) JMJ30-HA localization resembles that of H3K27me3 in the nucleus. Scale bar, 10 μm. (**e**) Image shows enlarged view of a nucleus. Scale bar, 2.5 μm.

transgenic line and the endogenous promoter-driven *pJMJ30::JMJ30-HA jmj30-2* line grown at 29 °C under LD conditions. We immunoprecipitated the epitope-tagged JMJ30-HA protein using anti-HA agarose to assess the level of JMJ30-HA binding across the *FLC* chromatin region. Compared with WT plants, we found that JMJ30-HA associates with *FLC* chromatin directly in both lines, with the P2 region near the transcriptional start site showing the highest levels of binding enrichment (Fig. 8a; Supplementary Fig. 8).

To further elucidate the mechanism underlying the positive regulation of *FLC* expression at elevated temperatures by JMJ30, we were interested in *JMJ30* mRNA and protein expression and stability at 22 °C and 29 °C. *JMJ30* mRNA diurnal expression has been previously reported[41,42]. Taking samples from WT seedlings grown at 22 °C and 29 °C under LD condition every 4 h, we found that *JMJ30* expression peaked approximately 4 h before dark for both conditions, and the peak levels in the *JMJ30* diurnal expression were not significantly affected by the temperature. However, we found that the width of the peak broadened under the 29 °C conditions (Fig. 8b), which could be due to prolonged expression or increased mRNA stability.

To test if the protein expression of JMJ30 is similarly affected, we did a western blot with total proteins extracted from *jmj30-2 pJMJ30::JMJ30-HA* using an anti-HA-HRP antibody. Under standard growth conditions (22 °C LD), the peak of the JMJ30-HA protein accumulation at the beginning of dark was slightly delayed compared with its mRNA expression, and JMJ30-HA was degraded quickly after that (Fig. 8c). At 29 °C, not only was the JMJ30-HA protein accumulation lengthened, it was also more stable as it persisted much longer than expected based on mRNA expression (Fig. 8b,c). To confirm this, we performed a protein stability assay by pre-treating the seedlings with cycloheximide to prevent *de novo* protein synthesis, and adding the proteasome inhibitor MG132 at the end of the light photoperiod. We collected the samples at different time points and found that the rapid degradation of JMJ30-HA at 22 °C was inhibited by the addition of the proteasome inhibitor MG132 (Supplementary Fig. 9), suggesting that the proteasome-dependent JMJ30-HA degradation is impaired at higher temperatures. These results suggested that the strongly prolonged JMJ30 expression at elevated temperatures may allow JMJ30 to bind and demethylate

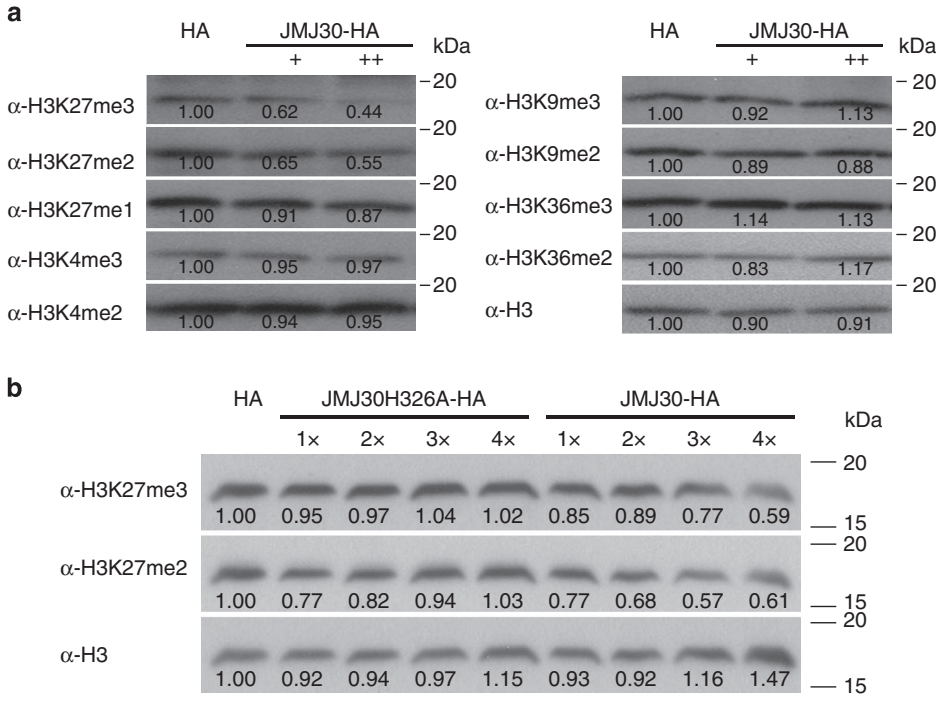

Figure 5 | JMJ30 demethylates H3K27me2/3 *in vitro*. (**a**) Immunoaffinity-purified JMJ30-HA was co-incubated with substrate calf thymus histone and cofactors Fe(II) ions and α-KG at 37 °C for 4 h. Immunoblot analysis of histone demethylase activity of JMJ30 was performed using antibodies indicated to the left. The anti-H3 antibody is used as loading control. (**b**) A mutated version of JMJ30-HA (JMJ30H326A-HA) was unable to demethylate H3K27me2/3 *in vitro* when a conserved Fe(II)-binding histidine residue in the JmjC domain was replaced by alanine. Numbers indicate relative band intensity compared with control reaction (HA) performed using an anti-HA precipitate from WT. At least two biological replicates were performed and one set of the data is shown here.

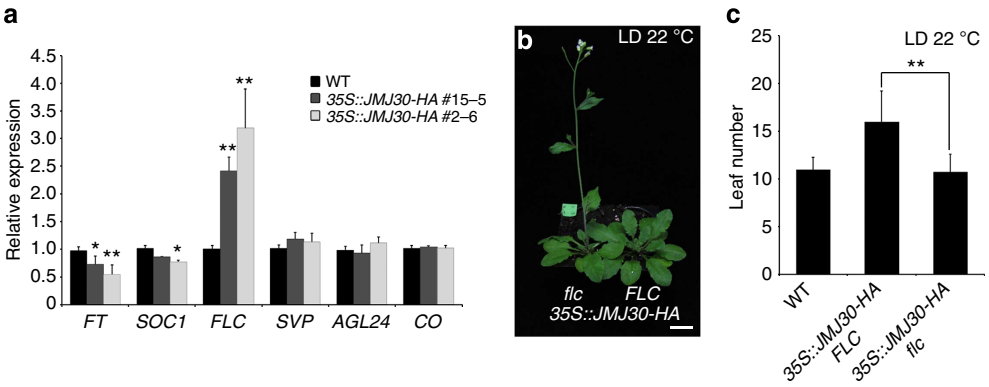

Figure 6 | Overexpression of JMJ30 leads to delayed flowering. (**a**) mRNA expression levels of flowering time genes in WT and two independent lines of *35S::JMJ30-HA*. Relative fold changes to WT are presented. Bars indicate s.d. of three biological replicates; two-tailed Student's *t*-test, $*P<0.05$, $**P<0.01$. (**b**) Introduction of *flc* mutation rescues the late-flowering phenotype of *35S::JMJ30-HA*. Scale bar, 1 cm. (**c**) Total primary rosette leaves before bolting in WT, *35S::JMJ30-HA* and *35S::JMJ30-HA flc* plants grown under LD 22 °C conditions were counted (two independent experiments with 20–50 plants each). Bars indicate s.d.; two-tailed Student's *t*-test, $**P<0.01$.

H3K27me3 at the *FLC* locus, thus maintaining a transcriptionally permissive chromatin status.

JMJ30-regulated genes are enriched for H3K27me3 targets. To investigate whether *JMJ30* overexpression and *jmj30 jmj32* loss-of-function mutants influence gene transcription at a global level, we performed expression profiling using NimbleGen 12 × 135K arrays. Compared with WT, 469 genes were downregulated and 657 genes were upregulated in *jmj30 jmj32* under 29 °C LD conditions (Supplementary Data 1, NCBI Gene Expression Omnibus GSE51898). On the other hand, 516 genes were upregulated and 588 genes were downregulated in *35S::JMJ30-HA* compared with WT (Supplementary Data 2). The transcriptome analyses suggested that despite only showing flowering phenotypes, the loss-of-function and overexpression of *JMJ30* did affect global expression profiles.

Previous studies identified that at least 25% (27.70% of genes analysed in our microarray) of the *Arabidopsis* genome is targeted by H3K27me3 (refs 33,52), and our study showed that JMJ30 and

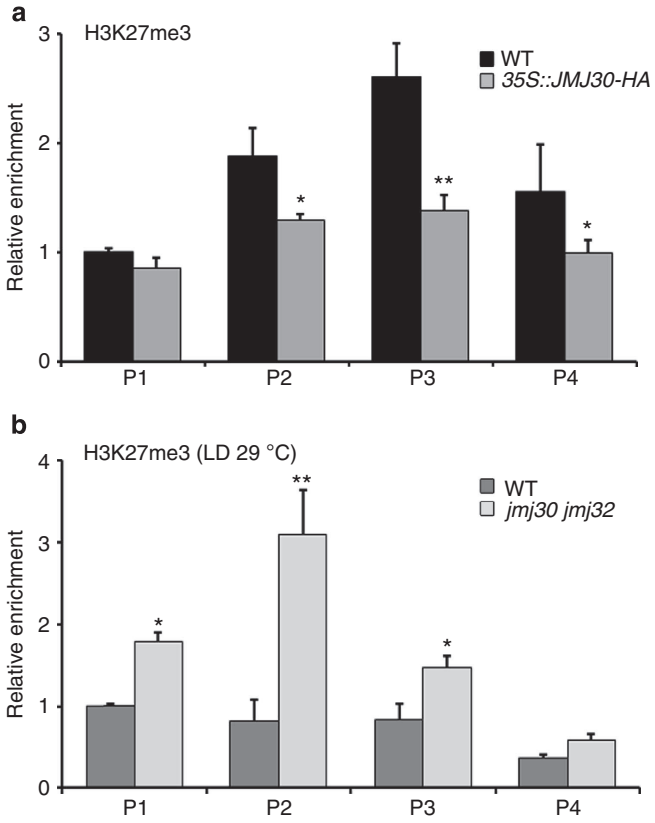

Figure 7 | The repressive H3K27me3 on the *FLC* locus is affected by JMJ30 and JMJ32. (**a**,**b**) ChIP analysis of H3K27me3 enrichment on the *FLC* locus in (**a**) 8 DAG WT and *35S::JMJ30-HA* seedlings grown under LD 22 °C conditions and (**b**) 8 DAG WT and *jmj30 jmj32* seedlings grown under LD 29 °C conditions. An anti-H3 antibody was used as a control. Bar indicates s.e.m. of three biological replicates; two-tailed Student's *t*-test, $*P<0.05$, $**P<0.01$.

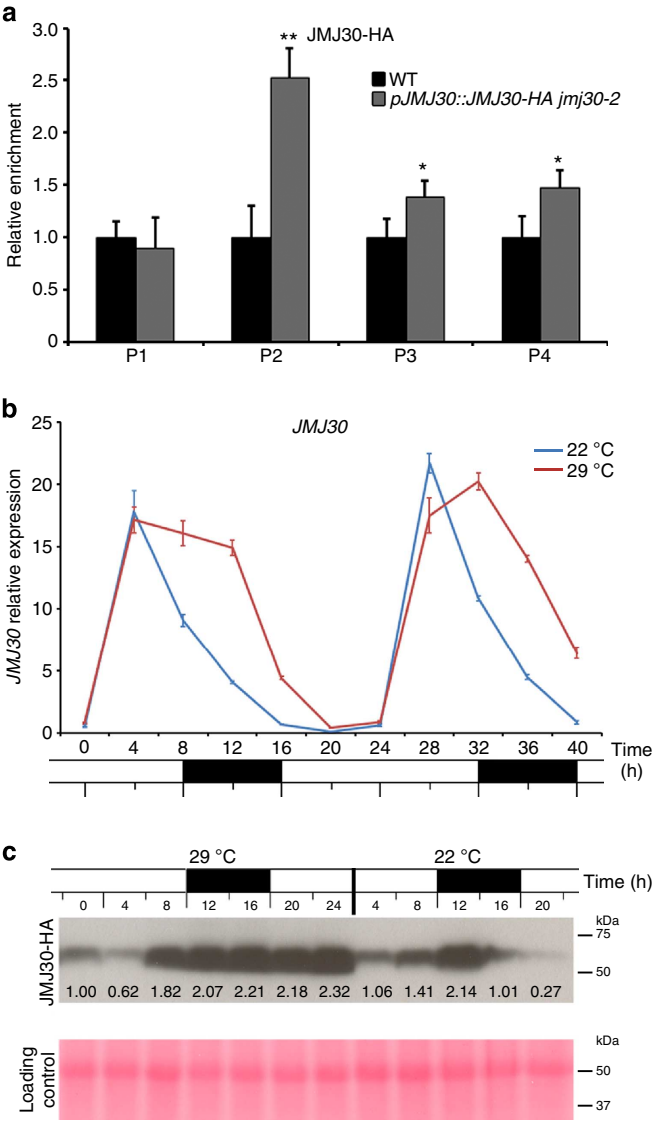

Figure 8 | Prolonged JMJ30 activity under elevated temperature directly regulates *FLC* expression. (**a**) ChIP analysis of JMJ30-HA enrichment at the *FLC* locus in 8 DAG WT and *jmj30-2 pJMJ30::JMJ30-HA* seedlings. JMJ30-HA directly binds near the transcriptional start site of the *FLC* locus. A mouse IgG was used as control. Bar indicates s.e.m. of three biological replicates; two-tailed Student's *t*-test, $*P<0.05$, $**P<0.01$. (**b**) *JMJ30* mRNA levels in WT seedlings grown under LD 22 °C and 29 °C conditions, measured over 40 h (h). Relative fold changes to 0 h are presented. Bars indicate s.d. of three biological replicates. (**c**) Relative JMJ30-HA protein levels over 24 h examined by western blot using anti-HA-HRP antibody. Total proteins from *jmj30-2 pJMJ30::JMJ30-HA* seedlings grown under LD 22 °C and 29 °C conditions were used. Ponceau Red-stained membrane is shown as a loading control. Numbers indicate relative band intensity compared with 29 °C 0 h sample. Two biological replicates were performed and one set of the data is shown here.

JMJ32 are H3K27me3 demethylases. We found that 193 of the 469 (41.15%) total downregulated genes in *jmj30 jmj32* and 213 of the 516 (41.28%) genes upregulated in *35S::JMJ30-HA* overlapped with reported H3K27me3-regulated genes (Fig. 9a, Supplementary Data 1 and 2)[33,52]. Moreover, the genes downregulated in *jmj30 jmj32* showed enrichment for PcG targets (41.15%, Fisher's exact test, P-value $= 3.499 \times 10^{-10}$) compared with the upregulated genes (201 out of 657, 30.59%, Fisher's exact test, P-value $= 0.0565$). Gene ontology analysis of the H3K27me3 targets affected by JMJ30/JMJ32 (shaded in Fig. 9a) revealed that, in terms of molecular function, genes involved in transcription factor activity (Fisher's exact test, P-value $= 8.899 \times 10^{-3}$) were more enriched, and there were slight enrichment in transcription, DNA-dependent genes in terms of biological process (Fisher's exact test, P-value $= 6.074 \times 10^{-2}$; Fig. 9b). The 40% correlation between reported H3K27me3 targets and our transcriptome profiling suggested that JMJ30/JMJ32-mediated gene regulation positively influences gene expression by demethylating the repressive H3K27me3, thereby contributing to gene de-repression.

Discussion

In this study, we revealed that the histone modifiers JMJ30 and JMJ32 demethylate H3K27me3 marks at the *FLC* locus to delay the repression of the floral repressor at elevated temperatures. In the flowering pathways, *FLC* is the central repressor that represses two floral integrators, *FT* and *SOC1*, in *Arabidopsis*[43]. We showed that JMJ30 specifically demethylates H3K27me2/3 *in vitro* (Fig. 5a,b) and *in vivo* (Supplementary Fig. 6). Moreover, *jmj30 jmj32* double mutant showed accelerated flowering when grown under 29 °C LD or SD conditions (Fig. 2c,d, Supplementary Fig. 2a,b), a temperature below the one used in basal thermotolerance experiments[53]. On the other hand, overexpression of *JMJ30-HA* led to an obvious late-flowering phenotype

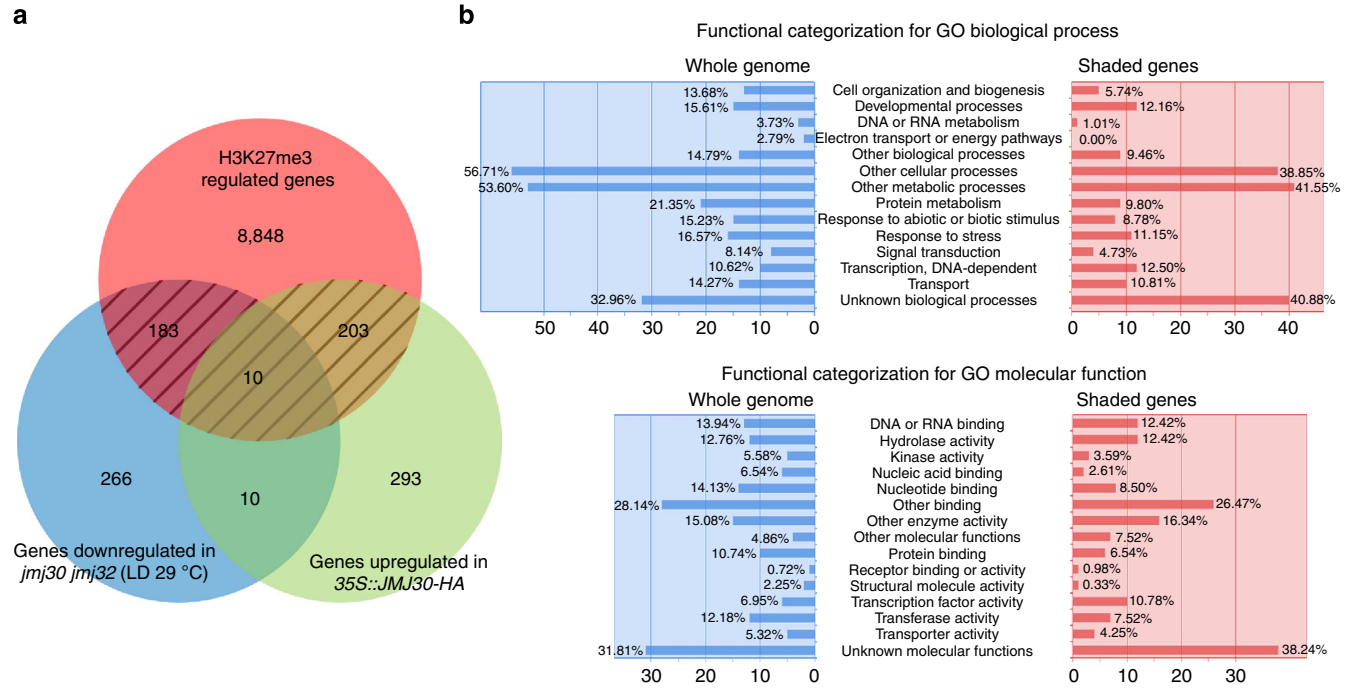

Figure 9 | Hundreds of genes are regulated by *JMJ30/JMJ32*. (**a**) Diagram showing overlap of genes downregulated in *jmj30 jmj32* grown under LD 29 °C conditions, genes upregulated in *35S::JMJ30-HA* and reported H3K27me3-regulated genes[33,52]. Genes showing a 1.5-fold change within a 90% confidence interval were considered to be differentially expressed. (**b**) Functional categorization for Gene Ontology of genes shaded in **a**.

(Supplementary Fig. 7a–d). The mutation of *fri flc* leads to early-flowering under LD (Fig. 1a,b) or SD[38] conditions with increased temperatures. Accordingly, in both *jmj30 jmj32* and *35S::JMJ30-HA* lines, we noticed that *FLC* expression was the most obviously affected (Figs 3a and 6a). The direct binding of JMJ30-HA to the transcriptional start site of the *FLC* locus shows that *FLC* is a direct target of JMJ30 (Fig. 8a; Supplementary Fig. 8). Moreover, the genetic rescue of the late-flowering phenotype of *JMJ30* overexpression by introducing the *flc* mutation strengthens the notion that JMJ30 functions through *FLC* to help regulate flowering time (Fig. 6b,c). Our work shows the importance of the balancing act between PcG-mediated histone methylation and JMJ30/JMJ32-mediated histone demethylation on H3K27 in controlling the expression of genes such as *FLC*.

Under the functional *FRI* background, *FRI jmj30 jmj32* showed only a modest decrease of *FLC* at 3-weeks-after-germination at 29 °C LD (Supplementary Fig. 10). A strong transcription activity driven by activators such as *FRI* may negatively affect the deposition of the repressive H3K27me3 marks at the *FLC* locus as previously suggested[54], possibly masking the effect of JMJ30/JMJ32. *FRI*-activated *FLC* is gradually silenced through vernalization with the accumulation of H3K27me3 (ref. 16). It would hence be interesting to study the effect of JMJ30/32 on vernalization under the *FRI* background.

JMJ30 transcript shows diurnal circadian rhythm (Fig. 8b)[41,42]. JMJ30/JMJ32-dependent *FLC* delayed repression at elevated temperatures led us to examine whether the higher activity of JMJ30 is mediated through increased expression levels or a shift in circadian rhythms. We found that *JMJ30* diurnal expression is increased by maintaining the high peak before dropping to start another cycle (Fig. 8b) and the protein is further stabilized (Fig. 8c; Supplementary Fig. 9). Although *FLC* itself is not controlled by circadian regulation, we reasoned that the increased accumulation of the JMJ30 protein at a higher temperature can help maintain the *FLC* locus in a transcriptionally permissive state. Our data showed that instability of JMJ30 protein at 22 °C is mediated by proteasomal degradation pathway, which is blocked by the proteasome inhibitor MG132 or when the plants are grown at 29 °C (Supplementary Fig. 9). Our future work includes the search for interacting partners of JMJ30 in its temperature-dependent behaviour.

Expression profiling showed that 396 out of thousands of H3K27me3-regulated genes are upregulated in *35S::JMJ30-HA* and/or downregulated in *jmj30 jmj32*. The fact that the expression profiles of many H3K27me3-regulated genes are not affected, suggests that JMJ30 and JMJ32 may only target a subset of H3K27me3-regulated genes. Because JMJ30 and JMJ32 contain only the catalytic JmjC domain, the activity of these histone modifiers may be dependent on the availability of a recruiter to the target genes. Furthermore, this JmjC domain-only group contains another member, JMJ31/AT5G19840, which has a different variant for one of its key α-KG-binding amino acids and is thus likely to be enzymatically inactive[51]. Hence, the biological function of JMJ31 remains to be elucidated.

In animals, the H3K27me3 demethylases are developmentally essential, and loss-of-function mutants of the demethylases usually lead to severe developmental defects and lethality. In mouse, JMJD3 inactivation results in perinatal lethality because of respiratory failure[55], whereas the loss of the zebrafish Utx1 leads to posterior developmental defects[56]. In *Caenorhabditis elegans*, the *utx-1* loss-of-function mutant leads to sterility and embryonic lethality[57], whereas loss of the JMJD3 homologue causes abnormal gonad development[34]. In *Arabidopsis*, one member of the KDM4/JHDM3/JMJD2 group, *REF6*, has been shown to target the floral inducer *FT*[29]. Because *FT* functions downstream of *FLC*, *ref6-1* is supposed to be epistatic to *jmj30-2 jmj32-1*, as was observed in the late-flowering phenotype of *ref6-1 jmj30-2 jmj32-1* (Supplementary Fig. 11). It is of note that the *ref6-1 jmj30-2 jmj32-1* triple mutant showed no severe developmental defects other than its late-flowering phenotype (Supplementary Fig. 11). The lack of phenotype suggests that other H3K27me3 demethylases exist in addition to these JMJ

proteins, that the feedback loop to the histone methylation is robust and flexible, or that the developmental plasticity is greater in plants than in animals.

JMJ30 and JMJ32 differ from REF6 both in their JmjC domain sequences and their lack of the JmjN domain[22]. Moreover, the JmjC domains of JMJ30, JMJ32 and REF6 showed considerable diversifications even among members of the same group, except for the highly conserved amino acids close to the Fe(II) and α-KG-binding residues[22]. Such variations within the catalytic domains of JMJ proteins have been reported in human JHDM1 and JMJD2A, both of which carry out H3K36me2 demethylation[58]. Thus, it is not uncommon for JMJ proteins with diverse variation within the JmjC domain to target the same substrate, as in the case of REF6, JMJ30 and JMJ32 in *Arabidopsis*. Crystal structures of JMJ30, JMJ32, REF6 and their cognate substrate (H3K27me3) may be helpful to verify substrate specificity-determining residues.

In addition to the floral integrators, *FT* and *SOC1*, FLC also binds and regulates many stress-responsive genes, such as the cold response genes *C-REPEAT/DRE BINDING FACTOR 1* (*CBF1*) and *CBF3* (ref. 59), and many genes involved in stress and stimulus response are implicated as target genes of JMJ30 and JMJ32 (Fig. 9b). It would be interesting to further study the roles of *JMJ30*, *JMJ32* and *FLC* in stress responses.

FLC is also known to mediate the temperature compensation mechanism of the circadian clock at elevated temperatures by lengthening the circadian period, possibly through regulating the expression of an MYB transcription factor *LUX ARRHYTHMO* (*LUX*)[60]. During circadian oscillation, the transcriptional feedback loop between the central clock genes *CIRCADIAN CLOCK ASSOCIATED 1* (*CCA1*), *LATE ELONGATED HYPOCOTYL* (*LHY*) and *TIMING OF CAB EXPRESSION 1* (*TOC1*) forms the core oscillator[61]. Two core clock genes, *CCA1* and *LHY*, directly bind and repress *JMJ30* (ref. 41), whereas JMJ30, in turn, promotes the expression of the morning-phased clock genes, *CCA1* and *LHY*[42], forming a negative feedback loop similar to the central *CCA1/LHY/TOC1* oscillation. Taken together, the interactions between *FLC*, *JMJ30* and the circadian clock genes provide a platform for crosstalk between the flowering pathway and circadian regulation to modulate plant responses to fluctuating temperatures.

One of the key players in the thermosensory pathway, the repressive H2A.Z occupancy controlling the accessibility of *PIF4*, mediates thermosensory responses by wrapping DNA more tightly at lower temperatures, thus negatively affecting *PIF4*-mediated transcription[8,9]. Although the heat-induced upregulation outcome of the H2A.Z-mediated mechanism fits the *FLC* expression profile, *FLC* does not seem to be a PIF4-regulated target gene[62]. On the other hand, recent publications showed that SVP, FLC and different splice variants of FLM form MADS-box heterocomplexes to control flowering time in response to ambient temperature changes[12–14]. The SVP-FLM-β complex delays flowering through the transcriptional repression of *FT* and *SOC1* at low temperatures, which is alleviated by the *FLM*-δ dominant-negative form at increased temperatures[13,14]. SVP may also form a complex with FLC to repress flowering at elevated temperatures, although this is less likely because SVP is rapidly degraded at elevated temperatures[13]. Taken together, our work suggests that JMJ30- and JMJ32-regulated *FLC* expression, in parallel with temperature-responsive H2A.Z nucleosome occupancy[9] and SVP-FLM cold-sensing pathways[13,14], may function to balance and coordinate flowering time in response to fluctuating temperatures.

A recent study showed that flowering in chrysanthemum is repressed at elevated temperatures through the downregulation of one of its floral inducers, *FLOWERING LOCUS T-like 3* (*FTL3*)[63]. Together with our results, this finding suggests that the need for a thermosensory balancing mechanism that represses flowering at elevated temperatures may be conserved, although the molecules involved in the process may differ. When plants are grown in an environment with fluctuating temperatures, the interplay between floral inductive and repressive signals plays a key role in determining the optimal flowering time for reproductive success. All in all, this study provides insights into the regulation of flowering time through *FLC* heat-inductive expression, which is partly achieved through the activity of H3K27 demethylases, JMJ30 and JMJ32.

Methods

Plant materials and growth conditions. All *Arabidopsis thaliana* plants used were in the background of the ecotype Columbia (Col). The *jmj32-1* (SALK_003313) allele was isolated from the SALK collections from ABRC. The alleles of *jmj30-1* (SAIL_811_H12)[41,42], *jmj30-2* (GK-454C10)[41,42] and *flc-3*[36] were described previously. Plants were grown in LDs (16-h light/8-h dark) or SDs (8-h light/16-h dark) at 22 °C or 29 °C. Genotyping primer sequences are shown in Supplementary Table 1. Total primary rosette leaves before bolting were counted to measure flowering time. Statistical analysis was performed using two-tailed Student's *t*-test.

Plasmid construction and plant transformation. To construct the *35S::JMJ30-HA* plasmid, the full-length *JMJ30* coding sequence was amplified by primer set XhoI-JMJ30_F and Bsp120I-JMJ30_R (Supplementary Table 2) and cloned into vectors pGREEN-35S-HA[64] using *Xho*I and *Bsp*120I restriction enzymes. Mutagenesis using the primers JMJ30-H326A-F and JMJ30-H326A-R produced the *35S::JMJ30H326A-HA* plasmid. The *35S::JMJ32-HA* plasmid was constructed similarly, using primer set XhoI-JMJ32_F and Bsp120I-JMJ32_R (Supplementary Table 2), and *35S::JMJ32H174A-HA* was constructed through mutagenesis using primers JMJ32-H174A-F and JMJ32-H174A-R.

For the *pJMJ30::JMJ30-GUS* and *pJMJ30::JMJ30-HA* plasmids, a 6.1-kb *JMJ30* genomic fragment (from −2,313 to +3,798; A of the start codon was set as +1) was cloned into pCR8 TOPO vector (Invitrogen) using primers JMJ30-FL_F and JMJ30-FL_R. An *Sfo*I restriction site was introduced in front of the *JMJ30* stop codon through mutagenesis using primers JMJ30-mut_F and JMJ30-mut_R (Supplementary Table 2). *GUS* or *HA* fragments were then inserted into the *Sfo*I site of the *pCR8-JMJ30* plasmid. Finally, *pJMJ30::JMJ30-GUS* and *pJMJ30::JMJ30-HA* in pCR8 were recombined into pEarleyGate303 and pHGW, respectively, using LR Clonase II (Invitrogen).

pJMJ32::JMJ32-GUS plasmid was constructed similarly to *pJMJ30::JMJ30-GUS*, differing only in that the 5.3-kb JMJ32 genomic fragment (from −3,215 to +2,084) was cloned using primer set JMJ32-FL_F and JMJ32-FL_R, and mutagenesis was performed using primers JMJ32-mut_F and JMJ32-mut_R (Supplementary Table 2).

Transgenic plants were generated by floral dipping with *Agrobacterium tumefaciens* (strain C58C1; with additional *pSOUP* helper plasmid for transformation of *pGREEN-35S::JMJ30-HA*)[65].

RNA extraction and expression analysis. For the tissue expression analysis of *JMJ30* and *JMJ32*, total RNA was isolated from young seedlings, rosette leaves, cauline leaves, stems and inflorescences. For the time-course flowering time gene expression analysis, samples were harvested from aerial parts of 5 DAG to 13 DAG seedlings for WT, *jmj30*, *jmj32* and *jmj30 jmj32*, and 1- to 3-week old seedlings for *FRI* and *FRI jmj30 jmj32* (collected at the end of the light photoperiod). Total RNA was extracted using the RNeasy plant mini kit (Qiagen) according to the manufacturer's instructions. 2 μg total RNA was used for reverse transcription using the Superscript III RT–PCR system (Invitrogen). RT–PCR with gene-specific primers (Supplementary Table 3) was performed using HotStarTaq DNA Polymerase (Qiagen) on a Thermocycler (Bio-Rad) for 15–25 cycles. Real-time quantitative PCR (qPCR) was performed on an ABI PRISM 7900HT sequence detection system (Applied Biosystems) using the KAPA SYBR FAST ABI Prism qPCR Master Mix (KAPA Biosystems). *Tip41-like* (AT4G34270) was used as an internal reference gene[66]. The relative expression of a gene of interest is calculated as $2^{-\Delta\Delta CT}$ [$\Delta\Delta C_T = \Delta C_T$ (experimental sample) − ΔC_T (control sample); $\Delta C_T = C_T$ (gene of interest)–C_T (*Tip41-like*)]. Statistical analysis was performed using two-tailed Student's *t*-test. The primer sequences are shown in Supplementary Table 3.

GUS staining. GUS staining was performed as previously described with slight modifications[67]. Briefly, plant tissues were fixed by incubating in ice-cold 90% acetone for 30 min and rinsed with rinsing solution (50 mM $NaPO_4$, pH 7.2, 0.5 mM $K_3Fe(CN)_6$ and 0.5 mM $K_4Fe(CN)_6$). The tissues were then stained in staining solution (50 mM $NaPO_4$, pH 7.2, 0.5 mM $K_3Fe(CN)_6$, 0.5 mM $K_4Fe(CN)_6$, 2 mM X-gluc) at 37 °C overnight. After staining, the tissues were placed in fixation

solution (50% ethanol, 5% acetic acid and 3.7% formaldehyde) at room temperature overnight and transferred to 100% ethanol the following day. For histological analysis, the tissues were mounted on slides with clearing solution (Hoyer's solution containing 30 ml water, 100 g chloral hydrate, 7.5 g gum Arabic, 5 ml glycerol) and observed under a SteREO Discovery.V12 Stereomicroscope (Zeiss) with images taken with an AxioCam ICc 3 (Zeiss).

ChIP assays. ChIP experiments were performed as previously described with minor modifications[67,68]. Briefly, total chromatin was extracted from 8 DAG seedlings (collected at the end of the light photoperiod) and immunoprecipitated using anti-HA (Santa Cruz Biotechnology, #sc-7392) and normal mouse IgG as a control (Santa Cruz Biotechnology, #sc-2025), or anti-H3K27me3 (Millipore, #07-449) and anti-H3 as a control (Abcam, #ab1791). Antibody dilutions of 1:200 were used (5 µl antibody in 1 ml of immunoprecipitation reaction). DNA fragments were recovered by phenol–chloroform extraction. qPCR with gene-specific primers (Supplementary Table 3) was performed on an ABI PRISM 7900HT sequence detection system (Applied Biosystems) using the KAPA SYBR FAST ABI Prism qPCR Master Mix (KAPA Biosystems). The results were first normalized to an internal control *Mutator-like* transposon (AT4G03870). For the histone modification ChIP, the relative enrichment was calculated by taking the ratio of DNA immunoprecipitated with anti-H3K27me3 antibody with that of anti-H3 antibody. Similarly, the ChIP relative enrichment of JMJ30-HA binding was calculated from the ratio between anti-HA antibody and normal mouse IgG immunoprecipitated DNA. Statistical analysis was performed using two-tailed Student's *t*-test.

Immunolocalization. The isolation of nuclei and *in situ* immunolocalization of chromatin proteins were performed as described with minor modifications[69]. Young leaves from *pJMJ30::JMJ30-HA* transgenic plants were fixed in ice-cold 4% formaldehyde Tris buffer for 20 min, rinsed and chopped into a fine suspension in LB01 buffer (15 mM Tris–HCl, pH 7.5, 2 mM EDTA, 0.5 mM spermine, 80 mM KCl, 20 mM NaCl, 0.1% Triton X-100). The sample suspension was air-dried on glass slides. Each slide was blocked with 1% BSA in 1 × PBS before incubating with mouse anti-HA antibody (Santa Cruz Biotechnology, #sc-7392) and later with CF555 goat anti-mouse IgG antibody (Biotium, #20030). A dilution of 1:200 is used for both primary and secondary antibodies. The slides were stained with DAPI and imaged with a Leica TCS SP5 confocal microscope (Leica).

Immunolocalization of protoplasts were performed as described[70]. Mouse anti-HA (Santa Cruz Biotechnology, #sc-7392) and rabbit anti-H3K27me3 (Millipore, #07-449) antibodies were used as primary antibodies, whereas CF555 goat anti-mouse IgG (Biotium, #20030) and CF488 goat anti-rabbit IgG antibodies (Biotium, #20012) were used as secondary antibodies. A dilution of 1:200 is used for both primary and secondary antibodies. The slides were stained with DAPI and imaged with a Leica TCS SPE confocal microscope (Leica).

***In vitro* histone demethylase assays.** Recombinant JMJ30-HA was transiently overexpressed in tobacco leaves and immunoaffinity-purified using anti-HA beads (Sigma, A2095). Histone demethylase assay was performed as previously described[25,29]. Briefly, the purified JMJ30-HA enzymes and substrate calf thymus histone (4 µg) were co-incubated in a 20-µl reaction mix (20 mM Tris–HCl, pH 7.5, 150 mM NaCl, 50 µM $Fe(NH_4)_2(SO_4)_2$, 1 mM α-KG, 2 mM ascorbate) for 4 h at 37 °C. The reaction products were analysed by western blotting using the following antibodies: anti-H3K27me3 (Millipore, #07-449), anti-H3K27me2 (Millipore, #07-452), anti-H3K27me1 (Millipore, #07-448), anti-H3K9me3 (Millipore, #07-442), anti-H3K9me2 (Millipore, #07-441), anti-H3K4me3 (Millipore, #07-473), anti-H3K4me2 (Millipore, #07-030), anti-H3K36me3 (Abcam, #ab9050), anti-H3K36me2 (Abcam, #ab9049) and anti-H3 (Abcam, #ab1791). A dilution of 1:1,000 is used for primary antibodies and 1:10,000 for secondary antibodies. Band intensity was calculated using ImageJ. Uncropped scans of western blot results are shown in Supplementary Fig. 13.

***In vivo* histone demethylase assays.** The protoplast transformation and *in vivo* histone demethylase assays were conducted as previously described[70]. Briefly, JMJ30-HA, JMJ30H326A, JMJ32-HA and JMJ32H174A were transiently overexpressed in *Arabidopsis* leaf protoplasts through polyethylene glycol (PEG)-mediated transformation. After one day, nuclei were isolated from the protoplasts and air-dried on the slide. Immunostaining was performed as described[69] by incubating each slide with mouse anti-HA (Santa Cruz Biotechnology, #sc-7392) and rabbit anti-H3K27me3 (Millipore, #07-449) antibodies, and then with CF555 goat anti-mouse IgG (Biotium, #20030) and CF488 goat anti-rabbit IgG antibodies (Biotium, #20012). A dilution of 1:200 is used for both primary and secondary antibodies. The slides were stained with DAPI and imaged with a Leica TCS SP8 confocal microscope (Leica). The intensities of at least 50 pairs of closely located JMJ-HA-transformed and non-transformed nuclei were analysed using ImageJ. Data were presented as a relative intensity of transformed/non-transformed nuclei and statistical analysis was performed using two-tailed Student's *t*-test.

Protein expression assays. Samples for the time-course JMJ30-HA protein expression experiment were harvested from aerial parts of 9 DAG *pJMJ30::JMJ30-HA* or *35S::JMJ30-HA* seedlings. The JMJ30-HA protein stability assay with CHX and MG132 was performed as described[13]. Total protein was extracted by grinding plant tissues in liquid nitrogen and resuspending in an equal volume of 2 × SDS loading buffer (4% SDS, 20% glycerol, 0.125 M Tris pH 6.8, 0.2% bromophenol blue, 200 mM β-mercaptoethanol). Protein samples were incubated at 95 °C for 10 min and then centrifuged for 10 min at 12,000 *g*. The supernatant was used for western blots using anti-HA-HRP (Santa Cruz Biotechnology, #sc-7392 HRP) using a dilution of 1:2,000. Band intensity was calculated using ImageJ. Uncropped scans of western blot results are shown in Supplementary Fig. 13.

Microarray analysis. For genome-wide expression analysis, two replicates of WT, *jmj30-2 jmj32-1* and *35S::JMJ30-HA* samples were analysed by NimbleGen 12 × 135K arrays (Roche). Total RNA was extracted from aerial parts of 13 DAG seedlings with the RNeasy plant mini kit (Qiagen), and double-stranded cDNA was synthesized using the SuperScript double-stranded cDNA synthesis kit (Invitrogen). cDNA samples were Cy3-labelled and hybridized following the manufacturer's instructions (Roche Nimblegen). Gene expression was analysed by Arraystar (DNAStar), and genes showing at least a 1.5-fold change within a 90% confidence interval were considered to be differentially expressed and were presented in Supplementary Data 1 and Supplementary Data 2. Gene enrichments with H3K27me3 target were tested with Fisher's exact test using R.

Dot blot. The specificity of the anti-histone antibodies was tested by dot blot (Supplementary Fig. 12). Different amount of biotin-labelled histone peptide are blotted onto a nitrocellulose membrane. Western blot analyses were then performed using the anti-histone antibodies: anti-H3K27me3 (Millipore, #07-449), anti-H3K4me3 (Millipore, #07-473) and anti-H3K36me3 (Abcam, #ab9050). A dilution of 1:1,000 is used for primary antibodies and 1:10,000 for secondary antibodies. The control experiment was probed using Strepavidin-HRP (Thermo Scientific Pierce, #21130) using a dilution of 1:1,000. The histone peptide used include: Biotinylated Histone H3 Peptide residues 1 – 21 (Epigentek, #R – 1004 – 100), Biotinylated Histone H3 Peptide residues 21 – 44 (Epigentek, #R – 1006 – 100), Biotinylated Trimethyl Histone H3K4 Peptide (Epigentek, #R – 1023 – 100), Biotinylated Trimethyl Histone H3K9 Peptide (Epigentek, #R – 1029 – 100), Biotinylated Trimethyl Histone H3K27 Peptide (Epigentek, #R – 1035 – 100) and Biotinylated Trimethyl Histone H3K36 Peptide (Epigentek, #R – 1050 – 100).

References

1. Kelly, A. E. & Goulden, M. L. Rapid shifts in plant distribution with recent climate change. *Proc. Natl Acad. Sci. USA* **105,** 11823–11826 (2008).
2. Samach, A. & Wigge, P. A. Ambient temperature perception in plants. *Curr. Opin. Plant Biol.* **8,** 483–486 (2005).
3. Wingler, A. Interactions between flowering and senescence regulation and the influence of low temperature in Arabidopsis and crop plants. *Ann. Appl. Biol.* **159,** 320–338 (2011).
4. He, Y. & Amasino, R. M. Role of chromatin modification in flowering-time control. *Trends Plant Sci.* **10,** 30–35 (2005).
5. Dennis, E. S. & Peacock, W. J. Epigenetic regulation of flowering. *Curr. Opin. Plant Biol.* **10,** 520–527 (2007).
6. Srikanth, A. & Schmid, M. Regulation of flowering time: all roads lead to Rome. *Cell. Mol. Life Sci.* **68,** 2013–2037 (2011).
7. Liu, C., Thong, Z. & Yu, H. Coming into bloom: the specification of floral meristems. *Development* **136,** 3379–3391 (2009).
8. Kumar, S. V. *et al.* Transcription factor PIF4 controls the thermosensory activation of flowering. *Nature* **484,** 242–245 (2012).
9. Kumar, S. V. & Wigge, P. A. H2A.Z-containing nucleosomes mediate the thermosensory response in Arabidopsis. *Cell* **140,** 136–147 (2010).
10. Blazquez, M. A., Ahn, J. H. & Weigel, D. A thermosensory pathway controlling flowering time in *Arabidopsis thaliana*. *Nat. Genet.* **33,** 168–171 (2003).
11. Lee, J. H. *et al.* Role of SVP in the control of flowering time by ambient temperature in Arabidopsis. *Genes Dev.* **21,** 397–402 (2007).
12. Gu, X. *et al.* Arabidopsis FLC clade members form flowering-repressor complexes coordinating responses to endogenous and environmental cues. *Nat. Commun.* **4,** 1947 (2013).
13. Lee, J. H. *et al.* Regulation of ambient temperature-responsive flowering by MADS-box transcription factor repressor complexes. *Science* **342,** 628–632 (2013).
14. Pose, D. *et al.* Temperature-dependent regulation of flowering by antagonistic FLM variants. *Nature* **503,** 414–417 (2013).
15. Seo, E. *et al.* Crosstalk between cold response and flowering in Arabidopsis is mediated through the flowering-time gene SOC1 and its upstream negative regulator FLC. *Plant Cell.* **21,** 3185–3197 (2009).
16. Angel, A., Song, J., Dean, C. & Howard, M. A polycomb-based switch underlying quantitative epigenetic memory. *Nature* **476,** 105–108 (2011).

17. Jiang, D., Wang, Y. & He, Y. Repression of FLOWERING LOCUS C and FLOWERING LOCUS T by the Arabidopsis polycomb repressive complex 2 components. *PLoS ONE* **3,** e3404 (2008).
18. Xu, Y. *et al.* A matrix protein silences transposons and repeats through interaction with retinoblastoma-associated proteins. *Curr. Biol.* **23,** 345–350 (2013).
19. Crevillen, P. & Dean, C. Regulation of the floral repressor gene FLC: the complexity of transcription in a chromatin context. *Curr. Opin. Plant Biol.* **14,** 38–44 (2011).
20. Jarillo, J. A., Pineiro, M., Cubas, P. & Martinez-Zapater, J. M. Chromatin remodeling in plant development. *Int. J. Dev. Biol.* **53,** 1581–1596 (2009).
21. Gan, E. S., Huang, J. & Ito, T. Functional roles of histone modification, chromatin remodeling and micrornas in arabidopsis flower development. *Int. Rev. Cell Mol. Biol.* **305,** 115–161 (2013).
22. Lu, F. *et al.* Comparative analysis of JmjC domain-containing proteins reveals the potential histone demethylases in Arabidopsis and rice. *J. Integr. Plant Biol.* **50,** 886–896 (2008).
23. Hong, E. H. *et al.* Temporal and spatial expression patterns of nine Arabidopsis genes encoding Jumonji C-domain proteins. *Mol. Cells* **27,** 481–490 (2009).
24. Inagaki, S. *et al.* Autocatalytic differentiation of epigenetic modifications within the Arabidopsis genome. *EMBO J.* **29,** 3496–3506 (2010).
25. Yang, W., Jiang, D., Jiang, J. & He, Y. A plant-specific histone H3 lysine 4 demethylase represses the floral transition in Arabidopsis. *Plant J.* **62,** 663–673 (2010).
26. Jeong, J. H. *et al.* Repression of FLOWERING LOCUS T chromatin by functionally redundant histone H3 lysine 4 demethylases in Arabidopsis. *PLoS ONE* **4,** e8033 (2009).
27. Yang, H. *et al.* A companion cell-dominant and developmentally regulated H3K4 demethylase controls flowering time in Arabidopsis via the repression of FLC expression. *PLoS Genet.* **8,** e1002664 (2012).
28. Liu, C., Lu, F., Cui, X. & Cao, X. Histone methylation in higher plants. *Annu. Rev. Plant Biol.* **61,** 395–420 (2010).
29. Lu, F. L., Cui, X., Zhang, S. B., Jenuwein, T. & Cao, X. F. Arabidopsis REF6 is a histone H3 lysine 27 demethylase. *Nat. Genet.* **43,** 715–U144 (2011).
30. Yu, X., Li, L., Guo, M., Chory, J. & Yin, Y. Modulation of brassinosteroid-regulated gene expression by Jumonji domain-containing proteins ELF6 and REF6 in Arabidopsis. *Proc. Natl Acad. Sci. USA* **105,** 7618–7623 (2008).
31. Saze, H., Shiraishi, A., Miura, A. & Kakutani, T. Control of genic DNA methylation by a jmjC domain-containing protein in *Arabidopsis thaliana*. *Science* **319,** 462–465 (2008).
32. Cho, J. N. *et al.* Control of seed germination by light-induced histone arginine demethylation activity. *Dev. Cell* **22,** 736–748 (2012).
33. Lafos, M. *et al.* Dynamic regulation of H3K27 trimethylation during Arabidopsis differentiation. *PLoS Genet.* **7,** e1002040 (2011).
34. Agger, K. *et al.* UTX and JMJD3 are histone H3K27 demethylases involved in HOX gene regulation and development. *Nature* **449,** 731–734 (2007).
35. Li, T. *et al.* Jumonji C domain protein JMJ705-mediated removal of histone H3 lysine 27 trimethylation is involved in defense-related gene activation in rice. *Plant Cell* **25,** 4725–4736 (2013).
36. Michaels, S. D. & Amasino, R. M. FLOWERING LOCUS C encodes a novel MADS domain protein that acts as a repressor of flowering. *Plant Cell* **11,** 949–956 (1999).
37. Michaels, S. D. & Amasino, R. M. Loss of FLOWERING LOCUS C activity eliminates the late-flowering phenotype of FRIGIDA and autonomous pathway mutations but not responsiveness to vernalization. *Plant Cell* **13,** 935–941 (2001).
38. Balasubramanian, S., Sureshkumar, S., Lempe, J. & Weigel, D. Potent induction of Arabidopsis thaliana flowering by elevated growth temperature. *PLoS Genet.* **2,** e106 (2006).
39. Li, D. *et al.* A repressor complex governs the integration of flowering signals in Arabidopsis. *Dev. Cell* **15,** 110–120 (2008).
40. Noh, B. *et al.* Divergent roles of a pair of homologous jumonji/zinc-finger-class transcription factor proteins in the regulation of Arabidopsis flowering time. *Plant Cell* **16,** 2601–2613 (2004).
41. Lu, S. X. *et al.* The Jumonji C domain-containing protein JMJ30 regulates period length in the Arabidopsis circadian clock. *Plant Physiol.* **155,** 906–915 (2011).
42. Jones, M. A. *et al.* Jumonji domain protein JMJD5 functions in both the plant and human circadian systems. *Proc. Natl Acad. Sci. USA* **107,** 21623–21628 (2010).
43. Searle, I. *et al.* The transcription factor FLC confers a flowering response to vernalization by repressing meristem competence and systemic signaling in Arabidopsis. *Genes Dev.* **20,** 898–912 (2006).
44. Winter, D. *et al.* An 'Electronic Fluorescent Pictograph' browser for exploring and analyzing large-scale biological data sets. *PLoS ONE* **2,** e718 (2007).
45. Bastow, R. *et al.* Vernalization requires epigenetic silencing of FLC by histone methylation. *Nature* **427,** 164–167 (2004).
46. Yoo, S. K. *et al.* CONSTANS activates SUPPRESSOR OF OVEREXPRESSION OF CONSTANS 1 through FLOWERING LOCUS T to promote flowering in Arabidopsis. *Plant Physiol.* **139,** 770–778 (2005).
47. Hepworth, S. R., Valverde, F., Ravenscroft, D., Mouradov, A. & Coupland, G. Antagonistic regulation of flowering-time gene SOC1 by CONSTANS and FLC via separate promoter motifs. *EMBO J.* **21,** 4327–4337 (2002).
48. Liu, C. *et al.* Direct interaction of AGL24 and SOC1 integrates flowering signals in Arabidopsis. *Development* **135,** 1481–1491 (2008).
49. Mathieu, O., Probst, A. V. & Paszkowski, J. Distinct regulation of histone H3 methylation at lysines 27 and 9 by CpG methylation in Arabidopsis. *EMBO J.* **24,** 2783–2791 (2005).
50. Lindroth, A. M. *et al.* Dual histone H3 methylation marks at lysines 9 and 27 required for interaction with CHROMOMETHYLASE3. *EMBO J.* **23,** 4286–4296 (2004).
51. Klose, R. J., Kallin, E. M. & Zhang, Y. JmjC-domain-containing proteins and histone demethylation. *Nat. Rev. Genet.* **7,** 715–727 (2006).
52. Zhang, X. *et al.* Whole-genome analysis of histone H3 lysine 27 trimethylation in Arabidopsis. *PLoS Biol.* **5,** e129 (2007).
53. Chen, J., Burke, J. J., Velten, J. & Xin, Z. FtsH11 protease plays a critical role in Arabidopsis thermotolerance. *Plant J.* **48,** 73–84 (2006).
54. Buzas, D. M., Robertson, M., Finnegan, E. J. & Helliwell, C. A. Transcription-dependence of histone H3 lysine 27 trimethylation at the Arabidopsis polycomb target gene FLC. *Plant J.* **65,** 872–881 (2011).
55. Burgold, T. *et al.* The H3K27 demethylase JMJD3 is required for maintenance of the embryonic respiratory neuronal network, neonatal breathing, and survival. *Cell Rep.* **2,** 1244–1258 (2012).
56. Lan, F. *et al.* A histone H3 lysine 27 demethylase regulates animal posterior development. *Nature* **449,** 689–694 (2007).
57. Vandamme, J. *et al.* The *C. elegans* H3K27 demethylase UTX-1 is essential for normal development, independent of its enzymatic activity. *PLoS Genet.* **8,** e1002647 (2012).
58. Chen, Z. *et al.* Structural insights into histone demethylation by JMJD2 family members. *Cell* **125,** 691–702 (2006).
59. Deng, W. *et al.* FLOWERING LOCUS C (FLC) regulates development pathways throughout the life cycle of Arabidopsis. *Proc. Natl Acad. Sci. USA* **108,** 6680–6685 (2011).
60. Edwards, K. D. *et al.* FLOWERING LOCUS C mediates natural variation in the high-temperature response of the Arabidopsis circadian clock. *Plant Cell* **18,** 639–650 (2006).
61. Nagel, D. H. & Kay, S. A. Complexity in the wiring and regulation of plant circadian networks. *Curr. Biol.* **22,** R648–R657 (2012).
62. Oh, E., Zhu, J. Y. & Wang, Z. Y. Interaction between BZR1 and PIF4 integrates brassinosteroid and environmental responses. *Nat. Cell Biol.* **14,** 802–809 (2012).
63. Nakano, Y., Higuchi, Y., Sumitomo, K. & Hisamatsu, T. Flowering retardation by high temperature in chrysanthemums: involvement of FLOWERING LOCUS T-like 3 gene repression. *J. Exp. Bot.* **64,** 909–920 (2013).
64. Hellens, R. P., Edwards, E. A., Leyland, N. R., Bean, S. & Mullineaux, P. M. pGreen: a versatile and flexible binary Ti vector for Agrobacterium-mediated plant transformation. *Plant Mol. Biol.* **42,** 819–832 (2000).
65. Clough, S. J. & Bent, A. F. Floral dip: a simplified method for Agrobacterium-mediated transformation of *Arabidopsis thaliana*. *Plant J.* **16,** 735–743 (1998).
66. Czechowski, T., Stitt, M., Altmann, T., Udvardi, M. K. & Scheible, W. R. Genome-wide identification and testing of superior reference genes for transcript normalization in Arabidopsis. *Plant Physiol.* **139,** 5–17 (2005).
67. Sun, B., Xu, Y., Ng, K. H. & Ito, T. A timing mechanism for stem cell maintenance and differentiation in the Arabidopsis floral meristem. *Genes Dev.* **23,** 1791–1804 (2009).
68. Ito, T., Takahashi, N., Shimura, Y. & Okada, K. A serine/threonine protein kinase gene isolated by an in vivo binding procedure using the Arabidopsis floral homeotic gene product, AGAMOUS. *Plant Cell Physiol.* **38,** 248–258 (1997).
69. Lysak, M., Fransz, P. & Schubert, I. Cytogenetic analyses of Arabidopsis. *Methods Mol. Biol. (Clifton, NJ)* **323,** 173–186 (2006).
70. Lee, M. H., Lee, Y. & Hwang, I. *In vivo* localization in Arabidopsis protoplasts and root tissue. *Methods Mol. Biol. (Clifton, NJ)* **1043,** 113–120 (2013).

Acknowledgements

We thank H. Yu for generously providing *flc-3* seeds, Y. Tamada and D. Buzas for their critical comments and discussions on this work, and *Arabidopsis* Biological Resource Center for providing the T-DNA insertion line of *JMJ30* and *JM32*. This work was supported by research grants to T.I. from Temasek Life Sciences Laboratory (TLL), the National Research Foundation, Prime Minister's Office, Singapore, under its Competitive Research Program (CRP Award No. NRF-CRP001-108) and PRESTO, Japan Science and Technology Agency, 4-1-8 Honcho Kawaguchi, Saitama, Japan. The funders had no role in study design, data collection and analysis, decision to publish, or preparation of the manuscript.

Author contributions

T.I. conceived the research. E.-S.G., T.I. and Y.X. designed the experiments. E.-S.G., J.-Y.W. and J.G.G. performed the experiments. W.-Y.W. participated in the confocal imaging. B.S. and J.H. participated in the ChIP assays. E.-S.G., Y.X. and T.I. wrote the paper. All authors discussed the results and made substantial contributions to the manuscript.

Additional information

Accession codes: The NimbleGen 12 × 135 K expression array data sets are deposited in the NCBI Gene Expression Omnibus (GEO) under the accession code GSE51898.

Supplementary Information accompanies this paper at http://www.nature.com/naturecommunications

Competing financial interests: The authors declare no competing financial interests.

Reprints and permission information is available online at http://npg.nature.com/reprintsandpermissions/

How to cite this article: Gan, E.-S. *et al.* Jumonji demethylases moderate precocious flowering at elevated temperature via regulation of *FLC* in *Arabidopsis*. *Nat. Commun.* 5:5098 doi: 10.1038/ncomms6098 (2014).

Plant and Cell Physiology Advance Access published April 3, 2015

PCP
PLANT & CELL PHYSIOLOGY

Review

Co-ordination of Flower Development Through Epigenetic Regulation in Two Model Species: Rice and Arabidopsis

Siyi Guo[1,3], Bo Sun[1,3], Liang-Sheng Looi[1,2], Yifeng Xu[1], Eng-Seng Gan[1,2], Jiangbo Huang[1,2] and Toshiro Ito[1,2,*]

[1]Temasek Life Sciences Laboratory, 1 Research Link, National University of Singapore, 117604, Republic of Singapore
[2]Department of Biological Sciences, National University of Singapore, 117604, Republic of Singapore
[3]These authors contributed equally to this work.
*Corresponding author: E-mail, itot@tll.org.sg; Fax, +65-6872-7007.
(Received November 17, 2014; Accepted February 24, 2015)

Angiosperms produce flowers for reproduction. Flower development is a multistep developmental process, beginning with the initiation of the floral meristems, followed by floral meristem identity specification and maintenance, organ primordia initiation, floral organ identity specification, floral stem cell termination and finally floral organ maturation. During flower development, each of a large number of genes is expressed in a spatiotemporally regulated manner. Underlying these molecular and phenotypic events are various genetic and epigenetic pathways, consisting of diverse transcription factors, chromatin-remodeling factors and signaling molecules. Over the past 30 years, genetic, biochemical and genomic assays have revealed the underlying genetic frameworks that control flower development. Here, we will review the transcriptional regulation of flower development in two model species: *Arabidopsis thaliana* and rice (*Oryza sativa*). We focus on epigenetic regulation that functions to co-ordinate transcription pathways in flower development.

Keywords: Arabidopsis • Epigenetic regulation • Floral homeotic protein • Flower development • Organ identity control • Rice.

Abbreviations: AG, AGAMOUS; AHL1–29, AT-HOOK MOTIF NUCLEAR-LOCALIZED PROTEIN 1–29; AP, APETALA; BRM, BRAHMA; CHR, CHROMATIN REMODELING; CLF, CURLY LEAF; *clk*, *clark kent*; DAD1, DELAYED ANTHER DEHISCENCE 1; DH1, DEGENERATED HULL1; DL, DROOPING LEAF; EMF2, EMBRYONIC FLOWER2; ESC, extra sex comb; E(Z), enhancer of zeste; F3H, FLAVANONE 3 HYDROXYLASE; FIE, FERTILIZATION INDEPENDENT ENDOSPERM; FIS2, FERTILIZATION INDEPENDENT SEED2; FLC, FLOWERING LOCUS C; FM, floral meristem; FT, FLOWERING LOCUS T; GIK, GIANT KILLER; GR, glucocorticoid receptor; HAT, histone acetyltransferase; HDA, histone deacetylase; HDAC1, histone deacetylase 1; H3K4, methylation of histone H3 lysine 4; H3K9, methylation of histone H3 lysine 9; H3K27, methylation of histone H3 lysine 27; H3K36, methylation of histone H3 lysine 36; HMT, histone methyltransferase; I-domain, Intervening domain; IM, inflorescence meristem; JA, jasmonic acid; JmjC, Jumonji-C; K-domain, Keratin-like domain; KNU, KNUCKLES; KYP, KRYPTONITE; LEC2, LEAFY COTYLEDON2; LFY, LEAFY; MEA, MEDEA; MRG1/2, MORF-RELATED GENE 1 and 2; MSI1–5, MULTICOPY SUPPRESSOR OF IRA1–5; PcG, Polycomb group; PI, PISTILLATA; PKL, PICKLE; PRC, Polycomb Repressive Complex; PRE, Polycomb-Responsive Element-like element; REF6, RELATIVE OF EARLY FLOWERING 6; RLE, Repressive LEC2 Element; SDG728, SET DOMAIN GROUP 728; SEP, SEPALLATA; SEU, SEUSS; SPL/NZZ, SPOROCYTLESS/NOZZLE; STK, SEEDSTICK; SYD, SPLAYED; sup, superman; SU(Z)12, suppressor of zeste 12; SWN, SWINGER; TEK, TRANSPOSABLE ELEMENT SILENCING VIA AT-HOOK; TPL, TOPLESS; trxG, trithorax group; TSS, transcription start site; ULT1, ULTRAPETALA1; VRN2, VERNALIZATION2; WUS, WUSCHEL.

Conservation and Diversification of Floral Homeotic Proteins in Arabidopsis and Rice

The model plant Arabidopsis has a typical eudicotyledon Brassicaceae flower with four types of floral organs arranged in concentric whorls: a first whorl of four sepals, a second whorl of four petals, a third whorl of six stamens and a fourth whorl of two fused carpels (**Fig. 1A**) (Smyth et al. 1990). In monocots, such as grasses, the floral architecture is distinct from that of eudicots (**Fig. 1B**). The spikelet is the primary unit of the inflorescence and comprises glumes (bract-like organs) and florets that lack sepals and petals (**Fig. 1B**). The number of florets in the spikelet varies among grass species. In rice, one spikelet contains a fertile floret and a pair of sterile lemmas (also known as empty glumes). The rice floret consists of a pair of bract-like organs (lemma and palea), two lodicules (equivalent to eudicot petals) in whorl 2, six stamens in whorl 3 and two carpels forming a pistil in whorl 4 . In Arabidopsis flowering, the shoot apical meristem converts into the inflorescence meristem (IM), which continuously produces the floral meristems (FMs) at lateral regions. During rice reproductive development, the IM initiates the primary branch meristems, followed by the secondary branch meristems, spikelet meristems and finally the FMs (**Fig. 1C**).

The genetic ABC model was introduced in 1991 based on studies of floral homeotic mutants in Arabidopsis and

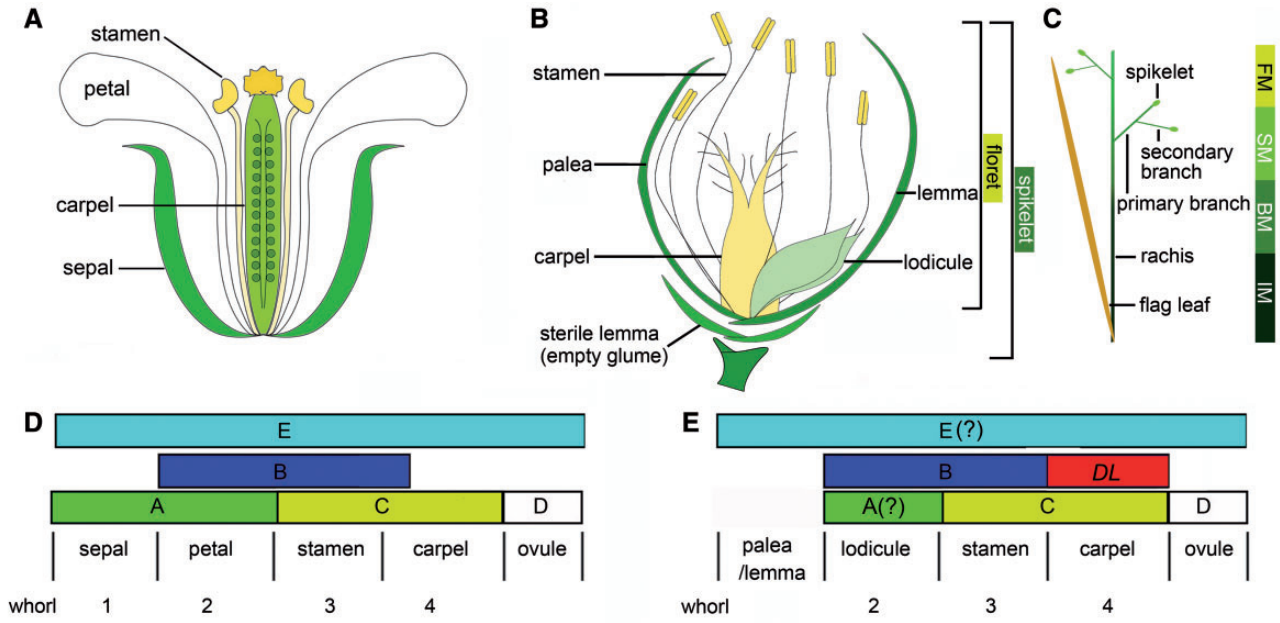

Fig. 1 Schematic representation of Arabidopsis and rice flowers and the genetic models of floral organ identity and determination in Arabidopsis and rice. (A) Arabidopsis flowers contain four concentric whorls of floral organs. From the outermost to innermost, these include: whorl 1, four sepals; whorl 2, four petals; whorl 3, six stamens; and whorl 4, two carpels. (B) Rice flowers are also composed of four concentric whorls of floral organs. From the outermost to innermost, these include: whorl 1, one palea and one lemma; whorl 2, two lodicules; whorl 3, six stamens; and whorl 4, one carpel. (C) Structure of the rice inflorescence. (D) The revised Arabidopsis ABC model. A-class genes, *APETALA1* (*AP1*) and *AP2*; B-class genes, *AP3* and *PISTILLATA* (*PI*); C-class gene, *AGAMOUS* (*AG*); D-class genes, *SEEDSTICK* (*STK*), *SHATTERPROOF1* (*SHP1*) and *SHP2*; and E-class genes, *SEPALLATA1* (*SEP1*), *SEP2*, *SEP3* and *SEP4*. (E) The rice organ identity model. B-class genes, *OsMADS2*, *OsMADS4* and *OsMADS16*; C-class genes, *OsMADS3* and *OsMADS58*; D-class gene, *OsMADS13*; and E-class genes, *OsMADS1*, *OsMADS5*, *OsMADS7*, *OsMADS8* and *OsMADS34*. *DL*, *DROOPING LEAF*.

Antirrhinum majus (Coen and Meyerowitz 1991, Ito 2011). Floral organ identity is determined by the combinatorial action of floral ABC-class homeotic proteins. Later, the ABC model was expanded to include the fourth and fifth classes: the D- and E-class genes (**Fig. 1E**). The E-class quadruple *sep1 sep2 sep3 sep4* mutant plants show all floral organs being transformed into leaves (Ditta et al. 2004). The E-class SEPALLATA (SEP) proteins form larger homo- and hetero-oligomeric complexes with A-, B-, C- and D-class proteins to specify the floral organ identities (Honma and Goto 2001, Jetha et al. 2014). Based on the quartet model, the A- and E-class complex [APETALA1 (AP1)–SEP] specifies the sepal identity; A-, B- and E-class proteins [AP1–SEP–AP3–PISTILLATA (PI)] specifies petals; the B-, C- and E-class complex [AGAMOUS (AG)–SEP–AP3–PI] specifies stamens; the C- and E-class complex (AG–SEP) specifies carpels; and the D- and E-class complex [SEEDSTICK (STK)–SEP] specifies ovules (Yanofsky et al. 1990, Jack et al. 1992, Mandel et al. 1992, Goto and Meyerowitz 1994, Honma and Goto 2001, Mendes et al. 2013). Moreover, E-class genes also function upstream of B- and C-class genes to regulate their expression (Kaufmann et al. 2009), possibly representing auto- and cross-regulation of the MADS proteins. Although SEP1–SEP4 generally function redundantly, SEP3 genetically has major functions. While *sep1 sep2 sep3* shows strong defects like B/C-class double mutants, *sep1 sep2 sep4* is phenotypically normal (Ditta et al. 2004). SEP1–SEP4 heterotetramer proteins have distinct binding properties to CArG-box pairs in vitro (Jetha et al. 2014). SEP3 shows binding to a larger range of distances between the CArG-boxes and thus presumably to a wider spectrum of target genes.

The ABC model basically holds true for reproductive development in rice; however, it remains unclear whether true A-class genes exist that determine the identity of the first- and second-whorl organs (Yoshida and Nagato 2011, Tanaka et al. 2013, Zhang and Yuan 2014). Further, the identities of the lemma and palea are controversial and are often considered to be non-floral bract- and prophyll-like organs, respectively. Rice tends to have duplicated BCDE-class genes derived from ancestral gene duplication events (Hirano et al. 2014). For example, there are two *PI* homologs, two AG homologs and five *SEP*-like genes in rice [*OsMADS1* and *LEAFY HULL STERILE1* (*LHS1*), *5*, *7*, *8* and *34*] (**Fig. 1E**) (Yamaguchi et al. 2006, Hirano et al. 2014). These duplicated genes are partially redundant but have functional diversifications based on their own expression patterns. Whether E-class functions are consevered in rice is controversial (Hirano et al. 2014). Independently of C-class genes, one YABBY type transcription factor, DROOPING LEAF (DL), plays an important role in specifying carpel identity and meristem determinacy. *DL* is mainly expressed in the presumptive region of carpel initiation in the FM and in the carpel primordia. The carpels of *dl* mutants homeotically transform into stamens in accordance with the expansion of B-class gene expression (**Fig. 1E**) (Yamaguchi et al. 2004).

Functional Specificity of Floral Homeotic Proteins

Overexpression of ABC genes was performed to assess the robustness of the ABC model with respect to its effect on floral organ identities (Jack et al. 1992, Mizukami and Ma 1992, Goto and Meyerowitz 1994). These experiments suggested that each class maintains functional specificity and can sufficiently induce downstream events when overexpressed. Chimeric domain-swapping analyses of ABC MADS proteins revealed that the MADS domains themselves are interchangeable. For example, the specificity of AP1 and AG is linked to the C-terminal region of the MADS domain and the I-domain [Intervening domain between MADS and the keratin-like (K) domain], while the specificity of AP3 and PI is linked to the I-domain and K-domain (Krizek and Meyerowitz 1996). These results indicate that functional specificity is conferred by protein complexes rather than the DNA binding specificity of individual proteins. A recent immunopurification assay of the whole complex revealed that SEP3 forms a complex of approximately 670 kDa, which is >10-fold greater than the predicted molecular weight of the SEP3 dimer (Smaczniak et al. 2012). MADS proteins assemble to form complexes with chromatin-remodeling factors including the SWI/SNF ATPases BRAHMA (BRM) and SPLAYED (SYD), the CHD remodeler PICKLE (PKL), the transcriptional co-repressors SEUSS (SEU) (Tamada et al. 2009) and LEUNIG-HOMOLOG (LUH), the histone demethylase RELATIVE OF EARLY FLOWERING 6 (REF6), and the ISWI-type remodelers CHROMATIN REMODELING 4 (CHR4), CHR11 and CHR17 (Smaczniak et al. 2012). Still, very little is known about functional multimeric complexes that specify specific cell types in each floral organ.

Mode of Action of Floral Homeotic Proteins

The mechanism by which ABC floral homeotic proteins control flower development has remained unknown for a long time. The homeotic genes are continuously expressed after organ identity is specified. The use of efficient inducible systems for ABC protein expression has shown that the homeotic genes control various aspects throughout the flower development. In the *ag-1 35S::AG-GR* line with inducible AG activity (a constitutive promoter-driven AG gene fused with a steroid-binding domain of the rat glucocorticoid receptor), a single dexamethasone treatment led to the nuclear accumulation of the AG–GR fusion protein for 2–3 d, resulting in the formation of leaf-like laminar stamens (Ito et al. 2004, Ito et al. 2007). To produce normal mature stamens, prolonged AG activity from stage 5–6 up to stage 10 is necessary. AG can induce normal stamens from organs originally fated to be petals at stage 5–6. However, if AG was induced after stage 7, microsporogenesis (pollen formation) was no longer induced, but petals had stalks, indicating that some late target genes of AG can be induced independently of early targets.

The initial AG expression starting from stage 3 is activated by the homeobox gene *WUSCHEL* (*WUS*) and the floral identity gene *LEAFY* (*LFY*) (Lenhard et al. 2001, Lohmann et al. 2001). For floral stem cell regulation, it is reported that AG may recruit CURLY LEAFY (CLF), a Polycomb group (PcG) protein on *WUS* from stage 3 for *WUS* repression (Liu et al. 2011) . However, the direct repression of *WUS* by AG is very mild because *WUS* is not fully terminated until stage 6 (Lenhard et al. 2001, Lohmann et al. 2001), and *35S::AG* lines still produce normal carpels (Mizukami and Ma 1992). Through direct induction of the C2H2 zinc finger repressor KNUCKLES (KNU), AG terminates *WUS* more effectively (Sun et al. 2009). In stage 6, AG induces *KNU*, which in turn terminates *WUS* expression. From stage 3 to stage 6, AG induces *KNU* over a 2 d period. This 2 d induction is timed by cell division-associated dilution of H3K27me3 on *KNU* chromatin, which is caused by the eviction of PcG protein from *KNU* PRE (Polycomb-Responsive Element-like element) by AG binding at the same site (Sun et al. 2014).

When the AG activity was continuously induced in stage 3 floral primordia of *ag-1 35S::AG-GR*, the flower showed carpelloid sepals in whorl 1, a reduced number of mature stamens in whorls 2 and 3, and carpels in whorl 4. When AG was induced at stage 4 (with only 1 d delay from stage 3 under 24 h light conditions) or later, the flower showed carpelloid sepals in whorl 1, ten stamens in whorls 2 and 3, four carpelloid sepals in whorl 4, ten stamens in whorls 5 and 6, and carpels in whorl 7 due to partial meristem indeterminacy. In the line with inducible RNA interference (RNAi) for AG, knockdown of AG at the middle stages of flower development led to branched-trichome formation on the surface of carpels. These results indicate that AG induces various targets throughout reproductive development, and further that AG represses leaf-specific genes in reproductive organs.

Downstream Targets of Floral Homeotic Proteins

The availability of expression profiling methods and the inducible lines has allowed the time-lapse analyses of downstream genes. Chromatin immunoprecipitation (ChIP) assays followed by quantitative PCR, tiling array screening or high-throughput sequencing have enabled the identification of direct target sites. Combined analyses of expression and genome-wide binding of the key floral transcription factors provide a holistic view of transcriptional networks. To date, whole genome-wide target analyses have been carried out for the ABCE-class transcription factors, AP1, AP2, AP3/PI, AG and SEP3 in addition to LFY (Kaufmann et al. 2009, Kaufmann et al. 2010, Yant et al. 2010, Winter et al. 2011, Wuest et al. 2012, O'Maoileidigh et al. 2013). The general finding of these genome-wide analyses was that floral transcription factors bind to a very large number of target sites (~1,500 for LFY and AP3/PI; ~2,000 for AP1, AP2 and AG; and ~4,000 for SEP3), and a limited portion of the bound genes exhibit expression changes in the presence/absence of the respective transcription factors. Generally speaking, the genetic combinatorial model has been supported by the target analyses. Over 60% of the genes bound by AP1 are also bound by SEP3 (Kaufmann et al. 2010). It will be interesting to determine

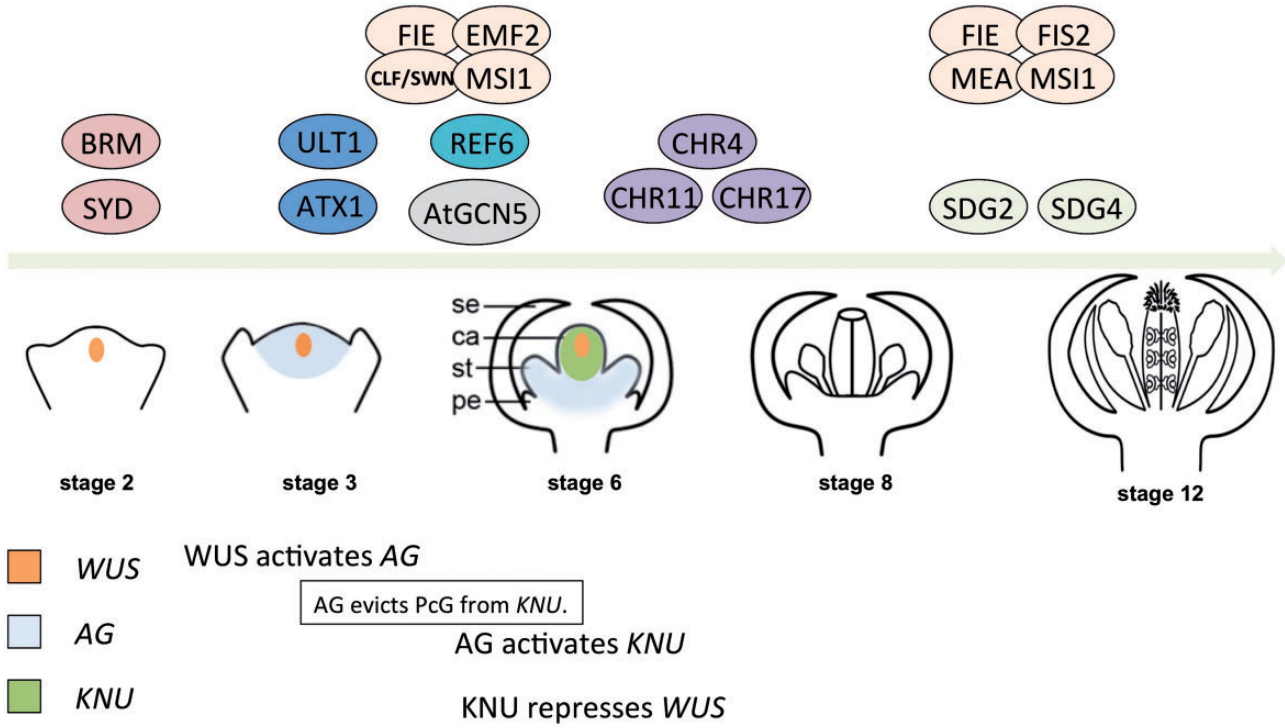

Fig. 2 Chromatin-remodeling factors in flower development and floral stem cell regulation. During flower development, various chromatin-remodeling factors modulate gene expression. In floral stage 1–2 (Smyth et al. 1990), the expression of floral homeotic B- and C-class genes is prevented by the EMF2–PRC2 complex. To reverse the repressive effects of Polycomb-mediated H3K27me3 repressive marks, LFY and SEP3 recruit the SWI/SNF chromatin-remodeling factors SYD and BRM to *AG* and *AP3* regulatory loci for their activation. Meanwhile, the trxG protein ULT1 interacts with ATX1 for the activation of *AG* and other MADS box genes. Beginning in floral stage 3, when the MADS box genes are induced, the chromatin-remodeling factors CHR4, 11 and 17 interact and form large complexes with AP1, PI, AP3, AG and SEPs. The JmjC-domain protein REF6, the demethylase of H3K27me3, interacts with AG and SEP3 to promote chromatin opening and facilitate AG, inducing the transcription of many downstream targets for the proper development of stamens and carpels. During male and female gametophyte development, SDG2, an H3K4 methyltransferase, may function in gene activation. In contrast, the FIS2–PRC2 complex plays a role in gene silencing during gametogenesis and seed development. In addition, SDG4, an H3K36 methyltransferase, is involved in pollen tube formation. For floral stem cell regulation, *AG* is activated by WUS and LFY from stage 3. It is known that AG may directly repress *WUS* from stage 3 by recruiting PcG to *WUS*. However, the direct repression of *WUS* by AG is mild because *WUS* is not fully terminated until stage 6. Through direct induction of the C2H2 zinc finger repressor KNU, AG terminates *WUS* more effectively in an indirect manner. In stage 6, AG induces *KNU*, which in turn shuts off *WUS* expression. From stage 3 to stage 6, AG induces *KNU* over a 2 d period. This 2 d induction is timed by cell division-associated dilution of H3K27me3 on *KNU* chromatin, which is caused by the eviction of PcG from *KNU* PRE by AG binding at the same site. In the AG/WUS regulatory pathway, the acetyltransferase AtGCN5 may function to regulate the proper expression patterns of both *AG* and *WUS*.

whether AP1 has SEP3-independent functions and whether SEP3 has AP1- and AG-independent functions. Analyses of the target genes of AP1, SEP3 and AG with high fidelity will help to answer these questions.

Floral homeotic proteins regulate many different types of genes, including transcription factors, hormone biosynthesis and signaling genes, and genes involved in cell growth and structure. The expression of each target gene is regulated in a cell-type-specific manner at precise stages of flower development. For example, AG directly induces the transcription of the SPOROCYTLESS/NOZZLE (SPL/NZZ) and KNU transcription factors at stage 6 in anther primordia to induce microsporogenesis and in FMs to terminate floral stem cell activities by repressing the stem cell-specifying gene *WUS*, respectively (Sun et al. 2009, Sun et al. 2014). In *ag-1 35S::AG-GR*, *SPL/NZZ* was induced within a few hours after the AG induction, while *KNU* started to be induced after a 2 d time lag (Sun et al. 2009, Sun et al. 2014). *SPL/NZZ* was detected in presumptive pollen sacs in the organ primordia of the *ag* mutant flowers only in certain developmental stages (Ito et al. 2004). This indicates that the transcriptional induction of *SPL/NZZ* depends on stage- and cell-type specific factors, which are developmentally regulated in an AG-independent manner. Therefore, AG induction in flowers at certain-stages (5–6) led to rapid induction of *SPL/NZZ*. In contrast, *KNU* induction depends on the cell-division-dependent changes of histone modification triggered by AG (**Fig. 2**) (Sun et al. 2009, Sun et al. 2014). AG binding sites on the *KNU* promoter are necessary for Polycomb recruitment (see the section 'H3K27 methylation and the Polycomb group complex) and the binding of AG causes the eviction of PcG from *KNU*, which leads to the delayed induction of *KNU*, associated with cell division-dependent dilution of the repressive status.

Additionally, AG induces the jasmonic acid (JA) biosynthetic gene *DELAYED ANTHER DEHISCENCE 1* (*DAD1*) after stage 10 in

developing stamen filaments (Ito et al. 2007). JA controls stamen maturation; filament elongation, anther opening and pollen maturation. A laminar stamen produced after temporal induction of *AG* is interpreted as an organ which has had *SPL/NZZ* expression but lacked stamen maturation genes including *DAD1*. In contrast, a petal with a stalk is an organ that has had the maturation genes but lacked *SPL/NZZ* expression. AP3/PI also regulates different targets in a stage-specific manner, including almost 1,000 genes in the early floral stages and approximately 500 different sets of genes during late flower development (Wuest et al. 2012).

Global profiling of target analysis was also carried out for the rice *SEP*-like gene *OsMADS1*. *OsMADS1* directly represses the expression of another *SEP*-like gene, *OsMADS34*, and various transcription factors, including class III homeodomain-leucine zipper member (OsHB4), BEL1-like member (OsBLH1), OsKANADI2 and OsKANADI4 (Khanday et al. 2013).

Epigenetic Regulation of Genes Located Upstream and Downstream of Floral Homeotic Protein-Encoding Genes

Epigenetic regulation is defined as heritable changes that are not caused by changes in the DNA sequence but rather by DNA methylation or histone modification, and these changes play key roles in flower development. Of the various histone modifications, histone lysine methylation is well studied and changes dynamically during flower development (Gan et al. 2013). Histone methylations can be generally divided into activating marks [the methylation of histone H3 lysine 4 (H3K4) and lysine 36 (H3K36)] and repressive marks [the methylation of histone H3 lysine 9 (H3K9) and lysine 27 (H3K27)] (Pien and Grossniklaus 2007, Gan et al. 2013). Antagonizing the establishment of histone methylation, lysine-specific demethylase1 (LSD1)- and Jumonji-C (JmjC)-domain proteins function to demethylate histones. In this section, their functions and histone-modifying enzymes in flower development are discussed (**Table 1**).

H3K9 methylation

SUVH4/KRYPTONITE (KYP) is an H3K9 histone methyltransferase (HMT) initially identified in a suppressor screen of the *superman* (*sup*) epi-alleles [the *clark kent* (*clk*) alleles], which have excessive cytosine methylation at the *SUP* locus (Jacobsen 1997). The phenotype of *clk* was rescued in the *kyp* mutant. As a repressive mark, H3K9me2 in Arabidopsis is associated with CpG DNA methylation and seems to be heterochromatin specific (Mathieu et al. 2005).

H3K9 methylation also influences floral organ maturation in rice. A rice homolog of *Su(var)3-9* is the *SET DOMAIN GROUP 728* (*SDG728*) H3K9 HMT. In the *SDG728* knockdown lines, seed size and weight were reduced, and the activities of a *Ty1-copia* element and *Tos17* retrotransposons were activated (Qin et al. 2010).

There are 21 JMJ proteins in both Arabidopsis and rice, which can be divided into five groups (Groups I, II, III, IV and V) (Sun and Zhou 2008). In rice, T-DNA insertion mutants of the histone H3K9 demethylase *JMJ706* affect spikelet development, including altered floral morphology and organ number (Sun and Zhou 2008). JMJ706 regulates the expression of *OsMADS47* and *DEGENERATED HULL1* (*DH1*), a putative lateral organ boundary-expressed transcription factor required for rice rudimentary glume formation. In the *jmj706* mutant, the expression of *OsMAD47* and *DH1* is reduced, which is associated with increased levels of H3K9me2/3 at the promoter and 5′ regions of *OsMAD47* and *DH1* (Sun and Zhou 2008).

H3K27 methylation and the Polycomb group complex

H3K27me3 is known as a repressive histone mark responsible for gene silencing at various developmental stages in both animals and plants. In Arabidopsis, H3K27me3 is catalyzed by PcG protein-containing complexes (Lafos et al. 2011). It has been found that Arabidopsis PcG comprises two subgroups: Polycomb Repressive Complex 1 (PRC1) and PRC2. Corresponding to *Drosophila* PRC2 components, which include extra sex comb (ESC), enhancer of zeste [E(Z)], suppressor of zeste 12 [SU(Z)12] and p55, Arabidopsis PRC2 has one ESC homolog [FERTILIZATION INDEPENDENT ENDOSPERM (FIE)]; three E(Z) homologs [CLF, SWINGER (SWN) and MEDEA (MEA)]; three SU(Z)12 homologs [VERN (VRN2), FERTILIZATION INDEPENDENT SEED2 (FIS2) and EMBRYONIC FLOWER 2 (EMF2)]; and five p55 homologs [MULTICOPY SUPPRESSOR OF IRA1–5 (MSI1–MSI5] (Pien and Grossniklaus 2007). At different developmental stages, these PRC2 proteins may form different heterocomplexes. The FIS complex, containing MEA/SWN, FIS2, FIE and MSI1, functions to silence target genes during early seed development and gametogenesis. The VRN complex, containing CLF/SWN, VRN2 and FIE, functions during vegetative development and the floral transition, whereas the EMF complex, containing FIE, MSI1, CLF/SWN and EMF2, functions during inflorescence development and flower organogenesis (Pien and Grossniklaus 2007).

In Arabidopsis, thousands of genes are regulated by the repressive mark H3K27me3, which is enriched in the transcribed regions (Zhang et al. 2007). Among these genes, a significant number are involved in transcriptional regulation for many developmental processes. In flower development, H3K27me3 targets floral-specific genes such as *AP3*, *PI*, *AG* and *SUP*. It is known that H3K27me3 is deposited by PcG; however, it is unclear how PcG is recruited to specific targets. The ASYMMETRIC LEAVES1 (AS1)–AS2 complex recruits PcG to *BREVIPEDICELLUS* (*BP*) and *KNOTTED-LIKE FROM ARABIDOPSIS THALIANA 2* (*KNAT2*) via direct interaction with FIE and CLF to silence these two genes in differentiating leaves (Lodha et al. 2013). During the floral transition, the key floral repressor *FLOWERING LOCUS C* (*FLC*) also needs to be silenced. Within the *FLC* locus, a PRE was identified in the region near the transcription start site (TSS) and the long first intron (Buzas et al. 2012). This PRE is reported to be involved in the transcriptional silencing of *FLC* expression. Discovered first in

Table 1 List of chromatin factors involved in Arabidopsis and rice flower development

Family	Name	Gene number	Molecular function	References
SWI/SNF2 type ATP-dependent chromatin remodelers	BRAHMA (BRM)	At2G46020	Interact with SYD, AP1 and SEP3 to form a complex to activate B- and C-class genes	Hurtado et al. (2006); Bezhani et al. (2007); Wu et al. (2012)
	SPLAYED (SYD)	At2G28290	Interact with SYD, AP1 and SEP3 to form a complex to activate B- and C-class genes	Wagner and Meyerowitz (2002); Kwon et al. (2005); Bezhani et al. (2007); Walley et al. (2008); Wu et al. (2012)
	CHROMATIN REMODELING 4 (CHR4)	At5G44800	Interact with AP1, AP3, PI, AG and SEP3 to form a large complex	Smaczniak et al. (2012); Li et al. (2014)
	CHROMATIN REMODELING 17 (CHR17)	At5G18620	Interact with AP1, AP3, PI, AG and SEP3 to form a large complex	Smaczniak et al. (2012); Li et al. (2014)
	CHROMATIN REMODELING 11 (CHR11)	At3G06400	Interact with AP1, AP3, PI, AG and SEP3 to form a large complex	Smaczniak et al. (2012); Li et al. (2014)
	PICKLE (PKL)	At2G25170	Control apical dominance, flowering, anther dehiscence and carpel polarity; repress embryonic traits during germination	Eshed et al. (1999); Henderson et al. (2004); Smaczniak et al. (2012; Zhang et al. (2014)
H3K27me3 demethylases	RELATIVE OF EARLY FLOWERING 6 (REF6)	At3G48430	H3K27me3-specific demethylase, component of the large complex containing AP1, AG and SEP3	Lu et al. (2011); Smaczniak et al. (2012)
Polycomb group (PcG) proteins	FERTILIZATION-INDEPENDENT ENDOSPERM (FIE)	At3G20740	Component of PRC2, WD40 motif-containing protein	Pien and Grossniklaus (2007)
	EMBRYONIC FLOWER 2 (EMF2)	At5G51230	Component of PRC2, VEFS domain-containing protein	Pien and Grossniklaus (2007)
	MULTICOPY SUPPRESSOR OF IRA1 (MSI1)	At5G58230	Component of PRC2, WD40 motif-containing protein	Pien and Grossniklaus (2007)
	CURLY LEAF (CLF)	At2G23380	Component of PRC2, H3K27me3 methyltransferase, involved in floral organ development	Pien and Grossniklaus (2007)
	SWINGER (SWN)	At4G02020	Component of PRC2, H3K27me3 methyltransferase, involved in floral organ development	Pien and Grossniklaus (2007)
	FERTILIZATION INDEPENDENT SEED 2 (FIS2)	At2G35670	Component of PRC2, homolog of Suppressor of zeste 12 [SU(Z)12], involved in seed development	Pien and Grossniklaus (2007)
H3K4 methyltransferases	HOMOLOG of TRITHORAX (ATX1)	At2G31650	H3K4 methyltransferase, recruited by ULT1 for AG activation	Alvarez-Venegas et al. (2003); Saleh et al. (2008)
	SET DOMAIN GROUP 2 (SDG2)	At4G15180	H3K4 methyltransferase, functions for gene activation during male and female gametogenesis	Berr et al. (2010)
H3K36 methyltransferases	SET DOMAIN GROUP 4 (SDG4)	At4G30860	H3K36 methyltransferase, involved in pollen tube formation	Thorstensen et al. (2008)
	SET DOMAIN GROUP 8 (SDG8)	At1G77300	H3K36 methyltransferase, involved in floral organ development and gametogenesis	Xu et al. (2008); Cazzonelli et al. (2009); Grini et al. (2009); Berr et al. (2010); Xu et al. (2015)
MADS transcription factors	AGAMOUS (AG)	At4G18960	C-class floral MADS-domain protein, evictor of PcG on KNU chromatin	Sun et al. (2014)
	SEPALLATA3 (SEP3)	At1G24260	E-class floral MADS-domain protein, recruiter of SYD and BRM for AG and AP3 activation	Wu et al. (2012)
	LEAFY (LFY)	At5G61850	Homeotic protein for floral induction, recruiter of SYD and BRM for AG and AP3 activation	Wu et al. (2012)
SAND-domain factors	ULTRAPETALA1 (ULT1)	At4G28190	TrxG group protein, antagonist of PcG and interactor with ATX1	Carles and Fletcher (2009)
WD40 repeats	TOPLESS (TPL) ABERRANT SPIKELET AND PANICLE1 (ASP1)	At1G15750 Os08g06480	Embryonic axis specification; cofactor in repressing ARRs, FT, B-, C- and E-class genes. Meristem specification and auxin response	Leibfried et al. (2005); Kieffer et al. (2006); Tamada et al. (2009); Dinh et al. (2012); Krogan et al. (2012); Yoshida et al. (2012)
Histone H3K9 methyltransferase	SET DOMAIN GROUP 728 (SDG728)	Os05g41172	Repress a *Ty1-copia* element and *Tos17* retrotransposons in seed development	Qin et al. (2010)
Histone H3K36 methyltransferase	SET DOMAIN GROUP 725 (SDG725)	Os02g34850	Regulate brassinosteroid-related genes	Sui et al. (2012)
Polycomb group proteins (PcG)	EMBRYONIC FLOWER 2 (OsEMF2b)	Os09g13630	Regulate E-class genes (OsMADS1 and OsMADS6) in flowering and floral organ identity control	Luo et al. (2009); Conrad et al. (2014)
JmjC domain-containing proteins	JUMONJI706 (JMJ706)	Os10g42690	Regulate *OsMAD47* and *DH1*	Sun and Zhou (2008)

Drosophila, the PRE is responsible for the recruitment of PcG to specific genes, possibly through DNA-binding proteins or non-coding RNAs (Sawarkar and Paro 2010, Simon and Kingston 2013). In contrast, the histone demethylases JMJ30 and JMJ32 are able to demethylate H3K27me3 at the *FLC* locus, thereby dampening its repression (Gan et al. 2014). In another example, it was found that a different 50 bp sequence located in the promoter region of *LEAFY COTYLEDON2* (*LEC2*) (Berger et al. 2011), a master regulator of seed development, may function as a putative PRE. Referred to as Repressive *LEC2* Element (RLE), this fragment was necessary for the silencing of *LEC2* by H3K27me3. When this 50 bp *RLE* sequence was introduced into the *FLAVANONE 3 HYDROXYLASE* (*F3H*) promoter, the *pF3H::GUS* reporter was silenced. Evidence for the existence of an Arabidopsis PRE is further supported by the existence of a 153 bp PRE-like sequence located in the promoter region of *KNU* (approximately 1 kb upstream of the *KNU* TSS) (Sun et al. 2014). Similarly, when this 153 bp fragment was inserted in the *F3H* promoter, the reporter activity of *pF3H::YFP* was silenced.

PcG-mediated H3K27me3 also plays a very important role in rice. Some rice homologs of PRC2 components have been studied, but only a T-DNA insertion mutant of *OsEMF2b* [a homolog of Su(z)12] showed altered flowering time and defective floral organs, including short panicles, anther indehiscence and multiple indeterminate ovaries (Luo et al. 2009). This phenotype was similar to those of some E-class gene mutants (*osmads1* and *osmads6*), which is consistent with the down-regulation of *OsMADS1* and *OsMADS6* in *emf2b*. This finding indicates that genes upstream of *OsMADS1* and *OsMADS6* are repressed by H3K27me3. Therefore, PRC2 may function in rice floral meristem determinacy through indirect regulation of the expression of SEP-like genes (Luo et al. 2009, Conrad et al. 2014). Rice T-DNA insertion mutants of other components of the PRC2 complex have no obvious phenotype, possibly due to genetic redundancy (Luo et al. 2009).

H3K4 methylation and the trithorax group complex

The histone modification H3K4me3 marks active chromatin. In Arabidopsis, H3K4me3 is catalyzed by trithorax group (trxG) proteins and predominantly accumulate in promoters and 5′ genic regions (Zhang et al. 2009). A well-studied trxG protein, ULTRAPETALA1 (ULT1), functions partially to induce *AG* in floral stem cells (Carles and Fletcher 2009). ULT1 has a SAND domain, which directly binds to *AG* regulatory sequences. Via direct interaction with another trxG component, ATX1/SDG27, ULT1 counteracts the PcG-repressive activity of CLF to modulate the H3K4 methylation status at the *AG* locus. *ATX1/SDG27* encodes an H3K4 HMT in Arabidopsis (Alvarez-Venegas et al. 2003). The null *atx1/sdg27* mutant exhibits homeotic conversion of floral organs, suggesting that *ATX1/SDG27* is also involved in floral organ identity. In *atx1/sdg27* mutants, lower expression levels of floral homeotic genes, including *AP1*, *AP2*, *AP3*, *PI* and *AG*, are observed, indicating that trxG has a positive role in floral organ identity control.

In addition to ULT1 and ATX1/SDG27, several other SDG proteins have also been reported to be H3K4 HMTs (Kim 2005, Saleh et al. 2008, Berr et al. 2009, Tamada et al. 2009, Berr et al. 2010). Among these SDG genes, the *sdg2* mutant displays a pollen and ovule sterility phenotype, although no floral organ identity defects are observed (Berr et al. 2010). Noticeably, in the *sdg2* mutant, the levels of H3K4me3 on *SPL/NZZ*, *BTB AND TAZ DOMAIN PROTEIN 3* (*BT3*) and *MSI1* loci are significantly decreased, indicating the important role of trxG in proper gametophytic development. AG is essential for the direct induction of *SPL/NZZ* (Ito et al. 2004). It is interesting to note that AG is involved in the changes in H3K4me3 status at the *SPL/NZZ* locus. Another SDG gene, *SDG4*, plays an important role in pollen tube growth (Thorstensen et al. 2008). In the *sdg4* mutant, pollen tubes grow much more slowly than those in wild-type plants, leading to severe male sterility. This finding indicates that SDG4 is capable of modulating the expression of genes that function in the growth of pollen tubes (Cartagena et al. 2008).

H3K36 methylation

H3K36me3, which enriches in the 5′ region of transcribed regions of genes (Roudier et al. 2011), marks active chromatin. The HMTs SDG7 and SDG8/ASHH2 are responsible for H3K36 methylation, the loss of which leads to pleiotropic developmental defects including floral organ abnormalities and gametophytic defects (Xu et al. 2008, Cazzonelli et al. 2009, Grini et al. 2009, Berr et al. 2010, Xu et al. 2015). *sdg8/ashh2* flowers display homeotic conversions such as sepal to carpel, petal to stamen and carpelloid organs, all of which might be due to spreading of the *AG* expression domain into whorls 1 and 2, in accordance with down-regulation of negative regulators of *AG* in *sdg8/ashh2*. Moreover, ovule and stamen development are also obviously affected (Grini et al. 2009), which is due to a substantial decrease in H3K36me3 at *MYB99* and *AtDMC1* loci, which are involved in embryo sac and pollen development, respectively. In rice, knockdown of the H3K36 HMT *SDG725* causes pleiotropic developmental defects, including dwarfism, erect leaves, and reduced spikelets and rachis branches (Sui et al. 2012).

Histone Acetylation

Histone acetylation is another indicator of an active genetic locus. There are multiple histone acetyltransferases (HATs) and histone deacetylases (HDAs) that add or remove acetyl groups on histones, respectively, in Arabidopsis (Pandey et al. 2002). One of the HATs, *AtGCN5*, is reported to be involved in multiple developmental processes (Bertrand et al. 2003). In the *atgcn5* mutant, the *WUS* expression domain is expanded beyond the organizing center, resulting in global defects in vegetative development. In addition to its roles in vegetative development, *AtGCN5* is further suggested to be involved in floral stem cell regulation. Terminal flowers are produced in *atgcn5* mutant plants, and the mutant flowers display homeotic transformation of petals into stamens and sepals into

filamentous structures. Ectopic carpels are also observed in *atgcn5* mutant flowers. These phenotypes could be attributed to the expansion of the expression domains of *AG* and *WUS*, suggesting that *AtGCN5* is required for the induction of negative regulators for *AG* and *WUS* (Bertrand et al. 2003).

Antagonizing the effect of HATs, *AtHD1/HDA19* is known to form a complex with *LUG–SEU* for the regulation of *AG* expression via removal of the acetylation mark from the *AG* locus (Tian and Chen 2001, Chen and Tian 2007). By repressing *AG* in whorl 1 and whorl 2, the *LUG–SEU–HDA19* complex maintains *AG* expression in the correct domain. In *lug seu* single or double mutants, *AG* is ectopically expressed throughout all floral organs, leading to homeotic conversion of sepals and petals into reproductive organs. HDA19 was also recently found to interact with AP2 and TOPLESS (TPL) (see below) for negative regulation of floral homeotic genes (Krogan et al. 2012).

Chromatin Remodeling Factors

In addition to the protein factors and complexes directly responsible for histone modification, other chromatin-remodeling factors and chromatin structural proteins also have indispensable roles in plant growth, including flower development. Here, their cross-talk and indirect roles in histone modification are discussed (**Table 1**).

GIANT KILLER and transposable element silencing via AT-HOOK

The nuclear matrix attachment regions are AT-rich DNA sequences and contribute to functional nuclear architecture in plants and animals (Cai et al. 2003, Ng et al. 2009). A series of matrix proteins with AT-hook DNA-binding motifs have been shown to bind to the DNA minor groove of the AT-rich MAR target sites, affecting the epigenetic state of target genes through direct structural changes in chromatin and/or recruitment of chromatin modifiers, such as the mammalian histone deacetylase 1 (HDAC1) (Cai et al. 2003, Han et al. 2008). The Arabidopsis genome contains AT-HOOK MOTIF NUCLEAR-LOCALIZED PROTEIN 1–29 (AHL1–29), some of which have been characterized (Matsushita et al. 2007, Ng et al. 2009, Xu et al. 2013, Xu et al. 2015). *AHL21/GIANT KILLER* (*GIK*), as a target of the floral homeotic protein AG, negatively regulates multiple genes downstream of AG, partially through the repressive histone modification H3K9me2. The direct GIK target genes include several key transcriptional regulators of organ patterning and differentiation during reproductive development, such as *ETT/ARF3* (Ng et al. 2009). GIK fine-tunes the expression of multiple targets of AG. Another AHL protein, AHL22, interacts with HDACs, and overexpression of AHL22 suppresses the expression of flowering activator *FLOWERING LOCUS T* (*FT*), resulting in a late-flowering phenotype (Yun et al. 2012). *AHL16/TRANSPOSABLE ELEMENT SILENCING VIA AT-HOOK* (*TEK*) was found to maintain genome integrity by silencing transposable elements and repeat-containing genes (Xu et al. 2013). TEK has a role in the maintenance of DNA methylation and histone deacetylation by interacting with Retinoblastoma-associated protein 46/48, FVE and MSI5 (Xu et al. 2013). TEK is also important for pollen wall formation, and loss of function of *tek* leads to male sterility due to the absence of nexine (Xu et al. 2013, Lou et al. 2014).

MORF-RELATED GENE 1 and 2

MORF-RELATED GENE 1 and 2 (MRG1/2) proteins have recently been found to bridge the two important histone modifications for proper transcription of target genes (Xu et al. 2015). MRG1/2 are Arabidopsis homologs of the highly conserved MRG15 (MORF4-related gene on chromosome 15) proteins. They contain a chromodomain at their N-termini, which is able to bind to H3K36me3 and recruit the HATs HISTONE ACETYLTRANSFERASE OF THE MYST FAMILY 1 and 2 (HAM1/2) to achieve 2-fold hypertranscription by increasing the histone acetylation level of target loci (Xu et al. 2015). The study mainly focused on the flowering time genes, which show quantitative effects in timing of flowering, and loss-of-function mutants did not have obvious phenotypes in reproductive development. However, because H3K36me3 is the prevalent mark for transcription and the *sdg8* mutant showed defects in floral organs, it is still possible that MRG1/2 may have fine-tuning roles in the transcriptional regulation of flower development genes.

SWI/SNF ATPases

SWI/SNF ATPases are important catalytic subunits involved in chromatin opening and transcription facilitation (Flaus et al. 2006, Hurtado et al. 2006, Bezhani et al. 2007, Wu et al. 2012). Arabidopsis contains four members of the SWI/SNF subfamily: SYD, BRM, CHR12 and CHR23. Double *chr12* and *chr23* mutants are embryonic lethal, while single mutants are indistinguishable from the wild type (Sang et al. 2012). The absence of either *SYD* or *BRM* caused pleiotropic developmental defects, including reduced petals and stamens, female sterility and reduced anther dehiscence (Wagner and Meyerowitz 2002, Kwon et al. 2006). The *brm* mutant also exhibited a unique root defect along with male sterility (Wagner and Meyerowitz 2002, Hurtado et al. 2006). Therefore, it seems that BRM and SYD are not completely functionally redundant and appear to control only a small subset of genes in common (Kwon et al. 2005, Bezhani et al. 2007). This phenotypic pleiotropy suggested that SNF2 chromatin-remodeling ATPases regulate the transcription of developmental genes (Peterson and Workman 2000). SYD is required for the up-regulation of *WUS* transcription in the shoot apical meristem (Kwon et al. 2005). The WUS homeodomain protein is expressed in the organizing center and signals overlying stem cells to maintain meristem homeostasis. *SYD* and *BRM* are redundantly required for the activation of *AP3* (B-class gene) and *AG* (C-class gene) in flower patterning via physical interaction with two direct transcriptional activators of class B- and C-class gene expression: LFY and SEP3 (Smaczniak et al. 2012, Wu et al. 2012). Homeotic conversion of floral organs and reduced expression of B-class genes are observed in the *brm* mutant, the *lfy-5 syd-1* double mutant and the *brm syd* double mutant. The *syd* mutant can partially

rescue the phenotype of the *clf* mutant, indicating that the function of the SWI/SNF ATPase might be similar to that of trxG proteins. SYD is also directly recruited to promoters to up-regulate positively the expression of selected genes downstream of the jasmonate and ethylene signaling pathways for resistance against biotic stress (Walley et al. 2008).

PICKLE

PKL, a member of the CHD3/4 family, contains a zinc finger homeodomain and two chromodomains arranged in tandem. It functions as an ATP-dependent chromatin-remodeling factor (Ho and Crabtree 2010). The *pkl* mutant exhibits spontaneous somatic embryogenesis with pickle-like, green, tuberous roots; reduced apical dominance; delayed flowering; anther dehiscence; and carpel polarity defects (Ogas 1997, Eshed et al. 1999, Henderson et al. 2004). In Arabidopsis, HDA6 and HDA19 may function together with PKL to remove acetylation marks (Li et al. 2005, Tanaka et al. 2008). PKL physically interacts with different types of transcription factors: PHYTOCHROME INTERACTING FACTOR 3 (PIF3) in light signaling, BRASSINAZOLE-RESISTANT 1 (BZR1) in BR signaling and SEP3 in floral organ identity control (Smaczniak et al. 2012, Zhang et al. 2014). In the root meristem, PKL functions antagonistically with PcG proteins to regulate meristematic growth, suggesting that H3K27me3 mark maintenance has an important role in fine-tuning the expression of meristematic genes (Hay et al. 2002, Aichinger et al. 2011). PKL may act indirectly by promoting the expression of PRC2 (Aichinger et al. 2009) or may bind directly to H3K27me3-enriched genes to affect acetylation levels (Zhang et al. 2012).

TOPLESS

The WD40 domain proteins TPL and TPL-related (TPR) interact directly and indirectly with transcription complexes involved in auxin and jasmonate signal transduction, meristem specification/maintenance and host defense (Szemenyei et al. 2008, Pauwels et al. 2010, Zhu et al. 2010). In the *tpl-1* dominant-negative mutant, loss of *TPL* causes up-regulation of the *AINTEGUMENTA*-like transcription factors *PLETHORA1/2* (*PLT1/2*), resulting in homeotic conversion of shoot tissue to root tissue at higher temperatures. This conversion occurs via antagonism of HD-ZIPIII transcription factors, which function to specify the apical fate (Smith and Long 2010). In the shoot apical meristem, WUS recruits TPL/TPR co-repressors to repress differentiation genes, hence ensuring stem cell specification (Kieffer et al. 2006). TPL/TPR further recruits HDAs to mediate histone deacetylation (Long et al. 2006), including type A Arabidopsis response regulator (ARR) genes, which are transcriptional targets of cytokinin signaling (D'Agostino et al. 2000, Leibfried et al. 2005). Several transcription factors, including *AP2* and *AGL15/18*, probably recruit *TPL* to repress *FT* transcription to regulate flowering time (Causier et al. 2012). *TPL* also plays an important role in floral organ specification. Recruitment of TPL/TPR by AP2 and LEU is necessary to define the boundary of whorls via spatial repression of the floral homeotic genes *AP3*, *PI* (B-class gene), *SEP3* (E-class gene) and *AG* (C-class gene) (Dinh et al. 2012, Krogan et al. 2012). In *tpl-1* and *tpl-1 ap2-2* −/+, both *AP3* expression and *SEP3* expression can be clearly detected in whorl 1 organs. By binding to the *AG* intron, *AP3* promoter and *SEP3* promoter, the AP2–TPL–HDA19 complex has been suggested to fine-tune *AG*, *AP3* and *SEP3* expression and restrict petal fate by maintaining the organ boundaries during organogenesis. In rice, ABERRANT SPIKELET AND PANICLE1 (ASP1) encodes a transcriptional co-repressor that is related to Arabidopsis TPL. The rice *asp1* mutant demonstrated pleiotropic phenotypes such as aberrant spikelet morphology, phyllotaxy disarrangement and dysfunction in auxin signaling (Yoshida et al. 2012).

Cross-Talk Between Chromatin Status and Gene Transcription

Unlike in animals, there are currently no known pioneer transcription factors in plants (Zaret and Carroll 2011). These transcription factors can bind to condensed chromatin and function to recruit chromatin-remodeling factors onto target genes for chromatin opening and transcription initiation. However, in Arabidopsis, the floral homeotic protein AG, which binds to the *KNU* promoter, triggers the progressive removal of H3K27me3 from the *KNU* locus, leading to subsequent transcriptional activation of *KNU* (Sun et al. 2014). It is known that AG binds to the CArG boxes located 1 kb upstream of *KNU*, and, coincidentally, that region harbors a PRE element, which is also bound by PcG protein. Through eviction of PcG from the *KNU* locus during stage 3 of flower development, the repressive H3K27me3 mark on the *KNU* TSS and gene body is progressively diluted through cell cycle progression. In this manner, *KNU* is induced at floral stage 6 for termination of floral stem cells. Another study also suggested that AG itself, from stage 3, may also recruit PcG for mild repression of *WUS* (Liu et al. 2011).

In other studies, several floral homeotic gene loci have been reported to be associated with the H3K27me3 demethylase REF6 (Lu et al. 2011). The *REF6* overexpression phenotype is similar to that of the *clf* and *tfl2* mutants, and the *ref6* mutant can partially rescue the curly leaf phenotype of *clf*. A recent study on the function of MADS-domain transcription factor complexes in Arabidopsis flower development suggested that AG protein complexes might contain REF6 (Smaczniak et al. 2012). This suggests that MADS-domain proteins may closely interact with chromatin-remodeling factors to facilitate chromatin opening and transcription initiation. Further evidence from the same study also indicates that SEP3 and REF6 are both included in a large complex, and PI may physically interact with chromatin remodelers of CHR4, CHR11 and CHR17, the ISWI-type nucleosome remodelers participating in genome-wide nucleosome distribution (Li et al. 2014). Furthermore, CHR4, CHR11 and CHR17 are also found in various complexes formed by AG, AP3, SEP3 and AP1 (Smaczniak et al. 2012). Possibly through interaction with REF6, AP1 is also suggested to be required for the removal of H3K27me3 from SEP3 in the very early stages of flower development.

In a very recent study on the dynamic regulation of chromatin accessibility by MADS-domain transcription factors in flower development, AP1 and SEP3 were suggested to bind their targets even before the target gene chromatins were fully open (Pajoro et al. 2014), suggesting that MADS-domain proteins may function as pioneer transcription factors. Furthermore, AP1 and SEP3 have been suggested to retain the ability to modulate the chromatin accessibility of their target genes, hence facilitating access to those genes by other transcription factors.

After the nucleosome structures open, the Mediator complex links transcriptional regulator binding at gene promoters with changes in the activation of RNA polymerase II (Conaway and Conaway 2011). The plant Mediator complex is estimated to be composed of >30 protein subunits (Mathur et al. 2011). Thus far, none of the Mediator subunit mutants has shown flower-specific defects; however, these subunits must play essential roles in transcriptional gene activation in flower development.

Summary and Future Perspectives

Studies of flower development over the last 30 years have revealed a large number of key regulatory genes and genetic networks. Floral organ identity and stem cell activity are regulated by the combinatorial action of floral homeotic proteins, which control different classes of transcription factors, hormone biosynthetic genes, signaling molecules and epigenetic regulators to control downstream events (**Fig. 2**). Studies have revealed that one homeotic protein can bind to thousands of target sites by forming higher order complexes. Homeotic proteins, transcription factors, hormones and epigenetic factors may converge and regulate the expression of multiple common downstream genes to perform complex developmental processes. These processes involve floral organ identity specification, floral organ formation and differentiation, and other important floral developmental programs including floral meristem maintenance and termination, floral organ patterning and boundary formation, and gametophytic development. During flower development the chromatin-remodeling factors appear to associate and bind to specific target genes to achieve spatiotemporal-specific expression in flower development. There are multiple balancing mechanisms that allow fine-tuning of gene expression in a single cell, and these mechanisms sometimes utilize antagonistic factors such as histone-modifying enzymes of the H3K27me3-depositing PcG complex, H3K27me3-removing JMJ histone demethylases, HATs and HDACs. However, several major questions remain, including (but not limited to) how each target is regulated in a temporal- and spatial-specific manner by particular complexes, how multimeric complexes are assembled at specific loci during flower development, how particular players co-ordinate the cross-talk between the intrinsic developmental program and extrinsic environmental cues, and how the robust and divergent effects of transcription factors, hormone signaling factors and chromatin factors are co-ordinated and converge to produce a robust genetic network for the formation of species-specific size, number and shape of floral organs downstream of the conserved ABC functions. Answering these questions in multiple model systems will allow us to understand fully the beauty of flower development.

Funding

This work was supported by Temasek Life Sciences Laboratory (TLL) [research grants to T.I.]; the National Research Foundation, Prime Minister's Office, Singapore under its Competitive Research Program [CRP Award No. NRF-CRP001-108]

Acknowledgements

The authors apologize that certain references could not be cited because of space limitations.

Disclosures

The authors have no conflicts of interest to declare.

References

Aichinger, E., Villar, C.B., Di Mambro, R., Sabatini, S. and Kohler, C. (2011) The CHD3 chromatin remodeler PICKLE and polycomb group proteins antagonistically regulate meristem activity in the Arabidopsis root. *Plant Cell* 23: 1047–1060.

Aichinger, E., Villar, C.B., Farrona, S., Reyes, J.C., Hennig, L. and Kohler, C. (2009) CHD3 proteins and polycomb group proteins antagonistically determine cell identity in Arabidopsis. *PLoS Genet.* 5: e1000605.

Alvarez-Venegas, R., Pien, S., Sadder, M., Witmer, X., Grossniklaus, U. and Avramova, Z. (2003) ATX-1, an Arabidopsis homolog of trithorax, activates flower homeotic genes. *Curr. Biol.* 13: 627–637.

Berger, N., Dubreucq, B., Roudier, F., Dubos, C. and Lepiniec, L. (2011) Transcriptional regulation of Arabidopsis LEAFY COTYLEDON2 involves RLE, a cis-element that regulates trimethylation of histone H3 at lysine-27. *Plant Cell* 23: 4065–4078.

Berr, A., McCallum, E.J., Alioua, A., Heintz, D., Heitz, T. and Shen, W.-H. (2010) Arabidopsis histone methyltransferase SET DOMAIN GROUP8 mediates induction of the jasmonate/ethylene pathway genes in plant defense response to necrotrophic fungi. *Plant Physiol.* 154: 1403–1414.

Berr, A., Xu, L., Gao, J., Cognat, V., Steinmetz, A., Dong, A. et al. (2009) SET DOMAIN GROUP25 encodes a histone methyltransferase and is involved in FLOWERING LOCUS C activation and repression of flowering. *Plant Physiol.* 151: 1476–1485.

Bertrand, C., Bergounioux, C., Domenichini, S., Delarue, M. and Zhou, D.-X. (2003) Arabidopsis histone acetyltransferase AtGCN5 regulates the floral meristem activity through the WUSCHEL/AGAMOUS pathway. *J. Biol. Chem.* 278: 28246–28251.

Bezhani, S., Winter, C., Hershman, S., Wagner, J.D., Kennedy, J.F., Kwon, C.S. et al. (2007) Unique, shared, and redundant roles for the Arabidopsis SWI/SNF chromatin remodeling ATPases BRAHMA and SPLAYED. *Plant Cell* 19: 403–416.

Buzas, D.M., Tamada, Y. and Kurata, T. (2012) FLC: a hidden polycomb response element shows up in silence. *Plant Cell Physiol.* 53: 785–793.

Cai, S., Han, H.J. and Kohwi-Shigematsu, T. (2003) Tissue-specific nuclear architecture and gene expression regulated by SATB1. *Nat. Genet.* 34: 42–51.

Carles, C.C. and Fletcher, J.C. (2009) The SAND domain protein ULTRAPETALA1 acts as a trithorax group factor to regulate cell fate in plants. *Genes Dev.* 23: 2723–2728.

Cartagena, J.A., Matsunaga, S., Seki, M., Kurihara, D., Yokoyama, M., Shinozaki, K. et al. (2008) The Arabidopsis SDG4 contributes to the regulation of pollen tube growth by methylation of histone H3 lysines 4 and 36 in mature pollen. *Dev. Biol.* 315: 355–368.

Causier, B., Ashworth, M., Guo, W. and Davies, B. (2012) The TOPLESS interactome: a framework for gene repression in Arabidopsis. *Plant Physiol.* 158: 423–438.

Cazzonelli, C.I., Cuttriss, A.J., Cossetto, S.B., Pye, W., Crisp, P., Whelan, J. et al. (2009) Regulation of carotenoid composition and shoot branching in Arabidopsis by a chromatin modifying histone methyltransferase, SDG8. *Plant Cell* 21: 39–53.

Chen, Z.J. and Tian, L. (2007) Roles of dynamic and reversible histone acetylation in plant development and polyploidy. *Biochim. Biophys. Acta* 1769: 295–307.

Coen, E.S. and Meyerowitz, E.M. (1991) The war of the whorls: genetic interactions controlling flower development. *Nature* 353: 31–37.

Conaway, R.C. and Conaway, J.W. (2011) Function and regulation of the Mediator complex. *Curr. Opin. Genet. Dev.* 21: 225–230.

Conrad, L.J., Khanday, I., Johnson, C., Guiderdoni, E., An, G., Vijayraghavan, U. et al. (2014) The Polycomb group gene EMF2B is essential for maintenance of floral meristem determinacy in rice. *Plant J.* 80: 883–894.

D'Agostino, I.B., Deruère, J. and Kieber, J.J. (2000) Characterization of the response of the Arabidopsis response regulator gene family to cytokinin. *Plant Physiol.* 124: 1706–1717.

Dinh, T.T., Girke, T., Liu, X., Yant, L., Schmid, M. and Chen, X. (2012) The floral homeotic protein APETALA2 recognizes and acts through an AT-rich sequence element. *Development* 139: 1978–1986.

Ditta, G., Pinyopich, A., Robles, P., Pelaz, S. and Yanofsky, M.F. (2004) The SEP4 gene of Arabidopsis thaliana functions in floral organ and meristem identity. *Curr. Biol.* 14: 1935–1940.

Eshed, Y., Baum, S.F. and Bowman, J.L. (1999) Distinct mechanisms promote polarity establishment in carpels of Arabidopsis. *Cell* 99: 199–209.

Flaus, A., Martin, D.M.A., Barton, G.J. and Owen-Hughes, T. (2006) Identification of multiple distinct Snf2 subfamilies with conserved structural motifs. *Nucleic Acids Res.* 34: 2887–2905.

Gan, E.-S., Xu, Y., Wong, J.-Y., Geraldine Goh, J., Sun, B., Wee, W.-Y. et al. (2014) Jumonji demethylases moderate precocious flowering at elevated temperature via regulation of FLC in Arabidopsis. *Nat. Commun.* 5: 5098.

Gan, E.S., Huang, J. and Ito, T. (2013) Functional roles of histone modification, chromatin remodeling and microRNAs in Arabidopsis flower development. *Int. Rev. Cell Mol. Biol.* 305: 115–161.

Goto, K. and Meyerowitz, E.M. (1994) Function and regulation of the Arabidopsis floral homeotic gene PISTILLATA. *Genes Dev.* 8: 1548–1560.

Grini, P.E., Thorstensen, T., Alm, V., Vizcay-Barrena, G., Windju, S.S., Jørstad, T.S. et al. (2009) The ASH1 HOMOLOG 2 (ASHH2) histone H3 methyltransferase is required for ovule and anther development in Arabidopsis. *PLoS ONE* 4: e7817.

Han, H.J., Russo, J., Kohwi, Y. and Kohwi-Shigematsu, T. (2008) SATB1 reprogrammes gene expression to promote breast tumour growth and metastasis. *Nature* 452: 187–193.

Hay, A., Kaur, H., Phillips, A., Hedden, P., Hake, S. and Tsiantis, M. (2002) The gibberellin pathway mediates KNOTTED1-type homeobox function in plants with different body plans. *Curr. Biol.* 12: 1557–1565.

Henderson, J.T., Li, H.-C., Rider, S.D., Mordhorst, A.P., Romero-Severson, J., Cheng, J.-C. et al. (2004) PICKLE acts throughout the plant to repress expression of embryonic traits and may play a role in gibberellin-dependent responses. *Plant Physiol.* 134: 995–1005.

Hirano, H.Y., Tanaka, W. and Toriba, T. (2014) Grass flower development. *Methods Mol. Biol.* 1110: 57–84.

Ho, L. and Crabtree, G.R. (2010) Chromatin remodelling during development. *Nature* 463: 474–484.

Honma, T. and Goto, K. (2001) Complexes of MADS-box proteins are sufficient to convert leaves into floral organs. *Nature* 409: 525–529.

Hurtado, L., Farrona, S. and Reyes, J. (2006) The putative SWI/SNF complex subunit BRAHMA activates flower homeotic genes in Arabidopsis thaliana. *Plant Mol. Biol.* 62: 291–304.

Ito, T. (2011) Coordination of flower development by homeotic master regulators. *Curr. Opin. Plant Biol.* 14: 53–59.

Ito, T., Ng, K.H., Lim, T.S., Yu, H. and Meyerowitz, E.M. (2007) The homeotic protein AGAMOUS controls late stamen development by regulating a jasmonate biosynthetic gene in Arabidopsis. *Plant Cell* 19: 3516–3529.

Ito, T., Wellmer, F., Yu, H., Das, P., Ito, N., Alves-Ferreira, M. et al. (2004) The homeotic protein AGAMOUS controls microsporogenesis by regulation of SPOROCYTELESS. *Nature* 430: 356–360.

Jack, T., Brockman, L.L. and Meyerowitz, E.M. (1992) The homeotic gene APETALA3 of Arabidopsis thaliana encodes a MADS box and is expressed in petals and stamens. *Cell* 68: 683–697.

Jacobsen, S.E. (1997) Hypermethylated SUPERMAN epigenetic alleles in Arabidopsis. *Science* 277: 1100–1103.

Jetha, K., Theissen, G. and Melzer, R. (2014) Arabidopsis SEPALLATA proteins differ in cooperative DNA-binding during the formation of floral quartet-like complexes. *Nucleic Acids Res.* 42: 10927–10942.

Kaufmann, K., Muino, J.M., Jauregui, R., Airoldi, C.A., Smaczniak, C., Krajewski, P. et al. (2009) Target genes of the MADS transcription factor SEPALLATA3: integration of developmental and hormonal pathways in the Arabidopsis flower. *PLoS Biol.* 7: e1000090.

Kaufmann, K., Wellmer, F., Muino, J.M., Ferrier, T., Wuest, S.E., Kumar, V. et al. (2010) Orchestration of floral initiation by APETALA1. *Science* 328: 85–89.

Khanday, I., Yadav, S.R. and Vijayraghavan, U. (2013) Rice LHS1/OsMADS1 controls floret meristem specification by coordinated regulation of transcription factors and hormone signaling pathways. *Plant Physiol.* 161: 1970–1983.

Kieffer, M., Stern, Y., Cook, H., Clerici, E., Maulbetsch, C., Laux, T. et al. (2006) Analysis of the transcription factor WUSCHEL and its functional homologue in Antirrhinum reveals a potential mechanism for their roles in meristem maintenance. *Plant Cell* 18: 560–573.

Kim, V.N. (2005) MicroRNA biogenesis: coordinated cropping and dicing. *Nat. Rev. Mol. Cell Biol.* 6: 376–385.

Krizek, B.A. and Meyerowitz, E.M. (1996) Mapping the protein regions responsible for the functional specificities of the Arabidopsis MADS domain organ-identity proteins. *Proc. Natl Acad. Sci. USA* 93: 4063–4070.

Krogan, N.T., Hogan, K. and Long, J.A. (2012) APETALA2 negatively regulates multiple floral organ identity genes in Arabidopsis by recruiting the co-repressor TOPLESS and the histone deacetylase HDA19. *Development* 139: 4180–4190.

Kwon, C.S., Chen, C. and Wagner, D. (2005) WUSCHEL is a primary target for transcriptional regulation by SPLAYED in dynamic control of stem cell fate in Arabidopsis. *Genes Dev.* 19: 992–1003.

Kwon, C.S., Hibara, K.-i., Pfluger, J., Bezhani, S., Metha, H., Aida, M. et al. (2006) A role for chromatin remodeling in regulation of CUC gene expression in the Arabidopsis cotyledon boundary. *Development* 133: 3223–3230.

Lafos, M., Kroll, P., Hohenstatt, M.L., Thorpe, F.L., Clarenz, O. and Schubert, D. (2011) Dynamic regulation of H3K27 trimethylation during Arabidopsis differentiation. *PLoS Genet.* 7: e1002040.

Leibfried, A., To, J.P., Busch, W., Stehling, S., Kehle, A., Demar, M. et al. (2005) WUSCHEL controls meristem function by direct regulation of cytokinin-inducible response regulators. *Nature* 438: 1172–1175.

Lenhard, M., Bohnert, A., Jurgens, G. and Laux, T. (2001) Termination of stem cell maintenance in Arabidopsis floral meristems by interactions between WUSCHEL and AGAMOUS. *Cell* 105: 805–814.

Li, H.C., Chuang, K., Henderson, J.T., Rider, S.D., Jr. Bai, Y., Zhang, H. et al. (2005) PICKLE acts during germination to repress expression of embryonic traits. *Plant J* 44: 1010–1022.

Li, G., Liu, S., Wang, J., He, J., Huang, H., Zhang, Y. et al. (2014) ISWI proteins participate in the genome-wide nucleosome distribution in Arabidopsis. *Plant J.* 78: 706–714.

Liu, X., Kim, Y.J., Müller, R., Yumul, R.E., Liu, C., Pan, Y. et al. (2011) AGAMOUS terminates floral stem cell maintenance in Srabidopsis by directly repressing WUSCHEL through recruitment of Polycomb group proteins. *Plant Cell* 23: 3654–3670.

Lodha, M., Marco, C.F. and Timmermans, M.C.P. (2013) The ASYMMETRIC LEAVES complex maintains repression of KNOX homeobox genes via direct recruitment of Polycomb-repressive complex2. *Genes Dev.* 27: 596–601.

Lohmann, J.U., Hong, R.L., Hobe, M., Busch, M.A., Parcy, F., Simon, R. et al. (2001) A molecular link between stem cell regulation and floral patterning in Arabidopsis. *Cell* 105: 793–803.

Long, J.A., Ohno, C., Smith, Z.R. and Meyerowitz, E.M. (2006) TOPLESS regulates apical embryonic fate in Arabidopsis. *Science* 312: 1520–1523.

Lou, Y., Xu, X.F., Zhu, J., Gu, J.N., Blackmore, S. and Yang, Z.N. (2014) The tapetal AHL family protein TEK determines nexine formation in the pollen wall. *Nat. Commun.* 5: 3855.

Lu, F., Cui, X., Zhang, S., Jenuwein, T. and Cao, X. (2011) Arabidopsis REF6 is a histone H3 lysine 27 demethylase. *Nat.e Genet.* 43: 715–U144.

Luo, M., Platten, D., Chaudhury, A., Peacock, W.J. and Dennis, E.S. (2009) Expression, imprinting, and evolution of rice homologs of the polycomb group genes. *Mol. Plant* 2: 711–723.

Mandel, M.A., Gustafson-Brown, C., Savidge, B. and Yanofsky, M.F. (1992) Molecular characterization of the Arabidopsis floral homeotic gene APETALA1. *Nature* 360: 273–277.

Mathieu, O., Probst, A.V. and Paszkowski, J. (2005) Distinct regulation of histone H3 methylation at lysines 27 and 9 by CpG methylation in Arabidopsis. *EMBO J.* 24: 2783–2791.

Mathur, S., Vyas, S., Kapoor, S. and Tyagi, A.K. (2011) The Mediator complex in plants: structure, phylogeny, and expression profiling of representative genes in a dicot (Arabidopsis) and a monocot (rice) during reproduction and abiotic stress. *Plant Physiol.* 157: 1609–1627.

Matsushita, A., Furumoto, T., Ishida, S. and Takahashi, Y. (2007) AGF1, an AT-hook protein, is necessary for the negative feedback of AtGA3ox1 encoding GA 3-oxidase. *Plant Physiol.* 143: 1152–1162.

Mendes, M.A., Guerra, R.F., Berns, M.C., Manzo, C., Masiero, S., Finzi, L. et al. (2013) MADS domain transcription factors mediate short-range DNA looping that is essential for target gene expression in Arabidopsis. *Plant Cell* 25: 2560–2572.

Mizukami, Y. and Ma, H. (1992) Ectopic expression of the floral homeotic gene AGAMOUS in transgenic Arabidopsis plants alters floral organ identity. *Cell* 71: 119–131.

Ng, K.H., Yu, H. and Ito, T. (2009) AGAMOUS controls GIANT KILLER, a multifunctional chromatin modifier in reproductive organ patterning and differentiation. *PLoS Biol.* 7: e1000251.

Ogas, J. (1997) Cellular differentiation regulated by gibberellin in the Arabidopsis thaliana pickle mutant. *Science* 277: 91–94.

O'Maoileidigh, D.S., Wuest, S.E., Rae, L., Raganelli, A., Ryan, P.T., Kwasniewska, K. et al. (2013) Control of reproductive floral organ identity specification in Arabidopsis by the C function regulator AGAMOUS. *Plant Cell* 25: 2482–2503.

Pajoro, A., Biewers, S., Dougali, E., Leal Valentim, F., Mendes, M.A., Porri, A. et al. (2014) The (r)evolution of gene regulatory networks controlling Arabidopsis plant reproduction: a two-decade history. *J. Exp. Bot.* 65: 4731–4745.

Pandey, R., Müller, A., Napoli, C.A., Selinger, D.A., Pikaard, C.S., Richards, E.J. et al. (2002) Analysis of histone acetyltransferase and histone deacetylase families of Arabidopsis thaliana suggests functional diversification of chromatin modification among multicellular eukaryotes. *Nucleic Acids Res.* 30: 5036–5055.

Pauwels, L., Barbero, G.F., Geerinck, J., Tilleman, S., Grunewald, W., Perez, A.C. et al. (2010) NINJA connects the co-repressor TOPLESS to jasmonate signalling. *Nature* 464: 788–791.

Peterson, C.L. and Workman, J.L. (2000) Promoter targeting and chromatin remodeling by the SWI/SNF complex. *Curr. Opin. Genet. Dev.* 10: 187–192.

Pien, S. and Grossniklaus, U. (2007) Polycomb group and trithorax group proteins in Arabidopsis. *Biochim. Biophys. Acta* 1769: 375–382.

Qin, F.J., Sun, Q.W., Huang, L.M., Chen, X.S. and Zhou, D.X. (2010) Rice SUVH histone methyltransferase genes display specific functions in chromatin modification and retrotransposon repression. *Mol. Plant* 3: 773–782.

Roudier, F., Ahmed, I., Berard, C., Sarazin, A., Mary-Huard, T., Cortijo, S. et al. (2011) Integrative epigenomic mapping defines four main chromatin states in Arabidopsis. *EMBO J.* 30: 1928–1938.

Saleh, A., Alvarez-Venegas, R., Yilmaz, M., Le, O., Hou, G., Sadder, M. et al. (2008) The highly similar Arabidopsis homologs of trithorax ATX1 and ATX2 encode proteins with divergent biochemical functions. *Plant Cell* 20: 568–579.

Sang, Y., Silva-Ortega, C.O., Wu, S., Yamaguchi, N., Wu, M.-F., Pfluger, J. et al. (2012) Mutations in two non-canonical Arabidopsis SWI2/SNF2 chromatin remodeling ATPases cause embryogenesis and stem cell maintenance defects. *Plant J.* 72: 1000–1014.

Sawarkar, R. and Paro, R. (2010) Interpretation of developmental signaling at chromatin: the Polycomb perspective. *Dev. Cell* 19: 651–661.

Simon, J.A. and Kingston, R.E. (2013) Occupying chromatin: Polycomb mechanisms for getting to genomic targets, stopping transcriptional traffic, and staying put. *Mol. Cell* 49: 808–824.

Smaczniak, C., Immink, R.G., Muino, J.M., Blanvillain, R., Busscher, M., Busscher-Lange, J. et al. (2012) Characterization of MADS-domain transcription factor complexes in Arabidopsis flower development. *Proc. Natl Acad. Sci. USA* 109: 1560–1565.

Smith, Z.R. and Long, J.A. (2010) Control of Arabidopsis apical–basal embryo polarity by antagonistic transcription factors. *Nature* 464: 423–426.

Smyth, D.R., Bowman, J.L. and Meyerowitz, E.M. (1990) Early flower development in Arabidopsis. *Plant Cell* 2: 755–767.

Sui, P., Jin, J., Ye, S., Mu, C., Gao, J., Feng, H. et al. (2012) H3K36 methylation is critical for brassinosteroid-regulated plant growth and development in rice. *Plant J.* 70: 340–347.

Sun, B., Looi, L.-S., Guo, S., He, Z., Gan, E.-S., Huang, J. et al. (2014) Timing mechanism dependent on cell division is invoked by Polycomb eviction in plant stem cells. *Science* 343.

Sun, B., Xu, Y., Ng, K.-H. and Ito, T. (2009) A timing mechanism for stem cell maintenance and differentiation in the Arabidopsis floral meristem. *Genes Dev.* 23: 1791–1804.

Sun, Q. and Zhou, D.X. (2008) Rice jmjC domain-containing gene JMJ706 encodes H3K9 demethylase required for floral organ development. *Proc. Natl Acad. Sci. USA* 105: 13679–13684.

Szemenyei, H., Hannon, M. and Long, J.A. (2008) TOPLESS mediates auxin-dependent transcriptional repression during Arabidopsis embryogenesis. *Science* 319: 1384–1386.

Tamada, Y., Yun, J.-Y., Woo, S.C. and Amasino, R.M. (2009) ARABIDOPSIS TRITHORAX-RELATED7 is required for methylation of lysine 4 of histone H3 and for transcriptional activation of FLOWERING LOCUS C. *Plant Cell* 21: 3257–3269.

Tanaka, M., Kikuchi, A. and Kamada, H. (2008) The Arabidopsis histone deacetylases HDA6 and HDA19 contribute to the repression of embryonic properties after germination. *Plant Physiol.* 146: 149–161.

Tanaka, W., Pautler, M., Jackson, D. and Hirano, H.Y. (2013) Grass meristems II: inflorescence architecture, flower development and meristem fate. *Plant Cell Physiol.* 54: 313–324.

Thorstensen, T., Grini, P., Mercy, I., Alm, V., Erdal, S., Aasland, R. et al. (2008) The Arabidopsis SET-domain protein ASHR3 is involved in stamen development and interacts with the bHLH transcription factor ABORTED MICROSPORES (AMS). *Plant Mol. Biol.* 66: 47–59.

Tian, L. and Chen, Z.J. (2001) Blocking histone deacetylation in Arabidopsis induces pleiotropic effects on plant gene regulation and development. *Proc. Natl Acad. Sci. USA* 98: 200–205.

Wagner, D. and Meyerowitz, E.M. (2002) SPLAYED, a novel SWI/SNF ATPase Homolog, controls reproductive development in Arabidopsis. *Curr. Biol.* 12: 85–94.

Walley, J.W., Rowe, H.C., Xiao, Y., Chehab, E.W., Kliebenstein, D.J., Wagner, D. et al. (2008) The chromatin remodeler SPLAYED regulates specific stress signaling pathways. *PLoS Pathog.* 4: e1000237.

Winter, C.M., Austin, R.S., Blanvillain-Baufume, S., Reback, M.A., Monniaux, M., Wu, M.F. et al. (2011) LEAFY target genes reveal floral regulatory logic, cis motifs, and a link to biotic stimulus response. *Dev. Cell* 20: 430–443.

Wu, M.-F., Sang, Y., Bezhani, S., Yamaguchi, N., Han, S.-K., Li, Z. et al. (2012) SWI2/SNF2 chromatin remodeling ATPases overcome polycomb repression and control floral organ identity with the LEAFY and SEPALLATA3 transcription factors. *Proc. Natl Acad. Sci. USA* 109: 3576–3581.

Wuest, S.E., Maoileidigh, D.S.O., Rae, L., Kwasniewska, K., Raganelli, A., Hanczaryk, K. et al. (2012) Molecular basis for the specification of floral organs by APETALA3 and PISTILLATA. *Proc. Natl Acad. Sci. USA* 109: 13452–13457.

Xu, L., Zhao, Z., Dong, A., Soubigou-Taconnat, L., Renou, J.-P., Steinmetz, A. et al. (2008) Di- and tri- but not monomethylation on histone H3 lysine 36 marks active transcription of genes involved in flowering time regulation and other processes in Arabidopsis thaliana. *Mol. Cell Biol.* 28: 1348–1360.

Xu, Y., Gan, E.S., Zhou, J., Wee, W.Y., Zhang, X. and Ito, T. (2015) Arabidopsis MRG domain proteins bridge two histone modifications to elevate expression of flowering genes. *Nucleic Acids Res.* 42: 10960–10974.

Xu, Y., Wang, Y., Stroud, H., Gu, X., Sun, B., Gan, E.S. et al. (2013) A matrix protein silences transposons and repeats through interaction with retinoblastoma-associated proteins. *Curr. Biol.* 23: 345–350.

Yamaguchi, T., Lee, D.Y., Miyao, A., Hirochika, H., An, G. and Hirano, H.Y. (2006) Functional diversification of the two C-class MADS box genes OSMADS3 and OSMADS58 in Oryza sativa. *Plant Cell* 18: 15–28.

Yamaguchi, T., Nagasawa, N., Kawasaki, S., Matsuoka, M., Nagato, Y. and Hirano, H.Y. (2004) The YABBY gene DROOPING LEAF regulates carpel specification and midrib development in Oryza sativa. *Plant Cell* 16: 500–509.

Yanofsky, M.F., Ma, H., Bowman, J.L., Drews, G.N., Feldmann, K.A. and Meyerowitz, E.M. (1990) The protein encoded by the Arabidopsis homeotic gene agamous resembles transcription factors. *Nature* 346: 35–39.

Yant, L., Mathieu, J., Dinh, T.T., Ott, F., Lanz, C., Wollmann, H. et al. (2010) Orchestration of the floral transition and floral development in Arabidopsis by the bifunctional transcription factor APETALA2. *Plant Cell* 22: 2156–2170.

Yoshida, A., Ohmori, Y., Kitano, H., Taguchi-Shiobara, F. and Hirano, H.-Y. (2012) ABERRANT SPIKELET AND PANICLE1, encoding a TOPLESS-related transcriptional co-repressor, is involved in the regulation of meristem fate in rice. *Plant J* 70: 327–339.

Yoshida, H. and Nagato, Y. (2011) Flower development in rice. *J. Exp. Bot.* 62: 4719–4730.

Yun, J., Kim, Y.S., Jung, J.H., Seo, P.J. and Park, C.M. (2012) The AT-hook motif-containing protein AHL22 regulates flowering initiation by modifying FLOWERING LOCUS T chromatin in Arabidopsis. *J. Biol. Chem.* 287: 15307–15316.

Zaret, K.S. and Carroll, J.S. (2011) Pioneer transcription factors: establishing competence for gene expression. *Genes Dev.* 25: 2227–2241.

Zhang, D., Jing, Y., Jiang, Z. and Lin, R. (2014) The chromatin-remodeling factor PICKLE integrates brassinosteroid and gibberellin signaling during skotomorphogenic growth in Arabidopsis. *Plant Cell* 26: 2472–2485.

Zhang, D. and Yuan, Z. (2014) Molecular control of grass inflorescence development. *Annu. Rev. Plant Biol.* 65: 553–578.

Zhang, H., Bishop, B., Ringenberg, W., Muir, W.M. and Ogas, J. (2012) The CHD3 remodeler PICKLE associates with genes enriched for trimethylation of histone H3 lysine 27. *Plant Physiol.* 159: 418–432.

Zhang, X., Bernatavichute, Y.V., Cokus, S., Pellegrini, M. and Jacobsen, S.E. (2009) Genome-wide analysis of mono-, di- and trimethylation of histone H3 lysine 4 in Arabidopsis thaliana. *Genome Biol.* 10: R62.

Zhang, X., Clarenz, O., Cokus, S., Bernatavichute, Y.V., Pellegrini, M., Goodrich, J. et al. (2007) Whole-genome analysis of histone H3 lysine 27 trimethylation in Arabidopsis. *PLoS Biol.* 5: e129.

Zhu, Z., Xu, F., Zhang, Y., Cheng, Y.T., Wiermer, M., Li, X. et al. (2010) Arabidopsis resistance protein SNC1 activates immune responses through association with a transcriptional corepressor. *Proc. Natl Acad. Sci. USA* 107: 13960–13965.

Nucleic Acids Research Advance Access published September 2, 2014

doi: 10.1093/nar/gku781

Arabidopsis MRG domain proteins bridge two histone modifications to elevate expression of flowering genes

Yifeng Xu[1], Eng-Seng Gan[1,2], Jie Zhou[1], Wan-Yi Wee[1], Xiaoyu Zhang[3] and Toshiro Ito[1,2,*]

[1]Temasek Life Sciences Laboratory, National University of Singapore, Singapore 117604, Republic of Singapore, [2]Department of Biological Sciences, National University of Singapore, Singapore 117543, Republic of Singapore and [3]Department of Plant Biology, University of Georgia, Athens, GA 30602-7271, USA

Received April 14, 2014; Revised July 30, 2014; Accepted August 18, 2014

ABSTRACT

Trimethylation of lysine 36 of histone H3 (H3K36me3) is found to be associated with various transcription events. In *Arabidopsis*, the H3K36me3 level peaks in the first half of coding regions, which is in contrast to the 3′-end enrichment in animals. The MRG15 family proteins function as 'reader' proteins by binding to H3K36me3 to control alternative splicing or prevent spurious intragenic transcription in animals. Here, we demonstrate that two closely related *Arabidopsis* homologues (MRG1 and MRG2) are localised to the euchromatin and redundantly ensure the increased transcriptional levels of two flowering time genes with opposing functions, *FLOWERING LOCUS C* and *FLOWERING LOCUS T (FT)*. MRG2 directly binds to the *FT* locus and elevates the expression in an H3K36me3-dependent manner. MRG1/2 binds to H3K36me3 with their chromodomain and interact with the histone H4-specific acetyltransferases (HAM1 and HAM2) to achieve a high expression level through active histone acetylation at the promoter and 5′ regions of target loci. Together, this study presents a mechanistic link between H3K36me3 and histone H4 acetylation. Our data also indicate that the biological functions of MRG1/2 have diversified from their animal homologues during evolution, yet they still maintain their conserved H3K36me3-binding molecular function.

INTRODUCTION

In eukaryotes, including plants, post-translational covalent modifications on histones play a pivotal role in controlling gene expression at the chromatin level. Different histone modifications act sequentially or in combination to confer distinct transcriptional outcomes. Although histone modifications are conserved to a large extent amongst eukaryotes, there is some divergence in terms of the distribution of these histone modifications in the genome and their biological functions between plants and animals. For example, in yeast, worms and mammals, trimethylation of lysine 36 of histone H3 (H3K36me3) preferentially marks the exons of transcribed genes and peaks at the 3′-end of the coding region, and it has been shown to be involved in various activities, including the control of alternative splicing and the prevention of spurious intragenic transcription (1–5). In contrast, the H3K36me3 level in *Arabidopsis* peaks at the 5′-end of the coding region, which resembles the distribution patterns of active transcription-linked histone modifications, H3K4me2/3 and acetylated H3 (6). This preferential enrichment at the first half of the coding region in plants suggests that the mechanism governing H3K36me3 deposition, and possibly its effect on transcriptional events, may differ between plants and other eukaryotes.

Whilst some histone modifications such as acetylation can directly modulate chromatin structures, an increasing body of evidence suggests that individual histone modifications, or a combination of them, may serve as a platform to recruit specific 'reader' proteins, which then determine the transcriptional outcome of the target genes. The yeast homologue of the human MORF4-related gene on chromosome 15 (MRG15), Esa1-associated factor 3 (Eaf3), was the first identified 'reader' for H3K36me3 (2–4). MRG15 proteins are highly conserved across multiple species, including fruit flies (*Drosophila melanogaster*), worms (*Caenorhabditis elegans*) and yeast (*Schizosaccharomyces pombe* and *Saccharomyces cerevisiae*) (7,8). The MRG15 family proteins contain the conserved chromodomain at its amino terminus, which binds to H3K36me3. Chromodomain and chromo-like domain (such as Tudor and PWWP domains) are protein modules that are found in many chromatin-related proteins in nucleoprotein complexes (9). They have been shown to recognise and bind to methylated-Lys at the histone tails and hence recruit the protein complexes to play an important role in histone modifications and chromatin-remodelling, which control the transcription status of a large number of genes. For example, the chromodomain of chromatin-binding proteins heterochromatin-binding protein 1 (HP1) and Polycomb (Pc) bind to methylated Lys9

*To whom correspondence should be addressed. Tel: +65 6872 7016; Fax: +65 6872 7007; Email: itot@tll.org.sg

and Lys27 of histone H3, respectively, directing heterochromatin formation and/or gene silencing (10–13). The chromodomain of human MRG15 and its homologue in yeast, Eaf3, which is unlike the typical chromodomain found in HP1 and Pc proteins, is assumed to be an auto-inhibited chromo barrel domain and binds to trimethylated H3K36 and H3K4 *in vitro* with a relatively weak affinity (2–4,14–16).

In addition to the chromodomain, all members of the MRG family proteins contain the MRG domain, which shares sequence similarity with the Mortality factor on chromosome 4 (MORF4), a cell-senescence protein in humans, and that may be involved in protein–protein interactions (2–4,8,17,18). Biochemical assays have shown that the animal MRG15 proteins and the yeast homologues associate with at least two independent and antagonising nucleoprotein complexes that contain either histone acetyltransferases (HAT) or histone deacetylases (HDAC) (2–4,18–20). In mouse and *Drosophila*, deletion or knockdown of *MRG15* genes cause embryonic-lethal phenotypes, whilst loss-of-function of *S. cerevisiae* Eaf3 and *S. pombe* Altered polarity mutant-13 (Alp13) are viable (21,22). The loss of *Alp13* in fission yeast causes growth arrest, sterility, defects in cell polarity and is associated with global hyperacetylation of histones and chromosome instability (22). Alp13 represses the expression of repeated regions and maintains the heterochromatin through the recruitment of histone deacetylation complexes to the repeat regions (23). Eaf3 in *S. cerevisiae* was suggested to suppress intragenic transcriptional initiation by recruiting the histone deacetylase complex to H3K36me3-containing nucleosomes (2–4). Eaf3 also specifically targets promoter regions of heat-shock and ribosomal protein genes for transcriptional activation through the recruitment of NuA4-dependent histone H4 acetylation complexes (24–26). Due to these dual functions, the deletion of *Eaf3* greatly alters the global genomic profile of histone modification, with increased acetylation levels at coding sequences and decreased acetylation levels at the promoter regions (21). *MRG-1*, an *MRG15* homologue in *C. elegans*, was recently reported to be involved in homologous chromosome pairing, which is independent of both the pairing centre and meiotic homologous recombination (27). These data suggest that the function of MRG15 family proteins have diversified in different species and participate in varied biological processes. The *Arabidopsis* genome contains two *MRG15* homologues with high similarities in their protein sequences (8). However, whether they maintain their functions as H3K36me3 readers and effectors and which biological process they are involved in are largely unknown.

Histone acetylation is one of the histone modifications that is well known to be linked with active transcription (28). Histone acetylation may neutralise a positive charge and thus weaken the interaction of the histone octamer with the negatively charged DNA and/or interfere with the higher-order packing of chromatin, which allow transcriptional regulators to gain access to the DNA with a larger chromatin area (28). Different families of HATs have distinct histone targets and are involved in different biological events (28). One well-studied family of the acetyltransferases responsible for histone acetylation is the MYST (for MOZ, Ybf2/Sas3, Sas2 and Tip60)-related HATs (29). MYST proteins contain the acetyl-CoA binding motif as well as a C2HC zinc finger motif that is important for HAT activity and interact with the MRG15 family proteins (18,20,29). The yeast MYST HAT Esa1 associates with the MRG15 protein Eaf3 to specifically target promoter regions of heat-shock and ribosomal protein genes for transcriptional activation (20,24–26). Thus, the substrate specificity of the MYST protein is likely conferred through association with additional complex subunits. The *Drosophila* HAT, MOF, associates with the MRG protein, MSL3, in a mutually dependent manner to target Histone H4 in the X-chromosome dosage compensation mechanism and autosomal transcription regulation (30,31). In *Arabidopsis*, there are two functionally redundant MYST family proteins, namely, HISTONE ACETYLTRANSFERASE OF THE MYST FAMILY 1 (HAM1) and HAM2 (32). HAM1 and HAM2 have HAT activity specific to H4K5 *in vitro* and *in vivo* (33,34). The double-mutant *ham1 ham2* is not viable, and mutation of either *ham1* or *ham2* did not show any defects in vegetative and reproductive stages (32). Interestingly, *ham1*/+ *ham2*/+ plants showed a reduction in the *FLOWERING LOCUS C* (*FLC*) expression level, with a reduction of H4K5 acetylation at the *FLC* locus (32,34), suggesting that HAM1 and HAM2 have essential functions in various developmental processes, including flowering control.

Flowering is a highly regulated biological process in *Arabidopsis*. At the centre of the flowering control is the floral repressor *FLC*, which integrates multiple inputs from different flowering pathways and functions to repress two downstream floral inducers, *FLOWERING LOCUS T* (*FT*) and *SUPPRESSOR OF OVEREXPRESSION OF CONSTANS 1* (*SOC1*). *FLC* expression is governed by multiple epigenetic regulators (35). The H3K36me3 marks have an active effect on the transcription of *FLC*, and the loss-of-function mutant of the H3K36-methyltransferase SET DOMAIN GROUP 8 (SDG8), a homologue of the yeast histone H3K36-methyltransferase *SET2*, causes a drastic decrease in the *FLC* expression (36–38). However, the exact mechanistic function of SDG8-mediated H3K36me3 on *FLC* expression is largely unknown. In this study, we show that MRG1 and MRG2 function redundantly as the H3K36me3 'reader' and 'effector' in the fine-tuning of transcription of flowering time genes *FLC* and *FT*. MRG1 and MRG2 bind to their targets and recruit histone acetyltransferase HAM1 and HAM2 complex to increase the histone H4 acetylation levels on the target loci, thereby making these loci more accessible to transcriptional machinery, hence bridging H3K36 methylation and histone H4 acetylation.

MATERIALS AND METHODS

Plant materials and growth conditions

All *Arabidopsis thaliana* plants used were in the background of the Columbia (Col) ecotype. The alleles of *mrg1-1* (SAIK_057762), *mrg2-1* (SALK_035089), *mrg2-2* (SK28487) and *mrg2-3* (GK-255G06) were isolated from the SALK, SK and GABI-Kat collections, respectively. The *sdg8* allele (*sdg8-2*) was described previously (38). The allele

of *sdg7* (SALK_131218) in which T-DNA is inserted in the exon 4 were isolated from SALK collections. Plants were grown in LDs (16-h light/8-h dark) at 23°C. Genotyping primer sequences are shown in Supplementary Table S1.

Plasmid construction and plant transformation

To construct *35S::MRG2-HA* and *35S::GFP-MRG2* plasmids, the full length *MRG2* coding sequence was amplified by primer set MRG2- MluI_F and MRG2-XmaI_R1, or MRG2-ApaI_F and MRG2-XmaI_R2, cloned into vectors *pGREEN-35S-HA* by using *MluI* and *XmaI* or *pGREEN-35S-GFP* by using *ApaI* and *XmaI*.

For *pMRG2::MRG2-GUS*, *pMRG2::HA-MRG2* and *pHAM1::HA-HAM1* plasmids, a ~7.2-kb *MRG2* genomic fragment (from −3406 to +3845; A of the start codon was set as +1) and a ~4.0-kb *HAM1* genomic fragment (from −1371 to +2579) amplified using primers gDMRG2-cacc_F and gDMRG2-XmaI_R or gDHAM1-cacc_F and gDHAM1_R were cloned into *pENTR/D-TOPO* vector (Invitrogen). SfoI restriction site was introduced after ATG or in front of the *MRG2* stop codon, or after ATG of HAM1 through mutagenesis using primers mMRG2-ATG-SfoI_F and mMRG2-ATG-SfoI_R, mMRG2-Stop-SfoI_F and mMRG2-Stop-SfoI_R, or mHAM1-ATG-SfoI_F and mHAM1-ATG-SfoI_R, respectively. *HA* or *GUS* fragments were then inserted into the *SfoI* site of the *pENTR/D-TOPO-gDMRG2* or *pENTR/D-TOPO-gDHAM1* plasmid. Finally, *gDMRG2-GUS*, *HA-gDMRG2* or *HA-gDHAM1* in *pENTR/D-TOPO* plasmids were recombined into *pBGW* or *pHGW* using LR Clonase II (Invitrogen), respectively.

For *pMRG1::MRG1-GUS* plasmid, a ~3.2-kb *MRG1* genomic fragment (from −321 to +2878) spanning to the neighbouring genes located to the upstream and downstream of *MRG1* was cloned into Topo-PCRII (Invitrogen) first using the primer set gDMRG1-NotI_F and gDMRG1_R. The genomic fragment was then released with *NotI* digestion and cloned into the modified *pENTR* vector. Mutagenesis was performed using the primers mMRG1-Stop-ScaI_F and mMRG1-Stop-ScaI_R. The *GUS* fragment was then inserted into the *ScaI* site of the *pENTR-gDMRG1* plasmid. Finally, *MRG1* in *pENTR* was recombined into *pBGW* using LR Clonase II (Invitrogen). All the vectors were verified by sequencing. Primer sequences are listed in Supplementary Table S1.

Transgenic plants were generated by floral dipping with *Agrobacterium tumefaciens* with the corresponding constructs. The additional *pSOUP* helper plasmid was co-transfected for the transformation of *pGREEN-35S::MRG2-HA* and *pGREEN-35S::GFP-MRG2*.

RNA extraction and expression analysis

For the tissue expression analysis of *MRG1* and *MRG2*, total RNAs were isolated from the root, juvenile rosette leaf, mature rosette leaf, cauline leaf, stem, flower bud, open flower and silique. For the flowering time gene expression analysis, the aerial parts of 6 day-after-germination (DAG) and 9 DAG seedlings were harvested at dusk (ZT16). For a time course assay over a 24-h-long day cycle, the aerial parts of 9 DAG seedlings were harvested every 2 or 4 h. The total RNAs were extracted using an RNeasy plant mini kit (Qiagen) according to the manufacturer's instructions. Approximately 500 ng total RNAs were used for reverse transcription with the Superscript III RT-PCR system (Invitrogen). Semi-quantitative PCR (semi-qPCR) with gene-specific primers (Supplementary Table S1) were performed using HotStarTaq DNA Polymerase (Qiagen) on a Thermocycler (Bio-Rad) at 25–35 cycles. Real-time qPCR was performed on ABI PRISM 7900HT sequence detection system (Applied Biosystems) using KAPA SYBR FAST ABI Prism qPCR Master Mix (KAPA Biosystems). The ubiquitously expressed *Tip41-like* (AT4G34270) (39) was used as an internal reference gene. Primer sequences were shown in Supplementary Table S1.

GUS staining

GUS staining was performed as previously described (40). Briefly, plant tissues were fixed with ice-cold 90% acetone for 30 min and rinsed with rinsing solution. The tissues were then incubated in staining solution at 37°C for approximately 8 h. After staining, the tissues were incubated in fixation solution overnight and washed with a serial of ethanol solution. For histological analysis, the tissues were mounted on slides with clearing solution, and images were taken with an AxioCam ICc 3 (Zeiss) under a SteREO Discovery.V12 Stereomicroscope (Zeiss).

Chromatin immunoprecipitation (ChIP) assays

ChIP experiments were performed as previously described with minor modifications (41). Briefly, total chromatin was extracted from 10 DAG seedlings and immuno-precipitated using anti-HA (Santa Cruz Biotechnology, #sc-7392) and normal mouse IgG as a control (Santa Cruz Biotechnology, #sc-2025), or anti-H3Ace3 (Millipore, #06-599), anti-H4K5Ace (Active Motif #39699), anti-H3K4me3 (Active Motif #61379) and anti-H3K36me3 (Active Motif #61021), with anti-H3 (Abcam, #ab1791) as a control. DNA fragments were recovered by phenol-chloroform extraction and ethanol precipitation. Quantitative PCR with locus-specific primers (Supplementary Table S1) was performed to measure the amounts of *FT* relative to that of the constitutively expressed *ACTIN2* (AT3G18780) on ABI PRISM 7900HT sequence detection system (Applied Biosystems) using KAPA SYBR FAST ABI Prism qPCR Master Mix (KAPA Biosystems).

Bimolecular fluorescence complementation (BiFC) assay

The full-length coding sequences for MRG1, MRG2, HAM1 and HAM2 were fused in frame with either the coding sequence for an N-terminal yellow fluorescent protein (YFP) fragment or for a C-terminal YFP fragment in the primary pSAT1 vectors (42). To detect the interaction in tobacco, leaves of 2- to 4-week-old tobacco plants were infiltrated with *Agrobacterium* containing the respective plasmid pairs (43). Epidermal cell layers were examined 2–4 days after infiltration and imaged with a Zeiss LSM 5 EXCITER upright laser scanning confocal microscope (Zeiss) (41).

Co-immunoprecipitation (Co-IP) assays

Co-IP experiments were performed as described previously with minor modifications (41). Briefly, 10-day-old seedlings (~2 g) expressing *pHAM1::HA-HAM1 35S::GFP-MRG2* or *pHAM1::HA-HAM1* were harvested and total proteins were extracted and immunoprecipitated with anti-GFP antibody (Invitrogen, #A-11122). The HA-HAM1 protein in the immunoprecipitates was detected by western blotting with anti-HA-HRP (Santa Cruz Biotechnology, #sc-7392).

Immunostaining and *in situ* proximity ligation assay

Isolation of nuclei and *in situ* immunolocalisation of chromatin proteins were performed as described with minor modifications (44). Young leaves from *sdg8*, *sdg7 sdg8*, wild-type or *pMRG2::HA-MRG2* transgenic plants were used for nuclei extraction. Sample suspension was air-dried on glass slides. Each slide was blocked with 1% BSA in 1x PBS before incubating with mouse anti-H3K36me3 (Active Motif #61021) and rabbit anti-H3K36me2 (Abcam, #ab9049), or with rabbit anti-HAM1/2 (Aviva, #ARP33345_P050) and mouse anti-HA (Santa Cruz Biotechnology, #sc-7392), rabbit anti-H3K36me3 (Abcam, #ab9050) and mouse anti-H3K4me3 (Active Motif #61379), and rabbit anti-H3K9me2 (Abcam, #ab1220). Later the slides were incubated with CF555 goat anti-mouse IgG (Biotium, #20030) and/or CF 488A goat anti-rabbit IgG (Biotium, #20010). Slides were stained with DAPI and imaged with Leica TCS SP5 confocal microscope (Leica).

The *in situ* proximity ligation assay (PLA) assay was carried out with Duolink II kits (Genome holdings) according to the manufacturer's instructions, with nuclei prepared with *pMRG2::HA-MRG2* transgenic plants, wild-type plants and *pMRG2::MRG2-HA* in a *sdg8* background, in a way similar to the *in situ* immunolocalisation assay. Mouse anti-HA (Santa Cruz Biotechnology, #sc-7392) and rabbit anti-H3K4me3 (Millipore, #07-473), rabbit anti-H3K36me3 (Abcam, #ab9050), rabbit anti-H3 (Abcam, #ab1791), rabbit anti-HAM1/2 (Aviva, #ARP33345_P050), rabbit anti-H3K9me2 (Abcam, #ab1220) or rabbit IgG (Santa Cruz, #SC-2027) were used as the primary antibodies. After washing, Duolink II PLA Probe anti–Mouse Plus (Genome holdings, #92001–0030) and Duolink II PLA Probe anti−Rabbit Minus (Genome holdings, #92005–0030) were applied as the probes. Duolink II Detection Reagents (Genome holdings, #92008–0030) were used to amplify the interaction signal, and the fluorescent signal was imaged with a Leica TCS SP5 confocal microscope (Leica).

Peptide pull-down assays

The chromodomain of MRG1 (1-131 aa) or MRG2 (1-130 aa) was cloned into *pGST-4T-1* (GE Healthcare) with the primer set GST-MRG1-CD-BamHI_F and GST-MRG1-CD-XmaI_R, or GST-MRG2-CD-BamHI_F and GST-MRG2-CD-XmaI_R. GST alone, GST-MRG1 CD or GST-MRG2 CD (1 μg) expressed in *E. coli* Rosetta was incubated in binding buffer [20 mM Tris-HCl pH 8.0, 250 mM NaCl, 1 mM EDTA, 0.5% NP-40, 1 mM phenylmethylsulfonyl fluoride, 1 mM DTT, 1x protease inhibitor cocktail (Roche)] with 10 μg of BSA and 1 μg biotinylated trimethylated histone H3K36 peptide (Epigentek, #R–1050–100), trimethyl histone H3K4 (Epigentek, #R–1023–100), trimethyl histone H3K9 (Epigentek, #R–1029–100), trimethyl histone H3K27 (Epigentek, #R–1035–100) or biotinylated unmodified histone H3 aa 22–44 (Epigentek, #R–1006–100) and biotinylated unmodified histone H3 aa 1–21 (Epigentek, # R–1004–100) immobilised on streptavidin-agarose. The beads were then washed with binding buffer and analysed by western blotting with antibodies against GST (Santa Cruz, #sc-138).

RESULTS

The *mrg1 mrg2* double mutant shows a late-flowering phenotype

In *Arabidopsis*, there are two closely related *MRG15* homologues *MRG1* (AT4G37280) and *MRG2* (AT1G02740) that share high sequence similarities (Supplementary Figure S1; (8)). We first identified the *mrg2-1* (SALK_035089) mutant, in which the T-DNA insertion in the fourth exon (Figure 1A) abolished the expression of the full-length transcript of *MRG2* (Figure 1B). Whilst the homozygous plants showed male and female sterility due to a meiosis defect, fertility was normal in other *mrg2* loss-of-function alleles, indicating that it is not linked with the *mrg2* mutation. We also identified the *mrg1-1* (SALK_057762) mutant, in which T-DNA is inserted in the first intron with no full-length transcript produced (Figure 1A and B). Although the single *mrg1-1* did not show any mutant phenotypes, *mrg1-1 mrg2-1* showed a late-flowering phenotype under long-day (LD) growth conditions (Figure 1C, Supplementary Figure S2A and B). We isolated two more T-DNA mutant alleles of *mrg2*, *mrg2-2* (SK28487) and *mrg2-3* (GK-255G06) (Figure 1A). T-DNA insertion in the first and ninth intron, respectively, abolished the production of the *MRG2* full-length transcript (Figure 1A and B, Supplementary Figure S2A, E), but they did not show any sterility phenotype. Consistent with *mrg1-1 mrg2-1*, *mrg1-1 mrg2-2* and *mrg1-1 mrg2-3* showed similar late-flowering phenotypes (Figure 1C and D, Supplementary Figure S2A–D). Moreover, introduction of the *pMRG2::HA-MRG2* transgene into *mrg1-1 mrg2-2* completely rescue the late-flowering phenotype in the *mrg1 mrg2* double mutant (Figure 1C and D). These results show that MRG1 and MRG2 are redundantly involved in flowering control. Due to the similarity in their phenotype, we used *mrg1-1 mrg2-2* (herein *mrg1 mrg2*) for all subsequent experiments.

MRG1 and MRG2 are required for higher expression levels of *FLC* and *FT*

To investigate which flowering genes are responsible for the late-flowering phenotype in *mrg1 mrg2*, we harvested the aerial parts of the seedlings at 9 DAG (day after germination, at the beginning of the dark photoperiod under LD conditions) just before the floral induction. We then compared the expression of a series of flowering time genes between WT and *mrg1 mrg2*. Whilst *AGL24*, *MAF1-5* and *SVP* were un-affected in *mrg1 mrg2* (Supplementary Figure

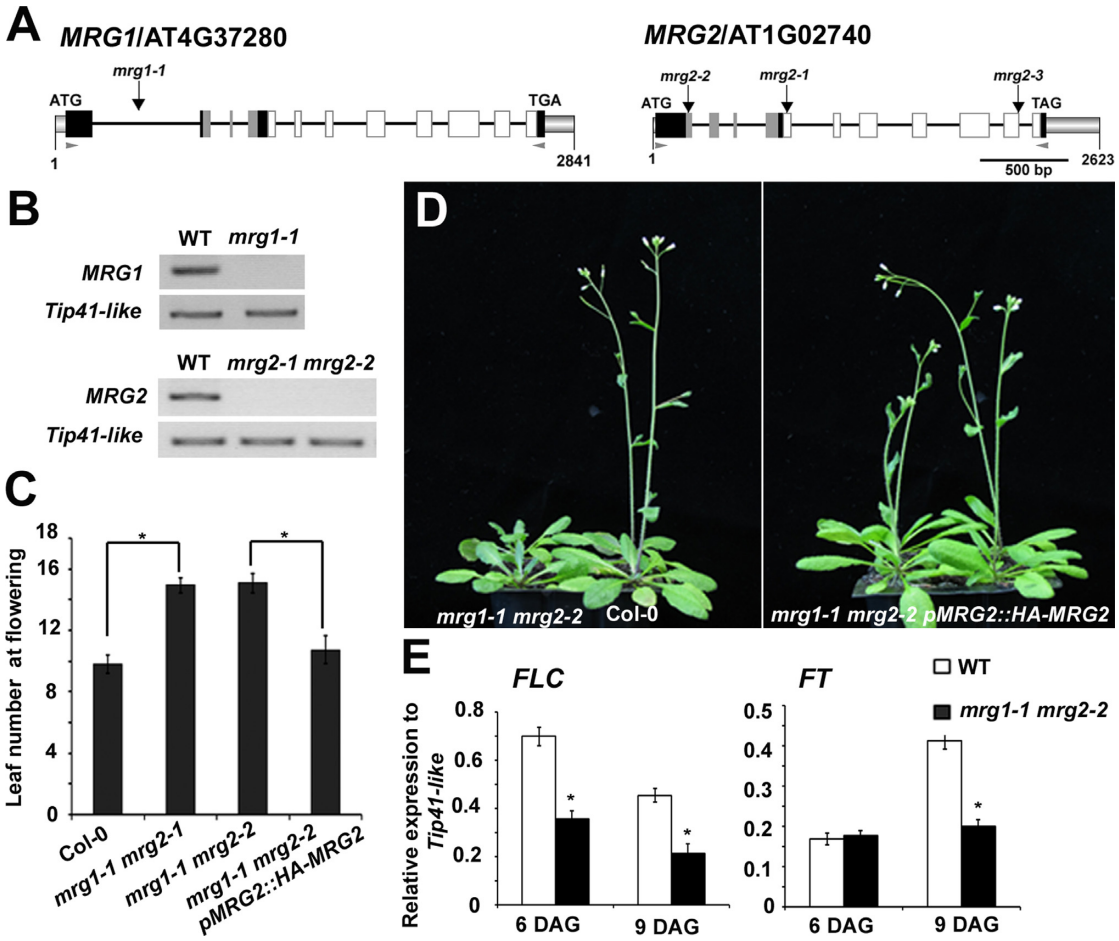

Figure 1. *MRG1* and *MRG2* are required for high transcriptional levels of *FT* and *FLC*. (**A**) Schematic drawings of the genomic structures of *MRG1* and *MRG2*. The smaller gray boxes indicate the 5′ and 3′ UTRs. Black lines indicate the introns. The larger boxes indicate exons with gray boxes and white boxes further showing the chromodomain and MRG domain coding regions, respectively. T-DNA insertional sites are marked by downward arrows above the schematic diagrams. The pairs of arrowheads on *MRG1 and MRG2* genomic structures indicate the position for the semi-quantitative RT-PCR primers designed to detect *MRG1* and MRG2 transcripts. Bar, 500 bp. (**B**) Semi-quantitative RT-PCR of *MRG1* and *MRG2* in Col wild-type (WT), *mrg1-1*, *mrg2-1* and *mrg2-2*, respectively. Primers are shown in A. Ubiquitously expressed *Tip41-like* gene (AT4G34270) was used as a control. (**C**) Total number of rosette leaves before bolting in Col WT, *mrg1-1 mrg2-1*, *mrg1-1 mrg2-2* and *mrg1-1 mrg2-2 pMRG2::HA-MRG2* plants grown in 16 h light/8 h dark long-day condition (LD) at 23°C were counted (two independent experiments with 15–20 plants each). *$P < 0.05$ with Student's *t*-test to indicate the difference of flowering time between Col WT and *mrg1-1 mrg2-1*, *mrg1-1 mrg2-2* and *mrg1-1 mrg2-2 pMRG2::HA-MRG2*. No significant difference between *mrg1-1 mrg2-2* and *mrg1-1 mrg2-3* ($P = 0.50$), Col WT and *mrg1-1 mrg2-2 pMRG2::HA-MRG2* ($P = 0.49$). (**D**) *mrg1-1 mrg2-2* bolted later than Col WT when grown in LD 23°C (2 plants each, left panel), and *pMRG2::HA-MRG2* rescued the late-flowering phenotype of *mrg1-1 mrg2-2* (right panel) grown at the same condition. (**E**) Quantitative RT-PCR-based expression levels of *FLC* and *FT* in 6 and 9 DAG seedlings of Col WT and *mrg1-1 mrg2-2* grown in LD 23°C. Bars indicate SD of three biological replicates. *$P < 0.05$ with Student's *t*-test.

S3A–G), *FLC*, *FT* and *SOC1* transcription levels were reduced approximately 2-fold in *mrg1 mrg2* (Figure 1E, Supplementary Figure S3H). As *SOC1* is one of the downstream targets of FT, the reduction of *SOC1* could be due to the indirect effect of loss-of-function of *mrg1* and *mrg2*. Because FT functions downstream of FLC, the *FT* reduction at 9 DAG may lead to late-flowering. Down-regulation of *FT* in spite of the reduced *FLC* expression in the mutant indicates that *FT* may be directly controlled by MRG1 and MRG2. To further characterise the transcriptional change of *FLC* and *FT* in *mrg1 mrg2*, we next compared their expression between WT and *mrg1 mrg2* plants at an earlier stage at 6 DAG, and found that *FLC* expression is reduced to half in *mrg1 mrg2* at both 6 DAG and 9 DAG (Figure 1E). Although *FT* showed a 2-fold decrease in expression at 9 DAG, the *FT* expression at 6 DAG was not affected (Figure 1E). *FT* is expressed at a relatively low level in the WT plant at 6 DAG compared with that at 9 DAG (45). Similar expression patterns of *FT* and *FLC* were also observed in the different allele *mrg1-1 mrg2-3* (Supplementary Figure S2F). These data suggest that two redundant *MRG1* and *MRG2* are essential in ensuring the maximum endogenous expression level of their putative targets *FT* and *FLC* but may not act in the initial transcriptional activation of *FT*. Transcriptional up-regulation by *MRG1* and *MRG2* on *FT* may require a threshold level of *FT* expression or the accumulation of the transcription-associated epigenetic marks, such as H3K36me3.

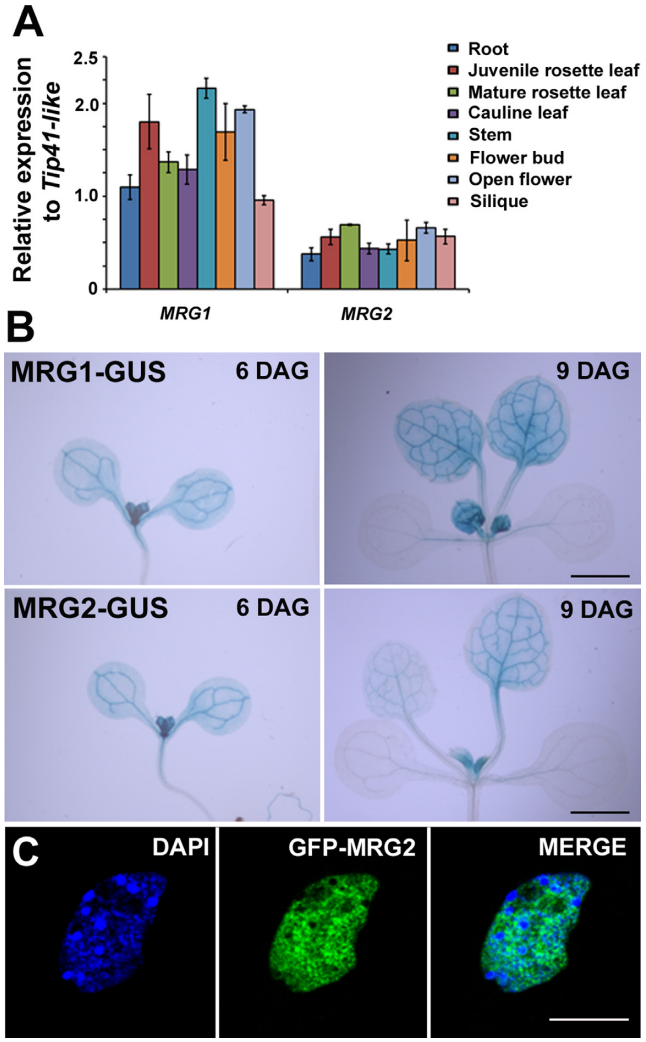

Figure 2. MRG1 and MRG2 are ubiquitously expressed and localised in euchromatin. (**A**) RT-qPCR-based expression levels of *MRG1* and *MRG2* in different tissues, including root, juvenile rosette leaf, mature rosette leaf, cauline leaf, stem, flower bud, open flower and silique. (**B**) Histochemical GUS staining of *pMRG1::MRG1-GUS* and *pMRG2::MRG2-GUS*. Seedlings at 6 and 9 DAG were stained for 8 h. Scale bar, 2 mm. (**C**) Immunolocalisation of GFP-MRG2 in the nuclei of a root cell of *35S::GFP-MRG2* transgenic line. Scale bar, 10 μm.

MRG1 and MRG2 are localised at euchromatin

Quantitative RT-PCR with RNA extracted from different tissues showed that *MRG1* and *MRG2* are ubiquitously expressed in the whole plants (Figure 2A). A GUS staining assay of plants harbouring the GUS fusion transgene *pMRG1::MRG1-GUS* and *pMRG2::MRG2-GUS* confirmed that *MRG1* and *MRG2* expression is detectable in all tissue types, especially in the vasculatures of true leaves and young leaf primordia (Figure 2B), which match the expression patterns of *FLC* and *FT*. The subcellular localisation of the MRG proteins was examined using the root of *35S::GFP-MRG2* transgenic plants. GFP-MRG2 was found to be localised in the euchromatic regions of the nucleus but not in the DAPI-dense heterochromatin (Figure 2C), consistent with the previous reports that MRG proteins function as chromatin remodelling factors (8).

MRG2 binds to H3K36me3 *in vitro* and *in vivo*

It has been shown that the chromodomain at the N-terminus of MRG15 homologues can bind to H3K36me3 in both yeast and humans and to H3K4me3 in yeast with low affinity (2–4,14–16). To check whether the chromodomain of *Arabidopsis* MRG proteins interacts directly with these modified histones, we cloned the N-terminal chromodomain (1–131 aa) of MRG1 and chromodomain (1–130 aa) of MRG2 to produce the GST-MRG1/2 chromodomain fusion proteins (MRG1-CD and MRG2-CD in Figure 3A) and performed a pull-down assay using different histone H3 peptides trimethylated at K4, K9, K27, K36, dimethylated at K36 or two unmodified histone H3 peptides (H3 1–21 and H3 21–44), all of which were biotin-labelled and immobilised on streptavidin agarose beads. Both of the chromodomains of MRG1 and MRG2 were found to bind to H3K36me2, H3K36me3 and H3K4me3 with different affinities, but not to the other histone modifications (H3K9me3 and H3K27me3) nor the unmodified histone H3 (Figure 3A). Thus, the histone-binding function of MRG1/2 to H3K36me2/3 is rather conserved across different species, but like the yeast homologue, they also bind to H3K4me3.

An *in situ* PLA provides another piece of evidence to support the model that MRG2 binding to histone H3 is mediated through H3K36me3 and/or H3K4me3 *in vivo*. An *in situ* PLA is able to detect the direct protein interaction with high sensitivity and specificity by integrating traditional immunolocalisation techniques with DNA-based signal amplification (46). We first carried out the immunofluorescence staining with antibody against HA-MRG2, MYST family HATs HAM1/2, H3K36me3 and H3K9me2, and confirmed that HA-MRG2 and HAM1/2 are co-localised at the euchromatin (Supplementary Figure S4C) in a similar pattern with the euchromatic histone modifications H3K4me3 and H3K36me3 (Supplementary Figure S4B), whilst H3K9me2 is specifically detectable at the heterochromatin region (Supplementary Figure S4A). Next, we performed *in situ* PLA assay with the tested antibodies. Using antibodies against HA and H3K4me3 and H3K36me3, the fluorescence signals of PLA were detected in the nuclei harvested from *pMRG2::HA-MRG2* plants but not in WT plants without the transgene (Figure 3B and C). The negative control, using an H3K9me2 antibody, showed there is no interaction between H3K9me2 and HA-MRG2 in transgenic plants. These results indicate the close localisation between MRG2 with H3K4me3 and H3K36me3 *in vivo* (Figure 3C).

MRG proteins function through SDG8-mediated H3K36me3

Immunostaining using the nuclei of wild-type and *sdg8* mutant leaf cells showed that mutation of the *Arabidopsis* H3K36 methyltransferase *SDG8* leads to a near complete abolishment of H3K36me3 and a slight reduction in H3K36me2 (Figure 4A) (37,38). The double mutant with another close homologue of *SDG8*, *sdg7 sdg8* fully abol-

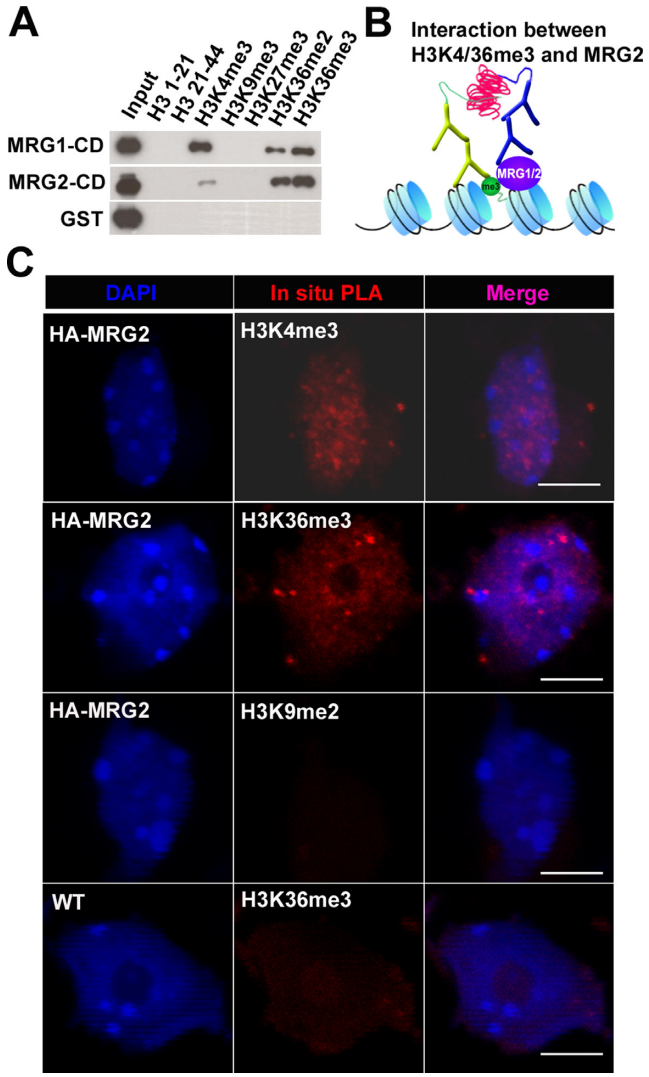

Figure 3. MRG2 directly binds to H3K36me3 *in vitro* and *in vivo*. (**A**) *In vitro* binding assay. Bacteria-expressed GST alone or GST-MRG1/2 chromodomains (MRG1-CD and MRG2-CD) were tested for binding to biotinylated unmodified histone H3 (H3 1–21 amino acid and H3 21–44 amino acid) or modified histone H3K4me3, H3K9me2, H3K27me3, H3K36me2 and H3K36me3 peptides immobilised on streptavidin-agarose. MRG1/2-CD were pulled down only by H3K4me3 and H3K36me2/3. GST was used as the negative control. (**B**) Schematic diagram showing *in situ* PLA assay between MRG2 and H3K4/36me3. (**C**) *In situ* PLA assay performed using anti-HA and anti-H3K4me3/H3K36me3 antibodies to show the interaction between HA-MRG2 and H3K4me3/H3K36me3. Blue, DAPI. Red, *in situ* PLA signals showing the interaction between HA-MRG2 and H3K4me3/H3K36me3. Purple, merge. Top two rows, *in situ* PLA assay using anti-HA and anti-H3K4me3/H3K36me3 antibodies in *pMRG2::HA-MRG2*; third row, *in situ* PLA assay between *pMRG2::HA-MRG2* and H3K9me2 as a negative control; bottom row, *in situ* PLA assay using anti-HA and anti-H3K36me3 antibodies in WT as a negative control. Scale bar, 5 μm.

ishes both the di- and tri-methylation marks at H3K36 (Figure 4A). In *sdg8* and *sdg7 sdg8, FLC* expression is almost fully abolished, suggesting that the H3K36me3 is essential for *FLC* expression (Figure 4B) (37). We found that H3K36me2, as in *Drosophila*, may function differently from H3K36me3 in *Arabidopsis*, because detectable, albeit dras-

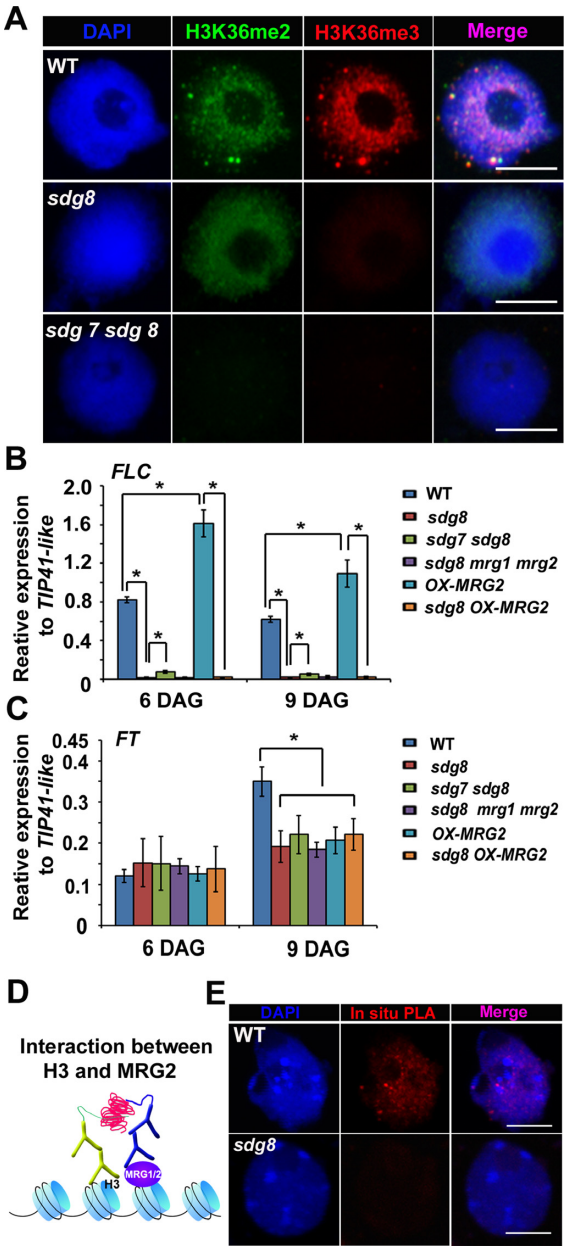

Figure 4. MRG1/2 function is dependent on H3K36me3. (**A**) Dual immunolocalisation of H3K36me2 and H3K36me3 in Col wild-type (WT, top panels), *sdg8* (middle panels) and *sdg7 sdg8* (bottom panels) nuclei. H3K36me2 (green) and H3K36me3 (red) were detectable using the respective antibodies in WT but not in *sdg7 sdg8*, whilst *sdg8* could still retain a reduced level of H3K36me2. Blue, DAPI. Scale bar, 5 μm. (B-C) RT-qPCR of *FLC* (**B**) and *FT* (**C**) expression in Col WT, *sdg8*, *sdg7 sdg8, sdg8 mrg1 mrg2, 35S::MRG2-HA* (*OX-MRG2*) and *sdg8 OX-MRG2*. Error bars indicate SD of three biological replicates. *$P < 0.05$ between *FLC* expression in Col WT and *sdg8*, *sdg8* and *sdg7 sdg8*, *OX-MRG2* and *sdg8 OX-MRG2*, Col WT and *OX-MRG2* at both 6 DAG and 9 DAG with Student's *t*-test. *$P < 0.05$ between *FT* expression in Col WT and other genotypes including *sdg8*, *sdg7 sdg8*, *sdg8 mrg1 mrg2*, *OX-MRG2* and *sdg8 OX-MRG2* at 9 DAG only. (**D**, **E**) The interaction between MRG2 and histone H3 is dependent on H3K36me3. Schematic diagram for *in situ* PLA assay between MRG2 and histone H3 (D). *In situ* PLA assay using anti-HA and anti-H3 antibodies in *pMRG2::HA-MRG2* WT showed positive signals (upper panels in E), whilst *in situ* PLA assay with *pMRG2::HA-MRG2 sdg8* showed no signals (lower panels in E). Scale bar, 5 μm. Blue, DAPI. Red, *in situ* PLA signals showing the interaction between HA-MRG2 and histone H3. Purple, merge.

tically reduced *FLC* expression was observed in *sdg7 sdg8* (Figure 4B) (47). Whilst *FLC* expression is reduced dramatically in *sdg8* mutant seedlings as well as in *sdg7 sdg8* at both DAG 6 and 9 (Figure 4B), the *FT* transcript is reduced to half at 9 DAG but not affected at 6 DAG in either *sdg8* or *sdg7 sdg8* (Figure 4C). These expression profiles of *FT* are similar to those observed in the *mrg1 mrg2* mutant (Figure 1E), suggesting that the SDG H3K36 methyltransferases and MRG proteins may function in the same pathway to regulate *FT*.

To test if the function of MRG1 and MRG2 requires H3K36 methylation, we performed genetic analyses. As the effects on *FLC* and *FT* in *sdg8* are as severe as those in *sdg7 sdg8*, we used the *sdg8* single mutant. In the *sdg8 mrg1 mrg2* triple mutant background, *FT* and *FLC* expression levels are similar to those in the *sdg8* single mutant (Figure 4B and C). This indicates that the function of *MRG1* and *MRG2* in flowering time control are dependent on *SDG8*-mediated H3K36me3. Overexpression of *MRG2* under the constitutive Cauliflower Mosaic Virus *p35S* promoter causes increased expression of *FLC* (∼2 and 1.5-folds in 6 and 9 DAG, respectively) and decreased expression of *FT* at 9 DAG (∼1.7-folds) (Figure 4B and C), leading to a late-flowering phenotype (Supplementary Figure S5). However, *35S::MRG2-HA* failed to affect the *FLC* transcript or flowering time in the *sdg8* mutant background (Figure 4B and Supplementary Figure S5), further confirming that the function of *MRG2* is dependent on SDG8. *FLC* reduction is more pronounced in *sdg8* than in *mrg1-1 mrg2-2* (Figures 1E and 4B), suggesting that H3K36me3 may have different effect in *FT* and *FLC* expression. It is possible that additional readers other than the MRG proteins, e.g. the PHD finger proteins, may prevent further down-regulation of *FLC* expression in *mrg1 mrg2* (48,49), and/or other H3K36me3-independent factors may maintain certain *FT* transcription level in *sdg8* and *mrg1 mrg2* (37,50–52).

Next, we tested whether the interaction of MRG proteins and histone H3 is dependent on H3K36me3 *in vivo*. We carried out the *in situ* PLA assay with antibodies for HA and histone H3 using *pMRG2::HA-MRG2* transgenic plants in the wild-type and *sdg8* mutant backgrounds. We observed positive signals that showed histone H3-MRG2 interaction in the wild-type background (Figure 4D and E). But the signals were abolished by the mutation of *sdg8* (Figure 4E), in which H3K36me3 is greatly decreased, whilst H3K4me3 and H3K36me2 are not changed or only moderately decreased (Figure 4A) (53,54), suggesting that MRG2 binding to histone H3 requires the H3K36me3 mark, whilst H3K4me3 and H3K36me2 are not sufficient to recruit MRG2 to histone H3 *in vivo*.

MRG2 directly binds to *FT* genomic regions

FT expression is controlled by CONSTANS (CO) and several other genes, including some histone modifiers involved in the activation and repression along the light-dark phase change (55). We next examined how MRG1 or MRG2 regulates *FT* expression during LD conditions. Taking samples from the aerial part of seedlings at 9 DAG, we showed that *FT* expression in *mrg1 mrg2* is decreased to approximately half at ZT 16 (the highest *FT* expression) and at most tested time points (Figure 5A). Interestingly, even at ZT 0 and ZT 24, at which the *FT* expression is at the lowest level during the entire light-dark cycle, the *FT* expression level in *mrg1 mrg2* is further reduced compared to WT (Figure 5A). In contrast, the *FT* expression level at 6 DAG did not show any obvious change between *mrg1 mrg2* and WT (Figure 1E). These results suggest that MRG1/2-mediated up-regulation may require pre-existing active transcription and the accumulation of the transcription-linked H3K36me3 mark to a certain level and that MRG1 and MRG2 may function continuously during the entire light-dark cycle once they have started.

To check if MRG2 directly regulates *FT* expression, we carried out ChIP assay with 9 DAG seedlings harvested at ZT16 and ZT24, in which *FT* expression is at the highest level and lowest level during the light-dark cycle, respectively. In both samples, the enrichment was detected in the regions of the promoter (*FT-P*) and exon 1 (*FT-E1*) but not in the region around intron 1 (*FT-I1*) (Figure 5B–D). Whilst the enrichment at ZT 16 is slightly higher than that ZT24, the difference is not so statistically significant. These results suggest that MRG2 directly binds to the *FT* locus throughout the day and night.

MRG2 interacts with HATs to induce H4 acetylation

We next compared the histone acetylation levels of histone H3 (H3Ace) and histone H4K5 (H4K5Ace), and the activation marks of H3K4me3 and H3K36me3 between WT and *mrg1 mrg2* seedlings (Figure 6A–C, Supplementary Figure S6A–C). For ease of sampling, we harvested the seedlings at 10 DAG and tested the histone modification at the *FT* locus. Interestingly, whilst the levels of H3K36me3 were not obviously changed in *mrg1 mrg2* (Figure 6B), the H3K4me3 levels were clearly reduced in all tested primers at the promoter, exon 1 and intron 1 (Supplementary Figure S6B). Both the levels of H3Ace and H4K5Ace were decreased in *mrg1 mrg2* compared to WT at the regions around the promoter and exon 1, but not at the intron 1 of the *FT* locus (Figure 6C, Supplementary Figure S6C), suggesting that the function of *MRG1* and *MRG2* in *Arabidopsis* is mediated through histone acetylation, and possibly H3K4me3. When we compared the distribution patterns of these histone modifications, H3K36me3 and H4K5Ace levels were peaked at the exon 1, whilst H3Ace and H3K4me3 showed higher levels at the promoter (Figure 6D). Thus, we checked the possible interaction between MRG1/2 and MYST HATs, HAM1/2 proteins, that catalyse H4K5Ace (33,34). First, we carried out bimolecular fluorescence complementation (BiFC) assay by transiently co-expressing a translational fusion of MRG1/2 to the N-terminal portion of YFP (MRG1/2-nYFP) and fusion of HAM1/2 to the C-terminal portion of YFP (HAM1/2-cYFP) in tobacco. We were able to detect fluorescence signal in the nuclei of tobacco epidermal cells whilst the control (MRG1/2-nYFP and vector cYFP, vector nYFP and HAM1/2-cYFP) did not show any signals, suggesting that the observed BiFC between MRG1/2-nYFP and HAM1/2-cYFP are specific (Supplementary Figure S7). In addition, using a rabbit antibody against both HAM1 and HAM2, together with the

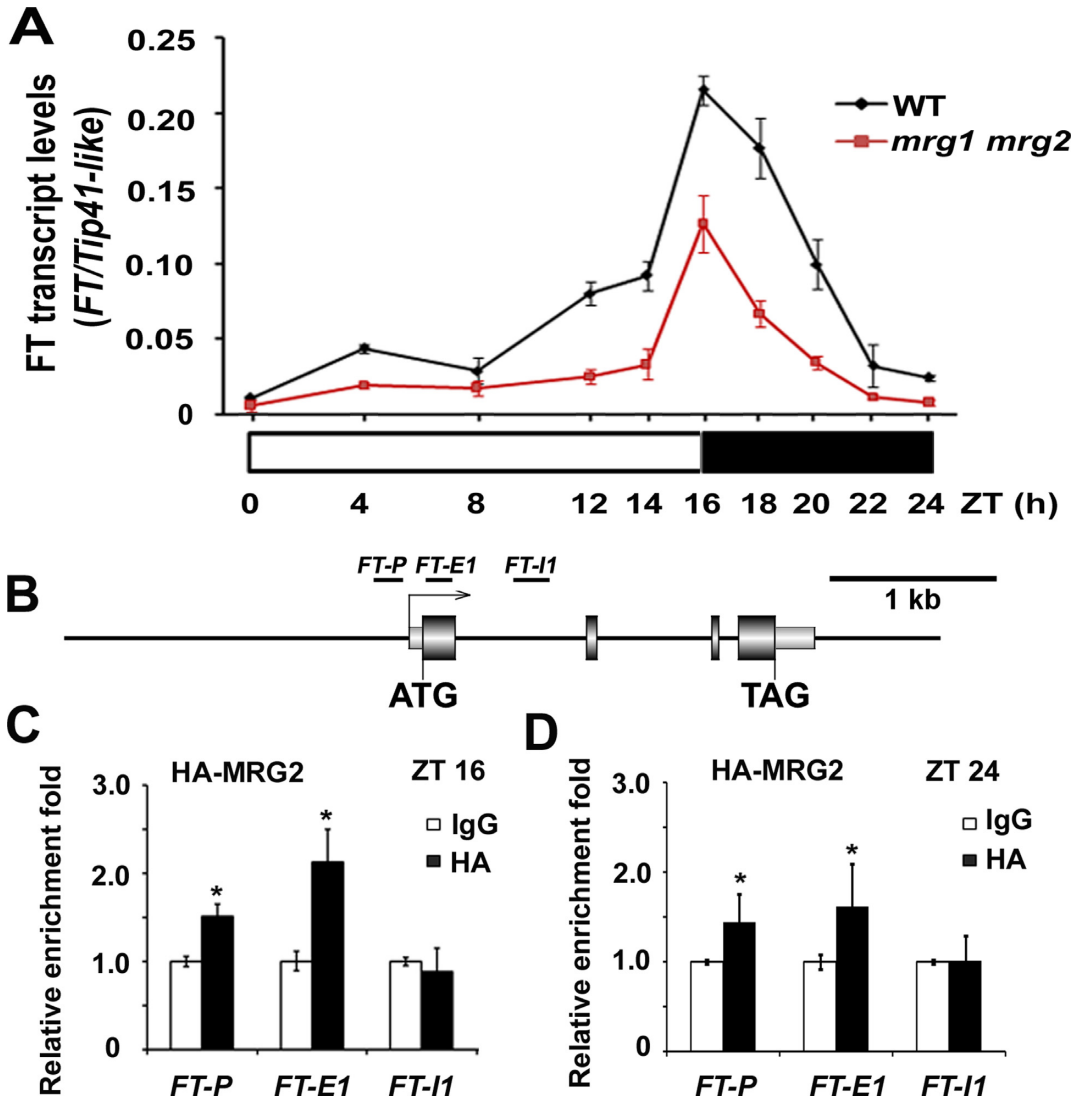

Figure 5. MRG2 binds directly to the *FT* locus. (**A**) *FT* mRNA levels in Col WT and *mrg1-1 mrg2-2* seedlings over a 24-h LD cycle. *FT* transcript levels were normalised to *Tip41-like*; bars indicate SD of triplicate measurements. White and dark bars below the x-axis indicate light and dark periods, respectively. One of two biological repeats with similar trends was shown. (**B**) Schematic drawing of the *FT* genome structure showing regions amplified by primers used for ChIP analysis. (**C–D**) ChIP analysis of HA-MRG2 enrichment at the *FT* locus at (C) ZT16 and (D) ZT24 with the *pMRG2::HA-MRG2* transgenic line. Amounts of the immunoprecipitated genomic fragments were measured by qPCR and normalised first to the endogenous control *ACTIN2 (ACT2)*. The fold enrichment of HA-MRG2 in each examined region was calculated by dividing the *ACT2*-normalised amount of the examined region from the sample with the anti-HA antibody by that with mouse IgG. Error bars indicate SD of six quantifications (three technical measurements of two biological replicates). *$P < 0.05$ with Student's *t*-test.

mouse HA antibody against HA-MRG2, we performed an *in situ* PLA assay. We detected positive signals, further indicating the direct interaction between MRG2 and HAM1/2 (Figure 7A and B). Furthermore, we prepared and transformed the genomic DNA fusion construct of *HAM*1 with HA inserted just after its ATG into *35S::GFP-MRG2* or wild-type plants. We performed Co-IP using the seedlings of *pHAM1::HA-HAM1 35S::GFP-MRG2*, with the seedling of *pHAM1::HA-HAM1* as the control. Indeed, anti-GFP antibody immunoprecipitated HA-HAM1 from the seedlings but not in the negative control with HA-HAM1 alone (Figure 7C). These results suggest that MRG proteins interact with HAM1/2 to induce histone H4 acetylation at the target loci that contained H3K36me3 (Figure 7D).

DISCUSSION

In this study, we have shown that *Arabidopsis MRG15* homologues *MRG1* and *MRG2* function redundantly to stimulate the amplitude of expression of the flowering time genes *FT* and *FLC* in an H3K36me3-dependent manner. Due to the epistatic relationship between *FLC* and *FT*, the mutant shows late-flowering phenotype, caused by *FT* reduction.

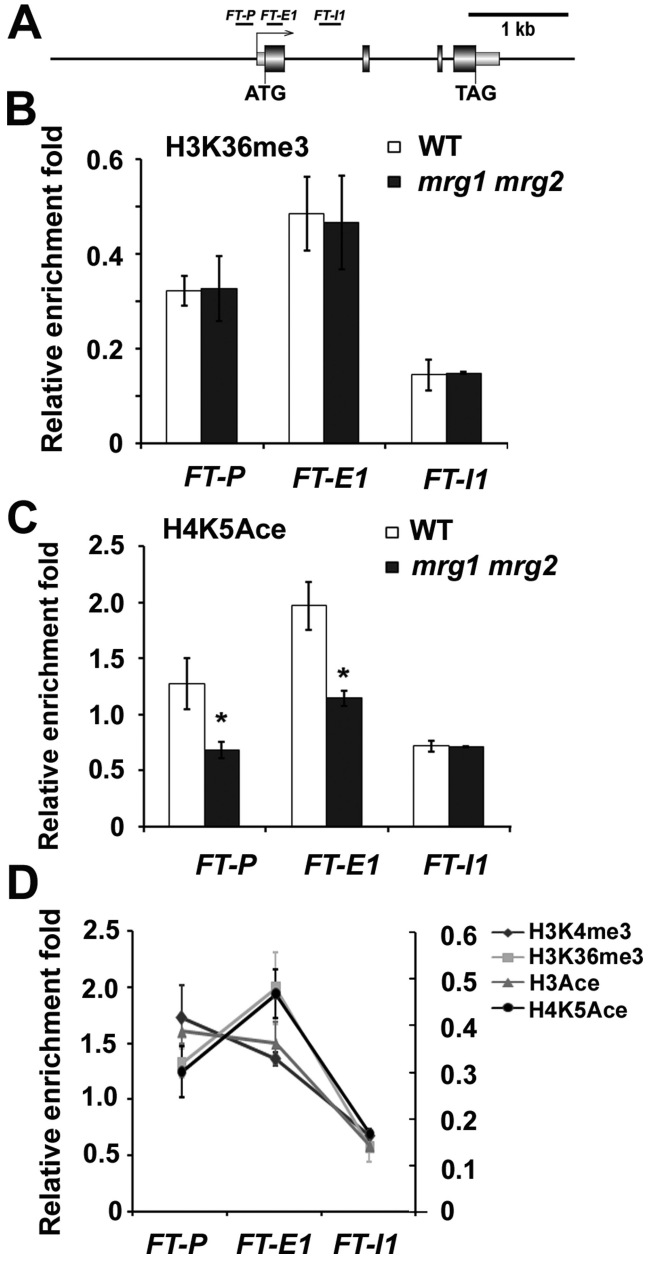

Figure 6. MRG1/2 maintain histone acetylation levels of the *FT* locus to ensure the high transcriptional level. (**A**) Schematic drawing of the *FT* genome structure showing regions amplified by primers used for ChIP analyses. (**B**, **C**) ChIP analyses of H3K36me3 (B), H4K5Ace (C). Enrichment at the *FT* locus in 10 DAG Col WT and *mrg1-1 mrg2-2* seedlings grown under LD 23°C. Amounts of the immunoprecipitated genomic fragments were measured by qPCR and normalised to the endogenous control *ACTIN2 (ACT2)*. White, WT; black, *mrg1 mrg2*. Bar indicates SD of six measurements (three measurements of two biological replicates) **P* < 0.05 with Student's *t*-test. (**D**) The distribution pattern of H3K4me3, H3K36me3, H3Ace and H4K5Ace in WT. Left Y-axis indicates relative enrichment fold of H3K4me3 and H4K5Ace, whilst right Y-axis indicates relative enrichment fold of H3K36me3 and H3Ace. It is based on the ChIP assays shown in B (for H3K36me3), C (for H4K5Ace) and Supplementary Figure S6B (for H3K4me3), S6C (for H3Ace).

MRG1/2 bridges H3K36me3 and histone acetylation to achieve higher levels of flowering gene expression

Two flowering time genes, *FT* and *FLC*, with the opposing functions in floral transition, are down-regulated in mutant *mrg1 mrg2* (Figure 1E, Supplementary Figure S2F). It is not uncommon that one epigenetic regulation controls these two genes with opposing functions. For example, PRC2-like complex, including H3K27 methyltransferases CURLY LEAF (CLF) and SWINGER (SWN), deposits H3K27me3 at both *FLC* and *FT* to repress its expression (56,57). *FT* expression levels are similarly reduced in *sdg8, mrg1 mrg2* and *sdg8 mrg1 mrg2* at 9 DAG (Figures 1E and 4C), which support the idea that MRG proteins function in the same pathway as H3K36 methyltransferase SDG8. One paradox was why the *sdg8* mutant showed an early flowering phenotype (37) despite reduced expression of *FT* at 9 DAG. It could be caused by a significant reduction of *FLC* or increased *FT* expression at later time points. We found that *FT* was indeed increased at 12 DAG for an unknown reason (Supplementary Figure S8). Such up-regulation of the *FT* transcript appears to be independent of *MRG1/2* because the early flowering phenotype of *sdg8* is epistatic to the overexpression of *MRG2* (Supplementary Figure S5). Our other genetic data of *sdg8 mrg1 mrg2* also suggested that *sdg8* is epistatic to *mrg1 mrg2* in flowering control. These data do not contradict the model that MRG1 and MRG2 bind to SDG8-mediated-H3K36me3 and function through the mark to control downstream activities.

The *sdg8* mutation has different locus-specific effects on gene expression (54,58,59). Whilst the transcription of *FT* in 9 DAG is similarly impaired in *sdg8* and *mrg1 mrg2* mutant plants (Figures 1E and 4C), the *sdg8* mutation has a drastic effect on *FLC* expression compared with *mrg1 mrg2* mutation (Figures 1E and 4B). It is of note that H3K27me3 coexists with H3K4me3 at the 5′-end nucleosome of *FLC* (50). As H3K36me2/3 were reported to inhibit PcG-mediated repressive mark H3K27me3 (51,52), it is possible that the loss of H3K36me3 (Figure 4A), and also the dramatic reduction of H3K36me2 level at the *FLC* locus (37), lead to the spreading or increased level of H3K27me3 at the *FLC* region, thus greatly reducing *FLC* expression. However, it is interesting to note that *FT* chromatin also has a bivalent structure, simultaneously carrying the active H3K4me3 and repressive H3K27me3 marks (56,57). Thus, it is likely that the different levels of H3K4me3 on *FLC* and *FT* regions, which is also responsible to prevent H3K27me3 (51), determine the different effects of *sdg8* mutation on *FT* and *FLC* expression. This speculation requires further detailed study in the dynamic change of epigenetic mark in inducible rescue lines.

MRG proteins directly bind to HAM1/2 acetyltransferase and bridge the two histone modifications, H3K36me3 and H4 acetylation (Figures 6 and 7, Supplementary Figure S7). The *ham1 ham2* double mutant is not viable, and the single mutation of either *ham1* or *ham2* did not show any defects in the vegetative and reproductive stages (32). Interestingly, *ham1/+ ham2/+* and RNAi knockdown plants showed the reduction in *FLC* expression levels, as observed in *mrg1 mrg2,* and both overexpression of *HAM1* and *MRG2* caused late flowering phenotype with the increased

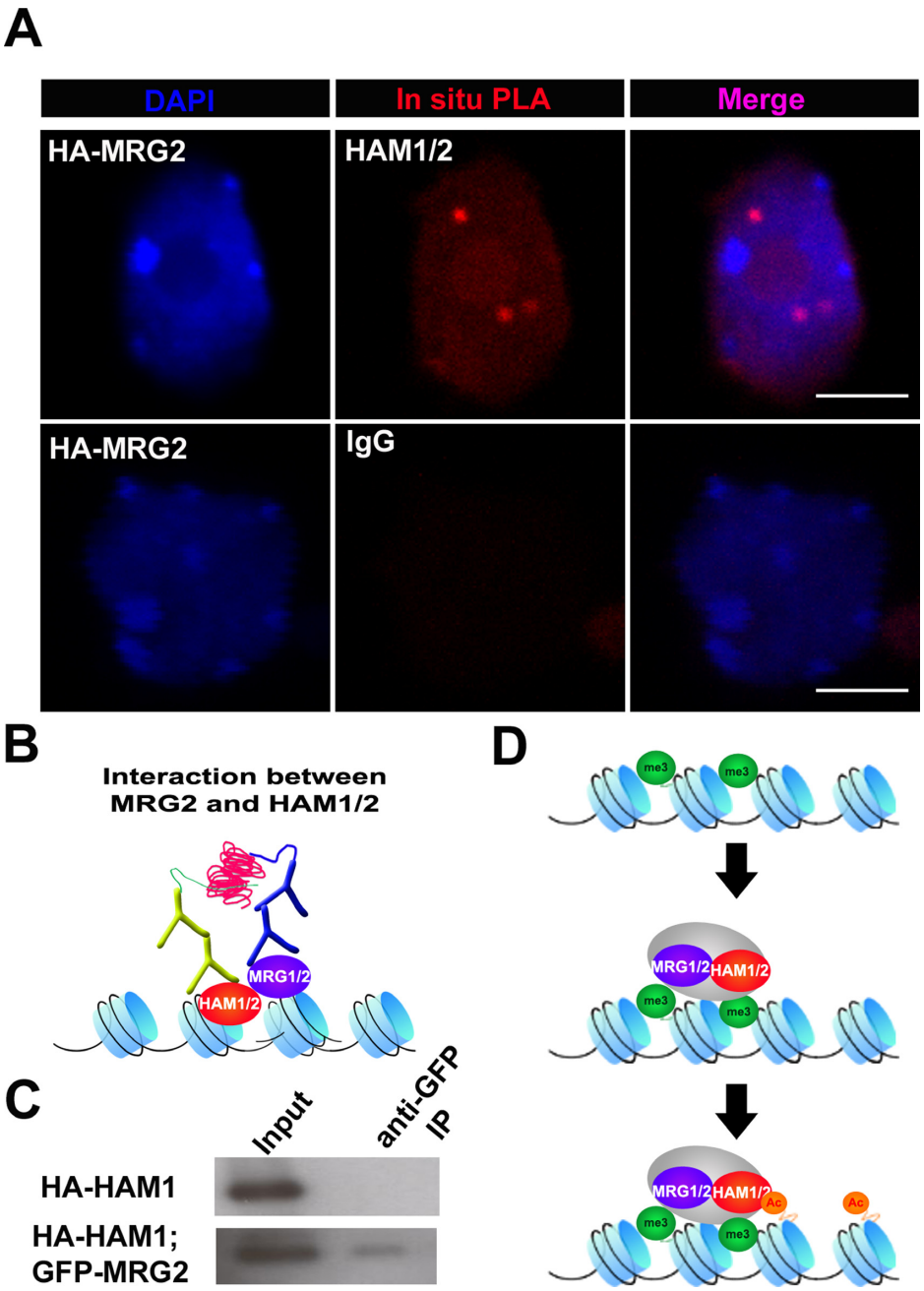

Figure 7. MRG1/2 recruits HAM1/2 to their targeted loci. (**A**) *In situ* PLA assay to show the interaction between MRG2 and HAM1/2. Blue, DAPI. Red, *in situ* PLA signal showing the interaction between HA-MRG2 and HAM1/2 (upper panels); the assay between HA-MRG2 and rabbit IgG was carried out as the negative control (lower panels). Purple, merge. Scale bar, 5 μm. (**B**) Schematic diagram for *in situ* PLA assay between MRG2 and HAM1/2. (**C**) Co-IP assay to show the interaction between MRG2 and HAM1. Total protein extracted from 10 DAG seedlings co-expressing *HA-HAM1* and *GFP-MRG2* or solely expressing *HA-HAM1* (as the negative control), were subjected to immunoprecipitation with anti-GFP antibody. HA-HAM1 protein in the immunoprecipitates was detected by western blotting using anti-HA-HRP antibody. (**D**) A working model for the control of the target genes by MRG1/2 through the recruitment of HAM1/2-containing complex to increase the histone acetylation level at the target loci.

FLC transcription (Figures 1E and 4B and Supplementary Figure S5) (32,34). These results suggest that the MRG proteins and the HAM acetyltransferases function together to regulate *FLC*.

We showed that the approximately 2-fold reduction of *FT* expression is correlated with a reduced level of H4K5Ace at the 5′ region of the *FT* locus in *mrg1 mrg2* seedlings (Figure 6C). In addition to H4K5Ace, we showed that the level of H3Ace is also decreased at the *FT* locus in the *mrg1 mrg2* mutant (Supplementary Figure S6C). As MYST family proteins specifically catalyse histone H4 acetylation, H4K5Ace may help to recruit other histone acetyltransferases to amplify the effect of histone acetylation in different histones. The similar distribution pattern between H3K36me3 and H4K5Ace but not with H3Ace or H3K4me3 on the *FT* locus also indicates that the change of H4K5Ace level could

be the direct effect of *mrg1 mrg2* mutation (Figure 6A–D, Supplementary Figure S6A–C). Further experiments using the inducible line of *MRG1/2* in the *mrg1 mrg2* mutant could provide a suitable system to check the sequential steps of histone modifications.

FT expression is controlled by CO in a rhythmic pattern in LD conditions (55). Whilst several genes, including some histone modifiers, are required for the activation and repression of *FT* along the light-dark phase change. Newly identified *SAP30 FUNCTION-RELATED 1/2* (*AFR1/2*) only represses *FT* transcription at ZT 16, at the end of the light photoperiod (60). *FT* transcription is first detectable in seedlings at 4 DAG and dramatically increases at approximately 9–10 DAG during the floral transition (45). It is interesting to note that at 6 DAG, we were unable to detect a difference in *FT* transcription levels between the seedlings of WT and *mrg1 mrg2* plants suggesting MRG1/2 function is dispensable for *FT* expression at the early developmental stage (Figure 1E). Such a difference is only detectable at later stages such as 9 DAG (Figure 1E). This suggests that, upon reaching a certain developmental stage (between 6 and 9 DAG), MRG1 and MRG2 begin acting on the *FT* locus, which then on affect *FT* expression throughout the day and night (Figure 5), unlike AFR1/2 which only regulates *FT* expression at ZT 16. MRG2 binding to H3K36me3 (Figure 3A–C) and the unaffected *FT* expression at 6 DAG suggest that the activating H3K36me3 epigenetic mark may need time to accumulate to recruit MRG1/2-containing complex to fine-tune transcription. The continuous binding of MRG2 to the *FT* locus during the light-dark cycle (Figure 5B–D) suggests that H3K36me3 is relatively stable throughout the day and night.

Conservation and divergence of plant MRG protein functions

Similar to its homologous MRG15 proteins, *in vivo* and *in vitro* assays confirmed that MRG1 and MRG2 can bind to H3K36me3. The MRG15 family proteins are evolutionarily conserved in yeast and animals, and the chromodomains of MRG15 and Eaf3 bind to trimethylated H3K36 and H3K4 *in vitro* with a relatively weak affinity (2–4,14–16). Consistently, we found that the binding specificity of plant MRG15 homologues to H3K36me3 is also relatively conserved during evolution. An *in vitro* pull-down assay showed that the chromodomain of MRG1/2 directly binds to trimethylated H3K36 as well as H3K4me3, but the binding affinity is relatively weak (Figure 3A). Yeast Eaf3 has been reported to interact with other protein partners (e.g. PHD proteins) and shows a wide range of binding strength (from unstable to robust) to H3K36-methylated nucleosomes, which suggests that the combinatorial action of Eaf3 and PHD proteins strengthens the binding affinity (61). It is likely that other chromatin- or DNA-binding proteins also help MRG proteins in binding to their target loci with higher affinity *in vivo*. Alternatively, such weak affinity may allow MRG-containing complexes to spread histone acetylation across the target loci, as implicated in the dosage compensation complex (62).

Although the *in vitro* data showed that the chromodomain of MRG2 can bind to both H3K4me3 and H3K36me3 (Figure 3A), the *in situ* PLA assay suggested that MRG2 binds to H3K36me3 specifically *in vivo* because the binding of MRG2 is completely abolished in the *sdg8* mutant, in which H3K36me3 is dramatically reduced, but H3K36me2 is still maintained albeit at a reduced level and H3K4me3 is intact (Figure 4A, D and E)(53,54). These data indicate that H3K36me3 is essential for MRG protein binding *in vivo*.

Whilst the human MRG15 and yeast Eaf3 are involved in both HATs and HDACs, most studies focus on the defects of its HDAC function because this effect is more obvious and the mutation effect is more severe (2–4,18–20). For example, in yeast, the deletion of *Eaf3* greatly alters the global genomic profile of histone acetylation, with increased acetylation levels at coding sequences and decreased acetylation levels at the promoter regions (21). However, these studies were rather focused on the function of Eaf3 binding to coding regions, recruiting an HDAC complex to H3K36me3-containing nucleosomes and thus prevents spurious intragenic transcription (2–4). Moreover, the loss of *Alp13*, the *MRG15* homologue in fission yeast, causes global hyperacetylation of histones and chromosome instability (22). Thus, the function of MRG15 and its homologues associated with HATs was overlooked, partly because the loss of the MRG mutants causes phenotypes that are more linked with elevated histone acetylation on a gene-specific level or globally.

The interaction between MRG1/2 and MYST family proteins HAM1/2, characterised by an *in situ* PLA assay, BiFC assay and Co-IP analysis (Figure 7A–C, Supplementary Figure S7), confirmed the protein interaction between MRG1/2 and HATs. Whilst we could detect the interaction between MRG2 and HDA6 when transiently co-overexpressed in tobacco (Supplementary Figure S9), the resulting effects with the locus-specific decreased acetylation suggested that *MRG1* and *MRG2* could have diversified from its homologues in animal and yeast and primarily function in the fine-tuning of transcription regulation associated with HATs. It is possible that MRG1/2 proteins recruit both HAT and HDAC dynamically, and loss-of-function of *mrg1 mrg2* leads to the disruption of a balance between these two counteracting activities, resulting in the reduction of histone acetylation levels and transcription. In human T cells, genome-wide mapping of HATs and HDACs binding showed that regions enriched with both HATs and HDACs are linked with active genes (63). They showed that in both active genes and primed genes (genes poised for expression later), inhibition of HDAC activity causes increased acetylation level at the promoter regions (63), rather than the reduced acetylation level we observed in *mrg1 mrg2* (Figure 6C, Supplementary Figure S6C). In addition, at active gene loci, HDAC physically interacts with the elongating form of RNA Pol II and is directly recruited to actively transcribed regions by RNA Pol II, which may bypass the need for H3K36me3 (63). Moreover, the histone deacetylase HDA6 in *Arabidopsis* is recruited to remove acetylated histone marks at the *FT* locus specifically at dusk under long-day conditions, thereby dampening *FT* mRNA expression after its transcriptional activation by CO. Mutation of the HDAC recruiter increases the histone acetylation level at the *FT* locus (60). As pertubation of HDAC generally leads to increased histone acetylation levels, the opposite effect of

the reduction of histone acetylation level at the *FT* locus in *mrg1 mrg2* mutant suggests that the function of MRG1/2 on *FT* is majorly dependent on its interaction with HATs.

The loss-of-function of *MRG1* and *MRG2* causes an approximately 2-fold decrease in the expression levels, together with the reduction of the histone acetylation levels at their target genes. It can be argued that the decreased *FT* expression is due to the decreased H3K4me3 and H3Ace. Although we have shown that H3K36me3 is essential for MRG2 binding to chromatin (Figure 4E), it is still possible that H3K4me3 is also necessary for MRG2-dependent expression of *FT*, as transcriptional regulation is mediated by complex cross-talk of multiple histone modifications. However, based on our results that MRG1/2 can form complex with the HATs specific for H4, HAM1/2, *in vitro* and *in vivo* (Figure 7 and Supplementary Figure S7) and co-localisation between H3K36me3 and H4 acetylation at the promoter region (Figure 6D), we favour the hypothesis that the binding of MRG proteins to H3K36me3 leads to the H4 acetylation for transcriptional induction and that the reduction of H3K4me3 and H3Ace levels in *mrg1 mrg2* could be the secondary effects of transcription reduction. This suggests that the MRG1/2 functions resemble the dosage compensation complex in *Drosophila* that contains MSL3 (MRG protein not belonging to the MRG15 subfamily) and MOF (MYST family HAT) (64,65). The binding of MRG2 to H3K36me3 at the target loci could facilitate the spread of histone acetylation through the recruitment of the MRG2-containing HAT complex, in a similar manner as the MSL3-containing dosage compensation complex (64,65).

In *Arabidopsis*, H3K36me3 co-localises with other activation marks, including H3K4me3 and H3K56Ace, at the active chromatin (6). This simultaneous occurrence of multiple epigenetic marks has no equivalent in *Drosophila, C. elegans* and humans (6). Moreover, in *Arabidopsis*, H3K36me3 peaks in the 5′-end of the coding region, which is in contrast to the 3′-end enrichment in other organisms (6). MRG1 and MRG2 may be involved in the association of H3K36me3 and histone acetylation marks. Indeed, at the *FT* locus, H4K5Ace distribution pattern is similar to that of H3K36me3 peaking at the 5′-end of the coding region (Figure 6D). Such a difference of the distribution pattern of H3K36me3 between plants and other organisms may be a result of co-evolution with the functional diversification of MRG15 proteins.

SUPPLEMENTARY DATA

Supplementary Data are available at NAR Online.

ACKNOWLEDGEMENT

We thank Aiwu Dong for communication on the *mrg2-1* mutant and for research discussion.
Author Contributions. T.I. conceived of the study, supervised and coordinated the study. Y.X., E.-S.G. J.Z. and T.I. designed the experiments. Y.X., E.-S.G. and W.-Y.W. performed the ChIP experiments, immunolocalisation analysis, *in situ* PLA assays and the microarray studies. Y.X., J.Z. and W.-Y.W. performed the genetic analysis. Y.X. and T.I. wrote the manuscript. All authors discussed the results and approved the final manuscript.

FUNDING

Temasek Life Sciences Laboratory (TLL) [to T.I.]; National Research Foundation Singapore under its Competitive Research Program [CRP Award No. NRF-CRP001-108].
Conflict of interest statement. None declared.

REFERENCES

1. Kolasinska-Zwierz,P., Down,T., Latorre,I., Liu,T., Liu,X.S. and Ahringer,J. (2009) Differential chromatin marking of introns and expressed exons by H3K36me3. *Nat. Genet.*, **41**, 376–381.
2. Carrozza,M.J., Li,B., Florens,L., Suganuma,T., Swanson,S.K., Lee,K.K., Shia,W.J., Anderson,S., Yates,J., Washburn,M.P. *et al.* (2005) Histone H3 methylation by Set2 directs deacetylation of coding regions by Rpd3S to suppress spurious intragenic transcription. *Cell*, **123**, 581–592.
3. Joshi,A.A. and Struhl,K. (2005) Eaf3 chromodomain interaction with methylated H3-K36 links histone deacetylation to Pol II elongation. *Mol. Cell*, **20**, 971–978.
4. Keogh,M.C., Kurdistani,S.K., Morris,S.A., Ahn,S.H., Podolny,V., Collins,S.R., Schuldiner,M., Chin,K., Punna,T., Thompson,N.J. *et al.* (2005) Cotranscriptional set2 methylation of histone H3 lysine 36 recruits a repressive Rpd3 complex. *Cell*, **123**, 593–605.
5. Luco,R.F., Pan,Q., Tominaga,K., Blencowe,B.J., Pereira-Smith,O.M. and Misteli,T. (2010) Regulation of alternative splicing by histone modifications. *Science*, **327**, 996–1000.
6. Roudier,F., Ahmed,I., Berard,C., Sarazin,A., Mary-Huard,T., Cortijo,S., Bouyer,D., Caillieux,E., Duvernois-Berthet,E., Al-Shikhley,L. *et al.* (2011) Integrative epigenomic mapping defines four main chromatin states in Arabidopsis. *EMBO J.*, **30**, 1928–1938.
7. Marin,I. and Baker,B.S. (2000) Origin and evolution of the regulatory gene male-specific lethal-3. *Mol. Biol. Evol.*, **17**, 1240–1250.
8. Bertram,M.J. and Pereira-Smith,O.M. (2001) Conservation of the MORF4 related gene family: identification of a new chromo domain subfamily and novel protein motif. *Gene*, **266**, 111–121.
9. Berger,S.L. (2007) The complex language of chromatin regulation during transcription. *Nature*, **447**, 407–412.
10. Jacobs,S.A. and Khorasanizadeh,S. (2002) Structure of HP1 chromodomain bound to a lysine 9-methylated histone H3 tail. *Science*, **295**, 2080–2083.
11. Nielsen,P.R., Nietlispach,D., Mott,H.R., Callaghan,J., Bannister,A., Kouzarides,T., Murzin,A.G., Murzina,N.V. and Laue,E.D. (2002) Structure of the HP1 chromodomain bound to histone H3 methylated at lysine 9. *Nature*, **416**, 103–107.
12. Min,J., Zhang,Y. and Xu,R.M. (2003) Structural basis for specific binding of Polycomb chromodomain to histone H3 methylated at Lys 27. *Genes Dev.*, **17**, 1823–1828.
13. Fischle,W., Wang,Y., Jacobs,S.A., Kim,Y., Allis,C.D. and Khorasanizadeh,S. (2003) Molecular basis for the discrimination of repressive methyl-lysine marks in histone H3 by Polycomb and HP1 chromodomains. *Genes Dev.*, **17**, 1870–1881.
14. Sun,B., Hong,J., Zhang,P., Dong,X., Shen,X., Lin,D. and Ding,J. (2008) Molecular basis of the interaction of Saccharomyces cerevisiae Eaf3 chromo domain with methylated H3K36. *J. Biol. Chem.*, **283**, 36504–36512.
15. Xu,C., Cui,G., Botuyan,M.V. and Mer,G. (2008) Structural basis for the recognition of methylated histone H3K36 by the Eaf3 subunit of histone deacetylase complex Rpd3S. *Structure*, **16**, 1740–1750.
16. Zhang,P., Du,J., Sun,B., Dong,X., Xu,G., Zhou,J., Huang,Q., Liu,Q., Hao,Q. and Ding,J. (2006) Structure of human MRG15 chromo domain and its binding to Lys36-methylated histone H3. *Nucleic Acids Res.*, **34**, 6621–6628.
17. Leung,J.K., Berube,N., Venable,S., Ahmed,S., Timchenko,N. and Pereira-Smith,O.M. (2001) MRG15 activates the B-myb promoter through formation of a nuclear complex with the retinoblastoma protein and the novel protein PAM14. *J. Biol. Chem.*, **276**, 39171–39178.
18. Pardo,P.S., Leung,J.K., Lucchesi,J.C. and Pereira-Smith,O.M. (2002) MRG15, a novel chromodomain protein, is present in two distinct multiprotein complexes involved in transcriptional activation. *J. Biol. Chem.*, **277**, 50860–50866.

19. Allard,S., Utley,R.T., Savard,J., Clarke,A., Grant,P., Brandl,C.J., Pillus,L., Workman,J.L. and Cote,J. (1999) NuA4, an essential transcription adaptor/histone H4 acetyltransferase complex containing Esa1p and the ATM-related cofactor Tra1p. *EMBO J.*, **18**, 5108–5119.
20. Eisen,A., Utley,R.T., Nourani,A., Allard,S., Schmidt,P., Lane,W.S., Lucchesi,J.C. and Cote,J. (2001) The yeast NuA4 and Drosophila MSL complexes contain homologous subunits important for transcription regulation. *J. Biol. Chem.*, **276**, 3484–3491.
21. Reid,J.L., Moqtaderi,Z. and Struhl,K. (2004) Eaf3 regulates the global pattern of histone acetylation in Saccharomyces cerevisiae. *Mol. Cell. Biol.*, **24**, 757–764.
22. Nakayama,J., Xiao,G., Noma,K., Malikzay,A., Bjerling,P., Ekwall,K., Kobayashi,R. and Grewal,S.I. (2003) Alp13, an MRG family protein, is a component of fission yeast Clr6 histone deacetylase required for genomic integrity. *EMBO J.*, **22**, 2776–2787.
23. Chen,E.S., Zhang,K., Nicolas,E., Cam,H.P., Zofall,M. and Grewal,S.I. (2008) Cell cycle control of centromeric repeat transcription and heterochromatin assembly. *Nature*, **451**, 734–737.
24. Reid,J.L., Iyer,V.R., Brown,P.O. and Struhl,K. (2000) Coordinate regulation of yeast ribosomal protein genes is associated with targeted recruitment of Esa1 histone acetylase. *Mol. Cell*, **6**, 1297–1307.
25. Vogelauer,M., Wu,J., Suka,N. and Grunstein,M. (2000) Global histone acetylation and deacetylation in yeast. *Nature*, **408**, 495–498.
26. Boudreault,A.A., Cronier,D., Selleck,W., Lacoste,N., Utley,R.T., Allard,S., Savard,J., Lane,W.S., Tan,S. and Cote,J. (2003) Yeast enhancer of polycomb defines global Esa1-dependent acetylation of chromatin. *Genes Dev.*, **17**, 1415–1428.
27. Dombecki,C.R., Chiang,A.C., Kang,H.J., Bilgir,C., Stefanski,N.A., Neva,B.J., Klerkx,E.P. and Nabeshima,K. (2011) The chromodomain protein MRG-1 facilitates SC-independent homologous pairing during meiosis in Caenorhabditis elegans. *Dev. Cell*, **21**, 1092–1103.
28. Lusser,A., Kolle,D. and Loidl,P. (2001) Histone acetylation: lessons from the plant kingdom. *Trends Plant Sci.*, **6**, 59–65.
29. Carrozza,M.J., Utley,R.T., Workman,J.L. and Cote,J. (2003) The diverse functions of histone acetyltransferase complexes. *Trends Genet.*, **19**, 321–329.
30. Smith,E.R., Pannuti,A., Gu,W., Steurnagel,A., Cook,R.G., Allis,C.D. and Lucchesi,J.C. (2000) The drosophila MSL complex acetylates histone H4 at lysine 16, a chromatin modification linked to dosage compensation. *Mol. Cell. Biol.*, **20**, 312–318.
31. Conrad,T., Cavalli,F.M., Holz,H., Hallacli,E., Kind,J., Ilik,I., Vaquerizas,J.M., Luscombe,N.M. and Akhtar,A. (2012) The MOF chromobarrel domain controls genome-wide H4K16 acetylation and spreading of the MSL complex. *Dev. Cell*, **22**, 610–624.
32. Latrasse,D., Benhamed,M., Henry,Y., Domenichini,S., Kim,W., Zhou,D.X. and Delarue,M. (2008) The MYST histone acetyltransferases are essential for gametophyte development in Arabidopsis. *BMC Plant Biol.*, **8**, 121.
33. Earley,K.W., Shook,M.S., Brower-Toland,B., Hicks,L. and Pikaard,C.S. (2007) In vitro specificities of Arabidopsis co-activator histone acetyltransferases: implications for histone hyperacetylation in gene activation. *Plant J.*, **52**, 615–626.
34. Xiao,J., Zhang,H., Xing,L., Xu,S., Liu,H., Chong,K. and Xu,Y. (2013) Requirement of histone acetyltransferases HAM1 and HAM2 for epigenetic modification of FLC in regulating flowering in Arabidopsis. *J. Plant Physiol.*, **170**, 444–451.
35. He,Y. (2012) Chromatin regulation of flowering. *Trends Plant Sci.*, **17**, 556–562.
36. Strahl,B.D., Grant,P.A., Briggs,S.D., Sun,Z.W., Bone,J.R., Caldwell,J.A., Mollah,S., Cook,R.G., Shabanowitz,J., Hunt,D.F. *et al.* (2002) Set2 is a nucleosomal histone H3-selective methyltransferase that mediates transcriptional repression. *Mol. Cell. Biol.*, **22**, 1298–1306.
37. Zhao,Z., Yu,Y., Meyer,D., Wu,C. and Shen,W.H. (2005) Prevention of early flowering by expression of FLOWERING LOCUS C requires methylation of histone H3 K36. *Nat. Cell Biol.*, **7**, 1256–1260.
38. Grini,P.E., Thorstensen,T., Alm,V., Vizcay-Barrena,G., Windju,S.S., Jorstad,T.S., Wilson,Z.A. and Aalen,R.B. (2009) The ASH1 HOMOLOG 2 (ASHH2) histone H3 methyltransferase is required for ovule and anther development in Arabidopsis. *PloS One*, **4**, e7817.
39. Czechowski,T., Stitt,M., Altmann,T., Udvardi,M.K. and Scheible,W.R. (2005) Genome-wide identification and testing of superior reference genes for transcript normalization in Arabidopsis. *Plant Physiol.*, **139**, 5–17.
40. Sun,B., Xu,Y., Ng,K.H. and Ito,T. (2009) A timing mechanism for stem cell maintenance and differentiation in the Arabidopsis floral meristem. *Genes Dev.*, **23**, 1791–1804.
41. Xu,Y., Wang,Y., Stroud,H., Gu,X., Sun,B., Gan,E.S., Ng,K.H., Jacobsen,S.E., He,Y. and Ito,T. (2013) A matrix protein silences transposons and repeats through interaction with retinoblastoma-associated proteins. *Curr. Biol.*, **23**, 345–350.
42. Lee,L.Y., Fang,M.J., Kuang,L.Y. and Gelvin,S.B. (2008) Vectors for multi-color bimolecular fluorescence complementation to investigate protein-protein interactions in living plant cells. *Plant Methods*, **4**, 24.
43. Sparkes,I.A., Runions,J., Kearns,A. and Hawes,C. (2006) Rapid, transient expression of fluorescent fusion proteins in tobacco plants and generation of stably transformed plants. *Nat. Protocol.*, **1**, 2019–2025.
44. Lysak,M., Fransz,P. and Schubert,I. (2006) Cytogenetic analyses of Arabidopsis. *Methods Mol. Biol.*, **323**, 173–186.
45. Kobayashi,Y., Kaya,H., Goto,K., Iwabuchi,M. and Araki,T. (1999) A pair of related genes with antagonistic roles in mediating flowering signals. *Science*, **286**, 1960–1962.
46. Koos,B., Andersson,L., Clausson,C.M., Grannas,K., Klaesson,A., Cane,G. and Soderberg,O. (2014) Analysis of protein interactions in situ by proximity ligation assays. *Curr. Top. Microbiol. Immunol.*, **377**, 111–126.
47. Bell,O., Wirbelauer,C., Hild,M., Scharf,A.N., Schwaiger,M., MacAlpine,D.M., Zilbermann,F., van Leeuwen,F., Bell,S.P., Imhof,A. *et al.* (2007) Localized H3K36 methylation states define histone H4K16 acetylation during transcriptional elongation in Drosophila. *EMBO J.*, **26**, 4974–4984.
48. Musselman,C.A., Avvakumov,N., Watanabe,R., Abraham,C.G., Lalonde,M.E., Hong,Z., Allen,C., Roy,S., Nunez,J.K., Nickoloff,J. *et al.* (2012) Molecular basis for H3K36me3 recognition by the Tudor domain of PHF1. *Nat. Struct. Mol. Biol.*, **19**, 1266–1272.
49. Vezzoli,A., Bonadies,N., Allen,M.D., Freund,S.M., Santiveri,C.M., Kvinlaug,B.T., Huntly,B.J., Gottgens,B. and Bycroft,M. (2010) Molecular basis of histone H3K36me3 recognition by the PWWP domain of Brpf1. *Nat. Struct. Mol. Biol.*, **17**, 617–619.
50. Saleh,A., Alvarez-Venegas,R. and Avramova,Z. (2008) Dynamic and stable histone H3 methylation patterns at the Arabidopsis FLC and AP1 loci. *Gene*, **423**, 43–47.
51. Schmitges,F.W., Prusty,A.B., Faty,M., Stutzer,A., Lingaraju,G.M., Aiwazian,J., Sack,R., Hess,D., Li,L., Zhou,S. *et al.* (2011) Histone methylation by PRC2 is inhibited by active chromatin marks. *Mol. Cell*, **42**, 330–341.
52. Yuan,W., Xu,M., Huang,C., Liu,N., Chen,S. and Zhu,B. (2011) H3K36 methylation antagonizes PRC2-mediated H3K27 methylation. *The Journal of biological chemistry*, **286**, 7983–7989.
53. Xu,L., Zhao,Z., Dong,A., Soubigou-Taconnat,L., Renou,J.P., Steinmetz,A. and Shen,W.H. (2008) Di- and tri- but not monomethylation on histone H3 lysine 36 marks active transcription of genes involved in flowering time regulation and other processes in Arabidopsis thaliana. *Mol. Cell. Biol.*, **28**, 1348–1360.
54. Palma,K., Thorgrimsen,S., Malinovsky,F.G., Fiil,B.K., Nielsen,H.B., Brodersen,P., Hofius,D., Petersen,M. and Mundy,J. (2010) Autoimmunity in Arabidopsis acd11 is mediated by epigenetic regulation of an immune receptor. *PLoS Pathog.*, **6**, e1001137.
55. Suarez-Lopez,P., Wheatley,K., Robson,F., Onouchi,H., Valverde,F. and Coupland,G. (2001) CONSTANS mediates between the circadian clock and the control of flowering in Arabidopsis. *Nature*, **410**, 1116–1120.
56. Jiang,D., Wang,Y., Wang,Y. and He,Y. (2008) Repression of FLOWERING LOCUS C and FLOWERING LOCUS T by the Arabidopsis Polycomb repressive complex 2 components. *PloS One*, **3**, e3404.
57. Oh,S., Park,S. and van Nocker,S. (2008) Genic and global functions for Paf1C in chromatin modification and gene expression in Arabidopsis. *PLoS Genet.*, **4**, e1000077.
58. Cazzonelli,C.I., Roberts,A.C., Carmody,M.E. and Pogson,B.J. (2010) Transcriptional control of SET DOMAIN GROUP 8 and CAROTENOID ISOMERASE during Arabidopsis development. *Mol. Plant*, **3**, 174–191.
59. Cazzonelli,C.I., Cuttriss,A.J., Cossetto,S.B., Pye,W., Crisp,P., Whelan,J., Finnegan,E.J., Turnbull,C. and Pogson,B.J. (2009)

Regulation of carotenoid composition and shoot branching in Arabidopsis by a chromatin modifying histone methyltransferase, SDG8. *Plant Cell*, **21**, 39–53.
60. Gu,X., Wang,Y. and He,Y. (2013) Photoperiodic regulation of flowering time through periodic histone deacetylation of the florigen gene FT. *PLoS Biol.*, **11**, e1001649.
61. Li,B., Gogol,M., Carey,M., Lee,D., Seidel,C. and Workman,J.L. (2007) Combined action of PHD and chromo domains directs the Rpd3S HDAC to transcribed chromatin. *Science*, **316**, 1050–1054.
62. Gelbart,M.E., Larschan,E., Peng,S., Park,P.J. and Kuroda,M.I. (2009) Drosophila MSL complex globally acetylates H4K16 on the male X chromosome for dosage compensation. *Nat. Struct. Mol. Biol.*, **16**, 825–832.
63. Wang,Z., Zang,C., Cui,K., Schones,D.E., Barski,A., Peng,W. and Zhao,K. (2009) Genome-wide mapping of HATs and HDACs reveals distinct functions in active and inactive genes. *Cell*, **138**, 1019–1031.
64. Morales,V., Regnard,C., Izzo,A., Vetter,I. and Becker,P.B. (2005) The MRG domain mediates the functional integration of MSL3 into the dosage compensation complex. *Mol. Cell. Biol.*, **25**, 5947–5954.
65. Bell,O., Conrad,T., Kind,J., Wirbelauer,C., Akhtar,A. and Schubeler,D. (2008) Transcription-coupled methylation of histone H3 at lysine 36 regulates dosage compensation by enhancing recruitment of the MSL complex in Drosophila melanogaster. *Mol. Cell. Biol.*, **28**, 3401–3409.

Timing Mechanism Dependent on Cell Division Is Invoked by Polycomb Eviction in Plant Stem Cells

Bo Sun, Liang-Sheng Looi, Siyi Guo, Zemiao He, Eng-Seng Gan, Jiangbo Huang, Yifeng Xu, Wan-Yi Wee, Toshiro Ito*

READ THE FULL ARTICLE ONLINE
http://dx.doi.org/10.1126/science.1248559

Cite this article as B. Sun *et al.*, *Science* **343**, 1248559 (2014). DOI: 10.1126/science.1248559

Introduction: In plants, leaves and flowers originate from the shoot apical meristem. In an indeterminate shoot apical meristem, stem cells persist for the life of the plant. In a determinate meristem, a certain number of organs are produced before the meristem is terminated; this characterizes the floral meristem derived from the shoot apical meristem. In *Arabidopsis*, stem cell identity is sustained by expression of the gene *WUSCHEL*. Expression of *WUSCHEL* can be terminated by the zinc finger protein KNUCKLES (KNU), with the result that stem cell identity is inactivated. *KNU* expression is induced by the floral homeotic protein AGAMOUS (AG), but that induction process requires ~2 days and invokes modification of histones resident at the *KNU* locus. Here, we show that the 2-day time lag is a consequence of a regulated molecular mechanism and that this mechanism can be embedded in a synthetic regulatory system to invoke a similar time lag.

Methods: For transgenic *Arabidopsis* plants, we accelerated or inhibited cell cycles with pharmacological agents and studied the resulting KNU expression in response to AG induction. We used chromatin immunoprecipitation to study the presence of Polycomb proteins on the *KNU* locus at specific times during flower development. We used insertional mutagenesis to alter the function of the Polycomb response element (PRE) and analyzed the response from a heterologous promoter in *Arabidopsis* cell cultures. We constructed a synthetic mimic in *Arabidopsis* floral buds of the AG function by using the DNA binding domain of the lactose operon repressor (lacI) with its cognate binding sites. To test the logic that the delay in downstream gene induction was caused by the need to evict Polycomb group (PcG) proteins from their residence, we simulated the competition between PcG proteins and DNA binding proteins by using lacI, designed transcription activator–like effector DNA binding proteins, and synthesized promoters in *Arabidopsis* cell lines.

Results: AG induces *KNU* with a time delay regulated by epigenetic modification. In wild-type plants, *KNU* expression begins in the center of the floral meristem and follows cell cycle progression. The binding sites for AG in the *KNU* upstream region are located within the PRE sequences required for the repressive histone modification. Binding of AG displaces PcG proteins, leading to the failure to maintain the repressive histone methylation. The combination of lacI operator sequences with a chimeric protein that contained the lacI DNA binding domain but lacked the activation domain was able to mimic the AG activity in *Arabidopsis* floral buds. We also reconstituted the cell division–dependent delayed-induction circuit in cell lines.

Discussion: Our results indicate that flower development in *Arabidopsis* employs cell division to provide stem cells with a window of opportunity to change fate. The competition we observed between repressive PcG proteins and an activating transcription factor may reflect a general mechanism. The logic of the molecular circuit we have uncovered here may impose timing control on diverse growth and differentiation pathways in plants and animals.

FIGURES IN THE FULL ARTICLE

SUPPLEMENTARY MATERIALS

Supplementary Text
Figs. S1 to S21
Tables S1 to S4
Full Reference List

RELATED ITEMS IN *SCIENCE*

X. Zhang, Delayed gratification—Waiting to terminate stem cell identity. *Science* **343**, 498–499 (2014). DOI: 10.1126/science.1249343

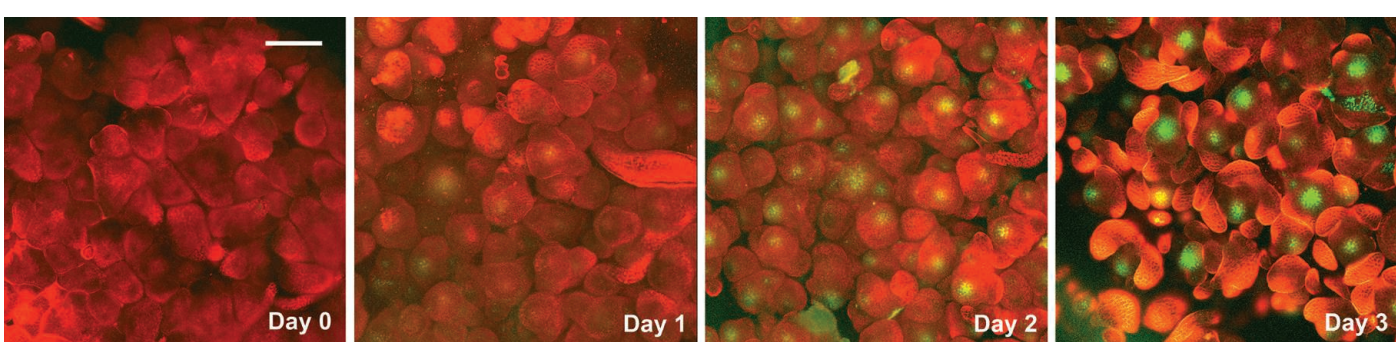

Induction of KNU in *Arabidopsis* floral meristems. Synchronized inflorescences imaged by confocal microscopy and reconstructed into three-dimensional projections (red stains by a fluorescence dye show the shapes of developing flowers). In an *Arabidopsis* line that has been engineered so that its floral development is both inducible and synchronized, KNU expression (green) begins 1 to 3 days after the activation of flower development. The delay is mediated by repressive histone methylation at the *KNU* locus. Upon activation, the transcription factor AG displaces Polycomb proteins, and the repressive histone marks are lost with cell cycle progression. Scale bar, 100 μm.

The list of author affiliations is available in the full article online.
*Corresponding author. E-mail: itot@tll.org.sg

Timing Mechanism Dependent on Cell Division Is Invoked by Polycomb Eviction in Plant Stem Cells

Bo Sun,[1] Liang-Sheng Looi,[1,2] Siyi Guo,[1] Zemiao He,[1,2] Eng-Seng Gan,[1,2] Jiangbo Huang,[1,2] Yifeng Xu,[1] Wan-Yi Wee,[1] Toshiro Ito[1,2]*

Plant floral stem cells divide a limited number of times before they stop and terminally differentiate, but the mechanisms that control this timing remain unclear. The precise temporal induction of the *Arabidopsis* zinc finger repressor KNUCKLES (KNU) is essential for the coordinated growth and differentiation of floral stem cells. We identify an epigenetic mechanism in which the floral homeotic protein AGAMOUS (AG) induces *KNU* at ~2 days of delay. AG binding sites colocalize with a Polycomb response element in the *KNU* upstream region. AG binding to the *KNU* promoter causes the eviction of the Polycomb group proteins from the locus, leading to cell division–dependent induction. These analyses demonstrate that floral stem cells measure developmental timing by a division-dependent epigenetic timer triggered by Polycomb eviction.

Multicellular developmental processes require the precise coordination of growth and differentiation. The growth and development of the aerial part of the plant depends on the continuous activity of stem cells that are maintained at the growing tips called the shoot apical meristem (SAM) (*1*). After floral transition, the SAM usually becomes an inflorescence meristem (IM) that generates floral meristems (FMs). In contrast to the continuous SAM and IM, the FM gives rise to a certain number of organs and loses its pool of stem cells during differentiation. Thus, in the vast majority of land plants, FMs are considered determinate meristems. However, the mechanisms that control when the cells stop dividing and terminally differentiate remain largely mysterious. In *Arabidopsis*, the homeodomain protein WUSCHEL (WUS) is expressed in a small group of cells at the center of the meristems (SAMs, IMs, and FMs) and is essential for maintenance of the stem cell pool (*2*). *WUS* expression is repressed by the C2H2-type zinc finger protein KNUCKLES (KNU) in the FM (*3*, *4*). The floral homeotic protein AGAMOUS (AG), which is directly induced by WUS in young floral buds, directly induces *KNU* ~2 days later to terminate FMs at the precise timing (Fig. 1, A and B) (*4*–*8*). Delayed or precocious *KNU* expression leads to the formation of extra or fewer organs, respectively (*4*). Here, we study the molecular mechanisms of these time-regulated delays in developmental programs.

KNU Induction Is Cell Division–Dependent

To examine the basis of the 2-day delay between AG and *KNU* induction, we used *ag-1 35S::AG-GR pKNU::KNU-GUS*, a *KNU* reporter line that expresses an AG construct that can be induced posttranslationally with dexamethasone (DEX) in the *ag-1* mutant (*4*). Roscovitine and olomoucine (cyclin-dependent kinase inhibitors) block cell cycle progression at the G_1-S and G_2-M phases, whereas aphidicolin (an inhibitor of DNA polymerase) blocks the cell cycle at the early S phase (*9*). Whereas the KNU-GUS reporter was induced ~2 days after DEX treatment in the AG inducible line, addition of cell cycle inhibitors prevented the *KNU* induction on day 2 (Fig. 1, C and D, and fig. S1). AG also induces *SPOROCYTELESS* (*SPL/NOZZLE*) at about the same developmental stage when *KNU* starts to express (*10*). However, *SPL* reporter expression was unaffected by olomoucine treatment (which had the strongest effect to *KNU*) in the AG inducible line (figs. S1 and S2). Thus, division-dependent time lag is required for AG's induction of *KNU* but not of *SPL*.

Phytohormones gibberellin and cytokinin, which accelerate cell cycle progression (*11*), increased the expression of a cyclin reporter construct in developing flowers (*11*) (fig. S3, A to C). In the inducible line of AG, treatment with these phytohormones alone did not induce the *KNU* reporter (fig. S3, D to F), but AG induction (through DEX) combined with phytohormone treatment showed precocious KNU-GUS activity within 24 to 36 hours (Fig. 1, E and F, and fig. S4).

To visualize *KNU* expression at the cellular level, we established a *KNU* fluorescence reporter in the inducible line of flower development, *ap1 cal 35S::AP1-GR pKNU::KNU-VENUS* (*12*), which enabled us to synchronize flower development of multiple floral buds. After the induction of flower development, *KNU* started to be expressed only in a limited number of cells with a time window of 1 and 3 days (fig. S5). The treatment with olomoucine or gibberellin to this line delayed or accelerated the induction timing of *KNU*, respectively, in a way that correlated with cell cycle progression (fig. S6). Cellular-level observation showed that *KNU* was induced in more cells by gibberellin treatment than the control on days 2 and 3, whereas no (on day 2) or fewer cells (on day 3) showed *KNU* induction when treated with olomoucine (Fig. 1, G to I, and fig. S7). Although we did not see any obvious phenotypic differences by the cell cycle manipulation until day 2, olomoucine and gibberellin delayed or accelerated the emergence of floral organ primordia on day 3, suggesting that cell division plays an important role in morphological changes in flower development (fig. S8; see supplementary text for details). The cell division of floral stem cells is not synchronized and occurs once in 18 to 36 hours in most of the cells (*13*). Together, these data indicate that *KNU* regulation may be controlled by an intrinsic cell division–based timer.

AG Displaces Polycomb Group Proteins from *KNU*

The *KNU* transcribed region carries the repressive histone modification trimethylation of lysine 27 of histone H3 (H3K27me3), which is established and maintained by Polycomb group (PcG) proteins (*14*, *15*). *KNU* activation by AG is associated with the loss of H3K27me3 (*4*). In PcG mutants, *KNU* is precociously expressed, and so is the *KNU* reporter line with a deletion in the *KNU* coding region carrying H3K27me3, suggesting that the mark has the commanding role for temporal regulation (*4*). Furthermore, the reduction of the H3K27me3 levels is AG-dependent (*4*), and the above-mentioned truncated reporter is expressed in *ag-1* (fig. S9). Thus, AG appears to temporal-specifically remove H3K27me3. To examine the mechanism underlying how AG affects the repressive marks on *KNU* in a cell division–dependent manner, we created tagged lines for the essential components of PcG, the ESC homolog FERTILIZATION-INDEPENT ENDOSPERM (FIE) and the structural homolog of Su(z)12, EMBRYONIC FLOWER2 (EMF2) (*16*, *17*). We first transformed the *pFIE::FIE-VENUS* and *pEMF2::EMF2-VENUS* constructs into the *fie-11/+* and *emf 2-1/+* heterozygous mutant lines, respectively, and obtained the rescued lines in the homozygous background for each mutation. Next, we introduced them into *ap1 cal 35S::AP1-GR* (*12*), which enabled us to harvest stage-specific floral buds (fig. S10, A to C). After one time of DEX treatment, floral buds were harvested to perform chromatin immunoprecipitation (ChIP) assays for FIE, EMF2, and AG [with an AG antibody (*4*)] at days 0, 1, and 2. We detected AG binding in the samples on days 1 and 2 at a region ~900 base pairs (bp) from the transcriptional start site, but not on day 0 (*4*) (fig. S11). In contrast, we detected moderate binding of FIE and EMF2 around a wider region of the *KNU* locus, including the AG binding sites on day 0 (Fig. 2, A and B, and fig. S12, A and B). From day 1 when AG binding started to be detected, the relative binding levels of FIE and EMF2 decreased to

[1]Temasek Life Sciences Laboratory, 1 Research Link, National University of Singapore, Singapore 117604, Republic of Singapore. [2]Department of Biological Sciences, National University of Singapore, Singapore 117543, Republic of Singapore.

*Corresponding author. E-mail: itot@tll.org.sg

the basal levels (Fig. 2B and figs. S11 and S12B). In the backgrounds containing the *ag-1* mutation, we detected continuous binding of FIE and EMF2 (Fig. 2C and fig. S12C). These results suggest that AG binds to the upstream region of *KNU* in a competitive manner with PcG proteins, evicting them from the locus, which would lead to the loss of H3K27me3 at the coding region.

KNU Upstream Regions Contain a Polycomb Response Element

PcG proteins are recruited to a specific site of target gene loci and then mediate the spread of H3K27me3 (*18*, *19*). Originally found in *Drosophila*, the Polycomb response element (PRE) is responsible for the recruitment of PcG to specific genes, possibly through DNA binding proteins or noncoding RNAs (*14*, *15*). The antagonistic localization of AG and PcG proteins on the same upstream region of *KNU* indicates that the region is necessary for the initial recruitment of PcG and, thus, for the prevention of ectopic *KNU* expression. To examine the function of PcG binding, we performed insertional mutagenesis of the PcG binding region of the *KNU-GUS* reporter construct (Fig. 2, D to H). When we inserted 6-bp unrelated nucleotide sequences immediately upstream of the first AG half-binding consensus sequence, the *KNU* reporter was ectopically expressed in the IMs of most of the independent transgenic lines (Fig. 2F and table S1). However, we observed no effects by the insertion of the same 6-bp fragment in 10- or 100-bp upstream regions (Fig. 2, G and H, and table S1). These results indicate that the region immediately adjacent to the first AG binding site may contain a PRE-like activity, which was at least partially perturbed by the insertion.

To further characterize the PRE-like activity of the *KNU* locus, we cloned the *KNU* upstream region containing the AG binding sites into a heterologous promoter, *pF3H*, with ubiquitous activity (*20*) and transformed the resulting constructs into *Arabidopsis* cultured cells (Fig. 3A). The shortest 153-bp fragment containing three AG binding sites retained the ability to almost fully silence the reporter expression, as did a longer fragment in the *KNU* upstream and the positive control *LEAFY COTYLEDON2* (*LEC2*) upstream region containing PRE-like activity (*20*) (Fig. 3, A to C, and fig. S13, A and B). High levels of H3K27me3 were deposited at the reporter coding region in transgenic lines containing the *KNU* 153-bp fragment but not in the negative control lines without any inserts (fig. S13C). These results suggest that the 153-bp fragment containing AG binding sites is sufficient to silence the heterologous promoter through the recruitment of PcG and deposition of H3K27me3 at the reporter coding region. Furthermore, the disruptive insertion, which caused the ectopic expression of the *KNU* reporter in plants, abolished the PRE activity in the cell line (Fig. 3, A and D).

To test whether the *KNU* PRE activity is transcription-dependent, we deleted the core promoter from the original constructs, abolishing the reporter expression regardless of the *KNU* PRE (fig. S13, D and E). Then, we tested the accumulation of the repressive marks by ChIP assay. We detected PRE-dependent accumulation of H3K27me3 in the reporter coding region (fig. S13F). This result indicates that the *KNU* PRE may have a transcription-independent activity in this context to recruit PcG and deposit the repressive marks.

Mimicking AG Functions by an Artificial Protein

The *KNU* PRE contains AG binding sites, and the binding of PcG and AG are complementary in flower development (Figs. 2, A to D, and 3A and figs. S11 and S12), leading to the AG-dependent reduction of the H3K27me3 marks (*4*). The Trithorax group (TrxG) transcriptional activator complexes counteract PcG activity and mediate the active H3K4 methylation marks (*14*). We examined the active marks at *KNU* in flower development by ChIP assays using the *ap1 cal 35S::AP1-GR* inflorescences. The *KNU* coding region contains both the H3K4me2 and H3K4me3 marks, and our sequential ChIP assays with antibodies for H3K27me3 and H3K4me3 showed that the *KNU* locus contains the bivalent marks (fig. S14). During flower development, we noticed a progressive decrease in the H3K27me3 levels consistent with *KNU* activation (*4*), whereas the H3K4me2 and H3K4me3 levels remained unchanged (fig. S14, B and C). Therefore, AG does not affect H3K4me2 and H3K4me3, but H3K27me3. The simplest explanation for these results may be that the AG functions to physically block the binding of the PcG proteins from PRE, causing the dilution of the epigenetic repressive status through cell division. A similar sustained silencing by PcG has been suggested in assays of the *Drosophila* heat shock–induced clonal analysis of PcG (*21*, *22*). Deletion of *Enhancer of Zeste* showed 2 to 3 days of delay

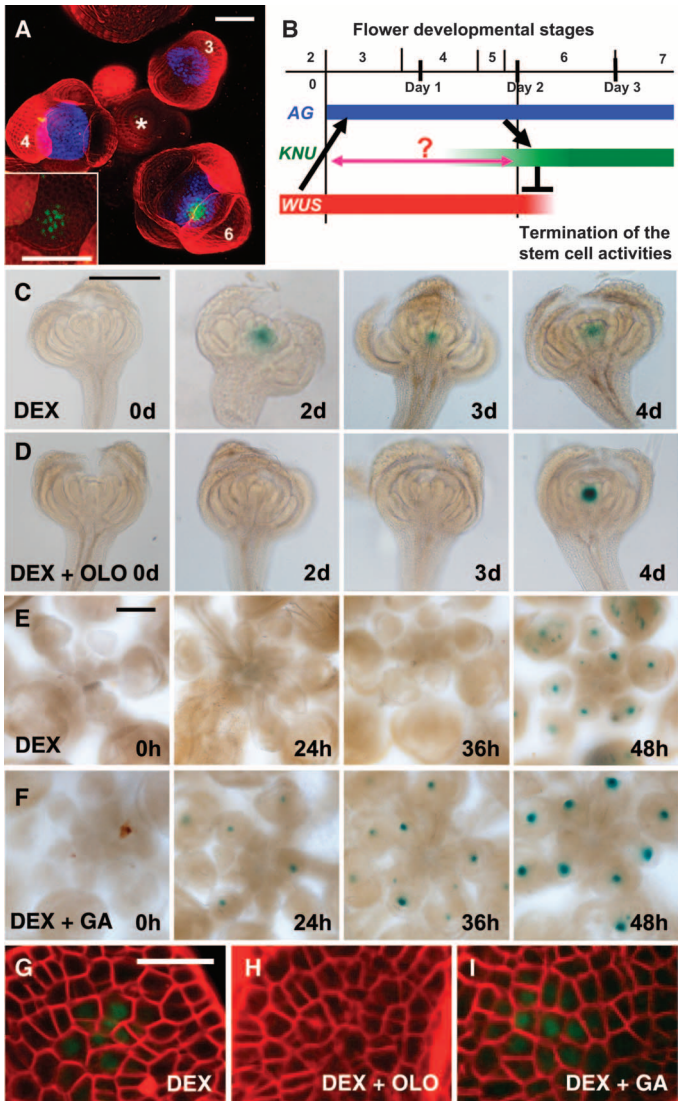

Fig. 1. KNU induction timing is cell division–dependent. (**A**) Confocal observations of the inflorescence doubly transgenic for *pAG::GFP* (blue) (*8*) and *pKNU::KNU-VENUS* (green), which rescues *knu-1*. *, SAM. Numbers, floral stages (*39*). (Inset) A higher magnification of the KNU-VENUS signal in a stage 5 to 6 floral bud. (**B**) Schematic diagram showing the developmental expression patterns of *AG*, *KNU*, and *WUS* in different floral stages. (**C** to **F**) GUS staining in *ag-1 35S::AG-GR pKNU::KNU-GUS* flowers at 0, 2, 3, and 4 days (C and D) or 0, 24, 36, and 48 hours (E and F) after treatment with 10 μM DEX alone (C and E), 10 μM DEX and 100 μM olomoucine (OLO) (D), or 10 μM DEX and 50 μM gibberellic acid 3 (GA) (F). For better penetration of the cell cycle inhibitors and phytohormones, we pretreated the lines with these compounds twice in total, 1 day before the DEX treatment and again in combination with DEX. (**G** to **I**) Confocal observation of *ap1 cal 35S::AP1-GR pKNU::KNU-VENUS*, 2 days after treatment with 1 μM DEX (G), 1 μM DEX and 100 μM OLO (H), or 1 μM DEX and 50 μM GA (I). Cells were stained with FM4-64 dye in (A) and (G) to (I). Scale bars, 50 μm (A and inset), 100 μm (C and D), 200 μm (E and F), and 20 μm (G to I).

before *HOX* misexpression was detected (*22*). To further examine the nature of the competitive binding between AG and PcG on the *KNU* locus, we tried to mimic the behavior of AG in vivo using an artificial protein (LacI-GR), which has the lactose operon repressor (lacI) DNA binding domain and a glucocorticoid hormone binding domain but no detectable transactivation activity (*23*–*25*) (Fig. 3E). In particular, two of the three AG half-binding consensus sequences on the *KNU* promoter were replaced by two *lac* operator (op) sequences, and the remaining one was mutated to prevent AG binding (Fig. 3E). We detected a clear DEX-dependent induction of *KNU* expression with a time lag of 3 days in most of the primary T1 transgenic plants and in selected T2 plants (Fig. 3, F to M, and tables S2 and S3). We noticed a weak basal level of expression without DEX treatment (Fig. 3, F and H to J), which may be caused by the weaker PRE-like activity due to the mutagenesis and/or the leaky effect of *35S::LacI-GR*. We further detected high levels of H3K27me3 on the coding region of the GUS reporter gene before the DEX treatment, and this level dropped on day 3 after the treatment (fig. S15). These results suggest that binding of the chimeric protein on the 2× op sequences can block the PcG complex binding and enable the expression of *KNU* through the removal of the repressive marks, which mimics the endogenous function of AG in *KNU* induction.

Creation of Cell Division–Dependent Epigenetic Timers

To test the logic of the timed induction of *KNU* based on the eviction of PcG proteins, we decided to reconstitute the "epigenetic timer" by simplifying the systems. We created a synthetic promoter combining the ubiquitous *pF3H* promoter and the short 50-bp PRE-like element of *LEC2* (*20*) (Fig. 3A) conjugated with two copies of op sequences in the 5′ and 3′ ends (fig. S16A). This chimeric reporter was silenced because of the PRE-like activity, but when the LacI-GR was induced, it should bind to the op sequences and physically interfere with factors binding to the PRE-like element, leading to their eviction and the subsequent induction of the reporter. After the DEX treatment, the fluorescence reporter was induced by 18 hours in the culture cells (fig. S16B). The reporter was resilenced in 24 hours after a single DEX treatment. When the cells were pretreated with olomoucine, the induction was delayed and observed by 24 hours (fig. S16C).

We further tested the inducibility of the silenced reporter containing the *KNU* PRE (Fig. 3, A to C) by cotransforming the AG protein, or a TAL (transcription activator–like) effector–based synthetic DNA binding protein (*26*), that is designed to recognize the sequences around the first AG binding site. Overexpression of AG by *35S::AG-GR* in the cultured cells could not activate the reporter (fig. S17), possibly because of the low binding affinity of the ectopically expressed AG to the *KNU* promoter. We then created and assayed the specific binding of the designer TAL by fusing the TAL DNA binding domain with a transcriptional activation domain (AD) and nuclear localization signal (NLS) (*26*). The transient assay in the leaf protoplasts revealed the specific induction of the endogenous *KNU*, showing that the TAL protein can bind to the upstream target sequence of *KNU* in vivo (fig. S18). We next induced the fusion protein between the TAL DNA binding domain, NLS, and the GR domain (which has no transcriptional activation domain) in the cultured cell lines containing the silenced reporter by *KNU* PRE (Fig. 4A). After a single DEX treatment, the reporter started to be induced in 20 hours, reached higher levels in 40 hours, and was resilenced in 60 hours (Fig. 4B). The induction was clearly delayed by the olomoucine pretreatment and observed by 60 to 70 hours (Fig. 4C). Accordingly, the ChIP assay in these cells showed

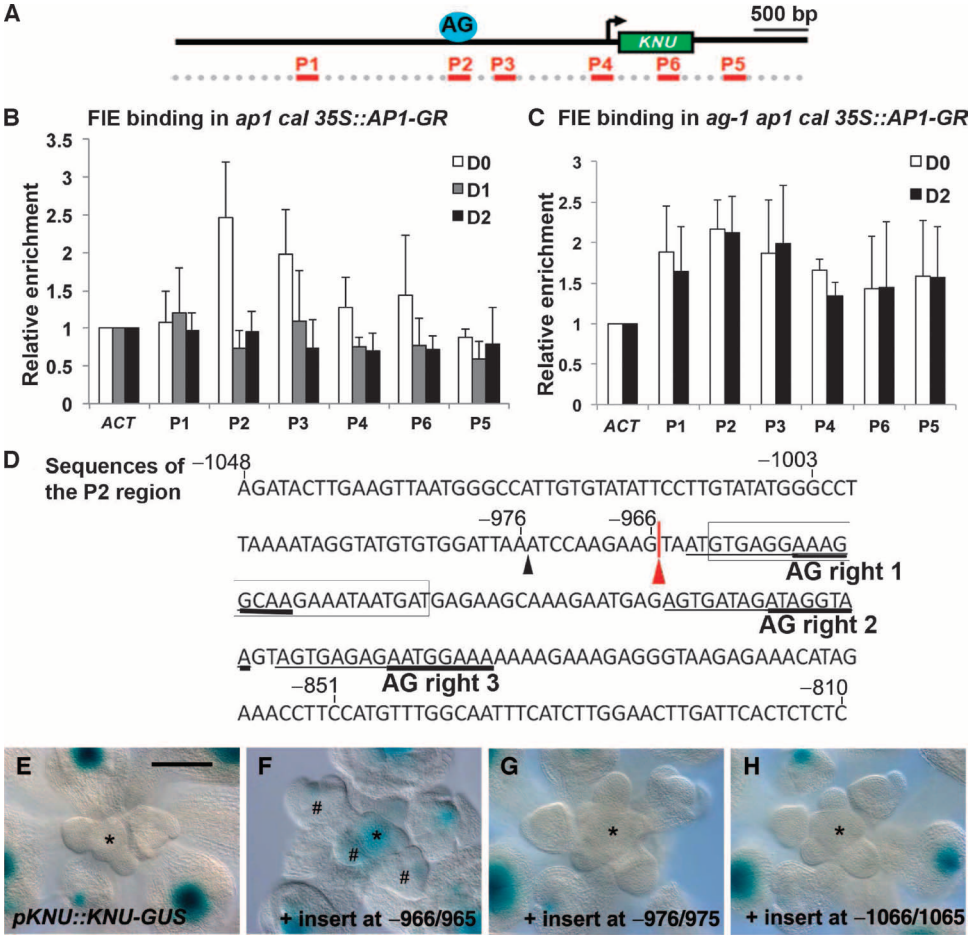

Fig. 2. Polycomb group protein binding on *KNU* and cis activities. (**A**) Schematic diagram of the *KNU* locus and primer sets P1 to P6 used for the ChIP assays in (B) and (C). (**B** and **C**) ChIP assays using *ap1 cal 35S::AP1-GR pFIE::FIE-VENUS* (B) and *ag-1 ap1 cal 35S::AP1-GR pFIE::FIE-VENUS* (C) inflorescences harvested 0, 1, and 2 days after a single 1 μM DEX treatment. Nuclear protein complexes were immunoprecipitated with an anti-GFP antibody, and the enriched DNA was used for quantitative PCR analysis. The *y* axis shows the relative enrichment with immunoglobulin G (IgG) as a control. The error bars represent SD based on three biological replicates. *ACTIN* (*ACT*) was used as a control gene for calibration. (**D**) Sequences of the *KNU* promoter, encompassing the P2 region from –1048 to –810 from the transcription start site (+1), which is bound by AG and PcG proteins. The 6-bp fragment (CATATG) was inserted at the position –966/–965 on the *KNU* promoter (red arrowhead). The three AG half-perfect binding consensus sequences are underlined (the full-length sequences are marked by thin lines). The boxed sequences show the target site for the TAL designer protein shown in Fig. 4. (**E** to **H**) GUS staining of the wild-type *pKNU::KNU-GUS* (E). The 6-bp insertion at the position –966/–965 caused ectopic and precocious *KNU* expression (shown by #) (F), whereas the same insertion at the –976/–975 [a small black arrowhead in (D)], 10 bp upstream (G) and –1066/–1065, 100 bp upstream sites (H) showed the same *KNU* expression pattern as the wild-type *pKNU::KNU-GUS* plants. *, IMs. Scale bar, 100 μm.

that H3K27me3 was reduced by 72 hours in the reporter coding region (fig. S19). When we fully blocked the cell cycle progression by the continuous olomoucine treatment, we did not observe the reporter induction (fig. S20). These results indicate that competitive eviction of PcG from PREs by DNA binding proteins leads to cell division–dependent delayed induction (Fig. 4D). The different timing in induction and resilencing in these two systems may be due to the different PRE-like elements and different affinities of LacI and TAL DNA binding domains to the target sites. In *Drosophila* flp–mediated recombination assay of PREs in different transgenes, excision of PREs from the reporter genes led to loss of silencing at various timing from 12 hours to 2 to 3 days of considerable longer delay (*27*, *28*). In *Arabidopsis*, LEAFY induces *AG* concomitantly through the recruitment of chromatin-remodeling adenosine triphosphatase by antagonizing PcG activities (*29*). Thus, the displacement of PcG proteins by competitive transcription factor binding may be a general mechanism with different cell division dependence (see supplementary text for PcG and cell division). An interesting future subject would be to determine the factors controlling the duration of this epigenetic timer and link with

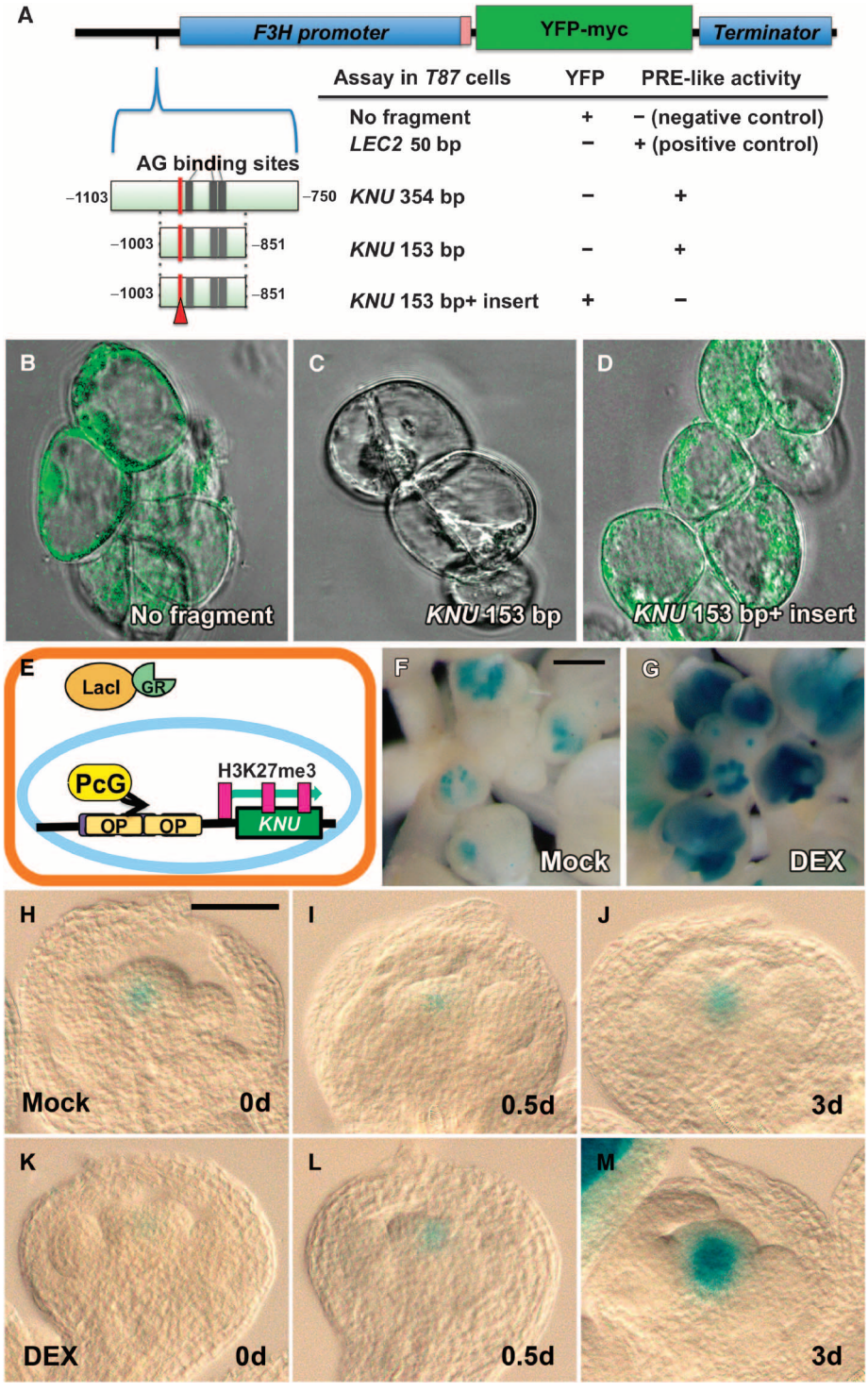

Fig. 3. Polycomb response element and simulation of AG. (**A**) Schematic diagram of the constructs to test the PRE activity of the fragment containing three AG binding sites (gray bars) on the *KNU* promoter and the disruptive insertion site that caused ectopic expression of the reporter in Fig. 2D (red arrowhead) and the summary of the assay in the *Arabidopsis* T87 culture cells. (**B** to **D**) T87 cells transgenic for the construct of *pF3H::YFP* alone (B) and the *pF3H::YFP* constructs conjugated with the 153-bp fragment, *pF3H-KNU PRE 153 bp::YFP* (C), and with the 153-bp fragment with the disruptive 6-bp insert, *pF3H-KNU PRE 153 bp+6 bp::YFP* (D). (**E**) Schematic diagram of the experiment to show that a chimeric protein with the lacI DNA binding domain (LacI) and glucocorticoid hormone binding domain (GR) partially mimics the function of AG to induce *KNU* expression by binding to the operator sequences (OP) upon DEX treatment and eviction of the PcG proteins. (**F** and **G**) GUS reporter staining 3 days after a single DEX treatment in T1 transgenic plants of *35S:: LacI-GR pKNU-OP::KNU-GUS* treated with mock (F) and 10 μM DEX (G). (**H** to **M**) Time course observation of T2 *35S::LacI-GR pKNU-OP::KNU-GUS* flowers treated with mock (H to J) or DEX (K to M) harvested at days 0 (H and K), 0.5 (I and L), and 3 (J and M) after a single 10 μM DEX treatment. Scale bars, 25 μm (B to D), 200 μm (F and G), and 50 μm (H to M).

cell cycle phase. This epigenetic timer can be used as a module to build time-responsive molecular circuits in synthetic biology.

Materials and Methods

Plant Materials and Chemical Treatments

All plants had the Landsberg *erecta* (L*er*) background and were grown at 22°C under continuous light. Plant photographs were taken with a stereomicroscope (Carl Zeiss MicroImaging GmbH). DEX (Sigma) treatments were conducted by inverting the plants and submerging the inflorescences for 1 min in a solution containing either 1 μM DEX (for *35S::AP1-GR*) or 10 μM DEX (for *35S::AG-GR, 35S::LacI-GR* and *35S::TAL-GR*) together with 0.015% Silwet L-77. The time of the initial DEX treatment was taken as day 0 or 0 hour. Cell cycle inhibitors and phytohormones, applied at final concentrations of 50 μM for roscovitine, 100 μM for olomoucine, 35 μM for aphidicolin, 500 μM for cytokinin [benzylaminopurine (BAP)], and 50 μM for gibberellic acid 3 (GA), were treated one time 24 hours before the DEX treatment for better penetration, as well as in combination with DEX at 0 hour. The mock treatments were conducted using the same method with the dipping solution without the chemicals.

For cultured cells, 10 μM DEX was applied directly into the liquid cell culture medium at 0 hour. For cell cycle manipulation, the cells were pretreated with dimethyl sulfoxide for mock or 50 μM olomoucine 1 day before the DEX treatment. Olomoucine was washed away at the time of DEX treatment or kept in the cultured medium for continuous treatment.

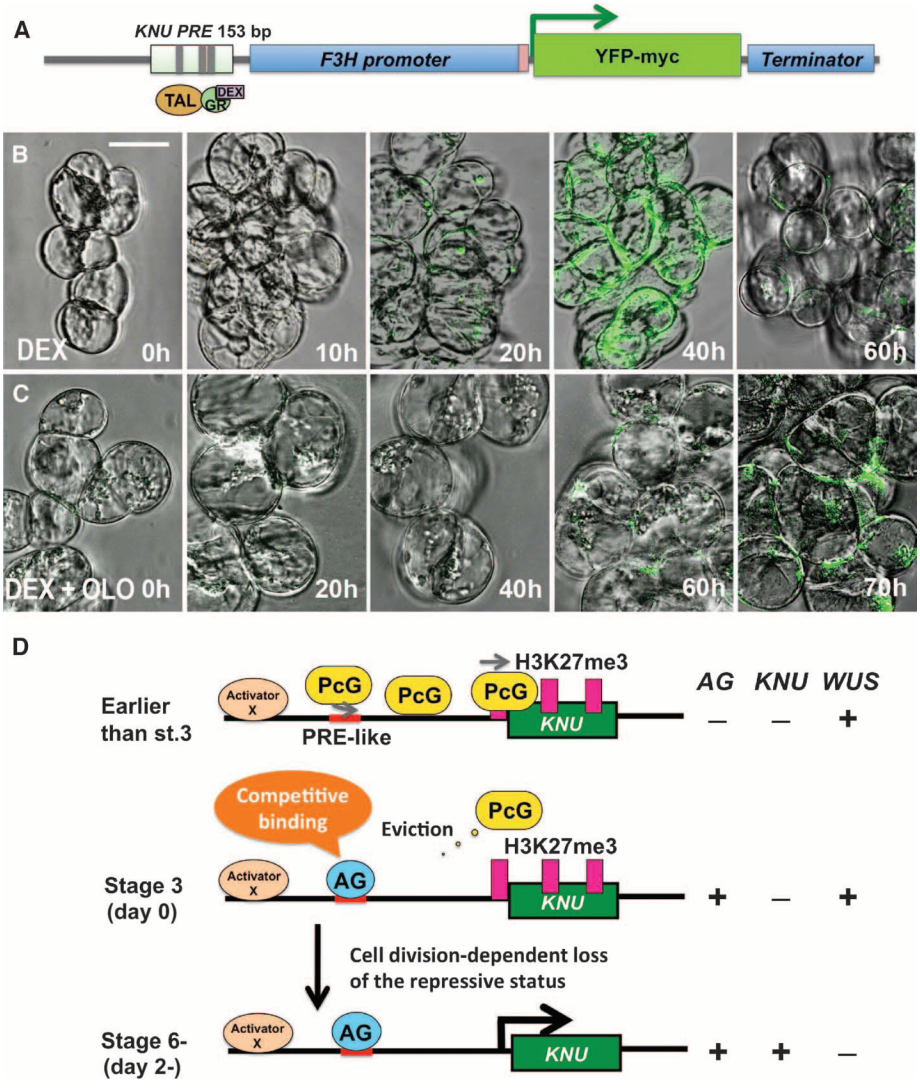

Fig. 4. Synthetic epigenetic timer and eviction model. (**A**) Schematic diagram of a synthetic epigenetic timer. *pF3H-KNU PRE 153 bp::YFP* was cotransformed with the *35S::TAL DNA binding domain-GR* (*TAL-GR*) construct, which targets the region around the first AG binding site (boxed sequences in Fig. 2D) in the *Arabidopsis* T87 culture cells. (**B** and **C**) Time course confocal microscopy observation of the T87 cells transgenic for the constructs shown in (A). The cells were observed at 0, 10, 20, 40, 60, and 70 hours after a single 10 μM DEX treatment. The cells were pretreated with mock (B) or 50 μM olomoucine (OLO) (C) 1 day before the DEX treatment, and the inhibitor was washed away at the time of the DEX treatment. Scale bar, 25 μm. (**D**) Schematic diagram of the *KNU* regulation. Earlier than stage 3 (corresponding to day 0 of *ap1 cal 35S::AP1-GR* floral buds), the *KNU* locus is covered by the H3K27me3 repressive mark, which is maintained by PcG. The *KNU* transcript cannot be induced because of the repressive marks. At stage 3, the AG protein, which is induced by WUS (*6*, *7*), directly binds to the *KNU* promoter competitively with PcG, leading to eviction of PcG from the *KNU* locus. The eviction of PcG leads to cell division–dependent loss of the repressive status of *KNU* and the timed induction. Subsequently, *WUS* transcription is repressed by KNU (*4*), and floral stem cell activity is terminated with perfect timing.

GUS Staining

GUS staining was performed as previously described (*30*) and observed in whole-mount samples in clearing solution with a Carl Zeiss MicroImaging stereomicroscope, or in paraffin sections with a Carl Zeiss Axioplan 2 microscope.

ChIP Assay

The ChIP experiments were performed as previously described (*31*) with slight modification. Inflorescences from *ap1 cal 35S::AP1-GR* were ground in liquid nitrogen and postfixed with 1% formaldehyde for 10 min. The chromatin was isolated and solubilized by sonication to generate DNA fragments with an average length of 400 bp. After incubation with salmon sperm DNA–protein A (for polyclonal antibody) or sperm DNA–protein G (for monoclonal antibody) agarose beads (Millipore), the solubilized chromatin was incubated overnight with anti-GFP (green fluorescent protein) antibody (Santa Cruz Biotechnology or Invitrogen), normal rabbit IgG (Santa Cruz Biotechnology), or anti-H3K27me3 antibody (Millipore or Abcam). The DNA fragments were recovered from the purified DNA-protein complexes and then used for enrichment tests by real-time polymerase chain reaction (PCR) analysis in triplicate. For the H3K27me3 ChIP, the ratio between the bound DNA after immunoprecipitation and the input DNA before immunoprecipitation was calculated for all the representative primer sets spanning the *KNU* genomic region, or for the primer sets on *GUS* or *yellow fluorescent protein* (*YFP*) reporters, and the ratios were plotted to show the relative changes in the levels of epigenetic marks. The relative enrichment for FIE and EMF2 proteins on the *KNU* locus was the ratio between the bound DNA after immunoprecipitation by anti-GFP over that by IgG. For sequential ChIP assay, cross-linked chromatin from the inflorescences was immunoprecipitated with monoclonal anti-H3K27me3 antibody (Abcam) as described above, except that chromatin was eluted in a solution of 30 mM dithiothreitol, 500 mM NaCl, and 0.1% SDS at 37°C (*32*). Eluted chromatin was subject to a second immunoprecipitation with monoclonal anti-H3K4me3 antibody (Abcam). In addition, a reversed sequential ChIP assay was performed in the sequence of application of anti-H3K4me3 antibody first, followed

by immunoprecipitation with anti-H3K27me3 antibody. For all ChIP experiments, the primers for the *Mu-like* transposon or the *ACT* gene were included as negative controls.

Vector Construction and Transgenic Selection

1) *pEMF2::EMF2-VENUS*, *pFIE::FIE-VENUS*, and *pKNU::KNU-VENUS* (fig. S21A) were produced as follows: The *EMF2* and *FIE* genomic regions were amplified from Col wild-type genomic DNA with the primer sets PSOKK131EMF2F/ PSOKK132EMF2R and PSOKK162FIEF/ PSOKK165FIER, respectively. The amplified *EMF2* and *FIE* genomic fragments were TA-cloned into pENTR-D TOPO vectors (Invitrogen). Subsequently, an Sfo I restriction site was introduced immediately before the stop codons of *EMF2* and *FIE* with the QuikChange Site-Directed Mutagenesis Kit (Stratagene). The *VENUS* fragment was generated by digestion of the vector *pRS316-VENUS* (*33*) with Sfo I. Then, the *VENUS* fragment flanked by Sfo I was introduced into the Sfo I sites in the above-mentioned *EMF2* or *FIE* genomic region, or Sfo I–digested *pKNU::KNU-GUS* (*4*) to replace the *GUS* fragment, to generate *pEMF2::EMF2-VENUS*, *pFIE::FIE-VENUS*, or *pKNU::KNU-VENUS*. Through LR reaction by Gateway LR Clonase II (Invitrogen), *pEMF2::EMF2-VENUS* or *pFIE::FIE-VENUS* was exchanged from the pENTR-D TOPO backbone to the destination vector pKGW (Invitrogen). *pKNU::KNU-VENUS* was exchanged from the pCR8 backbone to the destination vector CD3-694, pEarleyGate 303 (*4*).

2) Three *pKNU::KNU-GUS* lines with the 6-bp insertion at three different positions (fig. S21B) were produced as follows: First, a 996-bp *KNU* promoter fragment (from −1249 to −253 bp) flanked by Nde I sites, which contains the three AG binding sites, was cloned with the primer set PSOXYF68-KNU-NdeI-FP/ PSOXYF69-KNU-NdeI-RP into pCR8 GW TOPO vector by TA cloning (Invitrogen). To test the positional effect of 6-bp insertion, PCR mutagenesis using the primer sets PSOXYF393/394, PSOXYF397/398, and PSOZM204/205 were performed to introduce one extra Nde I site at three different positions inside the above-mentioned 996-bp *KNU* promoter fragment and named *pKNUM3* (−966/−965), *pKNUM5* (−976/−975), and *pKNUM7*(−1066/−1065), respectively. The resulting 1002-bp promoter fragments were digested from *pKNUM3*, *pKNUM5*, and *pKNUM7* by partial digestion with Nde I (to keep the internal Nde I site intact but not the flanking ones) and introduced into a pCR8-based modified *pKNU::KNU-GUS* vector (by Nde I) (*4*) to replace the specific endogenous *KNU* promoter region. Subsequently, the entire cassettes of *pKNUM3::KNU-GUS*, *pKNUM5::KNU-GUS*, and *pKNUM7::KNU-GUS* were recombined into the destination vector pKGW by the LR reaction (Invitrogen).

3) *35S::LacI-GR pKNU-OP::KNU-GUS* (fig. S21C) was constructed as follows: To prevent AG binding, a 996-bp *KNU* promoter fragment (from −1249 to −253 bp) flanked by Nde I sites was cloned from *pMutated KNU* with all three AG half binding sites mutated (from part ii) (*4*) into pCRII GW/TOPO vector and named *pCRII pMutated KNU NdeI*. Two copies of the op sequences were introduced to replace the second and third mutated AG half binding sites on pCRII *pMutated KNU NdeI* by four rounds of PCR mutagenesis with the primer sets PSOXYF399-OP1-F/ PSOXYF400-OP1-R, PSOXYF401-OP2-F/ PSOXYF402-OP2-R, PSOZM8MOP3_F/ PSOZM9MOP3_R, and PSOZM10MOP4_F/ PSOZM11 MOP4-R. Subsequently, the Nde I–flanked fragment harboring two copies of the op sequences was digested with Nde I and introduced into an Nde I–digested pCR8 *pKNU::KNU-GUS* to form the pCR8-based *pKNU-OP::KNU-GUS*. The resulting construct was further mutated by PCR with PSOZM50 KNUGUS NotI F/ PSOZM51 KNUGUS NotI R to create a Not I site after the *KNU* 3′ untranslated region for further cloning. The *35S::LacI-GR* fragment was obtained as follows: *LacI-GR* flanked by Sal I and Spe I was amplified by PCR with PSOZM12 LhGR_F/ PSOZM13 LhGR DB_R from vector pBJ36 (*34*). The *LacI-GR* was later introduced into the modified pGreen binary vector 0280 (*35*) with the same sites. The resulting pGreen-based product with a promoter and a terminator was further digested by Not I to obtain the Not I–flanked *35S::LacI-GR* fragment. Subsequently, the fragment was introduced into the Not I–digested vector pCR8 *pKNU-OP::KNU-GUS*, resulting in the entry vector pCR8 *35S::LacI-GR pKNU-OP::KNU-GUS*. The whole cassette was then recombined into pEarlygate303 CD3-694 (*36*) by the LR reaction (Invitrogen).

4) *pF3H::YFP* and *pF3H-RLE::YFP* (*RLE* from *LEC2*) (fig. S21D) were constructed as follows: The *YFP* fragment and terminator (*YFP CDS* followed by the *3myc* and *CaMV ter* fragments) was amplified by the primer set PSOZM161-YFP-F/ PSOZM133-CaMV-terR from *p1002-35S-YFP-3myc-CaMV* to generate the cassette *35S-YFP-3myc-CaMV*. The resulting cassette was then digested with Asc I and introduced into the modified pENTR-D TOPO p1002 to create the *p1002-YFP*. The *F3H* fragment was amplified from *Arabidopsis* L*er* genomic DNA by PSOZM153 F3HpF/ PSOZM154 F3Hp-35SR, which contains the sequences for the *35S* core promoter. The fragment was then digested with Bgl II and Xho I and introduced into the *p1002-YFP* vector to create *pF3H::YFP* (fig. S21D), and *F3H* is followed by the *35S* core promoter. *pF3H-RLE::YFP* (fig. S21D) was constructed by one round of PCR mutagenesis based on the template of *pF3H::YFP* with the primer set PSOZM159 F3H_iRLE F/ PSOZM160 F3H_iRLE R, resulting in the insertion of an *RLE* fragment (*20*) into *pF3H::YFP* to generate *pF3H-RLE::YFP*.

pF3H-KNU PRE 354bp::YFP and *pF3H-KNU PRE 153bp::YFP* were constructed based on *pF3H::YFP* as follows: To create *pF3H-KNU PRE 354bp::YFP* (fig. S21E), the 354-bp fragment flanked by Bgl II was first amplified with PSOZM142 KNU pro BglII F/ PSOZM206 KNU pro BglII R from *pKNU::KNU-GUS* (*4*). Then, the fragment was introduced into *p1002 pF3H::YFP* to generate *pF3H-KNU PRE 354bp::YFP*. To create *pF3H-KNU PRE 153bp::YFP* (fig. S21E), the 153-bp fragment flanked by Bgl II was first amplified with PSOZM142 KNU pro BglII F/ PSOZM143 KNU pro XhoI R from *pKNU::KNU-GUS* (*4*). Then, the fragment was introduced into *p1002 pF3H::YFP* to generate *pF3H-KNU PRE 153bp::YFP*.

5) *pF3H-KNU PRE 153bp+6bp insert::YFP*; *pOp-RLE-Op-F3H::YFP 35S::Lac-GR* (fig. S21F) were constructed as follows: For the *pF3H-KNU PRE 153bp+6bp insert::YFP* (fig. S21E), the 153-bp fragment was amplified from *pKNUM7*, which had an Nde I site at −1066/−1065. The fragment was introduced into *p1002 pF3H::YFP* to generate *pF3H-KNU PRE 153bp+6bp insert::YFP*. *pOp-RLE-Op-F3H::YFP* (fig. S21F) was created by two rounds of PCR mutagenesis with primer sets PSOZM175 F3H SopL F/ PSOZM176 F3H SopL R and PSOZM177 F3H SopR F/ PSOZM178 F3H SopR R sequentially to insert 1× op each into the 5′ and 3′ ends of the RLE sequences of *pF3H-RLE::YFP* to generate *pOp-RLE-Op-F3H::YFP*. *35S::LacI-GR* was constructed as follows: First, the *35S::LacI-GR-CaMVter* fragment was amplified by the primer set PSOZM187_35S_F/ PSOZM133CaMtR with pCR8 *pKNU-Op::KNU-GUS 35S::LacI-GR-CaMVter* as the template. Subsequently, the amplified fragment was digested with Asc I and introduced into pENTR-D TOPO p1002. The *CaMV* terminator was then replaced with the *Nos* terminator by mega-primer mutagenesis with the primer set PSOZM195_CaMV_NosF/PSOZM196_CaMV_NosR, resulting in the construct p1002 *35S::LacI-GR-Nos ter*. Next, the *pOp-RLE-Op-F3H::YFP* fragment was amplified with the primer set PSOZM153_F3Hp_F/ PSOZM193_CaMV_ter_NotIR. The fragment was later introduced into p1002 *35S::LacI-GR-Nos ter* through Bgl II and Not I sites to generate *pOp-RLE-Op-F3H::YFP 35S::LacI-GR* (fig. S21F).

6) *35S::TAL-GR* and *35S::TAL-AD* (fig. S21G) were created as follows: The *KNU* promoter 996-bp fragment, −1249 to −253 bp with an Nde I site on both ends, containing the three AG half binding sites, was input into an online tool (TAL Effector-Nucleotide Targeter, TALE-NT; http://boglabx.plp.iastate.edu/TALENT/). A 25-bp TALE sequence targeting the first AG half binding site was chosen as a good target site (Fig. 2D). TAL'C of pTAL1 vector (Addgene) contains NLSs and transactivation domain VP64 (AD). To create *35S::TAL-GR* (fig. S21G), a GR fragment including a hemagglutinin (HA) tag (861 bp) was first amplified from pGreen0281 plasmid (*35*) with the primer set PSOWY66_talBglIINdeIGR/ PSOZM192_talAsc1HA. Subsequently, the amplified fragment was used as a primer to anneal to pTAL1 vector (Addgene), amplifying the whole plasmid, resulting in replacement of the 105-bp transactivation domain VP64 (AD) with *GR* to generate the *pTAL1-NLS-GR*. Next, the chosen 25-bp TALE sequence was created by golden gate reaction (Addgene) into the *pTAL1-NLS-GR* destination

vector to generate *pTAL1-TALE-NLS-GR*, followed by exchanging the cassette of *TALE-NLS-GR* into binary vector pMDC32 by LR reaction (Invitrogen) to generate *35S::TAL-GR* (fig. S21G). *35S::TAL-AD* was constructed by using golden gate reaction (Addgene) of the chosen 25-bp TALE sequence into pTAL1 (Addgene) to generate *pTAL1-25bpTALE-NLS-AD*, followed by exchanging the cassette of *25bpTALE-NLS-AD* into binary vector pMDC32 by LR reaction (Invitrogen) to generate *35S::TAL-AD* (fig. S21G).

7) *35S* core promoter deletion (Δ*core promoter*) (fig. S21H) was created as follows: Both *pF3H::YFP* and *pF3H-KNU PRE 153bp::YFP* constructs were mutated by the KAPA PCR mutagenesis kit to delete 10 bp in the *35S* core promoter sequence using the PSOLS257-35sdel F/ PSOLS258-35sdelR primers. Subsequently, the transgenes were recombined into the destination vector KGW.

All clones from 1) to 7) (fig. S21) were fully sequenced for confirmation, and all the primers used for construction are listed in table S4. *pEMF2::EMF2-VENUS* and *pFIE::FIE-VENUS* (fig. S21A) were introduced into *ap1 cal 35S::AP1-GR*. All the *GUS* constructs from 2) and 3) (fig. S21, B and C) were introduced into wild-type L*er* plants using the floral dipping method mediated by *Agrobacterium*. *pEMF2::EMF2-VENUS* and *pFIE::FIE-VENUS* T1 transgenic plants were selected on an MS solid medium plate with the antibiotic kanamycin at a concentration of 50 μg/ml. All the *GUS* reporter transgenic plants were selected on soil with the herbicide Basta 15 (Bayer; 0.2% of the commercial solution). Constructs from 4) to 7) (fig. S21, D to H) were introduced into T87 cultured cells, and transformation was performed as described below.

Arabidopsis *Protoplast and Culture Cell Assay*

The transient gene expression assay using *Arabidopsis* mesophyll protoplasts was performed as previously described (*37*). The stable *Arabidopsis* transgenic culture cells were established using T87 suspensions cells (*38*). Briefly, the cells were maintained in JPL3 medium under continuous illumination at 22°C with rotary shaking at 120 rpm as previously described (*38*). To generate transgenic lines, 2-week-old T87 cells were sieved through a 500-μm stainless mesh and resuspended in B5 medium supplemented with 1 μM 1-naphthaleneacetic acid and sucrose (30 g/liter). Cell suspension was cultured under continuous illumination at 22°C with shaking at 120 rpm for 1 day. Then, 2.5 μl of overnight cultured *Agrobacterium* transformed with the appropriate vectors was added to the cell suspension and cultured for a further 2 days. After cocultivation, the cell suspension was washed twice with 10 ml of JPL3 medium supplemented with carbenicillin (200 μg/ml) by centrifugation at 100*g* for 2 min. Finally, cells were resuspended in 3 ml of JPL3 medium and spread over a selection JPL3 agar plate supplemented with carbenicillin (250 μg/ml) and selection drugs. After 2 weeks of culture, drug-resistant calli were transferred to fresh selection medium and maintained by subculture fortnightly. Kanamycin (30 μg/ml) and/or hygromycin B (12 μg/ml) were used for single/cotransformation on a plate. Kanamycin (25 μg/ml) and/or hygromycin B (7.5 μg/ml) were used for single/cotransformation in liquid medium. For reverse transcription PCR and ChIP assays, we used 1- to 2-week-old transgenic T87 suspension lines and collected ~0.2 ml of dry weight pellet by centrifugation at 100*g* for 2 min. For expression assay of the reporter lines, confocal microscopy images were taken with a Leica SP5 (as described below).

Confocal Microscopy Imaging

For the observation of the reporter lines in *Arabidopsis* inflorescences, the transgenic seeds were sowed on soil, and inflorescences were plucked and mounted on slides. The older floral buds were then carefully removed or spaced out to expose the SAM and early-stage floral buds. Dissected inflorescence was incubated with FM4-64 dye (50 μg/ml) for ~45 min on slides. Plants were imaged using a Zeiss LSM 510 upright (with motorized stage) confocal microscope with EC Plan-Neofluar 40×/1.30 oil differential interference contrast or Plan-Apochromat 20×/0.8 objective lens. GFP was stimulated with an argon laser at 488 nm at 60 to 70% of its output, with emission filtered using a 505- to 530-nm band-pass filter. VENUS was stimulated with an argon laser at 514 nm at 65 to 80% of its output, with emission filtered using a 530- to 600-nm band-pass filter. FM4-64 dye emission was filtered with a 585-nm long-pass filter. The z-stack was acquired using a 512-by-512–pixel frame, and the three-dimensional projections of the obtained z-stacks were then made with Zeiss LSM Image Brower version 4 and adjusted with Adobe Photoshop.

For the observation of T87 transgenic lines, 10 μl of cell suspension was mounted on slides and imaged using a Leica SP5 inverted confocal microscope with HCX PL APO 40×/1.25 objective lens. YFP was stimulated with an argon laser at 514 nm at 80% of its output, with emission filtered using a 520- to 550-nm band-pass filter. Images were acquired using 512 pixels by 512 pixels. Subsequently, images were made with Leica Application Suite Advanced Fluorescence v2.6.0 and adjusted with ImageJ v1.44 and Adobe Photoshop.

References and Notes

1. T. A. Steeves, I. M. Sussex, *Patterns in Plant Development* (Cambridge Univ. Press, Cambridge, ed. 2, 1989).
2. K. F. Mayer *et al.*, Role of *WUSCHEL* in regulating stem cell fate in the *Arabidopsis* shoot meristem. *Cell* **95**, 805–815 (1998). doi: 10.1016/S0092-8674(00)81703-1; pmid: 9865698
3. T. Payne, S. D. Johnson, A. M. Koltunow, *KNUCKLES* (*KNU*) encodes a C2H2 zinc-finger protein that regulates development of basal pattern elements of the *Arabidopsis* gynoecium. *Development* **131**, 3737–3749 (2004). doi: 10.1242/dev.01216; pmid: 15240552
4. B. Sun, Y. Xu, K. H. Ng, T. Ito, A timing mechanism for stem cell maintenance and differentiation in the *Arabidopsis* floral meristem. *Genes Dev.* **23**, 1791–1804 (2009). doi: 10.1101/gad.1800409; pmid: 19651987
5. M. F. Yanofsky *et al.*, The protein encoded by the *Arabidopsis* homeotic gene *agamous* resembles transcription factors. *Nature* **346**, 35–39 (1990). doi: 10.1038/346035a0; pmid: 1973265
6. J. U. Lohmann *et al.*, A molecular link between stem cell regulation and floral patterning in *Arabidopsis*. *Cell* **105**, 793–803 (2001). doi: 10.1016/S0092-8674(01)00384-1; pmid: 11440721
7. M. Lenhard, A. Bohnert, G. Jürgens, T. Laux, Termination of stem cell maintenance in *Arabidopsis* floral meristems by interactions between *WUSCHEL* and *AGAMOUS*. *Cell* **105**, 805–814 (2001). doi: 10.1016/S0092-8674(01)00390-7; pmid: 11440722
8. S. L. Urbanus *et al.*, In planta localisation patterns of MADS domain proteins during floral development in *Arabidopsis thaliana*. *BMC Plant Biol.* **9**, 5 (2009). doi: 10.1186/1471-2229-9-5; pmid: 19138429
9. S. Planchais, N. Glab, D. Inzé, C. Bergounioux, Chemical inhibitors: A tool for plant cell cycle studies. *FEBS Lett.* **476**, 78–83 (2000). doi: 10.1016/S0014-5793(00)01675-6; pmid: 10878255
10. T. Ito *et al.*, The homeotic protein AGAMOUS controls microsporogenesis by regulation of *SPOROCYTELESS*. *Nature* **430**, 356–360 (2004). doi: 10.1038/nature02733; pmid: 15254538
11. H. Stals, D. Inzé, When plant cells decide to divide. *Trends Plant Sci.* **6**, 359–364 (2001). doi: 10.1016/S1360-1385(01)02016-7; pmid: 11495789
12. F. Wellmer, M. Alves-Ferreira, A. Dubois, J. L. Riechmann, E. M. Meyerowitz, Genome-wide analysis of gene expression during early *Arabidopsis* flower development. *PLOS Genet.* **2**, e117 (2006). doi: 10.1371/journal.pgen.0020117; pmid: 16789830
13. G. V. Reddy, M. G. Heisler, D. W. Ehrhardt, E. M. Meyerowitz, Real-time lineage analysis reveals oriented cell divisions associated with morphogenesis at the shoot apex of *Arabidopsis thaliana*. *Development* **131**, 4225–4237 (2004). doi: 10.1242/dev.01261; pmid: 15280208
14. R. Sawarkar, R. Paro, Interpretation of developmental signaling at chromatin: The Polycomb perspective. *Dev. Cell* **19**, 651–661 (2010). doi: 10.1016/j.devcel.2010.10.012; pmid: 21074716
15. J. A. Simon, R. E. Kingston, Occupying chromatin: Polycomb mechanisms for getting to genomic targets, stopping transcriptional traffic, and staying put. *Mol. Cell* **49**, 808–824 (2013). doi: 10.1016/j.molcel.2013.02.013; pmid: 23473600
16. A. Katz, M. Oliva, A. Mosquna, O. Hakim, N. Ohad, FIE and CURLY LEAF polycomb proteins interact in the regulation of homeobox gene expression during sporophyte development. *Plant J.* **37**, 707–719 (2004). doi: 10.1111/j.1365-313X.2003.01996.x; pmid: 14871310
17. N. Yoshida *et al.*, EMBRYONIC FLOWER2, a novel polycomb group protein homolog, mediates shoot development and flowering in *Arabidopsis*. *Plant Cell* **13**, 2471–2481 (2001). doi: 10.2307/3871588; pmid: 11701882
18. Y. B. Schwartz *et al.*, Genome-wide analysis of Polycomb targets in *Drosophila melanogaster*. *Nat. Genet.* **38**, 700–705 (2006). doi: 10.1038/ng1817; pmid: 16732288
19. D. Schubert *et al.*, Silencing by plant Polycomb-group genes requires dispersed trimethylation of histone H3 at lysine 27. *EMBO J.* **25**, 4638–4649 (2006). doi: 10.1038/sj.emboj.7601311; pmid: 16957776
20. N. Berger, B. Dubreucq, F. Roudier, C. Dubos, L. Lepiniec, Transcriptional regulation of *Arabidopsis LEAFY COTYLEDON2* involves *RLE*, a *cis*-element that regulates trimethylation of histone H3 at lysine-27. *Plant Cell* **23**, 4065–4078 (2011). doi: 10.1105/tpc.111.087866; pmid: 22080598
21. D. Beuchle, G. Struhl, J. Müller, Polycomb group proteins and heritable silencing of *Drosophila* Hox genes. *Development* **128**, 993–1004 (2001). pmid: 11222153
22. J. Müller *et al.*, Histone methyltransferase activity of a *Drosophila* Polycomb group repressor complex. *Cell* **111**, 197–208 (2002). doi: 10.1016/S0092-8674(02)00976-5; pmid: 12408864

23. S. M. Hollenberg, R. M. Evans, Multiple and cooperative *trans*-activation domains of the human glucocorticoid receptor. *Cell* **55**, 899–906 (1988). doi: 10.1016/0092-8674(88)90145-6; pmid: 3191531
24. A. M. Lloyd, M. Schena, V. Walbot, R. W. Davis, Epidermal cell fate determination in *Arabidopsis*: Patterns defined by a steroid-inducible regulator. *Science* **266**, 436–439 (1994). doi: 10.1126/science.7939683; pmid: 7939683
25. L. Swint-Kruse, K. S. Matthews, Allostery in the LacI/GalR family: Variations on a theme. *Curr. Opin. Microbiol.* **12**, 129–137 (2009). doi: 10.1016/j.mib.2009.01.009; pmid: 19269243
26. T. Cermak *et al*., Efficient design and assembly of custom TALEN and other TAL effector-based constructs for DNA targeting. *Nucleic Acids Res.* **39**, e82 (2011). doi: 10.1093/nar/gkr218; pmid: 21493687
27. A. Busturia, C. D. Wightman, S. Sakonju, A silencer is required for maintenance of transcriptional repression throughout *Drosophila* development. *Development* **124**, 4343–4350 (1997). pmid: 9334282
28. A. K. Sengupta, A. Kuhrs, J. Müller, General transcriptional silencing by a Polycomb response element in *Drosophila*. *Development* **131**, 1959–1965 (2004). doi: 10.1242/dev.01084; pmid: 15056613
29. M. F. Wu *et al*., SWI2/SNF2 chromatin remodeling ATPases overcome polycomb repression and control floral organ identity with the LEAFY and SEPALLATA3 transcription factors. *Proc. Natl. Acad. Sci. U.S.A.* **109**, 3576–3581 (2012). doi: 10.1073/pnas.1113409109; pmid: 22323601
30. T. Ito, H. Sakai, E. M. Meyerowitz, Whorl-specific expression of the *SUPERMAN* gene of *Arabidopsis* is mediated by *cis* elements in the transcribed region. *Curr. Biol.* **13**, 1524–1530 (2003). doi: 10.1016/S0960-9822(03)00612-2; pmid: 12956955
31. T. Ito, N. Takahashi, Y. Shimura, K. Okada, A serine/threonine protein kinase gene isolated by an in vivo binding procedure using the *Arabidopsis* floral homeotic gene product, AGAMOUS. *Plant Cell Physiol.* **38**, 248–258 (1997). doi: 10.1093/oxfordjournals.pcp.a029160; pmid: 9150601
32. B. E. Bernstein *et al*., A bivalent chromatin structure marks key developmental genes in embryonic stem cells. *Cell* **125**, 315–326 (2006). doi: 10.1016/j.cell.2006.02.041; pmid: 16630819
33. M. G. Heisler *et al*., Patterns of auxin transport and gene expression during primordium development revealed by live imaging of the *Arabidopsis* inflorescence meristem. *Curr. Biol.* **15**, 1899–1911 (2005). doi: 10.1016/j.cub.2005.09.052; pmid: 16271866
34. Y. Eshed, S. F. Baum, J. V. Perea, J. L. Bowman, Establishment of polarity in lateral organs of plants. *Curr. Biol.* **11**, 1251–1260 (2001). doi: 10.1016/S0960-9822(01)00392-X; pmid: 11525739
35. R. P. Hellens, E. A. Edwards, N. R. Leyland, S. Bean, P. M. Mullineaux, pGreen: A versatile and flexible binary Ti vector for *Agrobacterium*-mediated plant transformation. *Plant Mol. Biol.* **42**, 819–832 (2000). doi: 10.1023/A:1006496308160; pmid: 10890530
36. K. W. Earley *et al*., Gateway-compatible vectors for plant functional genomics and proteomics. *Plant J.* **45**, 616–629 (2006). doi: 10.1111/j.1365-313X.2005.02617.x; pmid: 16441352
37. S. D. Yoo, Y. H. Cho, J. Sheen, *Arabidopsis* mesophyll protoplasts: A versatile cell system for transient gene expression analysis. *Nat. Protoc.* **2**, 1565–1572 (2007). doi: 10.1038/nprot.2007.199; pmid: 17585298
38. Y. Ogawa *et al*., Efficient and high-throughput vector construction and *Agrobacterium*-mediated transformation of *Arabidopsis thaliana* suspension-cultured cells for functional genomics. *Plant Cell Physiol.* **49**, 242–250 (2008). doi: 10.1093/pcp/pcm181; pmid: 18178967
39. D. R. Smyth, J. L. Bowman, E. M. Meyerowitz, Early flower development in *Arabidopsis*. *Plant Cell* **2**, 755–767 (1990). doi: 10.2307/3869174; pmid: 2152125

Acknowledgments: We thank H. Li and K. Kanehara for their experimental help, G. C. Angenent for the *pAG::GFP* seeds, D. Voytas for Golden Gate TAL effector kit (through Addgene), and RIKEN BRC for the *Arabidopsis* T87 culture cells. We thank H. Yu and F. Berger for their comments on the manuscript. This work was supported by a research grant to T.I. from Temasek Life Sciences Laboratory (TLL), PRESTO (Japan Science and Technology Agency, 4-1-8 Honcho Kawaguchi, Saitama, Japan), and the National Research Foundation Singapore under its Competitive Research Programme (CRP Award NRFCRP001-108). All the constructs made in this work are available from T.I. under a material transfer agreement with TLL.

Supplementary Materials

www.sciencemag.org/content/343/6170/1248559/suppl/DC1
Supplementary Text
Figs. S1 to S21
Tables S1 to S4
References (*40*–*44*)

15 November 2013; accepted 6 December 2013
10.1126/science.1248559

Chapter 22

Misexpression Approaches for the Manipulation of Flower Development

Yifeng Xu, Eng-Seng Gan, and Toshiro Ito

Abstract

The generation of dominant gain-of-function mutants through activation tagging is a forward genetic approach that complements the screening of loss-of-function mutants and that has been successfully applied to studying the mechanisms of flower development. In addition, the functions of genes of interest can be further analyzed through reverse genetics. A commonly used method is gene overexpression, where strong, often ectopic expression can result in an opposite phenotype to that caused by a loss-of-function mutation. When overexpression is detrimental, the misexpression of a gene using tissue-specific promoters can be useful to study spatial-specific function. As flower development is a multistep process, it can be advantageous to control gene expression, or its protein product activity, in a temporal and/or spatial manner. This has been made possible through several inducible promoter systems, as well as by constructing chimeric fusions between the ligand binding domain of the glucocorticoid receptor (GR) and the protein of interest. Upon treatment with a steroid hormone at a specific time point, the fusion protein can enter the nucleus and activate downstream target genes. All these methods allow us to genetically manipulate gene expression during flower development. In this chapter, we describe methods to produce the expression constructs, method of screening, and more general applications of the techniques.

Key words Overexpression, Misexpression, Promoter, Protein tagging, Activation tagging, Glucocorticoid receptor

1 Introduction

Over the last few decades, loss-of-function mutants produced by chemical, irradiation, and insertional mutagenesis have contributed greatly to our understanding of flower development. However, the screening for loss-of-function mutations (*see* Chapter 6), or the uncovering of gene function through the analysis of knockout mutants (*see* Chapter 20), is often hampered by genetic redundancy, i.e., where the activity of one gene can compensate for the loss of another. To circumvent this problem, plant transformation vectors containing multimerized transcriptional enhancers of the constitutive Cauliflower Mosaic Virus (CaMV) *35S* promoter have been used to generate dominant mutants, which typically result

José Luis Riechmann and Frank Wellmer (eds.), *Flower Development: Methods and Protocols*, Methods in Molecular Biology, vol. 1110, DOI 10.1007/978-1-4614-9408-9_22,

from the transcriptional activation, or over-expression, of genes in proximity of the resulting T-DNA insertions [1–3]. Thus, unlike the screening of loss-of-function mutants, such activation tagging lines can be screened in the T1 generation for phenotypic alterations resulting from enhanced gene function.

Once a floral regulator has been identified by forward or reverse genetics, its function can be further characterized by manipulating its expression in a number of ways. In addition to knocking out and reducing gene expression, the simplest and most commonly used approach is to overexpress the gene by placing it under the control of an ectopic and constitutive promoter, such as the CaMV *35S* promoter. Ectopic misexpression of a gene may result in a phenotype that helps to elucidate its functions at the cellular and organismal level. Whereas the analysis of a loss-of-function mutant might allow inferring that the affected gene is essential for a certain developmental function, overexpression studies can reveal whether such a gene is sufficient to carry out that function in a certain development context. For example, the ectopic expression of the floral organ identity gene *AGAMOUS* (*AG*) causes the homeotic transformation of perianth to reproductive organs, suggesting that it is sufficient to determine reproductive organ identity in the context of floral primordia [4].

Although useful and simple to apply, constitutive overexpression approaches have some limitations. Firstly, the CaMV *35S* promoter is often not completely constitutive, but rather exhibits both developmental and tissue specificity. One example is pollen, in which the promoter shows no or only very low activity [5]. Secondly, the high levels of transcript abundance that result from constitutive overexpression might mask temporal and spatial-specific effects, and/or may lead to lethality or sterility (which would make it impossible to obtain stable transformants). In other cases, the constitutive and ectopic expression of genes may lead to artificial phenotypes, by activating or repressing signalling cascades that are not normally linked with the gene's function. Thus, the molecular analyses of downstream cascades and phenotypic interpretation need to be carefully conducted and correlated with those of the corresponding loss-of-function mutants. Furthermore, to overcome the limitations of constitutive overexpression, several methods can also be employed to control gene expression in a temporal and/or spatial-dependent fashion.

Tissue-specific promoters and inducible promoter systems can be applied in different situations. Tissue-specific promoters restrict the activity of the transgenes to certain tissues, which allows assessing the function of a gene in specific cell types. In addition to directly driving a gene of interest under a specific promoter, two-component systems are also available, which utilize a trans-activator and the binding sites conjugated with a minimal promoter, such as the LhG4/*pOp* system [6, 7]. The LhG4 activator component

carries the DNA-binding domain of a mutant *lac* repressor and a transcriptional activation domain of the yeast GAL4 protein. The DNA-binding domain of a mutant *lac* repressor binds to the *lac* repressor-binding sites (*lac* operators or Op) with particularly high-affinity. Expression of the gene of interest, which has been placed under the control of the *lac* repressor binding sites, is thus determined by the expression pattern of the LhG4 activator, which is controlled by the chosen (tissue-specific) promoter. An important advantage of two-component systems is that they facilitate combinatorial experimental designs, where a number of genes of interest can be studied in different developmental contexts by generating and crossing the appropriate driver and reporter lines [8, 9].

In addition to tissue-specific expression, the ability to temporally modulate gene activity is essential to study downstream cascades and to identify immediate or direct effects of a gene in developmental processes. Chemical inducible systems are one of the solutions to temporally control transgene expression and/or activity, with those based on the glucocorticoid receptor (GR) being the most commonly used [10]. A one-component GR inducible strategy is suitable for nuclear-localized proteins, such as transcription factors and chromatin remodeling factors. In this case, the respective protein-coding sequence is translationally fused (at its N- or C-terminus) with the sequence coding for the GR ligand-binding domain. In transgenic plants, these chimeric transcription factors are retained in the cytoplasm by heat shock proteins in the absence of the ligand. Upon treatment of the tissue or cells with a glucocorticoid such as dexamethasone, the GR fusion protein is released from its cytoplasmic retention and imported into the nucleus, where it may be functionally active and thus activated. The addition of epitope tags, such as c-Myc or HA, at the N- or C-terminal end of the fusion protein is helpful for biochemical assays such as Chromatin Immunoprecipitation (ChIP) to examine the binding of a transcriptional regulator to specific target sites [11, 12]. Functionality of the fusion protein needs to be confirmed in the respective mutant background by phenotypic rescue upon dexamethasone induction. Furthermore, transgenic lines with an optimal inducibility need to be isolated, because the expression of transgenes can depend on, or be affected by, their place of insertion in the genome.

Two-component inducible promoter systems utilize GR-fused trans-activators and the corresponding binding sites, such as GR-LhG4/*pOp* to temporally activate transgenes [6, 13]. In this case, the GR domain is fused to the N-terminus of the synthetic transcription factor LhG4, whose expression is under the control of the constitutive CaMV *35S* promoter or of a tissue-specific promoter. Other chemically inducible two-component systems have also been successfully used. For instance, the GAG system utilizes a fusion protein between the Gal4 DNA binding domain, which binds to Gal4 UAS, and the VP16 activation domain,

followed by GR [14]. The estradiol-inducible XVE system is based on a fusion between the DNA binding domain of LexA, VP16 and an estradiol receptor ligand binding domain (ER) [15]. The ethanol-inducible AlcR/AlcA system is based on the transcriptional activator AlcR from *Aspergillus nidulans* and an AlcR-responsive promoter element, *alcA* [16].

This chapter describes our current protocols for activation tagging, as well as for the use of ectopic over-expression and tissue-specific expression of a gene of interest in flower development. In addition, the use of two different types of inducible systems, direct GR fusions to transcription factors (induction of protein activity) and the two-component LhG4-GR/*pOP* system (transcriptional induction), is described.

2 Materials

2.1 Construction of Expression Cassettes

1. Vectors (*see* Fig. 1).
2. cDNA prepared from tissue(s) expressing the gene of interest, or genomic DNA for tissue-specific promoters.
3. Competent cells of appropriate *E. coli* strains.
4. Luria–Bertani (LB) media (broth and agar plate).
5. Antibiotics for selection of plasmids in *E. coli*.
6. Oligonucleotide primers.
7. Restriction enzymes, *Taq* DNA polymerase, high fidelity and proofreading DNA polymerase, and T4 DNA ligase.

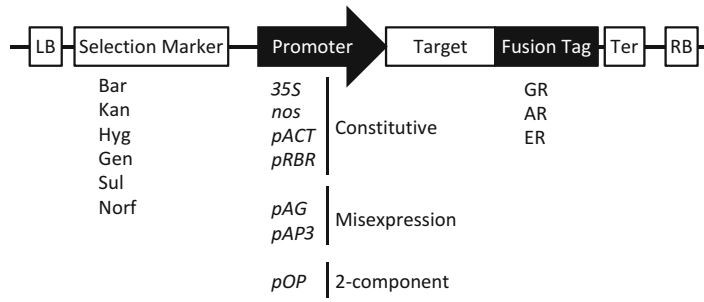

Fig. 1 Schematic representation of expression cassettes used for the misexpression of genes during flower development. Selection markers, promoters, gene fusions, transcriptional terminators (Ter), as well as Left Border (LB) and Right Border (RB) sequences are indicated. Selection markers: *Bar* Basta (or glufosinate), *Kan* Kanamycin, *Hyg* Hygromycin, *Gen* Gentamycin, *Sul* Sulfadiazine, *Norf* Norflurazon. Promoters: *35S* CaMV *35S*, *nos* Nopaline synthase promoter, *pACT ACTIN* promoter, *pRBR RETINOBLASTOMA-RELATED* promoter, *pAG AGAMOUS* promoter, *pAP3 APETALA3* promoter, *pOP lac* operators positioned upstream of a minimal promoter. Protein fusions: *GR* glucocorticoid receptor, *AR* androgen receptor, *ER* estrogen receptor

8. Agarose.
9. Gel extraction kit.
10. PCR purification kit.
11. Plasmid Miniprep kit.

2.2 Agrobacterium-Mediated Transformation of Arabidopsis

1. *Agrobacterium tumefaciens* strains.
2. Luria–Bertani (LB) media (broth and agar plate).
3. Antibiotics for selection of plasmids in *Agrobacteria*.
4. Infiltration medium: 5 % (w/v) (50 g/L) sucrose, 1× (4.4 g/L) Murashige & Skoog (MS) salt, 0.03 % (v/v) (300 μL/L) Silwet L-77.

2.3 Screening of Transgenic Plants

1. MS solid medium: 1× MS salts, 3 % sucrose, 0.8 % Phytagel™, pH 5.7 (adjusted with KOH).
2. Petri plates (100-mm square), around 40 mL of MS solid medium per plate.
3. Seed sterilization solution: freshly diluted bleach (10 % bleach) containing 0.01 % (v/v) Triton X-100.
4. 100 % ethanol and 95 % ethanol prepared with sterilized water.
5. Antibiotics for selection of transgenic plants.

2.4 Dexamethasone Induction and Protein Synthesis Inhibition Treatment

1. Plastic container.
2. Dexamethasone stock solution: 30 mM dexamethasone. Resuspend 23.55 mg of dexamethasone in 2 mL of ethanol. Store the stock solution at −20 °C, where it will last for at least 1 month.
3. Dexamethasone working solution: 0.5–25 μM (10 μM is often used as starting concentration) dexamethasone in deionized water with 0.015 % (v/v) Silwet L-77.
4. Cycloheximide stock solution: 10 mM cycloheximide in water. Solution can be stored in aliquots at −20 °C for several months.

2.5 Screening and Identification of Activation-Tagged Genes

1. Plant DNA extraction kit.
2. Restriction enzyme (*see* **Note 1**).
3. PCR purification kit.
4. T4 DNA ligase.
5. Competent *E. coli* cells.
6. Luria–Bertani (LB) media (broth and agar plate).

2.6 Observation of Phenotypes

1. Stereomicroscope.

3 Methods

3.1 Construction of Expression Cassettes

All cloning procedures are done in accordance with standard protocols [17]. A typical expression cassette flanked by the Left and Right Border is shown in Fig. 1.

3.1.1 Choice of Promoters

A good promoter of choice for overexpression is the Cauliflower Mosaic Virus (CaMV) *35S* promoter [18–20]. There are different versions of the promoter. We frequently use the double 35S promoter with success for strong ectopic expression [18]. Other constitutive promoters are also available, such as nopaline synthase (*nos*), octopine synthase (*ocs*), and mannopine synthase (*mas*) promoters [21–23], or promoters of housekeeping genes, such as actin (p*ACT*) or ubiquitin (p*UBQ*) [24, 25]. The *RETINOBLASTOMA-RELATED* promoter (*pRBR*) can be used to drive expression in the male and female gametophyte [26, 27], in which the *35S* promoter is only weakly active.

The phenotypes that result from constitutive overexpression of a gene may not represent its normal function in a native environment. Moreover, gene overexpression may cause plant lethality and sterility, making it impossible to obtain stable transformants. In these situations, using tissue-specific expression or misexpression might be a better choice. Typically, a clone containing 2–3 kb upstream of the transcriptional start site would be able to capture the endogenous expression of the gene. In some cases, regulatory elements are located in intragenic regions (as in the case of *AGAMOUS* (*AG*) and *SUPERMAN* (*SUP*) [28–30]) or in the 3′ untranslated or downstream regions of genes [31, 32]. Therefore, the use of the corresponding promoters to drive the expression of other genes would require including those regions in the constructs, to ensure proper expression patterns. *See* Table 1 for a list promoters used for studies in flower/meristem development.

For the two-component system, a gene of interest can be positioned downstream of the *pOP* promoter sequence. Depending on the need of the experiment, expression of the synthetic transcription factors LhG4 or LhG4-GR can be driven by the constitutive *35S* promoter or by tissue-specific promoters [7, 33]. Several different strategies can be used to combine the *pOP:GENE* construct and the *promoter::LhG4* construct *in planta*: the two constructs can be inserted into the same transformation vector; the two constructs could be used for sequential plant transformation (if they carry different selection markers); or doubly transgenic plants may be generated by crossing single transformants [8, 9].

3.1.2 Choices of Inducible Systems

Although dexamethasone-inducible GR fusions are the focus of this protocol, there are other chemical inducible systems that can be used, such as the dihydrotestosterone (DHT)-inducible

Table 1
Promoters used for misexpression studies in flower/meristem development

Gene	Expression pattern	References
ACTIN 4 (*ACT4*)	Ubiquitously expressed including developing pollen	[43]
RETINOBLASTOMA RELATED (*RBR*)	Ubiquitously expressed including developing pollen	[26, 27]
CLAVATA3 (*CLV3*)	In vegetative and floral stem cells	[44, 45]
UNUSUAL FLORAL ORGANS (*UFO*)	In shoot apical meristems and floral primordia at stages 1–3, restricted later to the junction between whorls 1 and 2	[45, 46]
CUP-SHAPED COTYLEDON2 (*CUC2*)	In meristems and organ boundaries, also in leaf margins	[47]
LEAFY (*LFY*)	Gradually increased in vegetative meristems and highly expressed in inflorescence and floral meristems	[45, 48]
AINTEGUMENTA (*ANT*)	Throughout emerging lateral organ primordia of all above-ground organs	[49, 50]
ASYMMETRIC LEAVES1 (*AS1*)	Throughout emerging lateral organ primordia of all above-ground organs	[51, 52]
FILAMENTOUS FLOWER (*FIL*)	In the peripheral region of vegetative and inflorescence meristems, later restricted to abaxial side of the vegetative and floral organ primordia	[7, 53, 54]
APETALA1 (*AP1*)	In floral meristems, later restricted to whorls 1 and 2 from stage 3 in developing flowers	[55, 56]
APETALA3 (*AP3*)	In whorls 2 and 3 from stage 3 in developing flowers	[52, 57]
AGAMOUS (*AG*)	In whorls 3 and 4 from stage 3 in developing flowers	[28]
CRABS CLAW (*CRC*)	In developing carpels and nectaries from stage 6	[58, 59]

Names of promoters, their expression patterns, and relevant references are given

Androgen Receptor (AR) [34] and the estradiol-inducible Estrogen Receptor (ER) [15]. These receptor tags can be fused with the protein-coding sequence directly in a one-component system, or with the activator in a two-component system such as LhG4-GR in the *pOP*/LhGR system [6]. Besides these chemical inducers, there are other inducible systems utilizing heat, cold, or alcohol (*see* Table 2), each with their own advantages and disadvantages. Although they are not the focus of this chapter, they are listed here for comparison.

The GR-based system is the most commonly used inducible system as glucocorticoid can easily permeate plant tissues and rapidly induces gene activation [14]. It can also be systematically transported, thus dexamethasone treatment can be done via spraying or dipping into a dexamethasone solution or planting on MS plates

Table 2
Inducible systems used to temporally control gene expression

Inducible system	Vector used	Mode of activation	References
GR fusion	pBI-ΔGR	Dexamethasone	[10, 60]
GVG/UAS	pBI101-GVG-UAS-Luc	Dexamethasone	[14]
pOP/LhGR	pBIN-LhGR-N, pOP6-GUS pBIN-LR-LhGR, pOP6-GUS pOPOff1	Dexamethasone	[6, 13]
AR fusion	pGREEN-35S-AR	Dihydrotestosterone	[34]
ER fusion	pSKM36-ESR2-ER	Estradiol	[43, 61]
XVE/OlexA	pER8	Estradiol	[15]
AlcR/AlcA	*alcR alcA::reporter*	Ethanol	[16]
pHSP18.2	pTT101 pGA482-pHSP18.2	Heat treatment (37 °C)	[62] [63]
CBF3/*pRD29A*	pMDC-CBF3 pFAJ-PAP1	Cold treatment (4 °C)	[40]

Names of vector used, their mode of activation, and relevant references are shown

containing dexamethasone [35]. On the other hand, estradiol is not easily transported in adult plants and hence, for local induction, an ER-based inducible system may be a better choice [36]. Another advantage of using these chemical inducers is that, at the concentration used, they are generally nontoxic to plants and show no observable pleiotropic physiological effect.

The ethanol-inducible AlcR/AlcA system is another system that can be easily applied to drive gene expression [16]. The inducer, ethanol, is nontoxic at the concentrations typically used. As ethanol evaporates quickly, ethanol vapor can be used for pulsed and local induction [37]. However, the volatility of ethanol means that it may also activate nearby plants during treatment. Extra care should also be taken when handling seedlings in an ethanol-sterilized environment.

Utilizing the heat-shock promoter *pHSP18.2*, genes can be induced simply by placing the plants in 37 °C condition for 1–2 h [38]. Compared to chemical treatment, heat treatment can be applied uniformly to plants at a large scale. Nevertheless, repeated heat-shock treatment may produce pleiotropic effects, especially affecting pollen development [39]. Unlike heat treatment, cold treatment can be used for a longer period in the CBF3/*pRD29A* system [40]. However, it should be noted that prolonged cold treatment impairs cell cycle progression and also causes pollen sterility [39].

3.1.3 Cloning Step

1. Amplify the coding region of the gene of interest using high fidelity DNA polymerase with cDNA (target gene) or gDNA (promoter) as the template (*see* **Note 2**).
2. Analyze the PCR amplification product by agarose gel electrophoresis, to check whether the size of the amplicon is correct, followed by extraction of the DNA fragment of interest from the gel with any gel extraction kit.
3. Digest amplicon and vector with appropriate restriction enzymes (*see* **Note 3**).
4. After the digestion reaction, cleanup the amplicon and the vector with a PCR purification kit if no big fragment is cut out. Otherwise, run the digestion products in a standard agarose gel and extract the DNA fragment(s) of interest with a gel extraction kit.
5. Ligate the vector with the insert (*see* **Note 4**).
6. Transform the ligation reaction using heat shock competent cells or by electroporation (*see* **Note 5**).
7. Add LB broth without antibiotic up to 1 mL and incubate for 1 h at 37 °C in a shaker at around 250 rpm. Spin down cells with a microcentrifuge at maximum speed. Pour off the supernatant. Resuspend the cell pellet with the residual LB Broth and spread on LB agar plates with the appropriate antibiotic. Incubate plates overnight at 37 °C.
8. Screen for positive clones by colony PCR, and transfer the clone into a culture tube with 3 mL of LB broth with the appropriate antibiotic. Incubate overnight at 37 °C in a shaker at around 250 rpm.
9. Extract the plasmid from the cells with a Miniprep kit according to the manual provided by the supplier.
10. Verify the plasmid sequence by Sanger DNA sequencing.

3.1.4 Activation Tagging

Many activation tagging vectors have been described in the literature and can be requested from the groups that generated them (*see* Table 3).

3.2 Transformation of Arabidopsis (Agrobacterium-Mediated Transformation)

1. Grow *Arabidopsis* on soil in trays or pots under a 16-h photoperiod at 22 °C. The plants are ready for transformation when their inflorescence stems are at least 5 cm in length. This occurs typically between 4 and 6 weeks after germination.
2. Transform an appropriate *Agrobacterium*-strain with the desired plant transformation vector, using either standard electroporation techniques or freeze-thaw transformation (*see* **Note 6**). After a recovery period of continuous shaking at 28 °C for 2–3 h, spread or streak the *Agrobacterium* cells onto LB agar plates containing the appropriate antibiotics for selection. Incubate at 28–30 °C for 2 days.

Table 3
Vectors used for activation tagging

Plasmid	Plant species	Plant selection	Reference
pPCVICEn4HPT	*Arabidopsis*, Petunia, Tobacco	Hygromycin	[1]
pSKI015	*Arabidopsis*	Basta	[2]
pSKI074	*Arabidopsis*	Kanamycin	[2]
pTag2B4A1	*Catharanthus*	Hygromycin	[64]
pGA2715	Rice	Hygromycin	[65]
pAG3202	Tomato	Kanamycin	[66]
pER16 (inducible)	*Arabidopsis*	Kanamycin	[67]

Names of plasmids, the plant species in which the vectors have been used, the selection markers for the isolation of transgenic plants, and relevant references are shown

3. Inoculate three individual colonies into 3 mL of LB Broth with the appropriate antibiotics. Incubate overnight at 28–30 °C with continuous shaking at around 250 rpm. in a standard orbital shaker.
4. Inoculate 500 mL of LB broth containing the appropriate antibiotics with 3 mL of the overnight culture. Grow overnight at 28–30 °C with continuous shaking until the culture reaches an OD_{600} of 1.0–1.5.
5. Harvest *Agrobacterium* cells by centrifugation at 8,000 × *g* for 15 min at room temperature. Resuspend the pellet with infiltration medium to an OD_{600} of 0.5–1.0.
6. Transfer 500 mL of the *Agrobacterium*-infiltration solution into a suitable plastic container. Trays or pots of *Arabidopsis* plants are placed upside down with the inflorescence submerged in the infiltration solution. Shake at 80 rpm on an orbital shaker for 3 min. Be careful not to let the soil contact the solution (*see* **Note 7**).
7. Cover the plants with plastic wrap to maintain high humidity and place transformed plants under low light intensity overnight.
8. Remove the plastic wrap and transfer the plants to growth room or chamber. Water the plants until they set seed. Allow the plants to dry gradually. Harvest dried seeds and store in a desiccator cabinet for at least 1 week.

3.3 Screening of Transformants

1. Sterilize T1 seeds for plating. Put T1 seeds in an appropriately sized tube and add approximately 10× volume of freshly prepared seed sterilization solution. Shake at high speed for 15 min.

Aspirate off liquid and rinse with approximately 10× volume of 95 % ethanol for three times.

2. Add around 10× volume of pure ethanol and pipette seeds onto filter paper (Whatman) to dry (*see* **Note 8**). Disperse dried seeds evenly onto MS medium plates with appropriate antibiotics.
3. Stratify the seeds by placing the plates at 4 °C in the dark for 2–5 days to synchronize germination, followed by placing the plates in a growth chamber at 22 °C with 16-h photoperiod.
4. Identify putative transgenic plants. Perform genotyping PCR, and assay for transgene expression by RT-PCR for verification. In the case of dexamethasone-inducible lines, select lines without any leaky phenotype (*see* **Note 9**).
5. Optional I: to screen the T1 transgenic plants for resistance to the herbicide Basta, the seeds also can be sown on soil and sprayed with 0.2 % (v/v) Basta solution after germination.
6. Optional II: perform Western blot analysis to identify lines that produce high levels of the fusion protein, using an antibody that recognizes the epitope tag introduced in the fusion protein (such as c-Myc or HA).

3.4 Dexamethasone Induction and Protein Synthesis Inhibition Treatment

Option 1: Grow seedlings on dexamethasone-containing MS plates for up to 21 days after germination. This approach leads to a sustained activation of the GR fusion protein and is thus not suitable for transient activation experiments.

1. Sterilize seeds and grow them on MS plates as described in Subheading 3.3. One set of MS plates contains dexamethasone at concentrations between 0.1 and 25 μM to test (*see* **Note 10**). Prepare another set of MS plates, which serve as controls, and replace the dexamethasone solution with an equal volume of ethanol.

Compare the phenotypes of the dexamethasone and mock-treated plants to identify phenotypic abnormalities likely caused by the activation of the GR fusion protein.

Option 2: Treat plants by submersion in dexamethasone-containing water. This approach is advisable for both transient and sustained inductions.

1. Freshly prepare a dexamethasone work solution and a mock-solution in which the dexamethasone stock solution is replaced with an equal volume of ethanol.
2. Submerge plants with an inflorescence shoot of around 5 cm into a plastic container with dexamethasone-containing or mock solutions. Shake at low speed (around 70 rpm) for 3 min to remove bubbles and allow the solution to penetrate thoroughly.

3. For sustained activation, treatments can be repeated daily (*see* **Note 11**). However, because a prolonged treatment with Silwet L-77 might have a toxic effect on plants, reduce its concentration after the initial treatment, or replace it with Triton X-100 (used at a concentration of 0.1 % (v/v)).
4. In transient activation experiments, 10 μM cycloheximide in water can be applied prior to or at the same time as the dexamethasone treatment, to inhibit de novo protein synthesis. This treatment is useful for testing whether gene expression changes are the result of a direct or indirect regulation of the transcription factor under study.

3.5 Screening and Determination of the Activation Tag

Screening of T1 seeds is done as described in Subheading 3.3. After selecting the lines with the desired phenotypes, it is important to determine the site of T-DNA insertion. This can be done through the method of Plasmid Rescue:

1. Extract genomic DNA from the transgenic lines (*see* **Note 12**).
2. Digest about 100 ng of purified genomic DNA with restriction enzyme (*see* **Note 1**).
3. Clean-up the digested genomic DNA with a PCR purification kit.
4. Use T4 DNA ligase to self-ligate the digested DNA at 16 °C at low concentration.
5. Clean-up the ligated plasmid with a PCR purification kit.
6. Transform the purified plasmid into competent *E. coli* cells.
7. Amplify the plasmid and analyze the flanking sequence by sequencing using the T-DNA specific primer.
8. Examine the genes located nearby the T-DNA insertion site (*see* **Note 13**).
9. Generate independent transgenic lines that overexpress the candidate gene(s) identified through activation tagging, to confirm its capability to cause the desired phenotype. The rescued plasmid can be transformed into plants if the full coding region of the gene is contained in it.

3.6 Observation of Phenotypes

After obtaining the desired lines, a phenotypic characterization is frequently done in plants of the T2 or T3 generation (*see* **Note 14**). *Arabidopsis* flower development can be divided into 12 stages during early development (Fig. 2) and another eight stages during late stage development after the bud opens [41]. Depending on the stage of development, observation of phenotypes may be done under a scanning electron microscope (*see* Chapters 7 and 13) or a stereomicroscope. Look for plants with floral phenotypes such as alteration of meristem structure or size, floral homeotic conversion, early or delayed termination of floral meristem, abnormalities in floral organ number, size, or shape, etc. It is also advisable to grow

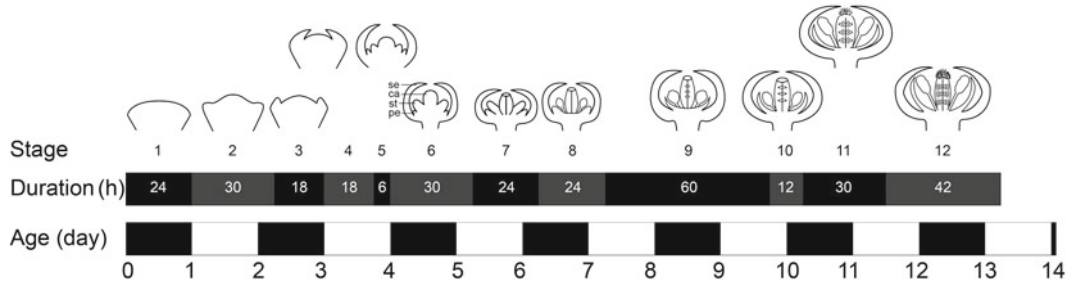

Fig. 2 Early *Arabidopsis* flower development. The duration of each stage is estimated to the nearest 6 h interval when wild-type Arabidopsis plants are grown at 25 °C under constant illumination [41]. Sizes of flower buds shown are not to scale

wild-type plants side by side to the transgenic lines as controls to account for potential environmental effects on plant growth and development.

4 Notes

1. The restriction enzyme to use depends on the activation tagging vector employed. For example, in pSKI015 and pSKI074, the restriction enzymes *Kpn*I, *Eco*RI, and *Hin*dIII can be used for the isolation of sequences next to the right border of the T-DNA [2].
2. For direct digestion of PCR products, the primers can be designed with a protective extension of two to four nucleotides at the 5′ end, depending on the restriction enzyme and the corresponding recognition site. Alternatively, to increase the efficiency of the restriction digestion, the amplicon can be inserted into TA cloning vectors (e.g., from Invitrogen or Promega) first.
3. To reduce the occurrence of self-ligation of the vector, Calf Intestinal Alkaline Phosphatase can be added to the restriction digestion mix to remove terminal phosphates from the DNA backbone.
4. Ligation reactions can be carried out with rapid ligation mixture at room temperature for a few minutes, or by standard conditions at 16 °C overnight. The total reaction volume is usually 5–10 μL. The amount of vector commonly used is 50 ng and the molar ratio of vector to insert is 1:3.
5. Prior to transformation into *E. coli* by electroporation, the DNA from the ligation reaction needs to be purified and desalted by ethanol precipitation and then resuspended in water.
6. Compared with the electroporation technique, freeze-thaw transformation is a much cheaper method. Thaw competent *Agrobacterium* cells on ice and add about 100 ng of plasmid to 250 μL of cell suspension. Incubate the mixture on ice for 5 min.

Transfer mixture to liquid nitrogen and incubate for 5 min. Incubate the mixture for another 5 min in a 37 °C water bath. Add 1 mL of LB Broth without antibiotics and shake for 2–4 h at 28 °C for recovery.

7. Nylon netting can be placed over the soil pot with seeds, to prevent the contact of soil with infiltration medium and to prevent plant from falling off into infiltration medium.
8. The head of a 1,000 μL pipette tip should be trimmed to make the size of the opening much bigger to pipette seeds easily. Filter tips are advised to prevent contaminations.
9. While dexamethasone-inducible regulation is tight, we sometimes observe leaky effects of fusion proteins in the absence of hormone. At least 20 independent lines should be characterized for optimal inducibility.
10. 10 μM dexamethasone is the standard concentration, although concentrations ranging from 0.1 to 25 μM have been used successfully. If treatments of 10 μM dexamethasone results in toxic effects to the plants, reduced dexamethasone concentrations should be tested.
11. In the case of *ag-1* 35S::AG-GR, inflorescences that were subjected to a single treatment with 10 μM dexamethasone solution, it was determined that the AG-GR protein was retained in the nucleus for up to 2–3 days [42]. For full rescue of the *ag* mutant phenotypes, at least four times of daily dexamethasone treatments was necessary.
12. High quality genomic DNA is important for successful cloning of the flanking sequence. Hence, we recommend using a suitable extraction kit following the manufacturer's instructions.
13. Four tandemly connected 35S enhancers of the *pPCVICEn4HPT* vector are active up to around 10 kb from the insertion site. If a gene showing enhanced expression cannot be found in the vicinity of the activation construct, consider that there may be an unannotated gene present, such as a gene coding for a noncoding small regulatory RNA or a gene coding for a small peptide.
14. Molecular analysis should be carried out in homozygous lines to prevent sample variation.

Acknowledgement

This work was supported by research grants to T.I. from Temasek Life Sciences Laboratory (TLL), the National Research Foundation Singapore under its Competitive Research Programme (CRP Award No. NRF-CRP001-108) and PRESTO, Japan Science and Technology Agency, 4-1-8 Honcho Kawaguchi, Saitama, Japan.

References

1. Walden R, Fritze K, Hayashi H, Miklashevichs E, Harling H, Schell J (1994) Activation tagging: a means of isolating genes implicated as playing a role in plant growth and development. Plant Mol Biol 26(5):1521–1528
2. Weigel D, Ahn JH, Blazquez MA, Borevitz JO, Christensen SK, Fankhauser C, Ferrandiz C, Kardailsky I, Malancharuvil EJ, Neff MM, Nguyen JT, Sato S, Wang ZY, Xia Y, Dixon RA, Harrison MJ, Lamb CJ, Yanofsky MF, Chory J (2000) Activation tagging in Arabidopsis. Plant Physiol 122(4):1003–1013
3. Ito T, Meyerowitz EM (2000) Overexpression of a gene encoding a cytochrome P450, CYP78A9, induces large and seedless fruit in Arabidopsis. Plant Cell 12(9):1541–1550
4. Mizukami Y, Ma H (1992) Ectopic expression of the floral homeotic gene AGAMOUS in transgenic Arabidopsis plants alters floral organ identity. Cell 71(1):119–131
5. Wilkinson JE, Twell D, Lindsey K (1997) Activities of CaMV 35S and nos promoters in pollen: implications for field release of transgenic plants. J Exp Bot 48(2):265–275
6. Moore I, Samalova M, Kurup S (2006) Transactivated and chemically inducible gene expression in plants. Plant J 45(4):651–683
7. Goldshmidt A, Alvarez JP, Bowman JL, Eshed Y (2008) Signals derived from YABBY gene activities in organ primordia regulate growth and partitioning of Arabidopsis shoot apical meristems. Plant Cell 20(5):1217–1230
8. Moore I, Galweiler L, Grosskopf D, Schell J, Palme K (1998) A transcription activation system for regulated gene expression in transgenic plants. Proc Natl Acad Sci U S A 95(1): 376–381
9. Baroux C, Blanvillain R, Betts H, Batoko H, Craft J, Martinez A, Gallois P, Moore I (2005) Predictable activation of tissue-specific expression from a single gene locus using the pOp/LhG4 transactivation system in Arabidopsis. Plant Biotechnol J 3(1):91–101
10. Lloyd AM, Schena M, Walbot V, Davis RW (1994) Epidermal cell fate determination in Arabidopsis: patterns defined by a steroid-inducible regulator. Science 266(5184): 436–439
11. Earley KW, Haag JR, Pontes O, Opper K, Juehne T, Song K, Pikaard CS (2006) Gateway-compatible vectors for plant functional genomics and proteomics. Plant J 45(4):616–629
12. Knop M, Siegers K, Pereira G, Zachariae W, Winsor B, Nasmyth K, Schiebel E (1999) Epitope tagging of yeast genes using a PCR-based strategy: more tags and improved practical routines. Yeast 15(10B):963–972
13. Craft J, Samalova M, Baroux C, Townley H, Martinez A, Jepson I, Tsiantis M, Moore I (2005) New pOp/LhG4 vectors for stringent glucocorticoid-dependent transgene expression in Arabidopsis. Plant J 41(6):899–918
14. Aoyama T, Chua NH (1997) A glucocorticoid-mediated transcriptional induction system in transgenic plants. Plant J 11(3):605–612
15. Zuo J, Niu QW, Chua NH (2000) Technical advance: an estrogen receptor-based transactivator XVE mediates highly inducible gene expression in transgenic plants. Plant J 24(2):265–273
16. Roslan HA, Salter MG, Wood CD, White MR, Croft KP, Robson F, Coupland G, Doonan J, Laufs P, Tomsett AB, Caddick MX (2001) Characterization of the ethanol-inducible alc gene-expression system in Arabidopsis thaliana. Plant J 28(2):225–235
17. Green MR, Sambrook J (2012) Molecular cloning: a laboratory manual, 4th edn. Cold Spring Harbor Laboratory Press, New York
18. Fang RX, Nagy F, Sivasubramaniam S, Chua NH (1989) Multiple cis regulatory elements for maximal expression of the cauliflower mosaic virus 35S promoter in transgenic plants. Plant Cell 1(1):141–150
19. Benfey PN, Chua NH (1990) The cauliflower mosaic virus 35S promoter: combinatorial regulation of transcription in plants. Science 250(4983):959–966
20. Benfey PN, Ren L, Chua NH (1990) Tissue-specific expression from CaMV 35S enhancer subdomains in early stages of plant development. EMBO J 9(6):1677–1684
21. Leisner SM, Gelvin SB (1988) Structure of the octopine synthase upstream activator sequence. Proc Natl Acad Sci U S A 85(8):2553–2557
22. DiRita VJ, Gelvin SB (1987) Deletion analysis of the mannopine synthase gene promoter in sunflower crown gall tumors and Agrobacterium tumefaciens. Mol Gen Genet 207(2–3): 233–241
23. An G (1986) Development of plant promoter expression vectors and their use for analysis of differential activity of nopaline synthase promoter in transformed tobacco cells. Plant Physiol 81(1):86–91
24. An YQ, McDowell JM, Huang S, McKinney EC, Chambliss S, Meagher RB (1996) Strong, constitutive expression of the Arabidopsis ACT2/ACT8 actin subclass in vegetative tissues. Plant J 10(1):107–121

25. Callis J, Raasch JA, Vierstra RD (1990) Ubiquitin extension proteins of Arabidopsis thaliana. Structure, localization, and expression of their promoters in transgenic tobacco. J Biol Chem 265(21):12486–12493
26. Johnston AJ, Kirioukhova O, Barrell PJ, Rutten T, Moore JM, Baskar R, Grossniklaus U, Gruissem W (2010) Dosage-sensitive function of retinoblastoma related and convergent epigenetic control are required during the Arabidopsis life cycle. PLoS Genet 6(6):e1000988
27. Borghi L, Gutzat R, Futterer J, Laizet Y, Hennig L, Gruissem W (2010) Arabidopsis RETINOBLASTOMA-RELATED is required for stem cell maintenance, cell differentiation, and lateral organ production. Plant Cell 22(6):1792–1811
28. Sieburth LE, Meyerowitz EM (1997) Molecular dissection of the AGAMOUS control region shows that cis elements for spatial regulation are located intragenically. Plant Cell 9(3):355–365
29. Busch MA, Bomblies K, Weigel D (1999) Activation of a floral homeotic gene in Arabidopsis. Science 285(5427):585–587
30. Ito T, Sakai H, Meyerowitz EM (2003) Whorl-specific expression of the SUPERMAN gene of Arabidopsis is mediated by cis elements in the transcribed region. Curr Biol 13(17): 1524–1530
31. Kaufmann K, Wellmer F, Muino JM, Ferrier T, Wuest SE, Kumar V, Serrano-Mislata A, Madueno F, Krajewski P, Meyerowitz EM, Angenent GC, Riechmann JL (2010) Orchestration of floral initiation by APETALA1. Science 328(5974):85–89
32. Ito T, Wellmer F, Yu H, Das P, Ito N, Alves-Ferreira M, Riechmann JL, Meyerowitz EM (2004) The homeotic protein AGAMOUS controls microsporogenesis by regulation of SPOROCYTELESS. Nature 430(6997): 356–360
33. Lenhard M, Bohnert A, Jurgens G, Laux T (2001) Termination of stem cell maintenance in Arabidopsis floral meristems by interactions between WUSCHEL and AGAMOUS. Cell 105(6):805–814
34. Sun B, Xu Y, Ng KH, Ito T (2009) A timing mechanism for stem cell maintenance and differentiation in the Arabidopsis floral meristem. Genes Dev 23(15):1791–1804
35. Geng X, Mackey D (2011) Dose-response to and systemic movement of dexamethasone in the GVG-inducible transgene system in Arabidopsis. Methods Mol Biol 712:59–68
36. Tornero P, Chao RA, Luthin WN, Goff SA, Dangl JL (2002) Large-scale structure-function analysis of the Arabidopsis RPM1 disease resistance protein. Plant Cell 14(2): 435–450
37. Maizel A, Weigel D (2004) Temporally and spatially controlled induction of gene expression in Arabidopsis thaliana. Plant J 38(1):164–171
38. Masclaux F, Charpenteau M, Takahashi T, Pont-Lezica R, Galaud JP (2004) Gene silencing using a heat-inducible RNAi system in Arabidopsis. Biochem Biophys Res Commun 321(2):364–369
39. Zinn KE, Tunc-Ozdemir M, Harper JF (2010) Temperature stress and plant sexual reproduction: uncovering the weakest links. J Exp Bot 61(7):1959–1968
40. Feng Y, Cao CM, Vikram M, Park S, Kim HJ, Hong JC, Cisneros-Zevallos L, Koiwa H (2011) A three-component gene expression system and its application for inducible flavonoid overproduction in transgenic Arabidopsis thaliana. PLoS One 6(3):e17603
41. Smyth DR, Bowman JL, Meyerowitz EM (1990) Early flower development in Arabidopsis. Plant Cell 2(8):755–767
42. Ito T, Ng KH, Lim TS, Yu H, Meyerowitz EM (2007) The homeotic protein AGAMOUS controls late stamen development by regulating a jasmonate biosynthetic gene in Arabidopsis. Plant Cell 19:3516–3529
43. Ikeda Y, Banno H, Niu QW, Howell SH, Chua NH (2006) The ENHANCER OF SHOOT REGENERATION 2 gene in Arabidopsis regulates CUP-SHAPED COTYLEDON 1 at the transcriptional level and controls cotyledon development. Plant Cell Physiol 47(11): 1443–1456
44. Fletcher JC, Brand U, Running MP, Simon R, Meyerowitz EM (1999) Signaling of cell fate decisions by CLAVATA3 in Arabidopsis shoot meristems. Science 283(5409):1911–1914
45. Deveaux Y, Peaucelle A, Roberts GR, Coen E, Simon R, Mizukami Y, Traas J, Murray JA, Doonan JH, Laufs P (2003) The ethanol switch: a tool for tissue-specific gene induction during plant development. Plant J 36(6):918–930
46. Durfee T, Roe JL, Sessions RA, Inouye C, Serikawa K, Feldmann KA, Weigel D, Zambryski PC (2003) The F-box-containing protein UFO and AGAMOUS participate in antagonistic pathways governing early petal development in Arabidopsis. Proc Natl Acad Sci U S A 100(14):8571–8576
47. Steiner E, Efroni I, Gopalraj M, Saathoff K, Tseng TS, Kieffer M, Eshed Y, Olszewski N, Weiss D (2012) The Arabidopsis O-linked N-acetylglucosamine transferase SPINDLY interacts with class I TCPs to facilitate cytokinin responses in leaves and flowers. Plant Cell 24(1):96–108

48. Blazquez MA, Soowal LN, Lee I, Weigel D (1997) LEAFY expression and flower initiation in Arabidopsis. Development 124(19):3835–3844
49. Elliott RC, Betzner AS, Huttner E, Oakes MP, Tucker WQ, Gerentes D, Perez P, Smyth DR (1996) AINTEGUMENTA, an APETALA2-like gene of Arabidopsis with pleiotropic roles in ovule development and floral organ growth. Plant Cell 8(2):155–168
50. Long J, Barton MK (2000) Initiation of axillary and floral meristems in Arabidopsis. Dev Biol 218(2):341–353
51. Eshed Y, Baum SF, Perea JV, Bowman JL (2001) Establishment of polarity in lateral organs of plants. Curr Biol 11(16):1251–1260
52. Tretter EM, Alvarez JP, Eshed Y, Bowman JL (2008) Activity range of Arabidopsis small RNAs derived from different biogenesis pathways. Plant Physiol 147(1):58–62
53. Sawa S, Watanabe K, Goto K, Liu YG, Shibata D, Kanaya E, Morita EH, Okada K (1999) FILAMENTOUS FLOWER, a meristem and organ identity gene of Arabidopsis, encodes a protein with a zinc finger and HMG-related domains. Genes Dev 13(9):1079–1088
54. Siegfried KR, Eshed Y, Baum SF, Otsuga D, Drews GN, Bowman JL (1999) Members of the YABBY gene family specify abaxial cell fate in Arabidopsis. Development 126(18): 4117–4128
55. Mandel MA, Gustafson-Brown C, Savidge B, Yanofsky MF (1992) Molecular characterization of the Arabidopsis floral homeotic gene APETALA1. Nature 360(6401):273–277
56. Ohno CK, Reddy GV, Heisler MG, Meyerowitz EM (2004) The Arabidopsis JAGGED gene encodes a zinc finger protein that promotes leaf tissue development. Development 131(5): 1111–1122
57. Tilly JJ, Allen DW, Jack T (1998) The CArG boxes in the promoter of the Arabidopsis floral organ identity gene APETALA3 mediate diverse regulatory effects. Development 125(9):1647–1657
58. Bowman JL, Smyth DR (1999) CRABS CLAW, a gene that regulates carpel and nectary development in Arabidopsis, encodes a novel protein with zinc finger and helix-loop-helix domains. Development 126(11):2387–2396
59. Alvarez JP, Goldshmidt A, Efroni I, Bowman JL, Eshed Y (2009) The NGATHA distal organ development genes are essential for style specification in Arabidopsis. Plant Cell 21(5):1373–1393
60. Simon R, Igeno MI, Coupland G (1996) Activation of floral meristem identity genes in Arabidopsis. Nature 384(6604):59–62
61. Che P, Lall S, Howell SH (2008) Acquiring competence for shoot development in Arabidopsis: ARR2 directly targets A-type ARR genes that are differentially activated by CIM preincubation. Plant Signal Behav 3(2):99–101
62. Matsuhara S, Jingu F, Takahashi T, Komeda Y (2000) Heat-shock tagging: a simple method for expression and isolation of plant genome DNA flanked by T-DNA insertions. Plant J 22(1):79–86
63. Yoshida K, Kasai T, Garcia MR, Sawada S, Shoji T, Shimizu S, Yamazaki K, Komeda Y, Shinmyo A (1995) Heat-inducible expression system for a foreign gene in cultured tobacco cells using the HSP18.2 promoter of Arabidopsis thaliana. Appl Microbiol Biotechnol 44(3–4):466–472
64. van der Fits L, Hilliou F, Memelink J (2001) T-DNA activation tagging as a tool to isolate regulators of a metabolic pathway from a genetically non-tractable plant species. Transgenic Res 10(6):513–521
65. Jeong DH, An S, Kang HG, Moon S, Han JJ, Park S, Lee HS, An K, An G (2002) T-DNA insertional mutagenesis for activation tagging in rice. Plant Physiol 130(4):1636–1644
66. Mathews H, Clendennen SK, Caldwell CG, Liu XL, Connors K, Matheis N, Schuster DK, Menasco DJ, Wagoner W, Lightner J, Wagner DR (2003) Activation tagging in tomato identifies a transcriptional regulator of anthocyanin biosynthesis, modification, and transport. Plant Cell 15(8):1689–1703
67. Zuo J, Niu QW, Frugis G, Chua NH (2002) The WUSCHEL gene promotes vegetative-to-embryonic transition in Arabidopsis. Plant J 30(3):349–359

CHAPTER THREE

Functional Roles of Histone Modification, Chromatin Remodeling and MicroRNAs in *Arabidopsis* Flower Development

Eng-Seng Gan[*,†], **Jiangbo Huang**[*,†], **Toshiro Ito**[*,†,1]

[*]Department of Biological Sciences, National University of Singapore, Singapore, Republic of Singapore
[†]Temasek Life Sciences Laboratory, 1 Research Link, National University of Singapore, Singapore, Republic of Singapore
[1]Corresponding author: e-mail address: itot@tll.org.sg

Contents

Abstract

Flowers are the reproductive units of angiosperms and originate from small number of stem cells maintained at the growing tips of shoots. Flower development is a multistep

International Review of Cell and Molecular Biology, Volume 305
ISSN 1937-6448
http://dx.doi.org/10.1016/B978-0-12-407695-2.00003-2

process starting from an environmental response, followed by the meristem identity change, termination of the stem cell activity, organ polarity control, organ identity determination, and organogenesis. It is regulated through many hard-wired genetic pathways, composed of transcription factors, signaling molecules, catalytic enzymes, and structural proteins. Epigenetic regulators play essential roles for the initiation and maintenance of the genetic pathways by controlling gene expression through chromosomes. Histone modification, ATP-dependent chromatin remodeling, and microRNAs are involved in the regulation of spatiotemporal-specific expression of huge numbers of genes that lead to patterning, specification, and morphogenesis of flowers. In contrast, DNA methylation mainly works for genome stability and integrity, silencing transposons, and repeats. This review will describe the recent progress on functional roles of epigenetic regulators and their crosstalks in *Arabidopsis* flower development.

1. INTRODUCTION

Flowers are determinate structures for reproduction in angiosperms, with sporophylls producing male and female gametophytes. From the induction of the vegetative to reproductive phase transition to the final maturation of a flower, floral induction and development are multistep processes. Upon reaching a certain developmental stage and perceiving the right environmental cues, *Arabidopsis* undergoes floral transition involving the repression of *FLOWERING LOCUS C* (*FLC*) and induction of *FLOWERING LOCUS T* (*FT*) (Liu et al., 2009a). The vegetative shoot apical meristem (SAM) is transformed into an inflorescence meristem (IM) and the plant starts to bolt. The IM identity is maintained by *TERMINAL FLOWER 1* (*TFL1*), while floral meristems develop at the periphery of the IM following a specific phylotaxy. The floral meristem is established by the floral meristem identity genes, which include *LEAFY* (*LFY*), *APETALA1* (*AP1*) and *CAULIFLOWER* (*CAL*), together with *UNUSUAL FLORAL ORGANS* (*UFO*). *Arabidopsis* floral meristems produce four concentric whorls of floral organs of fixed numbers, namely, four sepals, four petals, six stamens, and two fused carpels in the center. In contrast to the indeterminate SAMs and IMs, floral meristems are genetically programmed to terminate after the primordia of the carpels are formed (Ito, 2011; Sablowski, 2007).

Flower development is a multistep process. After the formation of the floral meristem, other genes that function in governing the abaxial–adaxial polarity and organogenesis also kick in to regulate the establishment of unique organ identities and differentiation of the floral organs. Floral organ identities are determined by the combinatorial action of floral homeotic

proteins (Alvarez-Buylla et al., 2010; Ito, 2011). Later in the flower development, flower maturation is promoted by various genetic pathways, including genes such as *AUXIN RESPONSE FACTOR 6* (*ARF6*), *ARF8*, and *DELAYED ANTHER DEHISCENCE1* (*DAD1*) that induce jasmonic acid production (Nagpal et al., 2005; Reeves et al., 2012). After fertilization, the carpels elongate into fruits called siliques, while the fertilized ovules develop into seeds, fulfilling the life cycle of the *Arabidopsis* plant.

The expression of all these genes needs to be tightly regulated in a temporal and spatial manner to produce a functional flower, thus ensuring successful reproduction of plants. In plants, DNA methylation, histone modifications, ATP-dependent chromatin remodeling, placement of histone variants, and noncoding RNA regulation play critically important roles in regulating gene expression. The epigenetic mechanisms regulating flowering time have been reviewed previously (Dennis and Peacock, 2007; He, 2009; Jarillo and Pineiro, 2011; Srikanth and Schmid, 2011). In this review, the roles of epigenetic mechanism are discussed with focus on the whole process of *Arabidopsis* flower development.

2. HISTONE MODIFICATION IN FLOWER DEVELOPMENT

The epigenetic trait is defined as "stably heritable phenotype resulting from changes in a chromosome without alterations in the DNA sequence" (Berger et al., 2009). In the nucleus, histone proteins help package the DNA strands into condensed chromatin. Around 147 base pairs of DNA wrap around one octameric nucleosome core consisting of two of each core histone H2A, H2B, H3, and H4. The linker histone H1 binds the nucleosome, locking the DNA into place. Histones can undergo a wide array of posttranslational modifications including, but not limited to, methylation, acetylation, phosphorylation, ubiquitination, and sumoylation. The N-terminal tails of histones, posttranslationally modified at selected residues, confer different regulatory signals, and some of the patterns have been shown to be closely linked to biological events, which is called the histone code (Strahl and Allis, 2000).

Approximately 30–40% of the core histone N-termini consists of the positively charged lysine and arginine residues. This fueled the spreading of the perception that the N-termini function primarily by binding to the DNA in the nucleosomes (Hansen et al., 1998). However, emerging evidence suggests that, rather than binding with DNA, the histone N-termini interacts with nonhistone regulatory proteins and form

multiprotein complexes. Many of these distinct histone H3 and H4 tail modifications lie so close to each other that they act sequentially or in combination to regulate unique biological outcomes (Strahl and Allis, 2000). The histone code hypothesis predicts that these covalent modifications might provide specific binding platforms, recruiting effector proteins, and allowing the inherent code to be interpreted into functional outcomes (Jenuwein and Allis, 2001; Liu et al., 2010). Hence this highlights the importance of the enzymatic complex responsible for establishment, maintenance, and removal of these types of epigenetic marks.

2.1. Histone methylation

One of the most well-studied histone modifications is histone methylation. Histone methylation plays an important role in diverse biological processes ranging from transcriptional regulation to heterochromatin formation (Liu et al., 2010). In plants, its importance in flower development is obvious as the loss-of-function mutants of components of this regulatory mechanism mis-express many floral genes in the leaves and/or different floral organs.

The histone mark is deposited by histone methyltransferase (HMTase), a family of proteins in the SET DOMAIN GROUP (SDG) that share the conserved SET domain. The SET domain has ~130 amino acids and was initially found in three *Drosophila melanogaster* proteins: SUPPRESSOR OF VARIEGATION 3–9 [SU(VAR)3–9] (Tschiersch et al., 1994), ENHANCER OF ZESTE [E(Z)] (Jones and Gelbart, 1993), and TRITHORAX (TRX) (Stassen et al., 1995), hence the name SET. This SET domain can catalyze histone lysine mono-, di-, or trimethylation of several lysine and arginine residues in the histones H3 and H4 (Pien and Grossniklaus, 2007). These lysine and arginine methylation states have been experimentally classified into two categories: depending on their effect on gene expression, there are repressive and activating marks. In general, methylated ninth and twenty-seventh lysine residues of histone H3 (H3K27 and H3K9) are considered repressive marks, while methylated fourth and thirty-sixth lysine residues (H3K4 and H3K36) are classified as activating marks (Pien and Grossniklaus, 2007).

Antagonizing the effect of histone methylation by the SET-domain protein are the histone demethylases. There are two types of demethylases, Lysine-specific demethylase1 (LSD1) and Jumonji-C (JmjC) domain-containing proteins, each functioning through different biochemical

mechanisms. In *Arabidopsis*, there are four LSD1 homologs, FLOWERING LOCUS D (FLD), LSD1-LIKE1 (LDL1), LDL2, and LDL3. LSD1 can remove methyl groups from mono- and dimethylated histones through FAD-dependent amine oxidation (Shi et al., 2004; Spedaletti et al., 2008). On the other hand, JmjC domain-containing proteins are able to demethylate all three mono-, di-, and trimethylated histone through hydroxylation using the cofactors Fe(II) ions and α-ketoglutarate (Liu et al., 2010; Tsukada et al., 2006). There are 21 JUMONJI (JMJ) proteins in the *Arabidopsis* genome, which can be categorized into five clades with some degree of conserved substrate specificity within each clade (Hong et al., 2009; Lu et al., 2008).

2.2. H3K9 methylation and DNA methylation

In *Arabidopsis*, there are nine *SU(VAR)3–9 HOMOLOGS* (*SUVH*) genes and five *SU(VAR)3–9 RELATED* (*SUVR*) genes (Thorstensen et al., 2011). Some of the members in this SU(VAR)3–9 family of HMTase have been shown to be involved in the methylation of H3K9, for example, SUVH2, SUVH4/KRYPTONITE (KYP), SUVH5, SUVH6, and SUVR2 (Ebbs and Bender, 2006; Ebbs et al., 2005; Jackson et al., 2002, 2004; Naumann et al., 2005; Thorstensen et al., 2006). Mutations of these HMTase not only cause a reduction of methylated H3K9, but also show loss of DNA methylation, and reduced gene silencing at some loci. In fact, more evidences are showing that H3K9 methylation, together with DNA methylation and histone deacetylation may form a self-reinforcing cycle of epigenetic events to silence gene expression (Fuks, 2005; To et al., 2011).

DNA cytosine methylation is maintained at CG context by DNA METHYLTRANSFERASE1 (MET1) (Kankel et al., 2003), and CHROMOMETHYLASE3 (CMT3) at CHG context (Lindroth et al., 2001), potentially at a semiconservative manner during DNA replication. Methylation at the nonsymmetrical CHH context requires DOMAINS REARRANGED METHYLASE 1 (DRM1) and DRM2 and CMT3 (Bartee et al., 2001; Cao and Jacobsen, 2002). Since CHH methylation does not have a template for maintenance, it must be methylated *de novo* after replication, and this is mediated through the RNA-directed DNA methylation (RdDM) pathway (Zhang and Zhu, 2011). Other components of the DNA methylation mechanism include ATP-dependent chromatin remodeling factors, methyl-cytosine binding proteins, and DNA glycosylases that act to remove methyl-cytosine (Furner and Matzke, 2011).

DNA methylation has been implicated to be important for genome stability and integrity, silencing transposons, and repeats at heterochromatin (Zhang et al., 2006). However, DNA methylation is also found at gene body of transcribed genes. Although the function of genic methylation is not very clear, some reports have suggested that it may prevent transcriptional initiation from cryptic promoters, at the cost of reduced elongation efficiency (Zilberman et al., 2007). Loss of MET1 or DNA glycosylase DEMETER (DME) causes floral abnormalities with altered floral organ number and the floral homeotic conversion (Choi et al., 2002; Finnegan et al., 1996). Double mutant of *met1 dme* have even more distinct severe phenotype (Xiao et al., 2003). Some of the floral homeotic conversion can be explained by the ectopic expression of floral homeotic genes *AGAMOUS* (*AG*) and *APETALA3* (*AP3*) in *met1* antisense plants (Finnegan et al., 1996). Furthermore, aberrant flower phenotypes such as reduced sepal number and unfused carpels are also seen in selfed lines of the mutant of chromatin remodeling ATPase, DECREASED DNA METHYLATION 1 (DDM1), indicating the importance of DNA methylation in flower development (Kakutani et al., 1996).

H3K9me2 is important for CMT3-mediated CHG methylation, and they are highly colocalized at the genome level (Bernatavichute et al., 2008; Feng and Jacobsen, 2011). Dimethylation of H3K9 is concentrated in the heterochromatin and has been shown to silence transposons and other repeat-containing genes that are constitutively repressed (Bernatavichute et al., 2008). However, there seem to be some mechanistic differences in the epigenetic silencing of H3K9me2 in the pericentromeric regions and euchromatic arms. In the pericentromeric heterochromatin, H3K9me2 is present in large blocks, while in the euchromatin, it is enriched in smaller regions with lower levels of H3K9me2 but higher levels of CHG methylation (Bernatavichute et al., 2008). Furthermore, compared to the constitutively silenced heterochromatin, H3K9 methylation seems to be regulated in a more dynamic manner at some loci in the euchromatic arms, providing another level of gene expression regulation.

Antagonizing the effect of H3K9 methylation is its demethylase INCREASE IN BONSAI METHYLATION 1 (IBM1)/JMJ25, first identified by a genetic screen for mutants that causes methylation-induced silencing of *BONSAI* (*BNS*) (Saze et al., 2008). The *ibm1* mutant causes extensive hypermethylation in thousands of genes, especially at long transcribed genes, whereas transposable elements are not affected (Inagaki et al., 2010; Miura et al., 2009). The varieties of developmental defects in

ibm1 are rescued in the mutants of H3K9 HMTase KYP/SUVH4 and the CHG methylase CMT3, showing the interplay between H3K9 methylation/demethylation and DNA methylation in regulating gene expression (Saze et al., 2008). As the methylation at the heterochromatin has the potential to spread by a self-reinforcing mechanism, presence of the H3K9 demethylase may function to prevent spreading of non-CG methylation into genic regions, hence ensuring genome integrity (Fahrner and Baylin, 2003; Richards and Elgin, 2002; Vermaak et al., 2003). Furthermore, it has been shown that IBM1 not only protects genes from silencing, but also targets components of the RdDM pathway, RNA-DEPENDENT RNA POLYMERASE 2 (RDR2) and DICER-LIKE 3 (DCL3), hence indirectly participating in RdDM-directed repression (Fan et al., 2012).

A long-standing mystery in the *met1* mutation is that *met1* shows not only CG hypomethylation, but also CHG hypermethylation in gene bodies at many loci. This suggests that MET1 may function to protect genes from CHG methylation. Only recently has it been shown that the MET1 activity is necessary for the expression of the functional histone demethylase IBM1 (Rigal et al., 2012). Two mRNA variants are transcribed from the *IBM1* gene. Simultaneous CG and CHG methylation mediated by MET1, CMT3, and KYP is required for the expression of the longer *IBM1-L* transcripts, which encodes the functional demethylase. Reduction of *IBM1-L* causes accumulation of H3K9me2, which induces a positive feedback of CHG methylation by CMT3, thereby silencing the gene. This may partly explain why some *met1* or *MET* antisense plants show *superman* (*sup*, *see below*)-like phenotype. Interestingly, the mutation of *IBM1* also causes floral organ abnormalities, pollen defects, and leaf deformation (Saze et al., 2008).

During floral induction, after a vernalization exposure to cold, the status of the repressive mark H3K9me2 increases at the flowering repressor *FLC* locus, hence allowing the plants to proceed into the reproductive state (He, 2009). LIKE HETEROCHROMATIN PROTEIN1/TERMINAL FLOWER 2 (LHP1/TFL2) is essential for the maintenance of the silenced *FLC* status by H3K9me2 after the plants returned to warm conditions (Sung and Amasino, 2004). The *FLC* locus is also targeted by small interfering RNAs (siRNAs) at its 3′ end where H3K9me2 is enriched (Swiezewski et al., 2007). Loss of the RNA POLYMERASE IV/NUCLEAR RNA POLYMERASE D1A (NRPD1A), RDR2, and DCL3 retards the production of the 24-nt siRNA, resulting in increased *FLC* transcript expression. Furthermore, H3K9me2 was reduced at the locus in a *dcl2*, *3*, *4* triple mutant (Swiezewski et al., 2007).

An AT-hook DNA binding protein, TRANPOSABLE ELEMENT SILENCING VIA AT-HOOK (TEK, AHL16) is shown to regulate *FLC* (Xu et al., 2013). Knockdown of *TEK* leads to reduced H3K9me2 and increased H3 acetylation particularly at the *Mutator-like* transposable element (TE) in the L*er FLC*, resulting in the TE transposition and a late flowering phenotype. Moreover, knockdown of *TEK* also causes transposition of other TEs, and increased expression of another floral repressor, *FWA* which contains two *SINE*-like repeats near its transcriptional start site. TEK directly binds to *FLC* and *FWA* and changes the chromatin conformation. TEK also associates with *Arabidopsis* homologs of the Retinoblastoma-associated proteins, FVE and MSI5, which mediate histone deacetylation (Ausin et al., 2004; Gu et al., 2011). This indicates that the AT-hook DNA binding protein TEK recruits epigenetic machinery to silence TE and repeat-containing flowering regulators (Fig. 3.1; Xu et al., 2013).

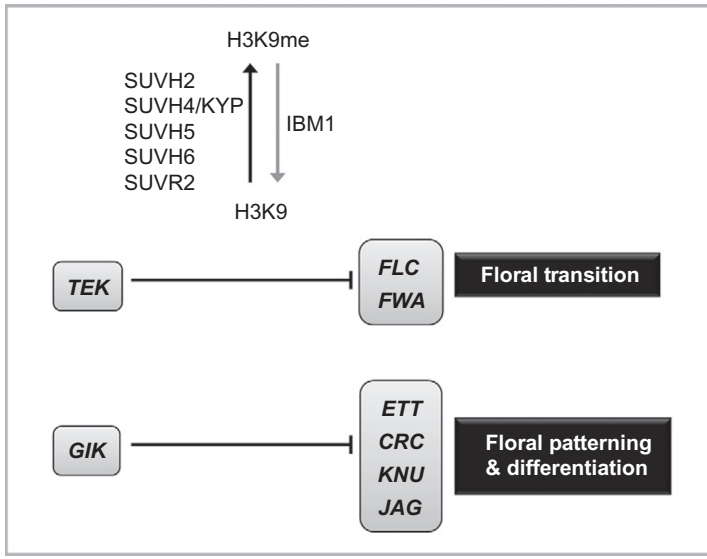

Figure 3.1 H3K9 can be methylated by the histone methyltransferase from the SU(VAR) 3–9 family and removed by IBM1. Its deposition at the loci is suggested to confer a repressive chromatin status, by forming a self-reinforcing cycle with DNA methylation complex and histone deacetylation complex. During floral transition, TEK regulates H3K9me2 deposition on *FLC* and *FWA* allowing the plant to transit from a vegetative to reproductive stage. Later during flower development, AG regulates *GIK* expression, which coordinates floral patterning and differentiation through H3K9me2-mediated repression of *ETT*, *CRC*, *KNU*, and *JAG*.

The H3K9 methyltransferase KYP was initially identified by suppressor screening of the *sup* epialleles, a zinc finger transcription factor that controls the boundary of the stamen and carpel whorls (Jacobsen and Meyerowitz, 1997; Sakai et al., 1995). These *clark kent* (*clk*) epialleles are hypermethylated at the *SUP* locus and its phenotype is rescued in the *kyp* mutant (Jackson et al., 2002; Jacobsen and Meyerowitz, 1997). On the other hand, in rice, H3K9 methylation plays an important role in floral organ development. Loss-of-function of the *IBM1* homolog in rice, *JMJ706* leads to increased di- and tri-methylation of H3K9 and affect the spikelet development, altering floral morphology, and organ number (Sun and Zhou, 2008). Some of the phenotypic changes include spikelets with depleted lemma and/or palea, spikelets with additional piece of palea, increased numbers of stamens and pistils, and vitrified tissues in some spikelets. The *jmj706* mutations lead to the increased H3K9me2/3 on the promoter and 5′ regions of *DEGENERATED HELL1* (*DH1*) and *OsMADS47*, which leads to their repression. The repression of *DH1* can account for part of the phenotype because mutation of *DH1* produces similar defects on palea and lemma formation (Sun and Zhou, 2008).

AG has been shown to be a master regulator of reproductive development (reviewed in Alvarez-Buylla et al., 2010; Ito, 2011). One of the direct target of AG, *GIANT KILLER* (*GIK*, *AHL21*) acts to fine-tune expression of key regulator of floral patterning and reproductive differentiation through histone modification (Ng et al., 2009). Overexpression of *GIK* shows stigmatic tissue outgrowth, shorter valves, and bipartite stigma with ectopic ovule growth which mimics the *auxin response factor4/ettin* (*ett*) phenotype. Detailed genetic and molecular analyses showed that GIK, an AT-hook type DNA binding protein, directly binds to the matrix attachment regions (MARs) of *ETT*. This binding causes repression of *ETT* expression by changing the chromatin conformation and inducing H3K9me2 accumulation at the same region. GIK also modulates the expression of other key floral development regulator such as *CRABS CLAW* (*CRC*), *JAGGED* (*JAG*), and *KNUCKLES* (*KNU*) possibly through similar mechanisms. Thus, by regulating *GIK* expression, AG coordinates floral patterning and reproductive differentiation through many genes including *ETT*, *CRC*, *KNU*, and *JAG* (Fig. 3.1; Ng et al., 2009).

2.3. H3K27 methylation and polycomb complex

2.3.1 Methyltransferase complex

H3K27 can be methylated by two complexes, one that monomethylate H3K27, and another regulates di- and trimethylation of H3K27.

H3K27me1 is a heterochromatic mark enriched in chromocenters (Mathieu et al., 2005). It is conferred by the redundant H3K27 mono-HMTases, *ARABIDOPSIS TRITHORAX-RELATED PROTEIN5* (*ATXR5*), and *ATXR6*, and it protects genomic integrity by preventing over replication of heterochromatin in *Arabidopsis* (Jacob et al., 2010). On the other hand, functioning in gene repression and developmental regulation, H3K27me3 is differently regulated throughout developmental stages, and is governed by the Polycomb group (PcG) proteins (Lafos et al., 2011; Zheng and Chen, 2011).

Two different PcG protein complexes have been characterized in detail: the polycomb repressive complex 1 (PRC1), and PCR2. In *Drosophila*, the PRC2 comprises of four core proteins, namely extra sex comb (ESC), enhancer of zeste (E(Z)), suppressor of zeste 12 (SU(Z)12), and p55. Like *Drosophila*, *Arabidopsis* PRC2 is also composed of four main proteins, but it has 12 homologs of *Drosophila* PRC2 subunits: three E(Z) homologs CURLY LEAF (CLF), MEDEA (MEA) and SWINGER (SWN); three SU(Z)12 homologs EMBRYONIC FLOWER 2 (EMF2), FERTILIZATION INDEPENDENT SEED2 (FIS2) and VERNALIZATION2 (VRN2); one ESC homolog FERTILIZATION INDEPENDENT ENDOSPERM (FIE); and the five p55 homologs MULTICOPY SUPRESSOR OF IRA1–5 (MSI1–5) (Pien and Grossniklaus, 2007). Genetic and molecular evidence suggests that these proteins form at least three PRC2-like complexes in different developmental context: the EMBRYONIC FLOWER (EMF), VERNALIZATION (VRN) and FERTILIZATION INDEPENDENT SEED (FIS) complexes. Although these complexes have clearly distinct functions, they do share some target genes. For instance, the FIS complex, which contains MEA/SWN, FIS2, FIE and MSI1, silences target genes during gametogenesis and early seed development, whereas the EMF complex, which probably contains CLF/SWN, EMF2, FIE, and MSI1, silences some of the same target genes including floral meristem and organ identity genes (see below) during subsequent sporophytic development. Similarly, *FLC* is silenced by both the VRN and the EMF complexes (Pien and Grossniklaus, 2007).

Around one fifth of the *Arabidopsis* genes are covered by the repressive H3K27me3 mark in seedlings (Zhang et al., 2007). The process of methylation through the SET domain HMTases is well defined, but knowledge on the process of recruitment to these sites is lagging behind. In *Drosophila*, there seems to be a set of *cis*-regulatory elements called Polycomb Repressive Element (PRE) that recruits DNA-binding proteins such as PLEIOHOMEOTIC (PHO),

ZESTE (Z), and GAGA factors (GAFs), which later bring the PRC2 complexes to these sites to exert transcriptional repression (Schwartz and Pirrotta, 2008). Similar PRE-like elements are found in mice and human. Just recently a short fragment in the upstream region of *LEAFY COTYLEDON2* gene was shown to have the PRE-like activity in *Arabidopsis* (Berger et al., 2011).

LEAFY COTYLEDON2 (LEC2) is a master regulator of seed development that is specifically expressed in the embryo in a short time frame. Promoter bashing experiment showed that 500-bp long sequence upstream of *LEC2* contains three *cis*-regulatory elements (Berger et al., 2011). Two of them are important for transcriptional activation, while the third one, named *Repressive LEC2 Element* (*RLE*) is necessary for the H3K27me3-mediated repression of *LEC2*. The *RLE* restricts *LEC2* transcription to the embryo. Furthermore, insertion of the 50-bp *RLE* to the *FLAVONONE 3-HYDROXYLASE* (*F3H*) promoter can trigger H3K27me3 deposition and repression of the *pF3H*::*GUS* reporter construct. This shows that *RLE* partially fulfilled the criteria of the PRE that it is able to generate a new binding site for PRC, create a site for H3K27me3 deposition, and induce repression of the corresponding gene (Schwartz and Pirrotta, 2008). During floral transition, *FLC* expression needs to be repressed. The region near the transcriptional start site and the long first intron in the *FLC* locus has been proposed to contain PRE-like elements that regulate *FLC* transcriptional states (Buzas et al., 2012).

2.3.2 Maintenance mechanism

After PRC2 establishes the H3K27me3 repressive mark, PRC1 functions to maintain the marks at the locus. It comprises LHP1/TFL2, AtRING1A/B (Chanvivattana et al., 2004) and AtBMI1A/B/C (Bratzel et al., 2010; Li et al., 2011). The PRC1 complex also modifies histones with its RING subunit, catalyzing histone H2A lysine 119 ubiquitination (H2AK119ub) (Bratzel et al., 2010). Loss-of-function of *Atbmi1a/b* causes dedifferentiation of vegetative tissues into callus-like structure. This phenotype mimics the double mutant of *clf swn* (Chanvivattana et al., 2004) and *vrn2 emf2* (Schubert et al., 2005), indicating that *AtBMI1* genes function in the same pathway as the PRC2 components and are required to maintain the differentiated state of somatic cells.

2.3.3 Demethylase

Although the HMTase of H3K27me3 has been reported for almost a decade, the discovery of its demethylase has not been as successful. This is mainly

because the H3K27me3 demethylase in animals, UBIQUITOUSLY TRANSCRIBED TETRATRICOPEPTIDE REPEAT X (UTX) and JMJD3, do not have close homologs in plants (Agger et al., 2007). Only very recently has RELATIVE OF EARLY FLOWERING 6 (REF6) been reported as the H3K27me3 demethylase in *Arabidopsis* (Lu et al., 2011). Overexpression of *REF6* causes phenotypes similar to the PRC2 mutant, *clf* and *tfl2*, showing defects in H3K27me3-mediated gene silencing. Through genetic crosses, REF6 has been also shown to act downstream of the H3K27me3 methyltransferase, and *ref6* mutant is able to slightly rescue the curly leaf phenotype of *clf*. However, the fact that *ref6* mutant phenotype is weaker than those of the metazoan counterpart hints that there might be more H3K27me3 demethylases waiting to be uncovered.

2.3.4 Target genes

During flower development, different genes need to be activated or repressed at specific stages. *LFY* and *AP1* encode transcription factors that determine the floral meristem identity in *Arabidopsis* and, with the aid of other factors, activate transcription of floral organ identity genes such as *AG*, *AP3*, and *PISTILLATA* (*PI*) (Parcy et al., 1998). Due to its importance for the transition from the SAM into an IM, *LFY* is tightly regulated and is repressed by PRC2 during embryo development. In the PRC2 mutant *fie*, early flowering of the mutant is likely due to the ectopic expression of *LFY* (Kinoshita et al., 2001). *Arabidopsis embryonic flower 1* (*emf1*) and *emf2* mutants skip the vegetative phase and flower soon after germination, suggesting there is a floral repression mechanism in wild-type plants that prevents flowering until maturity (Sung et al., 1992; Yang et al., 1995).

The repressive H3K27me3 mark not only function during floral induction through regulating *FLC* expression (Greb et al., 2007), and floral meristem identity through *LFY* (Kinoshita et al., 2001), it also participates in the organogenesis during flower development. The floral homeotic gene *AG* and the homeobox gene *SHOOTMERISTEMLESS* (*STM*) have been shown to be essential regulators of floral organogenesis and SAM maintenance, respectively (Bowman et al., 1989; Long et al., 1996). In vegetative stages, *CLF* binds to the *AG* locus, and its binding colocalizes with H3K27me3 marks to prevent ectopic expression of *AG* (Goodrich et al., 1997; Katz et al., 2004). The curly leaf phenotype of *clf* is due to the ectopic expression of *AG* in vegetative leaves, as the phenotype is rescued in the *clf ag* double mutant. Therefore, CLF acts as a repressor of floral homeotic genes during flower development. Similar phenotypes were observed when the

PRC1 component, LHP1/TFL2 is mutated. The curled-leaf phenotype of *tfl2* mutants is correlated with ectopic expression of the floral organ identity genes *AG* and *AP3* (Kotake et al., 2003). In the PRC2 and PRC1 loss-of-function mutant background, such as *clf swn* and *atbmi1a/b*, these marks were almost erased at the *AG* and *STM* locus (Bratzel et al., 2010; Schubert et al., 2006). The activation of the shoot stem cell regulator *STM* causes cells to dedifferentiate and form embryo-like structures.

Once the flower pattern is determined and the right amounts of cells are produced, the stem cells maintenance gene *WUSCHEL* (*WUS*) has to be repressed. This is achieved through the activation of *KNU* by AG, and then termination of *WUS* by KNU. Within a few days, the H3K27me3 at *KNU* locus drop drastically upon AG binding as the floral meristem proceeds from floral stage 3 to stage 6 (Sun et al., 2009). The reduction of H3K27me3 is cell cycle dependent. AG may bind to the *KNU* promoter competitively with the PRC proteins, leading to the passive dilution of the repressive status (Bo Sun and Toshiro Ito, unpublished data). In contrast, KNU may bind to the *WUS* promoter and facilitate the recruitment of the PRC complex, which would deposit the repressive H3K27me3 mark to the *WUS* locus (Bo Sun and Toshiro Ito, unpublished data). The termination of floral stem cells is spatio-temporally regulated to coincide with the formation of the female reproductive organs to ensure successful reproduction of plants (Fig. 3.2).

2.4. H3K4 methylation and trithorax

While transcriptional repression is associated with H3K9 and H3K27 methylation, the active transcription of genes depends on a permissive chromatin structure, and is associated with methylation of H3K4 and H3K36 and histone acetylation. In *Drosophila*, the Trx group (TrxG) mediates H3K4 methylation and counteracts transcriptional repression by PcG complex. In *Arabidopsis*, the TrxG family comprises 12 SDG genes. Five of the genes, *SDG8/ASHH2/EFS/CCR1*, *SDG25/ATXR7*, *SDG26/ASHH1*, *SDG27/ATX1* and *SDG30/ATX2*, are involved in flowering time regulation (Berr et al., 2009, 2010; Kim et al., 2005b; Pien et al., 2008; Saleh et al., 2008; Soppe et al., 1999; Tamada et al., 2009; Xu et al., 2008; Zhao et al., 2005).

Antagonizing the effect of H3K4 histone methyltransferase, the removal of this epigenetic mark is catalyzed by demethylases from both the LSD1 and JMJ proteins families. Many of the H3K4 demethylases have been reported to play a role in the floral induction pathway. From the LSD1 family, LDL1,

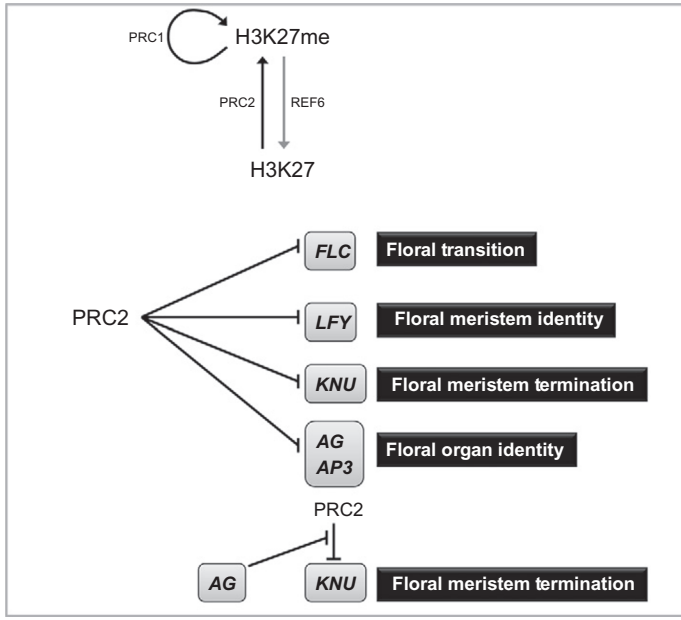

Figure 3.2 The repressive H3K27me3 is deposited by the polycomb repressive complex 2 (PRC2) which contains the E(Z) family members CLF, SWN, and MEA as the catalytic methyltransferase. REF6 and possibly other JMJ proteins, are the active demethylase for H3K27me3. This repressive mark is maintained by PRC1 complexes. H3K27me3 functions throughout the plant development, inducing floral transition (*FLC*), regulating floral meristem identity (*LFY*) and termination (*KNU*), and floral organ identity (*AG*, *AP3*). At stage 6 of flower development, AG induces *KNU* expression by preventing PRC-mediated repression on the *KNU* locus.

LDL2 and FLD play a role in partial redundancy to repress *FLC* expression. However, LDL1 and LDL2 appear to act independently of FLD in the silencing of *FWA*, indicating that there is target gene specialization within this histone demethylase family (Jiang et al., 2007). In addition to the LSD1 proteins, JMJ proteins from the KDM5/JARID1 family, including PKDM7B/JMJ14 (Lu et al., 2010; Yang et al., 2010), JMJ15 (Yang et al., 2012b), JMJ18 (Yang et al., 2012a) are also involved in flowering time regulation.

Besides functioning in the flowering pathway, ATX1 participates in early flower development (Alvarez-Venegas et al., 2003). Loss-of-function of *atx1* displays homeotic conversion of floral organs, such as stamenoid petals and stamens with stigmatic papillae, highlighting the fact that ATX1 may function in establishing floral organ identity. Consistently, downregulation

of several homeotic genes, *AP1*, *AP2*, and *AG*, and to a lesser extent, of *PI* and *AP3* was observed in *atx1* mutants, suggesting the role of ATX1 in maintaining the normal expression levels of these floral organ identity genes (Alvarez-Venegas et al., 2003).

Differing from the previously characterized TrxG proteins, the mutant of another TrxG protein, SDG2 does not show obvious flowering or floral organ identity phenotypes, but rather exhibits severe male and female gametogenesis defects (Berr et al., 2010). Ovules and pollens in *sdg2* mutants are largely sterile. This is because many genes essential for gametophyte development, such as *SPOROCYTELESS/NOZZLE* (*SPL/NZZ*), *BTB AND TAZ DOMAIN PROTEIN 3* (*BT3*), *MALE STERILITY 1* (*MS1*), *DYT1*, *MYB99*, *EDA31*, and *MEE65* are downregulated in the *sdg2* flower. Importantly, H3K4me3 was dramatically decreased at the *SPL/NZZ*, *BT3*, and *MS1* loci, highlighting the importance of this epigenetic mark in the proper development of gametophyte.

AG kicks in during floral meristem termination to turn off *WUS* expression and the timely activation of *AG* is partly mediated by ULTRAPETALA1 (ULT1) (Carles and Fletcher, 2009). ULT1 encodes a SAND domain protein with DNA-binding function but does not harbor an evident transcription activation domain. Rather, ULT1 acts as a TrxG component and binds to the *AG* regulatory sequences and recruits other TrxG components such as ATX1. ATX1-mediated H3K4 methylation can then be established to activate *AG* expression.

In the later stage of flower development, *Arabidopsis* SET-domain protein SDG4/ASHR3 is involved in stamen development. SDG4/ASHR3 interacts with the bHLH transcription factor ABORTED MICROSPORES (AMS), which helps bring SDG4/ASHR3 to the chromatin (Thorstensen et al., 2008). Furthermore, SDG4/ASHR3 also functions in the H3K4 and H3K36 methylation of gene regulation during fertilization (Cartagena et al., 2008). Pollen tube germination was not affected in the *sdg4* mutant; however, the pollen tube growth was much slower than those of wild type, which contribute to the sterility of the *sdg4* mutant.

2.5. H3K36 methylation and gene activation

Similar to H3K4 methylation, H3K36 methylation is also associated with gene activation. The HMTase for H3K36, SDG8/ASHH2/EFS/CCR1 have been shown to be involved in various developmental stages, regulating organ size, shoot branching, fertility, and carotenoid composition (Berr et al., 2010;

Cazzonelli et al., 2009; Grini et al., 2009; Soppe et al., 1999; Xu et al., 2008). SDG8 may function in floral organ identity establishment, as loss-of-function of the *sdg8/ashh2* mutants show homeotic conversions with carpeloid organs in whorls 2 and 3, or conversion of sepals to carpels and petals to stamen. Floral organ identity genes *AP1*, *AP3*, and *PI* are downregulated in the *sdg8/ashh2* inflorescences (Grini et al., 2009).

In the later organ maturation process, *sdg8/ashh2* also shows defects in ovule and embryo sac development, as well as anther development (Grini et al., 2009). In their ChIP experiments substantial decrease of H3K36me3 was observed but not H3K4me3 or H3K36me2 in *AP1*, *AtDMC1*, *MYB99*, each representing floral organ identify, embryo sac development, pollen development functions, respectively. This suggests that SDG8/ASHH2 controls multiple steps of flower development through regulating expression of these genes via H3K36 trimethylation.

2.6. Histone acetylation

Like methylation, histone acetylation is tightly regulated by the interplay between histone acetyltrasferases (HATs) and histone deacetylases (HDAs). It occurs at the N-terminals of histones. However, while methylation confers different transcriptional activity depending on the position and degree of methylation, acetylation primarily activates gene expression, possibly by charge neutralization of the lysines at histone tails hampering its interaction with DNA (Davie and Chadee, 1998) or serving as a new binding surface for recruitment of other proteins to the nucleosome (Dyson et al., 2001).

Arabidopsis has 18 putative HDAs. Different members of the HDA family have different functions. HDA6 is responsible for silencing transgenes, repetitive DNA, and rDNA loci (Aufsatz et al., 2002; Lippman et al., 2003; Murfett et al. 2001; Probst et al., 2004), whereas AtHD1/HDA19 is a putative global transcriptional regulator throughout *Arabidopsis* development (Tian and Chen, 2001; Tian et al., 2003).

LEC1, FUSCA3 (FUS3), and ABSCISIC ACID INSENSITIVE3 (ABI3) are key regulators during embryogenesis and should be repressed upon germination. This repression is partly mediated by the deacetylation by HDA6 and HDA19 (Tanaka et al., 2008). The single *hda6* mutant shows mild phenotype, but the further reduction of the HDAC activity by the treatment of a HDAC inhibitor in *hda6* causes post germination growth arrest and many embryonic genes are up-regulated. Moreover, double knockdown of *hda6* and *hda19* causes ectopic expression of *LEC1*, *FUS3*

and *ABI3*, which induces the formation of embryo-like structures on leaves. On the other hand, the growth arrest phenotype of the *hda6 hda19* double knockdown line is rescued in the *lec1* mutant background. Hence, it is proposed that upon germination, the HDAC complex containing HDA6 and HDA19 act redundantly to mediated repression of embryogenesis-related genes.

During floral induction, HDA6 also functions to deacetylate hence downregulating the expression of the floral repressor *FLC* (Yu et al., 2011). A *HDA6* mutant, *axe1–5*, and *HDA6*-RNAi displayed upregulation and hyperacetylation of *FLC* and consequently showed delayed-flowering phenotype. This late-flowering phenotype is rescued in the *flc* mutant background suggesting that the activity of HDA6 on flowering is *FLC* dependent. HDA6 interacts with another histone modifier FLD and together function to repress the floral repressor genes, *FLC*, *MADS AFFECTING FLOWERING 4* (*MAF4*) and *MAF5* during floral transition. The HDA6-mediated silencing of *FLC* and its homologs function through its corepressors MSI4/FVE and MSI5 (Gu et al., 2011). The FVE/MSI5–HDA6 complex not only targets *FLC* but also other RdDM targets such as *FWA* and transposable elements (*AtMU1*, *solo-LTR*). Recruitment of the FVE/MSI4–HDA6 HDAC to the target loci causes histone deacetylation, and further assists H3K9me2 deposition and DNA methylation at the loci. Besides regulating H3K9 methylation, we showed that the AT-hook DNA-binding protein TEK also interacts with the above-mentioned FVE and MSI5 in the HDAC, hence also participating in histone deacetylation (Xu et al., 2013). TEK and FVE not only share common binding sites in the *FLC* locus, the knockdown of *tek* also causes increased histone acetylation levels on *FLC*. They also regulate some other common targets such as *FWA* and *AtMU1*. Thus, it is likely that TEK binds specific loci and recruit FVE, MSI5 and histone deacetylase HDA6 to various target sites, which silences their expression.

In the SAM, WUS function to specify stem cell identity and the expression is normally limited to a few cells. However, in a mutant of a histone acetyltransferase, AtGCN5, the *WUS* expression domain is expanded (Bertrand et al., 2003). Mutation of *atgcn5* causes global reduction of acetylation and phenotypically causes floral homeotic conversion of late-arising flower and production of terminal flowers. The terminal flower phenotype resembles plant with overexpression of *AG*, and the conversion of whorl two organs into stamens hinted *AG* mis-expression at the outer two whorls. It is suggested that loss-of-function of *atgcn5* causes reduced expression of a

WUS repressor, leading to ectopic expression of *WUS*, which induces *AG* expression. A high level of *AG* at the IM later represses *WUS* expression producing terminal flowers (Bertrand et al., 2003).

During floral organogenesis, it has been previously shown that LEUNIG (LUG) and SEUSS (SEU) act as corepressors and function by repressing *AG* expression in the outer two floral whorls during flower development (Franks et al., 2002; Liu and Meyerowitz, 1995; Sridhar et al., 2004). In the single mutant of *lug* or *seu*, *AG* is expressed in all four whorls, causing partial homeotic conversion of the outer two whorls, and this phenotype is enhanced in the *lug seu* double mutant. During flower development, it was reported that antisense knockdown of *AtHD1/HDA19* causes ectopic expression of *SUP* and possibly other B function genes, resulting in extra stamen production and homeotic conversion (Tian and Chen, 2001; Tian et al., 2003). Further investigations showed that one pathway of the LUG–SEU-mediated repression is through histone deacetylation (Gonzalez et al., 2007). LUG repression is perturbed upon exposure to HDAC inhibitor, and LUG interacts with HDA19 directly. This suggests the importance of acetylation regulation in flower development.

Possibly functioning redundantly with LUG–SEU–HDA19 complex in negatively regulating *AG* expression, a recent report showed that AP2 recruits a corepressor TOPLESS (TPL) and the histone deacetylase HDA19 to the regulatory *AG* intron (Krogan et al., 2012). In the single loss-of-function mutant of *ap2*, *hda19* and quintuple mutant of *tpl topless related1–4*, *AG* expression is expanded to the outer whorls and carpeloid structures were produced. Moreover, AP2–TPL–HDA19 controls sepal petal identity by preventing the expression of B class gene into whorl 1. The complex binds to the *AP3* promoter directly but not *PI*. This is also supported by the genetic evidence that double mutant of *tpl ap2* and *tpl hda19* both increase the frequency of homeotic sepal-to-petal conversion found in *tpl* single mutant. AP2 further controls the sepal–petal boundary by directly repressing the E-class gene *SEPALLATA3* (*SEP3*) at whorl 1. These shows that histone deacetylation is used to finetune *AG* expression during organogenesis by LUG–SEU and AP2–TPL corepressors, while APL2-TPL-HDA19 further controls sepal–petal identity (Fig. 3.3).

2.7. Crosstalk of histone modifications

As reviewed above, a specific pattern of histone posttranslational modifications constitute a code that determines transcriptional outcomes. More complex

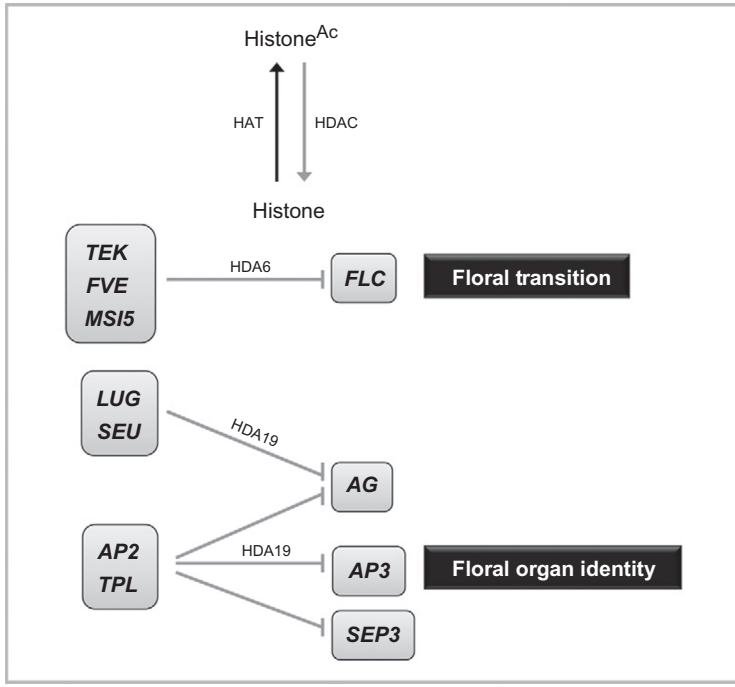

Figure 3.3 Acetylated histone marks confer a permissive chromatin status and are antagonized by the histone deacetylase complex (HDAC). The HDAC containing FVE/MSI5-TEK-HDA6 represses *FLC* during floral transition. LUG–SEU–HDA19 complex functions to repress *AG* expression at the outer two whorls. Possibly functioning redundantly with LUG–SEU, AP2–TPL also recruits HDA19 to the regulatory *AG* intron and represses *AG* expression. The AP2–TPL–HDA19 complex also controls sepal–petal identity by directly repressing *AP3* and *SEP3* at whorl 1.

scenarios arise when histone modifications act combinatorially in a context-dependent manner to facilitate the chromatin-mediated transcription. In some cases, the modification of one residue can alter the ability of a second residue to be implemented by its modifying enzyme (Lee et al., 2010b). Given that histone-modifying enzymes are often found in multisubunit complexes, modification of nearby residues can create binding sites for the components of the complex, helping to anchor an enzyme to a nucleosome.

During floral induction, a well-understood histone crosstalk is between histone acetylation and H3K4 methylation. The two histone modifications function together to control flowering time through regulating *FLC*. Increased levels of histone H3 acetylation and H3K4 trimethylation at *FLC*, *MAF4* and *MAF5* were found in both *axe1–5* (the *hda6* mutant) and *fld-6* plants (Yu et al., 2011). Their results also support a scenario in

which crosstalk between histone deacetylation and demethylation is mediated by physical association between HDA6 and FLD in the same complex.

Histone ubiquitylation also crosstalks with histone methylation. Regulating flowering time, H2Bub is required for the H3K4 and H3K36 hyperrmethylation of *FLC/MAF* loci (Cao et al., 2008). Each of the single mutation of the E3 homologs *HISTONE MONOUBIQUITINATION1* (*HUB1*) and *HUB2*, and double mutants of the two E2 homologs *UBIQUITIN CARRIER PROTEIN1* (*UBC1*) and *UBC2* causes decreased level of H3K4me3 and H3K36me2 in the chromatin of *FLC*, *MAF1*, *MAF4*, and *MAF5*, resulting in an early-flowering phenotype. On the other hand, histone H2Aub crosstalks with H3K27me3 to maintain the repressive status of target genes at a global level (Bratzel et al., 2010). The dedifferentiation phenotype found in the *atbmi1a/b* mutant phenocopies those seen in the *clf swn* mutants.

The PcG-mediated methylation of H3K27 and TrxG-mediated methylation of H3K4 are two contrasting histone marks. Thus, it is not surprising some form of crosstalk limits the deposition of one mark in the presence of the other. In *Drosophila*, the function of PcG is counteracted by the action of TrxG. ULT1 has been shown to limit H3K27me3 deposition and act as an activator of *AG* by catalyzing H3K4 trimethylation (Carles and Fletcher, 2009). At the same time, Trx genes such as *ULT1*, *ULT2*, and *PICKLE-RELATED 2* (*PKR2*) themselves are regulated by PRC2 (Bouyer et al., 2011). In *fie*, upregulated genes are positively correlated with loss of H3K27me3 and gain in H3K4me3, again highlighting the close antagonistic relation between these two marks (Bouyer et al., 2011). However, as with many biological systems, there are exceptions to the mutual exclusive deposition of these two marks. Bivalency of the activating H3K4me3 and repressive H3K27me3 mark on the same or nearby nucleosome does occur in some genes, such as *AG* and *FT*. It has been suggested that the bivalency of these two marks maintains the target genes in a "poised state," resulting in transcriptional silencing but allowing for fast reactivation upon commitment to differentiation (Bouyer et al., 2011).

3. CHROMATIN REMODELING IN FLOWER DEVELOPMENT

3.1. Mechanism of chromatin remodeling complex

ATP-dependent chromatin remodeling complexes are multisubunit complexes that alter DNA-histone interaction using ATP hydrolysis

(Varga-Weisz, 2001). The complex destabilizes nucleosome structures by introducing super helical torsion into DNA, and the final outcome may be changing nucleosome positions, histone modification, and/or histone removal. Ultimately, this would affect the accessibility of nucleosomal DNA.

One of the major classes of chromatin remodeling ATPases in *Arabidopsis* is the SWI/SNF complexes. The *Arabidopsis* genome encodes more than 40 SNF2-like proteins, including PICKLE (PKL), DDM1, SPLAYED (SYD) (Jarillo et al., 2009; Reyes et al., 2002).

3.2. Functions of chromatin remodeling in flower development

During meristem maintenance, FASCIATA 1 (FAS1) and FAS2, members of the chromatin assembly factor (CAF-1) complex and BRU1/MGO3/TSK are required to determine the correct spatial expression of *WUS*, preventing its ectopic expression outside the organizing center (Kaya et al., 2001). Mutations of *FAS* alter the expression pattern of *WUS* leading to altered shoot development. The SWI/SNF protein PKL is involved in the suppression of embryonic and meristematic genes during development. In leaf, PKL acts together with ASYMMETRIC LEAVES1 (AS1) to repress the *KNOX* genes, *STM*, *KNAT1*, *KNAT2*, and *KNAT6* in developing lateral organs (Ogas et al., 1999; Ori et al., 2000). In the inflorescence and floral meristems, the SNF2-class ATPase SYD is specifically recruited to the promoter region of *WUS* and regulates *WUS* expression (Kwon et al., 2005).

Besides meristem regulation, other chromatin remodeling factors play a role in regulating floral patterning. SYD and another SWI/SNF ATPase BRAHMA (BRM) share some redundant roles in this regulation (Bezhani et al., 2007; Wu et al., 2012). The *brm* mutant show severe flower abnormalities including homeotic transformations and reduced expression levels of *AP2*, *AP3*, and *PI* (Hurtado et al., 2006). *syd* enhances the floral phenotype of a weak *lfy* allele, suggesting SYD is a coactivator of *LFY*. SYD and BRM associate with the *AP3* and *AG* loci and the double knockdown of *syd brm* causes reduced *AG* and *AP3*, thus leading to homeotic conversion with sepal-like petals and stamens and defective carpels. Another component of CAF-1, MSI1 also functions in flower homeotic gene repression (Hennig et al., 2005).

Functioning in a genome-wide scale, DDM1 is a SNF2-like protein that is required for establishing genomic DNA methylation. Loss of DDM1 causes decrease in genome-wide cytosine methylation, especially in the repetitive region and heterochromatic regions. In terms of flower development,

loss of *ddm1* causes hypermethylation and silencing of *sup* and *ag*, whereas the *FWA* locus is hypomethylated and ectopically expressed (Jacobsen et al., 2000; Soppe et al., 2000).

A member of the immunophilin protein foldase family, CYCLOPHILIN71 (CYP71) containing apeptidylprolyl *cis–trans* isomerase catalytic domain and four WD40 repeats, functions in the maintenance of the silenced state of homeotic genes (Li and Luan, 2011; Li et al., 2007). *cyp71* shows reduced number of flowers due to the premature loss of meristematic activity. Moreover, floral organ numbers and morphology are also affected, with deformed petals, fewer sepals and stamens, and increased number of carpels (Li et al., 2007). The defects in leaf morphology are partly due to the ectopic expression of class I *KNOX* genes including *KNAT1*, *KNAT2*, and *STM*. Floral regulatory genes such as *AG*, *AP2* are also up-regulated in the *cyp71* leaves. At a molecular level, CYP71 interacts physically with histone H3 and LHP1, and is required for the association of LHP1 with the particular target loci. Interacting with LHP1 and FAS1, CYP71 may serve as a scaffolding protein that facilitates histone modification and deposition, which permit targeting the LHP1 associated complex onto chromatin (Li and Luan, 2011).

4. FUNCTION OF MICRORNAS IN FLOWER DEVELOPMENT

Since the first microRNA (miRNA) *lin-4* was identified from *Caenorhabditis. elegans* in 1993 (Lee et al., 1993), it has been found that the 21-nt short RNAs play crucial roles in the developmental processes in various organisms. The first plant miRNA was identified by genetic screening. With the help of bioinformatic analysis, hundreds of miRNAs have been investigated in plants. They function throughout the flower development, including regulation of flowering time, floral meristem determinacy, floral organ identity and floral patterning. In addition to miRNAs, other kinds of small RNAs, siRNAs have also been implicated in regulation of many developmental processes. Since few findings regarding the influence of siRNAs on flower development have been reported, here we mainly discuss functions of miRNAs in flowering and flower development.

4.1. miRNA biogenesis in *Arabidopsis*

Similar to protein-coding genes, miRNAs are transcribed from a transcriptional unit by RNA Polymerase II (Pol II). They have their own promoters that contain *cis*-elements and are regulated by various transcription factors.

MIR genes are first transcribed into primary miRNA (pri-miRNA), which carry 5′ cap, 3′ poly A and sometimes even intron, by Pol II (Bartel, 2004). After transcription, pri-miRNAs form hairpin structure due to partial self-complementary match. In the next step, pri-miRNAs are processed by Dicer-like 1 (DCL1) into miRNA duplexes via two sequential steps. In the first step, the secondary structure within the pri-miRNAs is recognized by DCL1 with the help of HYPONASTIC LEAVES 1 (HYL1) and SERRATE (SE). *HYL1* encode dsRNA-binding proteins (Hiraguri et al., 2005; Lu and Fedoroff, 2000). It has been shown that *hyl1* mutants lead to the accumulation of pri-miRNAs but decrease of pre-miRNAs (Hiraguri et al., 2005; Kurihara et al., 2006), and moreover that HYL1 protein directly interacts with DCL1, suggesting HYL1 may participate in the pri-miRNA to pre-miRNA processing through the recruitment of DCL1. SE is a C2H2 zinc finger protein, which has been shown to interact with HYL1 and the mutant of which causes increased level of pri-miRNAs (Lobbes et al., 2006; Yang et al., 2006a). Thus in the first step, the DCL1–HYL1–SE complex recognizes pri-miRNAs and releases the stem-loop region from the pri-mRNAs to generate precursor miRNA (pre-miRNA) (Han et al., 2004; Lobbes et al., 2006). In the second step, DCL1 alone releases the miRNA duplexes from the pre-miRNAs (Mateos et al., 2010; Song et al., 2010; Werner et al., 2010). Partial loss-of-function *dcl1* mutants reduce the accumulation of miRNAs and consequently exhibit multiple developmental defects (Jacobsen et al., 1999; Park et al., 2002; Ray et al., 1996; Reinhart et al., 2002). As DCL1 is involved in both the sequential steps, the *dcl1* null mutant shows decreased levels of pre-miRNAs while pri-miRNAs accumulate to higher levels (Kurihara and Watanabe, 2004; Kurihara et al., 2006).

In addition to miRNA processing, DCL1 is also required for the biogenesis of one class of siRNAs known as nat-siRNAs (Borsani et al., 2005; Katiyar-Agarwal et al., 2006), although the biochemical mechanism is unknown. Other homologs of DCL1, including DCL2, DCL3, and DCL4 are mainly responsible for processing long dsRNAs into siRNAs. It was shown that DCL4 also functions in the biogenesis of a few miRNAs in *Arabidopsis* (Rajagopalan et al., 2006). After the processing by the dicer complex, miRNAs undergo methylation on the 2′ -OH of the 3′ terminal nucleotide, which is important for the stabilization of miRNAs. A lack of methylation leads to uridylation and degradation of miRNAs. HUA ENHANCER 1 (HEN1), a methyltransferase identified from an enhancer screening of *ag-4*, has been shown to be responsible for the methylation of

miRNA duplexes (Bonnet et al., 2004; Chen et al., 2002). In the *hen1* mutant, the amount of miRNAs is reduced, and HEN1 is able to methylate miRNAs *in vitro* (Yu et al., 2005). The 2nt 3′ overhang of miRNA/miRNA* duplex, which is produced by DCL proteins, is necessary for the recognition by HEN1, since none of 1nt, 3nt, 4nt, or 5nt overhangs can be methylated (Yang et al., 2006b; Yu et al., 2005).

After the methylation step, the miRNA/miRNA* duplexes are exported from nucleus into cytoplasm by HASTY 1 (HTY1), which is an ortholog of Exportin-5 in animals (Bollman et al., 2003; Park et al., 2005). It has been suggested that methylation of miRNA duplexes could be a signal for exporting (Park et al., 2005).

In the cytoplasm, miRNA/miRNA* duplexes are loaded to RNA-induced silencing complex (RISC) assembly, which includes ARGONAUTE (AGO) proteins as key components. AGOs contain the PAZ domain, which binds to RNA, and the PIWI domain whose structure mimics RNaseH (Ma et al., 2004, 2005; Parker et al., 2004, 2005; Song et al., 2004). In *Arabidopsis*, there are10 genes in the AGO family, and most of them have RNA cleavage activity in their PIWI domains. When loaded to the RISC assembly, one strand of the miRNA duplex is cleaved by AGO to produce functional miRNAs. Which strand in the duplex will be cleaved is determined by the thermodynamic properties of their 5′ ends (Fig. 3.4; Khvorova et al., 2003; Schwarz et al., 2003).

4.2. miRNAs regulating floral transition

In plants, there are several endogenous and environmental pathways controlling the transition from vegetative to reproductive stages, including autonomous pathway, photoperiod pathway sensing the length of light cycle, gibberellin (GA) pathway functioning in the short-day condition, vernalization pathway in response to long exposure to low temperature and thermosensory pathway controlled by ambient temperature. All these pathways finally converge to a couple of flowering integrators and eventually activate of floral meristem identity genes. Many genes related to these pathways have been identified, some of which are regulated by miRNAs either directly or indirectly.

4.2.1 miR172 and miR156 regulate multiple flowering pathways

miR172 is one of the earliest miRNAs identified in plants (Park et al., 2002). It regulates the plant-specific transcription factor *AP2* and four *AP2*-like genes, including *TARGET OF EAT1* (*TOE1*), *TOE2*, *SCHNARCHZAPFEN*

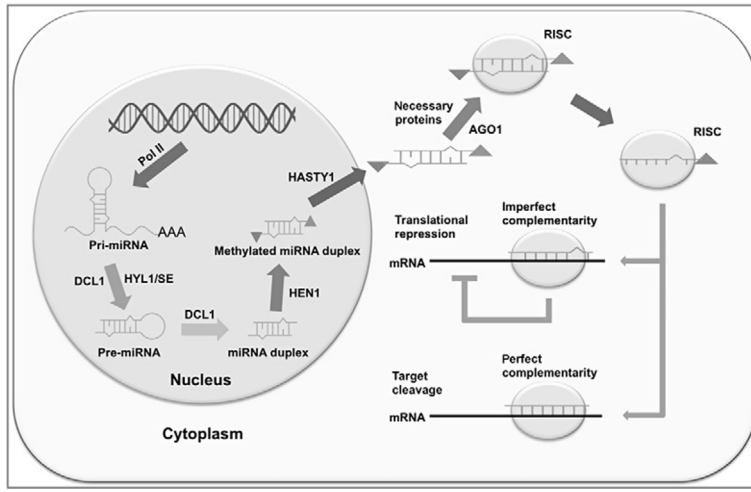

Figure 3.4 miRNA biosynthesis in plants. miRNAs are transcribed by RNA Pol II to produce pri-miRNAs. DCL1–HYL1–SE complex recognizes the secondary structure of pri-miRNAs and release the stem-loop structure. This stem-loop region are further processed by DCL1 to generate miRNA duplexes, followed by methylation at 3′-OH residues by HEN1. The methylated miRNA duplexes are exported from nucleus into cytoplasm by HASTY, a homolog of Exportin-5 in animals and recruit AGO and necessary proteins to form an RISC, where one strand of the duplex will be cleaved by AGO. The remaining miRNA guides the RISC assembly to target mRNA and cause either target cleavage or translational repression.

(*SNZ*), and *SCHLAFMÜTZE* (*SMZ*), which functions as flowering repressors. miR172 targets their coding regions near the 3′ end (Kim et al., 2006; Shigyo et al., 2006). In *Arabidopsis*, five *MIR172* loci have been identified. The expression of *miR172A*, *B*, and *C* genes increases during the floral transition, although the levels of *miR172D* and *E* remain low. (Aukerman and Sakai, 2003; Chen, 2004; Jung et al., 2007; Park et al., 2002; Schmid et al., 2003; Schwab et al., 2005), suggesting accumulation of miR172 may be necessary for floral transition. In fact, overexpression of miR172 causes early flowering, which are mediated by the reduction of four *AP2*-like genes targeted by miR172. Overexpression of any of these four *AP2*-like genes causes late flowering, whereas *toe1/toe2* mutants exhibit an early-flowering phenotype. Noticeably, plants that overexpress miR172 flowers earlier than the *toe1 toe2 smz snz* quadruple mutant (Mathieu et al., 2009), suggesting other targets of miR172 may also function to repress flowering. Furthermore, it has been suggested that AP2 may function as a flowering repressor, as overexpression of *AP2* causes late flowering (Chen, 2004). AP2 binds to the

regulatory regions of some flowering activators such as *SUPRESSOR OF OVEREXPRESSION OF CONSTANS1* (*SOC1*) and negatively regulates their expression (Yant et al., 2010). However, how the four AP2-like genes functions to repress flowering is still not clear.

As a flowering regulator, miR172 participates in multiple flowering pathways. Photoperiod affects expression of miR172 in a CONSTANS (CO)-independent GIGANTEA (GI) pathway. Level of miR172 decreases in *gi-2* but not in *co-2*. In a short-day condition, miR172 remains in a low level but is high in long-day condition (Jung et al., 2007). Interestingly, miR172 is also involved in the thermosensory flowering pathway. The expression level of miR172 increases in 23 °C compared with 16 °C (Lee et al., 2010a). SHORT VEGETATIVE PHASE (SVP) and FCA are key regulators of the thermosensory pathway (Blazquez et al., 2003). In *svp-32*, expression of miR172 is higher both in 16 and 23 °C compared with wild type (Lee et al., 2010a). The MADS domain protein SVP directly binds to the promoter of *MIR172A* and negatively regulates its transcript levels (Cho et al., 2012). FCA, as a RNA binding protein, binds to the flanking sequences of the stem-loop in pri-miR172 transcripts and regulates its processing (Jung et al., 2012). These results indicate that miR172 functions to adjust flowering time to adapt plants to the environmental changes.

miR172 is also regulated by two members of the SQUAMOSA PROMOTER BINDING PROTEIN LIKE (SPL) family, SPL9 and SPL10. Overexpression of *SPL9/10* leads to elevation of pri-miR172b and thus causes early flowering. SPL9/10 directly activate *MIR172B* by binding to its promoter (Wu et al., 2009). Interestingly, *SPL9/10* are targets of another miRNA, miR156. Level of miR156 is high in vegetative stage but low in reproductive stage, showing the opposite expression pattern to miR172. In addition to *SPL9/10*, *SPL3/4/5*, are also targeted by miR156 and function to activate floral meristem identity genes. Overexpression of miR156-resistant *SPL3/4/5* leads to early flowering (Fig. 3.5; Cardon et al., 1997; Gandikota et al., 2007; Wang et al., 2008; Wu and Poethig, 2006).

4.2.2 miR159 regulates gibberellin pathway

The GA signaling pathway is also affected by miRNAs. miR159 targets GAMYB-related genes, which are thought to be involved in the GA-dependent activation of floral meristem identity gene *LFY*. Overexpression of miR159 leads to a reduction in *LFY* transcript, resulting in late flowering in short-day condition (Achard et al., 2004). It has been shown that GAI and RGA, members of DELLA family transcription factors, are

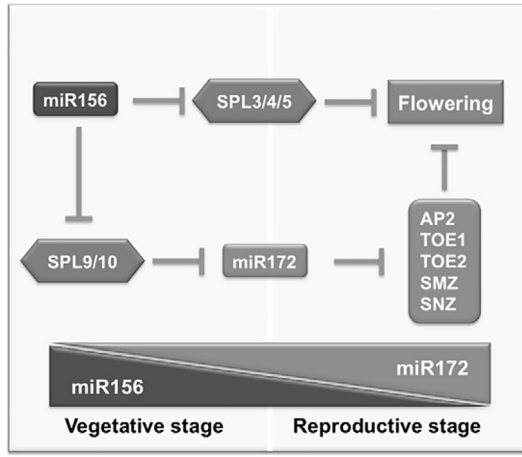

Figure 3.5 Regulatory roles of miR172 and miR156 in floral transition. miR172 and miR156 show inversely correlated expression pattern from vegetative to reproductive stages. Three targets of miR156, *SPL3/4/5*, function as a flowering repressor. *SPL9/10* are also repressed by miR156 and directly activate miR172. miR172 targets *AP2* and four *AP2*-like genes to induce flowering.

downregulated by GA signaling pathway, and function to repress miRNA159 (Achard et al., 2004). Either in the GA-deficient *ga1–3* mutant or in *gai* mutant, which is a dominant altered-function allele, the level of miR159 is reduced. Notably, treatment of GA is able to rescue the level of miR159 in *ga1–3* but bot in *gai*. At the same time, *ga1–3 gai rga* triple mutant has comparable levels of miR159 comparing to WT (Achard et al., 2004), revealing a complicated regulation of miR159 and GAMYB by the GA signaling. These results indicate that miR159 functions to mediate GA signaling to control flowering.

4.3. miRNAs controlling floral meristem determinacy

4.3.1 miR165/166 regulate HD-ZIP III genes to control floral meristem

miR165 and miR166 have been shown to control meristem behaviors and the abaxial–adaxial polarity of lateral organs. The mature miR165 and miR166 share nearly the same sequence except for one nucleotide. In *Arabidopsis*, two *MIR165* and six *MIR166* loci have been identified (Reinhart et al., 2002). Based on sequence analyses, miR165/166 are predicted to target the *class III HOMEODOMAIN-LEUCINE ZIPPER* (*HD-ZIP III*) genes, namely *REVOLUTA* (*REV*), *ATHB-9/PHAVOLUTA* (*PHV*),

ATHB-14/PHABULOSA (*PHB*), *ATHB-8*, and *ATHB-15/CORONA* (*CNA*), which function in meristem maintenance as well as regulating the lateral organs polarity. Their target sequences encode a part of the START domain of HD-ZIP III proteins with near-perfect complementarity (Jung and Park, 2007; Kim et al., 2005a; Tang et al., 2003). The mRNAs of *PHB* and *ATHB-15* have been shown to be cleaved at the miR165/166 target sequence in biochemical assays. Mutations in the START domains to lose the complementarity with miR165/166 cause dominant mutations.

In spite of the sequence similarity and conserved targets of these two miRNAs, there are some significant differences between them. Firstly, based on promoter driven GUS activities, individual *MIR166/165* genes exhibit distinct expression patterns in the developing flowers. For instance, miR166a is expressed in developing stamens, whereas miR166b is predominantly expressed developing in ovules and stigmas (Jung and Park, 2007). Secondly, overexpression of miR166 by activation tagging has been shown to reduce the mRNA levels of *ATHB-9/PHV*, *ATHB-14/PHB*, and *ATHB-15/CNA* and causes a phenotype resembling the *phv phb cna* triple mutant with enlarged SAMs (Kim et al., 2005a; Williams et al., 2005b), while overexpression of miR165 causes a concomitant downregulation of expression of all five HD-ZIP III genes and display prominent phenotypes reminiscent of loss-of-function mutants of *rev phb phv* and *rev/ifl1* with loss of SAMs (Zhou et al., 2007), indicating that miR165 and miR166 may have distinct effects on the regulation of their target genes. This could be due to different effectiveness of miR165 and miR166 on the cleavage of their target genes. In addition, different combinations of the loss-of-function for *HD-ZIP III* genes seem to result in the opposite SAM phenotypes, indicating that an accurate regulation of *HD-ZIP III* genes by miR165 and miR166 is essential for normal meristem formation. In flowers, both knockdown of *HD-ZIP III* genes by overexpression of miR165/166 and mis-expression of miR165/166 resistant *HD-ZIP III* genes lead to prolonged floral meristem activity (Ji et al., 2011). This also indicates that proper expression of *HD-ZIP III* genes is necessary to coordinate the balance between growth and differentiation in flowers.

It has been shown that two members of the AGO protein family, AGO1 and AGO10, the key components of RISC complexes, are responsible for incorporation of miR165/166 (Kidner and Martienssen, 2004; Liu et al., 2009b). Despite the similar small RNA binding specificities of these two AGO proteins, the *ago1* and *ago10* mutants have different effects on miR165/166 and their target genes. The amount of miR165/166 is reduced

in the *ago1* mutant, but increased in *ago10* (Kidner and Martienssen, 2004; Liu et al., 2009b). This has been explained by the fact that AGO 10 has higher binding affinity than AGO1 to miR165/166 but cannot functions normally, and thus act as a decoy to sequester miR165/166 to maintain the meristem (Zhu et al., 2011).

4.3.2 miR172 play a role in floral meristem determinacy via regulating AP2

The regulation of floral meristem determinacy by miR172 is mainly via its well-known target *AP2*, which is an A class organ identity gene determining the first whorl sepals and second whorl petals in the ABC model. AP2 may also regulates floral meristem determinacy mainly via two mechanisms, (1) as a repressor of C class gene *AG* and (2) as an activator of the meristem determinant gene *WUS*. AG controls floral meristem determinacy in addition to determine the reproductive identities, third whorl stamens and fourth whorl carpels as a C class gene. AG terminates the flower stem cell activity after the formation of carpel primordia through upregulation of *KNU* to terminate the expression of *WUS* (Sun et al., 2009). In *ap2–2*, the organ identities of the second and third whorls both become stamens (Bowman et al., 1991), which correspond to loss of A function and ectopic C function. However, the number of stamens in these two whorls is only one–two, which is supposed to be ten theoretically. This is probably due to the ectopic expression of *AG* causing precocious termination of stem cell, since *ap2–2 ag-4* partially rescue the organ number defects with an average of 5.4 stamens in whorls 2 and 3 (Sieburth et al., 1995). A dominant allele of *AP2* named *I28* shows deficient SAM and mimics *wus-1* (Wurschum et al., 2006). This suggests that AP2 functions to promote *WUS*, although the detailed mechanism is not clear.

Overexpression of miR172 causes *ap2–2* phenotype, whereas overexpression of miR172-resistant *AP2* leads to various indeterminate flowers: from one with infinite growth of stamens in the third and fourth whorls to an *ag-1*-like flower with bigger meristems (Zhao et al., 2007). Thus, miR172 may regulate the stem cell activity in developing flowers via regulating *AP2* in AG-dependent and independent pathways.

4.4. miRNAs controlling floral patterning

4.4.1 Floral organ polarity

During organ development, one of the most important programs is determination of the organ polarity, which leads to specification of tissues and

organs with their normal functions. Dozens of genes have been identified with polarized expression patterns and function in controlling organ polarity, including miR165/166-regulated *HD-ZIP III* genes. However, based on what have been shown, miR165/166 appears to mainly regulate the polarity of leaves, but not in flowers. Since overexpression of miR166 does not affect the flowers (Jung and Park, 2007) and plants overexpressing miR165 produce abnormal carpels which appears not to be caused by disruption of polarity (Zhou et al., 2007).

4.4.2 Organ boundary formation

The miR164 family contains three members, and functions redundantly to control the boundary of floral organ primordia by regulating two NAC-domain genes *CUP-SHAPED COTYLEDON1* (*CUC1*) *and CUC2*. CUC1 and CUC2 are redundantly required for the formation of floral organ boundaries. They are expressed at the boundaries between floral organ primordia in the same whorls and also in between whorls (Takada et al., 2001). The functions of CUC1 and CUC2 appear to be suppressing the cell proliferation at boundaries (Nikovics et al., 2006; Peaucelle et al., 2007; Sieber et al., 2007). The *cuc1 cuc2* double mutant produces flowers with defects in sepal and stamen separation (Aida et al., 1997). Overexpression of miR164 leads to the reduction of *CUC1* and *CUC2* transcripts, resulting in *cuc1 cuc2*–like flowers, with fused floral organs. This phenotype is rescued by expressing miR164-resistant *CUC2* (Mallory et al., 2004). It has been reported that the early-arising flowers of a loss-of-function allele of *MIR164C*, named *early extra petals 1* (*eep1*), produces extra petals, which is caused by the increased level of *CUC1* and *CUC2* (Baker et al., 2005). The increased number of petals may be due to the formation of extra boundaries. When combined with *mir164a* and *mir164b* mutants, the *mir164a mir164b mir164c* triple mutant exhibits a stronger phenotype, with increased number of sepals and petals, slightly fewer stamens and unfused carpels (Sieber et al., 2007). Although the product of the three members of miR164 family are very similar and are supposed to target the same genes, there are still some differences in their expression patterns (Sieber et al., 2007). Interestingly, it was found that miR164s do not function to restrict the spatial expression pattern of *CUC1* and *CUC2*, but just restrict their mRNA levels in the same domain. In fact, expressions of miR164 and *CUC1/2* in flowers are not complementary but overlapping (Sieber et al., 2007). This indicates that miR164s may function in the homeostatic maintenance of proper expression levels of *CUC* genes.

4.4.3 Trans-acting siRNAs affecting floral patterning

Trans-acting (ta) siRNAs are secondary siRNAs synthesized from noncoding transcript targeted by miRNAs (Peragine et al., 2004; Vazquez et al., 2004; Yoshikawa et al., 2005). *ETT*, which encodes a member of ARF family and functions to control the patterning of gynoecium (Remington et al., 2004), is regulated by a ta-siRNA from *TAS3* locus, *tasiR-ARF* (Allen et al., 2005; Williams et al., 2005a). The production and stability of tasiR-ARF require AGO7, DCL4, and RNA-DEPENDENT RNA POLYMERASE6 (RDR6) (Fahlgren et al., 2006; Hunter et al., 2006). Overexpression of tasiR-ARF-resistant *ETT* resembles the phenotype of *ago7* flowers, with short stamens producing little pollen (Hunter et al., 2006). Expression of tasiR-ARF-resistant *ETT* in *rdr6–15* background produces flowers with many severe defects (Fahlgren et al., 2006).

4.5. miRNAs regulating floral organ development

In *Arabidopsis*, the flowers consist of four sepals (first whorl), four petals (second whorl), six stamens (third whorl), and two fused carpels (fourth whorl). Based on genetic studies of some floral organ identity mutants, the ABC model was introduced 22 years ago and predicts that floral organ identities are determined by the combinatiorial action of ABC genes (Bowman et al., 1991; Coen and Meyerowitz, 1991). In this model, there are three classes of genes: A class including *AP1* and *AP2*, B class including *AP3* and *PI* and C class including *AG*. A class genes alone function in determine the sepal identity, and, in combination with B class genes, specify the petal identity. C class genes alone control the developmental program of carpels, and, together with B class genes, determine the stamen identity. All these three classes of genes have specific expression domain corresponding to their functions.

4.5.1 miR172 influences multiple floral organs via regulating AP2

miR172 functions in floral organ identity determination via regulating the A class gene *AP2*. Overexpression of miR172 leads to *ap2–2*-like phenotype, whereas overexpression of miR172-resistant *AP2* causes *ag*-like phenotype, which does not occur in overexpression of the wild-type copy of *AP2* (Chen, 2004). The finding of miR172 involved in floral organ development was first suggested by a mutagenesis screen using *ag-4*, which identifies *HEN1* functioning in miRNA processing and maturation. Regulation of *AP2* by miR172 is mainly via translation repression, since mRNA of *AP2* expressed through the 4 whorls but AP2 protein only locate in the first 2

whorls (Aukerman and Sakai, 2003; Chen, 2004), although cleavage of *AP2* mRNA by miR172 was also reported (Jung et al., 2007; Schwab et al., 2005).

4.5.2 miR159 is necessary for development of gynoeciums and stamens

The miR159 family contains three members and target three MYB genes *MYB33*, *MYB65*, and *MYB101* (Millar and Gubler, 2005). In flower development, MYB33 and MYB65 are expressed in developing anthers, pollen grains, and ovules, suggesting their functions in reproductive development (Gocal et al., 2001). Plants overexpressing miR159a produces flowers with stunted stamens and reduced fertility (Achard et al., 2004; Allen et al., 2007). The *mir159a mir159b* double mutant displays reduced fertility, and seeds with irregular shapes, although single mutant of each doesn't display any floral defects. Transgenic plant with miRNA-resistant version of *MYB33* resembles the *mir159a mir159b* double mutant. The loss of *MYB33* function partially suppresses the phenotype of *mir159a mir159b* double mutant. Furthermore, *mir159a mir159b myb33 myb65* quadruple mutant can fully rescues the developmental defects of the *mir159a mir159b* double mutant (Achard et al., 2004; Allen et al., 2007). In addition, Overexpression of a miRNA-resistant version of *MYB101* causes short petals, short stamens, and partial sterility (Palatnik et al., 2007). Thus, miR159 may functions to control the reproductive development via regulating the expression of *MYB33* and *MYB65*. In anther development and pollen microsporogenesis, miR159 is also regulated by gibberellin (GA) signaling (Achard et al., 2004).

Another interesting finding is that miR159 and miR319 show high sequence similarity, with 17 of the 21 nucleotides identical in the mature miRNAs (Palatnik et al., 2007). miR319 is able to target *MYB* genes *in vitro*, but not *in vivo* possibly due to the limited expression level and domain of miR319. On the other hand, miR159 only targets the *MYB*s but not TEOSINTE BRANCHED1, CYCLOIDEA, and PCF (TCP) transcription factors because of sequence complementarity (Palatnik et al., 2007).

4.5.3 miR319a regulates organ size and shape

There are three members in the miR319 family. It has been shown that miR319a function in controlling shape and size of floral organs by regulating the expression of the five members of the TCP transcription factor family: *TCP2*, *TCP3*, *TCP4*, *TCP10*, *TCP24* (Nag et al., 2009; Palatnik et al., 2003). TCP proteins are proposed to repress cell growth and promote cell differentiation (Crawford et al., 2004; Efroni et al., 2008; Luo et al., 1996,

1999; Nath et al., 2003). In flower, activity of miR319a::GUS is detected from stages 4–11, with strongest expression in developing petals. Loss-of-function mutant of *mir319a* leads to elevation of the levels of all the five TCPs, resulting in flowers with smaller petals and stamens than wild type (Nag et al., 2009). Among the five TCP factors, *TCP4* appears to be the key target of miR319a, since a *tcp4* allele, which contains a mutation in the miR319a binding site complementary to the *mir319a* mutation, can rescue the loss-of-function mutant of miR319 (Palatnik et al., 2007).

4.5.4 miR167 controls development of ovules and anthers

The miR167 family contains four members, which regulate the development of gynoecium and stamen by controlling two members of the ARFs: *ARF6* and *ARF8*. In the development of ovules and anthers, the expression patterns of *miR167* and *ARF6/ARF8* are mutually exclusive (Wu et al., 2006). The *arf6 arf8* double mutant produces short stamen filaments, poorly growing pollen, short stigmatic papillae, and leads to male and female sterility. This phenotype is phenocopied by overexpression of miR167 (Wu et al., 2006). In transgenic plants expressing miRNA-resistant versions of *ARF6* and *ARF8*, growth of ovule integuments is arrested, and anthers grows abnormally and failed to release pollen (Fig. 3.6; Wu et al., 2006).

	Floral transition	Floral meristem determinacy	Organ development	Floral patterning
miR156	●			
miR159	●		●	
miR164				●
miR165/166		●		●
miR167			●	
miR172	●	●	●	
miR319a			●	

Figure 3.6 Summary of functions of miRNAs in flower development. Some miRNAs have multiple functions during flower development, such as miR159 and miR172. Each developmental process involves several miRNAs.

5. CONCLUDING REMARKS

Recent genetic, reverse-genetic, genomic, and biochemical studies have shown that epigenetic regulators play essential roles for the initiation and maintenance of cell differentiation by controlling chromosomal status in flower development. Histone modification, ATP-dependent chromatin remodeling, and miRNAs are involved in the regulation of the spatiotemporal-specific expression of their target genes in multisteps of flower development. For the production of flowers in the right time with right number of functional organs, expression of thousands of genes is coordinated by the concerted actions of transcriptional factors and epigenetic regulators. Still little is known about the recruitment of epigenetic machinery to their specific targets in certain cell types. To understand the molecular details of their action in cell specification and maintenance, further analyses will be necessary including epigenetic assays in individual cell types in a specific developmental context. The *ap1 cal* mutant flowers with inducible AP1 activity enable us to harvest floral-stage specific samples and analyze dynamic change of epigenetic status in flower development (Sun et al., 2009; Wellmer et al., 2004). Cell sorting and affinity purification of nuclei from individual cell types also have been also successfully used using plants in which specific cells were labeled either by GFP markers or by biotin labeled nuclear envelop proteins (Birnbaum et al., 2005; Deal and Henikoff, 2010; Yadav et al., 2009).

REFERENCES

Achard, P., Herr, A., Baulcombe, D.C., Harberd, N.P., 2004. Modulation of floral development by a gibberellin-regulated microRNA. Development 131, 3357–3365.

Agger, K., Cloos, P.A., Christensen, J., Pasini, D., Rose, S., Rappsilber, J., Issaeva, I., Canaani, E., Salcini, A.E., Helin, K., 2007. UTX and JMJD3 are histone H3K27 demethylases involved in HOX gene regulation and development. Nature 449, 731–734.

Aida, M., Ishida, T., Fukaki, H., Fujisawa, H., Tasaka, M., 1997. Genes involved in organ separation in Arabidopsis: an analysis of the cup-shaped cotyledon mutant. Plant Cell 9, 841–857.

Allen, E., Xie, Z., Gustafson, A.M., Carrington, J.C., 2005. microRNA-directed phasing during trans-acting siRNA biogenesis in plants. Cell 121, 207–221.

Allen, R.S., Li, J., Stahle, M.I., Dubroue, A., Gubler, F., Millar, A.A., 2007. Genetic analysis reveals functional redundancy and the major target genes of the Arabidopsis miR159 family. Proc. Natl. Acad. Sci. USA 104, 16371–16376.

Alvarez-Buylla, E.R., Azpeitia, E., Barrio, R., Benitez, M., Padilla-Longoria, P., 2010. From ABC genes to regulatory networks, epigenetic landscapes and flower morphogenesis: making biological sense of theoretical approaches. Semin. Cell Dev. Biol. 21, 108–117.

Alvarez-Venegas, R., Pien, S., Sadder, M., Witmer, X., Grossniklaus, U., Avramova, Z., 2003. ATX-1, an Arabidopsis homolog of trithorax, activates flower homeotic genes. Curr. Biol. 13, 627–637.

Aufsatz, W., Mette, M.F., van der Winden, J., Matzke, M., Matzke, A.J., 2002. HDA6, a putative histone deacetylase needed to enhance DNA methylation induced by double-stranded RNA. EMBO J. 21, 6832–6841.

Aukerman, M.J., Sakai, H., 2003. Regulation of flowering time and floral organ identity by a MicroRNA and its APETALA2-like target genes. Plant Cell 15, 2730–2741.

Ausin, I., Alonso-Blanco, C., Jarillo, J.A., Ruiz-Garcia, L., Martinez-Zapater, J.M., 2004. Regulation of flowering time by FVE, a retinoblastoma-associated protein. Nat. Genet. 36, 162–166.

Baker, C.C., Sieber, P., Wellmer, F., Meyerowitz, E.M., 2005. The early extra petals1 mutant uncovers a role for microRNA miR164c in regulating petal number in Arabidopsis. Curr. Biol. 15, 303–315.

Bartee, L., Malagnac, F., Bender, J., 2001. Arabidopsis cmt3 chromomethylase mutations block non-CG methylation and silencing of an endogenous gene. Genes Dev. 15, 1753–1758.

Bartel, D.P., 2004. MicroRNAs: genomics, biogenesis, mechanism, and function. Cell 116, 281–297.

Berger, S.L., Kouzarides, T., Shiekhattar, R., Shilatifard, A., 2009. An operational definition of epigenetics. Genes Dev. 23, 781–783.

Berger, N., Dubreucq, B., Roudier, F., Dubos, C., Lepiniec, L., 2011. Transcriptional regulation of Arabidopsis LEAFY COTYLEDON2 involves RLE, a cis-element that regulates trimethylation of histone H3 at lysine-27. Plant Cell 23, 4065–4078.

Bernatavichute, Y.V., Zhang, X., Cokus, S., Pellegrini, M., Jacobsen, S.E., 2008. Genome-wide association of histone H3 lysine nine methylation with CHG DNA methylation in Arabidopsis thaliana. PLoS One 3, e3156.

Berr, A., Xu, L., Gao, J., Cognat, V., Steinmetz, A., Dong, A., Shen, W.H., 2009. SET DOMAIN GROUP25 encodes a histone methyltransferase and is involved in FLOWERING LOCUS C activation and repression of flowering. Plant Physiol. 151, 1476–1485.

Berr, A., McCallum, E.J., Menard, R., Meyer, D., Fuchs, J., Dong, A., Shen, W.H., 2010. Arabidopsis SET DOMAIN GROUP2 is required for H3K4 trimethylation and is crucial for both sporophyte and gametophyte development. Plant Cell 22, 3232–3248.

Bertrand, C., Bergounioux, C., Domenichini, S., Delarue, M., Zhou, D.X., 2003. Arabidopsis histone acetyltransferase AtGCN5 regulates the floral meristem activity through the WUSCHEL/AGAMOUS pathway. J. Biol. Chem. 278, 28246–28251.

Bezhani, S., Winter, C., Hershman, S., Wagner, J.D., Kennedy, J.F., Kwon, C.S., Pfluger, J., Su, Y., Wagner, D., 2007. Unique, shared, and redundant roles for the Arabidopsis SWI/SNF chromatin remodeling ATPases BRAHMA and SPLAYED. Plant Cell 19, 403–416.

Birnbaum, K., Jung, J.W., Wang, J.Y., Lambert, G.M., Hirst, J.A., Galbraith, D.W., Benfey, P.N., 2005. Cell type-specific expression profiling in plants via cell sorting of protoplasts from fluorescent reporter lines. Nat. Methods 2, 615–619.

Blazquez, M.A., Ahn, J.H., Weigel, D., 2003. A thermosensory pathway controlling flowering time in Arabidopsis thaliana. Nat. Genet. 33, 168–171.

Bollman, K.M., Aukerman, M.J., Park, M.Y., Hunter, C., Berardini, T.Z., Poethig, R.S., 2003. HASTY, the Arabidopsis ortholog of exportin 5/MSN5, regulates phase change and morphogenesis. Development 130, 1493–1504.

Bonnet, E., Wuyts, J., Rouze, P., Van de Peer, Y., 2004. Detection of 91 potential conserved plant microRNAs in Arabidopsis thaliana and Oryza sativa identifies important target genes. Proc. Natl. Acad. Sci. USA 101, 11511–11516.

Borsani, O., Zhu, J., Verslues, P.E., Sunkar, R., Zhu, J.K., 2005. Endogenous siRNAs derived from a pair of natural cis-antisense transcripts regulate salt tolerance in Arabidopsis. Cell 123, 1279–1291.

Bouyer, D., Roudier, F., Heese, M., Andersen, E.D., Gey, D., Nowack, M.K., Goodrich, J., Renou, J.P., Grini, P.E., Colot, V., Schnittger, A., 2011. Polycomb repressive complex 2 controls the embryo-to-seedling phase transition. PLoS Genet. 7, e1002014.

Bowman, J.L., Smyth, D.R., Meyerowitz, E.M., 1989. Genes directing flower development in Arabidopsis. Plant Cell 1, 37–52.

Bowman, J.L., Smyth, D.R., Meyerowitz, E.M., 1991. Genetic interactions among floral homeotic genes of Arabidopsis. Development 112, 1–20.

Bratzel, F., López-Torrejón, G., Koch, M., Del Pozo, J.C., Calonje, M., 2010. Keeping Cell Identity in Arabidopsis Requires PRC1 RING-Finger Homologs that Catalyze H2A Monoubiquitination. Curr. Biol. 20, 1853–1859.

Buzas, D.M., Tamada, Y., Kurata, T., 2012. FLC: a hidden polycomb response element shows up in silence. Plant Cell Physiol. 53, 785–793.

Cao, X., Jacobsen, S.E., 2002. Role of the arabidopsis DRM methyltransferases in de novo DNA methylation and gene silencing. Curr. Biol. 12, 1138–1144.

Cao, Y., Dai, Y., Cui, S., Ma, L., 2008. Histone H2B monoubiquitination in the chromatin of FLOWERING LOCUS C regulates flowering time in Arabidopsis. Plant Cell 20, 2586–2602.

Cardon, G.H., Hohmann, S., Nettesheim, K., Saedler, H., Huijser, P., 1997. Functional analysis of the Arabidopsis thaliana SBP-box gene SPL3: a novel gene involved in the floral transition. Plant J. 12, 367–377.

Carles, C.C., Fletcher, J.C., 2009. The SAND domain protein ULTRAPETALA1 acts as a trithorax group factor to regulate cell fate in plants. Genes Dev. 23, 2723–2728.

Cartagena, J.A., Matsunaga, S., Seki, M., Kurihara, D., Yokoyama, M., Shinozaki, K., Fujimoto, S., Azumi, Y., Uchiyama, S., Fukui, K., 2008. The Arabidopsis SDG4 contributes to the regulation of pollen tube growth by methylation of histone H3 lysines 4 and 36 in mature pollen. Dev. Biol. 315, 355–368.

Cazzonelli, C.I., Cuttriss, A.J., Cossetto, S.B., Pye, W., Crisp, P., Whelan, J., Finnegan, E.J., Turnbull, C., Pogson, B.J., 2009. Regulation of carotenoid composition and shoot branching in Arabidopsis by a chromatin modifying histone methyltransferase, SDG8. Plant Cell 21, 39–53.

Chanvivattana, Y., Bishopp, A., Schubert, D., Stock, C., Moon, Y.H., Sung, Z.R., Goodrich, J., 2004. Interaction of Polycomb-group proteins controlling flowering in Arabidopsis. Development 131, 5263–5276.

Chen, X., 2004. A microRNA as a translational repressor of APETALA2 in Arabidopsis flower development. Science 303, 2022–2025.

Chen, X., Liu, J., Cheng, Y., Jia, D., 2002. HEN1 functions pleiotropically in Arabidopsis development and acts in C function in the flower. Development 129, 1085–1094.

Cho, H.J., Kim, J.J., Lee, J.H., Kim, W., Jung, J.H., Park, C.M., Ahn, J.H., 2012. SHORT VEGETATIVE PHASE (SVP) protein negatively regulates miR172 transcription via direct binding to the pri-miR172a promoter in Arabidopsis. FEBS Lett. 586, 2332–2337.

Choi, Y., Gehring, M., Johnson, L., Hannon, M., Harada, J.J., Goldberg, R.B., Jacobsen, S.E., Fischer, R.L., 2002. DEMETER, a DNA glycosylase domain protein, is required for endosperm gene imprinting and seed viability in arabidopsis. Cell 110, 33–42.

Coen, E.S., Meyerowitz, E.M., 1991. The war of the whorls: genetic interactions controlling flower development. Nature 353, 31–37.

Crawford, B.C., Nath, U., Carpenter, R., Coen, E.S., 2004. CINCINNATA controls both cell differentiation and growth in petal lobes and leaves of Antirrhinum. Plant Physiol. 135, 244–253.

Davie, J.R., Chadee, D.N., 1998. Regulation and regulatory parameters of histone modifications. J. Cell. Biochem. 30–31 (Suppl.), 203–213.
Deal, R.B., Henikoff, S., 2010. A simple method for gene expression and chromatin profiling of individual cell types within a tissue. Dev. Cell 18, 1030–1040.
Dennis, E.S., Peacock, W.J., 2007. Epigenetic regulation of flowering. Curr. Opin. Plant Biol. 10, 520–527.
Dyson, M.H., Rose, S., Mahadevan, L.C., 2001. Acetyllysine-binding and function of bromodomain-containing proteins in chromatin. Front. Biosci. 6, D853–D865.
Ebbs, M.L., Bender, J., 2006. Locus-specific control of DNA methylation by the Arabidopsis SUVH5 histone methyltransferase. Plant Cell 18, 1166–1176.
Ebbs, M.L., Bartee, L., Bender, J., 2005. H3 lysine 9 methylation is maintained on a transcribed inverted repeat by combined action of SUVH6 and SUVH4 methyltransferases. Mol. Cell Biol. 25, 10507–10515.
Efroni, I., Blum, E., Goldshmidt, A., Eshed, Y., 2008. A protracted and dynamic maturation schedule underlies Arabidopsis leaf development. Plant Cell 20, 2293–2306.
Fahlgren, N., Montgomery, T.A., Howell, M.D., Allen, E., Dvorak, S.K., Alexander, A.L., Carrington, J.C., 2006. Regulation of AUXIN RESPONSE FACTOR3 by TAS3 ta-siRNA affects developmental timing and patterning in Arabidopsis. Curr. Biol. 16, 939–944.
Fahrner, J.A., Baylin, S.B., 2003. Heterochromatin: stable and unstable invasions at home and abroad. Genes Dev. 17, 1805–1812.
Fan, D., Dai, Y., Wang, X., Wang, Z., He, H., Yang, H., Cao, Y., Deng, X.W., Ma, L., 2012. IBM1, a JmjC domain-containing histone demethylase, is involved in the regulation of RNA-directed DNA methylation through the epigenetic control of RDR2 and DCL3 expression in Arabidopsis. Nucleic Acids Res. 40, 8905–8916.
Feng, S., Jacobsen, S.E., 2011. Epigenetic modifications in plants: an evolutionary perspective. Curr. Opin. Plant Biol. 14, 179–186.
Finnegan, E.J., Peacock, W.J., Dennis, E.S., 1996. Reduced DNA methylation in Arabidopsis thaliana results in abnormal plant development. Proc. Natl. Acad. Sci. USA 93, 8449–8454.
Franks, R.G., Wang, C., Levin, J.Z., Liu, Z., 2002. SEUSS, a member of a novel family of plant regulatory proteins, represses floral homeotic gene expression with LEUNIG. Development 129, 253–263.
Fuks, F., 2005. DNA methylation and histone modifications: teaming up to silence genes. Curr. Opin. Genet. Dev. 15, 490–495.
Furner, I.J., Matzke, M., 2011. Methylation and demethylation of the Arabidopsis genome. Curr. Opin. Plant Biol. 14, 137–141.
Gandikota, M., Birkenbihl, R.P., Hohmann, S., Cardon, G.H., Saedler, H., Huijser, P., 2007. The miRNA156/157 recognition element in the 3' UTR of the Arabidopsis SBP box gene SPL3 prevents early flowering by translational inhibition in seedlings. Plant J. 49, 683–693.
Gocal, G.F., Sheldon, C.C., Gubler, F., Moritz, T., Bagnall, D.J., MacMillan, C.P., Li, S.F., Parish, R.W., Dennis, E.S., Weigel, D., King, R.W., 2001. GAMYB-like genes, flowering, and gibberellin signaling in Arabidopsis. Plant Physiol. 127, 1682–1693.
Gonzalez, D., Bowen, A.J., Carroll, T.S., Conlan, R.S., 2007. The transcription corepressor LEUNIG interacts with the histone deacetylase HDA19 and mediator components MED14 (SWP) and CDK8 (HEN3) to repress transcription. Mol. Cell Biol. 27, 5306–5315.
Goodrich, J., Puangsomlee, P., Martin, M., Long, D., Meyerowitz, E.M., Coupland, G., 1997. A Polycomb-group gene regulates homeotic gene expression in Arabidopsis. Nature 386, 44–51.

Greb, T., Mylne, J.S., Crevillen, P., Geraldo, N., An, H., Gendall, A.R., Dean, C., 2007. The PHD finger protein VRN5 functions in the epigenetic silencing of Arabidopsis FLC. Curr. Biol. 17, 73–78.

Grini, P.E., Thorstensen, T., Alm, V., Vizcay-Barrena, G., Windju, S.S., Jorstad, T.S., Wilson, Z.A., Aalen, R.B., 2009. The ASH1 HOMOLOG 2 (ASHH2) histone H3 methyltransferase is required for ovule and anther development in Arabidopsis. PLoS One 4, e7817.

Gu, X., Jiang, D., Yang, W., Jacob, Y., Michaels, S.D., He, Y., 2011. Arabidopsis homologs of retinoblastoma-associated protein 46/48 associate with a histone deacetylase to act redundantly in chromatin silencing. PLoS Genet. 7, e1002366.

Han, M.H., Goud, S., Song, L., Fedoroff, N., 2004. The Arabidopsis double-stranded RNA-binding protein HYL1 plays a role in microRNA-mediated gene regulation. Proc. Natl. Acad. Sci. USA 101, 1093–1098.

Hansen, J.C., Tse, C., Wolffe, A.P., 1998. Structure and function of the core histone N-termini: more than meets the eye. Biochemistry 37, 17637–17641.

He, Y., 2009. Control of the transition to flowering by chromatin modifications. Mol. Plant 2, 554–564.

Hennig, L., Bouveret, R., Gruissem, W., 2005. MSI1-like proteins: an escort service for chromatin assembly and remodeling complexes. Trends Cell Biol. 15, 295–302.

Hiraguri, A., Itoh, R., Kondo, N., Nomura, Y., Aizawa, D., Murai, Y., Koiwa, H., Seki, M., Shinozaki, K., Fukuhara, T., 2005. Specific interactions between Dicer-like proteins and HYL1/DRB-family dsRNA-binding proteins in Arabidopsis thaliana. Plant Mol. Biol. 57, 173–188.

Hong, E.H., Jeong, Y.M., Ryu, J.Y., Amasino, R.M., Noh, B., Noh, Y.S., 2009. Temporal and spatial expression patterns of nine Arabidopsis genes encoding Jumonji C-domain proteins. Mol. Cells 27, 481–490.

Hunter, C., Willmann, M.R., Wu, G., Yoshikawa, M., de la Luz Gutierrez-Nava, M., Poethig, S.R., 2006. Trans-acting siRNA-mediated repression of ETTIN and ARF4 regulates heteroblasty in Arabidopsis. Development 133, 2973–2981.

Hurtado, L., Farrona, S., Reyes, J.C., 2006. The putative SWI/SNF complex subunit BRAHMA activates flower homeotic genes in Arabidopsis thaliana. Plant Mol. Biol. 62, 291–304.

Inagaki, S., Miura-Kamio, A., Nakamura, Y., Lu, F., Cui, X., Cao, X., Kimura, H., Saze, H., Kakutani, T., 2010. Autocatalytic differentiation of epigenetic modifications within the Arabidopsis genome. EMBO J. 29, 3496–3506.

Ito, T., 2011. Coordination of flower development by homeotic master regulators. Curr. Opin. Plant Biol. 14, 53–59.

Jackson, J.P., Lindroth, A.M., Cao, X., Jacobsen, S.E., 2002. Control of CpNpG DNA methylation by the KRYPTONITE histone H3 methyltransferase. Nature 416, 556–560.

Jackson, J.P., Johnson, L., Jasencakova, Z., Zhang, X., PerezBurgos, L., Singh, P.B., Cheng, X., Schubert, I., Jenuwein, T., Jacobsen, S.E., 2004. Dimethylation of histone H3 lysine 9 is a critical mark for DNA methylation and gene silencing in Arabidopsis thaliana. Chromosoma 112, 308–315.

Jacob, Y., Stroud, H., Leblanc, C., Feng, S., Zhuo, L., Caro, E., Hassel, C., Gutierrez, C., Michaels, S.D., Jacobsen, S.E., 2010. Regulation of heterochromatic DNA replication by histone H3 lysine 27 methyltransferases. Nature 466, 987–991.

Jacobsen, S.E., Meyerowitz, E.M., 1997. Hypermethylated SUPERMAN epigenetic alleles in arabidopsis. Science 277, 1100–1103.

Jacobsen, S.E., Running, M.P., Meyerowitz, E.M., 1999. Disruption of an RNA helicase/RNAse III gene in Arabidopsis causes unregulated cell division in floral meristems. Development 126, 5231–5243.

Jacobsen, S.E., Sakai, H., Finnegan, E.J., Cao, X., Meyerowitz, E.M., 2000. Ectopic hypermethylation of flower-specific genes in Arabidopsis. Curr. Biol. 10, 179–186.
Jarillo, J.A., Pineiro, M., 2011. Timing is everything in plant development. The central role of floral repressors. Plant Sci. 181, 364–378.
Jarillo, J.A., Pineiro, M., Cubas, P., Martinez-Zapater, J.M., 2009. Chromatin remodeling in plant development. Int. J. Dev. Biol. 53, 1581–1596.
Jenuwein, T., Allis, C.D., 2001. Translating the histone code. Science 293, 1074–1080.
Ji, L., Liu, X., Yan, J., Wang, W., Yumul, R.E., Kim, Y.J., Dinh, T.T., Liu, J., Cui, X., Zheng, B., Agarwal, M., Liu, C., Cao, X., Tang, G., Chen, X., 2011. ARGONAUTE10 and ARGONAUTE1 regulate the termination of floral stem cells through two microRNAs in Arabidopsis. PLoS Genet. 7, e1001358.
Jiang, D., Yang, W., He, Y., Amasino, R.M., 2007. Arabidopsis relatives of the human lysine-specific Demethylase1 repress the expression of FWA and FLOWERING LOCUS C and thus promote the floral transition. Plant Cell 19, 2975–2987.
Jones, R.S., Gelbart, W.M., 1993. The Drosophila Polycomb-group gene Enhancer of zeste contains a region with sequence similarity to trithorax. Mol. Cell Biol. 13, 6357–6366.
Jung, J.H., Park, C.M., 2007. MIR166/165 genes exhibit dynamic expression patterns in regulating shoot apical meristem and floral development in Arabidopsis. Planta 225, 1327–1338.
Jung, J.H., Seo, Y.H., Seo, P.J., Reyes, J.L., Yun, J., Chua, N.H., Park, C.M., 2007. The GIGANTEA-regulated microRNA172 mediates photoperiodic flowering independent of CONSTANS in Arabidopsis. Plant Cell 19, 2736–2748.
Jung, J.H., Seo, P.J., Ahn, J.H., Park, C.M., 2012. Arabidopsis RNA-binding protein FCA regulates microRNA172 processing in thermosensory flowering. J. Biol. Chem. 287, 16007–16016.
Kakutani, T., Jeddeloh, J.A., Flowers, S.K., Munakata, K., Richards, E.J., 1996. Developmental abnormalities and epimutations associated with DNA hypomethylation mutations. Proc. Natl. Acad. Sci. USA 93, 12406–12411.
Kankel, M.W., Ramsey, D.E., Stokes, T.L., Flowers, S.K., Haag, J.R., Jeddeloh, J.A., Riddle, N.C., Verbsky, M.L., Richards, E.J., 2003. Arabidopsis MET1 cytosine methyltransferase mutants. Genetics 163, 1109–1122.
Katiyar-Agarwal, S., Morgan, R., Dahlbeck, D., Borsani, O., Villegas Jr., A., Zhu, J.K., Staskawicz, B.J., Jin, H., 2006. A pathogen-inducible endogenous siRNA in plant immunity. Proc. Natl. Acad. Sci. USA 103, 18002–18007.
Katz, A., Oliva, M., Mosquna, A., Hakim, O., Ohad, N., 2004. FIE and CURLY LEAF polycomb proteins interact in the regulation of homeobox gene expression during sporophyte development. Plant J. 37, 707–719.
Kaya, H., Shibahara, K.I., Taoka, K.I., Iwabuchi, M., Stillman, B., Araki, T., 2001. FASCIATA genes for chromatin assembly factor-1 in arabidopsis maintain the cellular organization of apical meristems. Cell 104, 131–142.
Khvorova, A., Reynolds, A., Jayasena, S.D., 2003. Functional siRNAs and miRNAs exhibit strand bias. Cell 115, 209–216.
Kidner, C.A., Martienssen, R.A., 2004. Spatially restricted microRNA directs leaf polarity through ARGONAUTE1. Nature 428, 81–84.
Kim, J., Jung, J.H., Reyes, J.L., Kim, Y.S., Kim, S.Y., Chung, K.S., Kim, J.A., Lee, M., Lee, Y., Narry Kim, V., Chua, N.H., Park, C.M., 2005a. microRNA-directed cleavage of ATHB15 mRNA regulates vascular development in Arabidopsis inflorescence stems. Plant J. 42, 84–94.
Kim, S.Y., He, Y., Jacob, Y., Noh, Y.S., Michaels, S., Amasino, R., 2005b. Establishment of the vernalization-responsive, winter-annual habit in Arabidopsis requires a putative histone H3 methyl transferase. Plant Cell 17, 3301–3310.

Kim, S., Soltis, P.S., Wall, K., Soltis, D.E., 2006. Phylogeny and domain evolution in the APETALA2-like gene family. Mol. Biol. Evol. 23, 107–120.
Kinoshita, T., Harada, J.J., Goldberg, R.B., Fischer, R.L., 2001. Polycomb repression of flowering during early plant development. Proc. Natl. Acad. Sci. USA 98, 14156–14161.
Kotake, T., Takada, S., Nakahigashi, K., Ohto, M., Goto, K., 2003. Arabidopsis TERMINAL FLOWER 2 gene encodes a heterochromatin protein 1 homolog and represses both FLOWERING LOCUS T to regulate flowering time and several floral homeotic genes. Plant Cell Physiol. 44, 555–564.
Krogan, N.T., Hogan, K., Long, J.A., 2012. APETALA2 negatively regulates multiple floral organ identity genes in Arabidopsis by recruiting the co-repressor TOPLESS and the histone deacetylase HDA19. Development 139, 4180–4190.
Kurihara, Y., Watanabe, Y., 2004. Arabidopsis micro-RNA biogenesis through Dicer-like 1 protein functions. Proc. Natl. Acad. Sci. USA 101, 12753–12758.
Kurihara, Y., Takashi, Y., Watanabe, Y., 2006. The interaction between DCL1 and HYL1 is important for efficient and precise processing of pri-miRNA in plant microRNA biogenesis. RNA 12, 206–212.
Kwon, C.S., Chen, C., Wagner, D., 2005. WUSCHEL is a primary target for transcriptional regulation by SPLAYED in dynamic control of stem cell fate in Arabidopsis. Genes Dev. 19, 992–1003.
Lafos, M., Kroll, P., Hohenstatt, M.L., Thorpe, F.L., Clarenz, O., Schubert, D., 2011. Dynamic regulation of H3K27 trimethylation during Arabidopsis differentiation. PLoS Genet. 7, e1002040.
Lee, R.C., Feinbaum, R.L., Ambros, V., 1993. The *C. elegans* heterochronic gene lin-4 encodes small RNAs with antisense complementarity to lin-14. Cell 75, 843–854.
Lee, H., Yoo, S.J., Lee, J.H., Kim, W., Yoo, S.K., Fitzgerald, H., Carrington, J.C., Ahn, J.H., 2010a. Genetic framework for flowering-time regulation by ambient temperature-responsive miRNAs in Arabidopsis. Nucleic Acids Res. 38, 3081–3093.
Lee, J.S., Smith, E., Shilatifard, A., 2010b. The language of histone crosstalk. Cell 142, 682–685.
Li, H., Luan, S., 2011. The cyclophilin AtCYP71 interacts with CAF-1 and LHP1 and functions in multiple chromatin remodeling processes. Mol. Plant 4, 748–758.
Li, H., He, Z., Lu, G., Lee, S.C., Alonso, J., Ecker, J.R., Luan, S., 2007. A WD40 domain cyclophilin interacts with histone H3 and functions in gene repression and organogenesis in Arabidopsis. Plant Cell 19, 2403–2416.
Li, W., Wang, Z., Li, J., Yang, H., Cui, S., Wang, X., Ma, L., 2011. Overexpression of AtBMI1C, a polycomb group protein gene, accelerates flowering in Arabidopsis. PLoS One 6, e21364.
Lindroth, A.M., Cao, X., Jackson, J.P., Zilberman, D., McCallum, C.M., Henikoff, S., Jacobsen, S.E., 2001. Requirement of CHROMOMETHYLASE3 for maintenance of CpXpG methylation. Science 292, 2077–2080.
Lippman, Z., May, B., Yordan, C., Singer, T., Martienssen, R., 2003. Distinct mechanisms determine transposon inheritance and methylation via small interfering RNA and histone modification. PLoS Biol. 1, E67.
Liu, Z., Meyerowitz, E.M., 1995. LEUNIG regulates AGAMOUS expression in Arabidopsis flowers. Development 121, 975–991.
Liu, C., Thong, Z., Yu, H., 2009a. Coming into bloom: the specification of floral meristems. Development 136, 3379–3391.
Liu, Q., Yao, X., Pi, L., Wang, H., Cui, X., Huang, H., 2009b. The ARGONAUTE10 gene modulates shoot apical meristem maintenance and establishment of leaf polarity by repressing miR165/166 in Arabidopsis. Plant J. 58, 27–40.
Liu, C., Lu, F., Cui, X., Cao, X., 2010. Histone methylation in higher plants. Annu. Rev. Plant Biol. 61, 395–420.

Lobbes, D., Rallapalli, G., Schmidt, D.D., Martin, C., Clarke, J., 2006. SERRATE: a new player on the plant microRNA scene. EMBO Rep. 7, 1052–1058.
Long, J.A., Moan, E.I., Medford, J.I., Barton, M.K., 1996. A member of the KNOTTED class of homeodomain proteins encoded by the STM gene of Arabidopsis. Nature 379, 66–69.
Lu, C., Fedoroff, N., 2000. A mutation in the Arabidopsis HYL1 gene encoding a dsRNA binding protein affects responses to abscisic acid, auxin, and cytokinin. Plant Cell 12, 2351–2366.
Lu, F., Li, G., Cui, X., Liu, C., Wang, X.J., Cao, X., 2008. Comparative analysis of JmjC domain-containing proteins reveals the potential histone demethylases in Arabidopsis and rice. J. Integr. Plant Biol. 50, 886–896.
Lu, F., Cui, X., Zhang, S., Liu, C., Cao, X., 2010. JMJ14 is an H3K4 demethylase regulating flowering time in Arabidopsis. Cell Res. 20, 387–390.
Lu, F., Cui, X., Zhang, S., Jenuwein, T., Cao, X., 2011. Arabidopsis REF6 is a histone H3 lysine 27 demethylase. Nat. Genet. 43, 715–719.
Luo, D., Carpenter, R., Vincent, C., Copsey, L., Coen, E., 1996. Origin of floral asymmetry in Antirrhinum. Nature 383, 794–799.
Luo, D., Carpenter, R., Copsey, L., Vincent, C., Clark, J., Coen, E., 1999. Control of organ asymmetry in flowers of Antirrhinum. Cell 99, 367–376.
Ma, J.B., Ye, K., Patel, D.J., 2004. Structural basis for overhang-specific small interfering RNA recognition by the PAZ domain. Nature 429, 318–322.
Ma, J.B., Yuan, Y.R., Meister, G., Pei, Y., Tuschl, T., Patel, D.J., 2005. Structural basis for 5'-end-specific recognition of guide RNA by the *A. fulgidus* Piwi protein. Nature 434, 666–670.
Mallory, A.C., Dugas, D.V., Bartel, D.P., Bartel, B., 2004. MicroRNA regulation of NAC-domain targets is required for proper formation and separation of adjacent embryonic, vegetative, and floral organs. Curr. Biol. 14, 1035–1046.
Mateos, J.L., Bologna, N.G., Chorostecki, U., Palatnik, J.F., 2010. Identification of microRNA processing determinants by random mutagenesis of Arabidopsis MIR172a precursor. Curr. Biol. 20, 49–54.
Mathieu, O., Probst, A.V., Paszkowski, J., 2005. Distinct regulation of histone H3 methylation at lysines 27 and 9 by CpG methylation in Arabidopsis. EMBO J. 24, 2783–2791.
Mathieu, J., Yant, L.J., Murdter, F., Kuttner, F., Schmid, M., 2009. Repression of flowering by the miR172 target SMZ. PLoS Biol. 7, e1000148.
Millar, A.A., Gubler, F., 2005. The Arabidopsis GAMYB-like genes, MYB33 and MYB65, are microRNA-regulated genes that redundantly facilitate anther development. Plant Cell 17, 705–721.
Miura, A., Nakamura, M., Inagaki, S., Kobayashi, A., Saze, H., Kakutani, T., 2009. An Arabidopsis jmjC domain protein protects transcribed genes from DNA methylation at CHG sites. EMBO J. 28, 1078–1086.
Murfett, J., Wang, X.J., Hagen, G., Guilfoyle, T.J., 2001. Identification of Arabidopsis histone deacetylase HDA6 mutants that affect transgene expression. Plant Cell 13, 1047–1061.
Nag, A., King, S., Jack, T., 2009. miR319a targeting of TCP4 is critical for petal growth and development in Arabidopsis. Proc. Natl. Acad. Sci. USA 106, 22534–22539.
Nagpal, P., Ellis, C.M., Weber, H., Ploense, S.E., Barkawi, L.S., Guilfoyle, T.J., Hagen, G., Alonso, J.M., Cohen, J.D., Farmer, E.E., Ecker, J.R., Reed, J.W., 2005. Auxin response factors ARF6 and ARF8 promote jasmonic acid production and flower maturation. Development 132, 4107–4118.
Nath, U., Crawford, B.C., Carpenter, R., Coen, E., 2003. Genetic control of surface curvature. Science 299, 1404–1407.
Naumann, K., Fischer, A., Hofmann, I., Krauss, V., Phalke, S., Irmler, K., Hause, G., Aurich, A.C., Dorn, R., Jenuwein, T., Reuter, G., 2005. Pivotal role of AtSUVH2

in heterochromatic histone methylation and gene silencing in Arabidopsis. EMBO J. 24, 1418–1429.
Ng, K.H., Yu, H., Ito, T., 2009. AGAMOUS controls GIANT KILLER, a multifunctional chromatin modifier in reproductive organ patterning and differentiation. PLoS Biol. 7, e1000251.
Nikovics, K., Blein, T., Peaucelle, A., Ishida, T., Morin, H., Aida, M., Laufs, P., 2006. The balance between the MIR164A and CUC2 genes controls leaf margin serration in Arabidopsis. Plant Cell 18, 2929–2945.
Ogas, J., Kaufmann, S., Henderson, J., Somerville, C., 1999. PICKLE is a CHD3 chromatin-remodeling factor that regulates the transition from embryonic to vegetative development in Arabidopsis. Proc. Natl. Acad. Sci. USA 96, 13839–13844.
Ori, N., Eshed, Y., Chuck, G., Bowman, J.L., Hake, S., 2000. Mechanisms that control knox gene expression in the Arabidopsis shoot. Development 127, 5523–5532.
Palatnik, J.F., Allen, E., Wu, X., Schommer, C., Schwab, R., Carrington, J.C., Weigel, D., 2003. Control of leaf morphogenesis by microRNAs. Nature 425, 257–263.
Palatnik, J.F., Wollmann, H., Schommer, C., Schwab, R., Boisbouvier, J., Rodriguez, R., Warthmann, N., Allen, E., Dezulian, T., Huson, D., Carrington, J.C., Weigel, D., 2007. Sequence and expression differences underlie functional specialization of Arabidopsis microRNAs miR159 and miR319. Dev. Cell 13, 115–125.
Parcy, F., Nilsson, O., Busch, M.A., Lee, I., Weigel, D., 1998. A genetic framework for floral patterning. Nature 395, 561–566.
Park, W., Li, J., Song, R., Messing, J., Chen, X., 2002. CARPEL FACTORY, a Dicer homolog, and HEN1, a novel protein, act in microRNA metabolism in Arabidopsis thaliana. Curr. Biol. 12, 1484–1495.
Park, M.Y., Wu, G., Gonzalez-Sulser, A., Vaucheret, H., Poethig, R.S., 2005. Nuclear processing and export of microRNAs in Arabidopsis. Proc. Natl. Acad. Sci. USA 102, 3691–3696.
Parker, J.S., Roe, S.M., Barford, D., 2004. Crystal structure of a PIWI protein suggests mechanisms for siRNA recognition and slicer activity. EMBO J. 23, 4727–4737.
Parker, J.S., Roe, S.M., Barford, D., 2005. Structural insights into mRNA recognition from a PIWI domain-siRNA guide complex. Nature 434, 663–666.
Peaucelle, A., Morin, H., Traas, J., Laufs, P., 2007. Plants expressing a miR164-resistant CUC2 gene reveal the importance of post-meristematic maintenance of phyllotaxy in Arabidopsis. Development 134, 1045–1050.
Peragine, A., Yoshikawa, M., Wu, G., Albrecht, H.L., Poethig, R.S., 2004. SGS3 and SGS2/SDE1/RDR6 are required for juvenile development and the production of trans-acting siRNAs in Arabidopsis. Genes Dev. 18, 2368–2379.
Pien, S., Grossniklaus, U., 2007. Polycomb group and trithorax group proteins in Arabidopsis. Biochim. Biophys. Acta 1769, 375–382.
Pien, S., Fleury, D., Mylne, J.S., Crevillen, P., Inze, D., Avramova, Z., Dean, C., Grossniklaus, U., 2008. ARABIDOPSIS TRITHORAX1 dynamically regulates FLOWERING LOCUS C activation via histone 3 lysine 4 trimethylation. Plant Cell 20, 580–588.
Probst, A.V., Fagard, M., Proux, F., Mourrain, P., Boutet, S., Earley, K., Lawrence, R.J., Pikaard, C.S., Murfett, J., Furner, I., Vaucheret, H., Mittelsten Scheid, O., 2004. Arabidopsis histone deacetylase HDA6 is required for maintenance of transcriptional gene silencing and determines nuclear organization of rDNA repeats. Plant Cell 16, 1021–1034.
Rajagopalan, R., Vaucheret, H., Trejo, J., Bartel, D.P., 2006. A diverse and evolutionarily fluid set of microRNAs in Arabidopsis thaliana. Genes Dev. 20, 3407–3425.
Ray, A., Lang, J.D., Golden, T., Ray, S., 1996. SHORT INTEGUMENT (SIN1), a gene required for ovule development in Arabidopsis, also controls flowering time. Development 122, 2631–2638.

Reeves, P.H., Ellis, C.M., Ploense, S.E., Wu, M.F., Yadav, V., Tholl, D., Chetelat, A., Haupt, I., Kennerley, B.J., Hodgens, C., Farmer, E.E., Nagpal, P., Reed, J.W., 2012. A regulatory network for coordinated flower maturation. PLoS Genet. 8, e1002506.
Reinhart, B.J., Weinstein, E.G., Rhoades, M.W., Bartel, B., Bartel, D.P., 2002. MicroRNAs in plants. Genes Dev. 16, 1616–1626.
Remington, D.L., Vision, T.J., Guilfoyle, T.J., Reed, J.W., 2004. Contrasting modes of diversification in the Aux/IAA and ARF gene families. Plant Physiol. 135, 1738–1752.
Reyes, J.C., Hennig, L., Gruissem, W., 2002. Chromatin-remodeling and memory factors. New regulators of plant development. Plant Physiol. 130, 1090–1101.
Richards, E.J., Elgin, S.C., 2002. Epigenetic codes for heterochromatin formation and silencing: rounding up the usual suspects. Cell 108, 489–500.
Rigal, M., Kevei, Z., Pelissier, T., Mathieu, O., 2012. DNA methylation in an intron of the IBM1 histone demethylase gene stabilizes chromatin modification patterns. EMBO J. 31, 2981–2993.
Sablowski, R., 2007. Flowering and determinacy in Arabidopsis. J. Exp. Bot. 58, 899–907.
Sakai, H., Medrano, L.J., Meyerowitz, E.M., 1995. Role of SUPERMAN in maintaining Arabidopsis floral whorl boundaries. Nature 378, 199–203.
Saleh, A., Alvarez-Venegas, R., Yilmaz, M., Le, O., Hou, G., Sadder, M., Al-Abdallat, A., Xia, Y., Lu, G., Ladunga, I., Avramova, Z., 2008. The highly similar Arabidopsis homologs of trithorax ATX1 and ATX2 encode proteins with divergent biochemical functions. Plant Cell 20, 568–579.
Saze, H., Shiraishi, A., Miura, A., Kakutani, T., 2008. Control of genic DNA methylation by a jmjC domain-containing protein in Arabidopsis thaliana. Science 319, 462–465.
Schmid, M., Uhlenhaut, N.H., Godard, F., Demar, M., Bressan, R., Weigel, D., Lohmann, J.U., 2003. Dissection of floral induction pathways using global expression analysis. Development 130, 6001–6012.
Schubert, D., Clarenz, O., Goodrich, J., 2005. Epigenetic control of plant development by Polycomb-group proteins. Curr. Opin. Plant Biol. 8, 553–561.
Schubert, D., Primavesi, L., Bishopp, A., Roberts, G., Doonan, J., Jenuwein, T., Goodrich, J., 2006. Silencing by plant Polycomb-group genes requires dispersed trimethylation of histone H3 at lysine 27. EMBO J. 25, 4638–4649.
Schwab, R., Palatnik, J.F., Riester, M., Schommer, C., Schmid, M., Weigel, D., 2005. Specific effects of microRNAs on the plant transcriptome. Dev. Cell 8, 517–527.
Schwartz, Y.B., Pirrotta, V., 2008. Polycomb complexes and epigenetic states. Curr. Opin. Cell Biol. 20, 266–273.
Schwarz, D.S., Hutvagner, G., Du, T., Xu, Z., Aronin, N., Zamore, P.D., 2003. Asymmetry in the assembly of the RNAi enzyme complex. Cell 115, 199–208.
Shi, Y., Lan, F., Matson, C., Mulligan, P., Whetstine, J.R., Cole, P.A., Casero, R.A., 2004. Histone demethylation mediated by the nuclear amine oxidase homolog LSD1. Cell 119, 941–953.
Shigyo, M., Hasebe, M., Ito, M., 2006. Molecular evolution of the AP2 subfamily. Gene 366, 256–265.
Sieber, P., Wellmer, F., Gheyselinck, J., Riechmann, J.L., Meyerowitz, E.M., 2007. Redundancy and specialization among plant microRNAs: role of the MIR164 family in developmental robustness. Development 134, 1051–1060.
Sieburth, L.E., Running, M.P., Meyerowitz, E.M., 1995. Genetic separation of third and fourth whorl functions of AGAMOUS. Plant Cell 7, 1249–1258.
Song, J.J., Smith, S.K., Hannon, G.J., Joshua-Tor, L., 2004. Crystal structure of Argonaute and its implications for RISC slicer activity. Science 305, 1434–1437.
Song, L., Axtell, M.J., Fedoroff, N.V., 2010. RNA secondary structural determinants of miRNA precursor processing in Arabidopsis. Curr. Biol. 20, 37–41.

Soppe, W.J., Bentsink, L., Koornneef, M., 1999. The early-flowering mutant efs is involved in the autonomous promotion pathway of Arabidopsis thaliana. Development 126, 4763–4770.
Soppe, W.J., Jacobsen, S.E., Alonso-Blanco, C., Jackson, J.P., Kakutani, T., Koornneef, M., Peeters, A.J., 2000. The late flowering phenotype of fwa mutants is caused by gain-of-function epigenetic alleles of a homeodomain gene. Mol. Cell 6, 791–802.
Spedaletti, V., Polticelli, F., Capodaglio, V., Schinina, M.E., Stano, P., Federico, R., Tavladoraki, P., 2008. Characterization of a lysine-specific histone demethylase from Arabidopsis thaliana. Biochemistry 47, 4936–4947.
Sridhar, V.V., Surendrarao, A., Gonzalez, D., Conlan, R.S., Liu, Z., 2004. Transcriptional repression of target genes by LEUNIG and SEUSS, two interacting regulatory proteins for Arabidopsis flower development. Proc. Natl. Acad. Sci. USA 101, 11494–11499.
Srikanth, A., Schmid, M., 2011. Regulation of flowering time: all roads lead to Rome. Cell. Mol. Life Sci. 68, 2013–2037.
Stassen, M.J., Bailey, D., Nelson, S., Chinwalla, V., Harte, P.J., 1995. The Drosophila trithorax proteins contain a novel variant of the nuclear receptor type DNA binding domain and an ancient conserved motif found in other chromosomal proteins. Mech. Dev. 52, 209–223.
Strahl, B.D., Allis, C.D., 2000. The language of covalent histone modifications. Nature 403, 41–45.
Sun, Q., Zhou, D.X., 2008. Rice jmjC domain-containing gene JMJ706 encodes H3K9 demethylase required for floral organ development. Proc. Natl. Acad. Sci. USA 105, 13679–13684.
Sun, B., Xu, Y., Ng, K.H., Ito, T., 2009. A timing mechanism for stem cell maintenance and differentiation in the Arabidopsis floral meristem. Genes Dev. 23, 1791–1804.
Sung, S., Amasino, R.M., 2004. Vernalization in Arabidopsis thaliana is mediated by the PHD finger protein VIN3. Nature 427, 159–164.
Sung, Z.R., Belachew, A., Shunong, B., Bertrand-Garcia, R., 1992. EMF, an Arabidopsis Gene Required for Vegetative Shoot Development. Science 258, 1645–1647.
Swiezewski, S., Crevillen, P., Liu, F., Ecker, J.R., Jerzmanowski, A., Dean, C., 2007. Small RNA-mediated chromatin silencing directed to the 3' region of the Arabidopsis gene encoding the developmental regulator, FLC. Proc. Natl. Acad. Sci. USA 104, 3633–3638.
Takada, S., Hibara, K., Ishida, T., Tasaka, M., 2001. The CUP-SHAPED COTYLEDON1 gene of Arabidopsis regulates shoot apical meristem formation. Development 128, 1127–1135.
Tamada, Y., Yun, J.Y., Woo, S.C., Amasino, R.M., 2009. ARABIDOPSIS TRITHORAX-RELATED7 is required for methylation of lysine 4 of histone H3 and for transcriptional activation of FLOWERING LOCUS C. Plant Cell 21, 3257–3269.
Tanaka, M., Kikuchi, A., Kamada, H., 2008. The Arabidopsis histone deacetylases HDA6 and HDA19 contribute to the repression of embryonic properties after germination. Plant Physiol. 146, 149–161.
Tang, G., Reinhart, B.J., Bartel, D.P., Zamore, P.D., 2003. A biochemical framework for RNA silencing in plants. Genes Dev. 17, 49–63.
Thorstensen, T., Fischer, A., Sandvik, S.V., Johnsen, S.S., Grini, P.E., Reuter, G., Aalen, R.B., 2006. The Arabidopsis SUVR4 protein is a nucleolar histone methyltransferase with preference for monomethylated H3K9. Nucleic Acids Res. 34, 5461–5470.
Thorstensen, T., Grini, P.E., Mercy, I.S., Alm, V., Erdal, S., Aasland, R., Aalen, R.B., 2008. The Arabidopsis SET-domain protein ASHR3 is involved in stamen development and

interacts with the bHLH transcription factor ABORTED MICROSPORES (AMS). Plant Mol. Biol. 66, 47–59.
Thorstensen, T., Grini, P.E., Aalen, R.B., 2011. SET domain proteins in plant development. Biochim. Biophys. Acta 1809, 407–420.
Tian, L., Chen, Z.J., 2001. Blocking histone deacetylation in Arabidopsis induces pleiotropic effects on plant gene regulation and development. Proc. Natl. Acad. Sci. USA 98, 200–205.
Tian, L., Wang, J., Fong, M.P., Chen, M., Cao, H., Gelvin, S.B., Chen, Z.J., 2003. Genetic control of developmental changes induced by disruption of Arabidopsis histone deacetylase 1 (AtHD1) expression. Genetics 165, 399–409.
To, T.K., Kim, J.M., Matsui, A., Kurihara, Y., Morosawa, T., Ishida, J., Tanaka, M., Endo, T., Kakutani, T., Toyoda, T., Kimura, H., Yokoyama, S., Shinozaki, K., Seki, M., 2011. Arabidopsis HDA6 regulates locus-directed heterochromatin silencing in cooperation with MET1. PLoS Genet. 7, e1002055.
Tschiersch, B., Hofmann, A., Krauss, V., Dorn, R., Korge, G., Reuter, G., 1994. The protein encoded by the Drosophila position-effect variegation suppressor gene Su(var)3-9 combines domains of antagonistic regulators of homeotic gene complexes. EMBO J. 13, 3822–3831.
Tsukada, Y., Fang, J., Erdjument-Bromage, H., Warren, M.E., Borchers, C.H., Tempst, P., Zhang, Y., 2006. Histone demethylation by a family of JmjC domain-containing proteins. Nature 439, 811–816.
Varga-Weisz, P., 2001. ATP-dependent chromatin remodeling factors: nucleosome shufflers with many missions. Oncogene 20, 3076–3085.
Vazquez, F., Vaucheret, H., Rajagopalan, R., Lepers, C., Gasciolli, V., Mallory, A.C., Hilbert, J.L., Bartel, D.P., Crete, P., 2004. Endogenous trans-acting siRNAs regulate the accumulation of Arabidopsis mRNAs. Mol. Cell 16, 69–79.
Vermaak, D., Ahmad, K., Henikoff, S., 2003. Maintenance of chromatin states: an open-and-shut case. Curr. Opin. Cell Biol. 15, 266–274.
Wang, J.W., Schwab, R., Czech, B., Mica, E., Weigel, D., 2008. Dual effects of miR156-targeted SPL genes and CYP78A5/KLUH on plastochron length and organ size in Arabidopsis thaliana. Plant Cell 20, 1231–1243.
Wellmer, F., Riechmann, J.L., Alves-Ferreira, M., Meyerowitz, E.M., 2004. Genome-wide analysis of spatial gene expression in Arabidopsis flowers. Plant Cell 16, 1314–1326.
Werner, S., Wollmann, H., Schneeberger, K., Weigel, D., 2010. Structure determinants for accurate processing of miR172a in Arabidopsis thaliana. Curr. Biol. 20, 42–48.
Williams, L., Carles, C.C., Osmont, K.S., Fletcher, J.C., 2005a. A database analysis method identifies an endogenous trans-acting short-interfering RNA that targets the Arabidopsis ARF2, ARF3, and ARF4 genes. Proc. Natl. Acad. Sci. USA 102, 9703–9708.
Williams, L., Grigg, S.P., Xie, M., Christensen, S., Fletcher, J.C., 2005b. Regulation of Arabidopsis shoot apical meristem and lateral organ formation by microRNA miR166g and its AtHD-ZIP target genes. Development 132, 3657–3668.
Wu, G., Poethig, R.S., 2006. Temporal regulation of shoot development in Arabidopsis thaliana by miR156 and its target SPL3. Development 133, 3539–3547.
Wu, M.F., Tian, Q., Reed, J.W., 2006. Arabidopsis microRNA167 controls patterns of ARF6 and ARF8 expression, and regulates both female and male reproduction. Development 133, 4211–4218.
Wu, G., Park, M.Y., Conway, S.R., Wang, J.W., Weigel, D., Poethig, R.S., 2009. The sequential action of miR156 and miR172 regulates developmental timing in Arabidopsis. Cell 138, 750–759.
Wu, M.F., Sang, Y., Bezhani, S., Yamaguchi, N., Han, S.K., Li, Z., Su, Y., Slewinski, T.L., Wagner, D., 2012. SWI2/SNF2 chromatin remodeling ATPases overcome polycomb

repression and control floral organ identity with the LEAFY and SEPALLATA3 transcription factors. Proc. Natl. Acad. Sci. USA 109, 3576–3581.
Wurschum, T., Gross-Hardt, R., Laux, T., 2006. APETALA2 regulates the stem cell niche in the Arabidopsis shoot meristem. Plant Cell 18, 295–307.
Xiao, W., Gehring, M., Choi, Y., Margossian, L., Pu, H., Harada, J.J., Goldberg, R.B., Pennell, R.I., Fischer, R.L., 2003. Imprinting of the MEA Polycomb gene is controlled by antagonism between MET1 methyltransferase and DME glycosylase. Dev. Cell 5, 891–901.
Xu, L., Zhao, Z., Dong, A., Soubigou-Taconnat, L., Renou, J.P., Steinmetz, A., Shen, W.H., 2008. Di- and tri- but not monomethylation on histone H3 lysine 36 marks active transcription of genes involved in flowering time regulation and other processes in Arabidopsis thaliana. Mol. Cell Biol. 28, 1348–1360.
Xu, Y., Wang, Y., Stroud, H., Gu, X., Sun, B., Gan, E.-S., Ng, K.-H., Jacobsen, S., He, Y., Ito, T., 2013. An Arabidopsis Matrix Protein Silences Transposons and Transposon-Containing Floral Repressors through Direct Interaction with Retinoblastoma-Associated Proteins. Curr. Biol. 23 (4), 345–350.
Yadav, R.K., Girke, T., Pasala, S., Xie, M., Reddy, G.V., 2009. Gene expression map of the Arabidopsis shoot apical meristem stem cell niche. Proc. Natl. Acad. Sci. USA 106, 4941–4946.
Yang, C.H., Chen, L.J., Sung, Z.R., 1995. Genetic regulation of shoot development in Arabidopsis: role of the EMF genes. Dev. Biol. 169, 421–435.
Yang, L., Liu, Z., Lu, F., Dong, A., Huang, H., 2006a. SERRATE is a novel nuclear regulator in primary microRNA processing in Arabidopsis. Plant J. 47, 841–850.
Yang, Z., Ebright, Y.W., Yu, B., Chen, X., 2006b. HEN1 recognizes 21–24 nt small RNA duplexes and deposits a methyl group onto the 2′ OH of the 3′ terminal nucleotide. Nucleic Acids Res. 34, 667–675.
Yang, W., Jiang, D., Jiang, J., He, Y., 2010. A plant-specific histone H3 lysine 4 demethylase represses the floral transition in Arabidopsis. Plant J. 62, 663–673.
Yang, H., Han, Z., Cao, Y., Fan, D., Li, H., Mo, H., Feng, Y., Liu, L., Wang, Z., Yue, Y., Cui, S., Chen, S., Chai, J., Ma, L., 2012a. A companion cell-dominant and developmentally regulated H3K4 demethylase controls flowering time in Arabidopsis via the repression of FLC expression. PLoS Genet. 8, e1002664.
Yang, H., Mo, H., Fan, D., Cao, Y., Cui, S., Ma, L., 2012b. Overexpression of a histone H3K4 demethylase, JMJ15, accelerates flowering time in Arabidopsis. Plant Cell Rep. 31, 1297–1308.
Yant, L., Mathieu, J., Dinh, T.T., Ott, F., Lanz, C., Wollmann, H., Chen, X., Schmid, M., 2010. Orchestration of the floral transition and floral development in Arabidopsis by the bifunctional transcription factor APETALA2. Plant Cell 22, 2156–2170.
Yoshikawa, M., Peragine, A., Park, M.Y., Poethig, R.S., 2005. A pathway for the biogenesis of trans-acting siRNAs in Arabidopsis. Genes Dev. 19, 2164–2175.
Yu, B., Yang, Z., Li, J., Minakhina, S., Yang, M., Padgett, R.W., Steward, R., Chen, X., 2005. Methylation as a crucial step in plant microRNA biogenesis. Science 307, 932–935.
Yu, C.W., Liu, X., Luo, M., Chen, C., Lin, X., Tian, G., Lu, Q., Cui, Y., Wu, K., 2011. HISTONE DEACETYLASE6 interacts with FLOWERING LOCUS D and regulates flowering in Arabidopsis. Plant Physiol. 156, 173–184.
Zhang, H., Zhu, J.K., 2011. RNA-directed DNA methylation. Curr. Opin. Plant Biol. 14, 142–147.
Zhang, X., Yazaki, J., Sundaresan, A., Cokus, S., Chan, S.W., Chen, H., Henderson, I.R., Shinn, P., Pellegrini, M., Jacobsen, S.E., Ecker, J.R., 2006. Genome-wide high-resolution mapping and functional analysis of DNA methylation in arabidopsis. Cell 126, 1189–1201.

Zhang, X., Clarenz, O., Cokus, S., Bernatavichute, Y.V., Pellegrini, M., Goodrich, J., Jacobsen, S.E., 2007. Whole-genome analysis of histone H3 lysine 27 trimethylation in Arabidopsis. PLoS Biol. 5, e129.

Zhao, Z., Yu, Y., Meyer, D., Wu, C., Shen, W.H., 2005. Prevention of early flowering by expression of FLOWERING LOCUS C requires methylation of histone H3 K36. Nat. Cell Biol. 7, 1256–1260.

Zhao, L., Kim, Y., Dinh, T.T., Chen, X., 2007. miR172 regulates stem cell fate and defines the inner boundary of APETALA3 and PISTILLATA expression domain in Arabidopsis floral meristems. Plant J. 51, 840–849.

Zheng, B., Chen, X., 2011. Dynamics of histone H3 lysine 27 trimethylation in plant development. Curr. Opin. Plant Biol. 14, 123–129.

Zhou, G.K., Kubo, M., Zhong, R., Demura, T., Ye, Z.H., 2007. Overexpression of miR165 affects apical meristem formation, organ polarity establishment and vascular development in Arabidopsis. Plant Cell Physiol. 48, 391–404.

Zhu, H., Hu, F., Wang, R., Zhou, X., Sze, S.H., Liou, L.W., Barefoot, A., Dickman, M., Zhang, X., 2011. Arabidopsis Argonaute10 specifically sequesters miR166/165 to regulate shoot apical meristem development. Cell 145, 242–256.

Zilberman, D., Gehring, M., Tran, R.K., Ballinger, T., Henikoff, S., 2007. Genome-wide analysis of Arabidopsis thaliana DNA methylation uncovers an interdependence between methylation and transcription. Nat. Genet. 39, 61–69.

Nucleus 4:4, 1–3; July/August 2013; © 2013 Landes Bioscience

Flowering and genome integrity control by a nuclear matrix protein in Arabidopsis

Yifeng Xu,[1] Eng-Seng Gan,[1,2] Yuehui He[1,2] and Toshiro Ito[1,2,*]

[1]Temasek Life Sciences Laboratory (TLL); 1 Research Link; National University of Singapore; Singapore, Singapore; [2]Department of Biological Sciences; Faculty of Science; National University of Singapore; Singapore, Singapore

The matrix attachment regions (MARs) binding proteins could finely orchestrate temporal and spatial gene expression during development. In Arabidopsis, transposable elements (TEs) and TE-like repeat sequences are transcriptionally repressed or attenuated by the coordination of many key players including DNA methyltransferases, histone deacetylases, histone methyltransferases and the siRNA pathway, which help to protect genomic integrity and control multiple developmental processes such as flowering. We have recently reported that an AT-hook nuclear matrix binding protein, TRANSPOSABLE ELEMENT SILENCING VIA AT-HOOK (TEK), participates in a histone deacetylation (HDAC) complex to silence TEs and genes containing TE-like sequence, including *AtMu1*, *FWA* and *FLOWERING LOCUS C* (*FLC*) in L*er* background. We have shown that *TEK* knockdown causes increased histone acetylation, reduced H3K9me2 and moderate reduction of DNA methylation in the target loci, leading to the derepression of *FLC* and *FWA*, as well as TE reactivation. Here we discuss the role of *TEK* as a putative MAR binding protein which functions in the maintenance of genome integrity and in flowering control by silencing TEs and repeat-containing genes.

Keywords: MAR, AT-hook, transposable element, TEK, flowering time

Submitted: 05/12/13

Revised: 06/28/13

Accepted: 07/02/13

http://dx.doi.org/10.4161/nucl.25612

*Correspondence to: Toshiro Ito;
Email: itot@tll.org.sg

Extra View to: Xu Y, Wang Y, Stroud H, Gu X, Sun B, Gan ES, et al. A matrix protein silences transposons and repeats through interaction with retinoblastoma-associated proteins. Curr Biol 2013; 23:345-50; PMID:23394836; http://dx.doi.org/10.1016/j.cub.2013.01.030

The nuclear matrix is a supporting structural component that remains inside the nucleus after removal of basic proteins and histones. The interactions between chromatin and the nuclear matrix occur through AT-rich sequences of high affinity, named as matrix or scaffold attachment regions (MARs or SARs) (reviewed in 1). MARs are commonly found at the boundaries of transcription units or close to regulatory *cis*-elements, and function in several biological processes such as forming higher order chromosome structures, regulating gene expression and facilitating DNA replications. Not all potential MARs are associated with the nuclear matrix at all times; in fact, MARs are dynamically anchored to the nuclear matrix by MAR-binding proteins in cell-type and/or cell-cycle-dependent manners. AT-hook DNA-binding proteins are a kind of MAR-binding proteins and have a variable number of AT-hook motifs, which are characterized by a typical sequence pattern centered around a highly conserved tripeptide of Gly-Arg-Pro (GRP).[2] AT-hook motifs are able to bind to the minor grooves of stretches of MARs in a non-strictly sequence-specific manner, while common transcription factors usually bind to the major grooves.[3,4] In mammals, AT-motif is present in many proteins, including high-mobility group A (HMGA) proteins, a family of non-histone chromosomal proteins, and hBRG1 protein, a central ATPase of the human switching/sucrose non-fermenting (SWI/SNF) remodeling complex.[5] HMGA proteins act as architecture transcription factors to regulate many biological processes including growth, proliferation, differentiation and death, by binding to differently-spaced AT-rich DNA regions and/or interacting with several transcription factors.[3,4]

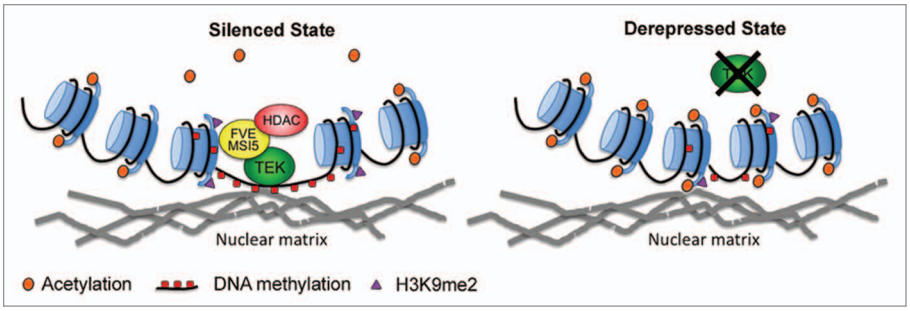

Figure 1. A model of TEK functions. TEK binds to specific targets and makes a protein complex with FVE/MSI5 and HDAC, which participates in histone deacetylation. Deacetylation of the target loci leads to transcriptional silencing. Once TEK action is abolished, the deacetylation process of its targets is blocked, resulting in the high acetylation level and reduced levels of both DNA methylation and H3K9 dimethylation at these loci, causing the transcriptional derepression of these targets.

In plants, AT-hook family proteins have evolved in a unique way by harboring an AT-hook motif together with an uncharacterized Plant and Prokaryotes Conserved (PPC) domain. The PPC domain is also found in prokaryotic proteins, but they do not contain the AT-hook motif.[6] The Arabidopsis genome contains a total of 29 AT-hook proteins (AHL1–29) and they have been shown to be involved in diverse processes, including hypocotyl elongation, flower development, gibberellin biosynthesis, leaf senescence, stem cell niche specification and root vascular tissue patterning.[6-9] Among these, *GIANT KILLER* (*GIK*)/*AHL21*, identified as a direct target of the floral homeotic protein AGAMOUS (AG), negatively fine-tune multiple targets downstream of AG to control patterning and differentiation of reproductive organs through repressive histone modifications.[7] We thoroughly analyzed the other AT-hook members, and found *TRANSPOSABLE ELEMENT SILENCING VIA AT-HOOK* (*TEK*)/*AHL16* to be of particular interest, based on its high expression in the reproductive tissues, and the late flowering phenotype upon its knockdown.

Transposable elements (TEs) were discovered as "jumping genes" half a century ago by Barbara McClintock.[10] Although they were primarily considered as parasites of host genome, recently a great amount of studies have uncovered the importance of TEs in genome function and evolution. TEs constitute a large fraction of most eukaryotic genomes including plants, e.g., 85% in maize and 17% in Arabidopsis. Activation of these "jumping genes" has a range of deleterious effects, including alterations of gene expression, gene deletions and insertions, and chromosome rearrangement. Epigenetic silencing helps to maintain genomic integrity by suppressing TE activities (reviewed in 11, 12). TEs are usually silenced by DNA methylation, repressive histone H3 lysine 9 dimethylation (H3K9me2), histone deacetylation and the presence of heterochromatic 24 nucleotides (nt) small interfering RNAs (siRNAs) that guide the RNA-directed DNA methylation (RdDM) machinery (reviewed in 13, 14). Recently, we have shown that the AT-hook DNA binding protein TEK is involved in the silencing of TEs and TE-like sequence containing genes, including L*er FLC* and *FWA*.[15]

The first noticeable phenotype in *TEK* knockdown plants is their extremely late flowering, which we later found that high expression of *FWA* and L*er FLC* is the main cause.[15] The heritable and T-DNA-independent late flowering phenotypes in F1 of *TEK* knockdown line crossed with WT or T2 progeny from self-fertilized T1 knockdown lines suggest that the effects of *TEK* knockdown are very likely linked with the epigenetic control of *FWA* and L*er FLC*. Indeed, the L*er FLC* allele contains a 1,224-bp insertion of a *Mutator*-like TE in the first intron, and *FWA* promoter contains SINE-related repeats, remnants of the TEs, both of which are subjected to siRNA-mediated repression.[16,17] In addition, ectopic expression of *FWA* in vegetative tissues is usually associated with loss of DNA methylation. However, bisulfite sequencing has only detected a slight reduction of DNA methylation in the CG, CHG and CHH contexts in the tandem repeats of *FWA* upon *TEK* knockdown.[15] Microarray analysis further revealed that together with *FLC* and *FWA*, 1,209 genes in total were upregulated at least 2-fold in *TEK* knockdown plants and among these, most (69%) are transposable element loci.[15] *AtMu1* is one of the TE genes upregulated in transgenic plants, and bisulfite sequencing also found that the percentages of methylated CG, CHG and CHH at *AtMu1* locus were only moderately decreased.[15] These data suggest that DNA methylation defect is neither the primary effect of *TEK* knockdown, nor the major cause of the upregulation of TE and TE-related genes. Instead, the levels of histone acetylation and H3K9me2 are dramatically changed upon *TEK* knockdown.[15] Consistent with this observation, yeast-two-hybrid assay, bimolecular fluorescence complementation (BiFC) analysis and co-immunoprecipitation assay have shown that TEK protein interacts with Retinoblastoma-associated protein FVE and its homolog MSI5, the components of histone deacetylation (HDAC) complexes.[15] Thus, we proposed that TEK is involved in protecting genome stability partly by recruiting FVE/MSI5-containing HDAC complexes to various target loci including *FLC, FWA* and TEs, which promotes a self-reinforcing cycle of histone deacetylation, DNA methylation and H3K9 dimethylation, leading to their transcriptional silencing. Upon TEK knockdown, the recruitment of histone deacetylation complex to the targets is abolished, resulting in the reduced levels of H3K9 dimethylation and DNA methylation, and the relatively higher levels of histone acetylation (summarized in **Fig. 1**).

The presence of the *Mutator*-like TE insertion is responsible for the inability of L*er FLC* to be activated by a functional *FRIGIDA* (a major determinant of natural flowering-time variation in Arabidopsis) and other *FLC* transcription activators. The high ectopic expression of L*er FLC* in the *amiTEK* lines prompted us to check whether the TE insertion was still present. Notably, the *Mutator*-like element is excised without leaving any footprint in all tested lines.[15] The transpositions of at least

two other DNA transposons, *CACTA* and *hAT*, were also observed in *amiTEK* plants by genomic Southern blots.[15] While the same epigenetic machinery could affect both transcription and transposition of TEs, the study of transposition of TEs is limited (reviewed in 18). TE transposition is usually only found after inbreeding of mutants impaired in DNA methylation, in some cases after several generations.[18] The immediate and dramatic burst of TE transposition was only detected at the combinational mutant of the loss of CG methylation and disruption of the siRNA pathway.[18] The transposition of TEs in *amiTEK* T1 lines, with the observation of the slight reduction of CG methylation, indicates the possibility that *TEK* knockdown affects the siRNA pathway in Arabidopsis.

The characterized function of Arabidopsis TEK is quite comparable to another well-studied AT-hook protein SATB1 in mammals. SATB1 acts as a global repressor of cell function in specific cell lineages. The binding of SATB1 affects the chromatin status of target genes, by inducing structural changes of chromatin[19,20] and/or recruitment of chromatin modifiers including HDAC1.[21,22] These chromatin modifiers have been proposed to suppress local or long-range gene expression through histone deacetylation and nucleosome remodeling at SATB1-bound MARs.[21] Chromatin immunoprecipitation analysis has revealed that TEK can directly bind to *FLC* and *FWA* loci and that *TEK* knockdown affects the matrix association of *FLC*.[15] This suggests that the function of *TEK* in TE repression is linked with its MAR binding activity. The derepression of a large number of TEs, a major component of heterochromatin, suggests possible change of boundary between heterochromatic and euchromatic regions due to disrupted nuclear matrix association. Future study of possible changes in the nuclear organization and chromatin conformation by manipulation of TEK activities can help us further understand how transcriptional regulation is mediated by dynamic nuclear organization and chromosomal interactions.

Disclosure of Potential Conflicts of Interest

No potential conflict of interest was disclosed.

Acknowledgments

This work was supported by research grants to T.I. and Y.H. from the Temasek Life Sciences Laboratory (TLL), the National Research Foundation Singapore under its Competitive Research Programme (CRP Award No. NRF-CRP001–108) and by a grant to T.I. from PRESTO, Japan Science and Technology Agency, 4–1-8 Honcho Kawaguchi, Saitama, Japan.

References

1. Gasser SM, Laemmli UK. A Glimpse at Chromosomal Order. Trends Genet 1987; 3:16-22; http://dx.doi.org/10.1016/0168-9525(87)90156-9
2. Aravind L, Landsman D. AT-hook motifs identified in a wide variety of DNA-binding proteins. Nucleic Acids Res 1998; 26:4413-21; PMID:9742243; http://dx.doi.org/10.1093/nar/26.19.4413
3. Reeves R, Nissen MS. The A.T-DNA-binding domain of mammalian high mobility group I chromosomal proteins. A novel peptide motif for recognizing DNA structure. J Biol Chem 1990; 265:8573-82; PMID:1692833
4. Reeves R. Molecular biology of HMGA proteins: hubs of nuclear function. Gene 2001; 277:63-81; PMID:11602345; http://dx.doi.org/10.1016/S0378-1119(01)00689-8
5. Singh M, D'Silva L, Holak TA. DNA-binding properties of the recombinant high-mobility-group-like AT-hook-containing region from human BRG1 protein. Biol Chem 2006; 387:1469-78; PMID:17081121; http://dx.doi.org/10.1515/BC.2006.184
6. Fujimoto S, Matsunaga S, Yonemura M, Uchiyama S, Azuma T, Fukui K. Identification of a novel plant MAR DNA binding protein localized on chromosomal surfaces. Plant Mol Biol 2004; 56:225-39; PMID:15604740; http://dx.doi.org/10.1007/s11103-004-3249-5
7. Ng KH, Yu H, Ito T. AGAMOUS controls GIANT KILLER, a multifunctional chromatin modifier in reproductive organ patterning and differentiation. PLoS Biol 2009; 7:e1000251; PMID:19956801; http://dx.doi.org/10.1371/journal.pbio.1000251
8. Matsushita A, Furumoto T, Ishida S, Takahashi Y. AGF1, an AT-hook protein, is necessary for the negative feedback of AtGA3ox1 encoding GA 3-oxidase. Plant Physiol 2007; 143:1152-62; PMID:17277098; http://dx.doi.org/10.1104/pp.106.093542
9. Zhou J, Wang X, Lee JY, Lee JY. Cell-to-cell movement of two interacting AT-hook factors in Arabidopsis root vascular tissue patterning. Plant Cell 2013; 25:187-201; PMID:23335615; http://dx.doi.org/10.1105/tpc.112.102210
10. McClintock B. The origin and behavior of mutable loci in maize. Proc Natl Acad Sci U S A 1950; 36:344-55; PMID:15430309; http://dx.doi.org/10.1073/pnas.36.6.344
11. Amasino R. Seasonal and developmental timing of flowering. Plant J 2010; 61:1001-13; PMID:20409274; http://dx.doi.org/10.1111/j.1365-313X.2010.04148.x
12. Crevillén P, Dean C. Regulation of the floral repressor gene FLC: the complexity of transcription in a chromatin context. Curr Opin Plant Biol 2011; 14:38-44; PMID:20884277; http://dx.doi.org/10.1016/j.pbi.2010.08.015
13. Zaratiegui M, Irvine DV, Martienssen RA. Noncoding RNAs and gene silencing. Cell 2007; 128:763-76; PMID:17320512; http://dx.doi.org/10.1016/j.cell.2007.02.016
14. Saze H, Kakutani T. Differentiation of epigenetic modifications between transposons and genes. Curr Opin Plant Biol 2011; 14:81-7; PMID:20869294; http://dx.doi.org/10.1016/j.pbi.2010.08.017
15. Xu Y, Wang Y, Stroud H, Gu X, Sun B, Gan ES, et al. A matrix protein silences transposons and repeats through interaction with retinoblastoma-associated proteins. Curr Biol 2013; 23:345-50; PMID:23394836; http://dx.doi.org/10.1016/j.cub.2013.01.030
16. Michaels SD, He Y, Scortecci KC, Amasino RM. Attenuation of FLOWERING LOCUS C activity as a mechanism for the evolution of summer-annual flowering behavior in Arabidopsis. Proc Natl Acad Sci U S A 2003; 100:10102-7; PMID:12904584; http://dx.doi.org/10.1073/pnas.1531467100
17. Gazzani S, Gendall AR, Lister C, Dean C. Analysis of the molecular basis of flowering time variation in Arabidopsis accessions. Plant Physiol 2003; 132:1107-14; PMID:12805638; http://dx.doi.org/10.1104/pp.103.021212
18. Bucher E, Reinders J, Mirouze M. Epigenetic control of transposon transcription and mobility in Arabidopsis. Curr Opin Plant Biol 2012; 15:503-10; PMID:22940592; http://dx.doi.org/10.1016/j.pbi.2012.08.006
19. Han HJ, Russo J, Kohwi Y, Kohwi-Shigematsu T. SATB1 reprogrammes gene expression to promote breast tumour growth and metastasis. Nature 2008; 452:187-93; PMID:18337816; http://dx.doi.org/10.1038/nature06781
20. Cai S, Han HJ, Kohwi-Shigematsu T. Tissue-specific nuclear architecture and gene expression regulated by SATB1. Nat Genet 2003; 34:42-51; PMID:12692553; http://dx.doi.org/10.1038/ng1146
21. Yasui D, Miyano M, Cai ST, Varga-Weisz P, Kohwi-Shigematsu T. SATB1 targets chromatin remodelling to regulate genes over long distances. Nature 2002; 419:641-5; PMID:12374985; http://dx.doi.org/10.1038/nature01084
22. Kumar PP, Purbey PK, Ravi DS, Mitra D, Galande S. Displacement of SATB1-bound histone deacetylase 1 corepressor by the human immunodeficiency virus type 1 transactivator induces expression of interleukin-2 and its receptor in T cells. Mol Cell Biol 2005; 25:1620-33; PMID:15713622; http://dx.doi.org/10.1128/MCB.25.5.1620-1633.2005

Plant Signaling & Behavior 8:8, e25006; August 2013; © 2013 Landes Bioscience

The AT-hook/PPC domain protein TEK negatively regulates floral repressors including *MAF4* and *MAF5*

Yifeng Xu,[1] Eng-Seng Gan[1,2] and Toshiro Ito[1,2,*]

[1]Temasek Life Sciences Laboratory (TLL); 1 Research Link; National University of Singapore; Singapore; [2]Department of Biological Sciences; Faculty of Science; National University of Singapore; Singapore

Keywords: transposable element, AT-hook, *Arabidopsis*, TEK, flowering time, male sterility

Epigenetic regulations of transposable elements (TEs) and TE-like repeat sequences help to protect genomic integrity and control various developmental processes, including flowering time. This complex action of gene silencing requires the coordination of many key players including DNA methylases, histone deacetylases and histone methyltranferases. We have recently reported that an AT-hook DNA binding protein, TRANSPOSABLE ELEMENT SILENCING VIA AT-HOOK (TEK), participates in silencing TEs and TE-like sequence containing genes, such as L*er FLOWERING LOCUS C* (*FLC*) and *FWA*. *TEK* knockdown in *amiTEK* plants causes increased histone acetylation, reduced H3K9me2 and DNA hypomethylation in the target loci, which ultimately leads to the upregulation of *FLC* and *FWA* as well as TE reactivation. In this report, we show that, besides *FLC*, other *FLC*-like genes *MADS AFFECTING FLOWERING 4* (*MAF4*) and *MAF5* are also upregulated in *amiTEK*. Here we discuss the role of the nuclear matrix protein TEK in the maintenance of genome integrity and in the control of flowering.

Transposable elements (TEs) constitute a large fraction of most eukaryotic genomes including plants. Activation of these "jumping genes" can disrupt genomic integrity by causing rearrangements and mutations. Epigenetic regulation helps to maintain genomic integrity by suppressing TE activities (for review see refs. 1 and 2). TEs are usually silenced by DNA methylation, repressive histone H3 lysine 9 dimethylation (H3K9me2) and histone deacetylation (for review see refs. 3 and 4). Although small-interfering RNAs (siRNAs) have been shown to trigger DNA methylation in certain TEs and repetitive sequences via the RNA-directed DNA methylation (RdDM) pathway,[5] the factors that provide locus specificity and mechanism on how TEs and repeats are targeted for histone modification remain unclear. Recently, we have shown that the AT-hook DNA binding protein TRANSPOSABLE ELEMENT SILENCING VIA AT-HOOK (TEK) is involved in the silencing of TEs and TE-like sequence containing genes, including L*er FLC* and *FWA*.[6]

Based on the yeast-two-hybrid assay, bimolecular fluorescence complementation (BiFC) assay and co-immunoprecipitation (Co-IP) assay, we have shown that TEK protein interacts with retinoblastoma-associated protein FVE and its homolog MSI5. Chromatin immunoprecipitation (ChIP) assay showed that TEK directly binds to a *FLC*-repressive regulatory region and the silencing repeats of *FWA*. We proposed that TEK is involved in protecting genome stability by recruiting FVE/MSI5-containing histone deacetylase (HDAC) complexes to various target loci including *FLC, FWA* and TEs, which promotes a self-reinforcing cycle of histone deacetylation, DNA methylation and H3K9 dimethylation, leading to their transcriptional silencing.

AT-hook DNA binding proteins are known to contribute to a functional nuclear architecture by binding to the nuclear matrix.[7-9] AT-hook motifs bind to the minor grooves in duplex DNA of matrix attachment regions (MAR) of target DNA sequences, which contain characteristic AT-rich DNA sequences.[10,11] The binding of AT-hook protein affects the chromatin status of target genes, by inducing structural changes of chromatin[12,13] and/or recruitment of chromatin modifiers including ACF, ISWI and HDAC1.[14,15] These chromatin modifiers have been proposed to suppress gene expression through histone deacetylation and nucleosome remodeling at SATB1-bound MARs.[14] Many plant AT-hook motif proteins have a plants and prokaryotes conserved (PPC) domain with unknown functions.[16] *Arabidopsis* genome contains 29 proteins in this family (AHL1-29) and till now only few of them have been studied for their biological functions.[16-18] Previously we identified a member of this family and a direct target of the floral homeotic protein AGAMOUS (AG), *GIANT KILLER* (*GIK*)/*AHL21*, negatively regulates various targets downstream of AG, controlling reproductive organs patterning and differentiation through repressive histone modifications.[17]

*Correspondence to: Toshiro Ito; Email: itot@tll.org.sg
Submitted: 03/25/13; Revised: 05/09/13; Accepted: 05/10/13
Citation: Xu, Y, Gan E-S, Ito T. The AT-hook/PPC domain protein TEK negatively regulates floral repressors including *MAF4* and *MAF5*. Plant Signal Behav 2013; 8: e25006; http://dx.doi.org/10.4161/psb.25006

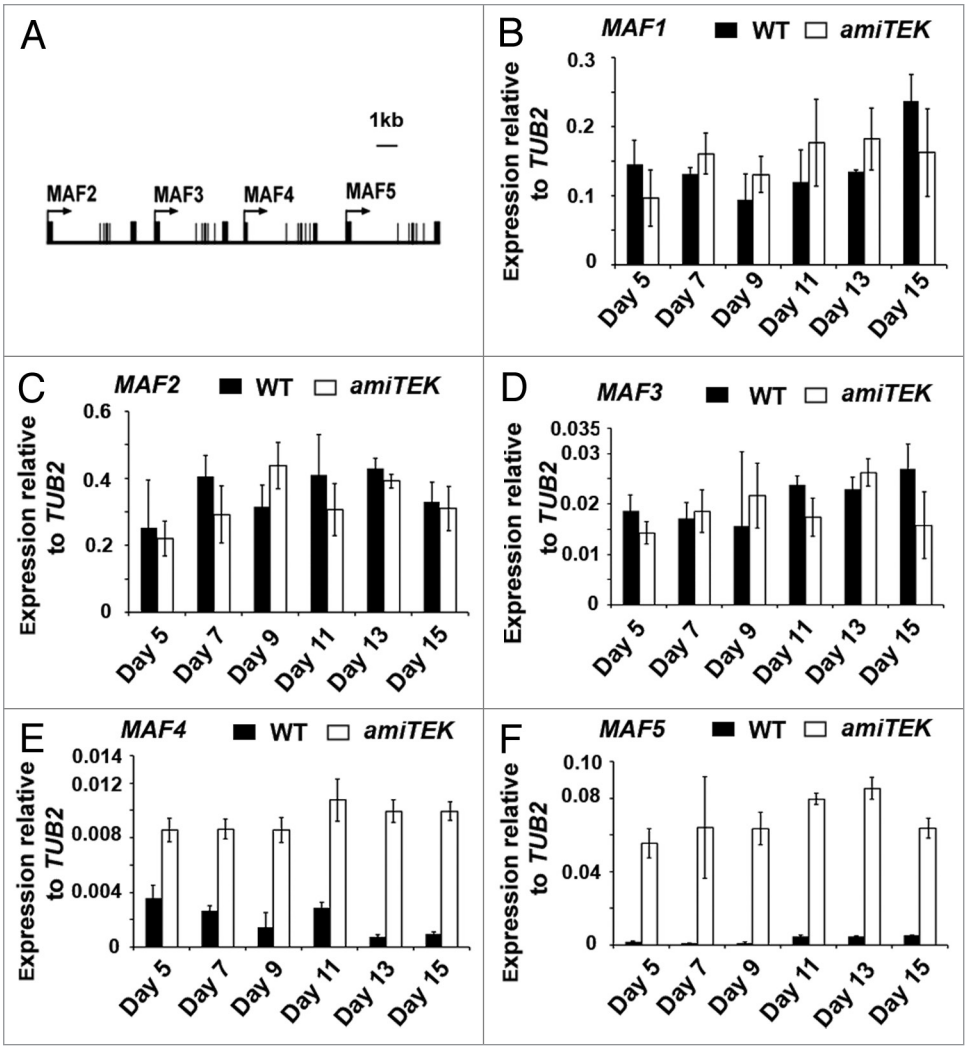

Figure 1. Upregulation of *MAF4* and *MAF5*, but not *MAF1*, *MAF2* and *MAF3* in *amiTEK* plants. (**A**) Schematic structure of the *MAF2–5* loci. (**B–F**) Relative mRNA expression levels of *FLC*-like flowering-time genes in DAG 5, 7, 9, 11, 13 and 15 wild-type L*er* plants and *amiTEK* plants. All error bars show the standard deviation based on three biological replicates. Relative mRNA expression levels of *MAF4* (**E**) and *MAF5* (**F**), but not *MAF1* (**B**), *MAF2* (**C**) and *MAF3* (**D**), were obviously increased in *amiTEK* plants.

We carefully analyzed the other members of the family and found *TEK*/*AHL16* to be of particular interest, not only because of its high expression in the reproductive tissues, but also its obvious late flowering phenotype in the knockdown mutants.

We first established *35S:amiTEK* transgenic lines and found the correlation between knockdown level of *TEK* mRNA and late flowering phenotypes. However, it is of note that the introduction of *35S::TEK-HA* (which does not contain the target site of *amiTEK)* into *35S::amiTEK* plants was unable to rescue the late flowering phenotype. We further noticed that the late flowering phenotype is transgene-independent heritable in both segregated T2 plants and F1 plants from *35S::amiTEK* crossed with wild-type plants, suggesting that the late flowering phenotype is linked with heritable epigenetic defects. To confirm that the late flowering phenotype of *35S::amiTEK* was really caused by the reduction of *TEK* mRNA, we changed the strategy of the rescue experiment. We prepared functional *35S::TEK-HA* transgenic lines first, then introduced *35S::amiTEK* construct into these plants. In a total of 20 T1 *35S::amiTEK 35S::TEK-HA* double transgenic plants, 95% (19 of 20 lines) showed normal flowering time, indicating that the defects caused by *35S::amiTEK* is *TEK*-specific. Detailed analysis showed that the loss of the silencing epigenetic marks on the *FWA* and *FLC* loci, which results in their de-repression, is the major cause for the heritable late flowering phenotype.

De-repressed *FWA* and *FLC* are the two major genes causing the late flowering phenotype in *35S::amiTEK* plants and we studied them in detail in the referred paper.[6] In addition to *FWA* and *FLC*, there are other flowering time genes affected in *TEK* knockdown lines. In *Arabidopsis*, there are five *FLC*-like genes which are proposed to function in flowering transition pathway. *MADS AFFECTING FLOWERING 1* (*MAF1*, also referred to as *FLM*) was proposed to function as a flowering repressor based on its overexpression lines.[19,20] The other four genes, *MAF2-5*, clustered tandemly at the bottom of chromosome 5 (**Fig. 1A**), also play roles in flowering time control as repressors at least in L*er*.[19,21] Through quantitative real-time PCR, we found that *MAF4* and *MAF5* are obviously increased in the *35S::amiTEK* plants, while *MAF1*, *MAF2* and *MAF3* are not significantly changed at the transcriptional level (**Fig. 1B–F**). Although further studies are required, the upregulation of *MAF4* and *MAF5* suggests that these genes may be regulated by a similar epigenetic mechanism, utilizing TEK-containing HDAC, as observed in *FLC* and *FWA* loci. The absence of repeat sequences and DNA methylation in *MAF4* and *MAF5* loci suggests that TEK can also function through repression pathways independently of DNA methylation.[22] On the other hand, *FLC*, *MAF4* and *MAF5*, but not *MAF1*, *MAF2* and *MAF3*, are reported to be repressed by Polycomb repressive complex 2 (PRC2) at the vegetative stages.[23] It will be interesting to study the cross-talk between HDAC and PRC2 pathways in the transcriptional regulation of *FLC*, *MAF4* and *MAF5*.

The L*er FLC* allele contains a 1,224-bp insertion of a *Mutator*-like TE in the first intron, which is subjected to siRNA mediated repression.[24,25] The presence of the TE insertion is responsible for the inability of L*er FLC* to be activated by a functional *FRIGIDA*

(*FRI*), because the insertion of this TE to a strong *FLC* allele causes it behaves like L*er FLC* allele.[24] In *amiTEK* L*er* plants, the *Mutator*-like element is excised without leaving any footprint.[6] This shows that precise excision could be a feature of such TEs in *Arabidopsis*, as well as in rice.[26] Thorough studies of the transposition locus and its sequence could provide information on the transposition mechanism. The *amiTEK* L*er* plants may also be useful for the studies of transposition of other DNA transposons. The transposition of at least two other DNA transposons, *CACTA* and *hAT*, were also observed by genomic Southern blots. Currently, when and how the DNA transposon excision and transposition occur are not well understood in plants. As the vegetative tissues of *amiTEK* plants are not chimerical in terms of cells with or without the *Mutator*-like TE at the L*er FLC* locus, we reasoned that the jumping had happened at or before the embryogenesis stage. It would be useful to utilize inducible *TEK* knockdown construct driven by cauliflower mosaic virus *35S* promoter or tissue-specific promoters and studying them in conjunction with the different mutants that causes TEs reactivation, to uncover the mechanism of DNA transposon transpositions: location and critical stage where and when transposition occur and key genes involved.

While we focused on the activation of TE and TE-like genes in *Arabidopsis* L*er* after knockdown of *TEK*, we also noticed some male sterility phenotype in the *TEK* knockdown plants and *TEK* loss-of-function mutants in all three tested ecotypes (Col, L*er* and Ws). This phenotype is consistent with the observation of high *TEK* expression in the stamen. Further studies will be necessary to uncover how *TEK* controls male fertility in *Arabidopsis*.

Disclosure of Potential Conflicts of Interest

No potential conflicts of interest were disclosed.

Acknowledgments

This work was supported by research grants to TI from Temasek Life Sciences Laboratory (TLL), the National Research Foundation Singapore under its Competitive Research Programme (CRP Award No. NRF-CRP001-108) and PRESTO, Japan Science and Technology Agency, 4-1-8 (Honcho Kawaguchi, Saitama, Japan).

References

1. Amasino R. Seasonal and developmental timing of flowering. Plant J 2010; 61:1001-13; PMID:20409274; http://dx.doi.org/10.1111/j.1365-313X.2010.04148.x
2. Crevillén P, Dean C. Regulation of the floral repressor gene FLC: the complexity of transcription in a chromatin context. Curr Opin Plant Biol 2011; 14:38-44; PMID:20884277; http://dx.doi.org/10.1016/j.pbi.2010.08.015
3. Zaratiegui M, Irvine DV, Martienssen RA. Noncoding RNAs and gene silencing. Cell 2007; 128:763-76; PMID:17320512; http://dx.doi.org/10.1016/j.cell.2007.02.016
4. Saze H, Kakutani T. Differentiation of epigenetic modifications between transposons and genes. Curr Opin Plant Biol 2011; 14:81-7; PMID:20869294; http://dx.doi.org/10.1016/j.pbi.2010.08.017
5. Lisch D. Epigenetic regulation of transposable elements in plants. Annu Rev Plant Biol 2009; 60:43-66; PMID:19007329; http://dx.doi.org/10.1146/annurev.arplant.59.032607.092744
6. Xu Y, Wang Y, Stroud H, Gu X, Sun B, Gan ES, et al. A matrix protein silences transposons and repeats through interaction with retinoblastoma-associated proteins. Curr Biol 2013; 23:345-50; PMID:23394836; http://dx.doi.org/10.1016/j.cub.2013.01.030
7. Aravind L, Landsman D. AT-hook motifs identified in a wide variety of DNA-binding proteins. Nucleic Acids Res 1998; 26:4413-21; PMID:9742243; http://dx.doi.org/10.1093/nar/26.19.4413
8. Morisawa G, Han-Yama A, Moda I, Tamai A, Iwabuchi M, Meshi T. AHM1, a novel type of nuclear matrix-localized, MAR binding protein with a single AT hook and a J domain-homologous region. Plant Cell 2000; 12:1903-16; PMID:11041885
9. Strick R, Laemmli UK. SARs are cis DNA elements of chromosome dynamics: synthesis of a SAR repressor protein. Cell 1995; 83:1137-48; PMID:8548801; http://dx.doi.org/10.1016/0092-8674(95)90140-X
10. Reeves R, Nissen MS. The A.T-DNA-binding domain of mammalian high mobility group I chromosomal proteins. A novel peptide motif for recognizing DNA structure. J Biol Chem 1990; 265:8573-82; PMID:1692833
11. Reeves R. Molecular biology of HMGA proteins: hubs of nuclear function. Gene 2001; 277:63-81; PMID:11602345; http://dx.doi.org/10.1016/S0378-1119(01)00689-8
12. Han HJ, Russo J, Kohwi Y, Kohwi-Shigematsu T. SATB1 reprogrammes gene expression to promote breast tumour growth and metastasis. Nature 2008; 452:187-93; PMID:18337816; http://dx.doi.org/10.1038/nature06781
13. Cai S, Han HJ, Kohwi-Shigematsu T. Tissue-specific nuclear architecture and gene expression regulated by SATB1. Nat Genet 2003; 34:42-51; PMID:12692553; http://dx.doi.org/10.1038/ng1146
14. Yasui D, Miyano M, Cai ST, Varga-Weisz P, Kohwi-Shigematsu T. SATB1 targets chromatin remodelling to regulate genes over long distances. Nature 2002; 419:641-5; PMID:12374985; http://dx.doi.org/10.1038/nature01084
15. Kumar PP, Purbey PK, Ravi DS, Mitra D, Galande S. Displacement of SATB1-bound histone deacetylase 1 corepressor by the human immunodeficiency virus type 1 transactivator induces expression of interleukin-2 and its receptor in T cells. Mol Cell Biol 2005; 25:1620-33; PMID:15713622; http://dx.doi.org/10.1128/MCB.25.5.1620-1633.2005
16. Fujimoto S, Matsunaga S, Yonemura M, Uchiyama S, Azuma T, Fukui K. Identification of a novel plant MAR DNA binding protein localized on chromosomal surfaces. Plant Mol Biol 2004; 56:225-39; PMID:15604740; http://dx.doi.org/10.1007/s11103-004-3249-5
17. Ng KH, Yu H, Ito T. AGAMOUS controls GIANT KILLER, a multifunctional chromatin modifier in reproductive organ patterning and differentiation. PLoS Biol 2009; 7:e1000251; PMID:19956801; http://dx.doi.org/10.1371/journal.pbio.1000251
18. Matsushita A, Furumoto T, Ishida S, Takahashi Y. AGF1, an AT-hook protein, is necessary for the negative feedback of AtGA3ox1 encoding GA 3-oxidase. Plant Physiol 2007; 143:1152-62; PMID:17277098; http://dx.doi.org/10.1104/pp.106.093542
19. Ratcliffe OJ, Nadzan GC, Reuber TL, Riechmann JL. Regulation of flowering in Arabidopsis by an FLC homologue. Plant Physiol 2001; 126:122-32; PMID:11351076; http://dx.doi.org/10.1104/pp.126.1.122
20. Scortecci KC, Michaels SD, Amasino RM. Identification of a MADS-box gene, FLOWERING LOCUS M, that represses flowering. Plant J 2001; 26:229-36; PMID:11389763; http://dx.doi.org/10.1046/j.1365-313x.2001.01024.x
21. Ratcliffe OJ, Kumimoto RW, Wong BJ, Riechmann JL. Analysis of the Arabidopsis MADS AFFECTING FLOWERING gene family: MAF2 prevents vernalization by short periods of cold. Plant Cell 2003; 15:1159-69; PMID:12724541; http://dx.doi.org/10.1105/tpc.009506
22. Shen H, He H, Li J, Chen W, Wang X, Guo L, et al. Genome-wide analysis of DNA methylation and gene expression changes in two Arabidopsis ecotypes and their reciprocal hybrids. Plant Cell 2012; 24:875-92; PMID:22438023; http://dx.doi.org/10.1105/tpc.111.094870
23. Jiang D, Wang Y, Wang Y, He Y. Repression of FLOWERING LOCUS C and FLOWERING LOCUS T by the Arabidopsis Polycomb repressive complex 2 components. PLoS ONE 2008; 3:e3404; PMID:18852898; http://dx.doi.org/10.1371/journal.pone.0003404
24. Michaels SD, He Y, Scortecci KC, Amasino RM. Attenuation of FLOWERING LOCUS C activity as a mechanism for the evolution of summer-annual flowering behavior in Arabidopsis. Proc Natl Acad Sci USA 2003; 100:10102-7; PMID:12904584; http://dx.doi.org/10.1073/pnas.1531467100
25. Gazzani S, Gendall AR, Lister C, Dean C. Analysis of the molecular basis of flowering time variation in Arabidopsis accessions. Plant Physiol 2003; 132:1107-14; PMID:12805638; http://dx.doi.org/10.1104/pp.103.021212
26. Shan X, Liu Z, Dong Z, Wang Y, Chen Y, Lin X, et al. Mobilization of the active MITE transposons mPing and Pong in rice by introgression from wild rice (Zizania latifolia Griseb.). Mol Biol Evol 2005; 22:976-90; PMID:15647520; http://dx.doi.org/10.1093/molbev/msi082

Current Biology 23, 345–350, February 18, 2013 ©2013 Elsevier Ltd All rights reserved http://dx.doi.org/10.1016/j.cub.2013.01.030

Report

A Matrix Protein Silences Transposons and Repeats through Interaction with Retinoblastoma-Associated Proteins

Yifeng Xu,[1] Yizhong Wang,[1,2] Hume Stroud,[3] Xiaofeng Gu,[1] Bo Sun,[1] Eng-Seng Gan,[1] Kian-Hong Ng,[1] Steven E. Jacobsen,[3,4] Yuehui He,[1,2,*] and Toshiro Ito[1,2,*]
[1]Temasek Life Sciences Laboratory (TLL), 1 Research Link, National University of Singapore, Singapore 117604, Singapore
[2]Department of Biological Sciences, Faculty of Science, National University of Singapore, 10 Science Drive 4, 117543, Singapore
[3]Department of Molecular, Cell and Developmental Biology
[4]Howard Hughes Medical Institute
University of California, Los Angeles, Los Angeles, CA 90095, USA

Summary

Epigenetic regulation helps to maintain genomic integrity by suppressing transposable elements (TEs) and also controls key developmental processes, such as flowering time [1–3]. To prevent TEs from causing rearrangements and mutations, TE and TE-like repetitive DNA sequences are usually methylated, whereas histones are hypoacetylated and methylated on specific residues (e.g., H3 lysine 9 dimethylation [H3K9me2]) [4, 5]. TEs and repeats can also attenuate gene expression [2, 6–8]. However, how various histone modifiers are recruited to target loci is not well understood. Here we show that knockdown of the nuclear matrix protein with AT-hook DNA binding motifs [9–11] TRANSPOSABLE ELEMENT SILENCING VIA AT-HOOK (TEK) in *Arabidopsis* Landsberg *erecta* results in robust activation of various TEs, the TE-like repeat-containing floral repressor genes *FLOWERING LOCUS C* (*FLC*) and *FWA* [1, 2, 12]. This derepression is associated with chromatin conformational changes, increased histone acetylation, reduced H3K9me2, and even TE transposition. TEK directly binds to an *FLC*-repressive regulatory region and the silencing repeats of *FWA* and associates with *Arabidopsis* homologs of the Retinoblastoma-associated protein 46/48, FVE and MSI5, which mediate histone deacetylation [13, 14]. We propose that the nuclear matrix protein TEK acts in the maintenance of genome integrity by silencing TE and repeat-containing genes.

Results and Discussion

TEK Knockdown Leads to Late Flowering

Matrix proteins with AT-hook DNA binding motifs bind to the AT-rich nuclear matrix attachment regions, possibly affecting the epigenetic state of target chromatin in animals and plants [15–17]. Some AT-hook proteins are known to regulate tissue-specific gene expression [15, 16] but very little is known about their functional mechanisms, especially in gene silencing. Most of the *Arabidopsis* AT-hook DNA binding proteins are dominantly expressed in root, but *AHL16* (*At2g42940*, we renamed it *TEK*) is preferentially expressed in the inflorescence meristem and young floral buds, as well as in seedling-stage vegetative meristems (the *Arabidopsis* eFP browser http://bbc.botany.utoronto.ca/efp; Figures 1A–1D and see Figure S1 available online). To study *TEK* functions, we created two artificial microRNA (amiRNA) constructs [18], *35S::amiTEKa* and *35S::amiTEKb*, to target the *TEK* coding and 3′ untranslated regions, respectively (Figure 1E). Transgenic lines for both constructs with strongly reduced *TEK* levels (20%–40% compared to the wild-type) showed late-flowering phenotypes in the Landsberg *erecta* (L*er*) ecotype background (Figures 1F–1I and S2A and S2B). About 40% of T_1 *35S::amiTEKb* plants showed extremely late flowering (Figures 1F). RNA levels of control genes including the closest homolog *AHL28* were unaffected (Figure S2C). Many T1 *amiTEK* transgenic plants also showed altered phyllotaxis, extra cauline leaves of larger size, and reduced fertility, in agreement with the expression pattern of *TEK* in the inflorescence meristem and reproductive organs (Figures 1D and 1J; data not shown) [19]. It is notable that none of the *35S::amiTEK* plants in the Colombia (Col) background showed late flowering (data not shown), suggesting that *TEK* knockdown may have accession-specific effects. We also identified *T-DNA* insertion mutants (*tek-1*, *tek-2*, and *tek-3*) in Col or Wassilewskija (Ws) (Figure S2D). These mutants were sterile, but they showed no obvious defects in flowering time (data not shown). Next, we confirmed that the late-flowering phenotype is accession dependent by backcrossing *tek-1* (in the Col background) into L*er*. Some homozygous plants started to exhibit late flowering after the fourth backcross (Figure S2E).

TEK Directly Controls *FLC* Expression and Chromatin Conformation

To examine what genes cause the delayed flowering in the *TEK* knockdown plants, we examined transcript levels of flowering regulators in stable and fertile *amiTEK* lines (they are called "*amiTEK*") (Figures 1K–1M and S2F–S2J). We found that *FLC*, a central floral repressor (reviewed in [20]), was dramatically upregulated (Figure 1K), whereas the levels of *FLC* downstream flowering integrators, including *AGL24*, *SOC1*, and *FT* [20], were moderately decreased (Figures 1L–1M and S2F). Furthermore, transcript levels of the *FLC* upstream factors such as the putative histone H3 lysine 4 demethylase FLD, FVE, and FRI LIKE 1 (FRL1) were not significantly changed (Figures S2G–S2J), indicating direct regulation of *FLC* by TEK.

To test whether TEK directly binds to *FLC* chromatin, we performed chromatin immunoprecipitation (ChIP) using the lines expressing the functional TEK with epitope tags driven by a ubiquitous promoter or the native *TEK* promoter. Enrichment with a primer set spanning 5′ end of the first intron (region c), essential for *FLC* silencing [21], was detected (Figures 2A, 2B, S3A, and S3B). Because *TEK* encodes an AT-hook DNA binding matrix protein, we next tested whether nuclear matrix association of *FLC* is affected in *amiTEK*. DNA attached to nuclear matrix is enriched by washing purified nuclei with high salt buffer [16]. We detected a dramatic increase in the ratio of free DNA to nuclear matrix-attached DNA in *amiTEK* compared to wild-type (Figures 2A and 2C). These results

*Correspondence: dbshy@nus.edu.sg (Y.H.), itot@tll.org.sg (T.I.)

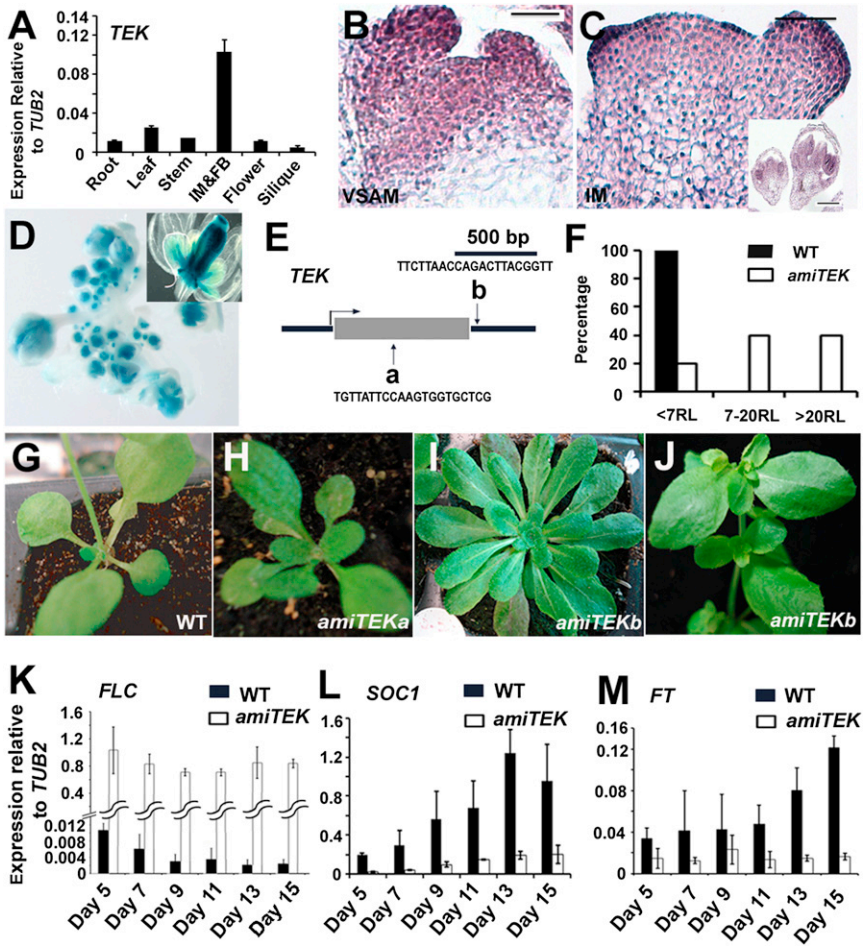

Figure 1. *TEK* Knockdown Leads to Significant *FLC* Derepression and Late Flowering

(A) The relative expression of *TEK* to *TUBULIN2 (TUB2)* in root, leaf, stem, inflorescence meristem, and young flower bud (IM&FB), flower, and silique. (B and C) In situ hybridization of *TEK* in the vegetative shoot apical meristem (VSAM) 10 days after germination (DAG 10) (B), the inflorescence meristem (IM) (C), and young floral buds (inset). Scale bars represent 25 μm for (B) and 50 μm for (C). (D) Spatial expression pattern of *pTEK*::*TEK-GUS* (β-glucuronidase) in the reproductive tissues. *TEK* is highly expressed in the whole inflorescence and ovules and anthers of a developing flower (inset). (E) The locations and target sequences of the artificial *TEK* knockdown constructs a and b. (F–J) Knockdown of *TEK* by *amiTEKa* and *amiTEKb* caused late flowering. Distribution of late-flowering phenotypes of 80 T_1 lines with *amiTEKb* under continuous light growth condition is shown by the number of rosette leaves (RL) (F), wild-type L*er* plant (G), a *35S::amiTEKa* plant (H), and *35S::amiTEKb* plants (I) and (J). (K–M) Expression analyses of *FLC* (K), *SOC1* (L), and *FT* (M) relative to *TUB2* in DAG 5, 7, 9, 11, 13, and 15 in wild-type L*er* (WT) and *amiTEK* plants. Error bars represent SD based on three biological replicates.

suggest that TEK is necessary for the association of *FLC* chromatin with the nuclear matrix for silencing.

TEK Knockdown Leads to Reduced H3K9me2 and Increased H3 Acetylation

Next, we compared histone modifications in wild-type and *amiTEK* by ChIP. We found that in wild-type seedlings, the repressive mark H3K9me2 was enriched in *FLC*, especially at the TEK binding site (region c) and 3′ region of the intron 1 (region e) (Figures 2A and 2D). This enrichment was abolished in *amiTEK* (Figures 2D and S3C). In contrast, the activation mark H3 acetylation (H3Ac) was increased in *amiTEK* compared with wild-type (Figures 2E, S3D, and S3E). Notably, another repressive mark, histone H3 lysine 27 trimethylation (H3K27me3), was not primarily changed in *amiTEK* (Figure 2F and S3F). Together, these data suggest that TEK may function through H3K9 dimethylation and histone deacetylation.

TEK Knockdown Leads to Robust Derepression of TEs and Even Transposition of the *Mutator*-like TE from L*er FLC*

We performed global transcriptional analyses in *amiTEK* using the *Arabidopsis* oligonucleotide microarray (NimbleGen, Roche). We detected 1,209 genes including *FLC* upregulated and 416 genes downregulated in *amiTEK* seedlings compared with wild-type ($p < 0.05$) (Figure 3A, Table S1, NCBI Gene Expression Omnibus GSE39158). Among the upregulated genes, around 69% were TEs. Drastic upregulation of various retrotransposons and DNA transposons [22–24] was confirmed in two independent *amiTEK* lines (Figure 3B).

To further confirm TE activation upon the loss of *TEK* function, we performed RNA-sequencing using the *tek-1* inflorescences showing late-flowering phenotypes. It showed that 75 TEs were upregulated over 4-fold compared to the wild-type L*er* ($p < 0.05$ cutoff) (Table S2). We also detected an overlap of upregulated protein-coding genes between *amiTEK* and the introgressed *tek-1* (Figure S4A, Table S3). Moderate activation of several representative TEs as well as *FLC* was further confirmed in the seedling of introgressed *tek-1* homozygous lines (Figure S4B) but not in the original Col background (data not shown). These show that TEK is essential for TE silencing in L*er*.

The L*er FLC* allele contains a *Mutator*-like insertion in the first intron, which silences *FLC* expression [2, 6] (Figure 3C). The significant derepression of L*er FLC* in *amiTEK* prompted us to check whether the TE insertion was still present. Strikingly, it was lost in four randomly picked T_1 lines with late-flowering phenotypes (Figures 3C and 3D). Sequencing of the excision sites of 12 independent lines (from two transformation experiments) showed that all lines have the exact same sequences as Col (data not shown), suggesting that the excision happened multiple times at the same position. In rice, one *Mutator*-like element has been reported to be excised without footprint [25]. Thus, the precise excision is likely to be a common feature in *Arabidopsis* and rice. Furthermore, the excision and transposition of the *Mutator*-like TE and two other DNA transposons *CACTA* and *hAT* were confirmed in two independent lines by genomic Southern blots (Figure 3E, marked as black arrows; Figure S4C). TEK binding to *FLC* was detected at a region about 1 kb upstream of the *Mutator*-like TE in both Col and L*er*

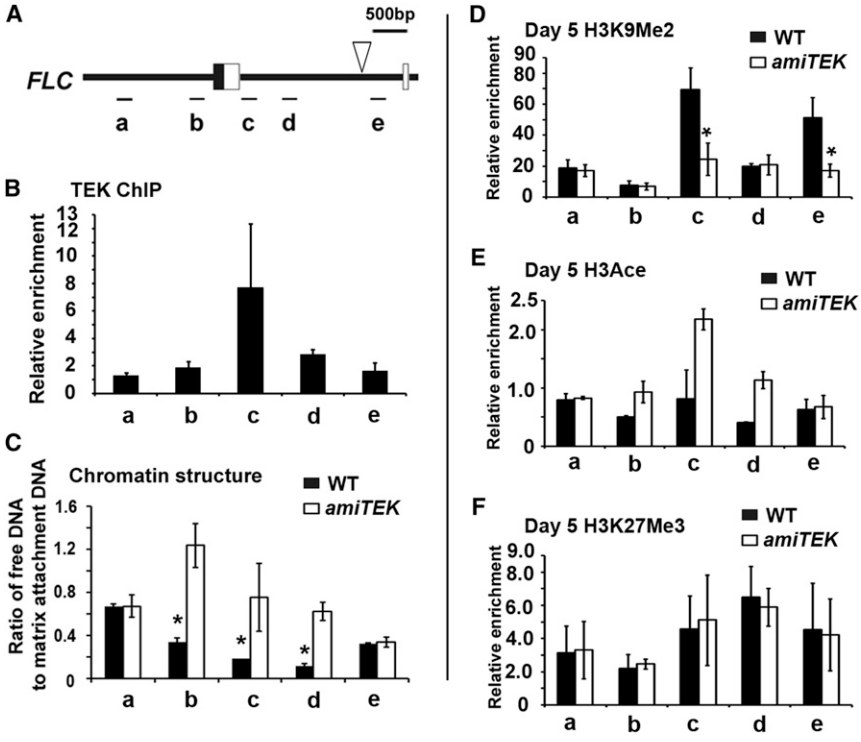

Figure 2. TEK Binds to *FLC* Chromatin, Mediates Histone Modification, and Maintains Chromatin Structure at the *FLC* Locus

(A) Schematic structure of the *FLC* locus showing the 5′ untranslated region (black box) and first two exons (white boxes). Letters a to e in (A)–(F) represent the amplicons examined by qPCR. White triangle, 1.2 kb TE insertion in L*er*. (B) Binding of TEK to *FLC* analyzed by ChIP using *pTEK::TEK-YFP* inflorescences. (C) *TEK* knockdown changed the matrix association of *FLC*. (D–F) Relative fold enrichment of epigenetic marks at *FLC*, H3K9me2 (D), H3 acetylation (E), and H3K27me3 (F) using the aerial parts of DAG 5 plants. Error bars represent SD based on three biological replicates in (B)–(D) and (F) and on two biological replicates in (E). Asterisks indicate statistically significant differences (paired Student's t test, $p < 0.05$) between samples in WT and *amiTEK*.

(Figures 2B and S3B), suggesting that TEK may be involved in *FLC* silencing, independently of TE silencing. Thus, *FLC* activation may have contributed to the TE transposition and vice versa.

The Repeat-Containing *FWA* Gene Is Also Derepressed and Contributes to Late-Flowering in *amiTEK*

We also found that the expression of *FWA*, which contains two tandem repeats of a *SINE*-like element near its transcription start site [8], was ectopically induced in *amiTEK* (Figures S4D–S4F). To see whether the late-flowering phenotype is attributed to ectopic expression of both *FLC* and *FWA*, we performed vernalization treatment (an extended period of cold exposure) on *amiTEK* because vernalization represses *FLC*, but not *FWA* (Figures S4E and S4F) [26]. The vernalization-treated *amiTEK* flowered earlier than those without treatment but still flowered later than wild-type (Figure S4D). These suggest that both *FLC* and *FWA* contribute to late flowering in *amiTEK*.

Because that ectopic expression of *FWA* in vegetative tissues and derepression of TEs are reportedly associated with loss of DNA methylation [12], we used bisulfite sequencing to examine DNA methylation of *FWA*. Methylation at CG, CNG, and CHH was reduced in the tandem repeats of *FWA* in *amiTEK* (Figure 3F). However, these reductions are not as great as those found in the *epi* mutant allele of *fwa*, in which DNA methylation was almost abolished [12]. At *AtMu1*, which is related to the *Mutator*-like TE at L*er FLC*, the percentages of methylated CG, CNG, and CHH were also moderately decreased (Figure S4G).

Next, we examined the histone modification state at *FWA*. The level of H3K9me2 was reduced in the tandem repeats (region b) of *FWA* in *amiTEK* (Figures S4H and S4I). The acetylation level was increased significantly in region b and moderately in region a (Figures 3G and 3H), whereas the H3K27me3 level did not show any obvious change (Figure S4J). The change in histone acetylation at *FWA* appears greater than the change in DNA methylation in *amiTEK*, suggesting that histone deacetylation may play a greater role in *FWA* silencing. The ChIP assays using *pTEK::TEK-YFP* confirmed that TEK directly binds to the repeated sequences of *FWA* (Figure 3I), suggesting that *FWA* is a direct TEK target.

TEK Associates with FVE and Its Homolog MSI5, Components of HDAC Corepressor Complexes

To understand the causal link between TEK and histone modifications, we performed yeast two-hybrid assays to examine the interaction of TEK with various histone-modification factors, including HDAC, FVE, MSI5, and Polycomb group proteins. We found that TEK interacted with FVE and MSI5, but not with others (Figure 4A and data not shown). The interactions were further confirmed in plant cells by bimolecular fluorescence complementation (BiFC). Fluorescence was observed in the nuclei of onion epidermal cells only when TEK and FVE or TEK and MSI5 constructs were coinjected (Figure 4B). Moreover, we carried out coimmunoprecipitation experiments to confirm the in vivo association of TEK with FVE/MSI5 using the seedlings expressing the TEK-YFP and FVE-FLAG/MSI5-FLAG. We found that anti-FLAG (recognizing FVE-FLAG and MSI5-FLAG) coimmuoprecipitated TEK-YFP from the seedlings (Figure 4C). Together, these show that TEK is in a complex with FVE/MSI5 in *Arabidopsis*.

Because both FVE and MSI5, *Arabidopsis* homologs of the mammalian Retinoblastoma-associated protein 46/48, are components of histone deacetylation complexes that silence *FLC*, TEs (e.g., *AtMu1*) and repetitive sequence-containing loci (e.g., *FWA*) [14], the TEK-FVE/MSI5 complex is likely to bind to TEs. However, we were unable to detect significant ChIP enrichments of TEK at TEs (data not shown). This might be due to weak binding abilities of AT-hook proteins. In *Brassica*, it has been shown that SINE-like repeats are highly associated with nuclear matrix [27]. Taken together, we propose that the nuclear matrix protein TEK associates with the FVE/MSI5 complex and binds to various target sites of

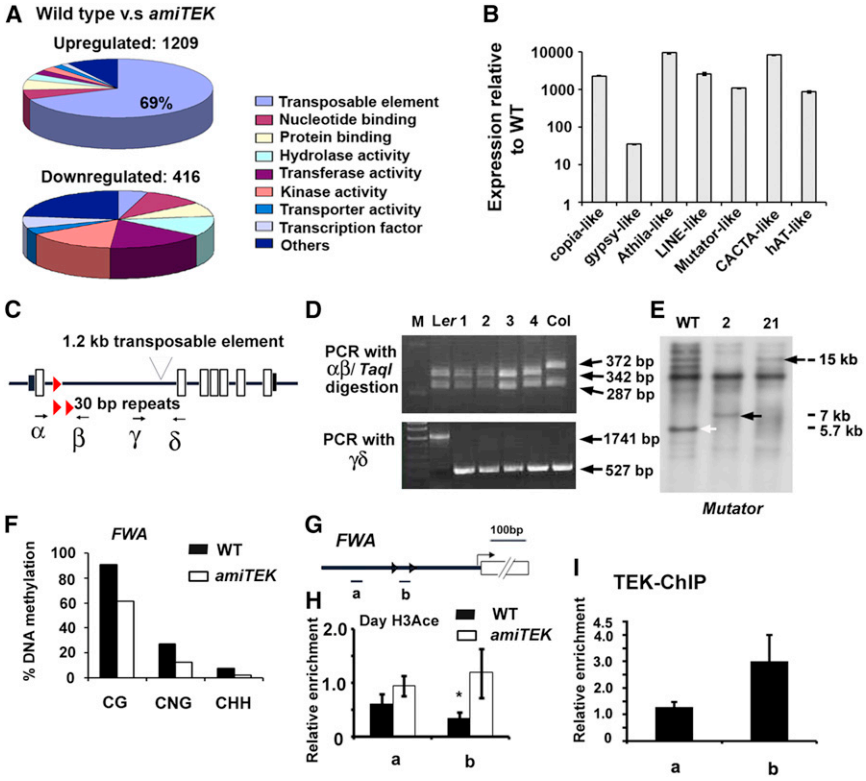

Figure 3. *TEK* Knockdown Causes TE Derepression and TE Transposition from L*er FLC*

(A) Pie chart of microarray results comparing *amiTEK* and wild-type L*er* plants at DAG 5. (B) The relative ratio of TE transcript levels in *amiTEK* and wild-type representative. TEs: *Copia-like (AT5G43800)*, *gypsy-like (AT5G33050)*, *Athila-like (AT5G32306)*, *LINE-like (AT3G43436)*, *Mutator-like (AT1G33460)*, *CACTA-like (AT5G45082)*, and *hAT-like (AT2G05700)*. (C and D) The *Mutator*-like element in the intron 1 of L*er FLC* was lost in *amiTEK*. Black and white boxes, untranslated and coding regions, respectively. Arrowheads, the 30 bp repeat in the intron 1 (one in L*er* and two in Col). In four randomly picked late-flowering plants in the L*er* background (1–4), the 1.2 kb TE was absent (D). (E) A genomic Southern blot showed that the *Mutator*-like TE in *FLC* (white arrow) was excised and translocated in *amiTEK* (lines 2 and 21, black arrows). (F) Bisulfite sequencing showed that cytosine methylation levels of CG, CHG, and CHH at *FWA* were decreased in *amiTEK*. (G) Schematic structure of *FWA*. Arrowheads, the *SINE*-like direct repeats. Letters a and b show regions tested in (H) and (I). (H) H3 acetylation levels were increased in *amiTEK*. Asterisk indicates statistically significant difference (paired Student's t test, $p < 0.05$) between samples. (I) Binding of TEK to *FWA* by ChIP using *pTEK::TEK-YFP* inflorescences. Error bars represent SD based on three biological replicates.

TEs and repeat-containing genes, leading to histone deacetylation and, thus, gene silencing (Figure 4D).

We compared the upregulated genes in *amiTEK* with those in the mutants for the DNA methyltransferase MET1 and the histone deacetylase HDA6 [28–30]. Significant overlap of genes silenced by TEK, MET1, and HDA6 was detected, including some of siRNA-directed DNA methylation targets (Figures S4K and S4L). These indicate the cooperative action of DNA methylation, histone deacetylation, and TEK. In addition, HDA6 can directly interact with MET1 [31], indicating that TEK may act as a part of large protein complexes including histone deacetylase as well as DNA methyltransferase.

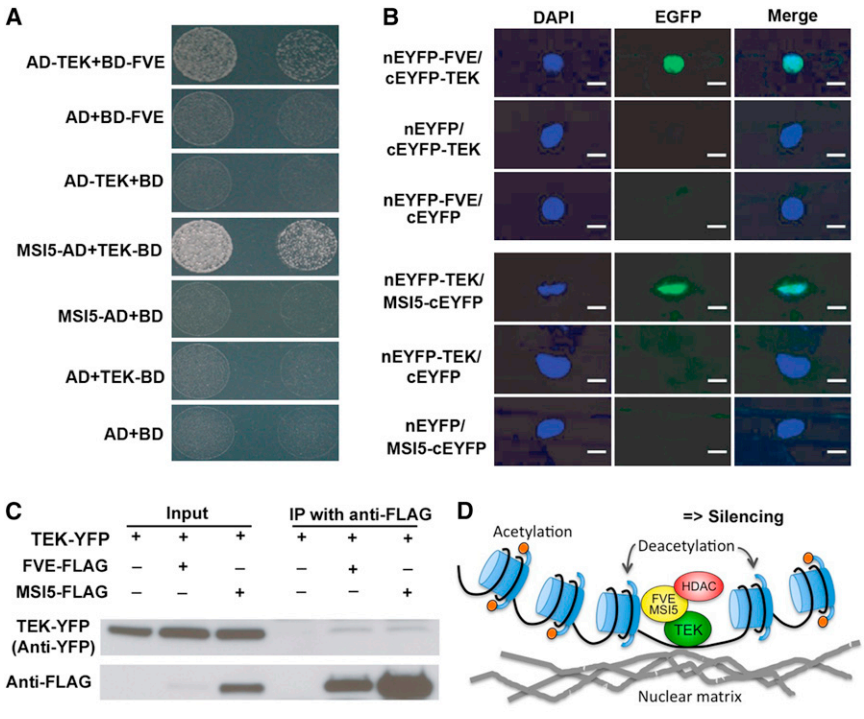

Figure 4. TEK Directly Associates with FVE and MSI5

(A) Interaction of TEK with FVE and MSI5 analyzed by yeast two-hybrid assay. Full-length TEK, FVE, or MSI5 was fused to GAL4 activation (AD) and/or DNA binding domains (BDs), respectively. Yeast colonies harboring these fusion constructs and/or empty vectors, as indicated, were grown on selective media. Yeast growth was detected only when the combinations of TEK and FVE or TEK and MSI5 were cotransformed. (B) BiFC analysis of TEK association with FVE and MSI5 in onion epidermal cells. Green signal indicates the binding of TEK with FVE or MSI5 in the nuclei. DAPI (4',6-diamidino-2-phenylindole) staining indicates nuclei. Scale bar represents 20 μm. (C) Coimmunoprecipitation of TEK with FVE and MSI5 in seedlings. Total proteins extracted from the *TEK-YFP* line (a negative control), F_1 of the doubly hemizygous *TEK-YFP* and *FVE-FLAG*, and F_1 of *TEK-YFP* and *MSI5-FLAG* were immunoprecipitated with anti-FLAG agarose beads. The TEK-YFP protein was specifically detected in the anti-FLAG precipitates from the F_1 seedlings expressing FVE-FLAG or MSI5-FLAG. (D) A model of TEK function. TEK binds to specific targets and forms a protein complex with FVE/MSI5, which participates in histone deacetylation. Deacetylation of the target locus leads to transcriptional silencing.

In summary, our data show that *TEK* acts in the maintenance of genomic integrity by silencing TEs and repeat-containing genes through epigenetic machinery. In *tek* insertional mutants in the Col and WS backgrounds, *FLC* was not derepressed, in contrast to *FLC* derepression in the *fve* mutant in the Col background [13]. The different ecotypic effects of *tek* mutations and *amiTEK* in Col and L*er* suggest that these two ecotypes may have different susceptibility to the loss of TEK activities. This may be due to presence of redundant genes that can substitute for *TEK*, downstream effectors of TEK or a parallel pathway for silencing in Col and WS (but not in L*er*). Such accession-specific effects have been reported in epigenetic regulation including differentially expressed small RNAs and genome imprinting in *Arabidopsis* [23, 32]. Further studies are needed to identify the genetic modifier(s) in different ecotypes.

Supplemental Information

Supplemental Information includes four figures, four tables, and Supplemental Experimental Procedures and can be found with this article online at http://dx.doi.org/10.1016/j.cub.2013.01.030.

Acknowledgments

We thank Arabidopsis TAIR (http://arabidopsis.org) for information and materials and also H. Yu and F. Berger for valuable comments on the manuscript. This work was supported by research grants to T.I. from Temasek Life Sciences Laboratory (TLL), the National Research Foundation Singapore under its Competitive Research Programme (CRP Award NRF-CRP001-108), and PRESTO, Japan Science and Technology Agency, 4-1-8 Honcho Kawaguchi, Saitama, Japan. The work in Y.H.'s laboratory was supported by a grant from the Singapore Ministry of Education (AcRF Tier 2; T207B3105), CRP Award NRF-CRP001-108, and TLL. The research in the S.E.J. laboratory was supported by National Science Foundation Grant MCB-1121245. Illumina sequencing was performed at the UCLA BSCRC BioSequencing Core Facility. H.S. was supported by a Fred Eiserling and Judith Lengyel Graduate Doctorate Fellowship. S.E.J. is an Investigator of the Howard Hughes Medical Institute.

Received: August 4, 2012
Revised: December 12, 2012
Accepted: January 11, 2013
Published: February 7, 2013

References

1. Liu, J., He, Y., Amasino, R., and Chen, X. (2004). siRNAs targeting an intronic transposon in the regulation of natural flowering behavior in Arabidopsis. Genes Dev. *18*, 2873–2878.
2. Gazzani, S., Gendall, A.R., Lister, C., and Dean, C. (2003). Analysis of the molecular basis of flowering time variation in Arabidopsis accessions. Plant Physiol. *132*, 1107–1114.
3. Law, J.A., and Jacobsen, S.E. (2010). Establishing, maintaining and modifying DNA methylation patterns in plants and animals. Nat. Rev. Genet. *11*, 204–220.
4. Zaratiegui, M., Irvine, D.V., and Martienssen, R.A. (2007). Noncoding RNAs and gene silencing. Cell *128*, 763–776.
5. Saze, H., and Kakutani, T. (2011). Differentiation of epigenetic modifications between transposons and genes. Curr. Opin. Plant Biol. *14*, 81–87.
6. Michaels, S.D., He, Y., Scortecci, K.C., and Amasino, R.M. (2003). Attenuation of FLOWERING LOCUS C activity as a mechanism for the evolution of summer-annual flowering behavior in Arabidopsis. Proc. Natl. Acad. Sci. USA *100*, 10102–10107.
7. Lippman, Z., Gendrel, A.V., Black, M., Vaughn, M.W., Dedhia, N., McCombie, W.R., Lavine, K., Mittal, V., May, B., Kasschau, K.D., et al. (2004). Role of transposable elements in heterochromatin and epigenetic control. Nature *430*, 471–476.
8. Kinoshita, Y., Saze, H., Kinoshita, T., Miura, A., Soppe, W.J., Koornneef, M., and Kakutani, T. (2007). Control of FWA gene silencing in Arabidopsis thaliana by SINE-related direct repeats. Plant J. *49*, 38–45.
9. Reeves, R., and Nissen, M.S. (1990). The A.T-DNA-binding domain of mammalian high mobility group I chromosomal proteins. A novel peptide motif for recognizing DNA structure. J. Biol. Chem. *265*, 8573–8582.
10. Yasui, D., Miyano, M., Cai, S.T., Varga-Weisz, P., and Kohwi-Shigematsu, T. (2002). SATB1 targets chromatin remodelling to regulate genes over long distances. Nature *419*, 641–645.
11. Cai, S., Han, H.J., and Kohwi-Shigematsu, T. (2003). Tissue-specific nuclear architecture and gene expression regulated by SATB1. Nat. Genet. *34*, 42–51.
12. Soppe, W.J., Jacobsen, S.E., Alonso-Blanco, C., Jackson, J.P., Kakutani, T., Koornneef, M., and Peeters, A.J. (2000). The late flowering phenotype of fwa mutants is caused by gain-of-function epigenetic alleles of a homeodomain gene. Mol. Cell *6*, 791–802.
13. Ausín, I., Alonso-Blanco, C., Jarillo, J.A., Ruiz-García, L., and Martínez-Zapater, J.M. (2004). Regulation of flowering time by FVE, a retinoblastoma-associated protein. Nat. Genet. *36*, 162–166.
14. Gu, X., Jiang, D., Yang, W., Jacob, Y., Michaels, S.D., and He, Y. (2011). Arabidopsis homologs of retinoblastoma-associated protein 46/48 associate with a histone deacetylase to act redundantly in chromatin silencing. PLoS Genet. *7*, e1002366.
15. Han, H.J., Russo, J., Kohwi, Y., and Kohwi-Shigematsu, T. (2008). SATB1 reprogrammes gene expression to promote breast tumour growth and metastasis. Nature *452*, 187–193.
16. Ng, K.H., Yu, H., and Ito, T. (2009). AGAMOUS controls GIANT KILLER, a multifunctional chromatin modifier in reproductive organ patterning and differentiation. PLoS Biol. *7*, e1000251.
17. Yun, J., Kim, Y.S., Jung, J.H., Seo, P.J., and Park, C.M. (2012). The AT-hook motif-containing protein AHL22 regulates flowering initiation by modifying FLOWERING LOCUS T chromatin in Arabidopsis. J. Biol. Chem. *287*, 15307–15316.
18. Schwab, R., Ossowski, S., Riester, M., Warthmann, N., and Weigel, D. (2006). Highly specific gene silencing by artificial microRNAs in Arabidopsis. Plant Cell *18*, 1121–1133.
19. Alves-Ferreira, M., Wellmer, F., Banhara, A., Kumar, V., Riechmann, J.L., and Meyerowitz, E.M. (2007). Global expression profiling applied to the analysis of Arabidopsis stamen development. Plant Physiol. *145*, 747–762.
20. Amasino, R. (2010). Seasonal and developmental timing of flowering. Plant J. *61*, 1001–1013.
21. He, Y., Michaels, S.D., and Amasino, R.M. (2003). Regulation of flowering time by histone acetylation in Arabidopsis. Science *302*, 1751–1754.
22. Singer, T., Yordan, C., and Martienssen, R.A. (2001). Robertson's Mutator transposons in A. thaliana are regulated by the chromatin-remodeling gene Decrease in DNA Methylation (DDM1). Genes Dev. *15*, 591–602.
23. Zhai, J.X., Liu, J., Liu, B., Li, P.C., Meyers, B.C., Chen, X.M., and Cao, X.F. (2008). Small RNA-directed epigenetic natural variation in Arabidopsis thaliana. PLoS Genet. *4*, e1000056.
24. Tsukahara, S., Kobayashi, A., Kawabe, A., Mathieu, O., Miura, A., and Kakutani, T. (2009). Bursts of retrotransposition reproduced in Arabidopsis. Nature *461*, 423–426.
25. Gao, D. (2012). Identification of an active Mutator-like element (MULE) in rice (Oryza sativa). Mol. Genet. Genomics *287*, 261–271.
26. Johanson, U., West, J., Lister, C., Michaels, S., Amasino, R., and Dean, C. (2000). Molecular analysis of FRIGIDA, a major determinant of natural variation in Arabidopsis flowering time. Science *290*, 344–347.
27. Tikhonov, A.P., Lavie, L., Tatout, C., Bennetzen, J.L., Avramova, Z., and Deragon, J.M. (2001). Target sites for SINE integration in Brassica genomes display nuclear matrix binding activity. Chromosome Res. *9*, 325–337.
28. Aufsatz, W., Mette, M.F., van der Winden, J., Matzke, M., and Matzke, A.J. (2002). HDA6, a putative histone deacetylase needed to enhance DNA methylation induced by double-stranded RNA. EMBO J. *21*, 6832–6841.
29. Zilberman, D., Gehring, M., Tran, R.K., Ballinger, T., and Henikoff, S. (2007). Genome-wide analysis of Arabidopsis thaliana DNA methylation uncovers an interdependence between methylation and transcription. Nat. Genet. *39*, 61–69.
30. To, T.K., Kim, J.M., Matsui, A., Kurihara, Y., Morosawa, T., Ishida, J., Tanaka, M., Endo, T., Kakutani, T., Toyoda, T., et al. (2011). Arabidopsis

HDA6 regulates locus-directed heterochromatin silencing in cooperation with MET1. PLoS Genet. *7*, e1002055.

31. Liu, X., Yu, C.W., Duan, J., Luo, M., Wang, K., Tian, G., Cui, Y., and Wu, K. (2012). HDA6 directly interacts with DNA methyltransferase MET1 and maintains transposable element silencing in Arabidopsis. Plant Physiol. *158*, 119–129.
32. Gehring, M., Bubb, K.L., and Henikoff, S. (2009). Extensive demethylation of repetitive elements during seed development underlies gene imprinting. Science *324*, 1447–1451.